P-401

NASA Contractor Report 3883

Program LRCDM2, Improved Aerodynamic Prediction Program for Supersonic Canard-Tail Missiles With Axisymmetric Bodies

Marnix F. E. Dillenius

CONTRACT NAS1-16770
APRIL 1985

Date for general release April 1987

NASA

NASA Contractor Report 3883

Program LRCDM2, Improved Aerodynamic Prediction Program for Supersonic Canard-Tail Missiles With Axisymmetric Bodies

Marnix F. E. Dillenius
Nielsen Engineering & Research, Inc.
Mountain View, California

Prepared for
Langley Research Center
under Contract NAS1-16770

National Aeronautics
and Space Administration

Scientific and Technical
Information Branch

1985

TABLE OF CONTENTS

LIST OF SYMBOLS

$b/2$	exposed fin semispan
c	fin local chord
c_r	fin root chord
$c_{s.e.}$	fin side edge or tip chord
cc_n	span loading
C_ℓ	rolling-moment coefficient about x_B-axis, positive right fin down, looking forward, moment/$(q_\infty S_{ref} L_{ref})$
C_m	pitching-moment coefficient about y_B-axis, nose up positive, moment/$(q_\infty S_{ref} L_{ref})$
C_n	yawing-moment coefficient about z_B-axis, nose to right positive, moment/$(q_\infty S_{ref} L_{ref})$
C_N	normal-force coefficient, $C_N = \sqrt{C_Z^2 + C_Y^2}$, $C_N = C_Z$ when $\phi = 0$
C_p	pressure coefficient, $(p - p_\infty)/q_\infty$
C_X	force coefficient along x_B-axis, force/$(q_\infty S_{ref})$
C_Y	force coefficient along y_B-axis, force/$(q_\infty S_{ref})$
C_Z	force coefficient along z_B-axis, force/$(q_\infty S_{ref})$
$K_{v,LE}$	proportionality factor relating normal force to suction along leading edge
$K_{v,SE}$	proportioanlity factor relating normal force to suction along side edge
ℓ	body length
L_{ref}	reference length
M_∞	free-stream Mach number
p	local static pressure
p_∞	free-stream static pressure
q_∞	free-stream dynamic pressure

S_{ref}	reference area
u,v,w	axial, lateral, and upward velocity components along body coordinates (x_B,y_B,z_B)
V_R	magnitude of resultant velocity
V_∞	free-stream velocity
x	distance along local chord measured from leading edge
y	distance along span measured from root chord
y_v	lateral position of fin-edge vortex measured from root chord, Section 2.4
$z_{\ell,\Gamma}$	distance of fin-edge vortex above plane of the fin Section 2.4
x_B,y_B,z_B	body-axis coordinate system with origin at nose tip, x_B along body longitudinal axis, see sketches in Sections 2.1 and 2.4
x_M	axial coordinate of moment center in body axis system
x_W,y_W,z_W	wing coordinate system parallel to x_B,y_B,z_B system but with origin on body longtudinal axis at axial location of leading edge of root chord of finned section, see sketch in Section 2.4
α	angle of pitch, Equation (3), degrees
α_c	included angle of attack, degrees; angle between free-stream velocity vector and body longitudinal axis, x_B
α_ℓ	angle of attack seen by a fin including effects of free stream and deflection angle, Equation (1), degrees
$\alpha_{F,\ell}$	local flow angle of attack at fin leading edge, includes body and external-vortex effects
β	angle of sideslip, Equation (3), degrees
γ	ratio of specific heats, $\gamma = 1.4$ for air
δ	fin deflection angle, degrees; flow deflection angle, Section 2.6

ε	lateral flow angularity on a local surface
θ	fin thickness envelope angle measured in streamwise direction relative to fin mean plane, Section 2.6; also angle between one segment in a strip on a body and body centerline, Section 2.6.2, degrees
ϕ	angle of roll, positive right fin down, looking forward, degrees; for a cruciform fin layout, $\phi = 0$ corresponds to right fin in horizontal plane and vertical fin in plane of symmetry
μ	Mach angle, $\mu = \sin^{-1}(1/M)$, M is Mach number
ν	Prandtl-Meyer flow angle

Subscripts and Abbreviations

[AIC]	matrix containing Aerodynamic Influence Coefficients FVN
Æ	aspect ratio
Bern	Bernoulli
corr	corrected
CP	center of pressure measured from root chord leading edge
F	fin
ℓ	local
lower, ℓ	bottom surface of an airfoil
LE	leading edge
min	minimum value
SE	side edge
TE	trailing edge
upper, u	top surface of an airfoil
2D, 2-D	two-dimensional
3D, 3-D	three-dimensional

1. INTRODUCTION

Designs of new air-to-air and other tactical missiles are aimed at high maneuverability, low structural weight, and conformal or submerged carriage. The speed range includes the low and high supersonic Mach numbers. Angles of attack can be high enough to cause formation of body and fin shed vorticity. The missiles may be equipped with planar and cruciform fin layouts, monoplane wing/interdigitated tail fins, or low profile finned sections all with various planform shapes. Accurate prediction of loading distributions and component loadings are required for stability and control and for aeroelastic analyses.

In response to the above needs, program LRCDM2 was developed for supersonic missiles with axisymmetric bodies and up to two finned sections. The fin planforms may have breaks in sweep but must be flat. This program is capable of predicting pressure distributions and component loads acting on the entire configuration including effects of body and fin vorticity. It is the result of an evolutionary process starting with the set of programs DEMON2 (Ref. 1) which was automated and specialized to configurations with bodies of revolution in program NSWCDM (Ref. 2). These analytic programs make use of supersonic paneling and line-singularity methods coupled with vortex-tracking theory. DEMON2 was developed under sponsorship of NASA/Langley Research Center and the Air Force Flight Dynamics Laboratory; NSWCDM was sponsored by the Naval Surface Weapons Center.

The work described in this report is concerned with improvements and extensions to NSWCDM in connection with fin- and afterbody-shed vorticity, reducing computation time, and extending the Mach number and angle of attack ranges. The resulting computer program is called LRCDM2. This work was supported by the Supersonic Aerodynamics Branch of

NASA/Langley Research Center under Contract NAS1-16770 with Mr. Jerry Allen as Technical Representative.

On the basis of recent user experience with programs DEMON2 and NSWCDM (for example, Refs. 3 and 4), the following specific tasks were performed to improve and extend the usable range of program NSWCDM.

Task 1.- Add an afterbody vortex-shedding model; the afterbody and tail-fin pressure and loading calculations shall include afterbody vorticity effects.

Task 2.- Add routines for determining fin leading- and/or side-edge vorticity characteristics in a form compatible with the vortex tracking routines; these vortices are to be included in the vortex trajectory calculations along the afterbody and tail section.

Task 3.- Reduce computer time by saving the influence coefficient matrix and other characteristics associated with the forward- and tail-finned sections; modify the program to run multiple angles of attack and roll for one Mach number.

Task 4.- Extend range of applicability in terms of Mach number (up to Mach 6) and angles of attack (up to 25°) by investigating practical means for combining two-dimensional nonlinear hypersonic and shock expansion theories with three-dimensional linear theory to account for interference.

As part of the above tasks, predictions were compared with available measurements in order to evaluate the improvements and extensions. In addition, fin layouts were made more flexible and may include low-profile quadriform and triform layouts. Program modifications for the latter were carried out for the U.S. Army Missile Command*.

---

*Work performed for Mr. Dave Washington, DRSMI-RDK, Redstone Arsenal, Alabama, under Purchase Order No. DAA H01-82-P-1224.

The updated program LRCDM2 treats a complete missile configuration from nose tip to body base in a series of steps. Fins and wings alone can also be analyzed by this program. A special program designated BDYSHD models afterbody vortex shedding and can be used with LRCDM2 and vortex tracking module VPATH2 to account for the effects of afterbody vortices on the tail fin pressures and loads.

In this report, the methods of approach to accomplish the tasks are given. Comparisons between predictions and experiment are described. Limitations and recommendations are given in the concluding remarks. The appendices contain user-oriented program documentation including a description of program flow, input and output, program limitations and a sample case. Additional analytical details are described in the remaining appendices.

2. METHODS OF APPROACH

This section contains brief descriptions of the nature of and the need for an afterbody vortex-shedding model, the basic underlying theoretical approach of an existing vortex-shedding program NOSEVTX, and the modifications and improvements required for use with program LRCDM2 resulting in companion program BDYSHD. The use of programs LRCDM2 and BDYSHD in the automated stepwise treatment of a complete missile configuration is described. This is followed by a discussion of the updated treatment for fin-edge vorticity and the modifications performed to reduce computer running time. A description is given of preliminary methods to extend the Mach number range of applicability of LRCDM2. Where necessary, additional details are given in appendices.

2.1 Afterbody Vortex-Shedding Model

Configurations with long afterbody sections (length between forward and tail fins $\geq$ 10 diameters) will shed afterbody vortices for angles of attack in excess of 10°. The following sketch depicts two vortex feeding sheets on the afterbody of an unrolled missile at included angle of attack α_c. The body coordinate system (x_B, y_B, z_B) with origin at the nose tip is indicated but the tail fins are not shown. The actual shape and starting locations of the feeding sheets are influenced by the flow conditions and external vortices (if present) generated by the forebody and the canard fins.

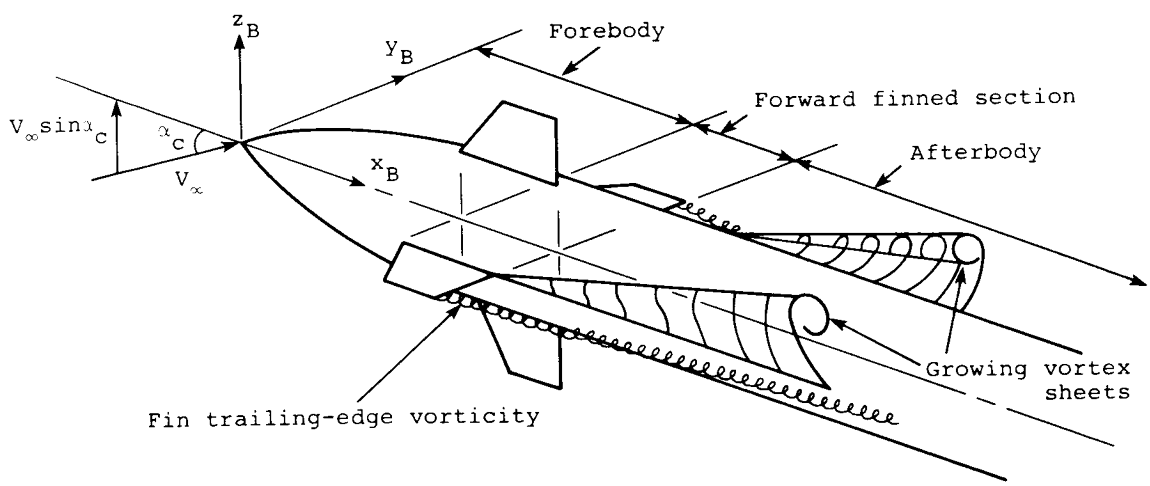

Only two fin trailing edge vortices are shown but more may exist. In the afterbody vortex model, the growing vortex sheets will be represented by a multitude of vortices called vortex clouds.

It is mentioned in Reference 3 that the lack of afterbody vorticity in program DEMON2 (on which NSWCDM and LRCDM2 are based) may affect predicted rolling moment for angles of attack in excess of about 12° for a forward control canard-tail wind tunnel model. Similar observations are listed in Reference 2 in connection with overall normal forces in pitch. Afterbody vortices will affect the forces and moments acting on the afterbody. In addition, the vortices will induce effects on the tail fins with the attendant modifications to the fin loadings. Thus, an afterbody vortex shedding module was developed from an existing program called NOSEVTX and adapted for optional use with LRCDM2.

The supersonic vortex shedding program NOSEVTX was developed for application to forebodies. The basic features are described in Reference 5 and program details are given in Reference 6. The method is essentially based on a modified Stratford separation criteria applied to circumferential pressure distributions on the body which are calculated with potential flow methods including effects of external vortices. Strengths of the shed or separated vortices are related to the square of the resultant flow velocity calculated at points on the body. The shed vortices form a vortex cloud.

2.2 Program BDYSHD

Program NOSEVTX (Ref. 6) was modified and arrangements made to suit the needs of program LRCDM2 and to decrease running time in the application to axisymmetric bodies. The new afterbody vortex shedding program is called BDYSHD. User-oriented program details are given in Appendix B. Program BDYSHD has the following new features.

1. The body source-paneling method is replaced with the source and doublet line-singularity method described in References 1 and 7 in order to decrease computation time appreciably; the allowable body cross-sectional shapes are limited to axisymmetric cross sections and the bodies consist of a nose followed by a cylinder.

2. Files are created to exchange calculated forces and moments between programs LRCDM2 and BDYSHD at the beginning and end of the afterbody section.

3. Files are created to exchange external vortex strengths and lateral locations between LRCDM2 and BDYSHD at the beginning and end of the afterbody section.

4. Effects of included angle of attack and angle of roll are incorporated and afterbody loads are calculated in rolled and unrolled body coordinate systems.

5. The latest modifications and improvements to NOSEVTX, performed under Contract NAS1-17027 since its description in Reference 6, have been incorporated in BDYSHD. These include refinements in the determination of the flow separation locations based on the Stratford criteria described in Reference 6 and an improved vortex core model. In the application to treatment of afterbodies (length of body between forward and tail-finned sections), program BDYSHD starts the analysis with a set of forebody vortices (if present) and forward fin-edge vortices.

The resulting program BDYSHD can be run as a stand-alone program to treat bodies of revolution at supersonic speeds. Additionally, it can be employed as a companion to LRCDM2 to model vortex shedding from axisymmetric afterbodies as an option. If the latter is the case, the stepwise calculation procedure used in LRCDM2 is interrupted by the job control cards at the end of the first three steps that treat the forebody and the canard section. Program BDYSHD is then called to handle the afterbody. After completion, program LRCDM2 is called again to treat the tail section. The procedure is described in more detail below.

2.3 Use of Programs LRCDM2 and BDYSHD in Stepwise Procedure

The stepwise series or sequence of calculations employs the following program or modules.

Program or Module	Purpose
LRCDM2 (contains executive routine)	Compute pressures and loads acting on axisymmetric forebody or afterbody (neglecting afterbody vortices) and one finned section; LRCDM2 makes use of line singularities and paneling methods as summarized in References 2 and 4 and described with more details in Reference 1; latest modifications are given elsewhere in this report.
VPATH2 (module of LRCDM2)	Calculate vortex paths and vortex induced effects for cases with or without cruciform fins mounted on axisymmetric bodies; method is based on slender body theory and makes use of path integration scheme as described in References 1, 2, and 4.
BDYSHD (separate program)	Over length of afterbody (i.e., between forward- and tail-fin sections), generate body-shed vortices and compute loads acting on afterbody; if this program is used, the afterbody calculations in LRCDM2 are not used; details of the vortex shedding method are given in References 5 and 6.

In the application to a complete configuration consisting of a forward set and tail set of fins mounted on an axisymmetric body, program LRCDM2 performs the following six steps in conjunction with module VPATH2 and optionally with program BDYSHD. Except for step 3a, the executive routine in LRCDM2 performs the stepwise procedure and arranges for the appropriate data exchanges. The optional step 3a, engagement of program BDYSHD, is performed with job control language. Also note that in the treatment of a tail finner (one finned section at body base), program LRCDM2 is set to perform the first three steps only.

Step 1.- Analyze forebody and forward-finned section or wing; effects of forebody shed vorticity (determined from built-in data base) are included up to finned section; compute and save control point coordinates and calculate loads on forward fins without vortex effects.

Step 2.- Using module VPATH2, track vortices through forward-finned section, compute and save their effects on the fins; in this process the vortex paths may move in a crossflow plane or their paths can be made to lie parallel to body centerlines (the latter scheme is recommended).

Step 3.- Include effects of forebody vortices in loadings acting on forward-finned section and determine fin-edge vorticity characteristics; add force and moment coefficients for the configuration up to the canard trailing edge.

Step 3a.- (OPTIONAL) Stop program LRCDM2 and continue with program BDYSHD to treat afterbody from forward-finned section to leading edge of tail-finned section; data sets containing loading and vortex information are exchanged at the start and the end of this run between programs LRCDM2 and BDYSHD.

Step 4.- Continue with LRCDM2 to compute and save control point coordinates and calculate loads on tail fins without effects of forebody, canard, or afterbody vortices; if step 3a is not exercised, coordinates of points on the afterbody at which pressures will be calculated are also calculated and stored.

Step 5.- If step 3a is not performed, track forebody and forward-fin vortices from forward-finned section along afterbody and through the tail section; compute and save vortex effects on afterbody and tail fins by another application of VPATH2; if program BDYSHD (step 3a) was used to treat the afterbody, VPATH2 tracks all (including afterbody) vortices through the tail section; along the tail fins, the vortex paths may move in the crossflow plane or their paths can be made to lie parallel to the body centerline (the latter scheme is recommended).

Step 6.- Include effects of external vortices in the loadings acting on tail fins; if step 3a was not used, compute afterbody loads including effects of forebody and forward-fin vorticity; compute and list forces and moments acting on complete configuration.

In the above steps, program LRCDM2 has been arranged to exchange data sets containing control point coordinates and vortex path information between fin-geometric and fin-load calculation routines and module VPATH2 without user intervention. When program BDYSHD is engaged, however, indices in the input data for LRCDM2 and BDYSHD arrange for data set exchanges between the two programs. Actual program running details are given in Appendices A and B describing program LRCDM2 and program BDYSHD, respectively.

The following sketch depicts the stepwise procedure superimposed on a typical configuration with and without the application of program BDYSHD. The scheme without the use of the latter program is indicated on the side of the configuration. The optional sequence shown at the top includes

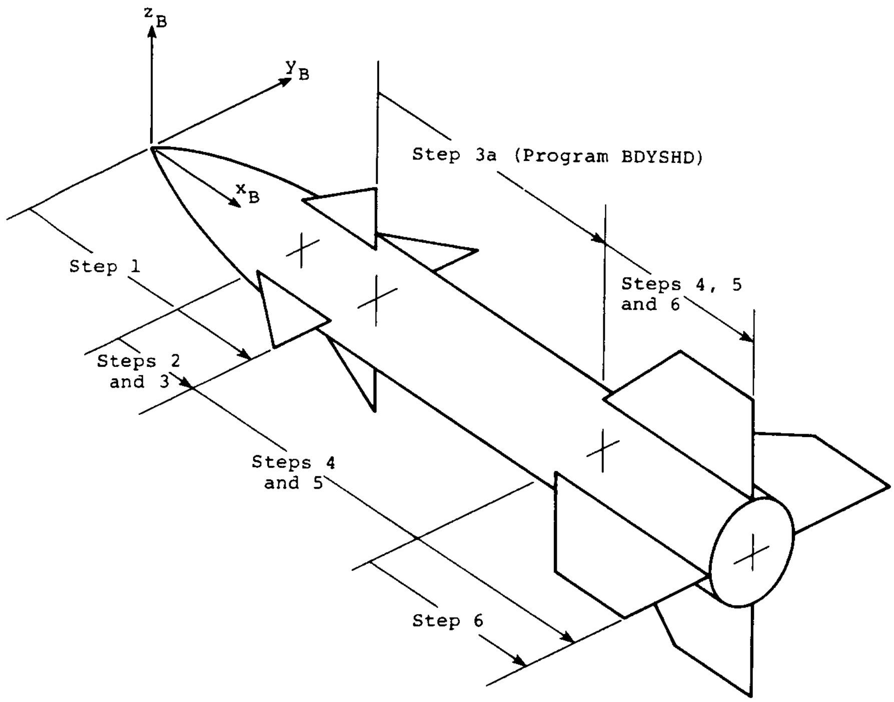

program BDYSHD to treat the afterbody. The body coordinate system is also shown. Note that steps 1, 3, 4, and 6 involve the body and fin routines of program LRCDM2 and steps 2 and 5 are performed by the vortex tracking module VPATH2. Step 3a involves the afterbody vortex-shedding program BDYSHD . If the configuration of interest is a tail finner (one finned section at the base), steps 1 through 3 only are engaged.

2.4 Fin Leading- and Side-Edge Vorticity Characteristics

Fins can develop leading- and side-edge separation vorticity as the angle of attack is increased. If the side edges are long, vorticity can be generated along the edge for angles of attack as low as 5°. Along the leading edges, vorticity can be generated at supersonic speeds provided the edge lies aft of the Mach cone from the root leading edge (subsonic leading edge). In any event, the leading- and side-edge vortices may combine and form a pattern of strong vorticity located above the trailing edge. In the case of a missile, the forward fins may generate leading- and/or side-edge vortices which stream aft along the afterbody and tail section and influence the pressures on those components.

For fins with leading- and/or side-edge flow separation, program LRCDM2 is capable of determining the augmentation to fin normal force from the suction distributions along those edges. This approach is based on the Polhamus suction analogy discussed in Appendix C of Reference 1. The actual method has been updated to account for arbitrary fin dihedral (or cant) angle and fin location on the body. The modifications are described in Section C.2 of Appendix C in this report. In addition, along the leading and/or side edges the growing vorticity strength is calculated as a function of spanwise distance by means of lifting line theory and the distribution of suction. Only a portion of the suction, determined by vortex lift factor $K_{v,LE}$ for the leading edge and factor $K_{v,SE}$ for the side edge, is converted to normal force. Estimates for these factors are given in Reference 8. These factors are required as input by program LRCDM2 and have default values $K_{v,LE} = 0.5$ and $K_{v,SE} = 1.0$. The leading- and side-edge forces are included in the overall force and moment calculation for a given configuration. At the trailing edge of the fin, the leading and/or side edge vortex is elevated above the fin plane as illustrated in the following sketch. One fin of the forward-finned section is shown attached to a body. The body coordinate system (x_B, y_B, z_B) and wing coordinate system (x_W, y_W, z_W) are also indicated. The dihedral or cant angle for a horizontal fin is zero. The fin leading edge

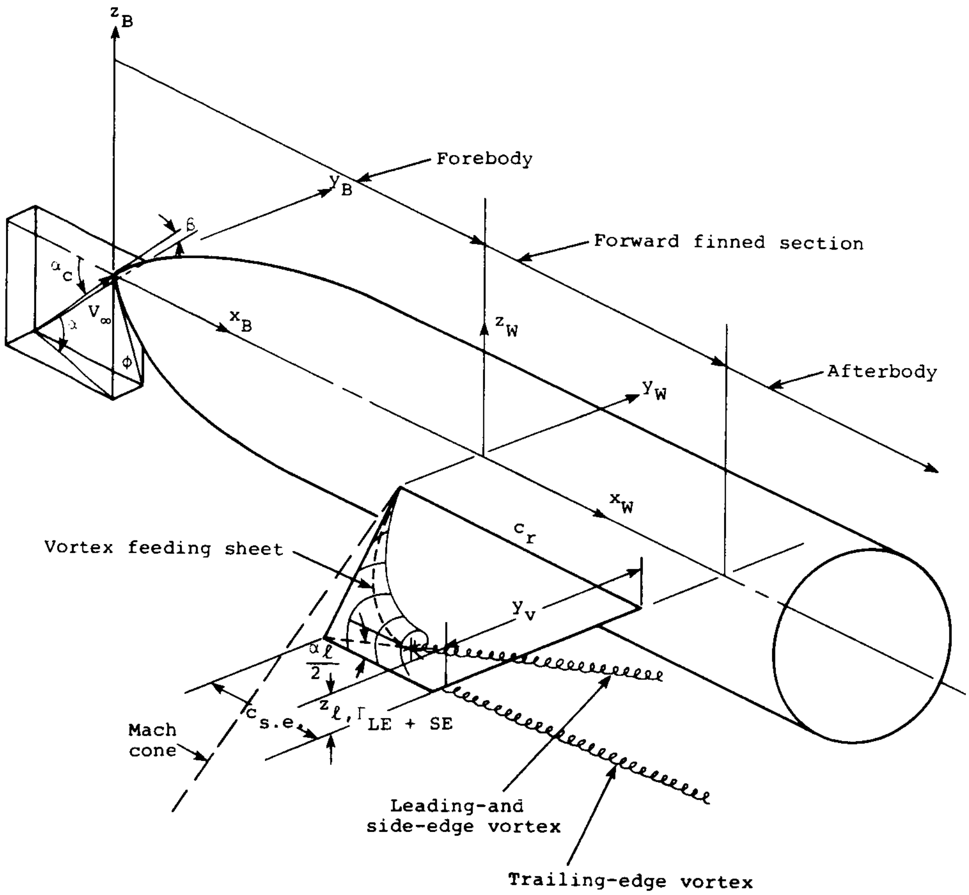

lies aft of the Mach cone (it is subsonic) and the side edge has nonzero length. The angle of pitch seen by the fin is high enough to cause formation of strong leading- and side-edge vorticity. A vortex feeding sheet forms and at the fin trailing edge it is fully developed. At this position, the vortex system can be represented by a concentrated discrete vortex. The lateral position y_v is taken as the center of gravity or the moment center of the suction distributions along the leading and side edges. This distance, as measured from the fin root chord, is given by Equation (C-9) in Appendix C of this report. Its position above the fin plane can be represented by considering the concentrated vortex to emanate from the forward corner of the side edge along a straight line directed by one-half of the angle of pitch α_ℓ seen by the fin. In this process, the upward motion of the vortex is in a plane normal to the fin. This is an approximation often made for a fin attached to a body in accordance with a concept originated by Bollay (Ref. 9). For a vertical fin, one half of the angle of sideslip is applied to determine the displacement of the leading- and/or side-edge vortex from the fin plane. For rolled fins, the upwash due to angle of pitch α, angle of sideslip β, and fin deflection angle δ is determined first and recast into a local fin angle of attack α_ℓ. One half of this angle is then used in the vortex displacement calculation. Thus, for a fin with nonzero side edge the elevation of the vortex is given by

$$\left.\begin{aligned} z_{\ell,\Gamma_{LE+SE}} &= c_{s.e.} \tan \frac{\alpha_\ell}{2} \\ \alpha_\ell &= \sin^{-1}(\sin\delta + \sin\alpha \cos\phi_f - \sin\beta \sin\phi_f) \end{aligned}\right\} \quad (1)$$

where $c_{s.e.}$ is the tip or side-edge chord and ϕ_f is the dihedral or cant angle of the fin as shown in Section C.2 of Appendix C.

For a fin with zero side-edge length (one half of a delta wing), the lateral location of the leading-edge vortex is assumed to correspond to the center of gravity or moment center of the suction along that edge. As a first approximation, the displacement (elevation) of the vortex is based on the root chord c_r of the fin

$$z_{\ell,\Gamma_{LE}} = c_r \tan \frac{\alpha_\ell}{2} \quad (2)$$

Angles α and β are related to the included angle of attack α_c and angle of roll ϕ in accordance with the pitch-roll tranformation

$$\begin{aligned} \sin\alpha &= \sin\alpha_c \cos\phi \\ \sin\beta &= \sin\alpha_c \sin\phi \end{aligned} \tag{3}$$

described on page 5 of Reference 10. Angles α_c, α, β, and ϕ are indicated in the previous sketch. Program LRCDM2 has been arranged to read in multiple sets of α_c and ϕ as described in the next section.

In addition to the leading-edge and/or side-edge vortex, the sketch also shows one trailing-edge vortex. This vortex is associated with the attached-flow span loading (also described in Appendix C) as opposed to the separated-flow edge load augmentation. Presently, program LRCDM2 computes the leading- and/or side-edge vortex and retains the one or more trailing edge vortices calculated from the fin span-load distribution for attached flow. It would be better to compute a total span-load distribution including the leading-edge force augmentation and the side-edge force augmentation spread out over some distance inward from the tip. Such a span load distribution may look as follows on a fin. Coordinate y is the lateral distance from the root chord and b/2 is the semispan.

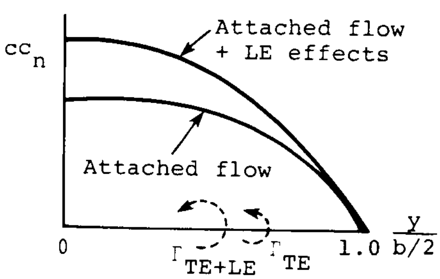

No side edge

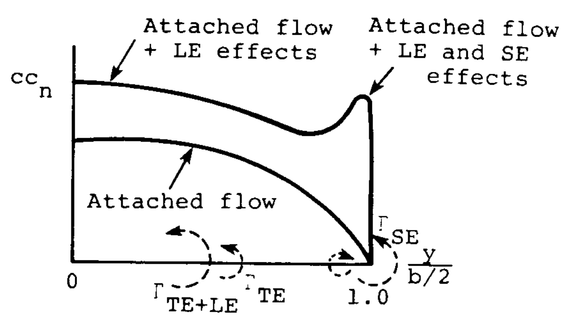

With side edge

Based on the total span load distribution, cc_n, several concentrated discrete vortices can be computed. The number will depend on the extrema in the span load distribution in accordance with the method described in Appendix C. This procedure is presently not sufficiently developed for inclusion in LRCDM2.

In any event, the strengths and positions of the fin leading- and/or side-edge vortex and the one or more trailing-edge vortices are now known. They will be included either in the vortex tracking step 5 (VPATH2) or they will be included in step 3a (BDYSHD) if afterbody vortex shedding is to be considered as an option. For a configuration with a tail-finned section, all of the vortices (body nose vortices if present, forward-fin edge vortices and afterbody vortices if generated) are included in the tail-fin loading calculations in step 6.

2.5 Reduction in Computation Time for Program LRCDM2

When program LRCDM2 is applied to a complete configuration consisting of a forward-finned section (canard or wing) and tail-finned section mounted on an axisymmetric body, an aerodynamic influence coefficient matrix is calculated for the forward fins and interference shell, and in general a different matrix is generated for the tail fins and interference shell. The aerodynamic influence coefficient matrix [AIC] contains coefficients FVN. In the sketch below, the forward- and tail-finned sections are covered with a sparse layout of constant u-velocity panels. Only one fin and one-quarter of the interference shell are shown covered with panels. As described in Reference 1, the aerodynamic influence coefficient FVN represents the normal velocity per unit strength induced by one panel at the control point of its own or another panel.

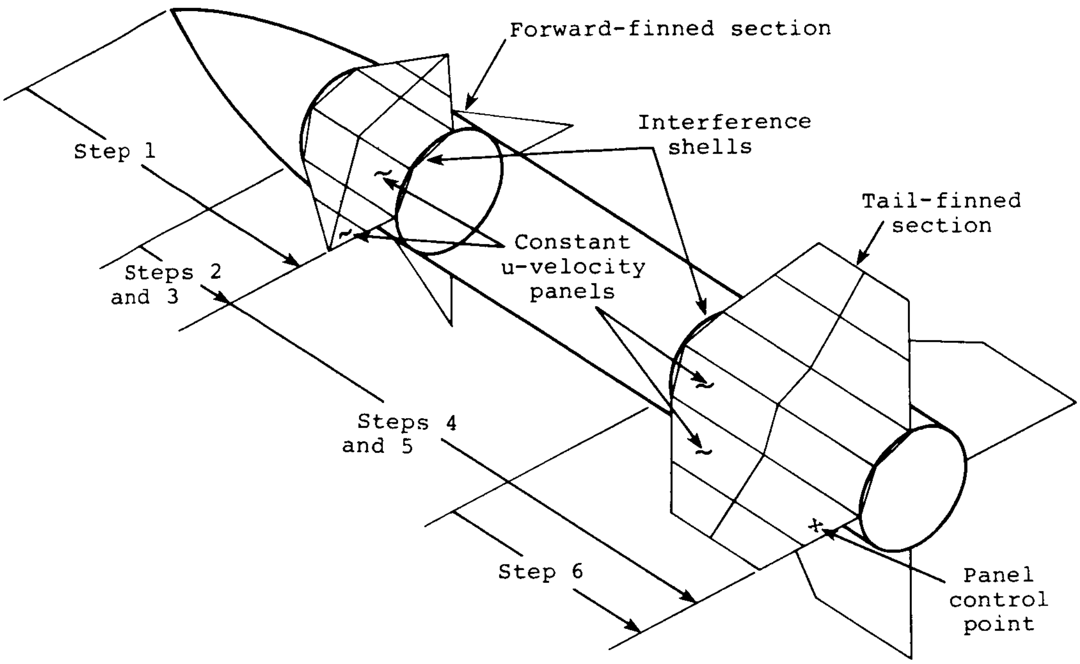

The matrix build-up for the forward fins and interference shell is performed in step 1 of the stepwise procedure described in Section 2.3. For the tail section, the operation is performed in step 4.

The aerodynamic influence coefficients are functions only of the configuration geometry and free-stream Mach number. In order to facilitate use of program LRCDM2 and to reduce computation time the following features have been incorporated. In the process of performing calculations for multiple included angles of attack α_c and/or angles of roll ϕ at one Mach number, the aerodynamic influence coefficients are saved during the calculation for the first combination of α_c and ϕ. Specifically, in step 1 the triangulated [AIC] for the forward fins and interfernece shell is saved on temporary storage device

TAPE9. In step 4, the triangulated [AIC] for the tail fins and interference shell is saved on temporary storage device TAPE10. The triangulating procedure is performed by subroutine PAS001 of LRCDM2. The respective triangulated [AIC]'s for the forward- and tail-finned sections are then read in during the calculation for the next set of α_c and ϕ and so forth until all combinations have been run. The included angles of attack α_c and/or the angles of roll ϕ for which computations are to be made are read in all at once at the beginning of a multiple run.

2.6 Shock-Expansion/Linear Theory and Newtonian/ Linear Theory Combinations for Pressure Distributions

In an effort to investigate practical methods for extending the applicable range of Mach number of program NSWCDM (Ref. 2), two schemes were developed and implemented as pressure calculation options in LRCDM2 for preliminary testing. At present, the two methods are limited to cases with attached shocks. The methods have been tested only on a rectangular wing, a delta wing, and an ogive cylinder body. The two methods will now be summarized. Further details are given later in this section.

The first scheme, first suggested by Carlson in Reference 11 for wings, involves shock-expansion (tangent wedge) theory for calculating pressure coefficients along chordwise or longitudinal strips on the surfaces of a fin or body, respectively. The nonlinear shock-expansion theory is valid for all supersonic Mach numbers provided the shock is attached. The flow deflection angles, δ, required by this two-dimensional nonlinear theory and shown for a fin in the sketch below, are determined from the geometry of the surface (streamwise slope θ) and then modified by correction angles

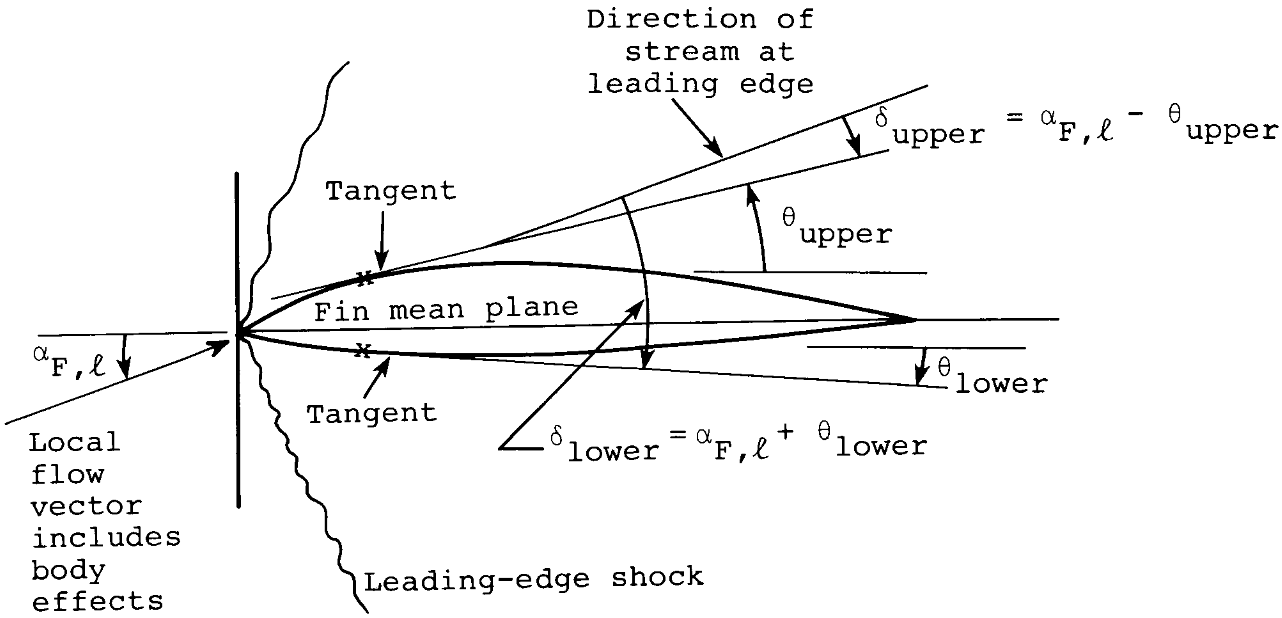

determined from two- and three-dimensional linear theory. With two-dimensional linear theory, the pressure is proportional to the flow deflection angle. In program LRCDM2, the three-dimensional linear theory is made up of the supersonic paneling method on the fins and the interference shell on the body, and the supersonic line singularity method used to model the body. The correction angles can be viewed as a correction to account for mutual interference effects between the individual strips on a given fin, between the fin and other fins and between the fin and the body. In addition, the correction angles may include effects induced by external vortices. The modified flow deflection angles then include a geometric component and an interference component based on local interference flow velocities. The updated angles are then used to compute corrected pressure coefficients by means of the shock-expansion formulation. This method is limited to cases when the shock is attached to the wing leading edge or body nose.

In the second scheme, the pressure coefficients are calculated with the simplest form of Newtonian or impact theory. This nonlinear theory is valid only for high supersonic Mach numbers ($M_\infty > 5$). The flow angles, δ, required by this theory are modified in the same manner as used with shock-expansion (tangent wedge) theory. Corrected pressures are then calculated with the updated angles used in the impact pressure formulations.

The essential differences between the nonlinear and linear theories and the optional combined theory pressure calculation procedures implemented in program LRCDM2 will now be described in more detail.

2.6.1 Two dimensional nonlinear and linear pressure coefficients.- The differences in pressure coefficients predicted by two-dimensional shock-expansion and linear theories can be illustrated as follows for a planar surface inclined to the free stream.

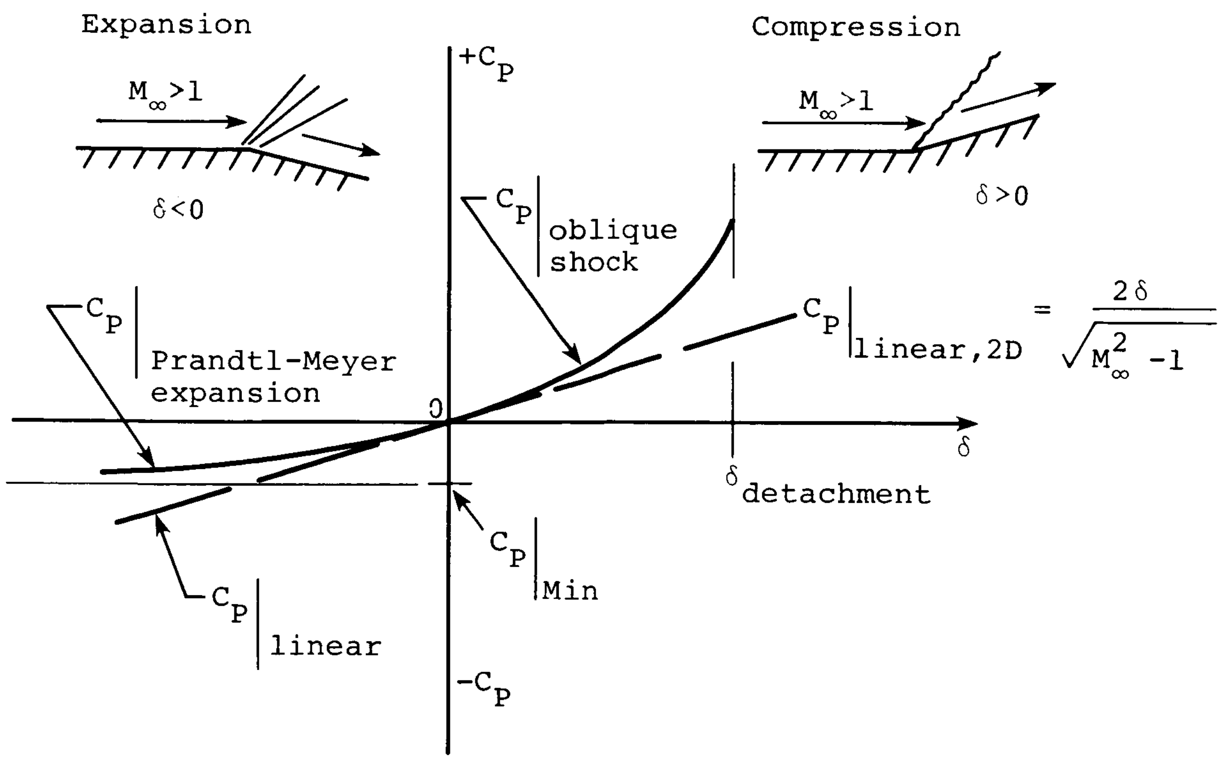

In the above sketch, the pressure coefficient calculated for the compression case ($\delta > 0$) with two-dimensional oblique shock relationships (Appendix D) increases nonlinearly with deflection angle δ up to shock detachment. The pressures are appreciably higher than those obtained with two-dimensional linear theory which relates the pressures directly to the deflection angle. For negative deflection angles, the pressures calculated with two-dimensional expansion relationships (Appendix D) are also higher than the two-dimensional linear theory pressures. For large expansion angles, the expansion (Prandtl-Meyer) formulation will automatically limit the pressure coefficient to

$$C_P\Big|_{min} = \frac{p - p_\infty}{q_\infty} = -\frac{2}{\gamma M_\infty^2} \tag{4}$$

which corresponds to zero static pressure ($p = 0$).

The simplest linear theory (two-dimensional) relates the pressure coefficient directly to the flow deflection angle as indicated in the sketch. For Mach numbers larger than 1, there are no bounds on the pressure coefficient calculated this way. However, the three-dimensional linear theory imbedded in program LRCDM2 provides three components of perturbation or interference velocities u, v, and w aligned with the body coordinate system (x_B, y_B, z_B). The velocities can be used in a linear pressure-velocity relationship

$$C_P\Big|_{lin} = -\frac{2u}{V_\infty} \tag{5}$$

or the isentropic Bernoulli pressure-velocity formulation

$$C_P\Big|_{Bern.,3D} = \frac{2}{\gamma M_\infty^2}\left\{\left[1 + \frac{\gamma - 1}{2} M_\infty^2 \left(1 - \frac{V_R^2}{V_\infty^2}\right)\right]^{\frac{\gamma}{\gamma-1}} - 1\right\} \tag{6}$$

where γ = 1.4 for air. The resultant velocity ratio is given by

$$\frac{V_R^2}{V_\infty^2} = 1 + \frac{2u}{V_\infty} \cos\alpha_c - \frac{2v}{V_\infty} \sin\alpha_c \sin\phi$$

$$+ \frac{2w}{V_\infty} \sin\alpha_c \cos\phi + \frac{u^2 + v^2 + w^2}{V_\infty^2} \qquad (7)$$

where α_c is the included angle of attack and ϕ is the angle of roll as defined earlier in Equation (3) of Section 2.4. The perturbation or interference velocity components due to three-dimensional linear theory can be unduly large in magnitude and cause the term in the square brackets in Equation (6) to become negative. In program LRCDM2, the pressure coefficient is set equal to $C_P\big|_{min}$, Equation (4), when the following condition holds.

$$1 + \frac{\gamma - 1}{2} M_\infty^2 \left(1 - \frac{V_R^2}{V_\infty^2}\right) \leq 0 \qquad (8)$$

Therefore, Bernoulli pressure coefficients obtained with the three-dimensional linear theory built into LRCDM2 have some nonlinear character by virtue of its formulation, Equation (6), and they are artificially limited with regard to the minimum pressure. Later we will consider only the Bernoulli pressures in connection with linear theory.

Finally, the simplest form of the Newtonian or impact theory pressure coefficient is given by (γ = ratio of specific heats)

$$C_P\Big|_{Newtonian} = 2 \sin^2\delta, \quad \left.\begin{matrix} M_\infty >> 1 \\ \gamma = 1 \end{matrix}\right\} \qquad (9)$$

Portions of the fins and/or body that do not "see" the on-coming stream experience zero pressure coefficient (Ref. 12) or more correctly zero pressure (Ref. 13). In the treatment presently implemented in program LRCDM2, the pressure coefficient is set equal to zero for negative flow deflection angles δ (expansions). For such cases, in the limit for high Mach numbers ($M_\infty > 5$), both the pressure coefficient as well as the static pressure approach the value zero.

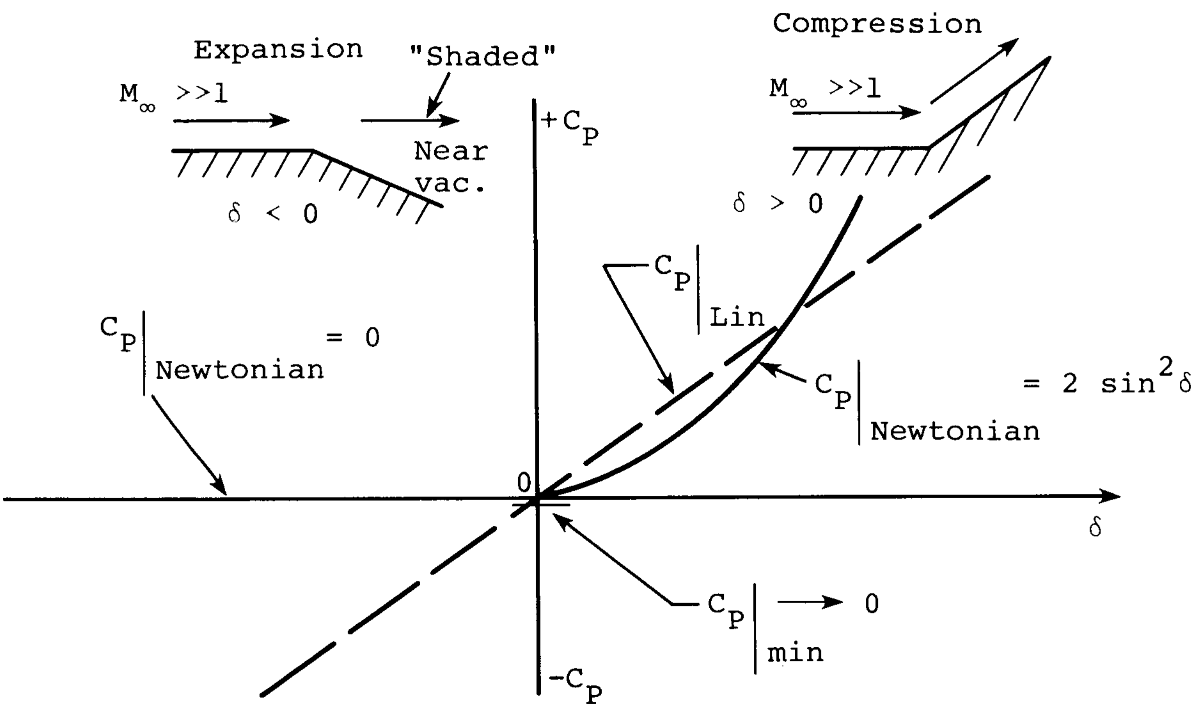

A comparison between the Newtonian and two-dimensional linear pressure coefficient is schematically shown above for a planar surface inclined to the free stream.

2.6.2 Procedure for calculating corrected nonlinear pressure coefficients on the fins and body.- The optional computation of pressures acting on the fins in accordance with combined nonlinear/linear theory is accomplished by means of a modified version of strip theory. This option is selected by setting index N2DPRF=2 in Namelist $INPUT of program LRCDM2.

The actual procedure, implemented in subroutine SPECPR for the fins, consists of the following stages. The procedure followed on the body is very similar and is described later.

In essense, the procedure consists of the following stages.

1. Apply nonlinear two-dimensional strip theory on fins and body, compute local Mach numbers, pressure ratios, etc.

2. Perform three-dimensional linear analysis of the fins and body; that is, solve for panel and line singularity strengths used to model the fins and body.

3. Update local Mach numbers calculated in the first stage using results from the second stage.

4. Recompute the two-dimensional pressure coefficients using the updated local Mach numbers.

The details of this procedure will now be described.

Nonlinear two-dimensional strip theory is performed on the top and bottom of the fin airfoil using shock-expansion and Newtonian theory. The former is described in Appendix D and the latter simply uses Equation (9). The spanwise locations of the strips coincide with the chordwise rows of control points of the constant u-velocity panels distributed over the fin. At the leading edge of each strip, a local angle of attack, $\alpha_{F,\ell}$, is calculated in a manner similar to Equation (1) including effects of free stream, body line-singularities and external vortex effects if present. The actual fin profile is approximated by straight line segments at each spanwise strip as shown in Figure D.1 of Appendix D. An asymmetric airfoil is broken up into equal longitudinal segments as shown below.

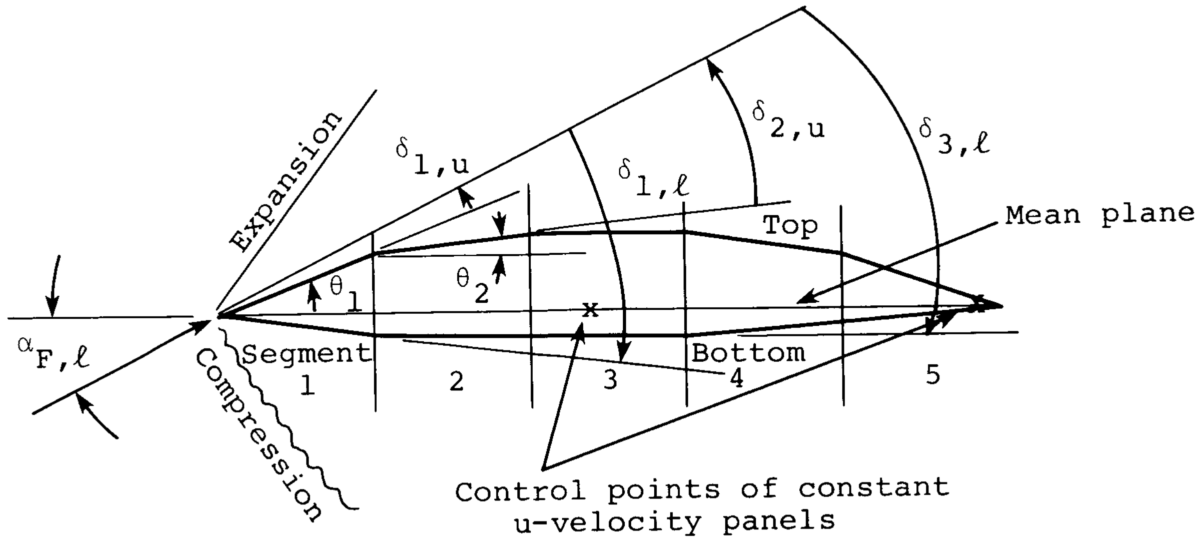

Angles $\delta_{1,u}$, $\delta_{1,\ell}$, and $\delta_{2,u}$, $\delta_{2,\ell}$ etc. are used directly with the Newtonian formulation. Two control points are shown for the case of two chordwise constant u-velocity panels. For shock expansion, the analysis starts with angles $\delta_{1,u}$ and $\delta_{1,\ell}$ for conditions on segment 1. For the case shown, there is an oblique shock attached to the leading edge on the bottom and an expansion wave on the top. Beyond this station Prandtl-Meyer expansion theory is employed using the actual profile angles θ_1, θ_2 etc. input by the user. If index N2DPRF is set equal to 1, the two kinds of nonlinear pressure coefficients are computed in this way and no further corrections are made. In any event, the value of the Prandtl-Meyer flow angle ν associated with the two-dimensional expansion flow and the value of the flow deflection angle δ for Newtonian theory are saved at the control point locations for the top and bottom surface of the fin. In addition, the ratio of total pressure behind the oblique shock to the free stream total pressure is also saved for each strip for use later in the computation of the corrected shock-expansion pressure coefficients.

The two-dimensional interference-free pressure coefficients based on the shock-expansion relationships and the Newtonian theory valid at high Mach numbers will be corrected for three-dimensional interference effects on the top and bottom surfaces of the fin at the panel control points. The essential idea of defining a new effective deflection angle was originated by Carlson in Reference 11 for the shock-expansion method. Here, the effective deflection angle concept is also applied to the Newtonian pressure method. First, an equivalent flow turning angle is calculated as follows. It is based on the notion of approximating the difference between the interference-free two-dimensional nonlinear theory (shock expansion or Newtonian) and three-dimensional nonlinear theory including interference effects by the difference between interference-free two-dimensional linear theory and three-dimensional linear theory including interference effects.

In equation form, this statement can be expressed as

[2-D nonlinear theory] + [(3-D linear theory)

- (2-D linear theory)] ≅ [3-D nonlinear theory] (10)

The local longitudinal or axial perturbation velocity in accordance with two-dimensional, linear theory is given by

$$\frac{u_{2D}}{V_\infty} = -\frac{1}{\sqrt{M_\infty^2 - 1}}\,\delta \tag{11}$$

where δ is the angle (in radians) between the oncoming stream and the top or bottom surface of the fin (or body) at the control point of a constant u-velocity panel. This relationship is based on the pressure coefficient for two-dimensional flow (shown in the first sketch of Section 2.6.1) and the two-dimensional relationship given by Equation (5). The corresponding local Mach numbers for interference-free, two-dimensional flow as formulated by Carlson in Reference 11 is expressed as

$$M_{2D} = M_\infty \left(1 + \frac{u_{2D}}{V_\infty}\right) \tag{12}$$

and the Prandtl-Meyer angle ν_{2D} associated with this Mach number is calculated with Equation (D.7) of Appendix D. In subroutine SPECPR, this equation is programmed as function FNU. The local Mach number for three-dimensional flow on the top and bottom of the fin at the panel control points includes inteference effects and is given in Reference 11 as follows.

$$M_{3D} = \frac{M_\infty \left(1 + \frac{u_{3D,\ell}}{V_\infty}\right)}{\cos \varepsilon} \tag{13}$$

The angle ε is the lateral flow angle measured in a plane tangent to the local surface at the panel control point as shown in the sketch below. It is the angle between the local streamline or flow direction and the streamwise direction on the fin.

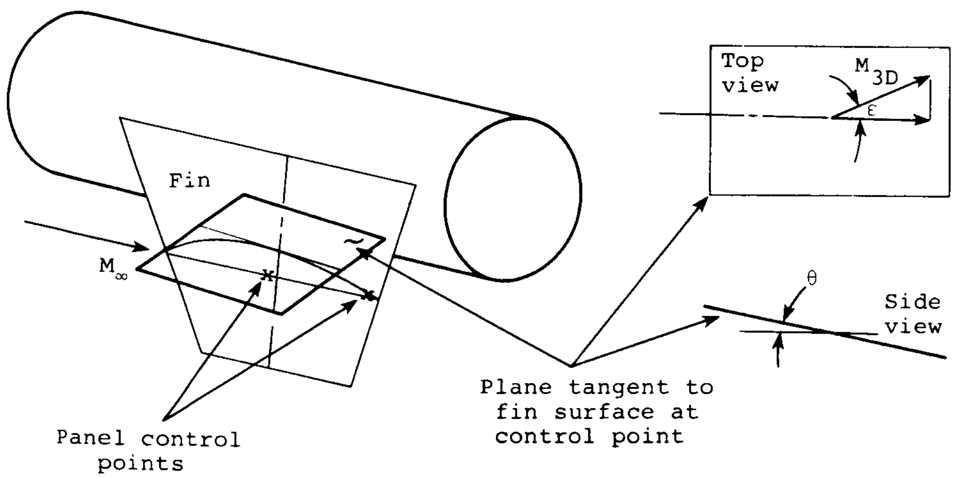

The local axial perturbation velocity component $u_{3D,\ell}$ is obtained from three-dimensional linear theory and includes contributions from all constant u-velocity panels on the fin(s) and interference shell, source panels for fin thickness, and the line singularities modeling the body. Component $u_{3D,\ell}/V_\infty$ is parallel to the mean plane and is calculated as UTOTA and UTOTB in routine SPECPR for the upper and lower fin surfaces, respectively. Therefore, by using Equation (13), the Mach number M_{3D} is made to correspond to the three-dimensional flow determined from linear theory calculated at the panel control points for the upper (and lower) surfaces of the fin. The tangent plane shown in the sketch corresponds to one of the strip segments inclined at angle δ with respect to the free stream. Lateral deflection angle ε can be determined from

$$\varepsilon = \tan^{-1} \frac{V_{F,\ell} + v_{3D,\ell}}{U_{F,\ell} + u_{3D,\ell}} \tag{14}$$

Quantity $V_{F,\ell}$ is the lateral velocity component parallel to the fin mean plane calculated as VFINL in routine SPECPR and represents effects of free stream including fin deflection angle. The perturbation lateral velocity component $v_{3D,\ell}$ in the fin local coordinate system (also parallel to fin mean plane) includes contributions from all constant u-velocity panels, planar source panels for fin thickness, body singularities and external vortices if present. Component $U_{F,\ell}$ (UFINL) is the axial component due to free stream parallel to the fin mean plane. The axial or longitudinal component $u_{3D,\ell}$ is discussed above in connection with Equation (13). The Prandtl-Meyer angle ν_{3D} is related to Mach number M_{3D} by means of Equation (D.7) shown in Appendix D.

The equivalent turning angle (or flow correction angle) is now defined as

$$\Delta\nu = \nu_{2D} - \nu_{3D} \tag{15}$$

where ν_{2D} and ν_{3D} are related to the Mach numbers M_{2D} and M_{3D}, Equations (12) and (13), respectively. The values of Prandtl-Meyer angles ν calculated and saved at the panel control points during the first stage are then corrected as follows.

$$\nu_{corr} = \nu - \Delta\nu \tag{16}$$

The flow deflection angles δ calculated and saved during the first stage for the Newtonian theory are also corrected to give an effective deflection angle

$$\delta_{corr} = \delta + \Delta\nu \tag{17}$$

The shock-expansion pressure coefficient is now recomputed in accordance with the method described in Appendix D using the updated local Mach number, Equations (D.10) and (D.23). It is based on ν_{corr} given by Equation (16). The saved total pressure ratios are included in this process. Likewise, the Newtonian pressure coefficients are recalculated in accordance with Equation (9) using δ_{corr} from Equation (17). Because the flow is usually accelerated, both of the corrections should generally tend to lower the nonlinear pressure coefficients calculated in the first stage.

In the application of three-dimensional linear theory (i.e., constant u-velocity and source panel methods) to delta wings, the perturbation velocities can become large in magnitude near the wing tip. In order to keep the lateral perturbation velocity component $v_{3D,\ell}$ within reasonable bounds, the sidewash is arbitrarily limited to

$$\left. \begin{array}{l} v_{3D,\ell}\Big|_{limit} = \left| \dfrac{v_{3D,\ell}}{u_{3D,\ell}} \right| u_{2D} \\ \text{for } v_{3D,\ell} \geq 0.5\ V_\infty \end{array} \right\} \qquad (18)$$

with the order of magnitude of the two-dimensional axial component given by Equation (11). This process is also performed in subroutine SPECPR of program LRCDM2. If subroutine SHKEXP (Appendix D) detects a strip with a detached shock at the leading edge, the linear and Bernoulli pressure coefficients calculated from linear theory at the panel control points in the strip are used instead in the subsequent fin loading calculation.

On the body, the optional computation of pressure coefficients with combined nonlinear/linear theory is selected by setting index N2DPRB=2 in Namelist $INPUT of program LRCDM2. In essence, the same procedure employed on the fins is repeated along longitudinal strips on the surface of the body from the nose tip to the base. A layout of longitudinal strips is indicated schematically below. Each segment or

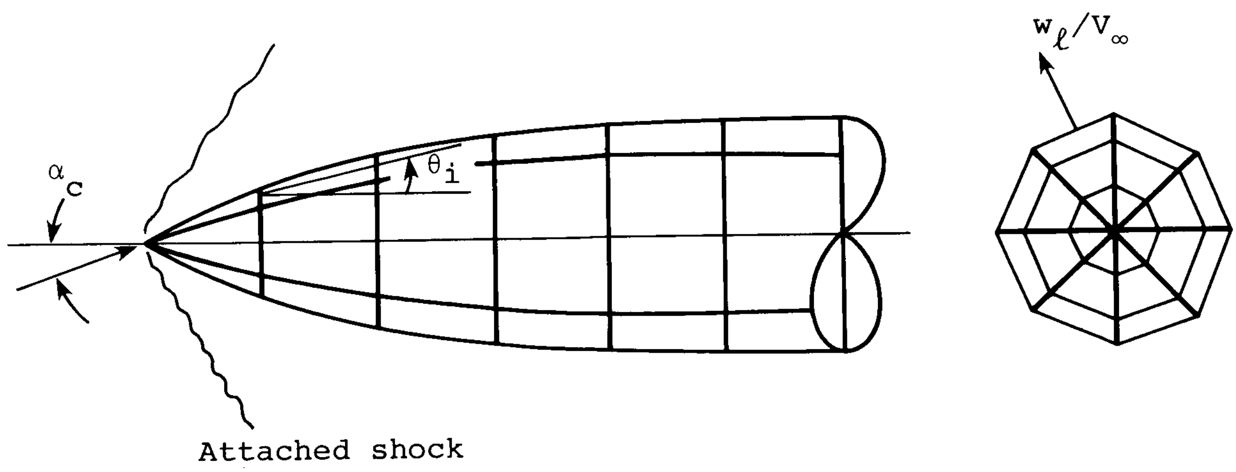

panel in a strip makes angle θ_i (shown out of plane) with the body centerline. These angles are input by the user. Subroutine BDYPR of program LRCDM2 defines a local angle of attack, α_ℓ, for each segment by computing the velocity component normal to the plane of the segment. This normal component, w_ℓ, includes a contribution of free stream and effects of external vorticity if present. Flow deflection angles δ are then defined as the angle between the local flow velocity vector and the plane of the segment. For each longitudinal strip, the pressure coefficients are determined in accordance with shock expansion (tangent wedge) and Newtonian theory during the first stage as described above for the fins. If N2DPRB is set equal to 1, the nonlinear pressure coefficients are not corrected as described above. For N2DPRB=2, the perturbation velocity components involved in the determination of the equivalent turning angle $\Delta\nu$ include contributions from the body line singularities, external vortices, and for the portions of the body next to the fins, effects of constant u-velocity panels on the fins and interference shell are also included. Equation (18) is used for the body as well to limit the local lateral velocity component.

3. COMPARISONS

In order to make an assessment of the accuracy of the updates and extensions to program NSWCDM (Ref. 2), some comparisons between results predicted with the new program LRCDM2 and experimental data are given in this section. First, results obtained for a triform configuration are discussed. A calculation example showing the effects of vortex shedding on afterbody load is discussed. Overall forces and moments acting on a forward control canard-tail wind tunnel model are calculated with and without afterbody vortex shedding and compared with measurements for a case with roll control. The nonlinear/linear combined theories are tested against measured pressure distributions on a rectangular and delta wing and on an ogive cylinder forebody.

3.1 Forces and Moments Acting on Triform Fin Configuration

Program LRCDM2 has been arranged to handle a variety of fin layouts including a new option for triform fins. Figure 1 shows an example comprising one set of triform tail fins attached to an ogive-cylinder body. Forces and moments measured on this configuration were taken from Reference 14 and are shown in Figure 2 by the open symbols. Results predicted by LRCDM2 using the linear theory Bernoulli pressure coefficient option are indicated by the solid symbols. Data are shown for two roll angles, $\phi = 0°$ and $90°$. Note that for $\phi = 0°$, the configuration is actually rolled 180° relative to the orientation shown in Figure 1. The orientations of the free-stream velocity component in the crossflow plane are shown at the top of the figure for the two roll angles. Positive directions of the normal force coefficient, C_Z, and side force coefficient, C_Y, are also indicated.

At zero roll and for the range of angles of attack shown, the measured normal force and pitching moment (positive nose up) are almost linear although the former shows a nonlinear increment most likely due to forebody vortices for α_c greater than 8°. Agreement between experiment and prediction is quite good. It should be noted here that program LRCDM2 is equipped with a data base containing symmetric forebody separation characteristics described in Reference 1. Effects of these vortices are included in the fin loads. On the forebody, only the lateral velocity components induced by the vortices are included in the pressure calculations resulting

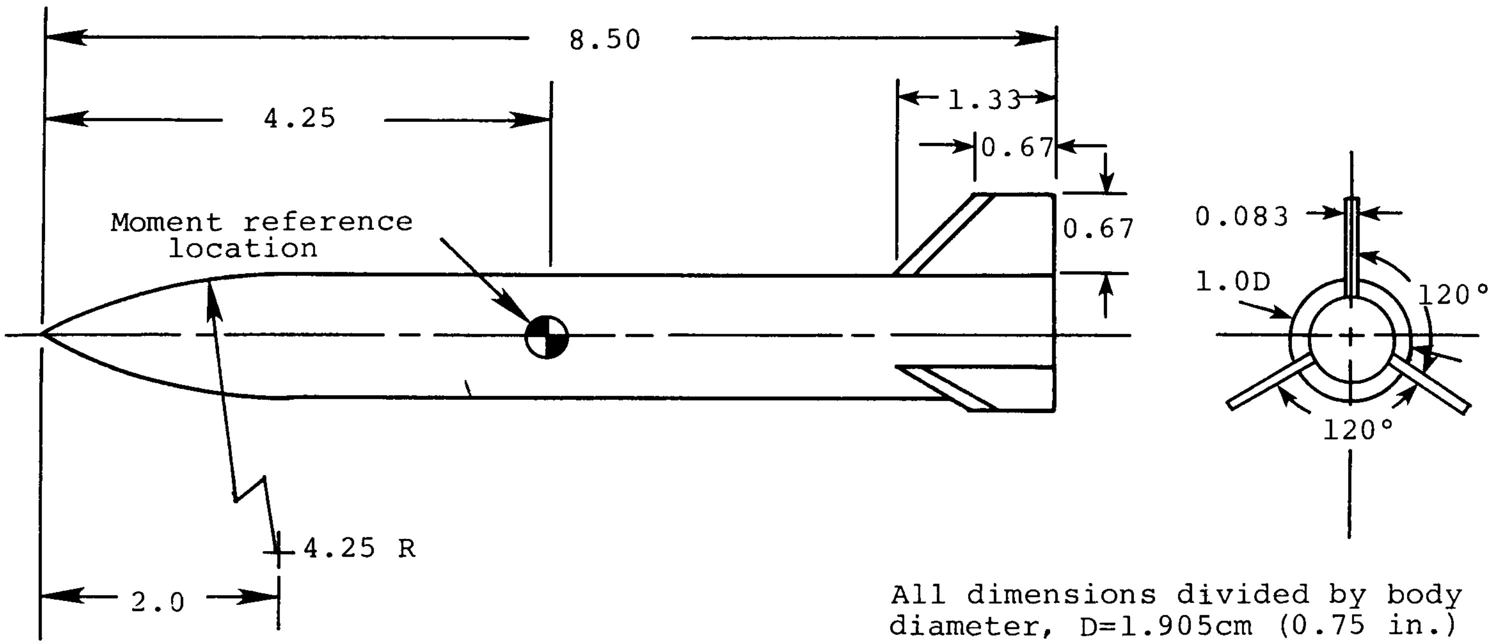

All dimensions divided by body diameter, D=1.905cm (0.75 in.)

Figure 1.- Triform ogive-cylinder configuration.

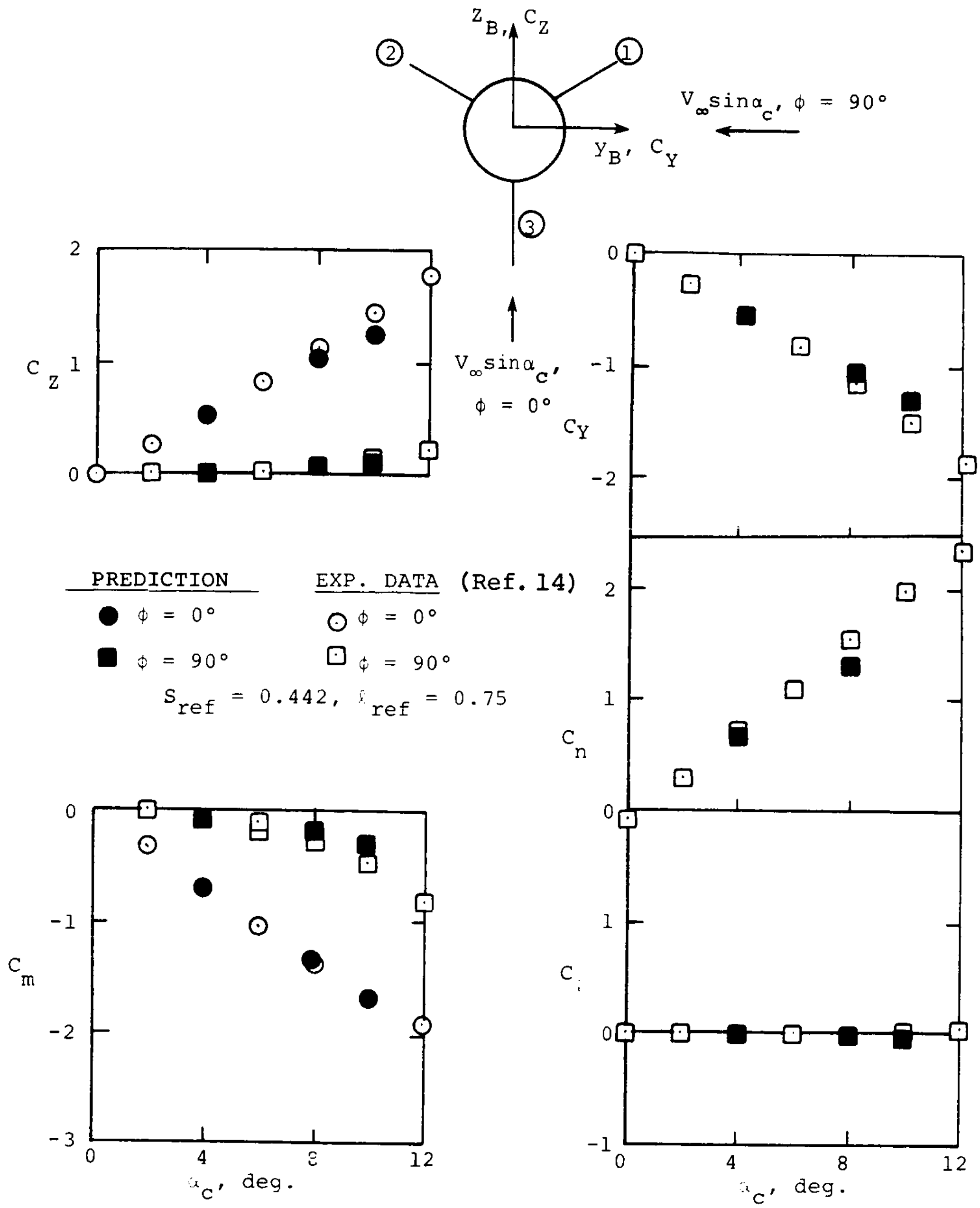

Figure 2.- Forces and moments acting on triform ogive-cylinder configuration, $M_\infty = 1.5$.

in underpredicted forebody loads when vortices are present (also refer to Appendix C, Section C.4). This deficiency in the present version of LRCDM2 shows up for α_c in excess of about 8°.

When the triform configuration is in pure sideslip ($\phi = 90°$), it is seen that the measured normal force, C_Z, and pitching moment, C_m, are nonzero and are predicted well by LRCDM2. For this condition, the side force, C_Y, and yawing moment, C_n (positive nose to right), are dominant and also show the effects of the aforementioned forebody vortices. Rolling moment is negligible. These lateral characteristics are also predicted well by the present version of LRCDM2. The calculations were performed with a sparse layout of three chordwise and five spanwise constant u-velocity panels on the fins. A layout of three lengthwise with 12 circumferential panels was used on the interference shell covering the body along the length of the fin root chord.

3.2 Forces and Moments Acting on TF-4 Wind Tunnel Model

The geometrical details of the NASA/LRC canard-controlled model designated TF-4 are shown in Figure 3. Here, only the king-size tail fin will be considered because of its pronounced effects on the overall longitudinal and lateral aerodynamic characteristics. Comparisons between extensive experimental data supplied by J. M. Allen and A. B. Blair, Jr. of the Supersonic Branch at the NASA/Langley Research Center and the earlier program NSWCDM are shown in Reference 4. The results discussed below are aimed at showing the effects of afterbody vortex shedding on the afterbody loads with zero control, and on the overall lateral characteristics for the case with roll control.

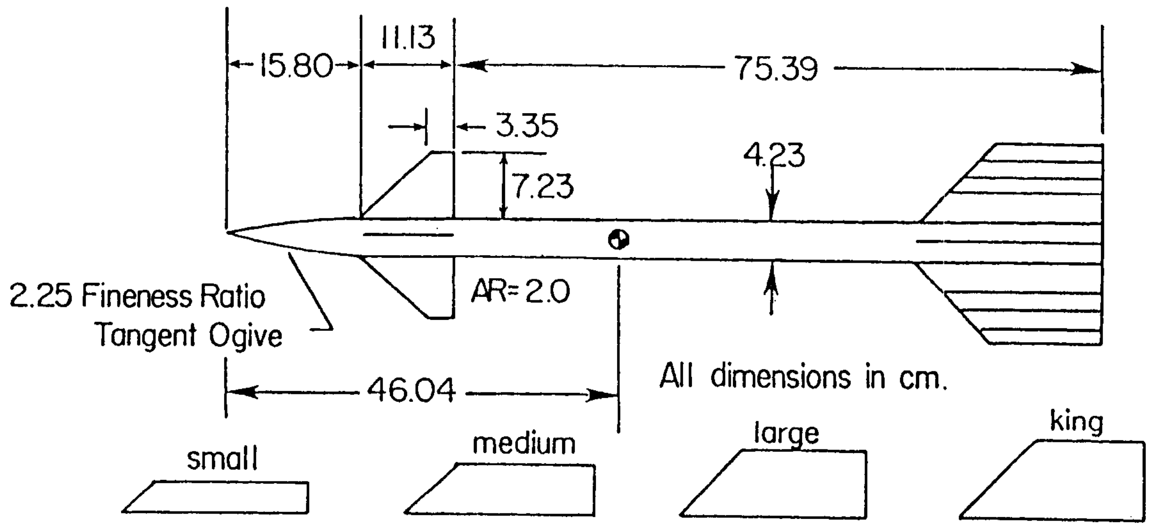

TAIL	small	medium	large	king
Root Chord	21.59	21.59	21.59	21.59
Tip Chord	18.21	16.15	13.87	12.55
Semi-span	3.38	5.44	7.72	9.04
AR	0.34	0.57	0.87	1.06

Tail Fin Details

Figure 3.- NASA/LRC wind tunnel model TF-4 with different tail fins.

3.2.1 Normal force on afterbody.- In order to illustrate program operation and to assess the magnitude of the loading acting on the 13-caliber afterbody, program LRCDM2 was applied to the unrolled TF-4 configuration with and without afterbody vortex shedding. For this calculation, the included angle of attack α_c is 20° and the Mach number M_∞ equals 1.6.

At this angle of attack, the data bases built into subroutine BDYVTX of program LRCDM2 generate two symmetric forebody vortices. In addition, for this case, the wake of the horizontal canard fins consist of four (two for each fin) discrete vortices as calculated by subroutine SPNLD at the end of step 3 of the stepwise procedure described in Section 2.3. Thus, at the axial location of the trailing edges of the canard, program LRCDM2 has generated six vortices. Typically, the set of discrete vortices are positioned in the crossflow plane as shown below. For this case with zero roll angle and zero fin deflection angles, the vertical fins are unloaded. The trailing-edge vortices are determined from

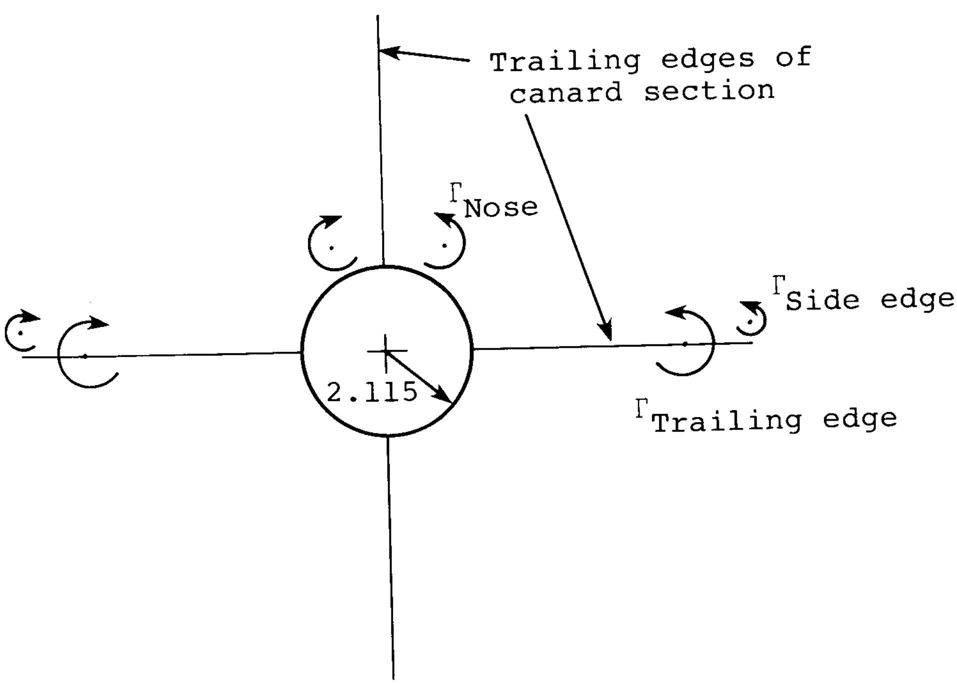

the attached flow span loading and the side-edge vortices (Section 2.4) are related to the Polhamus vortex-lift analogy as described in Appendix C.

The set of vortices can be tracked down the afterbody without shedding of afterbody vortices in accordance with step 5. The determination of the vortex paths and the calculation of the velocities induced by the vortices as they stream aft and above the afterbody is performed by module VPATH2 of LRCDM2. The calculation of pressures at points on the afterbody surface as well as the pressure integration for forces and moments is implemented in subroutine BDYPR of program LRCDM2. On the other hand, companion program BDYSHD (Section 2.2 and Appendix B) can be employed to compute the loads acting on the afterbody including effects of afterbody vortex shedding. This operation is schematically indicated as step 3a in the sketch of Section 2.3. In this process, program BDYSHD reads in the strengths and lateral locations of the set of vortices at the canard trailing edge. The rate of vortex shedding, the pressure distributions and the vortex paths determined by BDYSHD are thus influenced by the vortices generated by the forebody and canard fins. At the end of the afterbody, the six canard-section vortices and the additional vortices shed by the afterbody are positioned as shown below. Note that in this symmetric picture, the body-nose vortices are "captured" by the many afterbody vortices in the two vortex clouds. However, the canard fin vortices have traveled a fair distance above the afterbody.

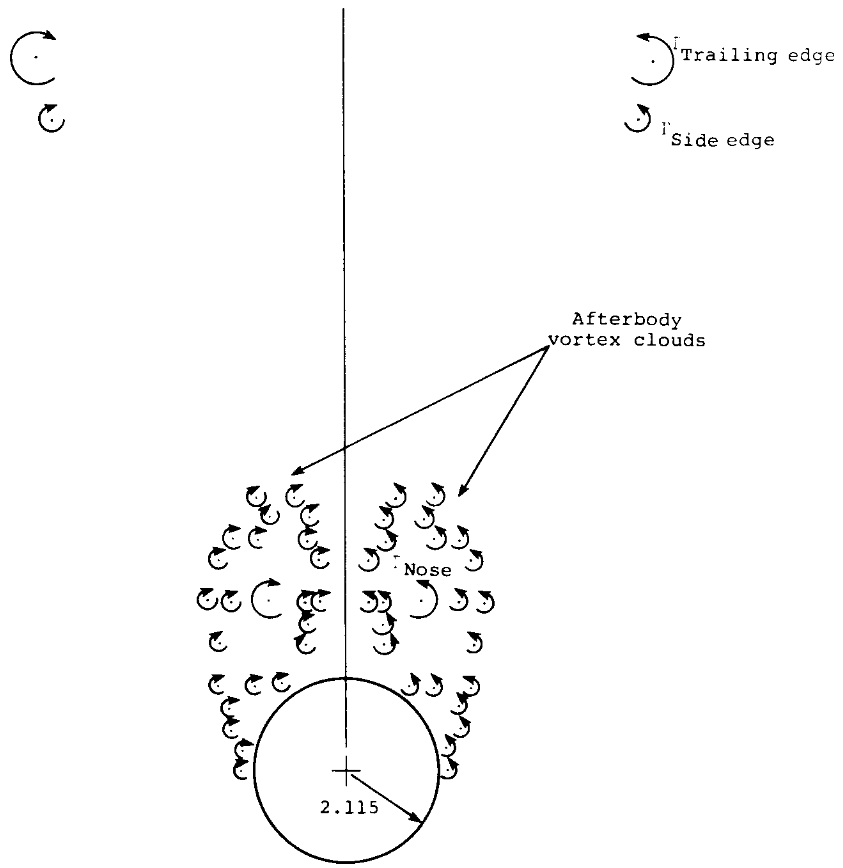

The distributions of normal force acting on the TF-4 afterbody calculated with and without vortex shedding are shown in Figure 4. The upper curve represents the normal force distribution calculated by BDYSHD using the laminar option for afterbody vortex shedding under the influence of canard-section vorticity. If the turbulent option is used, the calculated normal force will be lower in magnitude. Most of the added normal force is generated towards the aft portion of the afterbody. Simple constant crossflow-drag coefficient calculations do not include effects of upstream vortices and would result in a constant distribution of normal force of higher magnitude. The lower curve is generated by LRCDM2 and reflects the download effects of the forebody and canard

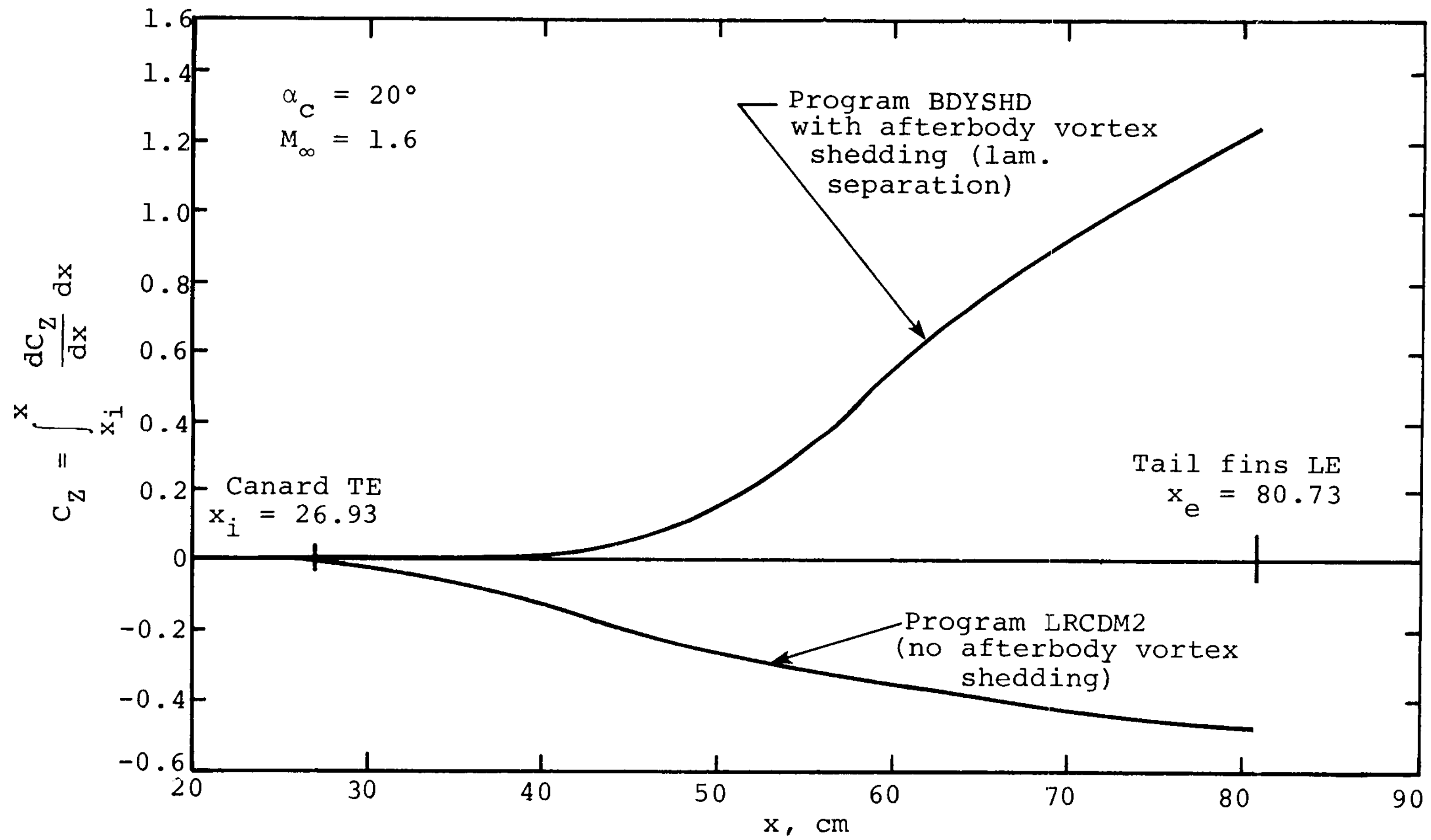

Figure 4.- Normal force build-up on axisymmetric afterbody of TF-4 in the presence of canard vortices, zero control deflection, $\phi = 0°$.

fin vortices. The net effect of accounting for afterbody vortex shedding by the optional inclusion of step 3a (BDYSHD) is to add about 1.7 to the normal force acting on the entire configuration. This amount is about 10% of the total normal force acting on the TF-4 with small tails.

3.2.2 Roll control.- Data were also obtained on the TF-4 for roll control. The right horizontal canard fin of the TF-4 configuration shown in Figure 3 is deflected 5° trailing edge down and the left horizontal canard fin is deflected -5° trailing edge up. Comparisons between experimental data taken at the Supersonic Branch of NASA/LRC and results calculated by program LRCDM2 are shown in Figure 5. The Mach number is 2.5 and the configuration is unrolled, $\phi = 0°$.

Normal-force coefficient, C_N, and pitching-moment coefficient, C_m, are given in Figure 5(a) as a function of included angle of attack, α_c. The measured normal force (open symbols) shows some nonlinear behavior throughout the range of α_c. Measured pitching moment (open symbols) is somewhat nonlinear for α_c up to about 6°. For low angles of attack, the oppositely deflected horizontal canard fins produce vortices of the same sense (or direction) which travel aft along the afterbody and produce an asymmetric flow field at the tail section. At the higher angles of attack, afterbody vortex shedding can occur and add to the vortex field as described later.

Program LRCDM2 was applied with (for $\alpha_c = 10°$, and 15°) and without (for $\alpha_c = 0°$, 5°, 10°, and 15°) the optional afterbody vortex shedding companion program BDYSHD. The difference between the two predictions (solid symbols) are neglible and both results match the experimental data well. Note that in this case the increment in normal force coefficient acting on the afterbody due to vortex shedding is considerably smaller than that for the undeflected canard fin

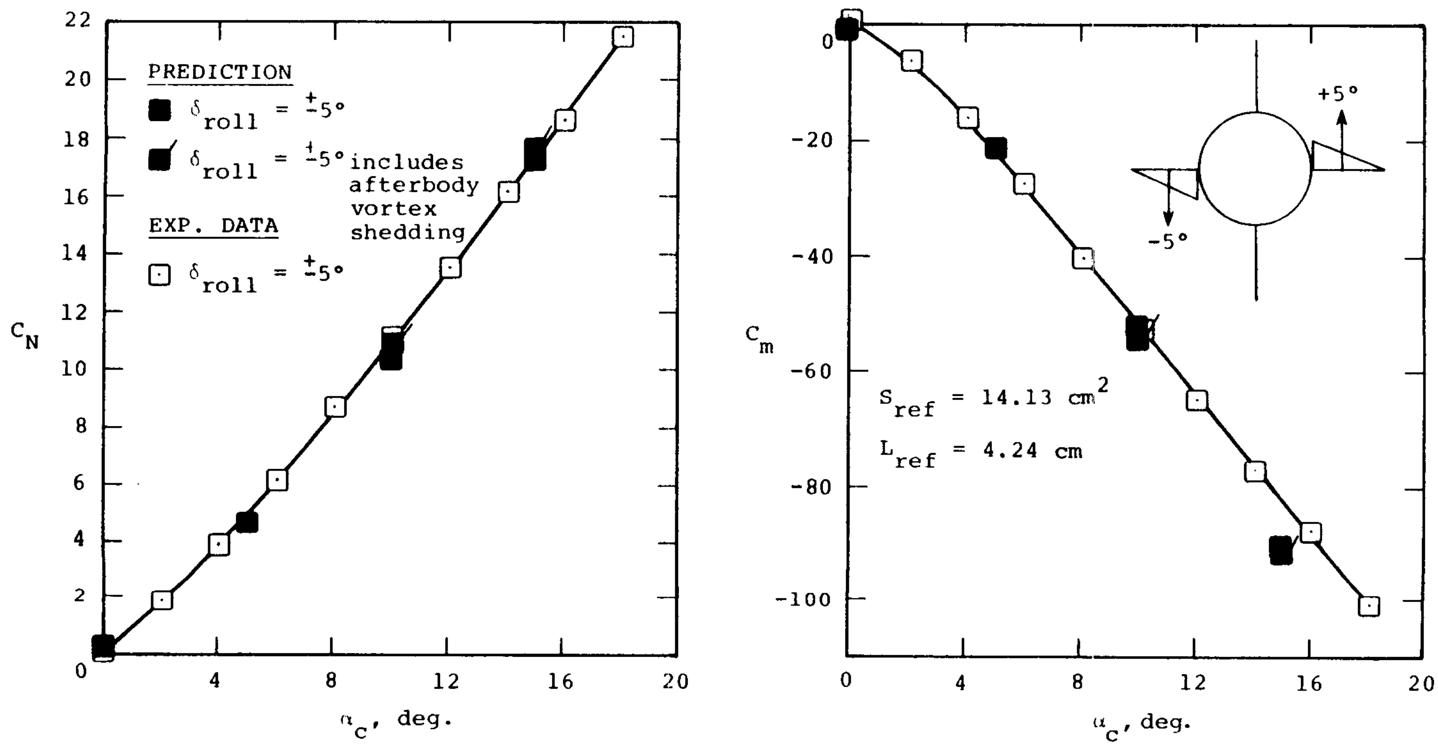

(a) Normal force and pitching moment coefficients.

Figure 5.- Aerodynamic forces acting on TF-4 model, $M_\infty = 2.5$, $\phi = 0°$. Forward fins with roll control, king-size tail fins.

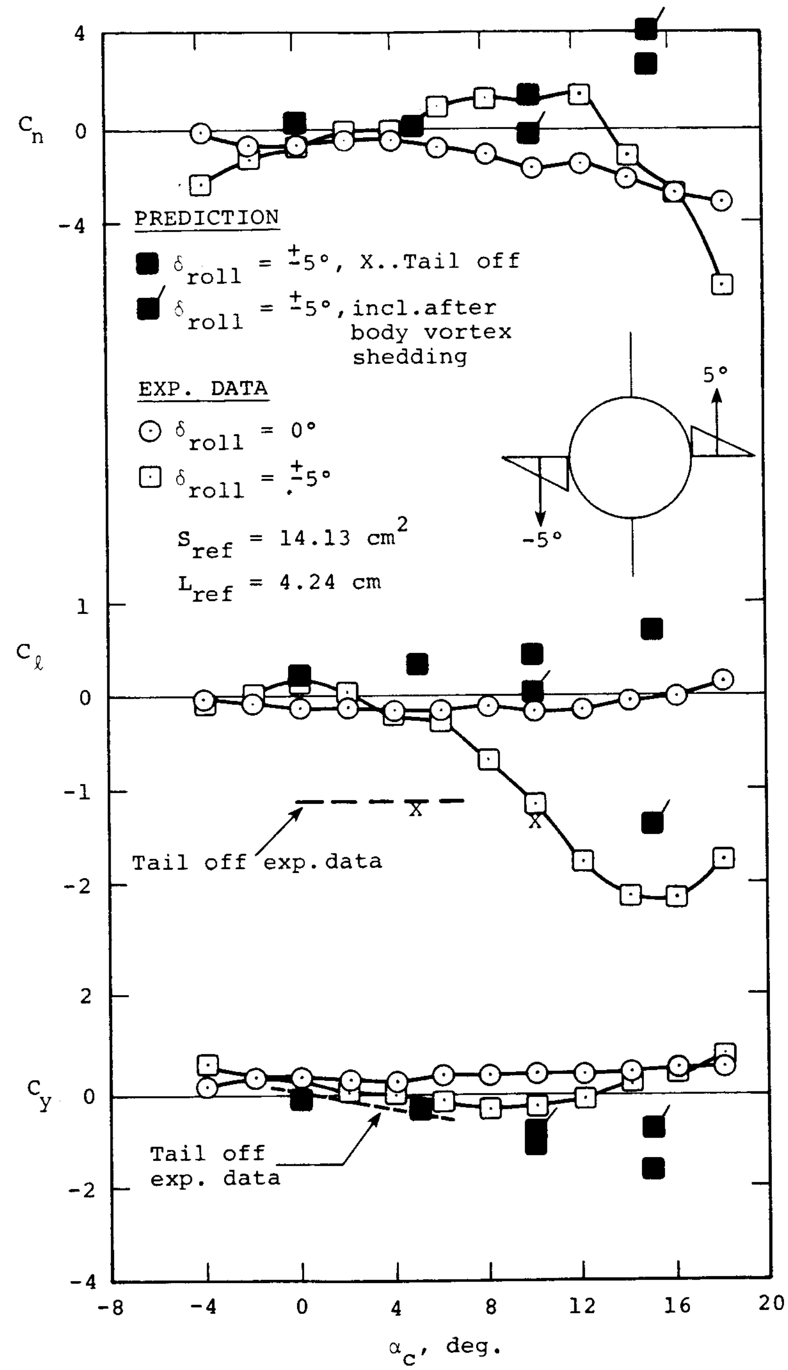

(b) Yawing moment, rolling moment and side force coefficients

Figure 5.- Concluded.

case described in the previous section. This is due in part to the asymmetric vortex field generated by the canard section for roll control. In addition, the forces and moments for this case are mostly due to the lifting surfaces (including the king-size tails).

The lateral aerodynamic characteristics are shown in Figure 5(b) with and without roll control. Measured yawing moment, C_n, rolling moment, C_ℓ, and side force, C_Y, indicate strong nonlinearities. The experimentally measured tail-off rolling moment is also indicated. It is seen that the effect of adding the king-size tail fins is to cancel the roll control of the canard fins up to about α_c equal to 6°. For higher angles of attack, the measured rolling moment exhibits nonlinear behavior and actually exceeds the rolling moment generated by the canards alone for α_c greater than 11°. In addition, some yawing moment is generated with roll control which changes sign as the angle of attack is increased. Little side force is measured. For low angles of attack, the vortices generated by the oppositely deflected canard fins induce unbalanced (asymmetric) loads on each of the king-size tail fins resulting in an adverse rolling moment. For angles of attack above 10°, the induced tail-fin rolling moment changes direction and actually adds to the canard rolling moment.

The negative tail-off rolling moment is predicted well by the tail-off results (indicated by the crosses) calculated by LRCDM2. At the lower angles of attack (α_c = 0°, 5°), the overall rolling moment calculated without afterbody vortex shedding is near zero and as such the interactions between the canard fins and the king-size tail fins are handled well by LRCDM2. However, the predictions without afterbody vortex shedding fail to predict the nonlinear behavior above 6° angle of attack. Afterbody vortex shedding becomes important at angles of attack in excess of 10° for the length of afterbody (13 calibers) under consideration. The predicted vortex field at the end of the afterbody (i.e., at the leading edge of the tail section) for α_c = 15° including effects of afterbody vortex shedding is indicated below.

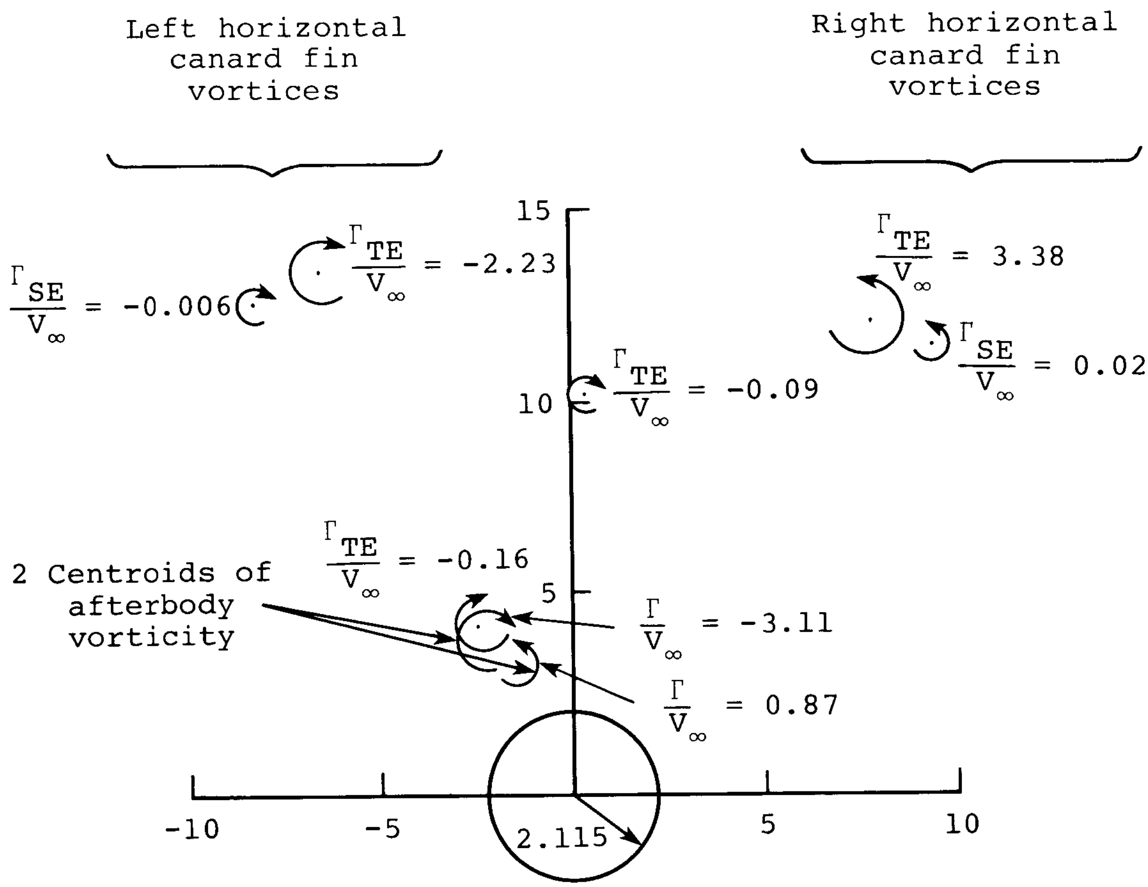

The afterbody vortex clouds are represented in the sketch by their centroids in the upper left quarter near the upper tail fin. The lower vertical canard fin trailing-edge vortex (Γ_{TE}/V_∞ = -0.16) has come up around the body and is trapped by the afterbody vortices. The actual crossflow vortex picture can be found in the sample case output of companion program BDYSHD in Appendix A and the vortex strengths and locations are also specified at the beginning of the output for step 5. The important point is that the sums of the strengths of the afterbody vortices (centroid strengths) are of same order of magnitude as the trailing-edge vortices of the deflected horizontal canard fins. The afterbody vortices tend to induce a side force (to the left) on the upper tail fin and to unload the left horizontal tail fin more than the right horizontal tail fin.

The calculated rolling moment, including the afterbody vortex shedding option (flagged solid symbols) using laminar separation, definitely follows the nonlinear trend. However, the predicted departure from the near zero level lags the experimental data by about 4° in angle of attack. Furthermore, the predicted side force also appears to benefit from the afterbody vortex shedding option. The predicted yawing moment is a little erratic with the afterbody vortex shedding option. Note that the maximum measured yawing-moment coefficient magnitude is only about 5% or less of the maximum measured pitching moment coefficient. The side-force coefficient magnitude is also about 5% of the measured normal-force coefficient. Furthermore, for zero canard fin deflection ($\delta_{roll} = 0°$), the measured yawing- and rolling-moment coefficients and the side-force coefficients indicated by the open circles should be zero for all angles of attack. This is an indication of some experimental error especially for α_c greater than 10°. A small error in measured and predicted side force either on the tail fins or afterbody can cause an appreciable contribution to the yawing moment.

Presently, the normal force acting on a deflected fin is not resolved into the z_B and x_B directions to give contributions to the C_Z and C_X force coefficient components. The axial (C_X) component would also generate a contribution to the yawing moment. Since the normal forces on the right and left horizontal fins are not equal in this case involving roll control, an additional net yawing moment would result from the canard section as the included angle of attack is increased from zero degrees. This contribution to the overall yawing is not accounted for in the present version of LRCDM2. In any event, the change in sign of the yawing moment as α_c is increased is presently not predicted. Note again that the magnitude of the yawing moment is but a few percent of the pitching moment shown in Figure 5(a).

All of the above predictions were obtained with a relatively sparse paneling layout (four chordwise by six spanwise on canard and tail fins). The actual calculation for $\alpha_c = 15°$ is given as the sample case in Appendix A and the results based on linear theory and the Bernoulli pressure method are used in all of the predictions shown here. On a CDC 7600, time required by LRCDM2 to perform this calculation including the optional engagement of companion program BDYSHD is 65 CPU sec.

3.3 Pressure Distributions Acting on Æ = 2 Rectangular Wing

In support of an effort aimed at developing numerical methodologies for analysis of wing/body configurations at supersonic speeds (Ref. 15), the Bernoulli and one of the nonlinear/linear pressure calculation methods implemented in program LRCDM2 were applied to the rectangular wing shown in Figure 6. This aspect ratio 2 wing was mounted on a dogleg sting and one side of the bevelled wing was instrumented with pressure orifices. The attitude of the assembly could be rotated 180° to enable measurement of pressures on the windward and leeward surfaces of the wing. The tests were performed by Stallings and Lamb at NASA/LRC and the results for this and other wings are contained in Reference 16.

Pressure distributions acting on the upper and lower surfaces of the wing are shown in Figure 7. Angle of attack is 10.3° and the Mach number equals 2.86. In Figure 7(a), the variation of pressure coefficients with spanwise distance is

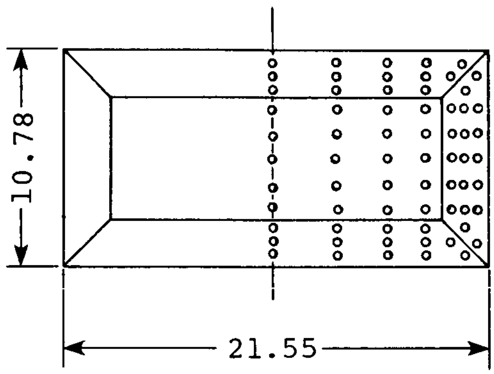

(a) Pressure tap layout (Ref. 16)

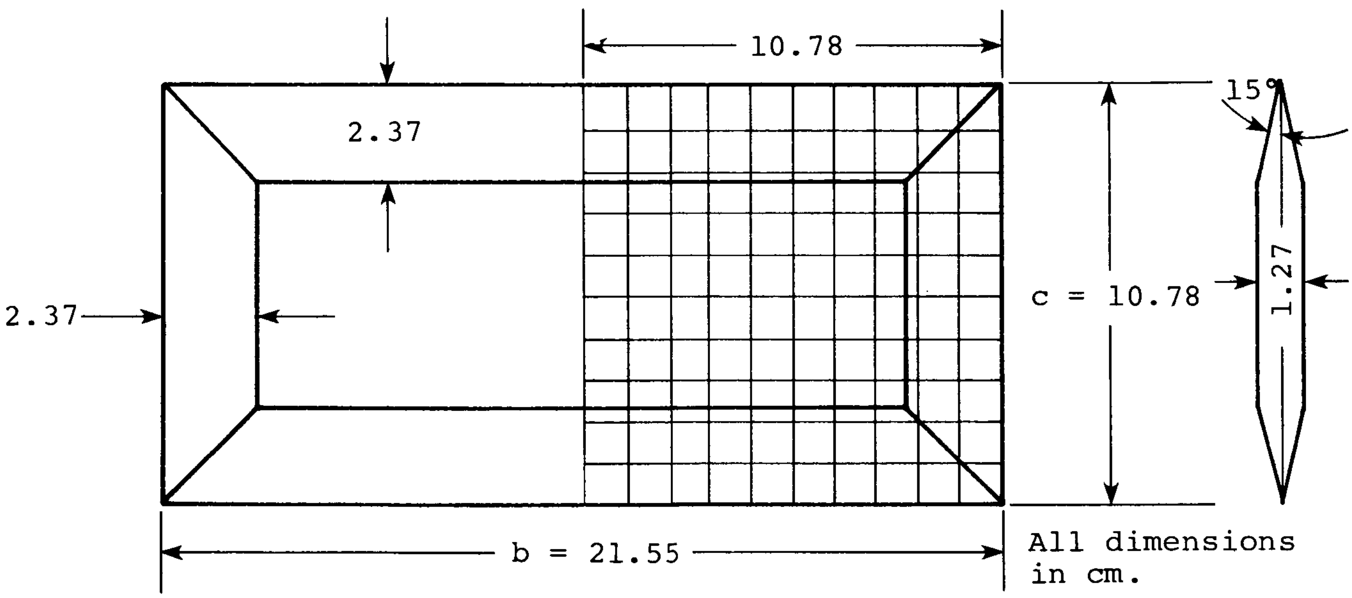

(b) Geometrical details and 10 x 10 paneling layout for prediction.

Figure 6.- AR = 2 rectangular wing, bevelled on the edges.

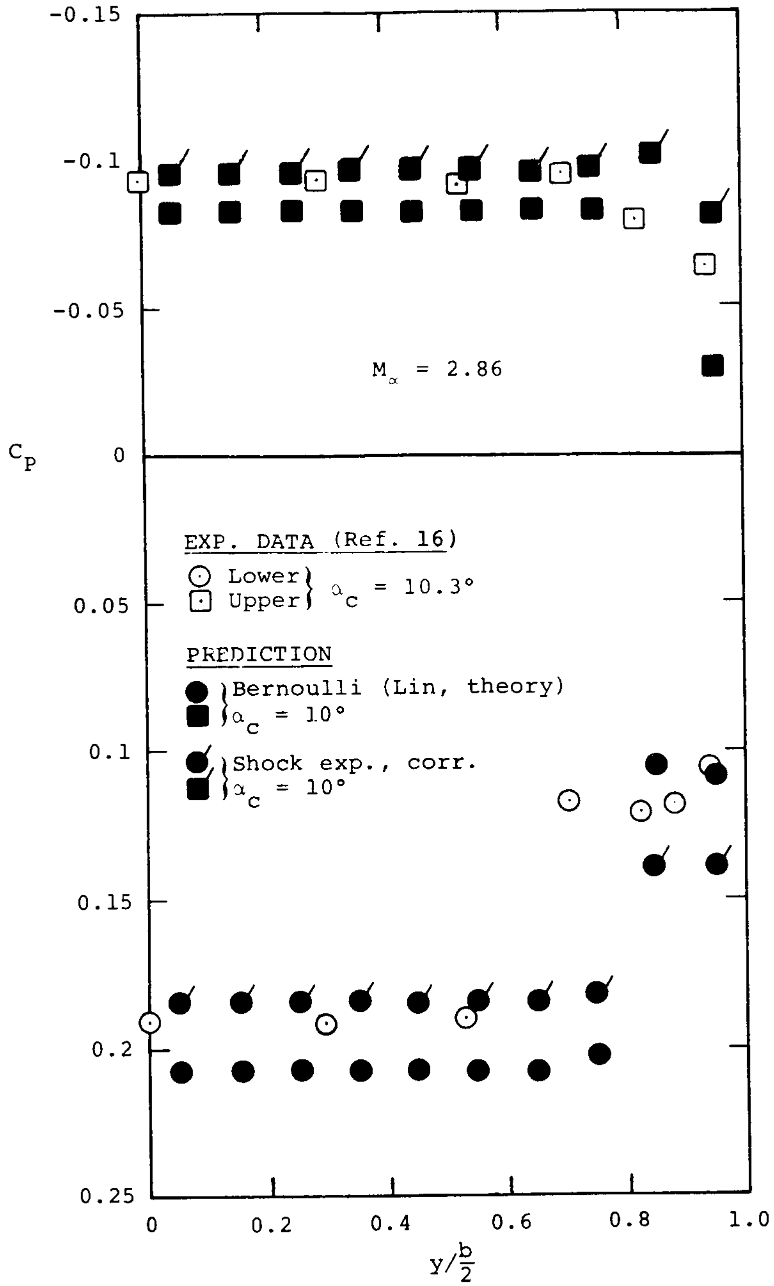

(a) Spanwise pressure distributions on upper and lower surfaces, x/c = 0.5

Figure 7.- Pressure distributions acting on Æ = 2.

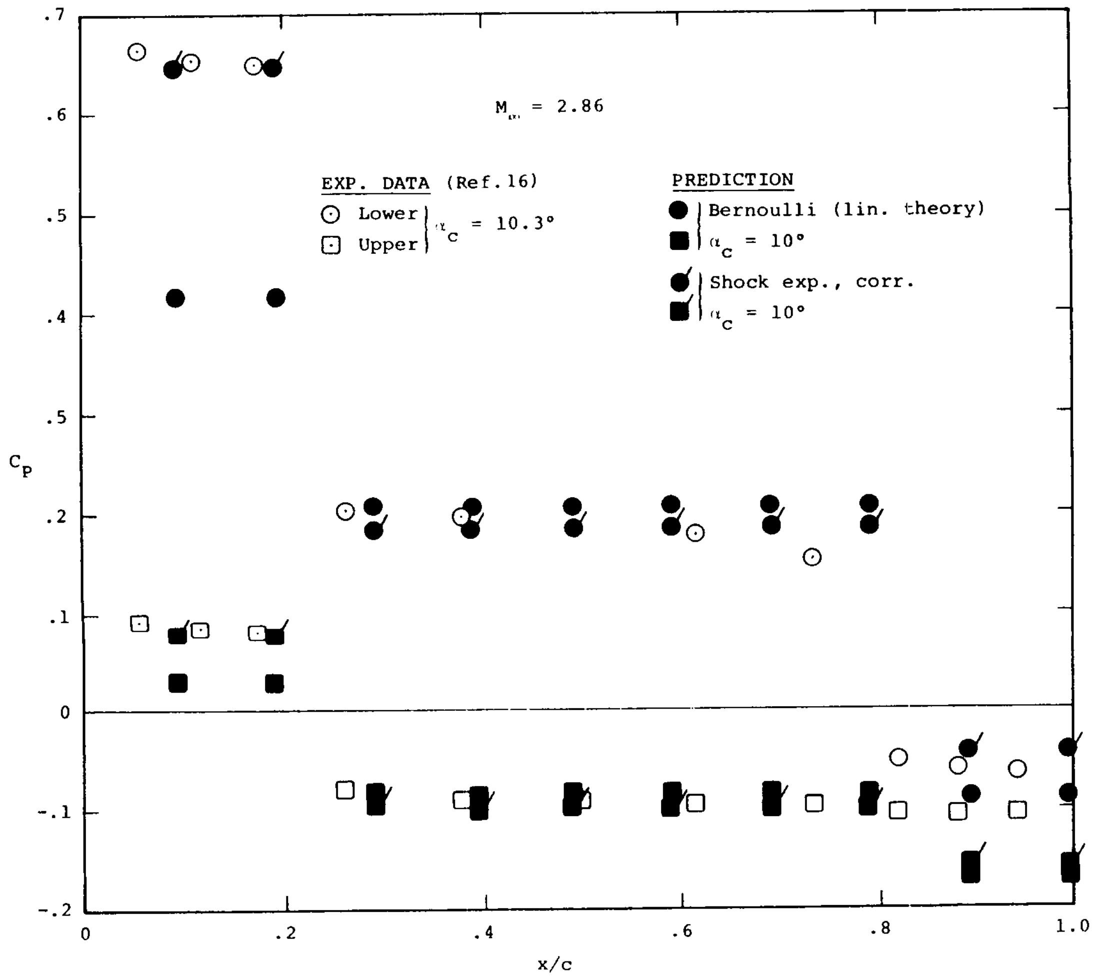

(b) Chordwise pressure distribution on upper and lower surfaces, $\frac{y}{b/2} = 0.53$

Figure 7.- Concluded.

indicated at the midchord position on the wing. The effects of the bevel near the side edge can be most clearly seen in the measured windward pressures (open symbols). The bevelled portion spans from y/(b/2) = 0.78 to the side edge. Inboard of this region, the measured pressures are practically constant.

The predictions generated by LRCDM2 are based on a 10-chordwise by 10-spanwise layout of constant u-velocity panels to model lift and the same layout of source panels are used to model thickness as shown in Figure 6(b). In addition, 10 spanwise strips with 10 segments in each were employed for the shock-expansion analysis. All predictions were performed for 10° angle of attack. The results marked Bernoulli in Figure 7(a) are based on linear theory. Thus, the perturbation velocities substituted in the Bernoulli pressure coefficient, Equation (5), are induced by all the panels distributed over the wing. The panel strengths were obtained from satisfying the flow-tangency boundary condition at the constant u-velocity control points (see Ref. 1 for details). In this instance, the calculated Bernoulli pressure coefficients are within 10% of the experimental data. The predicted results designated shock expansion, corrected, are based on shock-expansion strip theory with the flow angles corrected for interference by linear theory as described in Section 2.6.2. The pressure coefficients predicted this way match the measured values even better especially inboard of the bevelled section. Note that in terms of loading pressures ($\Delta C_P = C_{P_\ell} - C_{P_u}$), both methods give about the same answers except on the bevel.

The chordwise pressure distributions indicated in Figure 7(b) show the strong effects of the bevelled portion from the leading edge up to chordwise location x/c equal to 0.22. The spanwise station of this pressure distribution is approximately at half semi-span. On the upper and lower sides, the pressures are positive on the leading-edge bevel with half angle 15°. For 10.3° angle of attack both surfaces of this bevelled portion are compression surfaces. Near the trailing edge, only the lower or windward side is affected by the bevelled edge. On account of the presence of a strong oblique shock attached to the leading edge, the Bernoulli pressure method based on linear theory underestimates the pressure coefficients on the upper and lower surface by about 40% up to the flat portion of the wing. The corrected shock-expansion pressure method matches the experimental data much better near the leading edge. On the flat portion, both methods match the measured pressure level well. On the bevel at the trailing edge, both methods predict lower than measured pressure coefficients on the upper or suction surface. This is most likely due to boundary layer separation effects. On the lower or windward side, the corrected shock-expansion method matches experiment somewhat better. It should be mentioned that the flow correction angles calculated in accordance with Section 2.6.2 are small due to the two-dimensional nature of the flow in this case. However, the corrected shock-expansion method consistently provides the better predictions for pressure coefficients.

3.4 Pressure Distributions and Normal Force Acting on Æ = 1 Delta Wing

In order to compare in detail the differences between pressure coefficients calculated with the linear, nonlinear and combined nonlinear/linear theory methods, program LRCDM2 was applied to the aspect ratio 1 delta wing shown in Figures 8, 9, and 10. This delta wing has a 4 percent circular arc (biconvex) streamwise airfoil.

Figures 8 and 9 contain pressure distributions used in Reference 11 to test the shock expansion/linear theory concept originated by Carlson. The Mach number is 4.6 for all cases shown here so that the leading edge of the delta wing is just supersonic. The dashed line just inside the leading edge of

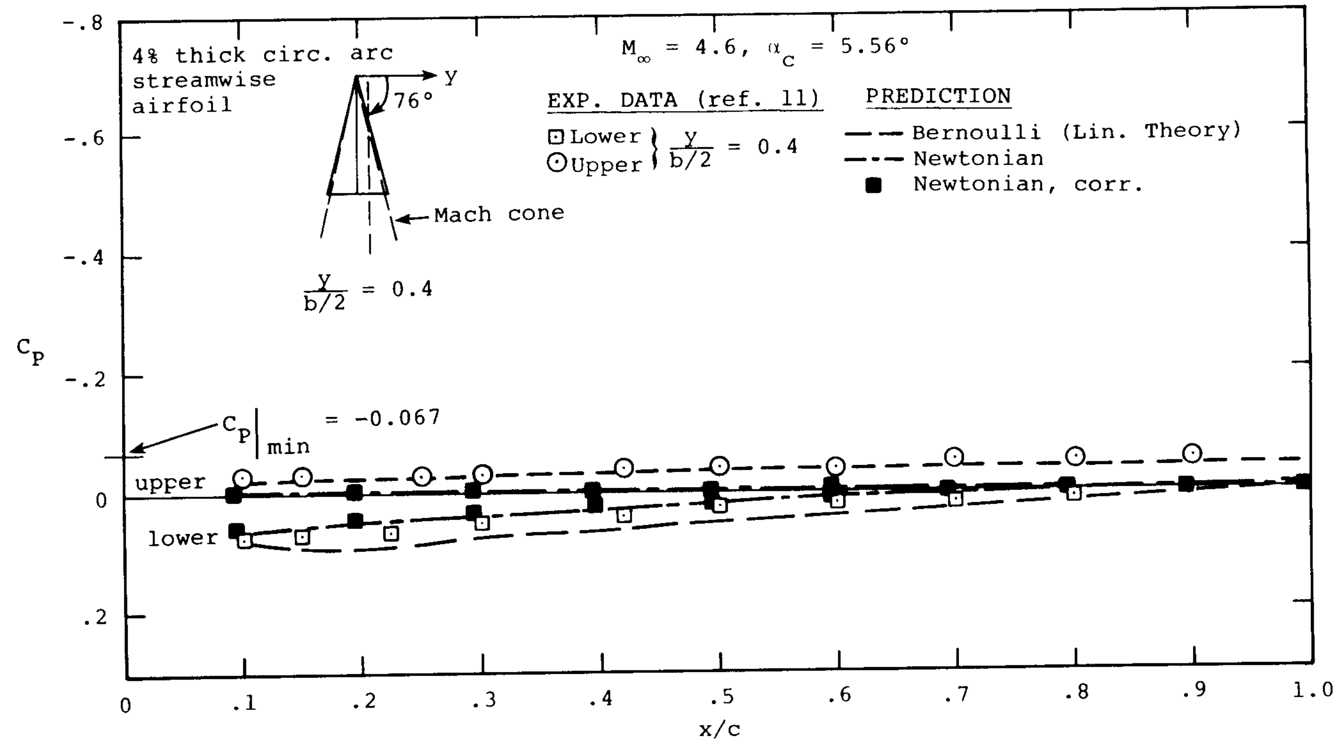

(a) $\frac{y}{b/2} = 0.4$, Bernoulli and Newtonian predictions

Figure 8.- Chordwise pressure distributions on upper and lower surfaces of $A\!\!R = 1$ delta wing, $M_\infty = 4.6$, $\alpha_c = 5.56°$.

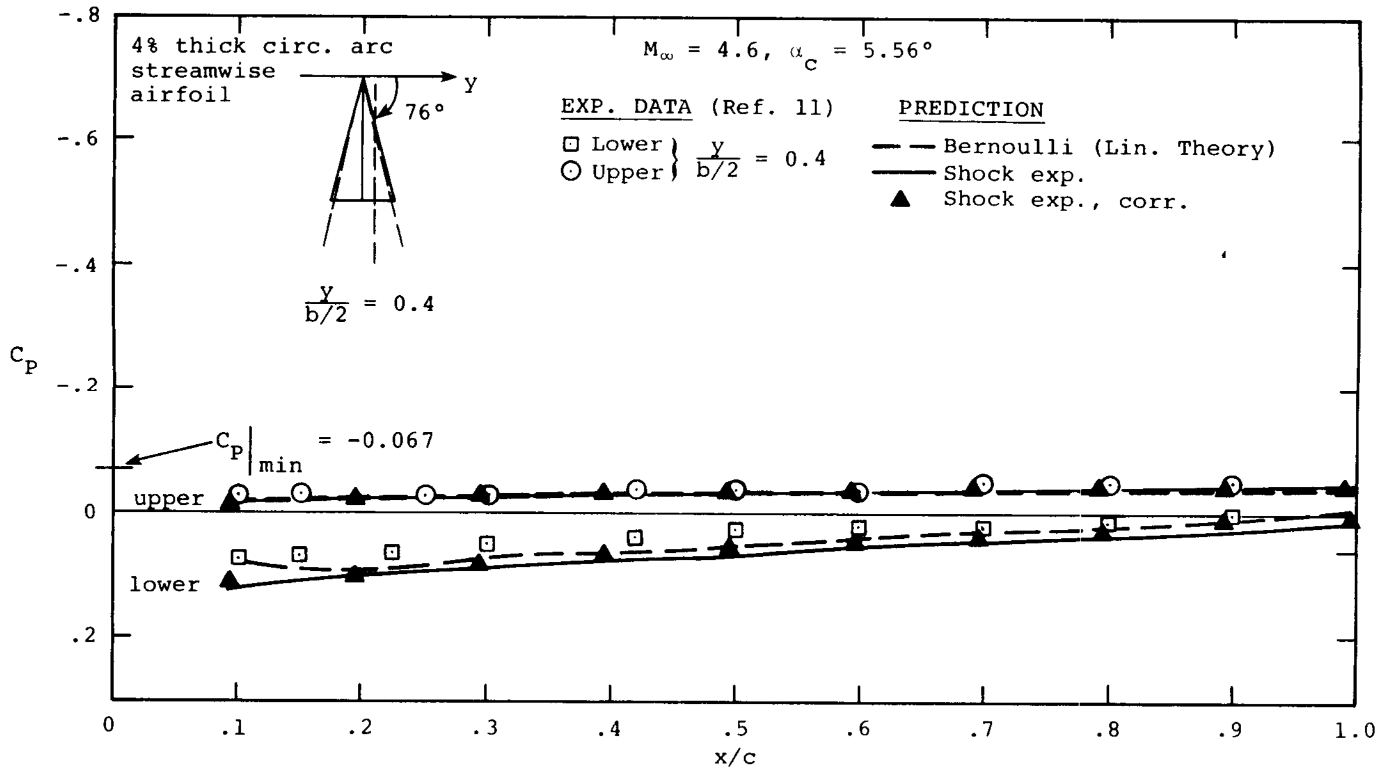

(b) $\frac{y}{b/2}$ = 0.4, Bernoulli and shock expansion predictions

Figure 8.- Continued.

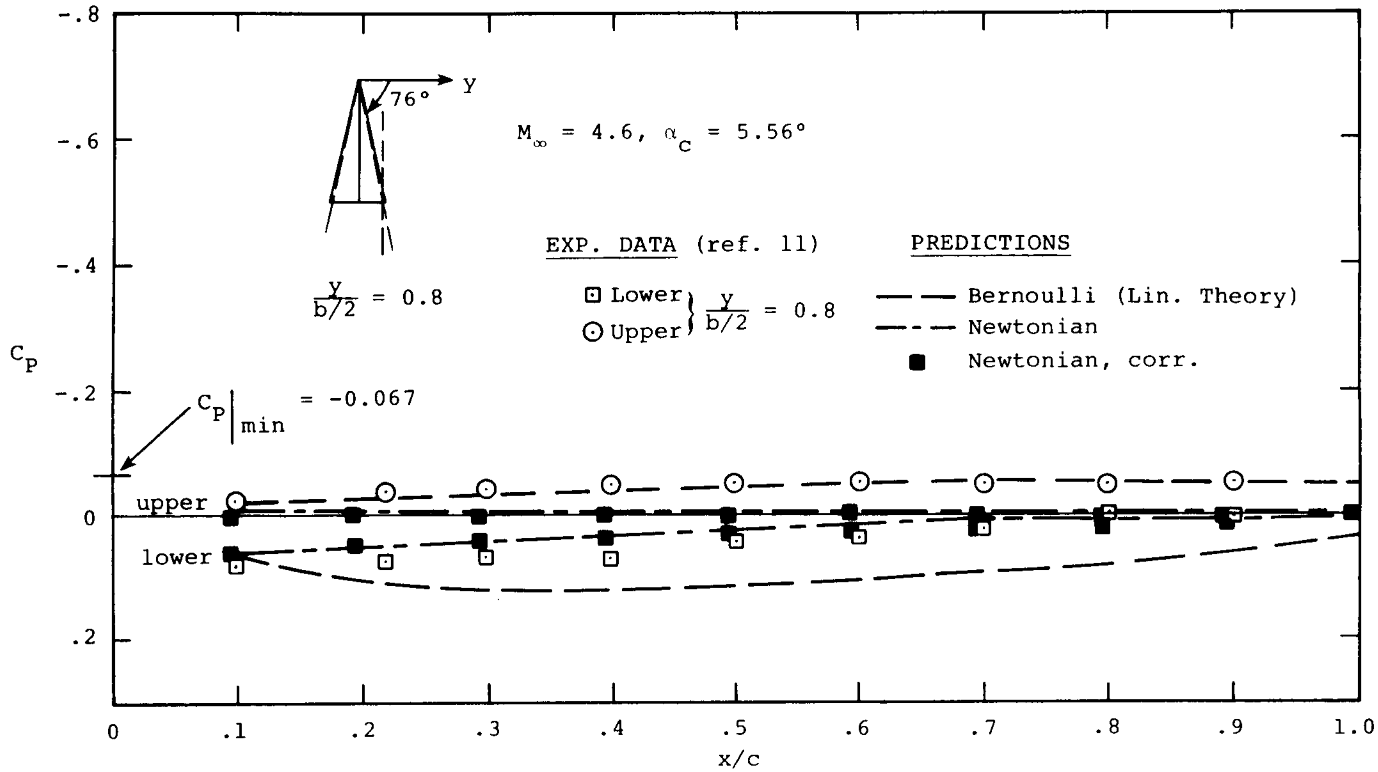

(c) $\frac{y}{b/2}$ = 0.8, Bernoulli and Newtonian predictions

Figure 8.- Continued.

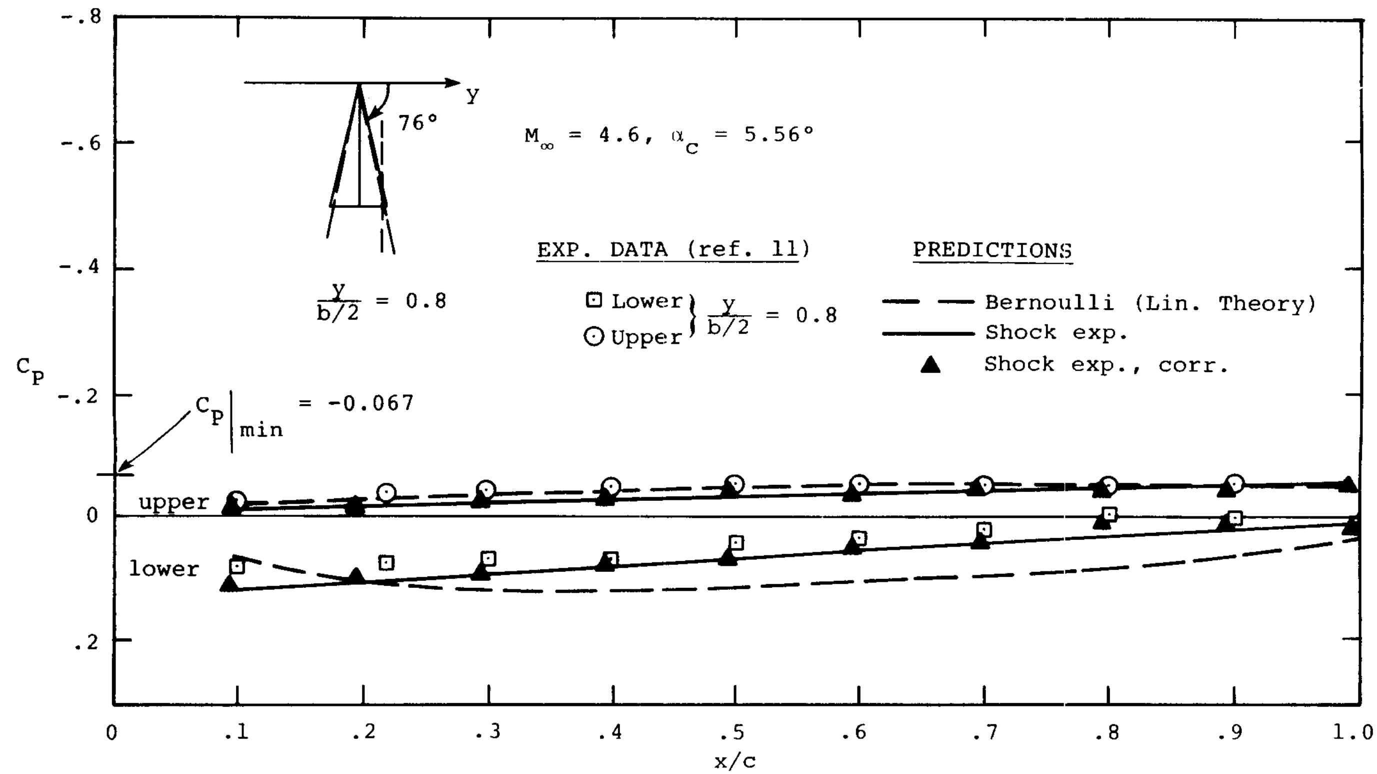

(d) $\frac{y}{b/2}$ = 0.8, Bernoulli and shock expansion predictions

Figure 8.- Concluded.

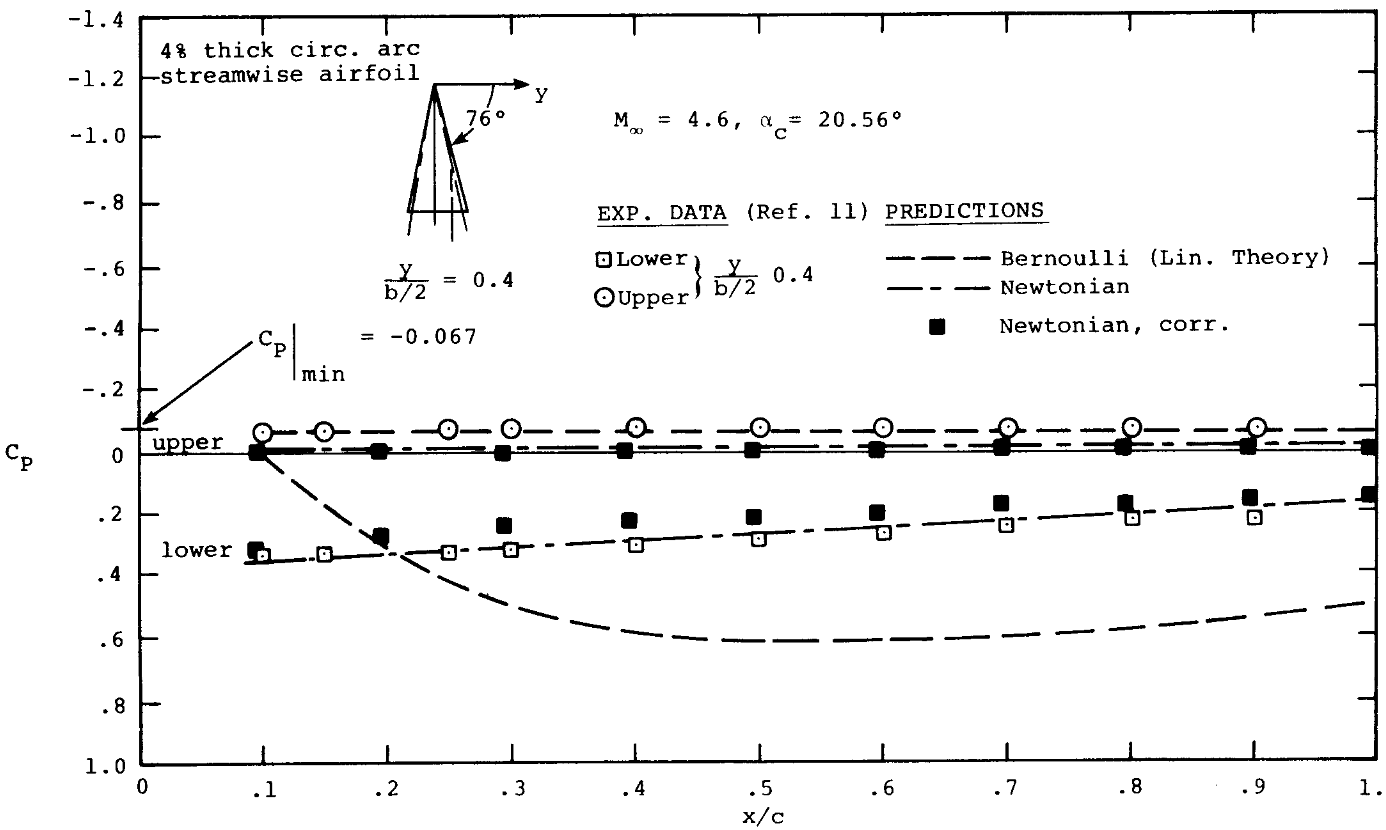

(a) $\frac{y}{b/2}$ = 0.4, Bernoulli and Newtonian predictions

Figure 9.- Chordwise pressure distributions on upper and lower surfaces of Æ = 1 delta wing, M_∞ = 4.6, α_c = 20.56°.

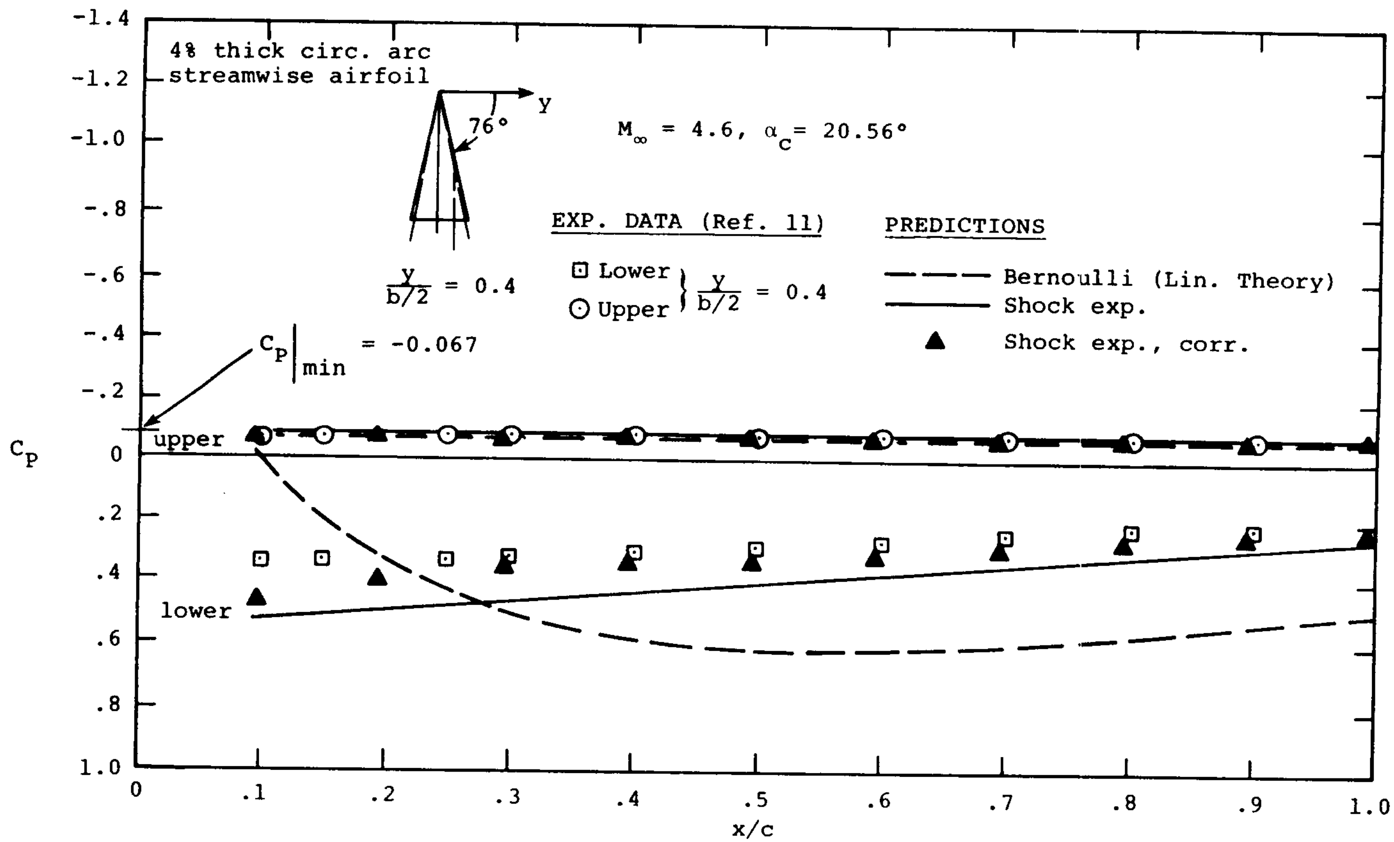

(b) $\frac{y}{b/2}$ = 0.4, Bernoulli and shock expansion predictions

Figure 9.- Continued.

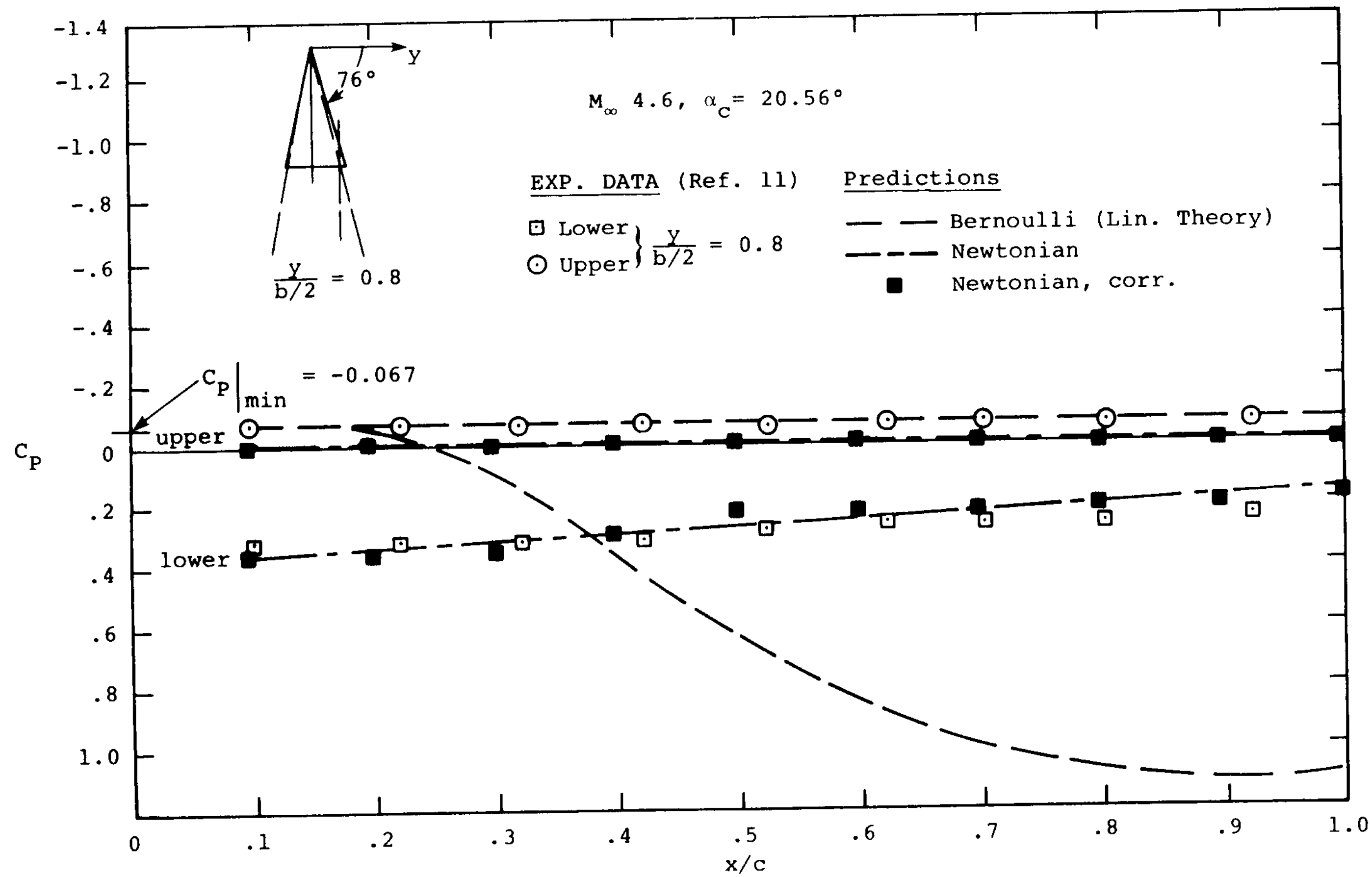

(c) $\frac{y}{b/2}$ = 0.8, Bernoulli and Newtonian predictions

Figure 9.- Continued.

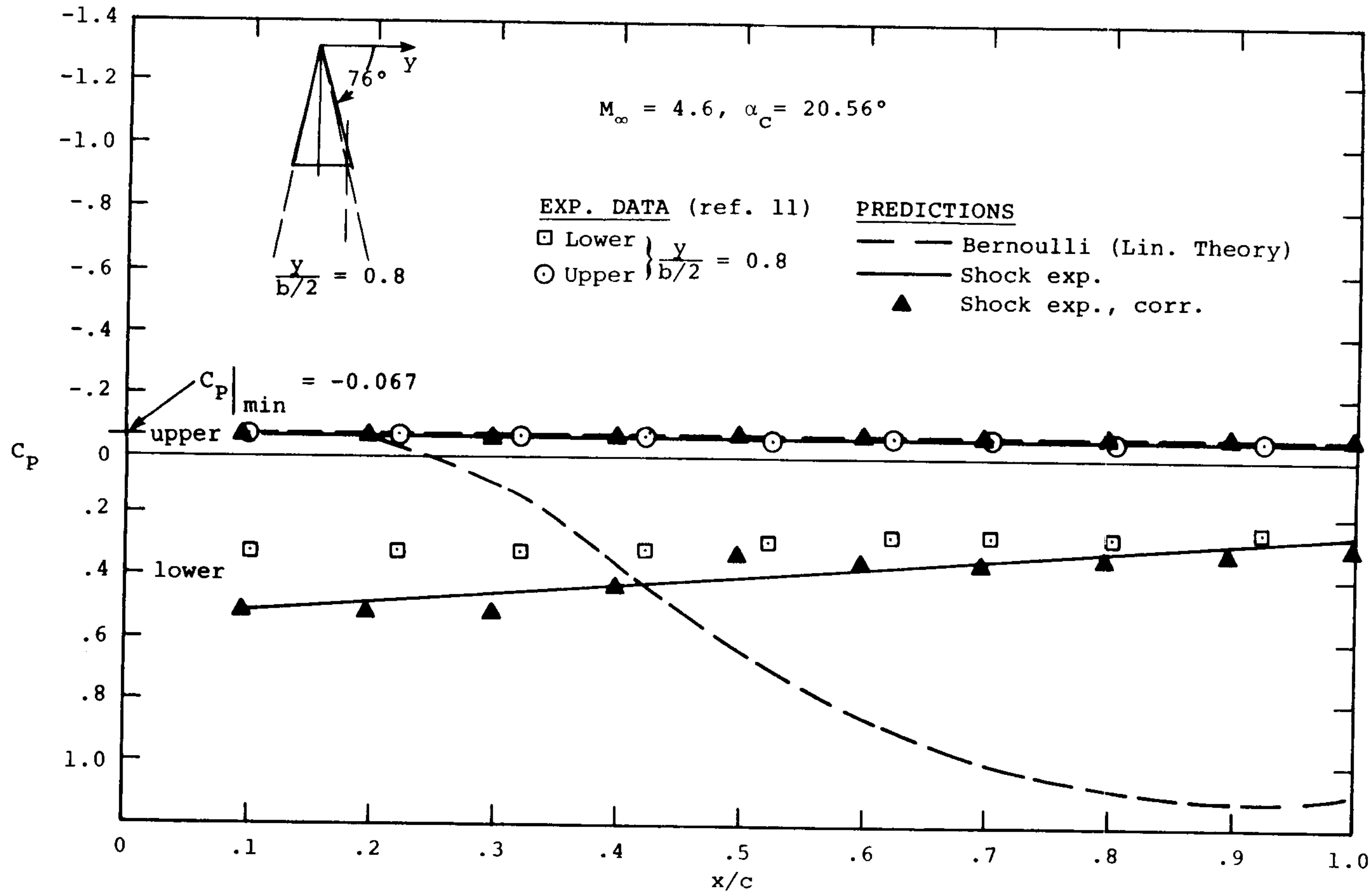

(d) $\frac{y}{b/2} = 0.8$, Bernoulli and shock expansion predictions

Figure 9.- Concluded.

the delta wing corresponds to the Mach cone associated with the free-stream Mach number. Therefore, the attached shock condition required by the shock-expansion method built into LRCDM2 is satisfied. In Figures 8(a,b) and 8(c,d), the pressure distributions are given for a low angle of attack of 5.56° at the 40 percent and 80 percent semispan stations, respectively. Pressure distributions at the same stations are shown in Figures 9(a,b) and 9(c,d) for a high angle of attack of 20.56°.

The results predicted by LRCDM2 were obtained with a layout of 10-chordwise by 5-spanwise constant u-velocity panels to model linear theory lift and 10 chordwise by 5-spanwise planar source panels to account for linear theory thickness. The nonlinear and combined theories are applied to five chordwise strips on the top and bottom surfaces with 10 segments on each strip. The results are categorized as follows.

1. Shock expansion: pressure coefficients calculated with shock-expansion theory uncorrected for interference effects, refer to Section 2.6.1 and Appendix D. (solid line)

2. Bernoulli (linear theory): pressure coefficients calculated in accordance with Equation (6) and with the required perturbation velocities induced by the linear theory paneling method(s). (dashed line)

3. Newtonian: pressure coefficients determined from Equation (9) on the windward side with $C_P = 0$ on the leeward side. (long dash, short dash line)

4. Shock expansion, corrected: category 1 pressure coefficients are corrected for interference effects with combined nonlinear/linear theory as described in Section 2.6.2. (solid triangles)

5. Newtonian, corrected: category 3 pressure coefficients are corrected for interference effects with combined nonlinear/linear theory as described in Section 2.6.2. (solid rectangles)

The Bernoulli and Newtonian results are indicated on Figures 8(a), 8(c) and 9(a), 9(c). The Bernoulli results are shown again with the shock expansion results on Figures 8(b), 8(d) and 9(b), 9(d).

In Figures 8(a) and 8(b), the measured chordwise pressure distributions (open symbols) on the upper and lower surfaces at the 40 percent midspan station do not exhibit any irregularities. The magnitudes of the pressure coefficients are low due to the low angle of attack and high Mach number. On the windward side, the Newtonian pressure predictions shown in Figure 8(a) appears to match the data best while the Bernoulli and shock-expansion methods shown in Figure 8(b) overestimate the measured pressure coefficients slightly. The corrected nonlinear pressures are not much different from the uncorrected ones. On the upper surface, the experimental data is only slightly above the value of the minimum pressure coefficient, Equation (4), and still below the zero level. The uncorrected and corrected Newtonian pressure coefficients are both zero by definition. The Bernoulli, uncorrected and corrected shock-expansion pressure coefficients match the data well. Nearer the wing tip, the levels of the measured pressure (open symbols) shown in Figures 8(c) and 8(d) are about the same as those at the 40 percent semispan location. On the windward or lower side, the Bernoulli pressures based on linear theory definitely overestimate the experimental data except near the leading edge. The uncorrected and corrected shock expansion and Newtonian pressure calculation methods agree well with the data. On the upper surface, the Newtonian based predictions are zero again whereas the experimental pressure coefficients approaches the minimum value especially near the trailing edge. The Bernoulli, uncorrected and corrected shock expansion pressure coefficients all appear to match the data well. Note that the surface area near the wing tip rapidly diminishes and that the inboard pressures have larger effect on the overall normal force. Also, as far as the linear theory is concerned, the calculated pressures become infinite at the wing tip. This characteristic will be more pronounced at the high angle of attack.

The effect of high angle of attack is shown in Figure 9. At the 40 percent semispan location, Figures 9(a) and 9(b), the measured pressure coefficients (open symbols) almost lie on straight lines. On the lower surface, the Bernoulli pressure coefficients are much higher than the experimental pressure coefficients except near the leading edge where the Bernoulli prediction approaches the zero level. This behavior is due to unrealistic (high) values of resultant flow velocity calculated with linear theory and substituted into the Bernoulli Equation (6). In Figure 8(a) and 8(b), this behavior was not evident because the angle of attack is low. The corrected shock-expansion method shown in Figure 9(b) definitely improves agreement with experiment but the uncorrected Newtonian results shown in Figure 9(a) matches the windward data best. On the suction or upper surface, the level of the measured pressure coefficients is at the minimum. The Bernoulli, uncorrected and corrected shock-expansion pressure coefficients are also at the minimum level. Note that the Bernoulli pressure coefficients derived from linear theory are limited to the minimum value in accordance with Section 2.6.1. Again, the uncorrected and corrected Newtonian pressure coefficients are set at zero.

Near the wing tip, Figures 9(c) and 9(d), the effect of angle of attack is felt even more by the linear theory for the Mach number under consideration. On the lower or windward surface, the Bernoulli method actually predicts negative values for pressure coefficient. The resultant flow velocity predicted by linear theory is very large near the leading edge and decreases too rapidly towards the trailing edge. This is mostly due to the high angle of attack and partially due to the high Mach number. The uncorrected and corrected Newtonian pressure method shown in Figure 9(c) match the data best on the lower surface. The corrected shock-expansion pressure coefficients indicated on Figure 9(d) are now affected by the arbitrary limitation on sidewash set by Equation (18) in that the calculated correction is not effective. On the upper surface the measured pressure coefficients are at their minimum and so are the calculated Bernoulli, uncorrected and corrected shock-expansion pressure coefficients. The uncorrected and corrected Newtonian pressure coefficients are at zero.

The chordwise pressure distributions, some of which are discussed above, were integrated over the upper and lower surfaces of the Æ = 1 delta wing to give the normal force coefficients as a function of angle of attack. In Figure 10 the normal-force coefficient and the location of the center of pressure measured from the wing apex and normalized by the root chord are shown as a function of angle of attack. The experimental data (open symbols) was taken from Reference 11. For angles of attack up to 12°, the Bernoulli method based on linear theory matches the normal force data well. However, the center of pressure calculated by that method lies aft of the measured location and the error grows larger with α_c. This is typical of linear theory in the application to wings at high Mach number, the total normal force often is estimated well but the distribution of that force is faulty. The uncorrected and corrected Newtonian normal-force predictions (open and solid rectangles) are low at the low and high angles of attack for which results were calculated. This is due to the forced zero pressure coefficient value on the upper surface of the wing. This "shadow flow" approximation holds better at Mach

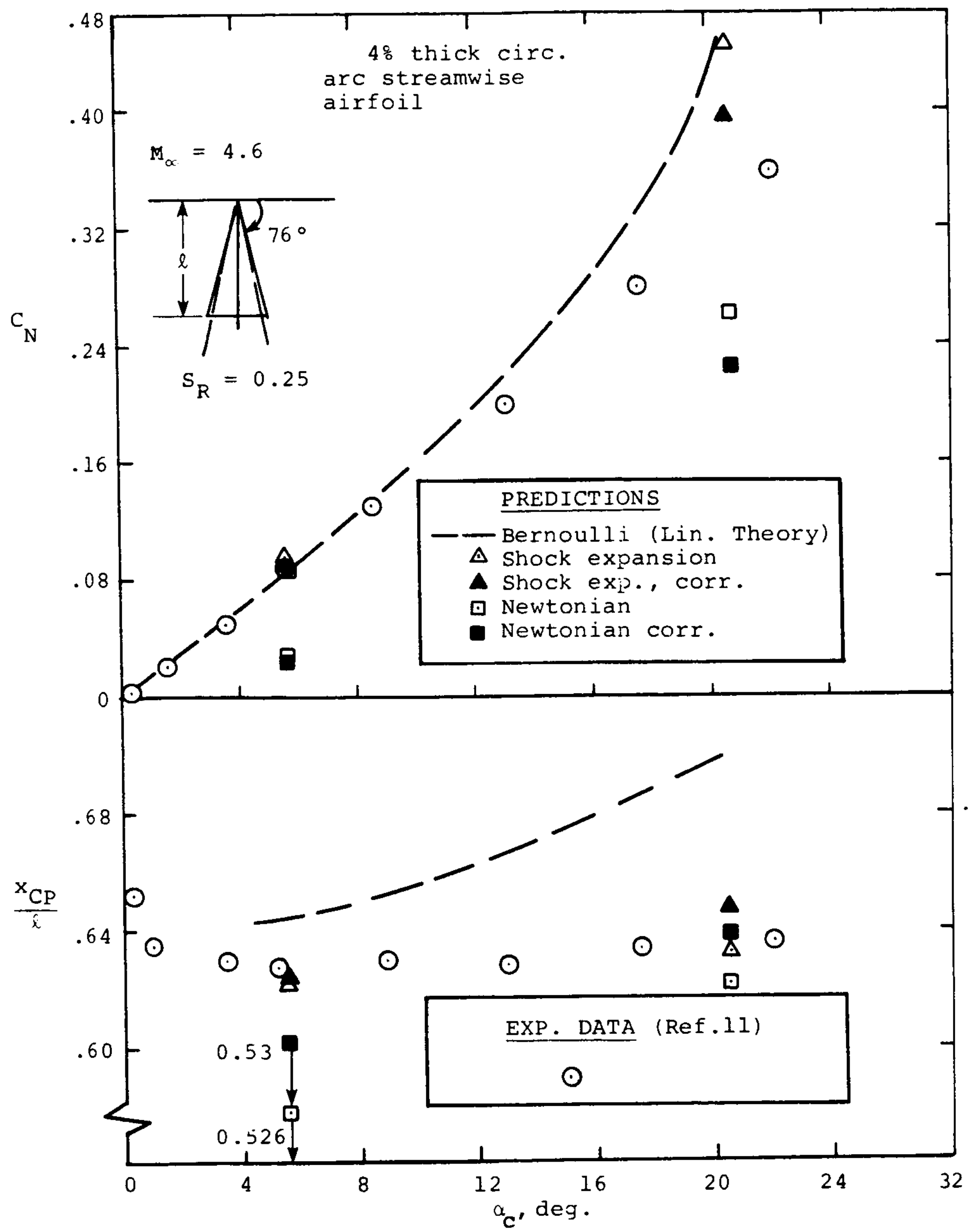

Figure 10.- Normal-force coefficient and center of pressure location for AR = 1 delta wing as a function of angle of attack, $M_{\infty} = 4.6$.

numbers in excess of 5. The center of pressure predicted by the Newtonian method is far forward of the measured level at the low angle of attack and matches the data coincidentally at the high angle. The uncorrected and corrected shock-expansion method (open and solid triangles) match the normal force and center of pressure data well at the low angle of attack. At the high angle, the agreement in normal force is definitely better with the corrected shock expansion method. Center of pressure is not affected much by the correction. In summary, the corrected shock-expansion pressure coefficient method appears to give the best results for the delta wing under consideration at $M_\infty = 4.6$ for both low and high angles of attack. On the windward side only, the pressure coefficients are predicted well by the Newtonian pressure methods. At the Mach number under consideration, the Bernoulli results agree fairly well with measured pressures and normal force at low angle of attack only.

3.5 Pressure Distributions on Ogive Cylinder

In addition to applying the Bernoulli (linear theory), nonlinear and nonlinear/linear pressure coefficient prediction methods to a rectangular and delta wing, program LRCDM2 was applied to the ogive cylinder with pointed nose shown in Figure 11.

Experimental pressure coefficients are shown for the upper and lower meridians of the pointed ogive-cylinder by the open symbols. At zero angle of attack, the pressures should be the same. It can be seen that the pressures overshoot the zero level past the tangency point.

The predictions were obtained with a distribution of 50 line source/sinks to model the linear volume effects of the body. Presently, LRCDM2 cannot treat a body alone. Therefore, a wing with a one-chordwise by one-spanwise panel layout is positioned at the body base. The circumferential number of

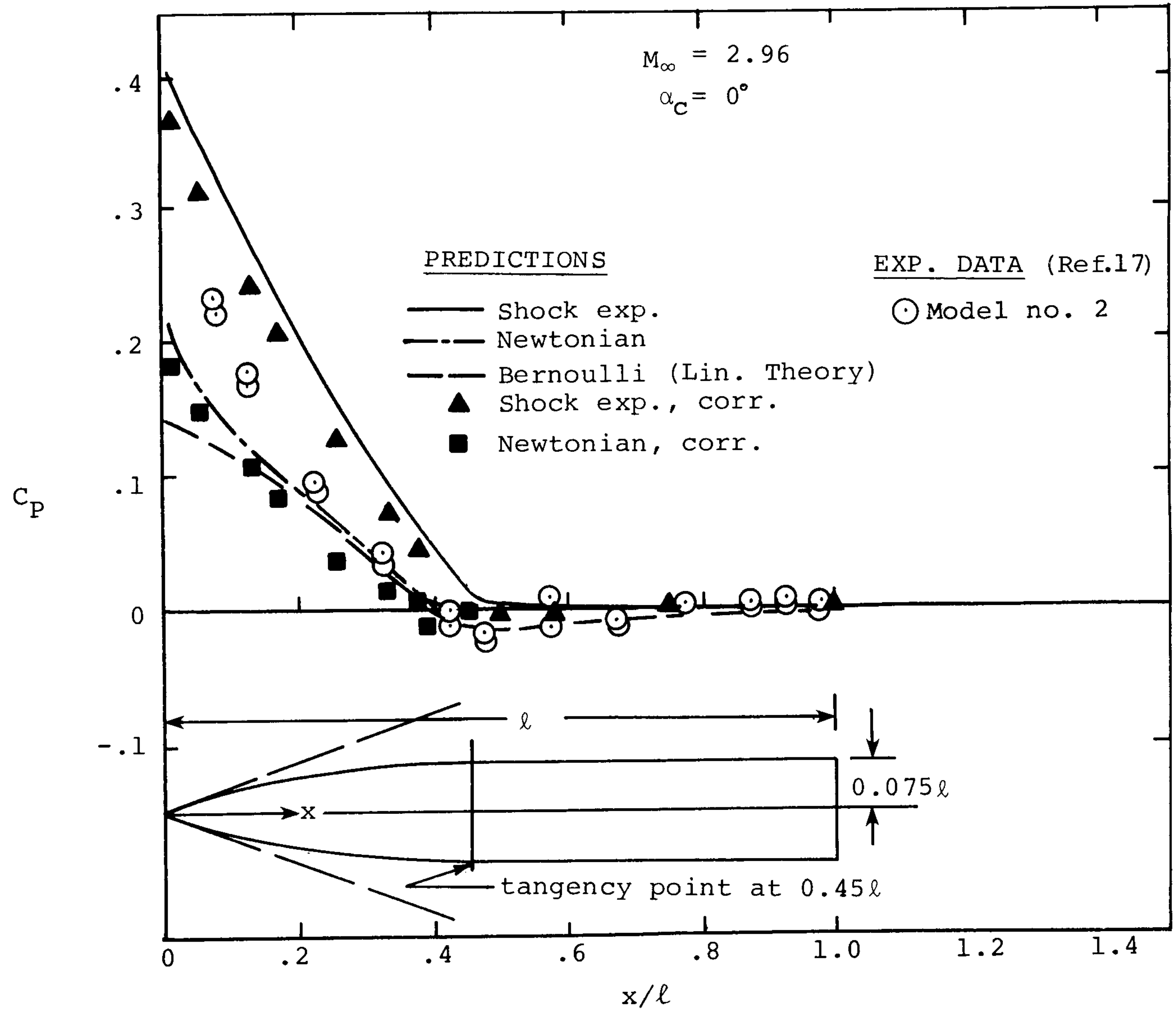

Figure 11.- Pressure distributions acting on upper and lower meridians of an ogive-cylinder at zero angle of attack, M_∞ = 2.96.

strips is determined by index NBDCR in namelist \$INPUT. For this symmetric case there were NBDCR (=4) plus one equals 5 strips laid out as shown below. This downstream view shows

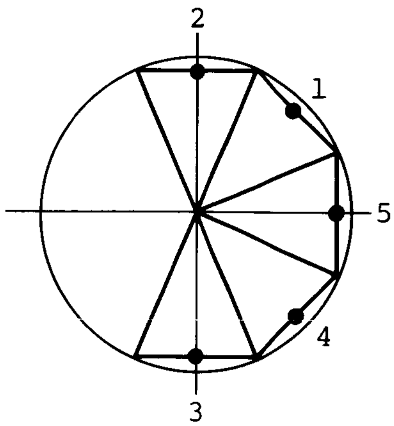

the first segments in each strip. The numbers correspond to the sequence of pressure point locations actually printed in the program output. Each strip had 20 segments in it to cover the body from the nose to the base. For the case at hand at zero angle of attack, the pressures will be the same along all strips. Before discussing the comparisons between the predicted and measured pressure coefficients, the locations of the conical shock and Mach cone will be indicated. This is followed by some general comments regarding the effects of shock location on the pressures acting on the body.

For the case at hand, the following conditions exist.

$\theta_{nose} = 18.93°$ at $x_B = 0$ $\qquad M_\infty = 2.96$

$\mu = 19.75°$, $\mu = \sin(1/M_\infty)$ $\qquad \theta_{shock} = 29°$ from conical shock tables

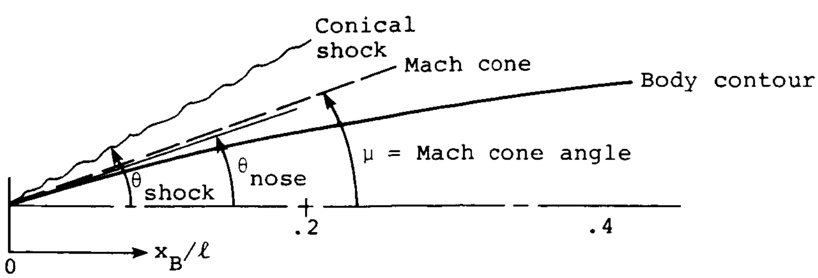

At zero angle of attack, the Mach cone associated with linear theory (also indicated in Figure 11) lies close to the body contour. For Mach numbers higher than 3.08, the body slope will exceed the Mach cone semi-vertex angle. In that case, subroutine BDYGEN of program LRCDM2 will replace the portion of the nose contour lying outside of the Mach cone with a conical portion with slightly smaller semi-vertex angle than the Mach cone so that the linear body analysis can be performed. For the conditions shown above, the conical shock lies within one radius of the body surface up to about 20% body length behind the pointed nose.

The methods using shock expansion (Sections 2.6.1, 2.6.2, and Appendix D) require the condition of an attached shock. Whether the shock is attached or not, the pressures near the nose of any body in supersonic flow are generally not predicted well by linear theory. This characteristic is a function of how close the body surface is to the shock. For slender bodies at zero angle of attack, the Mach number can be relatively high before linear theory breaks down and nonlinear theory takes over. As the angle of attack is increased, the windward side of the body is affected first by the nonlinear shock properties. Under these conditions, the linear theory will underpredict the pressures acting on the windward portion of any body.

In Figure 11, the Bernoulli pressure coefficients (dashed line) based on linear theory underestimate the experimental data up to about 20% body length. From there on to the body base, the Bernoulli pressure match the data very well including the overshoot.

The uncorrected shock-expansion method (solid line) definitely overestimates the pressure coefficients and approaches the zero level just about at the tangency point. The corrected shock-expansion pressure coefficients (solid triangles) are closer to the experimental data but are still high. Note that for this case involving zero angle of attack, the correction as determined by the method described in Section 2.6.2 is due to the difference in the Mach numbers M_{2D} and M_{3D} with the lateral flow angle ε equal to zero. The over-estimation is not unexpected since the shock-expansion method used here is actually based on a tangent-wedge solution applicable to wing type configurations. The tangent-cone solution is better for applications to axisymmetric bodies and will generate lower pressure coefficients on the body surface immediately behind the conical shock. As a matter of fact, for Mach number equal to 2.96 and using nose tip half angle $\theta_{nose} = 18.93°$, the tangent-cone pressure coefficient is about 0.26 compared to 0.41 for the tangent-wedge pressure coefficient. These values of pressure coefficients are valid at the body nose or wing leading edge, respectively.

The Newtonian predictions generally underestimate the pressure coefficients on the nose. In this case, the uncorrected and corrected Newtonian methods are definitely not applicable due to the low Mach number under consideration.

In summary, for the application to an ogive cylinder and probably to other body shapes as well, the Bernoulli method based on linear theory gives good agreement except for approximately one-half of the nose length in this case. The distance from the nose tip to good agreement with data is a function of the proximity of the nose shock to the surface. If the shock lies within about one body radius from the body surface, the Bernoulli predictions will underestimate the pressure coefficients. The shock-expansion methods presently employed in LRCDM2 overestimate the pressure coefficients. The agreement with experimental data will be improved by replacing the tangent-wedge with a tangent-cone approach. The Mach number at hand is too low for simple Newtonian theory.

4. CONCLUSIONS

Program LRCDM2 was developed from an existing computer program NSWCDM for detailed static aerodynamic loading analysis of supersonic missiles with axisymmetric bodies and up to two finned sections (tail or canard-tail configurations). The extensions and improvements incorporated in LRCDM2 include an optional afterbody vortex-shedding method, handling of canard fin leading- and/or side-edge vortices in the vortex tracking scheme, and the capability for analyzing a given configuration in one run for a set of included angles of attack and roll angle for the same Mach number. In addition, two combinations of nonlinear/linear theories for extending the range of applicability in terms of Mach number are built into program LRCDM2.

Comparisons with experimental data and a calculative example involving afterbody loads are given to assess the new features. The program is tested successfully against measured overall forces and moments acting on a triform tail-finned configuration. The new afterbody vortex-shedding option is applied to a canard-controlled configuration with a long afterbody. The results indicate that accuracy has been substantially improved for total rolling moment for the case with roll control. Initial tests of the nonlinear/linear approaches give good agreement for pressures acting on a rectangular wing and a delta wing with attached shocks for Mach numbers up to 4.6 and angles of attack up to 20°. In particular, the axial center-of-pressure location is predicted well with the corrected shock-expansion pressure method for the delta wing at M_∞ = 4.6. On bodies, the methods need further assessment and the tangent-wedge theory should be replaced with the tangent-cone method.

To the extend that program LRCDM2 has been tested, the following sets of recommendations are listed. The first set is concerned with theoretical aspects and the second set involves improvements to the structure of the computer program to make it more efficient and user friendly. The third set of recommendations are neither theoretical nor program-structure oriented but extend the capabilities of LRCDM2.

With regard to improvements to the present theoretical methods built into LRCDM2, the following should be considered.

1. The methods used to compute Bernoulli pressures on the forebody at high angles of attack under the influence of external vortices should be improved (refer to Section 3.1 and Appendix C, Section C.4).

2. At high angles of attack, the fin trailing-edge vorticity associated with attached flow and the leading- and/or side-edge vorticity due to flow separation need to be reconsidered in relation to each other. This will require an accurate and fast method for calculating span loading under the influence of moving vortices (refer to Section 2.4).

3. The representation of the canard-fin wake in terms of a limited number of concentrated, discrete vortices is not accurate for cases involving tail fins positioned a short distance (e.g., one to two canard-fin chords) behind the canard section; in these cases the canard fin wakes are not fully rolled up and are better modeled by a distribution of vortices lying in a nonplanar vortex-wake sheet allowed to deform (roll up) between the canard section and the tail section.

4. The vortex tracking scheme and the vortex effects calculation method (module VPATH2) should be enhanced with a simple vortex-core model to improve the vortex-path calculations and vortex-induced velocities when vortices are close together or close to the body surface or fins; companion

program BDYSHD used optionally for afterbody vortex-shedding effects is already equipped with a vortex-core model. In addition, a study should be made of the effects of including the center vortex in the image scheme that is used in both programs.

5. The combined nonlinear/linear pressure coefficient methods must be tested further for fins on a body; on the body, the tangent-cone solution should be incorporated.

The following computer program oriented modifications will reduce computation time and make program LRCDM2 more user friendly.

1. Save aerodynamic influence coefficients for velocity and pressure calculations at the panel control points and body pressure calculation points; similar coefficients for the panel strength calculations are already saved; additional computer time reduction will result with the saving of the influence coefficients for use with the pressure calculations especially when performing calculations for a set of included angles of attack and/or roll angle.

2. In addition to the above, the following geometrical quantities can be saved for multiple included angles of attack and/or roll calculations:

a. panel corner coordinates
b. panel control point coordinates
c. panel leading- and trailing-edge sweep angles

3. In order to reduce core storage requirements, the present panel strength calculation scheme should be modified to an out-of-core solution method employing a blocked matrix and an iterative solution approach.

4. Program LRCDM2 should be equipped with warnings in the program output to indicate:

a. number of constant u-velocity panels selected for modeling fin lift and interference on body is out of bounds

b. number of planar source panels selected for modeling fin thickness is out of bounds

c. excessive number of pressure points on the body surface

5. Input to LRCDM2 can be simplified further and a common input module should be incorporated.

6. Additional computer time can be saved by eliminating the forward-fin loading calculations performed in step 1 for cases without formation of forebody vortices. The forward fin loadings are calculated in step 3 and included in the overall force and moment calculation.

The following two items would extend the capabilities of program LRCDM2.

1. Presently the fin-thickness model can only handle planar or cruciform fins; the source paneling layout routines need to be updated to handle arbitrary fin location on the body and arbitrary fin dihedral (or cant) angle.

2. The normal force acting on a deflected fin needs to be resolved into the directions of the rolled body-axis coordinate system; the overall axial force and the yawing moment will receive added contributions.

REFERENCES

1. Dillenius, M. F. E. and Nielsen, J. N.: Computer Programs for Calculating Pressure Distributions Including Vortex Effects on Supersonic Monoplane or Cruciform Wing-Body-Tail Combinations With Round or Elliptical Bodies. NASA CR-3122, Apr. 1979.

2. Dillenius, M. F. E. and Smith, C. A.: Final Report - Program NSWCDM, Aerodynamic Prediction Program for Cruciform Canard-Axisymmetric Body-Cruciform Tail Missiles at Supersonic Speeds. NEAR TR 217 (Contract No. N70921-79-C-A365), Nielsen Engineering & Research, Inc., Apr. 1980.

3. Allen, J. M.: Comparison of Analytical and Experimental Supersonic Aerodynamic Characteristics of a Forward Control Missile. AIAA Paper No. 81-0398, 19th Aerospace Sciences Meeting, St. Louis, MO, Jan. 1981.

4. Dillenius, M. F. E., Hemsch, M. J., Sawyer, W. C., Allen, J. M., and Blair, A. B., Jr.: Comprehensive Missile Aerodynamics Programs for Preliminary Design. AIAA Paper No. 82-0375, 20th Aerospace Sciences Meeting, Orlando, FL, Jan. 1982.

5. Mendenhall, M. R.: Predicted Vortex Shedding from Noncircular Bodies in Supersonic Flow. J. Spacecraft and Rockets, Vol. 13, No. 5, Sept.-Oct. 1981, pp. 385-392.

6. Mendenhall, M. R. and Perkins, S. C., Jr.: Prediction of Vortex Shedding from Circular and Noncircular Bodies in Supersonic Flow. NASA CR-3754, Jan. 1984.

7. Dillenius, M. F. E., Goodwin, F. K., and Nielsen, J. N.: Prediction of Supersonic Store Separation Characteristics. Vol. I - Theoretical Methods and Comparisons with Experiment. AFFDL-TR-76-41, Vol. I, May 1976.

8. Mendenhall, M. R. and Nielsen, J. N.: Effect of Symmetrical Vortex Shedding on the Longitudinal Aerodynamic Characteristics of Wing-Body-Tail Combinations. NASA CR-2473, Jan. 1975.

9. Bollay, W. A.: Nonlinear Wing Theory and Its Application to Rectangular Wings of Small Aspect Ratio. ZAMM, 19, 1939.

10. Nielsen, J. N.: Missile Aerodynamics. McGraw-Hill Book Co., 1960.

11. Carlson, H. W.: A Modification to Linearized Theory for Prediction of Pressure Loadings on Lifting Surfaces at High Supersonic Mach Numbers and Large Angles of Attack. NASA TP-1406, Feb. 1979.

12. Truitt, R. W.: Hypersonic Aerodynamics. Ronald Press Co., New York, 1959, p. 5.

13. Chenyi, G. G.: Introduction to Hypersonic Flow. Translated and Edited by R. F. Probstein, Academic Press, New York and London, 1961, p. 41.

14. Goodwin, F. K., Dillenius, M. F. E., and Mullen, J., Jr.: Prediction of Supersonic Store Separation Characteristics Including Fuselage and Stores of Noncircular Cross Section. Vol. I - Theoretical Methods and Comparisons with Experiment. AFWAL-TR-80-3032, Vol. I, Nov. 1980.

15. Nielsen, J. N. and Kuhn, G. D.: Final Report - Studies of Vorticity Effects by the Euler Equations with Emphasis on Supersonic Flow Fields. NEAR TR 310 (Contract N00014-82-C-0391), Nielsen Engineering & Research, Inc., Oct. 1983.

16. Stallings, R. L., Jr. and Lamb, M.: Wing-Alone Aerodynamic Characteristics for High Angles of Attack at Supersonic Speeds. NASA TP-1889, July 1981.

17. Landrum, E. J.: Wind-Tunnel Pressure Data at Mach Numbers From 1.6 to 4.63 for a Series of Bodies of Revolution at Angles of Attack from -4° to 60°. NASA TM X-3558, Oct. 1977.

APPENDIX A
PROGRAM LRCDM2

TABLE OF CONTENTS

APPENDIX A

PROGRAM LRCDM2

A.1 INTRODUCTION

The purpose of this appendix is to describe computer program LRCDM2 with emphasis on the information the user must supply and the general understanding of the program. In essence, program LRCDM2 computes pressure distributions at points on the surfaces of a complete supersonic configuration comprising a forward- (canard) and tail-finned section attached to an axisymmetric body. The analysis embodied in the computer program is based on supersonic paneling and line singularity methods coupled with vortex-tracking theory. Details of the theoretical methods are given in References 1 and 2, and the latest modifications and extensions are given in this report.

For a complete configuration, the program proceeds through an automated series of six steps to analyze the forebody and forward-finned section, the afterbody, and the tail-finned section. If the configuration consists of a body with a set of tail fins, only the first three steps are employed.

The use of LRCDM2 and optional afterbody vortex-shedding program BDYSHD (Appendix B) in the stepwise procedure is described in Section 2.3 of the main part of this report. An executive routine organizes this procedure and also manages the exchanges of data sets containing point coordinates, vortex-induced velocity components, component loads, etc. In this process, effects of forebody and forward-fin vortex wakes are included in the pressure distributions and loads. Effects of afterbody vortex shedding on the afterbody loads and tail-fin loads can be included by the optional engagement of program BDYSHD described in Appendix B. Detailed components loadings and overall forces and moments are obtained from the calculated pressure distributions. On the fins, the Polhamus suction-to-normal force conversion is included in the fin force and moment calculations as described in Appendix C of this report.

In the following, descriptions are given of the types of geometry and flow conditions that can be treated by LRCDM2. The calculation procedure is listed in accordance with the automated stepwise procedure described in Section 2.3. Details of the internal data exchanges are specified. Program operation, including types of computer machines the program has actually been run on, is discussed. Known program limitations and precautions are listed. Input and output descriptions are keyed to specific steps of the stepwise procedure. Finally, a sample case is given including the use of optional afterbody vortex-shedding program BDYSHD.

The text in the main part and the appendices of this report refer to subroutine names used in connection with the procedures implemented in LRCDM2. The calling sequence of all the subroutines of program LRCDM2 is shown in Figure A.1. The source listings of the subroutines contain comment cards, following the subroutine name card, stating their purpose. Throughout most of the subroutines, additional comment cards point out the flow of calculations and/or operations performed in the particular subroutine.

A.2 CONFIGURATION GEOMETRICAL CHARACTERISTICS

The bodies must have (or are assumed to have) circular cross sections. In general, the body is composed of a nose section with varying radius followed by a cylindrical section with constant radius. The nose section may have the following shapes (the choice is set by control index BCODE in namelist $BODY, read in by subroutine BDYGEN as described in Section A.7):

BCODE	Forebody Shape
0	Parabolic
1	Sears-Haack*
2	Tangent-ogive
3	Ellipsoidal
4	Conical

If the body nose is not pointed and/or if the Mach number is high enough to cause the body-nose contour or a portion thereof to lie outside the Mach cone with its apex at the nose tip, subroutine BDYGEN will replace that forebody portion with a conical portion. The surface of this conical replacement is made to lie just inside the Mach cone so that the body solution can proceed.

The effects of the following fin geometrical and other characteristics can be accounted for:

- Up to four planar (flat) fins in a given finned section in planar, triform, cruciform, and low-profile layouts
- Control deflection angle
- Fin location on body contour and fin dihedral (or cant) angle arbitrary
- Leading-edge shape: Straight line which may be swept or it can be composed of straight line elements with different sweeps
- Trailing-edge shape: Straight line which may be swept or it can be composed of straight line elements with different sweeps
- Thickness: Accounted for by specifying streamwise slopes

---

*Ashley, H. and Landahl, M.: Aerodynamics of Wings and Bodies. Addison-Wesley Publishing Co., Inc. 1965, pp. 180-181.

- Taper: Uniform or broken
- Mean camber surface: Planar
- Side edges: Straight but not necessarily streamwise

In the stepwise procedure of Section 2.3, program LRCDM2 treats one finned section at a time. If the configuration of interest has only a tail-finned section (tail finner), steps 1 through 3 are used to analyze the body and tail fins.

A.3 FLOW CONDITIONS

The executive routine of program LRCDM2 reads in a series of included angles of attack, α_c, and angles of roll, ϕ, for one Mach number*. The approximate ranges of applicability of the present version of LRCDM2 are given in the following table.

Ranges of Flow Parameters

Parameter	Symbol	Range
Mach number	M_∞	1.05 - 6.0
Angle of attack	α_c	0 - 25°
Roll angle	ϕ	0 - 360°
Fin deflection angle	δ	±20°

The high Mach number capability is due to the incorporation of combined nonlinear/linear pressure coefficient calculation methods described in Section 2.6 of this report. However, these methods are preliminary in nature in their present form. The linear theory Bernoulli pressure method is valid up to $M_\infty = 2.5$. For configurations with long afterbodies (length of body between forward fins and tail fins in excess of 10 calibers) effects of afterbody vortex shedding become

*If program BDYSHD for optional afterbody vortex-shedding modeling is engaged, calculations are performed for one α_c and one ϕ only.

important for included angles of attack in excess of 10°. The afterbody vortex shedding companion program BDYSHD (Appendix B) can be optionally run in conjunction with LRCDM2. It is applicable up to the onset of supercritical crossflow Mach number and/or unsteady vortex formation.

A.4 AUTOMATED STEPWISE CALCULATION PROCEDURE WITH DATA EXCHANGES

The present version of program LRCDM2 contains routines for computing pressures and loads acting on the forebody, the fins, and the portion of body of either the forward- or tail-finned sections, and on the afterbody in the absence of afterbody shed vortices. In addition, program LRCDM2 contains routines called collectively module VPATH2 for calculating vortex paths along the configuration and for determining vortex-induced effects at points on the components. The calling sequence of all subroutines of program LRCDM2 is shown in Figure A.1. A cross reference map of all the common blocks is given in Figure A.2 and the subroutines themselves are cross-referenced in Figure A.3. References will be made later to the fixed or rolled body coordinate system (x_B, y_B, z_B) shown in Figure A.4.

Optionally, program LRCDM2 can call separate program BDYSHD (Appendix B) by means of job control and program organized data exchanges to model the effects of afterbody vorticity. A complete configuration is treated as follows by multiple applications of program LRCDM2 and its module VPATH2 as managed by the executive routine. The optional use of program BDYSHD is also described.

The following sketch depicts the stepwise procedure superimposed on a typical configuration with and without the application of program BDYSHD. The scheme without the use of the latter program is indicated on the side of the configuration. The optional sequence shown at the top includes program

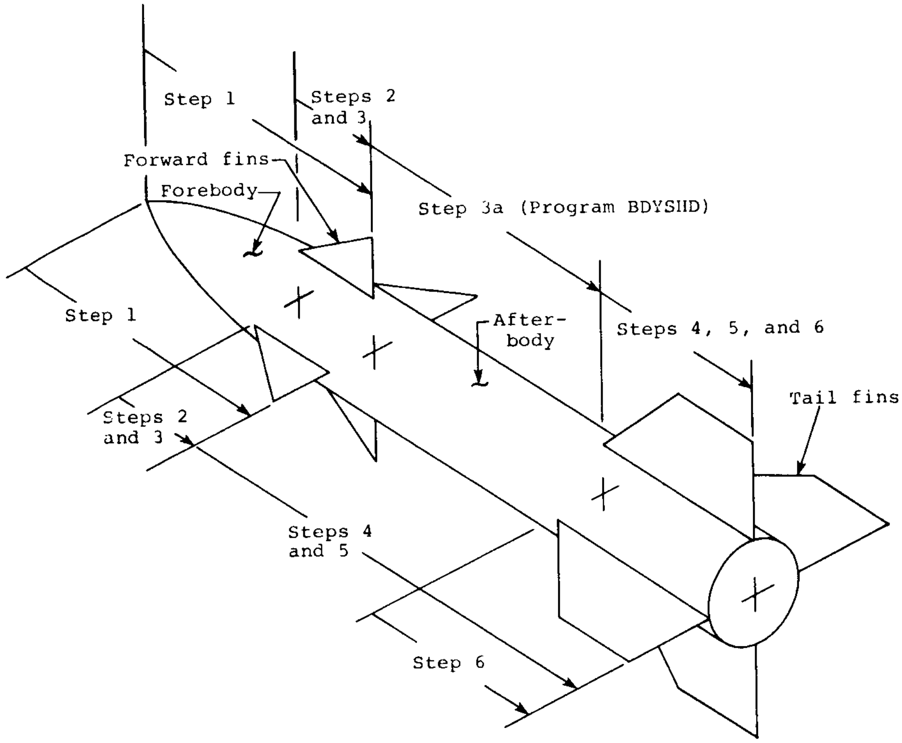

BDYSHD to treat the afterbody. Note that steps 1, 3, 4, and 6 involve the body and fin routines of program LRCDM2, and steps 2 and 5 are performed by the routines of vortex-tracking module VPATH2. Step 3a involves the afterbody vortex-shedding program BDYSHD. If the configuration of interest is a tail finner, steps 1 through 3 only are employed.

The executive routine of program LRCDM2 reads in the included angles of attack and angles of roll. Input associated with the forward fins, tail fins, and body are transferred to and saved in a data set on TAPE2. The executive routine then proceeds to manage the stepwise procedure as follows. References are made to certain control indices described later in the input description, Section A.7.

Step 1

Consider the forward fins mounted on the body. The body is modeled from its nose to the base by line singularities along the body longitudinal axis. Lifting-surface routine DEMON2 is called by the executive routine with index NCPOUT in namelist $INPUT set equal to one. This step first generates the coordinates of the control points associated with the constant u-velocity panels distributed on the forward fins and the body-interference shell. The cylindrical interference shell has constant cross section and covers the body from the leading edge to the trailing edge of the forward-finned section. The number of control points and the sets of coordinates are stored in a data set on TAPE4. There are NWBP sets of coordinates where NWBP is the total number of control points on the forward fins and interference shell.

The program proceeds to compute the pressure distributions on the body up to the forward-finned section. If the included angle of attack is sufficiently high and the forebody is long enough, the effects of forebody vorticity will be accounted for in the body pressures*. The forces and moments acting on the forebody portion are obtained from integrating the pressure distributions. They are expressed in the unrolled and rolled body coordinate systems shown later in the output description.

The forebody force and moment coefficients computed at this stage serve as the first values in the summing procedure for overall force and moment coefficients acting on the complete configuration. This operation is performed by subroutine TOLDS.

The strengths of the constant u-velocity panels and subsequently the pressure distributions and loadings on the forward fins are calculated in this step without the effects

*Refer to Limitations and Precaution Section A.6 in connection with a deficiency in the forebody loading when body nose vortices are present.

of forebody vorticity. These fin loadings are not included in the summing procedure. At the end of this step, the strengths and positions of the forebody vortices in the crossflow plane at the leading edge (beginning) of the forward-finned section are stored in a data set on TAPE8.

Step 2

Vortex path module VPATH2 is now employed by the executive routine to track the nose vortices over the forward-finned section. In the input for this step, indices NCPIN and NVLOUT should both be set equal to one. The former causes the data set on TAPE4 containing the control points of the forward fins and interference shell to be entered, and the latter generates a velocity data set which will be described shortly. The input to this step also includes the strengths and positions of the forebody vortices from the data set on TAPE8 generated in step 1. These vortices are tracked back to the trailing edge (end) of the forward-finned section. It is possible to make the vortices lie parallel to the body centerline as described in the input section (recommended procedure, refer to Limitations and Precautions Section A.6).

After the vortex paths have been calculated, the perturbation velocities induced by the forebody vortices are determined at the control points of the forward fins and interference shell. These velocity components are stored on a data set on TAPE7 when index NVLOUT is set equal to one, as mentioned earlier. The vortex-induced velocities are calculated as if the forward fins are not present in accordance with the procedure described in Section C.4 of Appendix C.

Step 3

Subroutine DEMON2 is called again by the executive routine which sets NVLIN=1 and NCPOUT=0 in namelist $INPUT. The value of the first index instructs the program to read in velocity components induced by the forebody vortices at the control points on the forward fins and the interference shell. This information was generated in step 2 by module VPATH2 and stored in a data set on TAPE7. The strengths of the constant u-velocity panels are then recalculated as well as the pressure distributions, forces and moments on the forward fins and on the body covered by the interference shell. The force and moment coefficients acting on the forward-finned section are added to those calculated for the forebody in step 1.

At this stage, the output also contains specifications for the concentrated vortices associated with the fin edges. Trailing-edge vortex strengths and positions calculated from the span load distribution using Bernoulli-type loading pressures and the characteristics of vortices from the fin leading- and/or side-edge calculated from the linear pressure loading are stored in a data set on TAPE8 and will be used later in either step 3a or step 5.

Step 3a (Optional)

When index NBSHED in namelist $INPUT is set equal to 1, the force and moment coefficients summed over the forebody and forward-finned section are printed in the output of program LRCDM2 at the end of step 3 and stored on TAPE9. Without this optional step, TAPE9 is used exclusively for storage of the aerodynamic influence coefficient array for the forward fins and interference shell.

Program BDYSHD (Appendix B) is called by the job control commands and besides reading its own input, the vortex data stored in TAPE8 is read in. This vortex data was generated by LRCDM2 and includes forebody and fin-edge vortex strengths and locations at the trailing-edge of the forward-finned section. These vortices form the initial vortex field for BDYSHD.

Under the influence of the upstream vortices, program BDYSHD computes pressure distributions at many axial stations from the forward-finned section up to the tail section. The Stratford criteria is applied to determine the location and strengths of additional vortices shed by the afterbody. In this process, many vortices are generated and form two vortex clouds. Incremental afterbody forces and moments are also computed.

At the end of the afterbody (corresponding to the leading edge of the tail-finned section), the vortex information on TAPE8 is expanded by the addition of afterbody vortices. If the number of afterbody vortices exceeds a number NVTRNS specified in the input for BDYSHD, the afterbody vortices are represented by two equivalent vortices at the two centroid locations of the afterbody vortex clouds. One will be in the counterclockwise (positive) sense and the other will be in the clockwise (negative) sense. The vortex data associated with the forebody and forward fins are stored separately from the afterbody vorticity on TAPE8. At the end of step 3a, the force and moment data on TAPE9 are updated and contain the sums of the force and moment coefficients calculated for the forebody, the forward-finned section (steps 1 through 3) and the afterbody.

<u>Step 4</u>

If step 3a was not exercised, the executive routine of program LRCDM2 calls subroutine DEMON2 to treat the tail-finned section as well as the afterbody. The body is flow modeled again from the nose to its base. In this step, effects of external vortices are not accounted for. Indices NCPOUT=1, NVLIN=0, and ITAIL=1 in namelist $INPUT for this step. In addition, quantity XSTART must be set equal to the axial location of the trailing edge of the forward-finned section. The first index causes routine DEMON2 to generate a data set, saved on TAPE4, which contains the number and sets of coordinates associated with control points on the tail fins and interference shell. Additionally, this data set contains the sets of coordinates specifying points on the afterbody surface between the forward fins and tail section at which pressures will be calculated. The tail-fin loadings calculated in this step do not include effects of forebody and canard-fin vorticity. No contributions are made to the summing procedure.

For the case with step 3a, program LRCDM2 is called by the job-control stream and reinitializes the force and moment coefficients in subroutine TOLDS by reading in the data on TAPE9. Subroutine DEMON2 reads input stored on TAPE2 at the start of the run. In the tail-section portion of this data, index ITAIL=1. In this case, only the calculated control point coordinates on the tail fins and interference shell are stored on TAPE4. Loadings are calculated on the tail-finned section excluding effects of any upstream vorticity. No contributions are made to the overall forces and moments.

Step 5

If step 3a was not performed, the executive routine calls VAPTH2 for the purpose of tracking the forebody and forward fin-edge vortices along the afterbody and through the tail-finned section. It is recommended to select VPATH2 input such that the vortex paths are made to lie parallel to the body centerline over the length of the tail section (refer to Section A.7). The strengths and positions of the vortices at the end of the forward-finned section are read in automatically from the data set on TAPE8 generated in step 3. Indices NCPIN=1 and NVLOUT=1 for this step. The value given to the first index causes the program to read in the data set on TAPE4 containing control and body pressure point coordinates generated in the previous step. Velocity components induced by the external vortices are calculated at the points given in this data set. The value given to the second index results in the generation of a data set stored on TAPE7 containing the vortex-induced velocity components.

If program BDYSHD (step 3a) was used to treat the afterbody, module VPATH2 tracks all vortices (including afterbody vortices) through the tail section only. Again, it is recommended to arrange the input to make the vortex paths be parallel to the body centerline. Vortex induced velocities are computed at the control points of the fins and interference shell of the tail section and stored on TAPE7. In this process, the velocity components induced by the external vortices are calculated with the tail fins not present in accordance with the description given in Section C.4 of Appendix C.

Step 6

Finally, the executive routine calls subroutine DEMON2 to compute loads acting on the tail fins including effects of upstream vortices. Indices NCPOUT and NVLIN are set equal to 0 and 1, respectively, by the executive routine, and ITAIL=1 in namelist $INPUT for the tail section stored on TAPE2. Therefore, subroutine DEMON2 reads in the data set stored on TAPE7 containing vortex effects calculated in the previous step.

If step 3a was not used, pressure distributions and loads acting on the afterbody are calculated by routine BDYPR of program LRCDM2. They will include effects of forebody and forward-fin vorticity.

The loads acting on the tail fins and interference shell are added to the loads acting on the afterbody, forward-finned section and forebody. The final sums represent the forces and moments acting on the complete configuration.

For the case with step 3a, the forces and moments calculated for the tail fins and interference shell in step 6 are added to the summed quantities read in from TAPE9 and transferred to subroutine TOLDS at the beginning of step 4. The final sums represent the loadings acting on the complete configuration. The loadings consist of normal force and side force coefficients, pitching moment, yawing moment, and rolling moment coefficients. The axial force coefficient due to the forebody only is also calculated. The loads are expressed in the rolled (or fixed) body coordinate system (x_B, y_B, z_B) and in the unrolled body coordinate system (x_B, y, z) shown in the output description.

A.5 PROGRAM OPERATION

Program LRCDM2 is written in FORTRAN IV language. The present version has been run on the following computer machines.

CDC CYBER 173
CDC CYBER 175
CDC CYBER 176
CDC 760 CYBER
CDC 7600
VAX 11/780

There is no overlay structure. Core requirement is about 270K octal words to load with array FVN dimensioned 24000 in blank COMMON of subroutine DEMON2 (also refer to the next section for possibility of adjusting the FVN dimension).

In addition to the standard input and output tapes (TAPE5=INPUT, TAPE6=OUTPUT), the program employs the following temporary storage devices.

TAPE2: input for steps 1 through 6 for a complete configuration

TAPE4: control point coordinates

TAPE7: vortex induced velocity components

TAPE8: body and fin vortex strengths and positions

TAPE9: aerodynamic influence coefficients for forward-finned section, or sums of force and moment coefficients acting on forebody and forward-finned section if program BDYSHD is used.

TAPE10: aerodynamic influence coefficients for tail-finned section

The aerodynamic influence coefficient data stored on TAPE9 and TAPE10 for a complete configuration are used repeatedly during calculations for multiple included angles of attack and/or roll.

Execution time is influenced by several factors. The primary influence is the number of constant u-velocity panels laid out on the lifting surfaces and interference shells of the forward- and tail-finned sections. Execution time in the vortex-tracking process is related to the length over which the vortex paths are to be calculated, the number of vortices, and the permissible error E5 allowed in these calculations. In addition, the number of included angles of attack and/or roll angle affects running time. Note that in the multiple angles case, running time is sharply reduced by saving the triangulated form of the aerodynamic influence coefficient matrix as presently arranged by LRCDM2 (refer to Section 2.5 of this report).

A representative execution time is provided by the sample case described at the end of this appendix. The case involves a complete configuration with canard control.

The angle of attack is sufficiently high to form afterbody vortices which influence the overall forces and moments as described in Section 3.2.2 of this report. With a reasonable number of panels and including the engagement of companion program BDYSHD, total running time on a CDC 7600 is about 65 seconds for one angle of attack and one Mach number.

A.6 LIMITATIONS AND PRECAUTIONS

Program LRCDM2 makes a number of assumptions about the missile configuration and flow field. Certain options have not been fully tested. In addition, there are input and program calculated variables that have maximum values which should not be exceeded. These matters are described below. References are made to namelists and variables described in the input descriptions, Section A.7.

1. The optional nonlinear/linear pressure coefficient methods based on shock-expansion and Newtonian theories have been tested only on wings and on an ogive cylinder. At the time of this writing, complete configurations have not been treated with the optional pressure coefficient calculation methods.

2. The Bernoulli pressure coefficient distributions calculated by subroutine BDYPR on the forebody and afterbody under the influence of external vortices suffer from a deficiency described in Section C.4 of Appendix C. In the present method, the external vortices only induce lateral velocity components and no axial velocity component. This problem does not exist in the afterbody loads calculated by optional program BDYSHD under the influence of shed and other external vortices. In the absence of afterbody shed vortices, subroutine BDYPR of

C-2

program LRCDM2 gives approximately the same results as program BDYSHD. Therefore, the deficiency mainly affects the loads on the forebody where the body nose vortices run close to the surface.

3. The body cross section inscribed by the interference shells associated with the forward-finned and tail-finned sections is assumed to have constant cross-sectional area. This shell is placed on the body from the leading edge to the trailing edge of each finned section. If the forward fins are attached to the nose of the configuration, the shell should match the layout radius (RA=RB specified in namelist $INPUT) as shown in the sketch below. The exposed fin semispan b/2, also specified in $INPUT, is indicated. In a case such as this

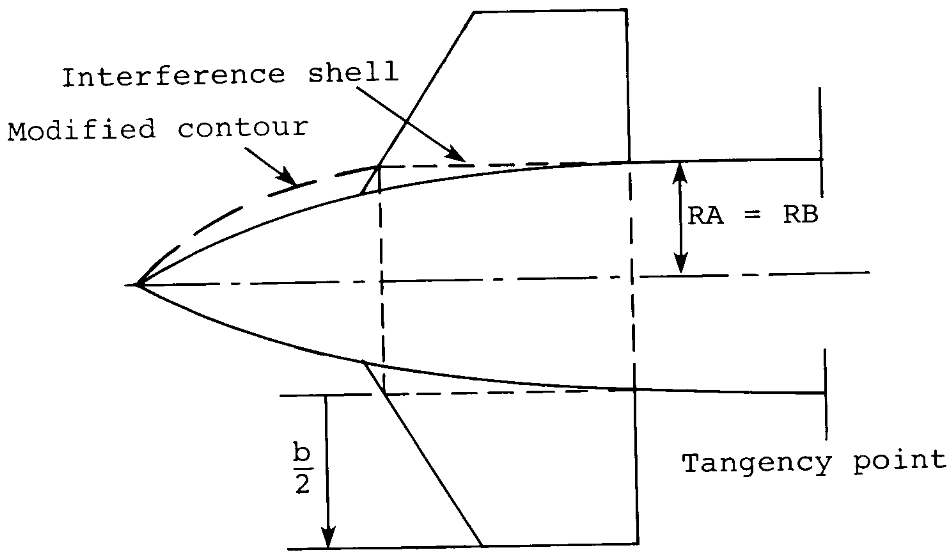

one, some care is required with regard to the forebody vortices if they are formed. Their lateral positions at the leading edge of the finned section must lie outside the radius of the interference shell. In this case, it may be better to alter the forebody contour so that the tangency point lies ahead or coincides with the axial location of the leading edge. An example of a modified contour is indicated by the curved dashed line.

4. The vortex tracking module VPATH2 cannot handle expanding or contracting body cross sections. Therefore, the body must be constant in radius over the fin sections and the afterbody.

5. In the specification of the number of constant u-velocity panels to be distributed on the forward or on the tail fins and respective interference shells in namelist $INPUT, the following limits must be kept in mind. For all fins and the interference shell, a maximum of 150 panels are available for either the forward or tail section. In the spanwise direction, the maximum number of panels is 19 for a fin. The number of panels on one interference shell must not exceed 100.

In the present version of program LRCDM2 the total number of panels on the fins and interference shell for a given finned section is set at 150 with the dimension of array FVN in blank COMMON set at 24,000 in subroutine DEMON2. Depending on available core storage, this dimension can be increased to a maximum of 62,000. The corresponding total number of panels is then 250. In namelist $BODY, the number of line sources/sinks and the number of line doublets (both specified by NXBODY) must not exceed 100.

6. The program has a symmetry option that considerably reduces the execution time for cases in which the flow field is symmetric relative to the configuration's vertical plane of symmetry. In the program, this situation exists only when the angle of roll, ϕ, is exactly zero and if the fins are undeflected*. Necessary input requirements to select this option are described in Section A.7. When this option is selected for a cruciform fin layout, loads are calculated on the right-hand side forward and tail fins only. Loads on the left fins are set equal to those on the right symmetric fins.

It is necessary to impose a small but finite angle of roll (ϕ = 0.001°) when treating an asymmetric case such as the following. Consider a cruciform canard-body-cruciform-tail

*Fins can be deflected symmetrically as in the case for pitch control.

configuration at zero sideslip but with the forward fins deflected asymmetrically. When calculating loads on the tail fins it is necessary to include and panel all the fins even though the free-stream velocity vector lies in the vertical plane of symmetry of the configuration. This is because the asymmetric deflection of the forward fins produces an asymmetric flow field at the tail section giving rise to loads on all four tail fins.

7. The number of stations at which vortex coordinates are printed (index NIP in input for steps 2 and 5) cannot exceed 50.

8. A maximum magnitude is set by the program for the perturbation velocities induced by external vortices at the control points in the flow tangency condition and pressure calculations. Since these velocities are based on potential vortex theory, their values could assume large magnitudes if the vortices run close to the fins or body surface and cause undue influence. Consequently, their magnitude is limited to 0.35 V_∞. This value can be overridden by setting variable VRTMAX in namelist $INPUT and in the input to VPATH2 equal to the desired value.

9. Accuracy in the vortex trajectory calculation is controlled through a variable, E5, which specifies the permissible error in these calculations. Some care must be exercised in the choice of a value for E5. If its value is much smaller than 10^{-4}, computation time may become unduly long.

Subroutine DASCRU will reduce automatically the initial integration interval in attempting to track the vortex paths to the accuracy specified by the value of E5. The initial integration interval (distance between first two axial stations XIP) can be reduced by as much as a factor of 100 in order to provide results of the accuracy desired. If, after reducing the integration interval by 100, a solution to the specified accuracy is still not obtained by DASCRU, the program will stop and register STOP40. A faulty crossflow plane flow field can cause this problem. For example, specifying an initial vortex field with coordinates inside the body contour will definitely cause problems.

10. Vortex trajectory calculations may suffer from slight numerical errors when the body length is long. These are suspected to be caused by errors introduced by the integration scheme in subroutine DASCRU. This behavior can be observed when chasing a set of vortices, initially located symmetrically relative to the free-stream vector in the crossflow plane, along an axisymmetric body of considerable length (in excess of 25 body radii).

11. A further limitation occurs when a vortex comes very close to the plane of a fin. Module VPATH2 either will tend to move the vortex away from the lifting surface, or it may move it along the contour in an unrealistic fashion. The latter constitutes a limit to the theory. In reality, a vortex is made up of distributed vorticity with a core in which the lateral velocity component goes to zero towards the core center. Such a vortex structure passes right over (and/or under) the lifting surface in question. In a case such as this, it is recommended to make the vortex paths lie parallel to the body centerline as described in the input for module VPATH2 in steps 2 and 5.

12. Care must be taken with the use of control indices NOUT and NPR. A very large amount of diagnostic output is generated when these indices are set equal to one. This output should only be used for debugging purposes employing a minimum number of constant u-velocity panels such as two per fin and four on the circumference of the body interference shell.

On the other hand, setting output control index MINPRN nonzero results in minimum print containing only the input and the overall force and moment coefficients.

13. Subroutine BDYPR computes a number JCPT equal to the number of pressure points defined on the forebody in step 1 or on the afterbody in step 4. The number is set by NBDCR in $INPUT and the number of body rings calculated by the program. The number of control points (or constant u-velocity panels) on the fins and interference shell in a given finned section is NWBP. The sum of JCPT and NWBP must not exceed 500. The program will fail to run if the sum exceeds 500. The easiest remedy is to reduce the number of body singularities NXBODY in namelist $BODY.

14. If a portion of the forebody contour lies outside the Mach cone with its vertex at the nose tip, subroutine BDYGEN will change that contour portion to a conical contour lying just inside the Mach cone. In this way, the body solution will proceed and the pressure distribution on the first body ring will be calculated on the conical portion instead of the actual body contour. The body solution cannot proceed if the Mach cone from the nose tip lies inside the entire length of the body. In such a case, a message to that effect will appear in the output.

A.7 DESCRIPTION OF INPUT

This section describes the input required by program LRCDM2 for treating the forebody and forward-finned section (steps 1 through 3) and for treating the afterbody and tail-finned section (steps 4 through 6). The same variable names are used for steps 1 and 4 and for steps 2 and 5. The values required in steps 4 and 5 are those relevant to the afterbody and tail section. A control index and optional input only are required for step 3. Optional input and the END card constitute the input for step 6. The stepwise procedure is described earlier in Section A.4 of this appendix and in Section 2.3 in the main text of this report.

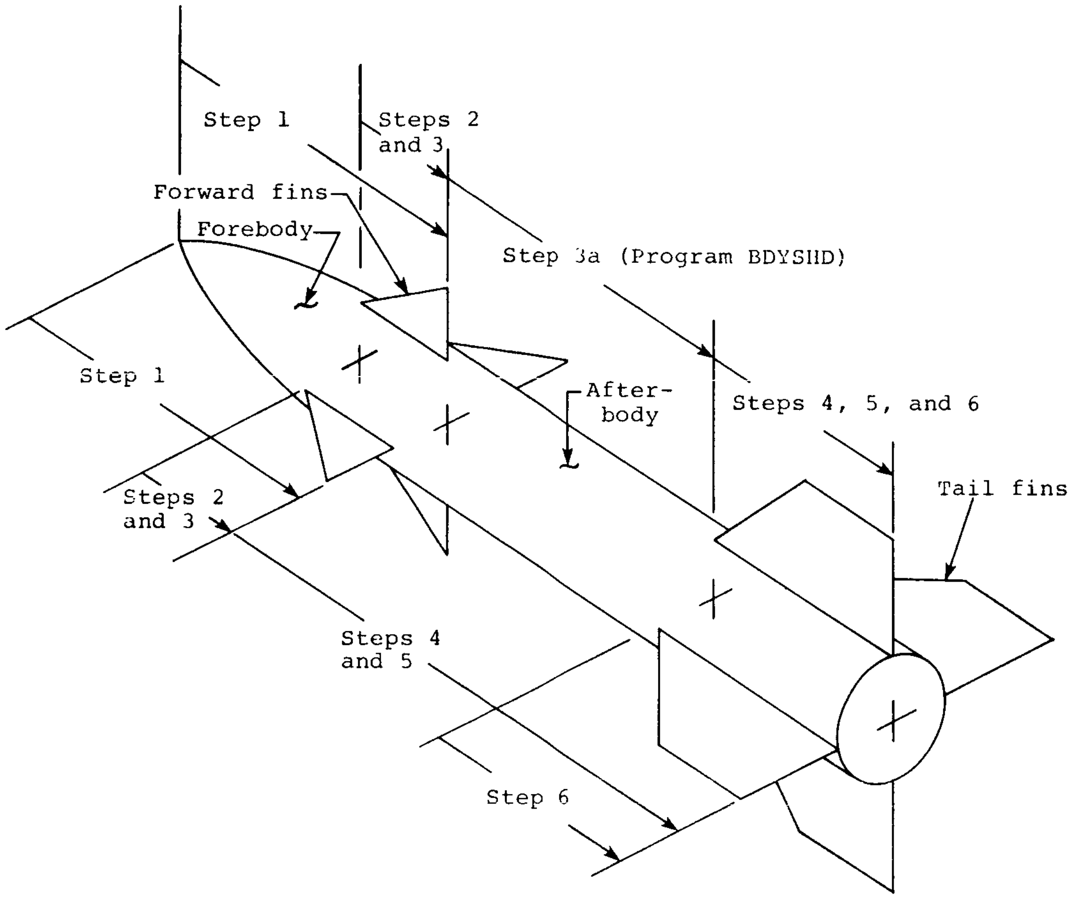

The steps are shown again in the above sketch. If companion program BDYSHD is employed as an option in step 3a, the input for steps 1 through 3 and the input for steps 4 through 6 is altered slightly. Input for BDYSHD is described in Appendix B.

For clarity, the input required for all runs and the input requirements for each step are described. All input variables are listed at the end of this section in their order of appearance for the first three steps. Most of the variable names are used again for the remaining steps. To run a complete configuration the inputs for each step are stacked in order and read in together.

A sample input is given in Figure A.5 in connection with the sample case which employs program BDYSHD. The details of this sample case are described later. It is concerned with a forward-control configuration with a cruciform set of forward fins and cruciform tail fins mounted on a slender axisymmetric body.

Description of First Cards Required for All Single Runs, Multiple Runs or Restart Runs

Item 1

This card is entered regardless of the step at which calculations start. It specifies the starting (NSTART) and ending (NSTOP) step desired. There are two possible choices for NSTART:

NSTART=1; calculations begin with step 1
NSTART=4; calculations begin with step 4

In particular, the latter choice is employed (with NSTOP=3) when companion program BDYSHD is used to treat the afterbody in step 3a thereby interrupting the LRCDM2 run at the end of step 3 and restarting LRCDM2 at step 4.

Cases with one finned section at the body base (tail finner) are treated with NSTART=1 and NSTOP=3.

The value of NSTOP should be given a value of 6 to ensure that the forward- and tail-finned sections of a complete configuration are examined completely. Calculations cease after the forward-finned section is examined when NSTOP=3. If NSTOP is given a value of 6, calculations stop after the tail-finned section is examined.

Item 2

This card contains the number of included angles of attack for multiple calculations.

Item 3

These cards contain the values of included angles of attack for which calculations are to be done.

Item 4

The number of angles of roll for each included angle of attack for which calculations are to be done are specified on this card.

Item 5

These cards contain the values of angles of roll for each included angle of attack for which calculations are to be done.

The included angle of attack, ALFS, is the angle α_C between the free-stream velocity vector and the body centerline (x_B-axis in Fig. A.4). Angle of roll, FEE, is also indicated by ϕ in the sketch below. The program computes pitch and sideslip angles in accordance with the pitch-roll transformation mentioned in Section 1-4 of Reference 10.

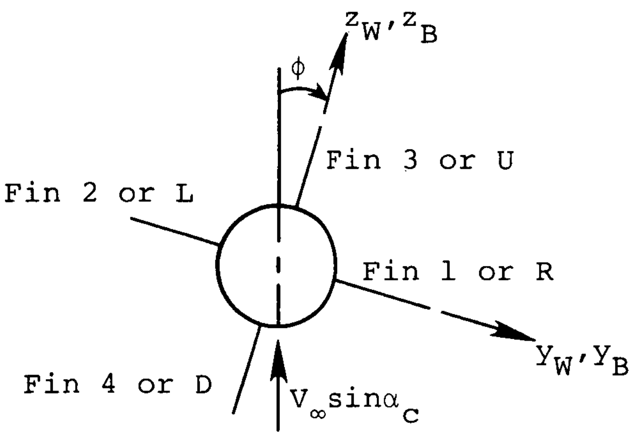

Description of Input Requirements for Step 1

Body nose with vortex effects and forward-finned section without vortex effects

Item 1 (step 1)

This first card serves as identification and may contain any alphanumeric information desired. This information is printed on the second page of the output.

Item 2 (step 1)

The second and following cards form the namelist $INPUT which specifies the geometrical parameters of the fins and interference shell associated with the forward-finned section. These parameters include the fin leading-edge and trailing-edge sweeps, semispan and root chord. For a planar or cruciform fin alone, the root chord is the wing centerline or the cruciform fin junction. In the case of a fin-body combination, the root chord is the straight line formed by the junction of the fin and the body. This line must be parallel to the body centerline. The semispan is measured from the root chord. The root chord leading edge is at the same axial station for all fins.

This namelist also contains the fin-deflection angles and the number of chordwise and spanwise constant u-velocity panels for each fin. The spanwise number, MSWR etc., may differ from one fin to another but the chordwise number NCW is the same for all. Similar information is specified for the layout of planar source panels*. The number of body interference panels on the circumference, NBDCR, is also included in this namelist. The specification of the latter also determines

*Present version of LRCDM2 handles thickness effects only for planar or cruciform fin layouts.

whether or not a body is present. The number of body interference panels in the axial direction is specified by NCWB. The total number of constant u-velocity panels, NWBP, for one finned section is given by the relation

NWBP = [NCW(MSWR+MSWL+MSWU+MSWD) + NCWB(NBDCR)]

and cannot exceed 150 unless the dimension of array FVN in blank COMMON is increased in subroutine DEMON2. The dimension equals the square of NWBP.

The body cross section must be circular with constant radius where the fins are attached. The value of the body cross-sectional radius must be given to both RA and RB. Furthermore, the value of ERATIO must be set equal to one. The body interference length, BIL, is the body length spanned by the fins. Fin interference loading is calculated over this length. Length BIL is taken equal to the fin root chord CRP.

Control index NDRAG must equal 1. This result in the calculation of in-plane forces for the suction distributions and consequently the fin normal-force augmentations and fin-edge vorticity characteristics. Index NBSHED controls the optional use of companion program BDYSHD for handling afterbody vortex shedding.

In addition, more control indices including a minimum output option set by MINPRN, free-stream Mach number, and reference quantities SREF and REFL are read in. Breaks in leading-edge and/or trailing-edge sweeps are also allowed if the configuration is a wing or cruciform wing alone at zero sideslip or if the configuration consists of a fin-body combination. This option is governed by control index LVSWP. Angles SWLEP, SWTEP, SWLEV, and SWTEV need not be specified if LVSWP $\neq$ 0.

Control indices N2DPRB and N2DPRF activate the optional nonlinear pressure coefficient calculation methods. Indices NCPOUT, NVLIN, and ITAIL play an important part in the calculation procedure built into the program as described earlier in this appendix and in Section 2.3 of this report. The axial location of the moment center, x_M, must be specified in the body coordinate system (x_B, y_B, z_B) with origin at the nose as shown in Figure A.4.

Angles PHIDIH ($=\phi_f$) and THETIT ($=\theta$) apply to cases involving four interdigitated or low-profile fin layouts with a vertical plane of symmetry. For cruciform or triform layouts, the default values are to be used. In the latter case, the fin root location angle and fin cant angles must be specified. Angles THETR, THETL, etc. locate the fin root chords on the body contour. Programmed default values correspond to planar or cruciform fin layouts. In addition, angles PHIFR, PHIFL, etc. correspond to the fin dihedral or cant angles. Default values correspond to planar or cruciform cases. For an interdigitated or low-profile fin layout, nonzero input angles PHIDIH and THETIT automatically determine the fin root location and fin can angles.

Special notes are given at the beginning and at the end of the namelist $INPUT description with regard to input setups for symmetric flow conditions and for cases with fin deflections.

<u>Item 3</u> (step 1)

This item pertains only to a wing alone or cruciform wing alone at zero sideslip. This optional input is required when there are breaks in the wing sweep or if the constant u-velocity panel side edges are to be laid out with user-determined unequal stepwise spacings. Variable YR is the distance from the root chord to the outboard panels side edges. Therefore, the first value for YR is zero. The last value for YR must equal wing semispan, B2, specified in the namelist $INPUT. In effect, this specification positions the panel outboard side edges on the right wing. The sweep angles are positive for wings with sweptback leading and trailing edges.

In the following Items 4, 5, 6, and 7, references are made to right, left, upper, and lower fins of a planar or cruciform fin layout. A sketch shown later in the itemized list of input variables relates the fin designations for the cruciform case to the fin designations for an arbitrary (interdigitated or low profile) fin layout.

Item 4 (step 1)

The optional input of this item is associated with a fin-body combination with breaks in leading-edge and/or trailing-edge sweeps. Also, this input is used for the configuration if the constant u-velocity panel side edges are to be laid out with user-determined unequal spacings. Variable YRT is the distance from the fin root chord to the outboard constant u-velocity panel edges on the right fin. The first value should equal 0.0 and the last value for YRT equals the exposed fin semispan, B2; the latter is specified in the namelist $INPUT. The sweep angles are positive for right fins with sweptback leading and trailing edges.

Item 5 (step 1)

This optional input accompanies Item 4 and is associated with the left fin. Variable YLT is the distance from the wing root chord to the outboard constant u-velocity panel edges on the left fin. The first value should equal 0.0 and the last value for YLT equals the negative exposed fin semispan, -B2. The sweep angles are negative for left fins with sweptback leading and trailing edges.

Item 6 (step 1)

The information in this optional item accompanies Items 4 and 5 if the configuration is a cruciform fin-body combination. Again, this input should only be used if there are breaks in the fin sweep or if the panel side edges are to be laid out with user-determined unequal spacings. Variable ZUT is the distance from the fin root chord to the outboard constant u-velocity panel edges on the upper fin. The first value should equal 0.0 and the last equals the exposed fin semispan, B2V. The latter is specified in namelist $INPUT. The sweep angles are positive for upper fins with sweptback leading and trailing edges.

Item 7 (step 1)

This optional information is the last of the four inputs associated with a cruciform fin-body combination if there are breaks in sweep or if the constant u-velocity panel side edges are to be laid out with user determined spacings; see Items 4 through 6. Variable ZDT is the distance from the fin root chord to the outboard constant u-velocity panel edges on the lower fin. The first value should equal 0.0 and the last value for ZDT must equal -B2V. The sweep angles are negative for lower fins with sweptback leading and trailing edges.

Item 8 (step 1)

This item is concerned with the specification of the layout and strengths of the planar source panels employed to model thickness of the lifting surfaces. This item is required only when NTDAT in Item 2 of step 1 ($INPUT) is set equal to 1. Basically, the planar source panels are laid out in the same manner used to layout the constant u-velocity panels. However, in this case the distance out to the outboard panel edge is now measured from the body centerline and not the root chord of the fin under consideration. Presently, the fin thickness option can only be selected for cases with planar or cruciform fin layouts. Breaks in sweep are handled by control index LVSWT in the same way control index LVSWP handles breaks in sweep in the layout of constant u-velocity panels.

The strengths of the planar source panels are related directly to the streamwise slopes which are specified in Item 8c of this step. Note that quantity THET is the tangent of the streamwise thickness envelope angle, THET=$\tan\theta_s$. For fins without or with breaks in sweep or user-specified distances to the outboard edges, the thickness slopes must be specified for all fins unless the flow conditions give rise to the symmetric (right to left) case. In the latter case, only the right horizontal fin of a planar or cruciform fin layout needs to be modeled for thickness. The present version of LRCDM2 cannot handle thickness effects for arbitrary fin layouts.

Item 9 (step 1)

The input cards for this item form the namelist $BODY which contains information for the body with circular cross section of the configuration under consideration. If the integer NBDCR in namelist $INPUT under Item 2 for this step is specified to be nonzero, a body must be present. The information in this input includes specification of body geometry parameters and it is read in by subroutine BDYGEN. The length of the nose, LNOSE, determines the body length over which the radius is changing as a function of the body axial coordinate. The actual nose configuration is governed by control index, BCODE, which selects preprogrammed forebody shapes described earlier in connection with geometrical characteristics, Section A.2 of this appendix.

Normally the body length, LBODY, should at least equal the axial distance from the body nose to the trailing edges of the finned section under consideration. If the trailing edges are swept back, length LBODY should be taken to include the trailing edge of the tip chords or side edges of the fins at hand. For a complete configuration with two finned sections, quantity LBODY is set equal to the entire body length.

The minimum number of body modeling singularities NXBODY can be determined as follows. Let the density (line sources and line doublets/unit body length) be determined by the number of constant u-velocity panels in the chordwise direction on the fins divided by the root chord (or length of fin-body junction). Then, number NXBODY equals the density times body length. Number NXBODY should never exceed 100.

Item 10 (step 1)

This input is concerned with the optional strip theory approach for calculating shock-expansion and Newtonian pressure coefficients along longitudinal strips on the surface of the body. Refer to Section 2.6.2 of this report. Each strip is composed of segments (100 maximum) making angle THETA relative to the body centerline. Near the nose, these angles are nonzero and positive. Segment slope angles need to be specified for one strip only since the body is axisymmetric.

Item 11 (step 1)

This optional input is required only when variable NVRTX, specified in namelist $INPUT, is nonzero. In fact, NVRTX is the number of external, two-dimensional vortices whose influences are to be included in the pressure and loading calculations. Each vortex is assumed to be infinite in length and to be parallel to the body centerline. Therefore, with each vortex there is associated a nondimensional strength, GAMMA, and nondimensional crossflow plane coordinates, YVRTX,ZVRTX, given in the body or wing coordinate system shown in Figure A.4. These quantities are input in subroutine VRTVEL. Note: This optional external vortex input is used for research purposes only. Normally, program LRCDM2 employs module VPATH2 to account for the presence of external vortices.

Item 12 (step 1)

This new input is concerned with the optional strip theory approach for calculating shock-expansion and Newtonian pressure coefficients along longitudinal strips on the upper and lower surfaces of the fins. Refer to Section 2.6.2 of this report. The number of strips on the upper and lower exposed fin surfaces is equal to the number of constant u-velocity panels in the spanwise direction of each fin (MSWR, MSWL, etc. in namelist $INPUT). Each strip has 100 segments maximum. Angles THETA are the angles of the segments in the upper surface strips measured relative to the fin mean plane. Angles THETAB are the angles of the lower surface strips measured relative to the mean plane. Near the leading edge both angles are nonzero and positive. Near the trailing edge, these angles are usually negative. The segment-angle data is to be specified for each fin of a finned section unless the case at hand is symmetric, i.e., zero roll and cruciform or planar fins are under consideration.

Description of Input Requirements for Step 2

Track vortices past forward-finned section

Item 1 (step 2)

The first card serves as identification and may contain any alphanumeric information desired. This information is printed on the first page of the output.

Item 2 (step 2)

The second card contains indices concerning the body and fin geometry, control indices governing the input of control-point coordinates, the generation of velocity components, the amount of output, and the option to print plots for debugging purposes in the program generated output.

Item 3 (step 2)

This card contains the end points for each body section for which coefficients describing a meridian will be given (Item 4). Usually, only one end point is required; that is, one body section with constant radius cylindrical cross section will be considered.

Item 4 (step 2)

For each body section, a set of coefficients (7 maximum) are specified on this card. They are members of the polynomial shown below and programmed in subroutine SHAPE.

$$r = C_1 + C_7 \sqrt{C_2 x^2 + C_3 x + C_4} + C_5 x + C_6 x$$

Here C_1 through C_7 are the coefficients, and r is the local body radius. In the present program, bodies of constant radius only are considered. Consequently, only coefficient C_1 is nonzero. It equals the radius (RA = RB specified in $INPUT, Item 2 of step 1) of the cylindrical cross section body.

Item 5 (step 2)

The coordinates of the fin planform corner points are read in if a set of cruciform or planar fins is present. Only one fin needs to be described. The XF and YF coordinates are shown in the example shown below; XF is measured from the body nose and YF is measured from the body centerline.

In the application of vortex tracking module VPATH2 to a finned section (with constant radius body), the fin layouts are limited to planar (for zero angle of roll) and cruciform. In addition, the fin planform is limited to delta or cropped delta shapes. Swept-back trailing edges cannot be treated.

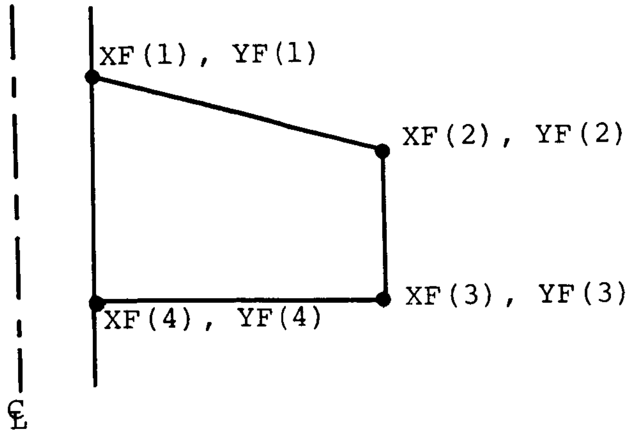

Note: The axial coordinate of the trailing edge of the root chord must be slightly larger than the axial coordinate of the trailing edge of the side edge. That is, the trailing edge must be swept forward slightly.

If the finned section has an arbitrary fin layout and/or fin planform, the vortices cannot be tracked through the section. In such a case, the paths of the vortices should be taken parallel to the body centerline by proper selection of the variables in Items 7 and 8 for this step.

Item 6 (step 2)

This card contains the permissible error, E5, used in a criterion on the integration scheme programmed in subroutine DASCRU. This card also reads in the upper bound, VRTMAX, imposed on the magnitude of the external vortex-induced velocity components.

Item 7 (step 2)

Quantity NIP is the number of axial stations over the length of the configuration along which the vortices are tracked. Vortex positions will be printed out at these stations. Module VPATH2 actually determines the axial positions of these stations. In addition, the vortex lateral coordinates computed at these stations are used for calculating vortex-induced effects at body and fin control points.

Item 8 (step 2)

The beginning (XBEGIN) and ending (XEND) axial locations of the length of configuration along which the vortices are to be tracked are listed on this card. These distances are measured from the body nose. In step 2, it is possible to "freeze" the paths of the forebody vortices through the forward-finned section in a direction parallel to the body centerline (recommended procedure). This is accomplished by setting NIP=1 in Item 7 and setting XBEGIN=XEND=leading edge of forward-finned section (XWLE in $INPUT, Item 2 for step 1).

Item 9 (step 2)

This optional input is specified when NCPIN of Item 2 is read in as zero. The number NCP is the number of field points at which vortex-induced velocity components are to be computed on the basis of the vortices being in the presence of the body only (refer to Section C.4 of Appendix C).

Item 10 (step 2)

If the value of NCP in Item 9 is nonzero, these cards contain the coordinates, in the body coordinate system (x_B,y_B,z_B), shown in Figure A.4, of the field points at which vortex-induced effects are to be computed. Note: In normal operation index NCPIN of Item 2 is set equal to 1 and the information of Items 9 and 10 is read in by means of a data set stored on TAPE4.

Description of Input Requirements for Step 3

Forward-finned section with vortex effects

Item 1 (step 3)

The integer variable NVORT is used to control the influence of the nose vortices. It has been observed that nose vorticity may disperse over the forward-finned section. Since the present model for nose vorticity is incapable of representing such a situation, the user has the option of ignoring the existence of nose vorticity downstream of the forward-finned section. The options are:

NVORT=0: Nose vortices, if present, are tracked over the entire configuration.

NVORT=1: Nose vortices are ignored downstream of the trailing edge of the root chord of the forward fins.

Item 2 (step 3)

The optional input concerned with the optional strip theory approach for calculating nonlinear pressure coefficients on the forward fins, Items 12(a), 12(b), 12(c), and 12(d) for step 1, are repeated here if the option is used.

Description of Input Requirements for Optional Step 3a (Program BDYSHD)

Afterbody with vortex shedding

The input for this optional step is described in Appendix B concerned with the companion program BDYSHD. If this program is engaged as described in Section A.4 (with NBSHED=1 in namelist $INPUT for step 1), care must be taken with the inputs for steps 4 and 5 described below. As mentioned later, XSTART in namelist $INPUT for step 4 should be set equal to the axial location of the tail-section leading edge. Quantity XBEGIN in Item 8 of step 5 should also be set equal to the axial location of the tail-section leading edge.

Description of Input Requirements for Step 4

Afterbody and tail section without vortex effects

Input values required for step 4 are associated with the same variable names as the input values for step 1 and they are entered in the same order. The particular values required are those relevant to the afterbody and tail section. Namelist $BODY need not be repeated for a full configuration provided the body length LBODY is set equal to the entire body length in Item 9 of step 1. If companion program BDYSHD is employed to treate the afterbody including vortex shedding effects, set NBSHED=1, and quantity XSTART should equal quantity XWLE (axial location of tail-fins root chord leading edge) in namelist $INPUT.

Description of Input Requirements for Step 5

Track vortices along afterbody and tail section

Input values required for step 5 have the same variable names and are entered in the same order as the input values for step 2. The particular values required are those relevant to the afterbody and tail section.

If companion program BDYSHD is employed to treat the afterbody including vortex shedding effects, set XBEGIN in Item 8 equal to the axial location of the leading edge of the tail section. In addition, by setting NIP=1 in Item 7 and XBEGIN=XEND=axial location of leading edge of tail section, the paths of all the vortices through the tail section are made to lie parallel to the body centerline (recommended procedure).

If BDYSHD is not used, XBEGIN should be set equal to the axial location of the trailing edge of the forward-finned section. The paths of the vortices along the afterbody are calculated and the vortex positions are printed at a number of stations given by index NIP. The vortex paths are made to lie parallel to the body through the tail section by setting XEND = axial location of the tail section leading edge.

Description of Input Requirements for Step 6

Afterbody and tail section with vortex effects

Item 1 (step 6)

The optional input concerned with the strip theory approach for calculating nonlinear pressure coefficients on the tail fins, Items 12(a) through 12(d) for step 4 are repeated here if the option is used.

Item 2 (step 6)

This item contains the required final card with END in the first three columns.

All input will now be listed in order of appearance including the format and algebraic symbols if applicable.

INPUT VARIABLES FOR PROGRAM LRCDM2

Program Variable	Format	Comments
List of Input Variables Required for All Runs		
Item 1	(2I5)	Beginning and ending steps in calculation.
NSTART		Step at which calculations are started.
NSTOP		Step after which calculations are stopped.

Item 2 (I5)

NALF — Number of values to be used in included angle of attack sweep.

Item 3 (8F10.4)

ALFS(N) — α_c — Values to be used in included angle of attack sweep (N=1 through NALF), degrees.

Item 4 (I5)

NFEE — Number of values to be used in roll angle sweep.

Item 5 (8F10.4)

FEES(N) — ϕ — Values to be used in roll angle sweep (N=1 through NFEE), degrees.

Note: For unrolled configurations, set FEES(N) equal to 0.001 for following cases.

1. For a set of planar or cruciform tail fins subjected to asymmetric oncoming flow such as that induced by asymmetrically deflected canard fins.

2. For any triform fin layout.

List of Input Variables for Step 1

The following four variables are used below in the description of the input variables for step 1. The terms "right" and "left" refer to an observer looking forward.

MSWRP: Number of panels in spanwise direction on right fin + 1; MSWRP = MSWR + 1

MSWLP: Number of panels in spanwise direction on left fin + 1; MSWLP = MSWL + 1

MSWUP: Number of panels in spanwise direction on upper fin + 1; MSWUP = MSWU + 1

MSWDP: Number of panels in spanwise direction on lower fin + 1; MSWDP = MSWD + 1

Also see notes at the end of namelist $INPUT for variables marked with "*".

Program Variable	Format	Comments
Item 1	(20A4)	Any alphanumeric information may be put on this card for identification of the calculation.
Item 2	(namelist)	Namelist $INPUT.
BIL		Length of body influenced by fins to account for interference. For fins with unswept trailing edges and for wing-alone cases, BIL=CRP, default = 0.0.
B2	b/2	Exposed fin semispan of horizontal or upper right or lower left fins, dimensional.
B2V		Exposed fin semispan of vertical or upper left or lower right fins, dimensional, default is 0.0.
CRP	c_r	Root chord of horizontal or lower left or upper right fins, dimensional.
CRPV		Root chord of vertical or upper left or lower right fins, dimensional, default is 0.0.
DELD*	δ_d	Deflection angle of vertical lower or upper left fin. Postive: trailing edge to right or down, degrees, default is 0.0.
DELL*	δ_ℓ	Deflection angle of horizontal left or lower left fin. Positive: trailing edge down, degrees, default is 0.0.
DELR*	δ_r	Deflection angle of horizontal right or upper right fin. Postive: trailing edge down, degrees, default is 0.0.

DELU*	δ_u	Deflection angle of vertical upper or lower right fin. Positive: trailing edge to right or down, degrees, default is 0.0.
ERATIO		Ratio of RB over RA, specify equal to 1.0, default = 1.0.
FAC		FAC=0.95 Fraction of the constant u-velocity panel chord (which contains the centroid) where the control point is located.
FKLE	$K_{v,LE}$	Fraction of leading-edge suction converted to normal force, default is 0.5.
FKSE	$K_{v,SE}$	Fraction of side-edge suction converted to normal force, default is 1.0.
FMACH	M_∞	Free-stream Mach number.
ITAIL		ITAIL=0 Treat forebody and canards, steps 1 and 3, default value. ITAIL=1 Treat afterbody and tail section, steps 4 and 6.
JCPT		JCPT=0 Later calculated by program
LVSWP		LVSWP=0 No breaks in fin leading or trailing edges, or equal spanwise spacings of panel side edges, default value. LVSWP≠0 Up to 19 breaks in fin leading or trailing edges or up to 19 unequal spanwise spacings.

MINPRN	MINPRN=0 No print suppression, default value. MINPRN>0 Input and final results only are printed.
MSWD*	Number of spanwise constant u-velocity panels on the vertical lower or upper left fin; $1 \leq$ MSWD ≤ 19, default is 0.
MSWL*	Number of spanwise constant u-velocity panels on the horizontal left or lower left fin; $1 \leq$ MSWL ≤ 19, default is 0.
MSWR*	Number of spanwise constant u-velocity panels on horizontal right or upper right fin; $1 \leq$ MSWR ≤ 19.
MSWU*	Number of spanwise constant u-velocity panels on vertical upper or lower right fin; $1 \leq$ MSWU ≤ 19, default is 0.
NBDCR*	Number of constant u-velocity panels on the circumference of the body in the interference shell. NBDCR=0 No body present, default value. NBDCR>0 Body present (see Item 9). Note: select value divisible by 4. NBDCR will be halved by the program for symmetric cases.
NBDYPR	NBDYPR=1 Pressures to be calculated along body meridians, default is 0, use value 1.
NBSHED	NBSHED=0 Afterbody vortex shedding companion program BDYSHD is not used, default = 0.

	NBSHED=1	Companion program BDYSHD to be engaged after completion of step 3 for treatment of afterbody.
NCPOUT	NCPOUT=0	No control point coordinates written, default value.
	NCPOUT=1	Write coordinates (in body system) of control points on fins and body interference shell in data set (TAPE4), and continue the run.
	NCPOUT=2	Write coordinates (in body coordinate system) of control points on fins and body interference shell in data set (TAPE4), and stop the run (STOP77).
NCRX*	NCRX=0	Horizontal fins only present, default value.
	NCRX=1	Vertical fins in addition to horizontal fin surfaces present.
NCW*	Number of chordwise constant u-velocity panels on the fins.	
NCWB*	Number of constant u-velocity panels in the longitudinal direction on the surface of the body over the body interference length BIL, default is 0.	
NCWT	Number of fin thickness (source) panels in a chordwise row, default is 0.	
NDRAG	NDRAG=1	Include calculation of in-plane forces and fin trailing-edge vorticity, default = 0, set NDRAG=1.

NFVNPR	NFVNPR≠0 Print influence coefficient matrix FVN for debugging, default is 0.
NOLINP	NOLINP=0 Loadings calculated on the basis of linear pressures only, default value. NOLINP=1 Loadings calculated on the basis of linear and Bernoulli pressures, default = 0, set NOLINP=1.
NOUT	NOUT≠0 Print large amount of output for debugging, default is 0.
NPR	Same as NOUT, default is 0.
NPRESS	NPRESS=0 This value ensures that loadings are computed on the basis of the linear pressure relationship in addition to the Bernoulli pressure relationship. A value of zero is fixed in the program.
NTDAT	Number of sets of thickness data to be input in Item 8 below. (Presently applicable to planar or cruciform fin layouts only.) NTDAT=0 No thickness input data, default value. NTDAT=1 For horizontal fin, symmetric layout; or for cruciform fin, symmetric layout with layout on vertical fins same as on horizontal fins.
NTPR	NTPR=1 Print debug output from subroutine THKVEL, default is 0.
NVLIN	NVLIN=0 (for steps 1 and 4)

NVRTPL	Applicable to fixed external vortices only. NVRTPL=0 Component of velocity parallel to fin induced by vortices not included in Bernoulli loading pressures. NVRTPL=1 Loading pressure calculated including parallel component of vortex induced velocity, default value.
NVRTX	Number of external vortices with fixed positions present, NVRTX $\leq$ 10 (see Item 11), default is 0. This option is to be used for special purposes only.
N2DPRB	Index governing type of loading calculation performed on the body surface. N2DPRB=0 Linear and Bernoulli pressure coefficients, default value. N2DPRB=1 Shock expansion and impact (Newtonian) pressure coefficients. N2DPRB=2 Shock expansion and impact (Newtonian) pressure coefficients corrected with linear theory. For N2DPRB > 0, further input is required (Item 10).
N2DPRF	Index governing type of loading calculation performed on fin surfaces. N2DPRF=0 Linear and Bernoulli pressure coefficients, default value. N2DPRF=1 Shock expansion and impact (Newtonian) pressure coefficients.

		N2DPRF=2 Shock expansion and impact (Newtonian) pressure coefficients corrected with linear theory.
		For N2DPRF > 0, further input is required (Item 12).
PHIDIH	ϕ_F	Dihedral or cant angle associated with interdigitated or low-profile four fin layouts, default is 0.0 for cruciform or triform fin layouts, $0 \leq \phi_f \leq 90°$.
PHIFR		Dihedral angle of right upper fin, in degrees. Default is 0. See sketch below.
PHIFL		Dihedral angle or left lower fin, in degrees, default is 0.
PHIFU		Dihedral angle of right lower fin, in degrees. Default is 90.0.
PHIFD		Dihedral angle of left upper fin, in degrees. Default is 90.0.
PHIINT		Interdigitation angle, degrees, between front and rear finned sections. When viewed from the rear, this angle is positive when the front section is rotated clockwise with respect to the rear section. Default is 0.

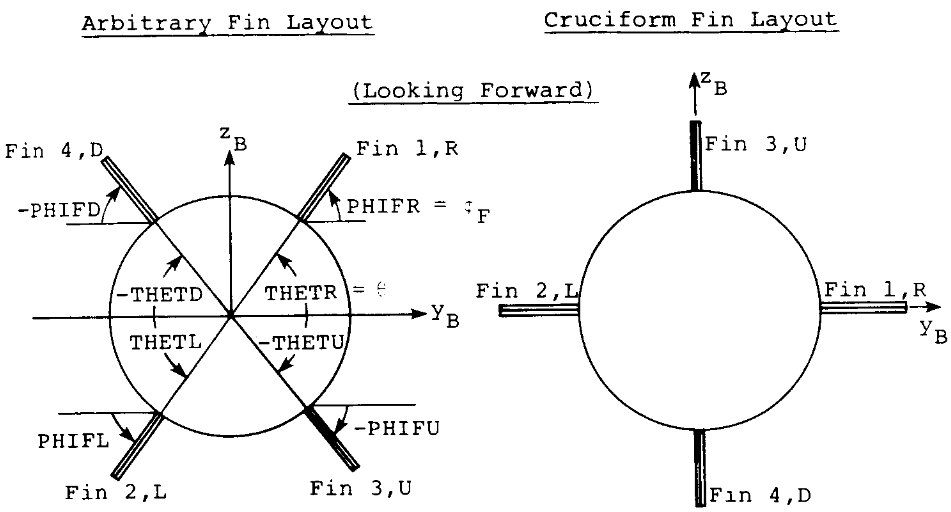

RA		Radius of cylindrical part of body, dimensional, default =0.0.
RB		RB=RA, default = 0.0.
REFL	L_{ref}	Reference length used in moment calculations, dimensional, default is 1.0.
SREF	S_{ref}	Reference area used in load calculations, dimensional, default is 1.0.
SWLEP		Horizontal or upper right and lower left fin leading-edge sweep angle measured in fin planform, positive for sweep back, degrees, default is 0.0.
SWLEV		Vertical or lower right and upper left fin leading-edge sweep angle measured in fin planform, positive for sweep back, degrees, default is 0.0.
SWTEP		Horizontal or upper right and lower left fin trailing-edge sweep angle measured in fin planform, positive for sweep back, degrees, default is 0.0.

SWTEV		Vertical or lower right and upper left fin trailing-edge sweep angle measured in fin planform, positive for sweep back, degrees, default is 0.0.
THETIT	θ	Location angle associated with interdigitated or low-profile four fin layouts, default is 0.0 for cruciform or triform fin layouts, $0 \leq \theta \leq 90°$.
THETR	also refer to preceding sketch	Polar angle of right upper fin in degrees, default is 0.0.
THETL		Polar angle of left lower fin, in degrees, default is 0.0.
THETU		Polar angle of right lower fin, in degrees, default is 90.0.
THETD		Polar angle of left upper fin, in degrees, default is 90.0.
TOLFAC		TOLFAC=1 Multiplication factor used in the evaluation of the tolerance, TLRNC, used in subroutine VELO.
VRTMAX		Maximum magnitude of vortex induced velocities included in flow tangency condition and pressure calculations, default is 0.35.
XM		x_B-coordinate of moment center in body-coordinate system, default is 0.0.

XSTART — Axial station (x_B-coordinate) aft of which body pressures are to be calculated, default is 0.0. <u>Note</u>: For steps 1-3 set XSTART=0.0. For steps 4-6 set XTART=canard T.E. location and if NBSHED=1, set XSTART=tail L.E. location.

XWLE — Axial location (x_B-coordinate) of fin root chord leading edge measured from body nose, default is 0.0.

ZM — z_B-coordinate of moment center in body coordinate system, default is 0.0.

*The following relations must hold:

1. NWBP=[NCW(MSWR+MSWL+MSWU+MSWD)+NCWB(NBDCR)]≤150.

2. Also, MSWR, MSWL, MSWU, and MSWD should be at least five for valid fin trailing-edge vorticity characteristics.

3. When running symmetric case, FEES(N) = 0.0 in Item 5 preceding step 1 input, and if fins are deflected symmetrically, set MSWL, MSWU, MSWD, and DELL, DELU, DELD as follows:

   a. for cruciform fins, MSWR≠0, set DELR≠0.0,
      set NCRX=0
      MSWL=0 DELL=DELR
      MSWU=0 DELU=0
      MSWD=0 DELD=0

   b. for arbitrary fin layout, MSWR≠0, MSWU≠0, 2 cases:

      - no fin deflection
        set NCRX=1
        MSWL=0
        MSWD=0

      - with fin deflection, set DELR≠0.0, DELU≠0.0
        set NCRX=1
        MSWL=MSWU DELD=DELR
        MSWD=MSWR DELL=DELU

<u>Item 3</u>	(3F10.5)	Optional input for planar or cruciform wing alone at zero side-slip (if $LVSWP \neq 0$). (Not used with fin-body combinations.)
YR(KJ)		Distance from wing root chord to the constant u-velocity panel outboard side edge on right wing, $1 \le KJ \le MSWRP$, $(MSWRP \le 20)$, YR(1)=0.0, YR(MSWRP)=B2.
VSWLER(KJ)		Leading-edge sweep of wing between YR(KJ-1) and YR(KJ), positive for sweep back, degrees, $1 \le KJ \le MSWRP$, $(MSWRP \le 20)$, VSWLER(1)=0.0.
VSWTER(KJ)		Trailing-edge sweep of wing between YR(KJ-1) and YR(KJ), positive for sweep back, degrees, $1 \le KJ \le MSWRP$, $(MSWRP \le 20)$, VSWTER(1)=0.0.
<u>Item 4</u>	(3F10.5)	Optional input for fin-body combination (if $LVSWP \neq 0$).
YRT(KJ)		Distance from fin root chord to the constant u-velocity panel outboard side edge on right horizontal or upper right fin, $1 \le KJ \le MSWRP$, $(MSWRP \le 20)$, YRT(1)=0.0, YRT(MSWRP)=B2.
VSWLER(KJ)		Leading-edge sweep of fin between YRT(KJ-1) and YRT(KJ), positive for sweep back, degrees, $1 \le KJ \le MSWRP$, $(MSWRP \le 20)$, VSWLER(1)=0.0.
VSWTER(KJ)		Trailing-edge sweep of fin between YRT(KJ-1) and YRT(KJ), positive for sweep back, degrees, $1 \le KJ \le MSWRP$, $(MSWRP \le 20)$, VSWTER(1)=0.0.
<u>Item 5</u>	(3F10.5)	Optional input for fin-body combination (if $LVSWP \neq 0$).

YLT(KJ)		Distance from fin root chord to the constant u-velocity panel outboard side edge on left horizontal or lower left fin, $1 \le KJ \le MSWLP$, $(MSWLP \le 20)$, YLT(1)=0.0, YLT(MSWLP)=-B2.
VSWLEL(KJ)		Leading-edge sweep of fin between YLT(KJ-1) and YLT(KJ), negative for sweep back, degrees, $1 \le KJ \le MSWLP$, $(MSWLP \le 20)$, VSWLEL(1)=0.0.
VSWTEL(KJ)		Trailing-edge sweep of fin between YLT(KJ-1) and YLT(KJ), negative for sweep back, degrees, $1 \le KJ \le MSWLP$, $(MSWLP \le 20)$, VSWTEL(1)=0.0.
<u>Item 6</u>	(3F10.5)	Optional input for cruciform fin-body combination (if $LVSWP \neq 0$).
ZUT(KJ)		Distance from fin root chord to the constant u-velocity panel outboard side edge on upper vertical or lower right fin, $1 \le KJ \le MSWUP$, $(MSWUP \le 20)$, ZUT(1)=0.0, ZUT(MSWUP)=B2V.
VSWLEU(KJ)		Leading-edge sweep of fin between ZUT(KJ-1) and ZUT(KJ), positive for sweep back, degrees, $1 \le KJ \le MSWUP$, $(MSWUP \le 20)$, VSWLEU(1)=0.0.
VSWTEU(KJ)		Trailing-edge sweep of fin between ZUT(KJ-1) and ZUT(KJ), positive for sweep back, degrees, $1 \le KJ \le MSWUP$, $(MSWUP \le 20)$, VSWTEU(1)=0.0
<u>Item 7</u>	(3F10.5)	Optional input for cruciform fin-body combination (if $LVSWP \neq 0$).
ZDT(KJ)		Distance from fin root chord to the constant u-velocity panel outboard side edge on lower fin, $1 \le KJ \le MSWDP$, $(MSWDP \le 20)$, ZDT(1)=0.0, ZDT(MSWDP)=-B2V

VSWLED(KJ)		Leading-edge sweep of fin between ZDT(KJ-1) and ZDT(KJ), negative for sweep back, degrees, $1 \leq KJ \leq MSWDP$, ($MSWDP \leq 20$), VSWLED(1)=0.0.
VSWTED(KJ)		Trailing-edge sweep of fin between ZDT(KJ-1) and ZDT(KJ), negative for sweep back, degrees, $1 \leq KJ \leq MSWDP$, ($MSWDP \leq 20$), VSWTED(1)=0.0.
Item 8		Optional thickness input data when NTDAT≠0. (presently applicable to planar or cruciform fin layouts only.)
Item 8(a)	(10I5)	Information in Items 8(a), 8(b), and 8(c) are read in by subroutine THKIN for the right horizontal fin.
MSWT		Number of source panels in the spanwise direction, $1 \leq MSWT \leq 19$.
LVSWT		LVSWT=0 No breaks in fin leading or trailing edges, or equal spanwise spacings of source panel sides, default is 0.
		LVSWT=1 Up to 19 breaks in fin leading or trailing edges or up to 19 unequal spanwise spacings.
NUNIS		NUNIS=0 Thickness distribution varies over the span.
		NUNIS=1 Thickness distribution constant over the span.
Item 8(b)	(3F10.5)	Optional input for LVSWT=1.
YTH(1,J)		Distance from body centerline to the source panel outboard side edge, $1 \leq J \leq MSWT+1$.

SWLET(J)		Leading-edge sweep of fin between YTH(1,J-1) and YTH(1,J), positive $1 \leq J \leq MSWT+1$.
SWTET(J)		Trailing-edge sweep of fin between YTH(1,J-1) and YTH(1,J), positive for sweep back, degrees, $1 \leq J \leq MSWT+1$.
<u>Item 8(c)</u>	(8F10.0)	Optional input specifying streamwise thickness slopes read in by subroutine THETIN in groups of NCWT values.
THET(K)		NUNIS=1: K=1, NCWT NUNIS=0: K=1, (NCWT*MSWT) <u>Note</u>: $1 \leq K \leq 400$
<u>Item 8(d)</u>		Optional thickness input for left fin. All input same as for right fin above, Items 8(a), (b), and (c).
<u>Item 8(e)</u>		Optional thickness input for upper fin when NCRX=1 in namelist $INPUT. Same input as for right fin, Items 8(a), (b), and (c).
<u>Item 8(f)</u>		Optional thickness input for lower fin when NCRX=1 in namelist $INPUT. All inputs same as for right fin, Items 8(a), (b), and (c).
<u>Item 9</u>	(namelist)	Namelist $BODY read in by subroutine BDYGEN. Required input when body with circular cross section is present, NBDCR≠0. <u>Note</u>: This input required for step 1 only.
NXBODY		Number of line source/sinks and line doublet singularities distributed along body centerline.

LNOSE — Length of nose part of body measured from nose tip, dimensional (real variable).

LBODY — Length of body, dimensional (real variable).

BCODE — Control index (integer) for specifying forebody shape over length LNOSE.

BCODE=0	Parabolic
BCODE=1	Sears-Haack
BCODE=2	Tangent ogive
BCODE=3	Ellipsoidal
BCODE=4	Conical

<u>Item 10</u> — Optional input for calculation of 2-D nonlinear pressures on body. Read when N2DPRB>0. Data required for one strip only since body is axisymmetric.

<u>Item 10(a)</u> (F10.5)

CONSTK — Constant used in Newtonian pressure coefficient, normally CONSTK=2.

<u>Item 10(b)</u> (I5)

NSEG — Number of 2-D segments used to describe body shape $2 \leq NSEG \leq 100$.

<u>Item 10(c)</u> (8F10.5)

THETA(J) — Slope angles of 2-D segments on body measured relative to body centerline in degrees. Eight values per card $1 \leq J \leq NSEG$.

Item 11	(8F10.5)	Optional input read by subroutine VRTVEL when the effect of fixed external vortices are considered, normally not used, $1 \leq NVRTX \leq 10$.
GAMMA(I)		Vortex strength divided by $(2\pi V_\infty a)$ where a is body radius RA, $1 \leq I \leq NVRTX$.
YVRTX(I)		y_B-coordinate of vortex, normalized by body radius, $1 \leq I \leq NVRTX$.
ZVRTX(I)		z_B-coordinate of vortex, normalized by body radius, $1 \leq I \leq NVRTX$. There will be NVRTX sets of vortex inputs.
Item 12		Optional input for calculation of 2-D nonlinear pressures on fins. Read when N2DPRF>0.
Item 12(a)	(F10.5)	
CONSTK		Constant used in Newtonian pressure coefficient, normally CONSTK=2.
Item 12(b)	(I5)	
NSEG		Number of 2-D segments used to describe fin profile, $2 \leq NSEG \leq 100$.
Item 12(c)	(8F10.5)	
THETA(J)		Slope angles of 2-D segments on upper surface of fin measured relative to fin chordal plane, degrees, $1 \leq J \leq NSEG$.
Item 12(d)		
THETB(J)		Slope angles of 2-D segments on lower surface of fin measured relative to fin chordal plane, degrees, $1 \leq J \leq NSEG$.

Note: Items 12(b) through 12(d) are repeated for each chordwise row of control points on each fin. That is, there are MSWR+MSWL+MSWD+MSWU repetitions of Items 12(b) through 12(d), $1 \leq J \leq NSEG$.

List of Input Variables for Step 2

Track body nose vortices along forward-finned section

Item 1 (20A4) Any alphanumeric information to identify the run.

Item 2 (8I10)

NS	Number of body sections for which coefficients C(I,J) are required, $1 \leq NS \leq 7$.
NF	Number of corner points used to define fin geometry, $1 \leq NF \leq 7$.
NCPIN	NCPIN=1 Read in control point and body pressure points from data set (TAPE4).
	NCPIN=0 Control points are not input via TAPE4.
NVLOUT	NVLOUT=1 Write velocities induced by moving vortices (and calculated in this program) on data set (TAPE7).
	NVLOUT=0 No such output.
NOUT	NOUT=1 Print additional output.
	NOUT=0 Minimum output.
IPLT	IPLT=0 No plots showing vortex positions in the output.
	IPLT=1 Vortex positions shown in crossflow planes.

Item 3	(7F105)	
XE(I)		Axial coordinates of the end of each body section, $1 \leq I \leq NS$.
Item 4	(8F10.5)	
C(I,J)		Coefficients in the body meridian equation, $1 \leq I \leq NS$, $1 \leq J \leq 7$. Only C(I,1) is non-zero. It equals the body radius, RA.
Item 5	(8F10.5)	Optional input concerning fin planform geometry when $NF \neq 0$.
XF(I)	specify in pairs	Axial coordinate of fin corner point, $1 \leq I \leq NF$.
YF(I)		Lateral coordinate of fin corner point, $1 \leq I \leq NF$.
Item 6	(8F10.5)	
E5		Error allowed in integration subroutine DASCRU. Use the value 0.01 or less.
VRTMAX		Maximum magnitude of vortex induced velocities, use the value 0.35.
Item 7	(8I10)	
NIP		Number of axial stations to be printed in output, $1 \leq NIP \leq 50$. Note: If XBEGIN=XEND set NIP=1.
Item 8	(8F10.5)	
XBEGIN		Axial location of vortex-tracking starting station. Note: If vortices are assumed to lie parallel to body centerline through forward-finned section in step 2, set XBEGIN=XEND and NIP=1 in Item 7. For step 5 refer to general description of input for that step given earlier.

XEND		Axial location of end station for vortex tracking.
<u>Item 9</u>	(8I10)	Next two items are optional input for NCPIN=0, only.
NCP		Number of control points and body pressure points or field points at which vortex induced velocities are to be calculated.
<u>Item 10</u>	(3F10.5)	Optional input when NCP≠0 specifying field point coordinates.
CPX		Body x_B-coordinate of field point, dimensional.
CPY		Body y_B-coordinate of field point, dimensional.
CPZ		Body z_B-coordinate of field point, dimensional.

List of Input Variables for Step 3

Forward-finned section with vortex effects

<u>Item 1</u>	(I5)	
NVORT		Integer flag read in by routine DEMON2 indicating how far along body the paths and influence of nose vortices are calculated. NVORT=0 Paths and influence calculated along entire body. NVORT=1 Paths and influence calculated to trailing edge of canard root chord only.
<u>Item 2</u>		Optional input for nonlinear pressure calculation on fins. If Items 12(a) through 12(d) were specified for step 1, they are repeated here.

Input Variables for Step 4

Same as for step 1 except this input is applied to the afterbody and tail section, Item 9 (NAMELIST $BODY) is excluded. Note: Set ITAIL=1. Also if NBSHED=1 in namelist $INPUT set XSTART=XWLE in $INPUT.

Input Variables for Step 5

Same as for step 2, applied to afterbody and tail section. Note: If NBSHED=1 in namelist $INPUT for step 4, set XBEGIN= axial location of the leading edge of the tail section; also refer to general description of input for this step given earlier with regard to running upstream vortices parallel to the body centerline through the length of the tail seciton (NIP≠0, XBEGIN=axial location of forward-finned section trailing edge, XEND=axial location of tail section leading edge).

List of Input Variables for Step 6

Item 1	Optional input for nonlinear pressure calculation on the fins. If items 12(a) through 12(d) were specified in step 4, they are repeated here.
Item 2	End card with "END" punched in first three columns.

The input deck must be terminated by a card with "END" punched in the first three columns.

A.8 DESCRIPTION OF OUTPUT

This section contains a description of the output generated by program LRCDM2 for a typical case involving a complete forward-fin, body, tail-fin combination. Hence, this output corresponds to a case where NSTART has a value of 1 and NSTOP has a value of 6. The output control index MINPRN specified in namelist $INPUT equals 0. If it is set equal to 1, only the input data and the overall force and moment coefficients are printed.

A sample output is shown in Figure A.7. It is the program output for the forward-controlled configuration used as the sample case discussed in Section A.9 of this appendix. This sample case includes output generated by program BDYSHD described in Appendix B. Thus, program LRCDM2 first runs steps 1 through 3, program BDYSHD runs optional step 3a, and LRCDM2 resumes to run steps 4 through 6.

Large amounts of additional output are generated if print control indices NOUT and NPR are set nonzero. This additional output is provided as an aid in finding input and/or program problems. For the benefit of the user, references are made to specific subroutines from which portions of the output are printed. The subroutine names are shown in the subroutine calling sequence, Figure A.1. For clarity, the output is described separately for each step of the stepwise procedure described in Section A.4 of this appendix and in Section 2.3 of this report. The output generated by companion program BDYSHD for optional step 3a is discussed in Appendix B.

The following descriptions are concerned with the linear and Bernoulli pressure coefficient calculation methods. If the optional shock-expansion and Newtonian pressure coefficients are used, the pertinent headings in the output will indicate that fact.

The following coordinate systems will be mentioned in output descriptions.

1. Body coordinate system (x_B, y_B, z_B) with origin at the nose, Figure A.4; this system is also called rolled or body-fixed coordinate system.

2. Unrolled body coordinate system (x_B, y, z) also with origin at the nose and z in the plane formed by the free-stream velocity vector and the body centerline; lateral coordinate y is normal to this plane and points to the right as will be shown in a later sketch.

3. Wing coordinate system (x_W, y_W, z_W) parallel to (x_B, y_B, z_B) with origin on the body centerline at the axial location of the root chord leading edge of either the forward- or tail-finned section, Figure A.4.

4. Local fin coordinate system (x_F, y_F, z_F) with origin at the root chord leading edge, x_F directed aft along the root chord, y_F in the plane of the fin (inboard or outboard), and z_F normal to the fin plane (also refer to Appendix C, Section C.2).

A.8.1 Output From Step 1

The first page is the title page and the second page identifies both the step and the particular run. For this step the title "LOADS ON FORWARD FINS WITHOUT EFFECTS OF NOSE VORTICES" is printed at the top of the second page followed by the run descriptor entered in input Item 1 for this step.

Values of the variables in namelist $INPUT read in by subroutine DEMON2 are printed on the second and possibly third page. The values of the variables pertain to the forward-finned section. All dimensions in the output are the same as in the input. Any dimensional system is acceptable to the program as long as it is used consistently.

Fin-section geometry and the number of constant u-velocity panels in the chordwise (NCW) and spanwise (MSWR, MSWL, MSWU, MSWD) directions are listed on the next page. Fin geometry is repeated on the following page with flow conditions. Quantities ALFA and BETA correspond to angles of pitch, α, and sideslip, β, respectively, calculated by the program in accordance with Equation (3) in this report. They are calculated from the included angle of attack, α_c, and angle of roll, ϕ, specified singly or multiply in Items 3 and 5 required for all runs. Information concerning the geometrical layout of the planar source panels used to model thickness of the fins is then shown if the thickness option is used. On the next page, the specified fin streamwise thickness slopes are printed.

Coordinates of the control points generated by subroutine DEMON2 and associated with the constant u-velocity panels are printed next. These panels are distributed on the fins and the body-interference shell of the forward-finned section. The number of control points and the coordinates, expressed in the (x_B, y_B, z_B) system, are stored on a data set on TAPE4 for later use in step 2. There are NWBP sets of coordinates where NWBP is the number of control points on the forward fins and interference shell. The value of NWBP is given by the following relation.

NWBP=NCW(MSWR+MSWL+MSWU+MSWD)+NCWB(NBDCR)

Namelist $BODY, which is read in by subroutine BDYGEN, appears next. It is followed by the cylindrical coordinates and streamwise slopes of the body definition points. These coordinates are calculated by the program. The origin of each semi-infinite line singularity (linearly varying line source/ sink and linearly varying line doublet) used to represent the body is given under the heading TX. All axial coordinates are given in the body-coordinate system with origin at the nose, as shown in Figure A.4. The strengths of the singularities are related to coefficients T(I) for the line sources or sinks, and by TC(I) for the line doublets.

On the next pages, the output shows the surface pressures calculated on the circumference of the forebody. The forebody is the length of body up to the forward-finned section. The first page of the body loading output is marked ***STEP1 on the upper right hand corner. The pressures are calculated by subroutine BDYPR on rings centered on the axial locations listed under the heading XB in the body coordinate system. The ring at each axial location is given a BODY RING number which is written above the pressure point coordinates, perturbation velocity components involved, pressure coefficients, meridional body slopes, and pressure ratios. The pressures are calculated by subroutine BDYPR on the basis of both the linear and Bernoulli pressure-velocity relationships. The former is given by Equation (5) and the latter is given by Equation (6) in this report. Pressures based on shock expansion and Newtonian theories can be optionally calculated (refer to Section 2.6 of this report). If this is the case, the pressure headings are changed accordingly in all of the following output.

At the given axial station on the forebody, body-nose shed vorticity characteristics can appear ahead of the body pressure output if the included angle of attack is in excess of about 5 degrees and if the forebody length is sufficiently long. The vorticity is represented by two concentrated vortices located symmetrically with respect to the crossflow component of the free-stream velocity vector as shown in the sketch below. The vortex coordinates are specified in the unrolled body coordinate system and in the fixed body-coordinate system (rolled coordinates) nondimensionalized by the local body

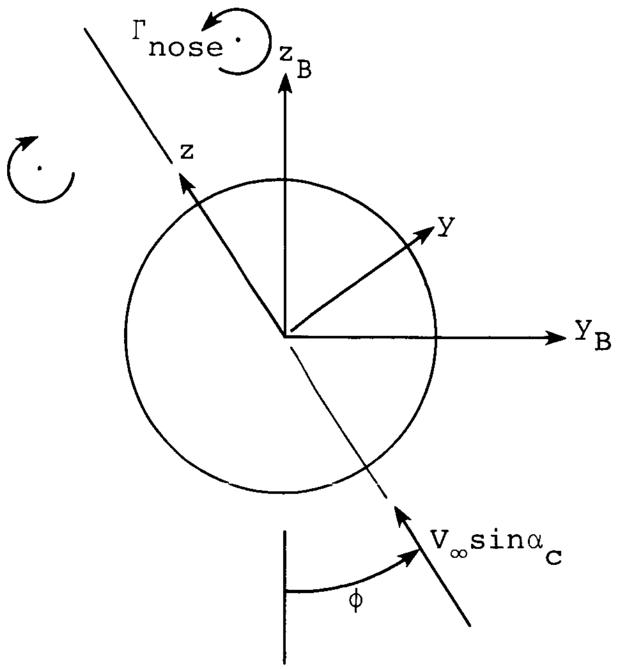

radius. The coordinate systems are discussed below. The vortex characteristics will change from one station to the next. The calculated pressures include effects of the body-nose vortices, if present*.

At the end of the output for each ring, the integrated loads on that ring are given in the unrolled body-axis and in the fixed or rolled body-axis coordinates for both linear loading and Bernoulli loading pressures. In addition, the cumulative body loads up to and including that ring are given. The relationship between the unrolled (x_B, y, z) and the rolled body-coordinate (x_B, y_B, z_B) system is shown above at a given body cross section. The x_B-axis is the same for both systems. If the angle of roll ϕ is zero, the two coordinate systems are the same.

---

*Refer to Limitations and Precaution Section A.6 in connection with a deficiency in the forebody pressures when under the influence of forebody vortices.

If body-nose vortices are generated on the forebody, their number, strengths and positions at the end of the forebody (i.e., at the beginning of the forward-finned section) are printed after the last forebody ring pressure distribution and loadings output. Positions are given in the body coordinate system (x_B, y_B, z_B) in dimensional units. Vortex strengths are divided by the free-stream velocity. This information is stored in a data set on TAPE8 for later use in step 2.

The accumulated body loads calculated in step 1, including the last ring on the forebody, are used as the first values in the summing procedure for the force and moment coefficients acting on the entire configuration. In program LRCDM2, the values for the force and moment coefficients are expressed in the unrolled body coordinate system (x_B, y, z) and in the rolled or fixed body coordinate system (x_B, y_B, z_B).

The next page in the output lists the calculated control point coordinates X,Y,Z for the constant u-velocity panels distributed on the fins. These coordinates are expressed in the wing-coordinate system (x_W, y_W, z_W) shown in Figure A.4. Perturbation velocities, induced at these points by the body sources/sinks and doublets, and lateral velocity components induced by vortices with their characteristics specified optionally in the input are also shown. The quantities BU,BV,BW are due to the body line singularities and VVRTX,WVRTX are due to the vortices specified in optional Item 10 of the input for step 1. These velocity components are also expressed in the wing coordinate system (x_W, y_W, z_W). Normally, velocities induced by moving vortices are calculated by module VPATH2 and printed later. Velocity components induced by the body singularities are calculated by subroutine VELCAL.

Coordinates of the control points associated with the body interference panels are given on the next page. They are also expressed in the wing coordinate system (x_W, y_W, z_W).

Velocity components THU, THV, and THW are induced by the planar source panels distributed on the fins to model thickness as an option.

The next pages are concerned with the Bernoulli pressure distributions acting on the fins calculated by subroutine SPECPR. In step 1, the fin pressures do not include effects of forebody vortices, if present. Perturbation velocity components UTOTA, VTOTA, and WTOTA and the pressure coefficient PRESSA ($=C_p$) act on the upper side of the horizontal fins. Perturbation velocity components UTOTB, VTOTB, and WTOTB and the pressure coefficient PRESSB ($=C_p$) act on the lower side of the horizontal fins. Coordinates X, Y, and Z correspond to the control points of the constant u-velocity panels on the fins and are expressed in the wing-coordinate system (x_W, y_W, z_W) shown in Figure A.4. The perturbation velocity components act along directions parallel to the wing- or body-coordinate systems. The Bernoulli pressure coefficient information is then given for the left (PRESSA) and right (PRESSB) sides of the vertical fins, looking forward.

For cases with interdigitated or low-profile fin layouts, the pressures acting on the surfaces of each fin are still given by PRESSA and PRESSB. The designation of the fins in an arbitrary layout is related to the designation of the fins in a cruciform layout as shown below.

Arbitrary Fin Layout

Cruciform Fin Layout

(Looking Forward)

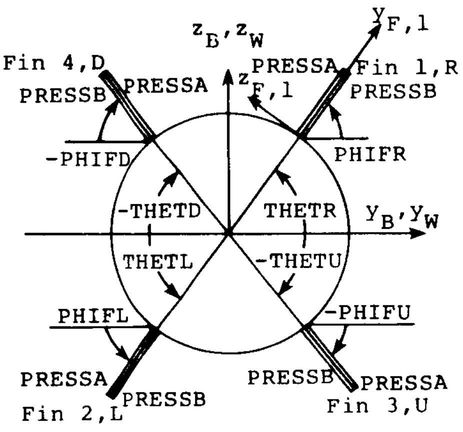

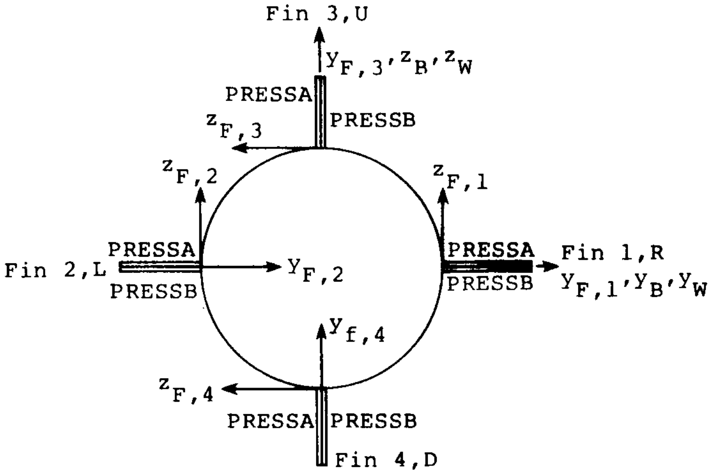

Pressure coefficients PRESSA and PRESSB are shown in the sketch on the sides of the fins where they act. The lateral fin local coordinate (y_F, z_F) are indicated for each fin for the cruciform case and for one fin for the arbitrary fin layout. Note that for the arbitrary case the fin planes do not coincide with y_B, y_W or z_B, z_W. However, the perturbation velocities are still expressed in the body- or wing-coordinate systems.

The Bernoulli loading pressures shown on the next pages are computed as PRESSB minus PRESSA (ΔC_P = DELTP, BERN.) for all fins, and the linear loading pressures (ΔC_P = DELTP, LIN.) are proportional to the strengths of the constant u-velocity panels on the fins.

Fin loading information is printed on the next pages. The first page is marked ***STEP1. First, the loadings calculated by subroutine SPECLD are based on the linear pressure loadings DELTP, LIN. The force and moment coefficients, spanwise loading and suction distributions are given for each fin as follows.

The heading specifies flow conditions and reference quantities including the moment center coordinates in the body system. It is followed by a list of the fin deflection angles, thrust coefficient, CTHR, acting in the negative x_W (or x_B) direction, force coefficient CZ in the z_W (or z_B) direction, force coefficient CY in the y_W (or y_B) direction, pitching moment CM (nose-up positive), yawing moment CLN (nose-to-right positive) and rolling-moment CLL (right-fin-down positive) coefficients. Values for the various loads, printed in the first column under the title "TOTAL" are the sum of the loads on the fins only. They do not include the carryover loads on the interference shell.

Force coefficients CZ,CY and moment coefficients CM,CLN are also printed for the interference shell which covers the body over the length covered by the fins. They are only representative of the lift carryover or interference from the fins. The actual loads acting on this section of body are computed by integrating the appropriate pressure distributions printed out later as part of step 3.

For convenience, the positive directions of the forces and moments expressed in the rolled or body-fixed system are indicated in the following sketch together with the rolled body- and wing-coordinate systems. So far, the loading coefficients have been expressed in the rolled body-axis system. The fin loading information is also specified in the unrolled body-axis system discussed earlier in connection with the forebody loads. For cases with zero roll angle ($\phi = 0°$), the two sets of force and moment coefficients are the same.

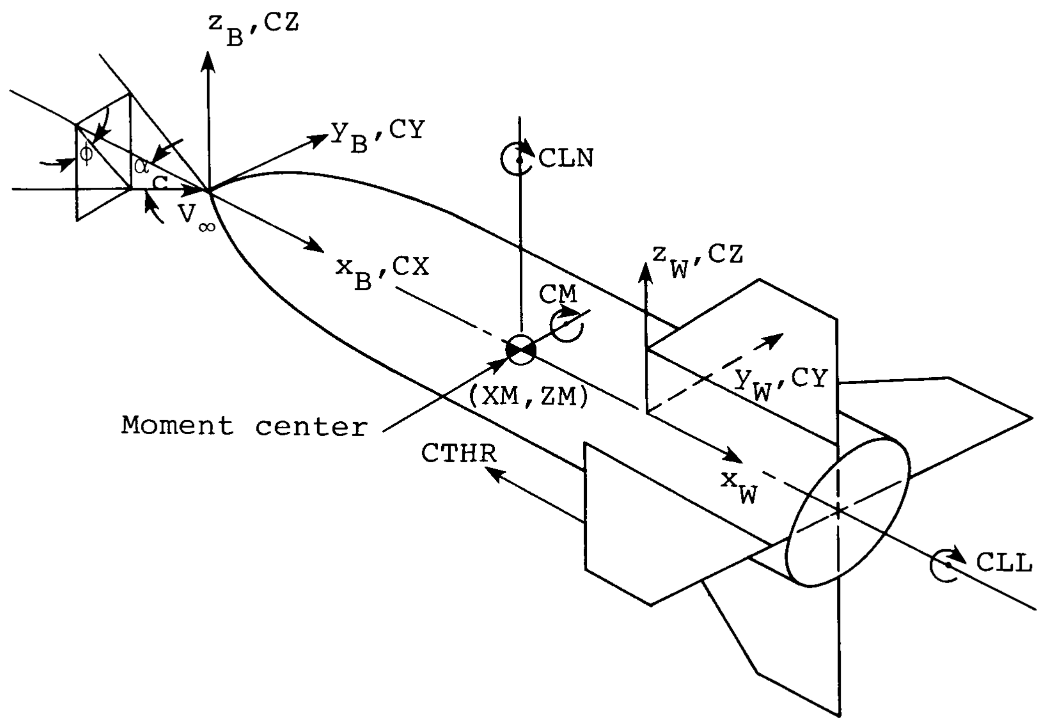

Under the heading SPANWISE DISTRIBUTIONS, the quantities of interest are the span loading CN*C/(2*B), and the suction distribution CS*C/(2*B) given as a function of the fraction of exposed fin semispan. These quantities are calculated in subroutine SPNLD. Parameter B is twice the exposed fin semi-span. Other important quantities are the leading- and side-edge augmentations CNADD to fin-normal force calculated from the suction distributions along those edges in accordance with Polhamus' suction-to-normal force conversion (refer to Appendix C, Section C.2). Proportion factors KVLE and KVSE are specified in namelist $INPUT. If the fin leading edge is supersonic, the suction and therefore the normal-force augmentation along that edge is zero. The contributions from the additional leading- and/or side-edge normal force(s) acting on the fin to the force and moment coefficients in the rolled and unrolled coordinates are printed (CYADD, CZADD, etc.). The points of action of the additional leading- and side-edge forces are indicated by XCG, YCG, and ZCG. On the leading edge, the additional force is located at the spanwise center of pressure of the suction distribution. On the side edge, the axial location is assumed to be at mid-chord.

The strengths and lateral positions of the vortices associated with the fin leading- and/or side-edge normal force augmentations are printed next. Coordinates Y, C.G. and Z, C.G. are given in the local fin system (y_F, z_F) shown in an earlier sketch and in the rolled body-coordinate system. These coordinates represent the lateral vortex locations at the trailing edge of the fin.

All of the above information is repeated for each fin in the finned section under consideration (forward section in step 1). Note again that for step 1, the effects of forebody vortices (if present) are not included. These effects will be included later in the output associated with step 3.

All loading computations are repeated by subroutine SPCLD on the basis of the Bernoulli loading pressures printed earlier. However, in this instance the characteristics of trailing-edge vorticity represented as one or more concentrated vortices are specified under the heading "T.E. FIN VORTICITY DUE TO ATTACHED FLOW." This vorticity is determined from the spanload distribution based on Bernoulli pressure loading (Appendix C, Section C.3) and is not related to the vorticity due to the force augmentations along the leading and side edges.

None of the loading or vortex information calculated during step 1 is included in the summing or storing of data. This will be done in step 3 when the effects of forebody vortices are included.

A.8.2 Output From Step 2

At the top of the first page of output from this step, the title "PATHS OF NOSE VORTICES OVER FORWARD FINS" is printed. This is followed by the run identifier entered as input Item 1 for step 2.

The next output appears only if body-nose vortices have been formed as part of step 1. Fin planform geometry (if specified) and flow conditions are given. The permissible error, E5, in the vortex path integration scheme is printed. This output is followed by a list of vortex strengths and lateral positions at the initial axial station (beginning of forward-finned section). Coordinates Y,VRTX and Z,VRTX and the axial locations are expressed in the rolled body-coordinate system (x_B, y_B, z_B). Vortex strengths are divided by the magnitude of the free stream and as such GAMMA/VINF is dimensional (unit of length). If the input specified in Items 7 and 8 allow the vortices to move in the crossflow plane, the vortex coordinates are given at a number (NIP) of axial stations. If the vortices are assumed to travel aft parallel to the body centerline (by setting NIP=1 and XBEGIN=XEND), the vortex coordinates are given for the first station only.

The next item in the output for step 2 is a listing of the coordinates of field points (or control points), read in be means of a data set on TAPE4, and the velocity components induced by the vortices at those points. If no body vortices were generated, the vortex effects will be zero. The coordinates and the velocity components are given in the rolled body-coordinate system (x_B, y_B, z_B). The vortex effects are calculated on the basis of the vortices in the presence of the body only (refer to Appendix C) and are stored in a data set on TAPE7. Finally, the updated body-nose vortex positions and strengths are shown and stored on TAPE8.

A.8.3 Output From Step 3

In step 3, as in step 1, loads are calculated on the forward-finned section. The only difference between the two steps is that the effects of nose vortices (if present) on the fins and interference shell are included in step 3 while they are omitted in step 1. Much of the output in step 3 appears similar to that in step 1. To the extent possible, repeat calculations are avoided in order to decrease program execution times. For example, the body singularity strengths and the loads on the forebody are calculated in step 1 only while the loads acting on the portion of body in the forward-finned section are determined only in step 3.

The title "LOADS ON FORWARD FINS WITH EFFECTS OF NOSE VORTICES" marks the beginning of the output for step 3. This is followed by the run identifier entered in input item 1 of step 1.

Values of the variables in namelist $INPUT are printed on the following pages. These values are the same, with the exception of NVLIN and NCPOUT, as used in step 1. These latter two variables have been set by the executive routine to read in the vortex-induced velocities, calculated in step 2, from a data set (NVLIN=1) and to not write the control point coordinates onto a data set (NCPOUT=0).

Immediately below the list of namelist $INPUT is a statement specifying whether or not the nose vortices are tracked past the forward-finned section. This is controlled by the variable NVORT entered as input to step 3. Body-nose vortex effects are calculated along the afterbody and tail section when NVORT has a value of zero. When NVORT is assigned a value of one, effects of nose vortices are neglected downstream of the trailing edge of the forward-finned section.

The fin section geometry characteristics, and flow conditions are printed again. Vortex-induced velocities at the panel control points (XCP,YCP,ZCP) are printed next. These velocity components are designated VVEL and WVEL and were calculated in step 2. The values should agree with the V and W values printed at the end of that step. In step 3, the point coordinates and velocity components are expressed in the wing coordinate system (x_W, y_W, z_W).

Pressure coefficients based on the Bernoulli expression, Equation (6), calculated at the control points of the panels on the fins are printed on the next pages. The meaning of above and below are discussed in the corresponding output description for step 1. This time, in step 3, the pressure coefficients (PRESSA, PRESSB) and pressure loadings (DELTP,LIN., DELP,BERN.) include contributions from the forebody vortices if present.

Fin loading information for step 3 is printed on the next pages. These loads are presented in the same manner as in step 1. The first set of loads is based on linear pressure loading, and the first page shows ***STEP3 in the right upper corner. The difference between the fin loads printed during step 1 and those printed during step 3 is that the former loads do not include effects induced by any nose vortices while the loads given in step 3 do include these vortex effects.

The leading- and side-edge fin normal-force augmentations and the associated fin-edge vortex characteristics are printed after the spanwise distributions for each fin of the forward-finned section. These quantities are calculated as part of the linear pressure loading method in accordance with Appendix C of this report and Appendix C of Reference 1. During step 3, the fin force and moment augmentations are added to the forebody force and moment coefficients calculated during step 1. In addition, the leading- and side-edge vortex characteristics are added to the data set on TAPE8.

The second set of loading information is based on the Bernoulli loading pressures. It is printed on a page marked ***STEP3. During step 3, the fin loads are added to the accumulated force and moment coefficients. The total load acting on a fin of a forward-finned section is given by the sum of the force or moment coefficient listed under the heading "BERNOULLI PRESSURE LOADS IN BODY SYSTEM" or "FOLLOWING ARE IN UNROLLED BODY-AXIS COORDINATE SYSTEM" and the corresponding additional force and moment coefficients due to leading- and/or side-edge normal-force augmentations calculated with the linear pressure loadings*. This information is printed a few pages earlier under the spanwise distributions output generated with linear pressure loading.

The trailing-edge vorticity characteristics shown under the heading "T.E. VORTICITY DUE TO ATTACHED FLOW" are added to the table of vortex strengths and positions on TAPE8 as listed at the end of the fin load output. Coordinates Y and Z under the heading "VORTEX INFORMATION WRITTEN ON TAPE8 FROM SUBROUTINE SPNLD" correspond to the rolled body coordinates y_B and z_B of the vortices at the trailing edge of the forward-finned section. The vortex strengths, GAMMA, are divided by free stream.

Finally, pressures and loads acting on the rings of the body interference shell are printed under the heading "PRESSURE COEFFICIENTS AT POINTS ON BODY MERIDIANS." This set of rings covers the length of body next to the fins of the forward-finned section and follows the rings on the forebody. The widths of the rings of the interference shell are set by body interference length BIL and axial paneling number NCWB both specified in namelist $INPUT, Item 2 for step 1. Coordinates XB, YB, and ZB are expressed in the rolled body coordinate system (x_B, y_B, z_B). Perturbation components UTOT, VTOT, and WTOT are also in that system and include contributions from body singularities, fin thickness panels, constant u-velocity panels on the fins and interference shell and external (forebody) vortices if present.

The final accumulated ring loads are added to the overall force and moment coefficients accumulated so far. If optional

---

*The NASA/LRC version of LRCDM2 prints the total fin forces under the Bernoulli pressure loads as CZFT,CYFT...etc. and CZFTU,CYFTU...etc. The sample case output shown later does not show these quantities.

afterbody vortex shedding program BDYSHD is engaged (step 3a), the forces and moments accumulated for the forebody and forward-finned section are printed under the heading "SUMMARY OF TOTAL LOADS" at the end of step 3. The output for optional step 3a is described in Appendix B.

A.8.4 Output From Step 4

If optional step 3a was engaged to handle the afterbody, the output for step 4 commences with a list of accumulated force and moment coefficients for the configuration up to the tail section. Without step 3a, this step marks the beginning of calculations on the afterbody and tail fins. The same type of information is printed in steps 4 through 6 as in steps 1 through 3 with minor differences. The output will be described in short.

Following the title "LOADS ON TAIL FINS WITHOUT VORTEX EFFECTS" the run descriptor, entered as input item 1 for this step, is printed. Namelist $INPUT is printed next followed by tail-section geometry, flow conditions, tail-fin planform and thickness information and namelist $BODY. The body parameters include the entire body length and should be the same as printed out for step 1.

Body dimensions and line-singularity information are printed next. This information is identical to that in step 1 and is repeated for convenience.

The next portion of the output shows the coordinates, in the rolled body-axis system, of the constant u-velocity panel control points distributed on the tail fins and interference shell. If optional step 3a was not engaged, this output is continued for points on the afterbody at which pressures will be calculated. These coordinates are stored on TAPE4 for later use in step 5. At the beginning of this output, the total number of coordinate sets is given and this number should not exceed 500.

Control point coordinates of the constant u-velocity panels distributed on the tail-fin surfaces are printed next, followed by the coordinates of the control points associated with the body interference panels. The formats of both of these are the same as for the corresponding output in step 1 and are accompanied by body induced velocities, fixed external vortex effects (normally not used here) and fin thickness effects, respectively.

The next pages contain the pressures acting at the control points of the constant u-velocity panels on the fins. The meanings of the headings are described earlier under output for step 1. In this step 4, effects of external vortices (from the forebody, forward-finned section, and optionally the afterbody) are not included.

Fin loading information for linear and Bernoulli loading pressures follow. The format is the same as used for steps 1 and 3. These tail-fin loads are without external vortex effects. None of the tail-fin loads and vortex information are either added to the accumulated forces and moments or saved.

A.8.5 Output From Step 5

The information shown in the output for step 5 is concerned with the tracking of and the effects induced by the forebody vortices (if present and if NVORT is set equal to zero in step 3) and the vortices originating from the fins of the forward-finned section. The kind of information given and the formats used are identical to those described for step 2.

Two cases are possible. In the first case, optional step 3a is not used and the output for step 5 covers the length of body from the trailing edge of the forward-finned section up to the tail section as a minimum. Vortex effects induced at points on the afterbody and tail section are printed at the end of this step. In the second case, optional step 3a is engaged and companion program BDYSHD tracks the forebody vortices (if present and if NVORT is set equal to zero in step 3) and the forward-fin vortices together with afterbody-shed vortices up to the tail section. In this case, the effects induced by the vortices at points on the tail section only are printed at the end of this step. In either case, the vortices can be allowed to move laterally through the tail section or the vortex paths can be made to lie parallel to the body centerline as described in the input for step 2 and step 5. In the latter case, the last body x_B-station listed corresponds to the leading edge of the tail section.

A.8.6 Output From Step 6

As a minimum, the output for this step is concerned with the loadings, including vortex-induced effects, acting on the tail section. This is the situation when optional step 3a is engaged in which case afterbody loads are calculated by program BDYSHD. If step 3a is not used, the loads are calculated on both the afterbody and tail section by program LRCDM2 in step 6 including vortex-induced effects. In both cases the output is similar to that described in step 3.

Input relevant to the tail section appears on the first few pages. This is followed by a list of vortex-induced perturbation velocities calculated in step 5. The coordinates XCP,YCP,ZCP correspond to the control points of the constant u-velocity panels on the tail fins and interference shell and are expressed in the rolled body coordinate system (x_B, y_B, z_B).

If optional step 3a is not used, this list also includes vortex-induced velocity components at points on the afterbody, and the surface pressures and body ring loads are presented next at program determined axial locations XB. The format is the same as that used for presenting the surface pressures on the forebody in step 1. These pressures and the integrated loads acting on the rings include vortex induced effects calculated in step 5.

For cases with optional step 3a, the next portion of output gives the Bernoulli pressures acting on both sides of the fins. This is followed by a list of the linear and Bernoulli loading pressures acting on the fins. The format of the pressure distribution output is described in detail for the output of step 1. In this step, effects induced by upstream vortices are included.

Tail-fin loads are given next, first using linear pressure loading and then Bernoulli pressure loading. These loads are presented in the same manner as the forward-finned section loads printed in step 1 so that comments made there apply here also. Again, these loads now include effects due to the upstream vortex flow field. The total load acting on one tail fin of the tail section is given by the sum of the force or moment coefficient listed under the heading "BERNOULLI PRESSURE LOADS IN BODY SYSTEM" or "FOLLOWING ARE IN UNROLLED BODY-AXIS COORDINATE SYSTEM" and the corresponding additional force and moment coefficients due to leading- and/or side-edge normal-force augmentations calculated with the linear pressure loading*. This latter information is printed a few pages earlier following the spanwise distributions output generated for linear pressure loading. The additional quantities appear under the headings "L.E. AUGMENTATION OF FIN NORMAL FORCE...ETC" and/or S.E. AUGMENTATION OF FIN NORMAL FORCE...ETC." The fin forces and moments are added to the forces and moments accumulated up to the tail section.

The next item of information printed in this step is the surface pressure distribution acting at the control points x_B, y_B, z_B of the body interference shell for the tail section. This shell covers the portion of the body from the leading

*See footnote on page A-73.

edge of the tail section to the trailing edge. The pressures are integrated to obtain loads acting on the rings centered at x_B. The loads summed over all the rings in the tail section are added to the accumulated force and moment coefficients.

Finally, the executive routine directs subroutine TOLDS to print the summary of total loads. Note that in the summing or accumulation process, only loads which include vortex effects are included (i.e., results from step 1 for the forebody, results from steps 3 and 6 for the finned sections and afterbody, or from optional step 3a for the afterbody). After printing the flow conditions, the total force and moment coefficients valid for the complete configuration under consideration are listed in the rolled and unrolled body-axis coordinate systems. These coordinate systems are described at the beginning of this section. The loads are calculated with the linear pressure/velocity relationship, Equation (5), and with the Bernoulli pressure/velocity relationship, Equation (6), respectively. On the basis of comparisons with experimental data, the Bernoulli results are considered the better of the two. It is also possible to employ optional nonlinear pressure coefficient calculation methods described in Section 2.6 of this report. The pressure headings will change accordingly.

A.9 SAMPLE CASE

In order to illustrate the use of program LRCDM2 and optional program BDYSHD, the input and output are supplied in this appendix for a case involving a canard-tail missile with forward roll control. References will be made to the stepwise procedure described in Section A.4 of this appendix.

The geometry of the sample case is associated with the TF-4 wind tunnel model with AR = 2 canard fins and AR = 1.06 "king" tail fins shown in Figure 3 of this report. The included angle of attack is high enough to cause formation of afterbody vortices. Thus, in this calculation companion program BDYSHD is engaged to account for afterbody-shed vortex effects on the afterbody loads under the influence of canard vortices, and BDYSHD will also generate the vortex field at the beginning of the tail section.

As shown in Figure 3, the configuration consists of an ogive nose followed by a cruciform canard section, cylindrical afterbody with constant radius and a cruciform tail section. The essential geometrical and modeling details are listed below together with the corresponding input variable names for the body, canard section and tail section.

Body

Nose length	LNOSE	9.518
Overall length	LBODY	102.32
Nose type	BCODE	2 (ogive)
Constant body radius	RA,RB	2.115
Number of singularities (line sources/sinks and line doublets)	NXBODY	50

Forward-Finned Section

(four fins in cruciform layout)

Fin root chord	CRP,CRPV	11.13
Leading-edge sweep angle	SWLEP,SWLEV	47.1°
Trailing-edge sweep angle	SWTEP,SWTEV	0.0°
Exposed fin span	B2,B2V	7.23
Interference shell length	BIL	11.13
Root chord L.E. location	XWLE	15.8
Deflection angles of left and right horizontal fins	DELL,DELR	-5.0,+5.0°
Number of constant u-velocity panels in chordwise direction	NCW	4 on each fin
Number of constant u-velocity panels in spanwise direction	MSWR,MSWL, MSWU,MSWD	6 on each fin
Number of constant u-velocity panels in longitudinal direction on interference shell	NCWB	4
Number of constant u-velocity panels on circumference of interference shell	NBDCR	12

Tail Finned Section

(four fins in cruciform layout)

Fin root chord	CRP,CRPV	21.59
Leading-edge sweep angle	SWLEP,SWLEV	45.0°
Trailing-edge sweep angle	SWTEP,SWTEV	0.0°
Exposed fin span	B2,B2V	9.04
Interference shell length	BIL	21.59
Root chord L.E. location	XWLE	80.73

The constant u-velocity paneling layout is the same as for forward-finned section.

Flow Conditions and Reference Quantities

Included angle of attack	ALFS (α_c)	15°
Angle of roll*	FEES (ϕ)	0.001
Free-stream Mach number	FMACH	2.5
Reference area	SREF	14.12
Reference length	REFL	4.23
Moment center	XM	46.04

All of the above information is included or used to generate the input shown in Figure A.5(a), A.5(b), and A.5(c) for the roll control case. All of the input data shown in these figures are read in together. The information listed in A.5(a) actually covers the geometry and other input for the canard and tail section. This data is stored on TAPE2 for later use. However, since NSTART=1 and NSTOP=3 (see Item 1 required for all runs), the calculations will be interrupted at the end of step 3. Index NBSHED is set equal to 1 signifying engagement of companion program BDYSHD. Figure A.5(b) shows the input for optional step 3a required by program BDYSHD described in Appendix B. This input also includes the body characteristics and number of singularities listed above except that LNOSE was chosen 15.8. This will not make any difference insofar as calculations on the afterbody are concerned. Finally, the remaining input required by LRCDM2 to perform steps 4 through 6 is indicated in Figure A.5(c).

---

*See note in input variable description following Item 5 required for all runs; in this case, the horizontal canard fins are deflected asymmetrically so ϕ = 0.001°.

Note that the portion of input in Figure A.5(a) read in by module VPATH2 does not contain any canard or tail fin corner coordinates. This information is not required if the vortices are assumed to lie parallel to the body centerline over the length spanned by the canard section and tail section, respectively (refer to input descriptions for steps 2 and 5).

The job control card stream suitable for use on a CDC 7600 computer is shown in Figure A.6. Basically, program LRCDM2 is run first with the first half of the data of Figure A.5(a) to handle the forebody and the canard section. Upon completion of step 3, program BDYSHD is called to perform step 3a concerned with afterbody vortex shedding using the data of Figure A.5(b). Finally, LRCDM2 is called again with the second half of the data of Figure A.5(a) stored on TAPE2 together with the data shown in Figure A.5(c) to treat the tail section. Data set transfers are organized automatically by the two programs.

The output generated by program LRCDM2 (with print control MINPRN=0 in $INPUT, Item 2 of input for steps 1 and 4) and by optional companion program BDYSHD (with print controls NPRNTS=NPRNTV=1 and program output plot control NPLOTV=3) is shown in Figures A.7(a), A.7(b), and A.7(c). A detailed description of LRCDM2 output is given in Section A.8 of this appendix. Output generated by BDYSHD is discussed in Appendix B.

The first figure contains the output for steps 1 through 3 containing information calculated by LRCDM2 for the forebody and canard section. The right and left horizontal fins are deflected asymmetrically for roll control. For the included angle of attack and forebody length, no forebody vortices are formed. Therfore, module VPATH2 computes zero vortex-induced vortex effects and the fin loading results calculated in step 1 are the same as those printed under step 3.

Since optional program BDYSHD is engaged to treat the afterbody, Figure A.5(a) concludes with a summary of the loads acting on the forebody and canard fins. The forebody loads are determined in step 1 and the canard section loads are calculated in step 3. The basic total load on a canard fin based on Bernoulli loading pressure is given in the output for step 3 under the heading "FIN LOADING INFORMATION" (with ***STEP3 in upper right corner) and subheading "BERNOULLI PRESSURE LOADS..." If the fin has a subsonic leading edge and/or nonzero length side edge, additional loads acting on those edges are calculated with the linear pressure loading and printed a few pages earlier under the heading "L.E. AUGMENTATION..." and/or "S.E. AUGMENTATION..." For example, the total force coefficient acting on the deflected right horizontal fin (Fin 1 or R) in the z_B-direction is made up of the following contributions:

basic: $CZ|_{Bernoulli} = 2.7760$ from fin loading information based on Bernoulli loading pressure

+

additional: $CZADD|_{S.E.} = 0.02325$ from fin loading information based on linear loading pressure

---

$$CZ|_{TOTAL} = 2.79925$$

The basic fin loadings can be calculated with linear or Bernoulli pressure loadings, the additional loadings are always calculated with linear pressure loadings. This procedure holds for all force and moment coefficients acting on fins of a finned section.

The output of Figure A.7(b) contains pressure distribution and vortex field information generated by companion program BDYSHD. Only a subset of the actual output is shown. The analysis starts at the canard trailing edge ($X \equiv x_B = 26.93$) with a set of vortices associated with the forebody and canard section. The vortex characteristics are specified next to the heading "INITIAL VORTICITY DISTRIBUTION." Vortex coordinates Y and Z are specified in the y_B and z_B directions, respectively (see Figure A.4). This information is generated by subroutine SPNLD in step 3 and transferred by means of a data set on TAPE8 to BDYSHD. The output includes optional crossflow plane plots showing the upstream and additional vortices shed from the afterbody in a schematic manner. These plots only serve to visualize the vortex field in the vicinity of the circular cross section afterbody shown as a collection of asterisks. At the end of this output, the final vortex field is indicated and the portion associated with the shed vortices is represented by the two centroids of shed vorticity. The listed force and moment coefficients acting on the afterbody are calculated on the basis of the Bernoulli pressure Equation (6) only. A list of the vortex field data set at the beginning of the tail section ($X = x_B = 80.73$), is printed. It is headed by the two afterbody vortex centroids. Note that this vortex field is not symmetric left to right. The loading and vortex field information is automatically transferred to program LRCDM2 for steps 4 through 6 by means of data sets stored on TAPE9 and TAPE8, respectively.

The printout shown in Figure A.7(c) is generated by program LRCDM2 for steps 4 through 6 of the stepwise procedure described in Section A.4 of this appendix. Because optional step 3a is exercised, the output for step 4 opens with the force and moment coefficients accumulated up to the tail section. This means that the afterbody loads calculated with companion program BDYSHD are added to the accumulated force and moment coefficients for the forebody and canard section.

For example, the force coefficients calculated with Bernoulli pressures and acting in the z_B-direction, CZB, as it appears in the list at the beginning of step 4 is obtained as follows.

$$
\begin{array}{r}
CZB|_{\text{step 3}} = 6.026 \\
+ \\
CZ|_{\text{step 3a}} = 0.40995 \\
\hline
CZB|_{\text{up to tail section}} = 6.436
\end{array}
$$

For this sample case, the output for step 4 (and step 6) is concerned with the tail section only since the afterbody is treated by companion program BDYSHD in step 3a. In step 4, 144 sets of control point coordinates are written onto TAPE4 for use in step 5. Coordinates XCP, YCP, and ZCP are expressed in the rolled body coordinate system x_B, y_B, and z_B, and they are associated with the control points of the constant u-velocity panels on the four tail fins and the interference shell. The total number, NWBP, of panels in the tail section is given by

$$
\begin{aligned}
\text{NWBP} &= \text{NCW(MSWR+MSWL+MSWU+MSWD)} \\
&\quad + \text{NCWB(NBDCR)} \\
&= 4(6+6+6+6) + 4(12) \\
&= 144
\end{aligned}
$$

where NCW,MSWR etc. are listed earlier in this section. The fin loading results printed in the remaining output for step 4 are calculated without the effects of canard-section and afterbody vorticity. Therefore, this calculation is for a set of tail fins mounted on a body with no flow asymmetry other than the fact that the roll angle is set equal to 0.001 as described earlier in this section. Thus, the fin loads are symmetric left to right and the vertical fin loads are near zero. Rolling moment coefficient for the tail fins, CLL, is near zero. None of these loadings are added to the accumulated force and moment coefficients.

In step 5, the effects at points on the tail section due to the vortex field transferred from step 3a (program BDYSHD) are calculated and printed by module VPATH2. In this instance, the paths of the vortices through the tail section are made to lie parallel to the body centerline. This is accomplished by setting NIP=1 and XBEGIN=XEND=80.73 in the input to step 5 [last portion of input shown in Figure A.5(a)]. The list of lateral vortex coordinates and vortex strengths at X=80.73 is the same as the list printed at the end of step 3a, Figure A.7(b).

In order to enlighten the program user, the vortex strengths and vortex numbers are given below together with the source of each vortex.

Vortex	GAMMA/VINF	Source
1	0.86923	Afterbody } centroid representation
2	-3.1134	Afterbody } centroid representation
3	0.021299	Right horizontal canard side edge
4	-0.0058798	Left horizontal canard side edge
5	3.3798	Right horizontal canard trailing edge
6	-2.2259	Left horizontal canard trailing edge
7	-0.093338	Upper vertical canard trailing edge
8	-0.16236	Lower vertical canard trailing edge

The next pages show the perturbation velocity components V and W (along y_B- and z_B-directions) induced by the set of vortices at the 144 control points on the interference shell and tail fins of the tail section. They are stored on TAPE7 for use in the final step 6. Note that the magnitude of the velocity components never exceeds 0.35, the default input value.

In step 6, program LRCDM2 computes the tail section loads including the effects of canard and afterbody vortices. The vortex-induced velocity components are printed under the heading "POINT COORDINATES AND PERTURBATION VELOCITIES CALCULATED BY PROGRAM VPATH2." They are the same as the ones printed at the end of step 5.

The calculated pressures and loads acting on the tail fins are now affected by the asymmetric vortex field. Consequently, in contrast with the results of step 4 the fin loads are no longer symmetric left to right, and the vertical fins now show nonzero loading. The basic tail-section rolling-moment coefficient, CLL, based on Bernoulli pressures is listed as -0.12915. In accordance with the description of output, Section A.8, the contributions due to tail-fin leading- and/or side-edge normal-force augmentations calculated on the basis of linear pressure loading must be added. In this case, the tail-fin leading edge is supersonic (as printed on the fin loading information page), and only the side edges add appreciable contributions. They are printed under the spanwise distributions of the linear pressure loads. The total rolling moment acting on the tail section including fin side-edge effects is obtained as follows.

$CLL|_{Bernoulli} = -0.12915$ basic rolling moment coefficient for four fins

$CLLADD|_{right\ fin\ S.E.} = -0.84428$ appreciable contribution

$CLLADD|_{left\ fin\ S.E.} = 0.93415$ appreciable contribution

$CLLADD|_{upper\ fin\ S.E.} = -0.00447$

$CLLADD|_{lower\ fin\ S.E.} = 0.0$ (not printed)

$CLL|_{total,\ fin\ tail\ section} = -0.04375$

The loads acting on the portion of body next to the fins is then printed. These loads include fin-lift carryover. Since the bodies are assumed circular in LRCDM2, no additional rolling moment is generated.

Finally, the overall force and moment coefficients acting on the entire configuration are listed. As stated earlier at the conclusion of Section A.8, the Bernoulli-pressure based results are considered most valid at least up to Mach number 2.5 or thereabouts. As an example, the tail-section rolling-moment coefficient calculated above (CLL=-0.04375) is added to the rolling moment coefficient listed at the beginning of step 4 (CLL=-1.1351) to give the listed overall value of -1.394. The other force and moment coefficients are added in the same manner. This concludes the output for the sample case. The calculated results are indicated by the flagged solid squares in Figures 5(a) and 5(b) of this report.

Figure A.1.- Subroutine calling sequence of program LRCDM2 including module VPATH2.

(pages 90 through 94)

FLOW CHART OF PROGRAM - LRCDM2

```
PROGRAM
 LRCDM2

   |-- INPUT
   |-- OUTPUT
   |-- TAPE10
   |-- TAPE2
   |-- TAPE4
   |-- TAPE5
   |-- TAPE6
   |-- TAPE7
   |-- TAPE8
   |-- TAPE9
   |-- TOLDS  ---- TAPE6
   |-- DEMON2 ---- TAPE2
   |           |-- TAPE4
   |           |-- TAPE6
   |           |-- TAPE7
   |           |-- TAPE8
   |           |-- VARIAB
   |           |-- SIN
   |           |-- COS
   |           |-- ASIN
   |           |-- TAN
   |           |-- SQRT
   |           |-- LAYOUT ---- COS
   |           |           |-- SIN
   |           |           |-- SQRT
   |           |           |-- TAN
   |           |-- THKIN  ---- TAPE2
   |           |           |-- EDGES
   |           |           |-- THETIN ---- TAPE2
   |           |-- THKOUT ---- TAPE6
   |           |-- THKLYT ---- TAPE6
   |           |           |-- TAN
   |           |-- BDYGEN ---- TAPE2
   |           |           |-- TAPE6
   |           |           |-- SQRT
   |           |           |-- ASIN
   |           |           |-- BODYR  ---- SQRT
   |           |           |-- SOURCE ---- TAPE6
   |           |           |            |-- SQRT
   |           |           |            |-- ALOG
   |           |           |-- DOUBLT ---- TAPE6
   |           |                        |-- SQRT
   |           |                        |-- ALOG
   |           |-- BDYPR  ---- TAPE2
   |           |           |-- TAPE4
   |           |           |-- TAPE6
   |           |           |-- TAPE7
   |           |           |-- ASIN
   |           |           |-- ATAN
   |           |           |-- ROTWF
   |           |           |-- SHKEXP ---- TAPE6
```

```
|           |           |           |-- SHKAGL ---- TAPE6
|           |           |           |           |-- SQRT
|           |           |           |           |-- ASIN
|           |           |           |           |-- ATAN
|           |           |           |           |-- SIN
|           |           |           |           |-- COS
|           |           |           |-- SIN
|           |           |           |-- ATAN
|           |           |           |-- SQRT
|           |           |-- COS
|           |           |-- SIN
|           |           |-- VELCAL ---- SQRT
|           |           |           |-- ATAN2
|           |           |           |-- SOURCE ---- TAPE6
|           |           |           |           |-- SQRT
|           |           |           |           |-- ALOG
|           |           |           |-- DOUBLT ---- TAPE6
|           |           |           |           |-- SQRT
|           |           |           |           |-- ALOG
|           |           |           |-- COS
|           |           |           |-- SIN
|           |           |-- BDYVTX ---- TAPE6
|           |           |           |-- SQRT
|           |           |           |-- SIN
|           |           |-- VORTEX
|           |           |-- SQRT
|           |           |-- ATAN2
|           |           |-- PRCOR  ---- SIN
|           |           |-- TOLDS  ---- TAPE6
|           |           |-- THKVEL ---- TAPE6
|           |           |           |-- VELOTH ---- TAPE6
|           |           |           |           |-- SQRT
|           |           |           |           |-- ALOG
|           |           |           |           |-- ATAN2
|           |           |-- VELNOR ---- TAPE6
|           |                       |-- ROTWF
|           |                       |-- ROTWB
|           |                       |-- VELO   ---- TAPE6
|           |                       |           |-- SQRT
|           |                       |           |-- ATAN2
|           |                       |           |-- ALOG
|           |                       |-- ROTFW
|           |                       |-- ROTBW
|           |-- VELCAL ---- SQRT
|           |           |-- ATAN2
|           |           |-- SOURCE ---- TAPE6
|           |           |           |-- SQRT
|           |           |           |-- ALOG
|           |           |-- DOUBLT ---- TAPE6
|           |           |           |-- SQRT
|           |           |           |-- ALOG
|           |           |-- COS
|           |           |-- SIN
|           |-- VRTVEL ---- TAPE2
|           |           |-- TAPE6
|           |-- VELNOR ---- TAPE6
|           |           |-- ROTWF
|           |           |-- ROTWB
|           |           |-- VELO   ---- TAPE6
|           |           |           |-- SQRT
```

```
|         |         |         |-- ATAN2
|         |         |         |-- ALOG
|         |         |
|         |         |-- ROTFW
|         |         |-- ROTBW
|         |
|         |-- ROTWB
|         |-- ROTWF
|         |-- OUT    ---- TAPE6
|         |-- PAS001
|         |-- THKVEL ---- TAPE6
|         |         |-- VELOTH ---- TAPE6
|         |                   |-- SQRT
|         |                   |-- ALOG
|         |                   |-- ATAN2
|         |
|         |-- PAS002
|         |-- FINVEL ---- TAPE6
|         |         |-- VELCAL ---- SQRT
|         |         |         |-- ATAN2
|         |         |         |-- SOURCE ---- TAPE6
|         |         |         |         |-- SQRT
|         |         |         |         |-- ALOG
|         |         |         |-- DOUBLT ---- TAPE6
|         |         |         |         |-- SQRT
|         |         |         |         |-- ALOG
|         |         |         |
|         |         |         |-- COS
|         |         |         |-- SIN
|         |         |-- VELNOR ---- TAPE6
|         |         |         |-- ROTWF
|         |         |         |-- ROTWB
|         |         |         |-- VELO   ---- TAPE6
|         |         |         |         |-- SQRT
|         |         |         |         |-- ATAN2
|         |         |         |         |-- ALOG
|         |         |         |
|         |         |         |-- ROTFW
|         |         |         |-- ROTBW
|         |         |
|         |         |-- ROTWF
|         |         |-- ROTFW
|         |-- SPECPR ---- TAPE2
|         |         |-- TAPE6
|         |         |-- VELCAL ---- SQRT
|         |         |         |-- ATAN2
|         |         |         |-- SOURCE ---- TAPE6
|         |         |         |         |-- SQRT
|         |         |         |         |-- ALOG
|         |         |         |-- DOUBLT ---- TAPE6
|         |         |         |         |-- SQRT
|         |         |         |         |-- ALOG
|         |         |         |
|         |         |         |-- COS
|         |         |         |-- SIN
|         |         |
|         |         |-- ROTWF
|         |         |-- SIN
|         |         |-- ASIN
|         |         |-- SHKEXP ---- TAPE6
|         |         |         |-- SHKAGL ---- TAPE6
|         |         |         |         |-- SQRT
|         |         |         |         |-- ASIN
|         |         |         |         |-- ATAN
|         |         |         |         |-- SIN
|         |         |         |         |-- COS
|         |         |         |
|         |         |         |-- SIN
|         |         |         |-- ATAN
|         |         |
```

```
|          |          |          |-- SQRT
|          |          |-- COS
|          |          |-- VELNOR ---- TAPE6
|          |          |          |-- ROTWF
|          |          |          |-- ROTWB
|          |          |          |-- VELO   ---- TAPE6
|          |          |          |          |-- SQRT
|          |          |          |          |-- ATAN2
|          |          |          |          |-- ALOG
|          |          |          |-- ROTFW
|          |          |          |-- ROTBW
|          |          |-- THKVEL ---- TAPE6
|          |          |          |-- VELOTH ---- TAPE6
|          |          |                     |-- SQRT
|          |          |                     |-- ALOG
|          |          |                     |-- ATAN2
|          |          |-- CPBERN
|          |          |-- SQRT
|          |          |-- ATAN2
|          |          |-- ATAN
|          |          |-- PRCOR  ---- SIN
|          |          |-- SPECLD ---- TAPE6
|          |                     |-- ROTBW
|          |                     |-- ROTWF
|          |                     |-- SIN
|          |                     |-- ROTFW
|          |                     |-- ATAN
|          |                     |-- TOLDS  ---- TAPE6
|          |                     |-- SPNLD  ---- TAPE6
|          |                                |-- TAPE8
|          |                                |-- SIN
|          |                                |-- COS
|          |                                |-- ATAN
|          |                                |-- ROTWF
|          |                                |-- ASIN
|          |                                |-- TAN
|          |                                |-- ROTFW
|          |                                |-- TOLDS    ---- TAPE6
|          |-- BDYAFT
|-- VPATH2 ---- TAPE2
|          |-- TAPE4
|          |-- TAPE6
|          |-- TAPE7
|          |-- TAPE8
|          |-- EOF
|          |-- SQRT
|          |-- SHAPE  ---- SQRT
|          |-- COS
|          |-- SIN
|          |-- ASIN
|          |-- DASCRU ---- F      ---- FCT    ---- COS
|          |                     |          |-- SQRT
|          |                     |-- SIMP   ---- F1
|          |                     |-- Z      ---- CSQRT
|          |                     |-- SHAPE  ---- SQRT
|          |                     |-- SQRT
|          |                     |-- PITROL ---- CSQRT
|          |                     |          |-- SIN
|          |                     |-- SYMFIN ---- SQRT
|          |                     |          |-- CSQRT
```

```
|           |                         |           |-- CLOG
|           |                         |           |-- ACOS
|           |                         |-- CRUCI  ---- TAPE6
|           |                         |           |-- FCT       ---- COS
|           |                         |           |                 |-- SQRT
|           |                         |           |-- SIMP      ---- F1
|           |                         |           |-- ACOS
|           |                         |           |-- COS
|           |                         |           |-- SIN
|           |                         |           |-- CSQRT
|           |                         |           |-- CEXP
|           |                         |           |-- CABS
|           |                         |           |-- SQRT
|           |                         |-- VOTEX  ---- Z         ---- CSQRT
|           |                         |-- COS
|           |-- PLOTVB ---- TAPE6
|           |           |-- COS
|           |           |-- SIN
|           |           |-- SQRT
|           |           |-- PLOTA2 ---- TAPE6
|           |           |             |-- PLOTA8 ---- TAPE6
|           |           |             |            |-- PLOTA6 ---- TAPE6
|           |           |             |            |             |-- ALOG10
|           |           |             |            |-- PLOTA5 ---- TAPE6
|           |           |             |-- PLOTA7
|           |           |-- PLOTA3 ---- COS
|           |                         |-- SIN
|           |                         |-- SQRT
|           |-- VVELS
|-- INTROT ---- TAPE6
|           |-- TAPE8
|           |-- COS
|           |-- SIN
|-- RESTRT ---- TAPE2
            |-- TAPE6
            |-- TAPE9
            |-- TOLDS  ---- TAPE6

PROGRAM
  END
```

Figure A.2.- Common Block cross reference map
for program LRCDM2.

(pages 96 through 99)

CROSS REFERENCE MAP PAGE = 1

SUBROUTINE NAME / COMMON BLOCKS	BDYGEN	BDYPR	BDYVTX	BODYR	CPBERN	CRUCI	DASCRU	DEMON2	DOUBLT	EDGES	FCT	FINVEL	F	INTROT	LAYOUT	LRCDM2	OUT	PASO01	PASO02	PITROL	PLOTA2	PLOTA3	PLOTA5	PLOTA6	PLOTA7	PLOTA8	PLOTV8	PLOTV2	PRCOR	RESTRT	ROTATE	SHAPE	SHKAGL	SHKEXP	SIMP	SOURCE	SPECLD	SPECPR	SPNLD	SYMFIN
BLK1						X							X							X																				X
BLK2													X																											
BPLTA1																					X				X	X		X												
BPLTA2																					X																			
BSCALE																					X					X		X												
BSCAL2																						X																		
BVEL		X						X				X																									X	X		
CTRANS	X	X						X				X				X																					X	X	X	
CX		X														X														X							X		X	
DBUGA																							X	X		X														
DIGTAT								X								X																								
ELLIPS		X						X				X			X																						X	X		
FINLE								X																															X	
FINSE								X																															X	
FINTE								X																															X	
FM														X		X																								
FRCDIS												X																									X		X	
ICVEL		X						X																														X		
INTRDT								X				X			X																						X	X	X	
NONLIN		X						X																										X			X	X		
OAFM		X						X				X																									X		X	
ONE	X	X			X			X				X			X																X						X	X	X	
PRINT	X	X						X																													X	X	X	
RSTART		X						X								X																								
SPCPRS												X																									X	X		
SPSANG	X	X			X			X				X																									X	X		
STACK	X							X								X														X									X	
SWEEPS		X						X				X			X																						X		X	
THKDAT		X						X																														X		
THKPAN																																								

CROSS REFERENCE MAP PAGE = 2

SUBROUTINE NAME / COMMON BLOCKS	BDYGEN	BDYPR	BDYVTX	BODYR	CPBERN	CRUCI	DASCRU	DEMON2	DOUBLT	EDGES	FCT	FINVEL	F	INTROT	LAYOUT	LRCDM2	OUT	PAS001	PAS002	PITROL
THREE		X						X				X								
THTAS																				
THVARG																				
THVELO								X												
TSPANS								X												
TWO	X	X		X					X											
UVCOND																				
VEL													X							
VORSPC		X						X												
VPTHVL		X						X				X				X				
VRTVX																				
VRTXV		X						X				X			X					
V																				
WBTR1	X	X																		
WBTR	X	X						X				X			X					
/ /						X		X			X									

SUBROUTINE NAME / COMMON BLOCKS	PLOTA2	PLOTA3	PLOTA5	PLOTA6	PLOTA7	PLOTA8	PLOTVB	PLOTV2	PRCOR	RESTRT	ROTATE	SHAPE	SHKAGL	SHKEXP	SIMP	SOURCE	SPECLD	SPECPR	SPNLD	SYMFIN
THREE																	X	X	X	
THTAS																				
THVARG																				
THVELO																				
TSPANS																				
TWO										X						X				
UVCOND																				
VEL												X								
VORSPC																				
VPTHVL																	X	X	X	
VRTVX																			X	
VRTXV																	X	X		
V																				
WBTR1																				
WBTR																	X		X	
/ /																				

CROSS REFERENCE MAP

SUBROUTINE NAME / COMMON BLOCKS	THETIN	THKIN	THKLYT	THKOUT	THKVEL	TOLDS	TRBIPW	VELCAL	VELNOR	VELOTH	VELO	VOTEX	VPATH2	VRTVEL	VVELS	Z
BLK1												X				
BLK2													X			
BPLTA1																
BPLTA2																
BSCALE																
BSCAL2																
BVEL								X						X		
CTRANS	X	X				X							X			
CX						X										
DBUGA																
DIGTAT																
ELLIPS																
FINLE																
FINSE																
FINTE																
FM						X										
FRCDIS																
ICVEL					X											
INTRDT									X							
NONLIN						X										
OAFM																
ONE			X				X	X	X		X			X		
PRINT													X			
RSTART																
SPCPRS																
SPSANG																
STACK						X		X					X			
SWEEPS																
THKDAT	X	X	X	X	X											
THKPAN			X		X											

CROSS REFERENCE MAP PAGE = 4

SUBROUTINE NAME / COMMON BLOCKS	THETIN	THKIN	THKLYT	THKOUT	THKVEL	TOLDS	TRBIPW	VELCAL	VELNOR	VELOTH	VELO	VOTEX	VPATH2	VRTVEL	VVELS	Z				
THREE																				
THTAS	X	X																		
THVARG					X					X										
THVELO										X										
TSPANS		X																		
TWO								X												
UVCOND									X		X									
VEL													X							
VORSPC														X						
VPTHVL																				
VRTVX																				
VRTXV														X						
V												X				X				
WBTR1																				
WBTR								X	X											
/ /													X							

Figure A.3.- Subroutine cross reference map for program LRCDM2.

(pages 102 through 107)

CROSS REFERENCE MAP PAGE = 1

SUBROUTINE NAME / EXTERNAL REFERENCES	BDYGEN	BDYPR	BDYVTX	BODYR	CPBERN	CRUCI	DASCRU	DEMON2	DOUBLT	EDGES	FCT	FINVEL	F	INTROT	LAYOUT	LRCDM2	OUT	PAS001	PAS002	PITROL	PLOTA2	PLOTA3	PLOTA5	PLOTA6	PLOTA7	PLOTA8	PLOTVB	PLOTV2	PRCORR	RESTRT	ROTATE	SHAPE	SHKAGL	SHKEXP	SIMP	SOURCE	SPECLO	SPECPR	SPNLD	SYMFIN
ACOS						X																																		X
ALOG10																								X																
ALOG									X																											X				
ASIN	X	X						X																									X					X	X	
ATAN2		X																																				X		
ATAN		X																															X	X			X	X	X	
BDYAFT								X																																
BDYGEN								X																																
BDYPR								X																																
BDYVTX		X																																						
BODYR	X																																							
CABS						X																																		
CEXP						X																																		
CLOG																																								X
COS		X				X		X			X		X	X	X							X					X				X		X					X	X	
CPBERN																																						X		
CRUCI													X																											
CSQRT						X														X																				X
DASCRU																																								
DEMON2																X																								
DOUBLT	X																																							
EDGES																																								
EOF																																								
FCT						X							X																											
FINVEL								X																																
F1																																			X					
F							X																																	
INPUT																X																								
INTROT																X																								
LAYOUT								X																																

CROSS REFERENCE MAP PAGE = 2

SUBROUTINE NAME / EXTERNAL REFERENCES	BDYGEN	BDYPRT	BDYVTX	BODYR	CPBERN	CRUCCI	DASCRU	DEMON2	DOUBLT	EDGES	FCT	FINVEL	F	INTROT	LAYOUT	LRCDM2	OUT	PAS001	PAS002	PITROL
OUTPUT																X				
OUT								X												
PAS001								X												
PAS002								X												
PITROL													X							
PLOTA2																				
PLOTA3																				
PLOTA5																				
PLOTA6																				
PLOTA7																				
PLOTA8																				
PLOTV8																				
PRCOR		X																		
RESTRT																X				
ROTBW																				
ROTFW												X								
ROTWB								X												
ROTWF		X						X				X								
SHAPE													X							
SHKAGL																				
SHKEXP		X																		
SIMP						X							X							
SIN		X	X			X		X						X	X					X
SOURCE	X																			
SPECLD																				
SPECPR								X												
SPNLD																				
SQRT	X	X	X	X		X		X	X		X		X		X					
SYMFIN													X							
TAN								X							X					

SUBROUTINE NAME / EXTERNAL REFERENCES	PLOTA2	PLOTA3	PLOTA5	PLOTA6	PLOTA7	PLOTA8	PLOTV8	PLOTV2	PRCOR	RESTRT	ROTATE	SHAPE	SHKAGL	SHKEXP	SIMP	SOURCE	SPECLD	SPECPR	SPNLD	SYMFIN
OUTPUT																				
OUT																				
PAS001																				
PAS002																				
PITROL																				
PLOTA2							X													
PLOTA3							X													
PLOTA5						X														
PLOTA6						X														
PLOTA7	X							X												
PLOTA8	X							X												
PLOTV8																				
PRCOR																				
RESTRT																		X		
ROTBW																	X			
ROTFW																	X		X	
ROTWB																				
ROTWF																	X	X	X	
SHAPE																				
SHKAGL														X						
SHKEXP																				
SIMP																		X		
SIN		X					X		X		X		X	X			X	X	X	
SOURCE																				
SPECLD																		X		
SPECPR																				
SPNLD																	X			
SQRT		X					X					X	X	X		X		X		X
SYMFIN																				
TAN																			X	

CROSS REFERENCE MAP PAGE = 3

SUBROUTINE NAME / EXTERNAL REFERENCES	BDYGEN	BDYPR	BDYVTX	BODYER	COPBRN	CRUCI	DASCRU	DEMON2	DOUBLT	EDGES	FCT	FINVEL	F	INTROT	LAYOUT	LRCDM2	OUT	PAS001	PAS002	PITROL
TAPE10																X				
TAPE2	X	X						X								X				
TAPE4		X						X								X				
TAPE5																X				
TAPE6	X	X	X			X		X	X			X		X		X	X			
TAPE7		X						X								X				
TAPE8								X						X		X				
TAPE9																X				
THETIN																				
THKIN								X												
THKLYT								X												
THKOUT								X												
THKVEL		X						X												
TOLDS		X														X				
VARIAB								X												
VELCAL		X						X				X								
VELNOR		X						X				X								
VELOTH																				
VELO																				
VORTEX		X																		
VOTEX													X							
VPATH2																X				
VRTVEL								X												
VVELS																				
Z													X							

SUBROUTINE NAME / EXTERNAL REFERENCES	PLOTA2	PLOTA3	PLOTA5	PLOTA6	PLOTA7	PLOTA8	PLOTVB	PLOTV2	PRCOR	RESTRT	ROTATE	SHAPE	SHKAGL	SHKEXP	SIMP	SOURCE	SPECLD	SPECPR	SPNLD	SYMFIN
TAPE10																				
TAPE2										X								X		
TAPE4																				
TAPE5																				
TAPE6	X		X	X		X	X	X		X			X	X		X	X	X	X	
TAPE7																				
TAPE8																			X	
TAPE9										X										
THETIN																				
THKIN																				
THKLYT																				
THKOUT																				
THKVEL																		X		
TOLDS										X							X		X	
VARIAB																				
VELCAL																		X		
VELNOR																		X		
VELOTH																				
VELO																				
VORTEX																				
VOTEX																				
VPATH2																				
VRTVEL																				
VVELS																				
Z																				

CROSS REFERENCE MAP PAGE = 4

SUBROUTINE NAME / EXTERNAL REFERENCES	THETIN	THKIN	THKLYT	THKOUT	THKVEL	TOLDS	TRBIPW	VELCAL	VELNOR	VELOTH	VELO	VOTEX	VPATH2	VRTVEL	VVELS	Z
ACOS																
ALOG10																
ALOG										X	X					
ASIN													X			
ATAN2								X		X	X					
ATAN																
BDYAFT																
BDYGEN																
BDYPR																
BDYVTX																
BODYR																
CABS																
CEXP																
CLOG																
COS								X					X			
CPBERN																
CRUCI																
CSQRT																X
DASCRU													X			
DEMON2																
DOUBLT								X								
EDGES		X														
EOF													X			
FCT																
FINVEL																
F1																
F																
INPUT																
INTROT																
LAYOUT																

CROSS REFERENCE MAP

PAGE = 5

SUBROUTINE NAME / EXTERNAL REFERENCES	THETIN	THKIN	THKLYT	THKOUT	THKVEL	TOLDS	TRBIPW	VELCAL	VELNOR	VELOTH	VELO	VOTEX	VPATH2	VRTVEL	VVELS	Z
OUTPUT																
OUT																
PAS001																
PAS002																
PITROL																
PLOTA2																
PLOTA3																
PLOTA5																
PLOTA6																
PLOTA7																
PLOTA8																
PLOTVB													X			
PRCOR																
RESTRT																
ROTBW									X							
ROTFW									X							
ROTWB									X							
ROTWF									X							
SHAPE													X			
SHKAGL																
SHKEXP																
SIMP																
SIN								X					X			
SOURCE								X								
SPECLD																
SPECPR																
SPNLD																
SQRT								X		X	X		X			
SYMFIN																
TAN			X													

CROSS REFERENCE MAP

PAGE = 6

SUBROUTINE NAME / EXTERNAL REFERENCES	THETIN	THKIN	THKLYT	THKOUT	THKVEL	TOLDS	TRBIPW	VELCAL	VELNOR	VELOTH	VELO	VOTEX	VPATH2	VRTVEL	VVELS	Z
TAPE10																
TAPE2	X	X											X	X		
TAPE4													X			
TAPE5																
TAPE6			X	X	X	X			X	X	X		X	X		
TAPE7													X			
TAPE8													X			
TAPE9																
THETIN		X														
THKIN																
THKLYT																
THKOUT																
THKVEL																
TOLDS																
VARIAB																
VELCAL																
VELNOR																
VELOTH					X											
VELO									X							
VORTEX																
VOTEX																
VPATH2																
VRTVEL																
VVELS													X			
Z												X				

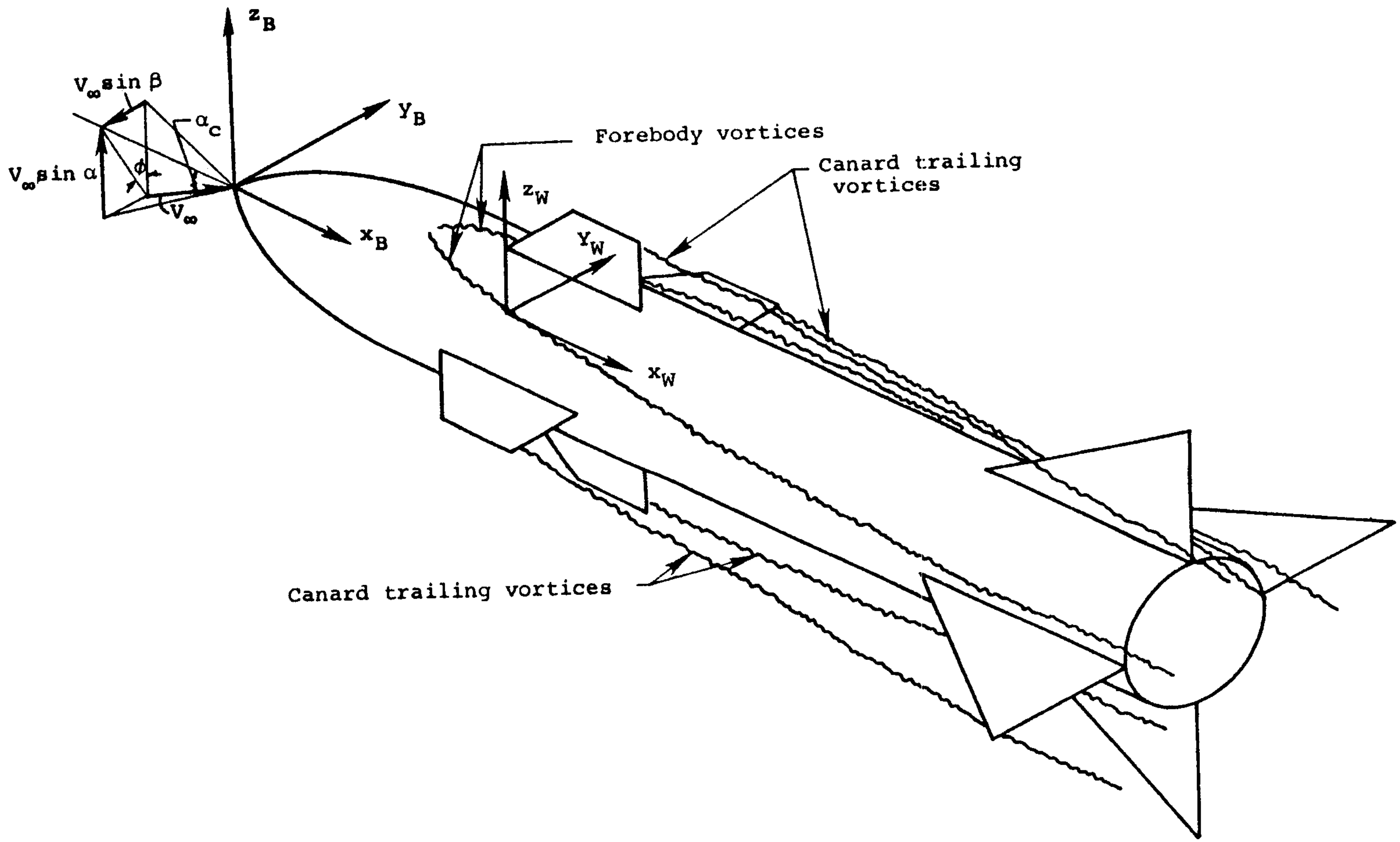

Figure A.4.- General axisymmetric body - cruciform forward fins - cruciform tail fin configuration at included angle of attack α_c and roll angle ϕ showing vortex field.

PRECEDING PAGE BLANK NOT FILMED

Figure A.5.- Input for TF-4 with king tails, roll control.

(pages 112 through 113)

```
    1     3
    1
15.0
    1
0.001
 NASA/LRC TF-4 WITH KING TAIL, FOREBODY AND CANARD SECTION   (ROLL CONTROL)
 $INPUT
 CRP=11.13,CRPV=11.13, SWLEP=47.1, SWLEV=47.1, B2=7.23, B2V=7.23,
 DELR=5.0, DELL=-5.0,
 RA=2.115,RB=2.115,
 NOLINP=1, NDRAG=1, NCRX=1, NBDYPP=1,
 FMACH=2.5,
 SREF=14.12, REFL=4.23, NCPOUT=1,
 XM=46.04, XWLE=15.8,
 NCW=4, MSWR=6, MSWL=6, MSWU=6, MSWD=6,
 NCWB=4, NBDCR=12, BIL=11.13,
 NBSHED=1,
 $END
 $BODY
 NXBODY=50, LNOSE=9.518, LBODY=102.32, BCODE=2,
 $END
 TRACK BODY NOSE VORTICES OVER CANARD SECTION, TF-4, KING TAIL
         1        0        1         1         0         0
26.93
2.115
0.001      0.35
         1
15.8       15.8
   0
 NASA/LRC TF-4 WITH KING TAIL, AFTERBODY AND TAIL SECTION
 $INPUT
 CRP=21.59, CRPV=21.59, SWLEP=45.0, SWLEV=45.0, B2=9.04, B2V=9.04,
 NCW=4, MSWR=6, MSWL=6, MSWU=6, MSWD=6,
 RA=2.115,RB=2.115,
 NCWB=4, NBDCR=12, BIL=21.59,
 NOLINP=1, NDRAG=1, NCRX=1,
 FMACH=2.5,NBSHED=1,
 SREF=14.12, REFL=4.23,
 NBDYPR=1, NCPOUT=1, ITAIL=1,
 XM=46.04, XWLE=80.73, XSTART=80.73,
 $END
 TRACK VORTICES ALONG AFTERBODY AND TAIL SECTION, TF-4, KING TAIL
         1        0        1         1         0         0
102.32
2.115
0.001      0.35
         1
80.73       80.73
END
```

(a) Steps 1-3 and steps 4-6 for later use

```
   0    0    1    1    0    0    1    2    1    8    0    0    0    0    0
   2    0    1    1    3    1    0
    VORTEX CHARACTERISTICS AT CANARD T.E.
  TF-4 WITH KING TAILS    ALPHA=15.0     PHI=0.001   MACH=2.5
14.12       4.23        46.04       102.32      4.23
15.0        0.001       277000.     1.0         2.5
26.93       80.73       2.115       1.05        0.0         1.0         0.25
0.1         0.0         0.0         0.0         0.0
    1
26.0
2.115
0.0
 26.93       35.39       43.85       52.31       60.77       69.23       77.69       80.73
0.0         0.0         0.0         0.0         0.0
 $BODY
 NXBODY=50, LNOSE=15.8, LBODY=102.32, BCODE=2,
 $END
```

(b) Step 3a, input for program BDYSHD

```
      4     6
      1
  15.0
      1
  0.001
```

(c) Remaining input for steps 4-6

```
BACKLOG                      0        0         0       0 CPU-HRS


NASA/AMES FL 7600. SCOPE 2.1.5 533   ( 12/17/82 ) 12/30/82        82364
SYS DEVICES 844/ 8/PF 819/ 2/   FLS=200K FLL=1750K MXS=160K MXL=1200K MXB=1357B

HH.MM.SS CPU SECOND ORIGIN
           08.05.57.ARS. YU      NASA - AMES - CF       508-3      11/21/82
08.05.41 00000.007 ARC.        -COMBO,T150,YD1,YL1,PN.
08.05.42 00000.014 USR.         ACCOUNT,RKRGDK,R0722C3.
08.05.44 00000.097 JOB.        -MOUNT,VSN=D0075C,SN=RKRGDK1.
08.06.48 00000.103 ARC.           RP320 -  EST  16  ASSIGNED
08.06.49 00000.115 ARC.           RP570 - VSN D0075C OF SET RKRGDK1 MOUNTED
08.06.49 00000.120 JOB.        -ATTACH,BLRCDM,ID=KLENKE,SN=RKRGDK1.
08.06.49 00000.121 ARC.           PF053 - LFN  IS   BLRCDM
08.06.50 00000.125 ARC.           PF254 - CYCLE     9 ATTACHED FROM SN=RKRGDK1
08.06.50 00000.126 JOB.        -ATTACH,BBDYSHD,ID=KLENKE,SN=RKRGDK1.
08.06.50 00000.126 ARC.           PF053 - LFN  IS   BBDYSHD
08.06.50 00000.131 ARC.           PF254 - CYCLE   10 ATTACHED FROM SN=RKRGDK1
08.06.50 00000.131 LOD.        -BLRCDM,PL=99999.
08.06.50 00000.139 ARC.           RP727 - VSN D0075C OF SET RKRGDK1 MOUNTED
08.07.59 00001.291 ARC.           LD610 - FLS REQUIRED TO LOAD - 0032663 OU.COG
08.07.59 00001.294 ARC.           LD603 - EXECUTION INITIATED OS.EXP           run steps 1-3
08.07.59 00001.294 USR.         FORTRAN LIBRARY 528             11/04/81       (LRCDM2)
08.08.46 00025.881 USR.             STOP
08.08.46 00025.881 USR.             156400    FINAL EXECUTION FL.
08.08.46 00025.881 USR.             24.586 CP SECONDS EXECUTION TIME.
08.08.46 00025.882 LOD.        -BBDYSHD,PL=99999.
08.08.46 00025.889 ARC.           RP727 - VSN D0075C OF SET RKRGDK1 MOUNTED
08.08.48 00026.555 ARC.           LD610 - FLS REQUIRED TO LOAD - 0024200 OU.COG
08.08.48 00026.557 ARC.           LD603 - EXECUTION INITIATED OS.EXP           run step 3a
08.08.48 00026.558 USR.         FORTRAN LIBRARY 528             11/04/81       (BDYSHD)
08.09.04 00038.669 USR.             STOP
08.09.04 00038.669 USR.             101600    FINAL EXECUTION FL.
08.09.04 00038.670 USR.             12.110 CP SECONDS EXECUTION TIME.
08.09.04 00038.670 LOD.        -BLRCDM,PL=99999.
08.09.06 00039.823 ARC.           LD610 - FLS REQUIRED TO LOAD - 0032663 OU.COG
08.09.06 00039.826 ARC.           LD603 - EXECUTION INITIATED OS.EXP           run steps 4-6
08.09.06 00039.826 USR.         FORTRAN LIBRARY 528             11/04/81       (LRCDM2)
08.09.38 00066.930 USR.             STOP
08.09.38 00066.930 USR.             156400    FINAL EXECUTION FL.
08.09.38 00066.931 USR.             27.102 CP SECONDS EXECUTION TIME.
08.09.38 00066.931 JOB.        -EXIT,U.
08.09.39 00066.938 ARC.           JM166 - MAXIMUM USER SCM          156400B WORDS
08.09.39 00066.939 ARC.           JM167 - MAXIMUM USER LCM          230000B WORDS
08.09.39 00066.939 ARC.           JM170 - MAXIMUM JS*IO LCM             240B BUFFERS
08.09.39 00066.939 ARC.           RM770 - MAXIMUM ACTIVE FILES                   7
08.09.39 00066.939 ARC.           RM771 - OPEN/CLOSE CALLS                      86
08.09.39 00066.940 ARC.           RM772 - DATA TRANSFER CALLS               10,609
08.09.39 00066.940 ARC.           RM773 - CONTROL/POSITIONING CALLS             49
08.09.39 00066.940 ARC.           RM774 - BM DATA TRANSFER CALLS             1,151
08.09.39 00066.940 ARC.           RM775 - BM CONTROL/POSITIONING CALLS         165
08.09.39 00066.940 ARC.           RM776 - QUEUE MANAGER CALLS                  207
08.09.39 00066.941 ARC.           RM777 - RECALL CALLS                         174
08.09.39 00066.941 ARC.           SCM               3 415.385  KWS
08.09.39 00066.941 ARC.           LCM               4 192.283  KWS
08.09.39 00066.942 ARC.           I/O                   0.155  MW
08.09.39 00066.942 ARC.           RMS                   5.953  MWS
08.09.39 00066.942 ARC.           USER                 62.999  SEC
08.09.39 00066.942 ARC.           JOB                  66.944  SEC
08.09.39 00066.942 ARC.           DIO                 460.938  KW
08.09.39 00066.942 ARC.           MAXS=0160K MAXL=0230K MAXB=0470B
08.09.39 00066.943 ARC.               .97 PRIORITY N ACCOUNTING UNITS =      $15.52
08.09.39 00066.943 ARC.           SC050 - 000352 SC/LC SWAPS
```

Figure A.6.- Typical job control language for use of program LRCDM2 with companion program BDYSHD.

PRECEDING PAGE BLANK NOT FILMED

PAGE A-114 INTENTIONALLY BLANK

(a) Steps 1-3, program LRCDM2

Figure A.7.- Sample case output for TF-4 with king tails, roll control.

(pages 118 through 168)

PRECEDING PAGE BLANK NOT FILMED

MISSILE DETAILED

AERODYNAMICS

PROGRAM

L R C D M 2

FOR NASA/LRC
SUPERSONIC BRANCH

DECEMBER, 1982

M.F.E.DILLENIUS D.KLENKE

NIELSEN
ENGINEERING AND RESEARCH, INC.
(415) 968-9457

STEP 1 LOADS ON FORWARD FINS WITHOUT EFFECTS OF NOSE VORTICES

NASA/LRC TF-4 WITH KING TAIL (D), FOREBODY AND CANARD SECTION

```
$INPUT
BIL     = .1113E+02,
B2      = .723E+01,
B2V     = .723E+01,
CRP     = .1113E+02,
CRPV    = .1113E+02,
DELD    = 0.0,
DELL    = -.5E+01,
DELR    = .5E+01,
DELU    = 0.0,
ERATIO  = .1E+01,
FAC     = .95E+00,
FKLE    = .5E+00,
FKSE    = .1E+01,
FMACH   = .25E+01,
ITAIL   = 0,
JCPT    = 0,
LVSWP   = 0,
MINPRN  = 0,
MSWD    = 6,
MSWL    = 6,
MSWR    = 6,
MSWU    = 6,
NBDCR   = 12,
NBDYPR  = 1,
NBSHED  = 1,
NCPOUT  = 1,
NCRX    = 1,
NCW     = 4,
NCWB    = 4,
NCWT    = 0,
NDRAG   = 1,
NFVNPR  = 0,
NOLINP  = 1,
NOUT    = 0,
NPR     = 0,
NPRESS  = 0,
NTDAT   = 0,
NTPR    = 0,
NVLIN   = 0,
NVRTPL  = 1,
NVRTX   = 0,
N2DPRB  = 0,
N2DPRF  = 0,
PHIDIH  = 0.0,
PHIFR   = 0.0,
PHIFL   = 0.0,
PHIFU   = .9E+02,
PHIFD   = .9E+02,
PHIINT  = 0.0,
RA      = .2115E+01,
RB      = .2115E+01,
REFL    = .423E+01,
SREF    = .1412E+02,
SWLEP   = .471E+02,
SWLEV   = .471E+02,
SWTEP   = 0.0,
SWTEV   = 0.0,
THETIT  = 0.0,
THETR   = 0.0,
THETL   = 0.0,
THETU   = .9E+02,
THETD   = .9E+02,
TOLFAC  = .1E+01,
VRTMAX  = .35E+00,
XM      = .4604E+02,
XSTART  = 0.0,
XWLE    = .158E+02,
ZM      = 0.0,
$END
```

FIN SECTION GEOMETRY DESCRIPTION

NO. OF CHORDWISE PANELS ON FINS PRESENT (NCW) = 4

FIN PROPERTY		FIN 1 OR R	FIN 2 OR L	FIN 3 OR U	FIN 4 OR D
NO. OF PANELS - SPANWISE	(MSW) =	6	6	6	6
ROOT CHORD	(CR) =	11.130	11.130	11.130	11.130
LEADING EDGE SWEEP	(SWLE) =	47.100	47.100	47.100	47.100
TRAILING EDGE SWEEP	(SWTE) =	0.000	0.000	0.000	0.000
EXPOSED SEMISPAN	(B2) =	7.230	7.230	7.230	7.230
FIN DIHEDRAL	(PHIF) =	0.000	0.000	90.000	90.000
BODY ANGLE OF FIN ATTACHMENT	(THET) =	0.000	0.000	90.000	90.000
FIN DEFLECTION	(DEL) =	5.000	-5.000	0.000	0.000
Y-INTERSECTION OF FIN TO BODY	(YBOD) =	2.115	-2.115	-.000	.000
Z-INTERSECTION OF FIN TO BODY	(ZBOD) =	0.000	-.000	2.115	-2.115

FIN GEOMETRY

TIP CHORD = 3.34959

ROOT CHORD = 11.13000

FIN SEMISPAN = 7.23000

LEADING EDGE SWEEP = 47.10000 DEGREES

TRAILING EDGE SWEEP = 0.00000 DEGREES

FLOW CONDITIONS

MACH = 2.50000 ALPHAC= 15.00000 PHI = .00100 ALFA = 15.00000 BETA = .00026

CRPT = 11.13000
CRPTV = 11.13000

CONTROL POINTS WRITTEN ON TAPE4 FROM SUBROUTINE DEMON2

I	XCPT	YCPT	ZCPT
1	18.928	2.7051	0.
2	21.551	2.7051	0.
3	24.175	2.7051	0.
4	26.799	2.7051	0.
5	19.915	3.9083	0.
6	22.215	3.9083	0.
7	24.515	3.9083	0.
8	26.815	3.9083	0.
9	20.902	5.1110	0.
10	22.878	5.1110	0.
11	24.855	5.1110	0.
12	26.831	5.1110	0.
13	21.888	6.3127	0.
14	23.541	6.3127	0.
15	25.194	6.3127	0.
16	26.847	6.3127	0.
17	22.873	7.5129	0.
18	24.203	7.5129	0.
19	25.533	7.5129	0.
20	26.863	7.5129	0.
21	23.855	8.7099	0.
22	24.863	8.7099	0.
23	25.871	8.7099	0.
24	26.880	8.7099	0.
25	18.928	-2.7051	0.
26	21.551	-2.7051	0.
27	24.175	-2.7051	0.
28	26.799	-2.7051	0.
29	19.915	-3.9083	0.
30	22.215	-3.9083	0.
31	24.515	-3.9083	0.
32	26.815	-3.9083	0.
33	20.902	-5.1110	0.
34	22.878	-5.1110	0.
35	24.855	-5.1110	0.
36	26.831	-5.1110	0.
37	21.888	-6.3127	0.
38	23.541	-6.3127	0.
39	25.194	-6.3127	0.
40	26.847	-6.3127	0.
41	22.873	-7.5129	0.
42	24.203	-7.5129	0.
43	25.533	-7.5129	0.
44	26.863	-7.5129	0.
45	23.855	-8.7099	0.
46	24.863	-8.7099	0.
47	25.871	-8.7099	0.
48	26.880	-8.7099	0.
49	18.928	0.	2.7051
50	21.551	0.	2.7051
51	24.175	0.	2.7051
52	26.799	0.	2.7051
53	19.915	0.	3.9083
54	22.215	0.	3.9083
55	24.515	0.	3.9083
56	26.815	0.	3.9083
57	20.902	0.	5.1110
58	22.878	0.	5.1110
59	24.855	0.	5.1110
60	26.831	0.	5.1110
61	21.888	0.	6.3127
62	23.541	0.	6.3127
63	25.194	0.	6.3127
64	26.847	0.	6.3127
65	22.873	0.	7.5129
66	24.203	0.	7.5129
67	25.533	0.	7.5129
68	26.863	0.	7.5129
69	23.855	0.	8.7099
70	24.863	0.	8.7099
71	25.871	0.	8.7099
72	26.880	0.	8.7099
73	18.928	0.	-2.7051
74	21.551	0.	-2.7051
75	24.175	0.	-2.7051
76	26.799	0.	-2.7051
77	19.915	0.	-3.9083
78	22.215	0.	-3.9083
79	24.515	0.	-3.9083
80	26.815	0.	-3.9083
81	20.902	0.	-5.1110
82	22.878	0.	-5.1110
83	24.855	0.	-5.1110
84	26.831	0.	-5.1110
85	21.888	0.	-6.3127
86	23.541	0.	-6.3127
87	25.194	0.	-6.3127
88	26.847	0.	-6.3127
89	22.873	0.	-7.5129
90	24.203	0.	-7.5129
91	25.533	0.	-7.5129
92	26.863	0.	-7.5129
93	23.855	0.	-8.7099
94	24.863	0.	-8.7099
95	25.871	0.	-8.7099
96	26.880	0.	-8.7099
97	18.443	1.9733	.52875
98	18.443	1.4446	1.4446
99	18.443	.52875	1.9733
100	18.443	-.52875	1.9733
101	18.443	-1.4446	1.4446
102	18.443	-1.9733	.52875
103	18.443	-1.9733	-.52875
104	18.443	-1.4446	-1.4446
105	18.443	-.52875	-1.9733
106	18.443	.52875	-1.9733
107	18.443	1.4446	-1.4446
108	18.443	1.9733	-.52875
109	21.226	1.9733	.52875
110	21.226	1.4446	1.4446
111	21.226	.52875	1.9733
112	21.226	-.52875	1.9733
113	21.226	-1.4446	1.4446
114	21.226	-1.9733	.52875
115	21.226	-1.9733	-.52875
116	21.226	-1.4446	-1.4446
117	21.226	-.52875	-1.9733
118	21.226	.52875	-1.9733
119	21.226	1.4446	-1.4446
120	21.226	1.9733	-.52875
121	24.008	1.9733	.52875
122	24.008	1.4446	1.4446
123	24.008	.52875	1.9733
124	24.008	-.52875	1.9733
125	24.008	-1.4446	1.4446
126	24.008	-1.9733	.52875
127	24.008	-1.9733	-.52875
128	24.008	-1.4446	-1.4446
129	24.008	-.52875	-1.9733
130	24.008	.52875	-1.9733
131	24.008	1.4446	-1.4446
132	24.008	1.9733	-.52875
133	26.791	1.9733	.52875
134	26.791	1.4446	1.4446
135	26.791	.52875	1.9733
136	26.791	-.52875	1.9733
137	26.791	-1.4446	1.4446
138	26.791	-1.9733	.52875
139	26.791	-1.9733	-.52875
140	26.791	-1.4446	-1.4446
141	26.791	-.52875	-1.9733
142	26.791	.52875	-1.9733
143	26.791	1.4446	-1.4446
144	26.791	1.9733	-.52875

```
$BODY
NXBODY  = 50.

LNOSE   = .9518E+01.

LBODY   = .10232E+03.

BCODE   = 2.

$END
```

PHYSICAL DIMENSIONS OF BODY AND LINE SINGULARITY STRENGTHS REPRESENTING THE BODY AT MACH= 2.5000 ALFAC= 15.0000

	X	R	DR/DX	TX	T(I)	TC(I)
1	0.0000	0.	.46751	0.	.34589	.11034
2	3.1314	1.1884	.29640	.40834	-.31104	-.80658E-01
3	5.1978	1.6959	.19588	1.3121	-.30893E-01	-.72376E-02
4	7.2643	2.0017	.10079	2.6778	-.41636E-01	-.15486E-01
5	9.3307	2.1142	.83352E-02	4.4864	.62544E-02	-.11892E-01
6	11.3971	2.1150	0.	6.5510	.25497E-01	-.46221E-02
7	13.4635	2.1150	0.	8.6175	.34224E-03	-.32877E-03
8	15.5300	2.1150	0.	10.684	.26558E-02	.85085E-03
9	17.5964	2.1150	0.	12.750	.88314E-03	.15202E-02
10	19.6628	2.1150	0.	14.817	.67952E-03	.16413E-02
11	21.7293	2.1150	0.	16.883	.40031E-03	.15407E-02
12	23.7957	2.1150	0.	18.950	.27314E-03	.13180E-02
13	25.8621	2.1150	0.	21.016	.18473E-03	.10582E-02
14	27.9285	2.1150	0.	23.082	.12958E-03	.80390E-03
15	29.9950	2.1150	0.	25.149	.92336E-04	.57904E-03
16	32.0614	2.1150	0.	27.215	.67019E-04	.39330E-03
17	34.1278	2.1150	0.	29.282	.49355E-04	.24817E-03
18	36.1943	2.1150	0.	31.348	.36838E-04	.14040E-03
19	38.2607	2.1150	0.	33.415	.27826E-04	.64483E-04
20	40.3271	2.1150	0.	35.481	.21249E-04	.14158E-04
21	42.3935	2.1150	0.	37.547	.16391E-04	-.16619E-04
22	44.4600	2.1150	0.	39.614	.12761E-04	-.33185E-04
23	46.5264	2.1150	0.	41.680	.10021E-04	-.39960E-04
24	48.5928	2.1150	0.	43.747	.79342E-05	-.40416E-04
25	50.6593	2.1150	0.	45.813	.63298E-05	-.37149E-04
26	52.7257	2.1150	0.	47.880	.50863E-05	-.32007E-04
27	54.7921	2.1150	0.	49.946	.41151E-05	-.26235E-04
28	56.8586	2.1150	0.	52.012	.33509E-05	-.20612E-04
29	58.9250	2.1150	0.	54.079	.27455E-05	-.15575E-04
30	60.9914	2.1150	0.	56.145	.22627E-05	-.11327E-04
31	63.0578	2.1150	0.	58.212	.18753E-05	-.79112E-05
32	65.1243	2.1150	0.	60.278	.15625E-05	-.52800E-05
33	67.1907	2.1150	0.	62.345	.13086E-05	-.33338E-05
34	69.2571	2.1150	0.	64.411	.11013E-05	-.19537E-05
35	71.3236	2.1150	0.	66.477	.93116E-06	-.10201E-05
36	73.3900	2.1150	0.	68.544	.79087E-06	-.42402E-06
37	75.4564	2.1150	0.	70.610	.67461E-06	-.72300E-07
38	77.5228	2.1150	0.	72.677	.57782E-06	.11041E-06
39	79.5893	2.1150	0.	74.743	.49688E-06	.18248E-06
40	81.6557	2.1150	0.	76.810	.42891E-06	.18719E-06
41	83.7221	2.1150	0.	78.876	.37159E-06	.15520E-06
42	85.7886	2.1150	0.	80.942	.32306E-06	.10720E-06
43	87.8550	2.1150	0.	83.009	.28181E-06	.56229E-07
44	89.9214	2.1150	0.	85.075	.24663E-06	.98192E-08
45	91.9879	2.1150	0.	87.142	.21651E-06	-.28342E-07
46	94.0543	2.1150	0.	89.208	.19064E-06	-.57081E-07
47	96.1207	2.1150	0.	91.275	.16835E-06	-.76742E-07
48	98.1871	2.1150	0.	93.341	.14907E-06	-.88497E-07
49	100.2536	2.1150	0.	95.407	.13236E-06	-.93853E-07
50	102.3200	2.1150	0.	97.474	0.	0.

PRESSURE COEFFICIENTS AT POINTS ON BODY MERIDIANS

BODY RING= 1

J	THETA, DEG.	XB	YB	ZB	UTOT	VTOT	WTOT	CP,LIN.	CP,BERN.	DR/DX	P/PINF. BERN.	P/PINF. LIN.
1	15.00000	2.09818	.82572	.22125	-.10464	.23442	.07330	.20929	.10723	.34976	1.46911	1.91563
2	30.00000	2.09818	.74032	.42742	-.08122	.16040	.10310	.16245	.06655	.34976	1.29116	1.71071
3	45.00000	2.09818	.60447	.60447	-.06111	.09606	.10655	.12223	.04098	.34976	1.17927	1.53475
4	60.00000	2.09818	.42742	.74032	-.04568	.04899	.09534	.09137	.02634	.34976	1.11525	1.39972
5	75.00000	2.09818	.22125	.82572	-.03598	.01920	.08213	.07196	.01914	.34976	1.08372	1.31484
6	90.00000	2.09818	-.00000	.85485	-.03267	0.00000	.07653	.06535	.01701	.34976	1.07442	1.28589
7	105.00000	2.09818	-.22125	.82572	-.03598	-.01920	.08213	.07196	.01914	.34976	1.08372	1.31483
8	120.00000	2.09818	-.42742	.74032	-.04568	-.04899	.09534	.09136	.02634	.34976	1.11524	1.39971
9	135.00000	2.09818	-.60447	.60447	-.06111	-.09606	.10655	.12222	.04097	.34976	1.17926	1.53473
10	150.00000	2.09818	-.74032	.42742	-.08122	-.16039	.10309	.16244	.06655	.34976	1.29114	1.71069
11	165.00000	2.09818	-.82572	.22125	-.10464	-.23442	.07330	.20928	.10722	.34976	1.46908	1.91560
12	180.00000	2.09818	-.85485	-.00000	-.12977	-.30437	.01049	.25954	.16693	.34976	1.73031	2.13550
13	195.00000	2.09818	-.82572	-.22125	-.15490	-.35358	-.08425	.30980	.24778	.34976	2.08403	2.35540
14	210.00000	2.09818	-.74032	-.42742	-.17832	-.36679	-.20128	.35664	.34753	.34976	2.52043	2.56031
15	225.00000	2.09818	-.60447	-.60447	-.19843	-.33438	-.32390	.39686	.45695	.34976	2.99914	2.73627
16	240.00000	2.09818	-.42742	-.74032	-.21386	-.25538	-.43185	.42773	.55913	.34976	3.44617	2.87130
17	255.00000	2.09818	-.22125	-.82572	-.22356	-.13836	-.50587	.44713	.63280	.34976	3.76851	2.95618
18	270.00000	2.09818	.00000	-.85485	-.22687	0.00000	-.53221	.45374	.65977	.34976	3.88649	2.98513
19	285.00000	2.09818	.22125	-.82572	-.22356	.13836	-.50587	.44713	.63281	.34976	3.76854	2.95619
20	300.00000	2.09818	.42742	-.74032	-.21386	.25539	-.43185	.42773	.55914	.34976	3.44623	2.87131
21	315.00000	2.09818	.60447	-.60447	-.19843	.33439	-.32390	.39687	.45696	.34976	2.99921	2.73630
22	330.00000	2.09818	.74032	-.42742	-.17832	.36680	-.20128	.35665	.34754	.34976	2.52049	2.56034
23	345.00000	2.09818	.82572	-.22125	-.15491	.35359	-.08425	.30981	.24779	.34976	2.08408	2.35542
24	360.00000	2.09818	.85485	.00000	-.12977	.30438	.01049	.25955	.16694	.34976	1.73035	2.13553

BODY LOADS ON RING 1 AT X= 2.09818

	UNROLLED BODY-AXIS COORDINATES		FIXED OR ROLLED BODY-AXIS COORDINATES	
	LINEAR LOADING	BERNOULLI LOADING	LINEAR LOADING	BERNOULLI LOADING
CX			.14422	.13936
CZ	.15426	.24446	.15426	.24446
CY	-.00000	-.00000	-.00000	-.00000
CM	1.60244	2.53949	1.60244	2.53949
CLN	-.00000	-.00000	-.00003	-.00004

CUMULATIVE BODY LOADS TO THIS STATION

	UNROLLED BODY-AXIS COORDINATES		FIXED OR ROLLED BODY-AXIS COORDINATES	
	LINEAR LOADING	BERNOULLI LOADING	LINEAR LOADING	BERNOULLI LOADING
CX			.14422	.13936
CZ	.15426	.24446	.15426	.24446
CY	-.00000	-.00000	-.00000	-.00000
CM	1.60244	2.53949	1.60244	2.53949
CLN	-.00000	-.00000	-.00003	-.00004

BODY RING= 2

J	THETA. DEG.	XB	YB	ZB	UTOT	VTOT	WTOT	CP.LIN.	CP.BERN.	DR/DX	P/PINF. BERN.	P/PINF. LIN.
1	15.00000	6.23104	1.80950	.48485	-.02296	.05279	.09931	.04592	-.01959	.14785	.91427	1.20090
2	30.00000	6.23104	1.62235	.93667	-.00189	-.02244	.07221	.00377	-.03708	.14785	.83778	1.01651
3	45.00000	6.23104	1.32465	1.32465	.01621	-.06724	.01792	-.03242	-.04252	.14785	.81395	.85818
4	60.00000	6.23104	.93667	1.62235	.03009	-.07409	-.04317	-.06019	-.04110	.14785	.82018	.73668
5	75.00000	6.23104	.48485	1.80950	.03882	-.04699	-.09020	-.07765	-.03770	.14785	.83505	.66030
6	90.00000	6.23104	-.00000	1.87333	.04180	-.00000	-.10777	-.08360	-.03609	.14785	.84212	.63425
7	105.00000	6.23104	-.48485	1.80950	.03882	.04699	-.09021	-.07765	-.03770	.14785	.83505	.66029
8	120.00000	6.23104	-.93667	1.62235	.03010	.07409	-.04317	-.06019	-.04110	.14785	.82018	.73666
9	135.00000	6.23104	-1.32465	1.32465	.01621	.06724	.01792	-.03242	-.04253	.14785	.81395	.85816
10	150.00000	6.23104	-1.62235	.93667	-.00188	.02245	.07220	.00377	-.03708	.14785	.83777	1.01649
11	165.00000	6.23104	-1.80950	.48485	-.02296	-.05278	.09930	.04591	-.01960	.14785	.91426	1.20088
12	180.00000	6.23104	-1.87333	-.00000	-.04557	-.14110	.08516	.09114	.01505	.14785	1.06586	1.39875
13	195.00000	6.23104	-1.80950	-.48485	-.06818	-.21981	.02627	.13637	.07123	.14785	1.31163	1.59662
14	210.00000	6.23104	-1.62235	-.93667	-.08926	-.26684	-.06890	.17852	.15017	.14785	1.65701	1.78100
15	225.00000	6.23104	-1.32465	-1.32465	-.10735	-.26680	-.18164	.21471	.24603	.14785	2.07640	1.93934
16	240.00000	6.23104	-.93667	-1.62235	-.12124	-.21520	-.28757	.24248	.34277	.14785	2.49961	2.06084
17	255.00000	6.23104	-.48485	-1.80950	-.12997	-.12003	-.36280	.25994	.41631	.14785	2.82138	2.13722
18	270.00000	6.23104	.00000	-1.87333	-.13295	-.00000	-.38999	.26589	.44397	.14785	2.94236	2.16327
19	285.00000	6.23104	.48485	-1.80950	-.12997	.12003	-.36281	.25994	.41632	.14785	2.82141	2.13723
20	300.00000	6.23104	.93667	-1.62235	-.12124	.21520	-.28758	.24248	.34278	.14785	2.49967	2.06085
21	315.00000	6.23104	1.32465	-1.32465	-.10736	.26680	-.18164	.21471	.24605	.14785	2.07646	1.93936
22	330.00000	6.23104	1.62235	-.93667	-.08926	.26685	-.06891	.17852	.15019	.14785	1.65706	1.78103
23	345.00000	6.23104	1.80950	-.48485	-.06819	.21981	.02626	.13638	.07124	.14785	1.31167	1.59664
24	360.00000	6.23104	1.87333	.00000	-.04557	.14111	.08516	.09115	.01506	.14785	1.06589	1.39877

BODY LOADS ON RING 2 AT X= 6.23104

	UNROLLED BODY-AXIS COORDINATES LINEAR LOADING	UNROLLED BODY-AXIS COORDINATES BERNOULLI LOADING	FIXED OR ROLLED BODY-AXIS COORDINATES LINEAR LOADING	FIXED OR ROLLED BODY-AXIS COORDINATES BERNOULLI LOADING
CX			.04691	.05437
CZ	.30418	.38650	.30418	.38650
CY	-.00000	.00000	-.00001	-.00001
CM	2.86267	3.63736	2.86267	3.63736
CLN	-.00000	.00000	-.00005	-.00006

CUMULATIVE BODY LOADS TO THIS STATION

	UNROLLED BODY-AXIS COORDINATES LINEAR LOADING	UNROLLED BODY-AXIS COORDINATES BERNOULLI LOADING	FIXED OR ROLLED BODY-AXIS COORDINATES LINEAR LOADING	FIXED OR ROLLED BODY-AXIS COORDINATES BERNOULLI LOADING
CX			.19113	.19373
CZ	.45844	.63096	.45844	.63096
CY	-.00000	-.00000	-.00001	-.00001
CM	4.46512	6.17686	4.46512	6.17686
CLN	-.00000	-.00000	-.00008	-.00011

BODY RING= 3

J THETA. XB YB ZB UTOT VTOT WTOT CP.LIN. CP.BERN. DR/DX P/PINF. P/PINF.

J	DEG.										BERN.	LIN.
1	15.00000	10.36390	2.04293	.54740	.02949	-.11457	.16579	-.05897	-.13714	0.00000	.39999	.74199
2	30.00000	10.36390	1.83164	1.05750	.04342	-.19844	.08192	-.08684	-.13184	0.00000	.42321	.62009
3	45.00000	10.36390	1.49553	1.49553	.05538	-.22915	-.03265	-.11076	-.11610	0.00000	.49204	.51540
4	60.00000	10.36390	1.05750	1.83164	.06456	-.19845	-.14722	-.12913	-.09494	0.00000	.58464	.43508
5	75.00000	10.36390	.54740	2.04293	.07033	-.11458	-.23110	-.14067	-.07635	0.00000	.66595	.38458
6	90.00000	10.36390	-.00000	2.11500	.07230	-.00000	-.26180	-.14460	-.06889	0.00000	.69859	.36736
7	105.00000	10.36390	-.54740	2.04293	.07033	.11457	-.23110	-.14067	-.07635	0.00000	.66596	.38458
8	120.00000	10.36390	-1.05750	1.83164	.06456	.19844	-.14723	-.12913	-.09494	0.00000	.58465	.43507
9	135.00000	10.36390	-1.49553	1.49553	.05538	.22915	-.03266	-.11077	-.11610	0.00000	.49206	.51539
10	150.00000	10.36390	-1.83164	1.05750	.04342	.19845	.08192	-.08684	-.13184	0.00000	.42322	.62007
11	165.00000	10.36390	-2.04293	.54740	.02949	.11458	.16579	-.05898	-.13714	0.00000	.39999	.74197
12	180.00000	10.36390	-2.11500	-.00000	.01454	.00000	.19649	-.02908	-.12875	0.00000	.43673	.87279
13	195.00000	10.36390	-2.04293	-.54740	-.00041	-.11457	.16579	.00083	-.10287	0.00000	.54993	1.00361
14	210.00000	10.36390	-1.83164	-1.05750	-.01434	-.19844	.08192	.02869	-.05540	0.00000	.75763	1.12552
15	225.00000	10.36390	-1.49553	-1.49553	-.02631	-.22915	-.03265	.05262	.01374	0.00000	1.06012	1.23020
16	240.00000	10.36390	-1.05750	-1.83164	-.03549	-.19845	-.14722	.07098	.09363	0.00000	1.40961	1.31052
17	255.00000	10.36390	-.54740	-2.04293	-.04126	-.11458	-.23110	.08252	.16019	0.00000	1.70084	1.36102
18	270.00000	10.36390	.00000	-2.11500	-.04323	-.00000	-.26180	.08646	.18641	0.00000	1.81555	1.37825
19	285.00000	10.36390	.54740	-2.04293	-.04126	.11457	-.23110	.08252	.16020	0.00000	1.70087	1.36103
20	300.00000	10.36390	1.05750	-1.83164	-.03549	.19844	-.14723	.07098	.09364	0.00000	1.40966	1.31053
21	315.00000	10.36390	1.49553	-1.49553	-.02631	.22915	-.03266	.05262	.01375	0.00000	1.06017	1.23021
22	330.00000	10.36390	1.83164	-1.05750	-.01435	.19845	.08192	.02869	-.05539	0.00000	.75766	1.12553
23	345.00000	10.36390	2.04293	-.54740	-.00041	.11458	.16579	.00083	-.10287	0.00000	.54995	1.00363
24	360.00000	10.36390	2.11500	.00000	.01454	.00000	.19649	-.02907	-.12875	0.00000	.43674	.87281

BODY LOADS ON RING 3 AT X= 10.36390

	UNROLLED BODY-AXIS COORDINATES		FIXED OR ROLLED BODY-AXIS COORDINATES	
	LINEAR LOADING	BERNOULLI LOADING	LINEAR LOADING	BERNOULLI LOADING
CX			0.00000	0.00000
CZ	.22705	.21564	.22705	.21564
CY	.00000	.00000	-.00000	-.00000
CM	1.91493	1.81873	1.91493	1.81873
CLN	.00000	.00000	-.00003	-.00003

CUMULATIVE BODY LOADS TO THIS STATION

	UNROLLED BODY-AXIS COORDINATES		FIXED OR ROLLED BODY-AXIS COORDINATES	
	LINEAR LOADING	BERNOULLI LOADING	LINEAR LOADING	BERNOULLI LOADING
CX			.19113	.19373
CZ	.68548	.84660	.68548	.84660
CY	-.00000	.00000	-.00001	-.00001
CM	6.38005	7.99558	6.38005	7.99558
CLN	-.00000	.00000	-.00011	-.00014

BODY RING= 4

J	THETA. DEG.	XB	YB	ZB	UTOT	VTOT	WTOT	CP.LIN.	CP.BERN.	DR/DX	P/PINF. BERN.	P/PINF. LIN.
1	15.00000	14.49675	2.04293	.54740	.01458	-.13411	.23874	-.02916	-.15747	0.00000	.31108	.87242
2	30.00000	14.49675	1.83164	1.05750	.02035	-.23230	.14056	-.04070	-.13815	0.00000	.39561	.82195
3	45.00000	14.49675	1.49553	1.49553	.02530	-.26824	.00644	-.05060	-.10236	0.00000	.55219	.77861
4	60.00000	14.49675	1.05750	1.83164	.02910	-.23230	-.12768	-.05820	-.05561	0.00000	.75672	.74536

5	75.00000	14.49675	.54740	2.04293	.03149	-.13412	-.22586	-.06298	-.01362	0.00000	.94043	.72445
6	90.00000	14.49675	-.00000	2.11500	.03231	-.00000	-.26180	-.06461	.00354	0.00000	1.01551	.71732
7	105.00000	14.49675	-.54740	2.04293	.03149	.13411	-.22586	-.06298	-.01361	0.00000	.94045	.72445
8	120.00000	14.49675	-1.05750	1.83164	.02910	.23230	-.12768	-.05820	-.05560	0.00000	.75675	.74536
9	135.00000	14.49675	-1.49553	1.49553	.02530	.26824	.00643	-.05060	-.10235	0.00000	.55222	.77861
10	150.00000	14.49675	-1.83164	1.05750	.02035	.23230	.14055	-.04070	-.13814	0.00000	.39563	.82194
11	165.00000	14.49675	-2.04293	.54740	.01458	.13412	.23874	-.02916	-.15747	0.00000	.31108	.87241
12	180.00000	14.49675	-2.11500	-.00000	.00839	.00000	.27467	-.01678	-.16045	0.00000	.29804	.92657
13	195.00000	14.49675	-2.04293	-.54740	.00220	-.13411	.23874	-.00441	-.14643	0.00000	.35937	.98072
14	210.00000	14.49675	-1.83164	-1.05750	-.00356	-.23230	.14056	.00713	-.11175	0.00000	.51108	1.03119
15	225.00000	14.49675	-1.49553	-1.49553	-.00852	-.26824	.00644	.01703	-.05372	0.00000	.76499	1.07453
16	240.00000	14.49675	-1.05750	-1.83164	-.01232	-.23230	-.12768	.02464	.02007	0.00000	1.08779	1.10778
17	255.00000	14.49675	-.54740	-2.04293	-.01471	-.13412	-.22586	.02941	.08559	0.00000	1.37446	1.12868
18	270.00000	14.49675	.00000	-2.11500	-.01552	-.00000	-.26180	.03104	.11224	0.00000	1.49104	1.13582
19	285.00000	14.49675	.54740	-2.04293	-.01471	.13411	-.22586	.02941	.08560	0.00000	1.37449	1.12869
20	300.00000	14.49675	1.05750	-1.83164	-.01232	.23230	-.12768	.02464	.02008	0.00000	1.08783	1.10778
21	315.00000	14.49675	1.49553	-1.49553	-.00852	.26824	.00643	.01704	-.05371	0.00000	.76503	1.07453
22	330.00000	14.49675	1.83164	-1.05750	-.00357	.23230	.14055	.00713	-.11175	0.00000	.51111	1.03120
23	345.00000	14.49675	2.04293	-.54740	.00220	.13412	.23874	-.00440	-.14643	0.00000	.35938	.98073
24	360.00000	14.49675	2.11500	.00000	.00839	.00000	.27467	-.01678	-.16045	0.00000	.29805	.92657

BODY LOADS ON RING 4 AT X= 14.49675

	UNROLLED BODY-AXIS COORDINATES		FIXED OR ROLLED BODY-AXIS COORDINATES	
	LINEAR LOADING	BERNOULLI LOADING	LINEAR LOADING	BERNOULLI LOADING
CX			0.00000	0.00000
CZ	.09399	.08718	.09399	.08718
CY	.00000	.00000	-.00000	-.00000
CM	.70091	.65010	.70091	.65010
CLN	.00000	.00000	-.00001	-.00001

CUMULATIVE BODY LOADS TO THIS STATION

	UNROLLED BODY-AXIS COORDINATES		FIXED OR ROLLED BODY-AXIS COORDINATES	
	LINEAR LOADING	BERNOULLI LOADING	LINEAR LOADING	BERNOULLI LOADING
CX			.19113	.19373
CZ	.77948	.93378	.77948	.93378
CY	-.00000	.00000	-.00001	-.00002
CM	7.08096	8.64568	7.08096	8.64568
CLN	-.00000	.00000	-.00012	-.00015

VORTEX INFORMATION WRITTEN ON TAPE8 FROM SUBROUTINE DEMON2

Y Z GAMMA/VINF

0

CONTROL POINT COORDINATES FOR 4 CHORDWISE BY 6 SPANWISE PANELS ON FIN 1 OR R, 6 SPANWISE ON FIN 2 OR L
AND 6 SPANWISE PANELS ON FIN 3 OR U 6 SPANWISE ON FIN 4 OR D

J	X(J)	Y(J)	Z(J)	BU(J)	BV(J)	BW(J)	VVRTX	WVRTX
1	3.12756	2.70508	0.00000	.54625E-02	-.18416E-02	.19099E+00	0.	0.
2	5.75131	2.70508	0.00000	.41013E-02	-.10153E-02	.19233E+00	0.	0.
3	8.37506	2.70508	0.00000	.32557E-02	-.75925E-03	.18945E+00	0.	0.
4	10.99881	2.70508	0.00000	.26420E-02	-.61564E-03	.18468E+00	0.	0.
5	4.11488	3.90832	0.00000	.52866E-02	-.37511E-02	.98555E-01	0.	0.
6	6.41492	3.90832	0.00000	.41109E-02	-.25673E-02	.10007E+00	0.	0.
7	8.71496	3.90832	0.00000	.33429E-02	-.19755E-02	.98861E-01	0.	0.
8	11.01500	3.90832	0.00000	.27542E-02	-.15403E-02	.96234E-01	0.	0.
9	5.10173	5.11099	0.00000	.51624E-02	-.47745E-02	.60585E-01	0.	0.
10	7.07821	5.11099	0.00000	.43852E-02	-.40910E-02	.62832E-01	0.	0.
11	9.05469	5.11099	0.00000	.35938E-02	-.31417E-02	.63009E-01	0.	0.
12	11.03118	5.11099	0.00000	.30300E-02	-.25527E-02	.61907E-01	0.	0.
13	6.08783	6.31274	0.00000	.58047E-02	-.71141E-02	.39940E-01	0.	0.
14	7.74100	6.31274	0.00000	.45928E-02	-.51054E-02	.42809E-01	0.	0.
15	9.39417	6.31274	0.00000	.43150E-02	-.51439E-02	.44096E-01	0.	0.
16	11.04734	6.31274	0.00000	.35008E-02	-.38351E-02	.44276E-01	0.	0.
17	7.07262	7.51291	0.00000	.72332E-02	-.10674E-01	.26192E-01	0.	0.
18	8.40291	7.51291	0.00000	.62352E-02	-.92169E-02	.29510E-01	0.	0.
19	9.73320	7.51291	0.00000	.44458E-02	-.56333E-02	.31575E-01	0.	0.
20	11.06349	7.51291	0.00000	.40770E-02	-.52175E-02	.32756E-01	0.	0.
21	8.05483	8.70993	0.00000	-.14064E-02	.84239E-02	.15686E-01	0.	0.
22	9.06308	8.70993	0.00000	.37560E-02	-.35577E-02	.18947E-01	0.	0.
23	10.07133	8.70993	0.00000	.75693E-02	-.12678E-01	.21375E-01	0.	0.
24	11.07959	8.70993	0.00000	.59535E-02	-.94870E-02	.23292E-01	0.	0.
25	3.12756	-2.70508	0.00000	.54626E-02	.18471E-02	.19099E+00	0.	0.
26	5.75131	-2.70508	0.00000	.41013E-02	.10208E-02	.19233E+00	0.	0.
27	8.37506	-2.70508	0.00000	.32556E-02	.76466E-03	.18945E+00	0.	0.
28	10.99881	-2.70508	0.00000	.26418E-02	.62101E-03	.18468E+00	0.	0.
29	4.11488	-3.90832	0.00000	.52868E-02	.37539E-02	.98555E-01	0.	0.
30	6.41492	-3.90832	0.00000	.41109E-02	.25699E-02	.10007E+00	0.	0.
31	8.71496	-3.90832	0.00000	.33428E-02	.19779E-02	.98861E-01	0.	0.
32	11.01500	-3.90832	0.00000	.27540E-02	.15426E-02	.96234E-01	0.	0.
33	5.10173	-5.11099	0.00000	.51627E-02	.47766E-02	.60585E-01	0.	0.
34	7.07821	-5.11099	0.00000	.43853E-02	.40927E-02	.62832E-01	0.	0.
35	9.05469	-5.11099	0.00000	.35937E-02	.31431E-02	.63009E-01	0.	0.
36	11.03118	-5.11099	0.00000	.30299E-02	.25540E-02	.61907E-01	0.	0.
37	6.08783	-6.31274	0.00000	.58052E-02	.71161E-02	.39940E-01	0.	0.
38	7.74100	-6.31274	0.00000	.45931E-02	.51070E-02	.42809E-01	0.	0.
39	9.39417	-6.31274	0.00000	.43151E-02	.51451E-02	.44096E-01	0.	0.
40	11.04734	-6.31274	0.00000	.35007E-02	.38361E-02	.44276E-01	0.	0.
41	7.07262	-7.51291	0.00000	.72339E-02	.10676E-01	.26192E-01	0.	0.
42	8.40291	-7.51291	0.00000	.62357E-02	.92187E-02	.29510E-01	0.	0.
43	9.73320	-7.51291	0.00000	.44461E-02	.56347E-02	.31575E-01	0.	0.
44	11.06349	-7.51291	0.00000	.40772E-02	.52185E-02	.32756E-01	0.	0.
45	8.05483	-8.70993	0.00000	-.14053E-02	-.84212E-02	.15686E-01	0.	0.
46	9.06308	-8.70993	0.00000	.37568E-02	.35600E-02	.18947E-01	0.	0.
47	10.07133	-8.70993	0.00000	.75700E-02	.12680E-01	.21375E-01	0.	0.
48	11.07959	-8.70993	0.00000	.59540E-02	.94886E-02	.23292E-01	0.	0.
49	3.12756	0.00000	2.70508	.95882E-02	-.33334E-05	-.16066E+00	0.	0.
50	5.75131	0.00000	2.70508	.30480E-02	-.33569E-05	-.15775E+00	0.	0.
51	8.37506	0.00000	2.70508	-.88941E-03	-.33066E-05	-.15552E+00	0.	0.
52	10.99881	0.00000	2.70508	-.27996E-02	-.32232E-05	-.15443E+00	0.	0.
53	4.11488	0.00000	3.90832	.11258E-01	-.17201E-05	-.86600E-01	0.	0.
54	6.41492	0.00000	3.90832	.41420E-02	-.17465E-05	-.77034E-01	0.	0.
55	8.71496	0.00000	3.90832	-.78184E-05	-.17254E-05	-.71729E-01	0.	0.
56	11.01500	0.00000	3.90832	-.22198E-02	-.16796E-05	-.69079E-01	0.	0.
57	5.10173	0.00000	5.11099	.14491E-01	-.10574E-05	-.64930E-01	0.	0.

58	7.07821	0.00000	5.11099	.73115E-02	-.10966E-05	-.53101E-01	0.	0.
59	9.05469	0.00000	5.11099	.22925E-02	-.10997E-05	-.44695E-01	0.	0.
60	11.03118	0.00000	5.11099	-.79704E-03	-.10805E-05	-.39599E-01	0.	0.
61	6.08783	0.00000	6.31274	.20316E-01	0.	-.64079E-01	0.	0.
62	7.74100	0.00000	6.31274	.12267E-01	0.	-.49143E-01	0.	0.
63	9.39417	0.00000	6.31274	.68106E-02	0.	-.39217E-01	0.	0.
64	11.04734	0.00000	6.31274	.22969E-02	0.	-.30686E-01	0.	0.
65	7.07262	0.00000	7.51291	.28989E-01	0.	-.75185E-01	0.	0.
66	8.40291	0.00000	7.51291	.20963E-01	0.	-.59954E-01	0.	0.
67	9.73320	0.00000	7.51291	.13445E-01	0.	-.44972E-01	0.	0.
68	11.06349	0.00000	7.51291	.85742E-02	0.	-.35524E-01	0.	0.
69	8.05483	0.00000	8.70993	.28878E-01	0.	-.69359E-01	0.	0.
70	9.06308	0.00000	8.70993	.27500E-01	0.	-.68282E-01	0.	0.
71	10.07133	0.00000	8.70993	.26302E-01	0.	-.67467E-01	0.	0.
72	11.07959	0.00000	8.70993	.19483E-01	0.	-.53669E-01	0.	0.
73	3.12756	0.00000	-2.70508	.13369E-02	-.33334E-05	-.15697E+00	0.	0.
74	5.75131	0.00000	-2.70508	.51546E-02	-.33569E-05	-.15571E+00	0.	0.
75	8.37506	0.00000	-2.70508	.74007E-02	-.33066E-05	-.15400E+00	0.	0.
76	10.99881	0.00000	-2.70508	.80835E-02	-.32232E-05	-.15319E+00	0.	0.
77	4.11488	0.00000	-3.90832	-.68464E-03	-.17201E-05	-.79095E-01	0.	0.
78	6.41492	0.00000	-3.90832	.40799E-02	-.17465E-05	-.71897E-01	0.	0.
79	8.71496	0.00000	-3.90832	.66936E-02	-.17254E-05	-.67775E-01	0.	0.
80	11.01500	0.00000	-3.90832	.77280E-02	-.16796E-05	-.65996E-01	0.	0.
81	5.10173	0.00000	-5.11099	-.41661E-02	-.10574E-05	-.55379E-01	0.	0.
82	7.07821	0.00000	-5.11099	.14589E-02	-.10966E-05	-.44917E-01	0.	0.
83	9.05469	0.00000	-5.11099	.48950E-02	-.10997E-05	-.38410E-01	0.	0.
84	11.03118	0.00000	-5.11099	.68570E-02	-.10805E-05	-.34492E-01	0.	0.
85	6.08783	0.00000	-6.31274	-.87058E-02	0.	-.49849E-01	0.	0.
86	7.74100	0.00000	-6.31274	-.30812E-02	0.	-.38931E-01	0.	0.
87	9.39417	0.00000	-6.31274	.18195E-02	0.	-.28928E-01	0.	0.
88	11.04734	0.00000	-6.31274	.47045E-02	0.	-.23015E-01	0.	0.
89	7.07262	0.00000	-7.51291	-.14522E-01	0.	-.53835E-01	0.	0.
90	8.40291	0.00000	-7.51291	-.84926E-02	0.	-.41518E-01	0.	0.
91	9.73320	0.00000	-7.51291	-.45531E-02	0.	-.33704E-01	0.	0.
92	11.06349	0.00000	-7.51291	-.41997E-03	0.	-.25088E-01	0.	0.
93	8.05483	0.00000	-8.70993	-.31689E-01	0.	-.86204E-01	0.	0.
94	9.06308	0.00000	-8.70993	-.19987E-01	0.	-.61164E-01	0.	0.
95	10.07133	0.00000	-8.70993	-.11163E-01	0.	-.42109E-01	0.	0.
96	11.07959	0.00000	-8.70993	-.75753E-02	0.	-.34694E-01	0.	0.

CONTROL POINT COORDINATES FOR BIP*S (FIN FRAME)

J	X(J)	Y(J)	Z(J)	THU(J)	THV(J)	THW(J)
97	2.64338	1.97332	.52875	0.	0.	0.
98	2.64338	1.44457	1.44457	0.	0.	0.
99	2.64338	.52875	1.97332	0.	0.	0.
100	2.64338	-.52875	1.97332	0.	0.	0.
101	2.64338	-1.44457	1.44457	0.	0.	0.
102	2.64338	-1.97332	.52875	0.	0.	0.
103	2.64338	-1.97332	-.52875	0.	0.	0.
104	2.64338	-1.44457	-1.44457	0.	0.	0.
105	2.64338	-.52875	-1.97332	0.	0.	0.
106	2.64338	.52875	-1.97332	0.	0.	0.
107	2.64338	1.44457	-1.44457	0.	0.	0.
108	2.64338	1.97332	-.52875	0.	0.	0.
109	5.42588	1.97332	.52875	0.	0.	0.
110	5.42588	1.44457	1.44457	0.	0.	0.
111	5.42588	.52875	1.97332	0.	0.	0.
112	5.42588	-.52875	1.97332	0.	0.	0.
113	5.42588	-1.44457	1.44457	0.	0.	0.
114	5.42588	-1.97332	.52875	0.	0.	0.
115	5.42588	-1.97332	-.52875	0.	0.	0.
116	5.42588	-1.44457	-1.44457	0.	0.	0.
117	5.42588	-.52875	-1.97332	0.	0.	0.
118	5.42588	.52875	-1.97332	0.	0.	0.
119	5.42588	1.44457	-1.44457	0.	0.	0.
120	5.42588	1.97332	-.52875	0.	0.	0.
121	8.20838	1.97332	.52875	0.	0.	0.
122	8.20838	1.44457	1.44457	0.	0.	0.
123	8.20838	.52875	1.97332	0.	0.	0.
124	8.20838	-.52875	1.97332	0.	0.	0.
125	8.20838	-1.44457	1.44457	0.	0.	0.
126	8.20838	-1.97332	.52875	0.	0.	0.
127	8.20838	-1.97332	-.52875	0.	0.	0.
128	8.20838	-1.44457	-1.44457	0.	0.	0.
129	8.20838	-.52875	-1.97332	0.	0.	0.
130	8.20838	.52875	-1.97332	0.	0.	0.
131	8.20838	1.44457	-1.44457	0.	0.	0.
132	8.20838	1.97332	-.52875	0.	0.	0.
133	10.99088	1.97332	.52875	0.	0.	0.
134	10.99088	1.44457	1.44457	0.	0.	0.
135	10.99088	.52875	1.97332	0.	0.	0.
136	10.99088	-.52875	1.97332	0.	0.	0.
137	10.99088	-1.44457	1.44457	0.	0.	0.
138	10.99088	-1.97332	.52875	0.	0.	0.
139	10.99088	-1.97332	-.52875	0.	0.	0.
140	10.99088	-1.44457	-1.44457	0.	0.	0.
141	10.99088	-.52875	-1.97332	0.	0.	0.
142	10.99088	.52875	-1.97332	0.	0.	0.
143	10.99088	1.44457	-1.44457	0.	0.	0.
144	10.99088	1.97332	-.52875	0.	0.	0.

VELOCITIES AND BERNOULLI PRESSURES AT CONTROL POINTS IMMEDIATELY ABOVE AND BELOW FIN SURFACE

J	X(J)	Y(J)	Z(J)	UTOTA	VTOTA	WTOTA	PRESSA	UTOTB	VTOTB	WTOTB	PRESSB
1	3.127561	2.705077	0.000000	.216337	-.228770	-.345975	-.216857	-.205412	.225087	-.345975	.619062
2	5.751312	2.705077	0.000000	.158327	-.125490	-.345975	-.180404	-.150125	.123460	-.345975	.494315
3	8.375062	2.705077	0.000000	.129779	-.068836	-.345975	-.151181	-.123269	.067320	-.345975	.420202
4	10.998812	2.705077	0.000000	.111498	-.029900	-.345975	-.129144	-.106217	.028672	-.345975	.368409
5	4.114882	3.908323	0.000000	.222483	-.237482	-.345975	-.218941	-.211910	.229980	-.345975	.638638
6	6.414921	3.908323	0.000000	.184812	-.148410	-.345975	-.198958	-.176590	.143276	-.345975	.582571
7	8.714959	3.908323	0.000000	.154034	-.083057	-.345975	-.174047	-.147348	.079106	-.345975	.504485
8	11.014998	3.908323	0.000000	.127677	-.035147	-.345975	-.147377	-.122171	.032070	-.345975	.423688
9	5.101730	5.110993	0.000000	.209948	-.225150	-.345975	-.214730	-.199623	.215601	-.345975	.607240
10	7.078212	5.110993	0.000000	.206999	-.167620	-.345975	-.210321	-.198229	.159438	-.345975	.656001
11	9.054694	5.110993	0.000000	.178560	-.097285	-.345975	-.192221	-.171372	.091001	-.345975	.592454
12	11.031176	5.110993	0.000000	.155154	-.043479	-.345975	-.173144	-.149095	.038374	-.345975	.522201
13	6.087825	6.312745	0.000000	.199075	-.215098	-.345975	-.210262	-.187465	.200869	-.345975	.575747
14	7.740997	6.312745	0.000000	.203323	-.165500	-.345975	-.208743	-.194137	.155289	-.345975	.642943
15	9.394169	6.312745	0.000000	.201568	-.111279	-.345975	-.205205	-.192938	.100991	-.345975	.674726
16	11.047341	6.312745	0.000000	.184835	-.052620	-.345975	-.194251	-.177833	.044950	-.345975	.634287
17	7.072615	7.512907	0.000000	.192277	-.209805	-.345975	-.207113	-.177811	.188458	-.345975	.550749
18	8.402905	7.512907	0.000000	.196007	-.162381	-.345975	-.205406	-.183536	.143947	-.345975	.609386
19	9.733195	7.512907	0.000000	.198227	-.109900	-.345975	-.203578	-.189335	.098633	-.345975	.661155
20	11.063485	7.512907	0.000000	.198193	-.057441	-.345975	-.201707	-.190039	.047006	-.345975	.684096
21	8.054830	8.709930	0.000000	.177676	-.184291	-.345975	-.197915	-.180489	.201139	-.345975	.549003
22	9.063082	8.709930	0.000000	.186067	-.150700	-.345975	-.199780	-.178555	.143585	-.345975	.590032
23	10.071335	8.709930	0.000000	.178968	-.104901	-.345975	-.192881	-.163829	.079545	-.345975	.567575
24	11.079587	8.709930	0.000000	.156338	-.049945	-.345975	-.174320	-.144431	.030971	-.345975	.505668
25	3.127561	-2.705077	0.000000	.147593	.154797	-.171663	-.175001	-.136667	-.151103	-.171663	.428879
26	5.751312	-2.705077	0.000000	.104195	.081806	-.171663	-.123580	-.095992	-.079764	-.171663	.323556
27	8.375062	-2.705077	0.000000	.083261	.043813	-.171663	-.092583	-.076748	-.042282	-.171663	.270514
28	10.998812	-2.705077	0.000000	.065002	.017399	-.171663	-.063240	-.059716	-.016154	-.171663	.221580
29	4.114882	-3.908323	0.000000	.141249	.150067	-.171663	-.169287	-.130676	-.142559	-.171663	.413140
30	6.414921	-3.908323	0.000000	.117897	.094406	-.171663	-.140686	-.109675	-.089266	-.171663	.366003
31	8.714959	-3.908323	0.000000	.096499	.052102	-.171663	-.111411	-.089813	-.048146	-.171663	.310997
32	11.014998	-3.908323	0.000000	.077711	.021710	-.171663	-.083353	-.072201	-.018621	-.171663	.258966
33	5.101730	-5.110993	0.000000	.124935	.133667	-.171663	-.152344	-.114609	-.124114	-.171663	.367964
34	7.078212	-5.110993	0.000000	.127102	.103137	-.171663	-.151198	-.118331	-.094951	-.171663	.393570
35	9.054694	-5.110993	0.000000	.109765	.060270	-.171663	-.128594	-.102578	-.053984	-.171663	.351968
36	11.031176	-5.110993	0.000000	.094087	.027051	-.171663	-.106945	-.088027	-.021943	-.171663	.308606
37	6.087825	-6.312745	0.000000	.113111	.122590	-.171663	-.138526	-.101500	-.108358	-.171663	.331431
38	7.740997	-6.312745	0.000000	.118573	.097100	-.171663	-.141683	-.109387	-.086886	-.171663	.365855
39	9.394169	-6.312745	0.000000	.120534	.067679	-.171663	-.141387	-.111904	-.057388	-.171663	.382974
40	11.047341	-6.312745	0.000000	.111222	.032817	-.171663	-.128916	-.104221	-.025144	-.171663	.361986
41	7.072615	-7.512907	0.000000	.106131	.117102	-.171663	-.129848	-.091663	-.095750	-.171663	.304354
42	8.402905	-7.512907	0.000000	.110019	.092982	-.171663	-.131641	-.097548	-.074545	-.171663	.330174
43	9.733195	-7.512907	0.000000	.112853	.063965	-.171663	-.132479	-.103961	-.052695	-.171663	.356895
44	11.063485	-7.512907	0.000000	.115291	.035139	-.171663	-.133770	-.107137	-.024702	-.171663	.371973
45	8.054830	-8.709930	0.000000	.091507	.091564	-.171663	-.108334	-.094318	-.108407	-.171663	.308117
46	9.063082	-8.709930	0.000000	.099906	.081161	-.171663	-.118168	-.092392	-.074041	-.171663	.313490
47	10.071335	-8.709930	0.000000	.099794	.062302	-.171663	-.116408	-.084654	-.036943	-.171663	.296161
48	11.079587	-8.709930	0.000000	.089056	.031846	-.171663	-.100216	-.077148	-.012869	-.171663	.274602
49	3.127561	0.000000	2.705077	.010588	.000005	-.163415	.039547	.010947	.000005	-.163802	.038843
50	5.751312	0.000000	2.705077	.008609	.000005	-.173344	.045941	.010685	.000005	-.175020	.041670
51	8.375062	0.000000	2.705077	.025821	.000005	-.201305	.013403	.038556	.000005	-.208157	-.011344
52	10.998812	0.000000	2.705077	.063858	.000005	-.254903	-.054970	.090490	.000005	-.262068	-.096488
53	4.114882	0.000000	3.908323	.011390	.000005	-.086962	.015689	.011488	.000005	-.087067	.015527
54	6.414921	0.000000	3.908323	.005061	.000005	-.079694	.026099	.005917	.000005	-.080386	.024572
55	8.714959	0.000000	3.908323	.002466	.000005	-.081492	.032281	.006222	.000005	-.083513	.025124
56	11.014998	0.000000	3.908323	.035063	.000005	-.156344	-.012237	.053565	.000005	-.161322	-.045250
57	5.101730	0.000000	5.110993	.014482	.000005	-.064920	.001206	.014501	.000005	-.064940	.001177

58	7.078212	0.000000	5.110993	.007879	.000005	-.054580	.010148	.008102	.000005	-.054760	.009775
59	9.054694	0.000000	5.110993	.003208	.000005	-.047808	.016671	.004338	.000005	-.048416	.014641
60	11.031176	0.000000	5.110993	.002846	.000005	-.052752	.019588	.007001	.000005	-.053870	.011614
61	6.087825	0.000000	6.312745	.020316	.000005	-.064079	-.010422	.020316	.000005	-.064079	-.010421
62	7.740997	0.000000	6.312745	.012249	.000005	-.049128	-.000795	.012285	.000005	-.049158	-.000854
63	9.394169	0.000000	6.312745	.006707	.000005	-.039161	.005787	.006914	.000005	-.039272	.005427
64	11.047341	0.000000	6.312745	.003123	.000005	-.033491	.010334	.003978	.000005	-.033721	.008734
65	7.072615	0.000000	7.512907	.028991	.000005	-.075187	-.022724	.028987	.000005	-.075183	-.022718
66	8.402905	0.000000	7.512907	.020963	.000005	-.059954	-.013216	.020963	.000005	-.059954	-.013216
67	9.733195	0.000000	7.512907	.013436	.000005	-.044967	-.004844	.013454	.000005	-.044977	-.004877
68	11.063485	0.000000	7.512907	.008527	.000005	-.035511	.000576	.008621	.000005	-.035536	.000403
69	8.054830	0.000000	8.709930	.028880	.000005	-.069362	-.024530	.028875	.000005	-.069357	-.024524
70	9.063082	0.000000	8.709930	.027502	.000005	-.068284	-.022374	.027498	.000005	-.068280	-.022368
71	10.071335	0.000000	8.709930	.026304	.000005	-.067467	-.020446	.026301	.000005	-.067466	-.020441
72	11.079587	0.000000	8.709930	.019481	.000005	-.053669	-.012847	.019484	.000005	-.053670	-.012853
73	3.127561	0.000000	-2.705077	.000344	.000005	-.159719	.061668	-.000028	.000005	-.160120	.062616
74	5.751312	0.000000	-2.705077	-.000402	.000005	-.171304	.065963	-.002487	.000005	-.172988	.071166
75	8.375062	0.000000	-2.705077	-.019306	.000005	-.199779	.117187	-.032049	.000005	-.206635	.151574
76	10.998812	0.000000	-2.705077	-.058571	.000005	-.253665	.230987	-.085209	.000005	-.260832	.314370
77	4.114882	0.000000	-3.908323	-.000810	.000005	-.079450	.038494	-.000920	.000005	-.079569	.038779
78	6.414921	0.000000	-3.908323	.003166	.000005	-.074553	.028057	.002299	.000005	-.075253	.030167
79	8.714959	0.000000	-3.908323	.004224	.000005	-.077536	.027014	.000459	.000005	-.079562	.035808
80	11.014998	0.000000	-3.908323	-.029551	.000005	-.153261	.133078	-.048061	.000005	-.158240	.184557
81	5.101730	0.000000	-5.110993	-.004151	.000005	-.055363	.035396	-.004181	.000005	-.055395	.035474
82	7.078212	0.000000	-5.110993	.000897	.000005	-.046391	.020769	.000663	.000005	-.046581	.021337
83	9.054694	0.000000	-5.110993	.003985	.000005	-.041520	.012284	.002844	.000005	-.042134	.014865
84	11.031176	0.000000	-5.110993	.003218	.000005	-.047644	.016579	-.000945	.000005	-.048764	.025656
85	6.087825	0.000000	-6.312745	-.008701	.000005	-.049844	.042620	-.008710	.000005	-.049854	.042644
86	7.740997	0.000000	-6.312745	-.003058	.000005	-.038912	.025480	-.003105	.000005	-.038950	.025596
87	9.394169	0.000000	-6.312745	.001928	.000005	-.028869	.010551	.001711	.000005	-.028986	.011042
88	11.047341	0.000000	-6.312745	.003883	.000005	-.025819	.005223	.003018	.000005	-.026051	.007042
89	7.072615	0.000000	-7.512907	-.014519	.000005	-.053832	.057308	-.014524	.000005	-.053838	.057322
90	8.402905	0.000000	-7.512907	-.008488	.000005	-.041514	.038173	-.008497	.000005	-.041522	.038196
91	9.733195	0.000000	-7.512907	-.004539	.000005	-.033696	.026051	-.004567	.000005	-.033711	.026118
92	11.063485	0.000000	-7.512907	-.000368	.000005	-.025074	.013329	-.000472	.000005	-.025102	.013553
93	8.054830	0.000000	-8.709930	-.031687	.000005	-.086202	.113141	-.031692	.000005	-.086207	.113154
94	9.063082	0.000000	-8.709930	-.019985	.000005	-.061162	.073246	-.019990	.000005	-.061166	.073258
95	10.071335	0.000000	-8.709930	-.011160	.000005	-.042107	.044214	-.011166	.000005	-.042110	.044228
96	11.079587	0.000000	-8.709930	-.007570	.000005	-.034692	.032885	-.007580	.000005	-.034695	.032908

ORIGINAL PAGE IS
OF POOR QUALITY

PRESSURE LOADINGS AT CONTROL POINTS

J	X(J)	Y(J)	Z(J)	DELTP.LIN.	DELTP.BERN.
1	3.127561	2.705077	0.000000	.843499	.835919
2	5.751312	2.705077	0.000000	.616904	.674718
3	8.375062	2.705077	0.000000	.506095	.571383
4	10.998812	2.705077	0.000000	.435431	.497553
5	4.114882	3.908323	0.000000	.868787	.857579
6	6.414921	3.908323	0.000000	.722804	.781529
7	8.714959	3.908323	0.000000	.602764	.678531
8	11.014998	3.908323	0.000000	.499696	.571064
9	5.101730	5.110993	0.000000	.819142	.821970
10	7.078212	5.110993	0.000000	.810457	.866322
11	9.054694	5.110993	0.000000	.699864	.784674
12	11.031176	5.110993	0.000000	.608498	.695344
13	6.087825	6.312745	0.000000	.773081	.786010
14	7.740997	6.312745	0.000000	.794921	.851686
15	9.394169	6.312745	0.000000	.789013	.879931
16	11.047341	6.312745	0.000000	.725336	.828539
17	7.072615	7.512907	0.000000	.740177	.757862
18	8.402905	7.512907	0.000000	.759087	.814792
19	9.733195	7.512907	0.000000	.775123	.864733
20	11.063485	7.512907	0.000000	.776463	.885803
21	8.054830	8.709930	0.000000	.716328	.746918
22	9.063082	8.709930	0.000000	.729243	.789811
23	10.071335	8.709930	0.000000	.685593	.760457
24	11.079587	8.709930	0.000000	.601540	.679988
25	3.127561	-2.705077	0.000000	.568519	.603880
26	5.751312	-2.705077	0.000000	.400374	.447136
27	8.375062	-2.705077	0.000000	.320018	.363097
28	10.998812	-2.705077	0.000000	.249436	.284820
29	4.114882	-3.908323	0.000000	.543850	.582428
30	6.414921	-3.908323	0.000000	.455145	.506689
31	8.714959	-3.908323	0.000000	.372624	.422408
32	11.014998	-3.908323	0.000000	.299823	.342319
33	5.101730	-5.110993	0.000000	.479089	.520308
34	7.078212	-5.110993	0.000000	.490867	.544768
35	9.054694	-5.110993	0.000000	.424685	.480563
36	11.031176	-5.110993	0.000000	.364227	.415551
37	6.087825	-6.312745	0.000000	.429221	.469957
38	7.740997	-6.312745	0.000000	.455919	.507537
39	9.394169	-6.312745	0.000000	.464877	.524361
40	11.047341	-6.312745	0.000000	.430885	.490902
41	7.072615	-7.512907	0.000000	.395587	.434202
42	8.402905	-7.512907	0.000000	.415135	.461815
43	9.733195	-7.512907	0.000000	.433628	.489374
44	11.063485	-7.512907	0.000000	.444855	.505743
45	8.054830	-8.709930	0.000000	.371649	.416452
46	9.063082	-8.709930	0.000000	.384596	.431658
47	10.071335	-8.709930	0.000000	.368897	.412569
48	11.079587	-8.709930	0.000000	.332408	.374818
49	3.127561	0.000000	2.705077	-.000719	-.000704
50	5.751312	0.000000	2.705077	-.004153	-.004270
51	8.375062	0.000000	2.705077	-.025471	-.024747
52	10.998812	0.000000	2.705077	-.053265	-.041518
53	4.114882	0.000000	3.908323	-.000195	-.000162
54	6.414921	0.000000	3.908323	-.001713	-.001527
55	8.714959	0.000000	3.908323	-.007513	-.007157
56	11.014998	0.000000	3.908323	-.037005	-.033012
57	5.101730	0.000000	5.110993	-.000037	-.000029
58	7.078212	0.000000	5.110993	-.000447	-.000373
59	9.054694	0.000000	5.110993	-.002261	-.002030
60	11.031176	0.000000	5.110993	-.008309	-.007974
61	6.087825	0.000000	6.312745	.000001	.000001
62	7.740997	0.000000	6.312745	-.000073	-.000059
63	9.394169	0.000000	6.312745	-.000414	-.000360
64	11.047341	0.000000	6.312745	-.001710	-.001601
65	7.072615	0.000000	7.512907	.000008	.000006
66	8.402905	0.000000	7.512907	-.000000	-.000000
67	9.733195	0.000000	7.512907	-.000038	-.000032
68	11.063485	0.000000	7.512907	-.000189	-.000173
69	8.054830	0.000000	8.709930	.000009	.000006
70	9.063082	0.000000	8.709930	.000009	.000007
71	10.071335	0.000000	8.709930	.000005	.000005
72	11.079587	0.000000	8.709930	-.000006	-.000005
73	3.127561	0.000000	-2.705077	.000744	.000947
74	5.751312	0.000000	-2.705077	.004171	.005203
75	8.375062	0.000000	-2.705077	.025486	.034387
76	10.998812	0.000000	-2.705077	.053276	.083382
77	4.114882	0.000000	-3.908323	.000220	.000285
78	6.414921	0.000000	-3.908323	.001734	.002110
79	8.714959	0.000000	-3.908323	.007530	.008794
80	11.014998	0.000000	-3.908323	.037019	.051479
81	5.101730	0.000000	-5.110993	.000060	.000079
82	7.078212	0.000000	-5.110993	.000469	.000568
83	9.054694	0.000000	-5.110993	.002280	.002581
84	11.031176	0.000000	-5.110993	.008325	.009077
85	6.087825	0.000000	-6.312745	.000018	.000024
86	7.740997	0.000000	-6.312745	.000094	.000115
87	9.394169	0.000000	-6.312745	.000435	.000491
88	11.047341	0.000000	-6.312745	.001729	.001819
89	7.072615	0.000000	-7.512907	.000010	.000014
90	8.402905	0.000000	-7.512907	.000018	.000023
91	9.733195	0.000000	-7.512907	.000057	.000067
92	11.063485	0.000000	-7.512907	.000209	.000224
93	8.054830	0.000000	-8.709930	.000009	.000013
94	9.063082	0.000000	-8.709930	.000009	.000013
95	10.071335	0.000000	-8.709930	.000011	.000014
96	11.079587	0.000000	-8.709930	.000020	.000023

FIN LOADING INFORMATION

*** STEP 1

MACH NUMBER =	.25000E+01
ANGLE OF ATTACK =	15.000 DEGREES
SIDE SLIP ANGLE =	.000 DEGREES
FIN AREA =	52.34373
REFERENCE AREA =	14.12000
REFERENCE LENGTH =	4.23000
EXPOSED FIN SPAN B/2=	7.23000
MOMENT CENTER: XM =	46.04000
ZM =	0.00000

LINEAR PRESSURE (U/VINF) LOADS IN BODY SYSTEM

	TOTAL	FIN 1 OR R	FIN 2 OR L	FIN 3 OR U	FIN 4 OR D	INTERF. SHELL
DEFL. ANGLE DEG. =		5.00000	-5.00000	0.00000	0.00000	
CTHR =	.68327E-01	.49335E-01	.19533E-01	-.27064E-03	-.27074E-03	
CZ =	4.1038	2.5707	1.5331	0.	0.	.58154
CY =	-.69007E-04	0.	0.	.29987E-01	-.30056E-01	-.10138E-04
CM =	22.666	14.176	8.4905	0.	0.	3.2168
CLN =	-.38198E-03	0.	0.	.15075	-.15113	-.56088E-04
CLL =	-1.2724	-3.1676	1.8489	.23113E-01	.23196E-01	.34388E-15

FOLLOWING ARE IN UNROLLED BODY-AXIS COORDINATE SYSTEM

CZU =	4.1038	2.5707	1.5331	-.52338E-06	.52458E-06	.58154
CYU =	.26187E-05	.44867E-04	.26758E-04	.29987E-01	-.30056E-01	.11440E-07
CMU =	22.666	14.176	8.4905	-.26310E-05	.26377E-05	3.2168
CLNU =	.13620E-04	.24742E-03	.14819E-03	.15075	-.15113	.55927E-07

NOTE: L.E. OF LEAD PANEL IN FIRST CHORDWISE ROW IS SUPERSONIC

SPANWISE DISTRIBUTIONS

------------------UPPER RIGHT OR RIGHT HORIZONTAL FIN--------------------

I	Y/(B/2)	CN*C/(2*B)	CT*C/(2*B)	CY1*C/(2*B)	CYTOT*C/(2*B)	CS*C/(2*B)	CSINT	YBAR	GAMNET(I)	GAMMA,LE/VINF	XLE
1	.08162	.21764	0.00000	0.00000	.00250	0.00000	0.00000	0.00000	-3.15103	0.00000	.63500
2	.24804	.21391	0.00000	0.00000	.00460	0.00000	0.00000	0.00000	.05282	0.00000	1.92985
3	.41438	.20034	0.00000	0.00000	.00530	0.00000	0.00000	0.00000	.19480	0.00000	3.22407
4	.58060	.17563	0.00000	0.00000	.00435	0.00000	0.00000	0.00000	.35559	0.00000	4.51731
5	.74660	.13964	0.00000	0.00000	.00363	0.00000	0.00000	0.00000	.51857	0.00000	5.80884
6	.91216	.09444	0.00000	0.00000	0.00000	0.00000	0.00000	0.00000	.65163	0.00000	7.09699
7	1.00000	0.00000							1.37763		

THRUST- AND SIDE-FORCE COEFFICIENTS IN PLANE OF THE FIN

SUMFX =CX..ACTS ON LEADING EDGE
SUMFY1=CY..ACTS ON LEADING EDGE
SUMFY2=CY..ACTS ON LEADING AND SIDE EDGE
SUMFT2=CY..ACTS ON SIDE EDGE

SUMFX = 0.
SUMFY1 = 0.
SUMFY2 = .50274E-01
SUMFT2 = .21231E-01

SIDE-EDGE DISTRIBUTION

JTIP	JSE	DISTANCE FROM LE /TIPCHORD	SUCTION FORCE PER UNIT LENGTH /(Q*TIPCHORD)	GAMMA,SE /VINF	YBAR	XSE
1	1	.25000	-.00110	.00020	7.23000	7.78041
2	2	.50000	-.00398	.00092	7.23000	8.61780
3	3	.75000	.01211	.00313	7.23000	9.45520
4	4	1.00000	.09984	.02130	7.23000	10.29260

S.E. AUGMENTATION OF FIN NORMAL FORCE FROM SUCTION CONVERSION IN PROPORTION WITH FACTOR
KVSE = 1.000

(LOCAL FIN)	(ROLLED BODY-AXIS)	(UNROLLED BODY-AXIS)
CNADD = .02325	CYADD = 0.00000	CYADD = .00000
	CZADD = .02325	CZADD = .02325
	CMADD = .11423	CMADD = .11425
	CLNADD = 0.00000	CLNADD = .00000

CLLADD	= -.05136		CLLADD	=	-.05136
XCG	= 25.2552		XCG	=	25.2552
YCG	= 9.3450		YCG	=	9.3450
ZCG	= 0.0000		ZCG	=	-.0002

**** T.E. FIN VORTICITY DUE TO SIDE EDGE FORCE AUGMENTATION

IVRT	GAMMA/VINF	Y.C.G. (LOCAL FIN)	Z.C.G. (LOCAL FIN)	Y.C.G. (BODY AXES)	Z.C.G. (BODY AXES)
1	.02130	7.23000	.59790	9.34500	.59790

------------------LOWER LEFT OR LEFT HORIZONTAL FIN--------------------

I	Y/(B/2)	CN*C/(2*B)	CT*C/(2*B)	CY1*C/(2*B)	CYTOT*C/(2*B)	CS*C/(2*B)	CSINT	YBAR	GAMNET(I)	GAMMA,LE/VINF	XLE
8	-.08162	.13939	0.00000	0.00000	-.00192	0.00000	0.00000	0.00000	2.01812	0.00000	.63500
9	-.24804	.13271	0.00000	0.00000	-.00182	0.00000	0.00000	0.00000	-.09593	0.00000	1.92985
10	-.41438	.11994	0.00000	0.00000	-.00166	0.00000	0.00000	0.00000	-.18401	0.00000	3.22407
11	-.58060	.10148	0.00000	0.00000	-.00111	0.00000	0.00000	0.00000	-.26612	0.00000	4.51731
12	-.74660	.07732	0.00000	0.00000	-.00087	0.00000	0.00000	0.00000	-.34850	0.00000	5.80884
13	-.91216	.05037	0.00000	0.00000	0.00000	0.00000	0.00000	0.00000	-.38878	0.00000	7.09699
14	-1.00000	0.00000							-.73479		

THRUST- AND SIDE-FORCE COEFFICIENTS IN PLANE OF THE FIN

SUMFX =CX..ACTS ON LEADING EDGE
SUMFY1=CY..ACTS ON LEADING EDGE
SUMFY2=CY..ACTS ON LEADING AND SIDE EDGE
SUMFT2=CY..ACTS ON SIDE EDGE

SUMFX = 0.
SUMFY1 = 0.
SUMFY2 = -.18233E-01
SUMFT2 = -.50575E-02

SIDE EDGE DISTRIBUTION

JTIP	JSE	DISTANCE FROM LE /TIPCHORD	SUCTION FORCE PER UNIT LENGTH /(Q*TIPCHORD)	GAMMA,SE /VINF	YBAR	XSE
1	5	.25000	.00057	-.00011	-7.23000	7.78041
2	6	.50000	.00209	-.00051	-7.23000	8.61780
3	7	.75000	-.00112	-.00072	-7.23000	9.45520
4	8	1.00000	-.02700	-.00588	-7.23000	10.29260

S.E. AUGMENTATION OF FIN NORMAL FORCE FROM SUCTION CONVERSION IN PROPORTION WITH FACTOR
KVSF = 1.000

(LOCAL FIN)			(ROLLED BODY-AXIS)			(UNROLLED BODY-AXIS)		
CNADD	=	.00611	CYADD	=	0.00000	CYADD	=	.00000
			CZADD	=	.00611	CZADD	=	.00611
			CMADD	=	.03003	CMADD	=	.03005
			CLNADD	=	0.00000	CLNADD	=	.00000
			CLLADD	=	.01350	CLLADD	=	.01350
			XCG	=	25.2552	XCG	=	25.2552
			YCG	=	-9.3450	YCG	=	-9.3450
			ZCG	=	-.0000	ZCG	=	.0002

**** T.E. FIN VORTICITY DUE TO SIDE-EDGE FORCE AUGMENTATION

IVRT	GAMMA/VINF	Y.C.G. (LOCAL FIN)	Z.C.G. (LOCAL FIN)	Y.C.G. (BODY AXES)	Z.C.G. (BODY AXES)
2	-.00588	-7.23000	.28965	-9.34500	.28965

------------------LOWER RIGHT OR UPPER VERTICAL FIN--------------------

I	Y/(B/2)	CN*C/(2*B)	CT*C/(2*B)	CY1*C/(2*B)	CYTOT*C/(2*B)	CS*C/(2*B)	CSINT	YBAR	GAMNET(I)	GAMMA.LE/VINF	XLE
15	.08162	-.00758	0.00000	0.00000	-.00001	0.00000	0.00000	0.00000	.10968	0.00000	.63500
16	.24804	-.00369	0.00000	0.00000	-.00002	0.00000	0.00000	0.00000	-.05629	0.00000	1.92985
17	.41438	-.00075	0.00000	0.00000	-.00000	0.00000	0.00000	0.00000	-.04247	0.00000	3.22407
18	.58060	-.00013	0.00000	0.00000	-.00000	0.00000	0.00000	0.00000	-.00911	0.00000	4.51731
19	.74660	-.00001	0.00000	0.00000	-.00000	0.00000	0.00000	0.00000	-.00167	0.00000	5.80884
20	.91216	.00000	0.00000	0.00000	0.00000	0.00000	0.00000	0.00000	-.00015	0.00000	7.09699
21	1.00000	0.00000							.00001		

THRUST- AND SIDE-FORCE COEFFICIENTS IN PLANE OF THE FIN

SUMFX =CX..ACTS ON LEADING EDGE
SUMFY1=CY..ACTS ON LEADING EDGE
SUMFY2=CY..ACTS ON LEADING AND SIDE EDGE
SUMFT2=CY..ACTS ON SIDE EDGE

SUMFX = 0.
SUMFY1 = 0.
SUMFY2 = -.65305E-04
SUMFT2 = .59962E-11

SIDE EDGE DISTRIBUTION

JTIP	JSE	DISTANCE FROM LE /TIPCHORD	SUCTION FORCE PER UNIT LENGTH /(Q*TIPCHORD)	GAMMA.SE /VINF	YBAR	XSE

1	9	.25000	.00000	0.00000	0.00000	7.78041
2	10	.50000	.00000	0.00000	0.00000	8.61780
3	11	.75000	.00000	0.00000	0.00000	9.45520
4	12	1.00000	.00000	0.00000	0.00000	10.29260

-------------------UPPER LEFT OR LOWER VERTICAL FIN--------------------

I	Y/(B/2)	CN*C/(2*B)	CT*C/(2*B)	CY1*C/(2*B)	CYTOT*C/(2*B)	CS*C/(2*B)	CSINT	YBAR	GAMNET(I)	GAMMA.LE/VINF	XLE
22	-.08162	.00758	0.00000	0.00000	.00001	0.00000	0.00000	0.00000	.10977	0.00000	.63500
23	-.24804	.00369	0.00000	0.00000	.00002	0.00000	0.00000	0.00000	-.05629	0.00000	1.92985
24	-.41438	.00076	0.00000	0.00000	.00000	0.00000	0.00000	0.00000	-.04248	0.00000	3.22407
25	-.58060	.00013	0.00000	0.00000	.00000	0.00000	0.00000	0.00000	-.00912	0.00000	4.51731
26	-.74660	.00001	0.00000	0.00000	.00000	0.00000	0.00000	0.00000	-.00169	0.00000	5.80884
27	-.91216	.00000	0.00000	0.00000	0.00000	0.00000	0.00000	0.00000	-.00017	0.00000	7.09699
28	-1.00000	0.00000							-.00003		

THRUST- AND SIDE-FORCE COEFFICIENTS IN PLANE OF THE FIN

SUMFX =CX..ACTS ON LEADING EDGE
SUMFY1=CY..ACTS ON LEADING EDGE
SUMFY2=CY..ACTS ON LEADING AND SIDE EDGE
SUMFT2=CY..ACTS ON SIDE EDGE

SUMFX = 0.
SUMFY1 = 0.
SUMFY2 = .65226E-04
SUMFT2 = .26827E-11

SIDE EDGE DISTRIBUTION

JTIP	JSE	DISTANCE FROM LE /TIPCHORD	SUCTION FORCE PER UNIT LENGTH /(Q*TIPCHORD)	GAMMA.SE /VINF	YBAR	XSE
1	13	.25000	.00000	0.00000	0.00000	7.78041
2	14	.50000	.00000	0.00000	0.00000	8.61780
3	15	.75000	.00000	0.00000	0.00000	9.45520
4	16	1.00000	.00000	0.00000	0.00000	10.29260

FIN LOADING INFORMATION

*** STEP 1

MACH NUMBER =	.25000E+01
ANGLE OF ATTACK =	15.000 DEGREES
SIDE SLIP ANGLE =	.000 DEGREES
FIN AREA =	52.34373
REFERENCE AREA =	14.12000
REFERENCE LENGTH =	4.23000
EXPOSED FIN SPAN B/2=	7.23000
MOMENT CENTER: XM =	46.04000
ZM =	0.00000

BERNOULLI PRESSURE LOADS IN BODY SYSTEM

	TOTAL	FIN 1 OR R	FIN 2 OR L	FIN 3 OR U	FIN 4 OR D	INTERF. SHELL
DEFL. ANGLE DEG. =		5.00000	-5.00000	0.00000	0.00000	
CTHR =	.68327E-01	.49335E-01	.19533E-01	-.27064E-03	-.27074E-03	
CZ =	4.4827	2.7760	1.7066	0.	0.	.58154
CY =	-.16259E-01	0.	0.	.26190E-01	-.42450E-01	-.10138E-04
CM =	24.663	15.233	9.4297	0.	0.	3.2168
CLN =	-.80453E-01	0.	0.	.13226	-.21271	-.56088E-04
CLL =	-1.3133	-3.4281	2.0623	.20344E-01	.32161E-01	.34388E-15

FOLLOWING ARE IN UNROLLED BODY-AXIS COORDINATE SYSTEM

CZU =	4.4827	2.7760	1.7066	-.45711E-06	.74088E-06	.58154
CYU =	-.16181E-01	.48451E-04	.29786E-04	.26190E-01	-.42450E-01	.11440E-07
CMU =	24.663	15.233	9.4297	-.23084E-05	.37125E-05	3.2168
CLNU =	-.80022E-01	.26587E-03	.16458E-03	.13226	-.21271	.55927E-07

NOTE: L.E. OF LEAD PANEL IN FIRST CHORDWISE ROW IS SUPERSONIC

SPANWISE DISTRIBUTIONS

------------------UPPER RIGHT OR RIGHT HORIZONTAL FIN---------------------

I	Y/(B/2)	CN*C/(2*B)	CT*C/(2*B)	CY1*C/(2*B)	CYTOT*C/(2*B)	CS*C/(2*B)	CSINT	YBAR	GAMNET(I)	GAMMA.LE/VINF	XLE
1	.08162	.23373	0.00000	0.00000	.00250	0.00000	0.00000	0.00000	-3.15103	0.00000	.63500
2	.24804	.22936	0.00000	0.00000	.00460	0.00000	0.00000	0.00000	.05282	0.00000	1.92985
3	.41438	.21605	0.00000	0.00000	.00530	0.00000	0.00000	0.00000	.19480	0.00000	3.22407
4	.58060	.19066	0.00000	0.00000	.00435	0.00000	0.00000	0.00000	.35559	0.00000	4.51731
5	.74660	.15210	0.00000	0.00000	.00363	0.00000	0.00000	0.00000	.51857	0.00000	5.80884
6	.91216	.10289	0.00000	0.00000	0.00000	0.00000	0.00000	0.00000	.65163	0.00000	7.09699
7	1.00000	0.00000							1.37763		

THRUST- AND SIDE-FORCE COEFFICIENTS IN PLANE OF THE FIN

SUMFX =CX..ACTS ON LEADING EDGE
SUMFY1=CY..ACTS ON LEADING EDGE
SUMFY2=CY..ACTS ON LEADING AND SIDE EDGE
SUMFT2=CY..ACTS ON SIDE EDGE

SUMFX = 0.
SUMFY1 = 0.
SUMFY2 = .50274E-01
SUMFT2 = .21231E-01

SIDE EDGE DISTRIBUTION

JTIP	JSE	DISTANCE FROM LE /TIPCHORD	SUCTION FORCE PER UNIT LENGTH /(Q*TIPCHORD)	GAMMA.SE /VINF	YBAR	XSE
1	1	.25000	-.00110	.00020	7.23000	7.78041
2	2	.50000	-.00398	.00092	7.23000	8.61780
3	3	.75000	.01211	.00313	7.23000	9.45520
4	4	1.00000	.09984	.02130	7.23000	10.29260

****T.E. FIN VORTICITY DUE TO ATTACHED FLOW*****

IVRT	GAMMA/VINF	Y.C.G. (LOCAL FIN)	Y.C.G. (BODY AXES)	Z.C.G. (BODY AXES)
3	3.37977	5.79887	7.91387	0.00000

------------------LOWER LEFT OR LEFT HORIZONTAL FIN--------------------

I	Y/(B/2)	CN*C/(2*B)	CT*C/(2*B)	CY1*C/(2*B)	CYTOT*C/(2*B)	CS*C/(2*B)	CSINT	YBAR	GAMNET(I)	GAMMA,LE/VINF	XLE
8	-.08162	.15394	0.00000	0.00000	-.00192	0.00000	0.00000	0.00000	2.01812	0.00000	.63500
9	-.24804	.14719	0.00000	0.00000	-.00182	0.00000	0.00000	0.00000	-.09593	0.00000	1.92985
10	-.41438	.13373	0.00000	0.00000	-.00166	0.00000	0.00000	0.00000	-.18401	0.00000	3.22407
11	-.58060	.11355	0.00000	0.00000	-.00111	0.00000	0.00000	0.00000	-.26612	0.00000	4.51731
12	-.74660	.08656	0.00000	0.00000	-.00087	0.00000	0.00000	0.00000	-.34850	0.00000	5.80884
13	-.91216	.05652	0.00000	0.00000	0.00000	0.00000	0.00000	0.00000	-.38878	0.00000	7.09699
14	-1.00000	0.00000							-.73479		

THRUST- AND SIDE-FORCE COEFFICIENTS IN PLANE OF THE FIN

SUMFX =CX..ACTS ON LEADING EDGE
SUMFY1=CY..ACTS ON LEADING EDGE
SUMFY2=CY..ACTS ON LEADING AND SIDE EDGE
SUMFT2=CY..ACTS ON SIDE EDGE

SUMFX = 0.
SUMFY1 = 0.
SUMFY2 = -.18233E-01
SUMFT2 = -.50575E-02

SIDE EDGE DISTRIBUTION

JTIP	JSE	DISTANCE FROM LE /TIPCHORD	SUCTION FORCE PER UNIT LENGTH /(Q*TIPCHORD)	GAMMA,SE /VINF	YBAR	XSE
1	5	.25000	.00057	-.00011	-7.23000	7.78041
2	6	.50000	.00209	-.00051	-7.23000	8.61780
3	7	.75000	-.00112	-.00072	-7.23000	9.45520
4	8	1.00000	-.02700	-.00588	-7.23000	10.29260

****T.E. FIN VORTICITY DUE TO ATTACHED FLOW*****

IVRT	GAMMA/VINF	Y.C.G. (LOCAL FIN)	Y.C.G. (BODY AXES)	Z.C.G. (BODY AXES)
4	-2.22595	-5.41287	-7.52787	-.00000

------------------LOWER RIGHT OR UPPER VERTICAL FIN--------------------

I	Y/(B/2)	CN*C/(2*B)	CT*C/(2*B)	CY1*C/(2*B)	CYTOT*C/(2*B)	CS*C/(2*B)	CSINT	YBAR	GAMNET(I)	GAMMA,LE/VINF	XLE
15	.08162	-.00645	0.00000	0.00000	-.00001	0.00000	0.00000	0.00000	.10968	0.00000	.63500
16	.24804	-.00332	0.00000	0.00000	-.00002	0.00000	0.00000	0.00000	-.05629	0.00000	1.92985
17	.41438	-.00071	0.00000	0.00000	-.00000	0.00000	0.00000	0.00000	-.04247	0.00000	3.22407
18	.58060	-.00012	0.00000	0.00000	-.00000	0.00000	0.00000	0.00000	-.00911	0.00000	4.51731
19	.74660	-.00001	0.00000	0.00000	-.00000	0.00000	0.00000	0.00000	-.00167	0.00000	5.80884
20	.91216	.00000	0.00000	0.00000	0.00000	0.00000	0.00000	0.00000	-.00015	0.00000	7.09699
21	1.00000	0.00000							.00001		

THRUST- AND SIDE-FORCE COEFFICIENTS IN PLANE OF THE FIN

SUMFX =CX..ACTS ON LEADING EDGE
SUMFY1=CY..ACTS ON LEADING EDGE
SUMFY2=CY..ACTS ON LEADING AND SIDE EDGE
SUMFT2=CY..ACTS ON SIDE EDGE

SUMFX = 0.
SUMFY1 = 0.
SUMFY2 = -.65305E-04
SUMFT2 = .59962E-11

SIDE EDGE DISTRIBUTION

JTIP	JSE	DISTANCE FROM LE /TIPCHORD	SUCTION FORCE PER UNIT LENGTH /(Q*TIPCHORD)	GAMMA,SE /VINF	YBAR	XSE
1	9	.25000	.00000	0.00000	0.00000	7.78041
2	10	.50000	.00000	0.00000	0.00000	8.61780
3	11	.75000	.00000	0.00000	0.00000	9.45520
4	12	1.00000	.00000	0.00000	0.00000	10.29260

****T.E. FIN VORTICITY DUE TO ATTACHED FLOW*****

IVRT	GAMMA/VINF	Y.C.G. (LOCAL FIN)	Y.C.G. (BODY AXES)	Z.C.G. (BODY AXES)
5	-.09334	1.98101	-.00000	4.09601

------------------UPPER LEFT OR LOWER VERTICAL FIN--------------------

I	Y/(B/2)	CN*C/(2*B)	CT*C/(2*B)	CY1*C/(2*B)	CYTOT*C/(2*B)	CS*C/(2*B)	CSINT	YBAR	GAMNET(I)	GAMMA,LE/VINF	XLE
22	-.08162	.01123	0.00000	0.00000	.00001	0.00000	0.00000	0.00000	.10977	0.00000	.63500
23	-.24804	.00498	0.00000	0.00000	.00002	0.00000	0.00000	0.00000	-.05629	0.00000	1.92985

24	-.41438	.00084	0.00000	0.00000	.00000	0.00000	0.00000	0.00000	-.04248	0.00000	3.22407
25	-.58060	.00014	0.00000	0.00000	.00000	0.00000	0.00000	0.00000	-.00912	0.00000	4.51731
26	-.74660	.00002	0.00000	0.00000	.00000	0.00000	0.00000	0.00000	-.00169	0.00000	5.80884
27	-.91216	.00000	0.00000	0.00000	0.00000	0.00000	0.00000	0.00000	-.00017	0.00000	7.09699
28	-1.00000	0.00000							-.00003		

THRUST- AND SIDE-FORCE COEFFICIENTS IN PLANE OF THE FIN

SUMFX =CX..ACTS ON LEADING EDGE
SUMFY1=CY..ACTS ON LEADING EDGE
SUMFY2=CY..ACTS ON LEADING AND SIDE EDGE
SUMFT2=CY..ACTS ON SIDE EDGE

SUMFX = 0.
SUMFY1 = 0.
SUMFY2 = .65226E-04
SUMFT2 = .26827E-11

SIDE EDGE DISTRIBUTION

JTIP	JSE	DISTANCE FROM LE /TIPCHORD	SUCTION FORCE PER UNIT LENGTH /(Q*TIPCHORD)	GAMMA.SE /VINF	YBAR	XSE
1	13	.25000	.00000	0.00000	0.00000	7.78041
2	14	.50000	.00000	0.00000	0.00000	8.61780
3	15	.75000	.00000	0.00000	0.00000	9.45520
4	16	1.00000	.00000	0.00000	0.00000	10.29260

****T.E. FIN VORTICITY DUE TO ATTACHED FLOW*****

IVRT	GAMMA/VINF	Y.C.G. (LOCAL FIN)	Y.C.G. (BODY AXES)	Z.C.G. (BODY AXES)
6	-.16236	-1.84585	.00000	-3.96085

CROSSFLOW VELOCITIES AT CONTROL POINTS INDUCED BY VORTICES AND THEIR IMAGES

IC	X,BODY	Y,BODY	Z,BODY	V	W
1	.18928E+02	.27051E+01	0.	0.	0.
2	.21551E+02	.27051E+01	0.	0.	0.
3	.24175E+02	.27051E+01	0.	0.	0.
4	.26799E+02	.27051E+01	0.	0.	0.
5	.19915E+02	.39083E+01	0.	0.	0.
6	.22215E+02	.39083E+01	0.	0.	0.
7	.24515E+02	.39083E+01	0.	0.	0.
8	.26815E+02	.39083E+01	0.	0.	0.
9	.20902E+02	.51110E+01	0.	0.	0.
10	.22878E+02	.51110E+01	0.	0.	0.
11	.24855E+02	.51110E+01	0.	0.	0.
12	.26831E+02	.51110E+01	0.	0.	0.
13	.21888E+02	.63127E+01	0.	0.	0.
14	.23541E+02	.63127E+01	0.	0.	0.
15	.25194E+02	.63127E+01	0.	0.	0.
16	.26847E+02	.63127E+01	0.	0.	0.
17	.22873E+02	.75129E+01	0.	0.	0.
18	.24203E+02	.75129E+01	0.	0.	0.
19	.25533E+02	.75129E+01	0.	0.	0.
20	.26863E+02	.75129E+01	0.	0.	0.
21	.23855E+02	.87099E+01	0.	0.	0.
22	.24863E+02	.87099E+01	0.	0.	0.
23	.25871E+02	.87099E+01	0.	0.	0.
24	.26880E+02	.87099E+01	0.	0.	0.
25	.18928E+02	-.27051E+01	0.	0.	0.
26	.21551E+02	-.27051E+01	0.	0.	0.
27	.24175E+02	-.27051E+01	0.	0.	0.
28	.26799E+02	-.27051E+01	0.	0.	0.
29	.19915E+02	-.39083E+01	0.	0.	0.
30	.22215E+02	-.39083E+01	0.	0.	0.
31	.24515E+02	-.39083E+01	0.	0.	0.
32	.26815E+02	-.39083E+01	0.	0.	0.
33	.20902E+02	-.51110E+01	0.	0.	0.
34	.22878E+02	-.51110E+01	0.	0.	0.
35	.24855E+02	-.51110E+01	0.	0.	0.
36	.26831E+02	-.51110E+01	0.	0.	0.
37	.21888E+02	-.63127E+01	0.	0.	0.
38	.23541E+02	-.63127E+01	0.	0.	0.
39	.25194E+02	-.63127E+01	0.	0.	0.
40	.26847E+02	-.63127E+01	0.	0.	0.
41	.22873E+02	-.75129E+01	0.	0.	0.
42	.24203E+02	-.75129E+01	0.	0.	0.
43	.25533E+02	-.75129E+01	0.	0.	0.
44	.26863E+02	-.75129E+01	0.	0.	0.
45	.23855E+02	-.87099E+01	0.	0.	0.
46	.24863E+02	-.87099E+01	0.	0.	0.
47	.25871E+02	-.87099E+01	0.	0.	0.
48	.26880E+02	-.87099E+01	0.	0.	0.
49	.18928E+02	0.	.27051E+01	0.	0.
50	.21551E+02	0.	.27051E+01	0.	0.
51	.24175E+02	0.	.27051E+01	0.	0.
52	.26799E+02	0.	.27051E+01	0.	0.
53	.19915E+02	0.	.39083E+01	0.	0.
54	.22215E+02	0.	.39083E+01	0.	0.
55	.24515E+02	0.	.39083E+01	0.	0.
56	.26815E+02	0.	.39083E+01	0.	0.
57	.20902E+02	0.	.51110E+01	0.	0.
58	.22878E+02	0.	.51110E+01	0.	0.
59	.24855E+02	0.	.51110E+01	0.	0.

60	.26831E+02	0.	.51110E+01	0.	0.
61	.21888E+02	0.	.63127E+01	0.	0.
62	.23541E+02	0.	.63127E+01	0.	0.
63	.25194E+02	0.	.63127E+01	0.	0.
64	.26847E+02	0.	.63127E+01	0.	0.
65	.22873E+02	0.	.75129E+01	0.	0.
66	.24203E+02	0.	.75129E+01	0.	0.
67	.25533E+02	0.	.75129E+01	0.	0.
68	.26863E+02	0.	.75129E+01	0.	0.
69	.23855E+02	0.	.87099E+01	0.	0.
70	.24863E+02	0.	.87099E+01	0.	0.
71	.25871E+02	0.	.87099E+01	0.	0.
72	.26880E+02	0.	.87099E+01	0.	0.
73	.18928E+02	0.	-.27051E+01	0.	0.
74	.21551E+02	0.	-.27051E+01	0.	0.
75	.24175E+02	0.	-.27051E+01	0.	0.
76	.26799E+02	0.	-.27051E+01	0.	0.
77	.19915E+02	0.	-.39083E+01	0.	0.
78	.22215E+02	0.	-.39083E+01	0.	0.
79	.24515E+02	0.	-.39083E+01	0.	0.
80	.26815E+02	0.	-.39083E+01	0.	0.
81	.20902E+02	0.	-.51110E+01	0.	0.
82	.22878E+02	0.	-.51110E+01	0.	0.
83	.24855E+02	0.	-.51110E+01	0.	0.
84	.26831E+02	0.	-.51110E+01	0.	0.
85	.21888E+02	0.	-.63127E+01	0.	0.
86	.23541E+02	0.	-.63127E+01	0.	0.
87	.25194E+02	0.	-.63127E+01	0.	0.
88	.26847E+02	0.	-.63127E+01	0.	0.
89	.22873E+02	0.	-.75129E+01	0.	0.
90	.24203E+02	0.	-.75129E+01	0.	0.
91	.25533E+02	0.	-.75129E+01	0.	0.
92	.26863E+02	0.	-.75129E+01	0.	0.
93	.23855E+02	0.	-.87099E+01	0.	0.
94	.24863E+02	0.	-.87099E+01	0.	0.
95	.25871E+02	0.	-.87099E+01	0.	0.
96	.26880E+02	0.	-.87099E+01	0.	0.
97	.18443E+02	.19733E+01	.52875E+00	0.	0.
98	.18443E+02	.14446E+01	.14446E+01	0.	0.
99	.18443E+02	.52875E+00	.19733E+01	0.	0.
100	.18443E+02	-.52875E+00	.19733E+01	0.	0.
101	.18443E+02	-.14446E+01	.14446E+01	0.	0.
102	.18443E+02	-.19733E+01	.52875E+00	0.	0.
103	.18443E+02	-.19733E+01	-.52875E+00	0.	0.
104	.18443E+02	-.14446E+01	-.14446E+01	0.	0.
105	.18443E+02	-.52875E+00	-.19733E+01	0.	0.
106	.18443E+02	.52875E+00	-.19733E+01	0.	0.
107	.18443E+02	.14446E+01	-.14446E+01	0.	0.
108	.18443E+02	.19733E+01	-.52875E+00	0.	0.
109	.21226E+02	.19733E+01	.52875E+00	0.	0.
110	.21226E+02	.14446E+01	.14446E+01	0.	0.
111	.21226E+02	.52875E+00	.19733E+01	0.	0.
112	.21226E+02	-.52875E+00	.19733E+01	0.	0.
113	.21226E+02	-.14446E+01	.14446E+01	0.	0.
114	.21226E+02	-.19733E+01	.52875E+00	0.	0.
115	.21226E+02	-.19733E+01	-.52875E+00	0.	0.
116	.21226E+02	-.14446E+01	-.14446E+01	0.	0.
117	.21226E+02	-.52875E+00	-.19733E+01	0.	0.
118	.21226E+02	.52875E+00	-.19733E+01	0.	0.
119	.21226E+02	.14446E+01	-.14446E+01	0.	0.

120	.21224E+02	.19733E+01	-.52875E+00	0.	0.
121	.24008E+02	.19733E+01	.52875E+00	0.	0.
122	.24008E+02	.14446E+01	.14446E+01	0.	0.
123	.24008E+02	.52875E+00	.19733E+01	0.	0.
124	.24008E+02	-.52875E+00	.19733E+01	0.	0.
125	.24008E+02	-.14446E+01	.14446E+01	0.	0.
126	.24008E+02	-.19733E+01	.52875E+00	0.	0.
127	.24008E+02	-.19733E+01	-.52875E+00	0.	0.
128	.24008E+02	-.14446E+01	-.14446E+01	0.	0.
129	.24008E+02	-.52875E+00	-.19733E+01	0.	0.
130	.24008E+02	.52875E+00	-.19733E+01	0.	0.
131	.24008E+02	.14446E+01	-.14446E+01	0.	0.
132	.24008E+02	.19733E+01	-.52875E+00	0.	0.
133	.26791E+02	.19733E+01	.52875E+00	0.	0.
134	.26791E+02	.14446E+01	.14446E+01	0.	0.
135	.26791E+02	.52875E+00	.19733E+01	0.	0.
136	.26791E+02	-.52875E+00	.19733E+01	0.	0.
137	.26791E+02	-.14446E+01	.14446E+01	0.	0.
138	.26791E+02	-.19733E+01	.52875E+00	0.	0.
139	.26791E+02	-.19733E+01	-.52875E+00	0.	0.
140	.26791E+02	-.14446E+01	-.14446E+01	0.	0.
141	.26791E+02	-.52875E+00	-.19733E+01	0.	0.
142	.26791E+02	.52875E+00	-.19733E+01	0.	0.
143	.26791E+02	.14446E+01	-.14446E+01	0.	0.
144	.26791E+02	.19733E+01	-.52875E+00	0.	0.

STEP 3 LOADS ON FORWARD FINS WITH EFFECTS OF NOSE VORTICES

NASA/LRC TF-4 WITH KING TAIL (D), FOREBODY AND CANARD SECTION

```
$INPUT
BIL     = .1113E+02,
B2      = .723E+01,
B2V     = .723E+01,
CRP     = .1113E+02,
CRPV    = .1113E+02,
DELD    = 0.0,
DELL    = -.5E+01,
DELR    = .5E+01,
DELU    = 0.0,
ERATIO  = .1E+01,
FAC     = .95E+00,
FKLE    = .5E+00,
FKSE    = .1E+01,
FMACH   = .25E+01,
ITAIL   = 0,
JCPT    = 96,
LVSWP   = 0,
MINPRN  = 0,
MSWD    = 6,
MSWL    = 6,
MSWR    = 6,
MSWU    = 6,
NBDCR   = 12,
NBDYPR  = 1,
NBSHED  = 1,
NCPOUT  = 0,
NCRX    = 1,
NCW     = 4,
NCWR    = 4,
NCWT    = 0,
NDRAG   = 1,
NFVNPR  = 0,
NOLINP  = 1,
NOUT    = 0,
NPR     = 0,
NPRESS  = 0,
NTDAT   = 0,
NTPR    = 0,
NVLIN   = 1,
NVRTPL  = 1,
NVRTX   = 0,
N2DPRB  = 0,
N2DPRF  = 0,
PHIDIH  = 0.0,
PHIFR   = 0.0,
PHIFL   = 0.0,
PHIFU   = .9E+02,
PHIFD   = .9E+02,
PHIINT  = 0.0,
RA      = .2115E+01,
RB      = .2115E+01,
REFL    = .423E+01,
SREF    = .1412E+02,
SWLEP   = .471E+02,
SWLEV   = .471E+02,
SWTEP   = 0.0,
SWTEV   = 0.0,
THETIT  = 0.0,
THETR   = 0.0,
THETL   = 0.0,
THETU   = .9E+02,
THETD   = .9E+02,
TOLFAC  = .1E+01,
VRTMAX  = .35E+00,
XM      = .4604E+02,
XSTART  = 0.0,
XWLF    = .158E+02,
ZM      = 0.0,
$END

*****    NOSE VORTICES ARE TRACKED ENTIRE LENGTH OF BODY
```

FIN SECTION GEOMETRY DESCRIPTION

NO. OF CHORDWISE PANELS ON FINS PRESENT (NCW) = 4

FIN PROPERTY		FIN 1 OR R	FIN 2 OR L	FIN 3 OR U	FIN 4 OR D
NO. OF PANELS - SPANWISE	(MSW) =	6	6	6	6
ROOT CHORD	(CR) =	11.130	11.130	11.130	11.130
LEADING EDGE SWEEP	(SWLE) =	47.100	47.100	47.100	47.100
TRAILING EDGE SWEEP	(SWTE) =	0.000	0.000	0.000	0.000
EXPOSED SEMISPAN	(B2) =	7.230	7.230	7.230	7.230
FIN DIHEDRAL	(PHIF) =	0.000	0.000	90.000	90.000
BODY ANGLE OF FIN ATTACHMENT	(THET) =	0.000	0.000	90.000	90.000
FIN DEFLECTION	(DEL) =	5.000	-5.000	0.000	0.000
Y-INTERSECTION OF FIN TO BODY	(YBOD) =	2.115	-2.115	-.000	.000
Z-INTERSECTION OF FIN TO BODY	(ZBOD) =	0.000	-.000	2.115	-2.115

FLOW CONDITIONS

MACH = 2.50000 ALPHAC= 15.00000 PHI = .00100 ALFA = 15.00000 BETA = .00026

CRPT = 11.13000
CRPTV = 11.13000

POINT COORDINATES AND PERTURBATION VELOCITIES CALCULATED BY PROGRAM VPATH2

IC	XCP	YCP	ZCP	VVEL(IC)	WVEL(IC)
1	3.12800	2.70510	0.00000	0.	0.
2	5.75100	2.70510	0.00000	0.	0.
3	8.37500	2.70510	0.00000	0.	0.
4	10.99900	2.70510	0.00000	0.	0.
5	4.11500	3.90830	0.00000	0.	0.
6	6.41500	3.90830	0.00000	0.	0.
7	8.71500	3.90830	0.00000	0.	0.
8	11.01500	3.90830	0.00000	0.	0.
9	5.10200	5.11100	0.00000	0.	0.
10	7.07800	5.11100	0.00000	0.	0.
11	9.05500	5.11100	0.00000	0.	0.
12	11.03100	5.11100	0.00000	0.	0.
13	6.08800	6.31270	0.00000	0.	0.
14	7.74100	6.31270	0.00000	0.	0.
15	9.39400	6.31270	0.00000	0.	0.
16	11.04700	6.31270	0.00000	0.	0.
17	7.07300	7.51290	0.00000	0.	0.
18	8.40300	7.51290	0.00000	0.	0.
19	9.73300	7.51290	0.00000	0.	0.
20	11.06300	7.51290	0.00000	0.	0.
21	8.05500	8.70990	0.00000	0.	0.
22	9.06300	8.70990	0.00000	0.	0.
23	10.07100	8.70990	0.00000	0.	0.
24	11.08000	8.70990	0.00000	0.	0.
25	3.12800	-2.70510	0.00000	0.	0.
26	5.75100	-2.70510	0.00000	0.	0.
27	8.37500	-2.70510	0.00000	0.	0.
28	10.99900	-2.70510	0.00000	0.	0.
29	4.11500	-3.90830	0.00000	0.	0.
30	6.41500	-3.90830	0.00000	0.	0.
31	8.71500	-3.90830	0.00000	0.	0.
32	11.01500	-3.90830	0.00000	0.	0.
33	5.10200	-5.11100	0.00000	0.	0.
34	7.07800	-5.11100	0.00000	0.	0.
35	9.05500	-5.11100	0.00000	0.	0.
36	11.03100	-5.11100	0.00000	0.	0.
37	6.08800	-6.31270	0.00000	0.	0.
38	7.74100	-6.31270	0.00000	0.	0.
39	9.39400	-6.31270	0.00000	0.	0.
40	11.04700	-6.31270	0.00000	0.	0.
41	7.07300	-7.51290	0.00000	0.	0.
42	8.40300	-7.51290	0.00000	0.	0.
43	9.73300	-7.51290	0.00000	0.	0.
44	11.06300	-7.51290	0.00000	0.	0.
45	8.05500	-8.70990	0.00000	0.	0.
46	9.06300	-8.70990	0.00000	0.	0.
47	10.07100	-8.70990	0.00000	0.	0.
48	11.08000	-8.70990	0.00000	0.	0.
49	3.12800	0.00000	2.70510	0.	0.
50	5.75100	0.00000	2.70510	0.	0.
51	8.37500	0.00000	2.70510	0.	0.
52	10.99900	0.00000	2.70510	0.	0.
53	4.11500	0.00000	3.90830	0.	0.
54	6.41500	0.00000	3.90830	0.	0.
55	8.71500	0.00000	3.90830	0.	0.
56	11.01500	0.00000	3.90830	0.	0.
57	5.10200	0.00000	5.11100	0.	0.
58	7.07800	0.00000	5.11100	0.	0.

59	9.05500	0.00000	5.11100	0.	0.
60	11.03100	0.00000	5.11100	0.	0.
61	6.08800	0.00000	6.31270	0.	0.
62	7.74100	0.00000	6.31270	0.	0.
63	9.39400	0.00000	6.31270	0.	0.
64	11.04700	0.00000	6.31270	0.	0.
65	7.07300	0.00000	7.51290	0.	0.
66	8.40300	0.00000	7.51290	0.	0.
67	9.73300	0.00000	7.51290	0.	0.
68	11.06300	0.00000	7.51290	0.	0.
69	8.05500	0.00000	8.70990	0.	0.
70	9.06300	0.00000	8.70990	0.	0.
71	10.07100	0.00000	8.70990	0.	0.
72	11.08000	0.00000	8.70990	0.	0.
73	3.12800	0.00000	-2.70510	0.	0.
74	5.75100	0.00000	-2.70510	0.	0.
75	8.37500	0.00000	-2.70510	0.	0.
76	10.99900	0.00000	-2.70510	0.	0.
77	4.11500	0.00000	-3.90830	0.	0.
78	6.41500	0.00000	-3.90830	0.	0.
79	8.71500	0.00000	-3.90830	0.	0.
80	11.01500	0.00000	-3.90830	0.	0.
81	5.10200	0.00000	-5.11100	0.	0.
82	7.07800	0.00000	-5.11100	0.	0.
83	9.05500	0.00000	-5.11100	0.	0.
84	11.03100	0.00000	-5.11100	0.	0.
85	6.08800	0.00000	-6.31270	0.	0.
86	7.74100	0.00000	-6.31270	0.	0.
87	9.39400	0.00000	-6.31270	0.	0.
88	11.04700	0.00000	-6.31270	0.	0.
89	7.07300	0.00000	-7.51290	0.	0.
90	8.40300	0.00000	-7.51290	0.	0.
91	9.73300	0.00000	-7.51290	0.	0.
92	11.06300	0.00000	-7.51290	0.	0.
93	8.05500	0.00000	-8.70990	0.	0.
94	9.06300	0.00000	-8.70990	0.	0.
95	10.07100	0.00000	-8.70990	0.	0.
96	11.08000	0.00000	-8.70990	0.	0.
97	2.64300	1.97330	.52875	0.	0.
98	2.64300	1.44460	1.44460	0.	0.
99	2.64300	.52875	1.97330	0.	0.
100	2.64300	-.52875	1.97330	0.	0.
101	2.64300	-1.44460	1.44460	0.	0.
102	2.64300	-1.97330	.52875	0.	0.
103	2.64300	-1.97330	-.52875	0.	0.
104	2.64300	-1.44460	-1.44460	0.	0.
105	2.64300	-.52875	-1.97330	0.	0.
106	2.64300	.52875	-1.97330	0.	0.
107	2.64300	1.44460	-1.44460	0.	0.
108	2.64300	1.97330	-.52875	0.	0.
109	5.42600	1.97330	.52875	0.	0.
110	5.42600	1.44460	1.44460	0.	0.
111	5.42600	.52875	1.97330	0.	0.
112	5.42600	-.52875	1.97330	0.	0.
113	5.42600	-1.44460	1.44460	0.	0.
114	5.42600	-1.97330	.52875	0.	0.
115	5.42600	-1.97330	-.52875	0.	0.
116	5.42600	-1.44460	-1.44460	0.	0.
117	5.42600	-.52875	-1.97330	0.	0.
118	5.42600	.52875	-1.97330	0.	0.
119	5.42600	1.44460	-1.44460	0.	0.
120	5.42600	1.97330	-.52875	0.	0.
121	8.20800	1.97330	.52875	0.	0.
122	8.20800	1.44460	1.44460	0.	0.
123	8.20800	.52875	1.97330	0.	0.
124	8.20800	-.52875	1.97330	0.	0.
125	8.20800	-1.44460	1.44460	0.	0.
126	8.20800	-1.97330	.52875	0.	0.
127	8.20800	-1.97330	-.52875	0.	0.
128	8.20800	-1.44460	-1.44460	0.	0.
129	8.20800	-.52875	-1.97330	0.	0.
130	8.20800	.52875	-1.97330	0.	0.
131	8.20800	1.44460	-1.44460	0.	0.
132	8.20800	1.97330	-.52875	0.	0.
133	10.99100	1.97330	.52875	0.	0.
134	10.99100	1.44460	1.44460	0.	0.
135	10.99100	.52875	1.97330	0.	0.
136	10.99100	-.52875	1.97330	0.	0.
137	10.99100	-1.44460	1.44460	0.	0.
138	10.99100	-1.97330	.52875	0.	0.
139	10.99100	-1.97330	-.52875	0.	0.
140	10.99100	-1.44460	-1.44460	0.	0.
141	10.99100	-.52875	-1.97330	0.	0.
142	10.99100	.52875	-1.97330	0.	0.
143	10.99100	1.44460	-1.44460	0.	0.
144	10.99100	1.97330	-.52875	0.	0.

** SPECPR **

VELOCITIES AND BERNOULLI PRESSURES AT CONTROL POINTS IMMEDIATELY ABOVE AND BELOW FIN SURFACE *** STEP 3

J	X(J)	Y(J)	Z(J)	UTOTA	VTOTA	WTOTA	PRESSA	UTOTB	VTOTB	WTOTB	PRESSB
1	3.127561	2.705077	0.000000	.216337	-.228770	-.345975	-.216857	-.205412	.225087	-.345975	.619062
2	5.751312	2.705077	0.000000	.158327	-.125490	-.345975	-.180404	-.150125	.123460	-.345975	.494315
3	8.375062	2.705077	0.000000	.129779	-.068836	-.345975	-.151181	-.123269	.067320	-.345975	.420202
4	10.998812	2.705077	0.000000	.111498	-.029900	-.345975	-.129144	-.106217	.028672	-.345975	.368409
5	4.114882	3.908323	0.000000	.222483	-.237482	-.345975	-.218941	-.211910	.229980	-.345975	.638638
6	6.414921	3.908323	0.000000	.184812	-.148410	-.345975	-.198958	-.176590	.143276	-.345975	.582571
7	8.714959	3.908323	0.000000	.154034	-.083057	-.345975	-.174047	-.147348	.079106	-.345975	.504485
8	11.014998	3.908323	0.000000	.127677	-.035147	-.345975	-.147377	-.122171	.032070	-.345975	.423688
9	5.101730	5.110993	0.000000	.209948	-.225150	-.345975	-.214730	-.199623	.215601	-.345975	.607240
10	7.078212	5.110993	0.000000	.206999	-.167620	-.345975	-.210321	-.198229	.159438	-.345975	.656001
11	9.054694	5.110993	0.000000	.178560	-.097285	-.345975	-.192221	-.171372	.091001	-.345975	.592454
12	11.031176	5.110993	0.000000	.155154	-.043479	-.345975	-.173144	-.149095	.038374	-.345975	.522201
13	6.087825	6.312745	0.000000	.199075	-.215098	-.345975	-.210262	-.187465	.200869	-.345975	.575747
14	7.740997	6.312745	0.000000	.203323	-.165500	-.345975	-.208743	-.194137	.155289	-.345975	.642943
15	9.394169	6.312745	0.000000	.201568	-.111279	-.345975	-.205205	-.192938	.100991	-.345975	.674726
16	11.047341	6.312745	0.000000	.184835	-.052620	-.345975	-.194251	-.177833	.044950	-.345975	.634287
17	7.072615	7.512907	0.000000	.192277	-.209805	-.345975	-.207113	-.177811	.188458	-.345975	.550749
18	8.402905	7.512907	0.000000	.196007	-.162381	-.345975	-.205406	-.183536	.143947	-.345975	.609386
19	9.733195	7.512907	0.000000	.198227	-.109900	-.345975	-.203578	-.189335	.098633	-.345975	.661155
20	11.063485	7.512907	0.000000	.198193	-.057441	-.345975	-.201707	-.190039	.047006	-.345975	.684096
21	8.054830	8.709930	0.000000	.177676	-.184291	-.345975	-.197915	-.180489	.201139	-.345975	.549003
22	9.063082	8.709930	0.000000	.186067	-.150700	-.345975	-.199780	-.178555	.143585	-.345975	.590032
23	10.071335	8.709930	0.000000	.178968	-.104901	-.345975	-.192881	-.163829	.079545	-.345975	.567575
24	11.079587	8.709930	0.000000	.156338	-.049945	-.345975	-.174320	-.144431	.030971	-.345975	.505668
25	3.127561	-2.705077	0.000000	.147593	.154797	-.171663	-.175001	-.136667	-.151103	-.171663	.428879
26	5.751312	-2.705077	0.000000	.104195	.081806	-.171663	-.123580	-.095992	-.079764	-.171663	.323556
27	8.375062	-2.705077	0.000000	.083261	.043813	-.171663	-.092583	-.076748	-.042282	-.171663	.270514
28	10.998812	-2.705077	0.000000	.065002	.017399	-.171663	-.063240	-.059716	-.016154	-.171663	.221580
29	4.114882	-3.908323	0.000000	.141249	.150067	-.171663	-.169287	-.130676	-.142559	-.171663	.413140
30	6.414921	-3.908323	0.000000	.117897	.094406	-.171663	-.140686	-.109675	-.089266	-.171663	.366003
31	8.714959	-3.908323	0.000000	.096499	.052102	-.171663	-.111411	-.089813	-.048146	-.171663	.310997
32	11.014998	-3.908323	0.000000	.077711	.021710	-.171663	-.083353	-.072201	-.018621	-.171663	.258966
33	5.101730	-5.110993	0.000000	.124935	.133667	-.171663	-.152344	-.114609	-.124114	-.171663	.367964
34	7.078212	-5.110993	0.000000	.127102	.103137	-.171663	-.151198	-.118331	-.094951	-.171663	.393570
35	9.054694	-5.110993	0.000000	.109765	.060270	-.171663	-.128594	-.102578	-.053984	-.171663	.351968
36	11.031176	-5.110993	0.000000	.094087	.027051	-.171663	-.106945	-.088027	-.021943	-.171663	.308606
37	6.087825	-6.312745	0.000000	.113111	.122590	-.171663	-.138526	-.101500	-.108358	-.171663	.331431
38	7.740997	-6.312745	0.000000	.118573	.097100	-.171663	-.141683	-.109387	-.086886	-.171663	.365855
39	9.394169	-6.312745	0.000000	.120534	.067679	-.171663	-.141387	-.111904	-.057388	-.171663	.382974
40	11.047341	-6.312745	0.000000	.111222	.032817	-.171663	-.128916	-.104221	-.025144	-.171663	.361986
41	7.072615	-7.512907	0.000000	.106131	.117102	-.171663	-.129848	-.091663	-.095750	-.171663	.304354
42	8.402905	-7.512907	0.000000	.110019	.092982	-.171663	-.131641	-.097548	-.074545	-.171663	.330174
43	9.733195	-7.512907	0.000000	.112853	.063965	-.171663	-.132479	-.103961	-.052695	-.171663	.356895
44	11.063485	-7.512907	0.000000	.115291	.035139	-.171663	-.133770	-.107137	-.024702	-.171663	.371973
45	8.054830	-8.709930	0.000000	.091507	.091564	-.171663	-.108334	-.094318	-.108407	-.171663	.308117
46	9.063082	-8.709930	0.000000	.099906	.081161	-.171663	-.118168	-.092392	-.074041	-.171663	.313490
47	10.071335	-8.709930	0.000000	.099794	.062302	-.171663	-.116408	-.084654	-.036943	-.171663	.296161
48	11.079587	-8.709930	0.000000	.089056	.031846	-.171663	-.100216	-.077148	-.012869	-.171663	.274602
49	3.127561	0.000000	2.705077	.010588	.000005	-.163415	.039547	.010947	.000005	-.163802	.038843
50	5.751312	0.000000	2.705077	.008609	.000005	-.173344	.045941	.010685	.000005	-.175020	.041670
51	8.375062	0.000000	2.705077	.025821	.000005	-.201305	.013403	.038556	.000005	-.208157	-.011344
52	10.998812	0.000000	2.705077	.063858	.000005	-.254903	-.054970	.090490	.000005	-.262068	-.096488
53	4.114882	0.000000	3.908323	.011390	.000005	-.086962	.015689	.011488	.000005	-.087067	.015527
54	6.414921	0.000000	3.908323	.005061	.000005	-.079694	.026099	.005917	.000005	-.080386	.024572
55	8.714959	0.000000	3.908323	.002466	.000005	-.081492	.032281	.006222	.000005	-.083513	.025124
56	11.014998	0.000000	3.908323	.035063	.000005	-.156344	-.012237	.053565	.000005	-.161322	-.045250
57	5.101730	0.000000	5.110993	.014482	.000005	-.064920	.001206	.014501	.000005	-.064940	.001177

58	7.078212	0.000000	5.110993	.007879	.000005	-.054580	.010148	.008102	.000005	-.054760	.009775
59	9.054694	0.000000	5.110993	.003208	.000005	-.047808	.016671	.004338	.000005	-.048416	.014641
60	11.031176	0.000000	5.110993	.002846	.000005	-.052752	.019588	.007001	.000005	-.053870	.011614
61	6.087825	0.000000	6.312745	.020316	.000005	-.064079	-.010422	.020316	.000005	-.064079	-.010421
62	7.740997	0.000000	6.312745	.012249	.000005	-.049128	-.000795	.012285	.000005	-.049158	-.000854
63	9.394169	0.000000	6.312745	.006707	.000005	-.039161	.005787	.006914	.000005	-.039272	.005427
64	11.047341	0.000000	6.312745	.003123	.000005	-.033491	.010334	.003978	.000005	-.033721	.008734
65	7.072615	0.000000	7.512907	.028991	.000005	-.075187	-.022724	.028987	.000005	-.075183	-.022718
66	8.402905	0.000000	7.512907	.020963	.000005	-.059954	-.013216	.020963	.000005	-.059954	-.013216
67	9.733195	0.000000	7.512907	.013436	.000005	-.044967	-.004844	.013454	.000005	-.044977	-.004877
68	11.063485	0.000000	7.512907	.008527	.000005	-.035511	.000576	.008621	.000005	-.035536	.000403
69	8.054830	0.000000	8.709930	.028880	.000005	-.069362	-.024530	.028875	.000005	-.069357	-.024524
70	9.063082	0.000000	8.709930	.027502	.000005	-.068284	-.022374	.027498	.000005	-.068280	-.022368
71	10.071335	0.000000	8.709930	.026304	.000005	-.067467	-.020446	.026301	.000005	-.067466	-.020441
72	11.079587	0.000000	8.709930	.019481	.000005	-.053669	-.012847	.019484	.000005	-.053670	-.012853
73	3.127561	0.000000	-2.705077	.000344	.000005	-.159719	.061668	-.000028	.000005	-.160120	.062616
74	5.751312	0.000000	-2.705077	-.000402	.000005	-.171304	.065963	-.002487	.000005	-.172988	.071166
75	8.375062	0.000000	-2.705077	-.019306	.000005	-.199779	.117187	-.032049	.000005	-.206635	.151574
76	10.998812	0.000000	-2.705077	-.058571	.000005	-.253665	.230987	-.085209	.000005	-.260832	.314370
77	4.114882	0.000000	-3.908323	-.000810	.000005	-.079450	.038494	-.000920	.000005	-.079569	.038779
78	6.414921	0.000000	-3.908323	.003166	.000005	-.074553	.028057	.002299	.000005	-.075253	.030167
79	8.714959	0.000000	-3.908323	.004224	.000005	-.077536	.027014	.000459	.000005	-.079562	.035808
80	11.014998	0.000000	-3.908323	-.029551	.000005	-.153261	.133078	-.048061	.000005	-.158240	.184557
81	5.101730	0.000000	-5.110993	-.004151	.000005	-.055363	.035396	-.004181	.000005	-.055395	.035474
82	7.078212	0.000000	-5.110993	.000897	.000005	-.046391	.020769	.000663	.000005	-.046581	.021337
83	9.054694	0.000000	-5.110993	.003985	.000005	-.041520	.012284	.002844	.000005	-.042134	.014865
84	11.031176	0.000000	-5.110993	.003218	.000005	-.047644	.016579	-.000945	.000005	-.048764	.025656
85	6.087825	0.000000	-6.312745	-.008701	.000005	-.049844	.042620	-.008710	.000005	-.049854	.042644
86	7.740997	0.000000	-6.312745	-.003058	.000005	-.038912	.025480	-.003105	.000005	-.038950	.025596
87	9.394169	0.000000	-6.312745	.001928	.000005	-.028869	.010551	.001711	.000005	-.028986	.011042
88	11.047341	0.000000	-6.312745	.003883	.000005	-.025819	.005223	.003018	.000005	-.026051	.007042
89	7.072615	0.000000	-7.512907	-.014519	.000005	-.053832	.057308	-.014524	.000005	-.053838	.057322
90	8.402905	0.000000	-7.512907	-.008488	.000005	-.041514	.038173	-.008497	.000005	-.041522	.038196
91	9.733195	0.000000	-7.512907	-.004539	.000005	-.033696	.026051	-.004567	.000005	-.033711	.026118
92	11.063485	0.000000	-7.512907	-.000368	.000005	-.025074	.013329	-.000472	.000005	-.025102	.013553
93	8.054830	0.000000	-8.709930	-.031687	.000005	-.086202	.113141	-.031692	.000005	-.086207	.113154
94	9.063082	0.000000	-8.709930	-.019985	.000005	-.061162	.073246	-.019990	.000005	-.061166	.073258
95	10.071335	0.000000	-8.709930	-.011160	.000005	-.042107	.044214	-.011166	.000005	-.042110	.044228
96	11.079587	0.000000	-8.709930	-.007570	.000005	-.034692	.032885	-.007580	.000005	-.034695	.032908

PRESSURE LOADINGS AT CONTROL POINTS

J	X(J)	Y(J)	Z(J)	DELTP.LIN.	DELTP.BERN.
1	3.127561	2.705077	0.000000	.843499	.835919
2	5.751312	2.705077	0.000000	.616904	.674718
3	8.375062	2.705077	0.000000	.506095	.571383
4	10.998812	2.705077	0.000000	.435431	.497553
5	4.114882	3.908323	0.000000	.868787	.857579
6	6.414921	3.908323	0.000000	.722804	.781529
7	8.714959	3.908323	0.000000	.602764	.678531
8	11.014998	3.908323	0.000000	.499696	.571064
9	5.101730	5.110993	0.000000	.819142	.821970
10	7.078212	5.110993	0.000000	.810457	.866322
11	9.054694	5.110993	0.000000	.699864	.784674
12	11.031176	5.110993	0.000000	.608498	.695344
13	6.087825	6.312745	0.000000	.773081	.786010
14	7.740997	6.312745	0.000000	.794921	.851686
15	9.394169	6.312745	0.000000	.789013	.879931
16	11.047341	6.312745	0.000000	.725336	.828539
17	7.072615	7.512907	0.000000	.740177	.757862
18	8.402905	7.512907	0.000000	.759087	.814792
19	9.733195	7.512907	0.000000	.775123	.864733
20	11.063485	7.512907	0.000000	.776463	.885803
21	8.054830	8.709930	0.000000	.716328	.746918
22	9.063082	8.709930	0.000000	.729243	.789811
23	10.071335	8.709930	0.000000	.685593	.760457
24	11.079587	8.709930	0.000000	.601540	.679988
25	3.127561	-2.705077	0.000000	.568519	.603880
26	5.751312	-2.705077	0.000000	.400374	.447136
27	8.375062	-2.705077	0.000000	.320018	.363097
28	10.998812	-2.705077	0.000000	.249436	.284820
29	4.114882	-3.908323	0.000000	.543850	.582428
30	6.414921	-3.908323	0.000000	.455145	.506689
31	8.714959	-3.908323	0.000000	.372624	.422408
32	11.014998	-3.908323	0.000000	.299823	.342319
33	5.101730	-5.110993	0.000000	.479089	.520308
34	7.078212	-5.110993	0.000000	.490867	.544768
35	9.054694	-5.110993	0.000000	.424685	.480563
36	11.031176	-5.110993	0.000000	.364227	.415551
37	6.087825	-6.312745	0.000000	.429221	.469957
38	7.740997	-6.312745	0.000000	.455919	.507537
39	9.394169	-6.312745	0.000000	.464877	.524361
40	11.047341	-6.312745	0.000000	.430885	.490902
41	7.072615	-7.512907	0.000000	.395587	.434202
42	8.402905	-7.512907	0.000000	.415135	.461815
43	9.733195	-7.512907	0.000000	.433628	.489374
44	11.063485	-7.512907	0.000000	.444855	.505743
45	8.054830	-8.709930	0.000000	.371649	.416452
46	9.063082	-8.709930	0.000000	.384596	.431658
47	10.071335	-8.709930	0.000000	.368897	.412569
48	11.079587	-8.709930	0.000000	.332408	.374818
49	3.127561	0.000000	2.705077	-.000719	-.000704
50	5.751312	0.000000	2.705077	-.004153	-.004270
51	8.375062	0.000000	2.705077	-.025471	-.024747
52	10.998812	0.000000	2.705077	-.053265	-.041518
53	4.114882	0.000000	3.908323	-.000195	-.000162
54	6.414921	0.000000	3.908323	-.001713	-.001527
55	8.714959	0.000000	3.908323	-.007513	-.007157
56	11.014998	0.000000	3.908323	-.037005	-.033012
57	5.101730	0.000000	5.110993	-.000037	-.000029
58	7.078212	0.000000	5.110993	-.000447	-.000373
59	9.054694	0.000000	5.110993	-.002261	-.002030
60	11.031176	0.000000	5.110993	-.008309	-.007974
61	6.087825	0.000000	6.312745	.000001	.000001
62	7.740997	0.000000	6.312745	-.000073	-.000059
63	9.394169	0.000000	6.312745	-.000414	-.000360
64	11.047341	0.000000	6.312745	-.001710	-.001601
65	7.072615	0.000000	7.512907	.000008	.000006
66	8.402905	0.000000	7.512907	-.000000	-.000000
67	9.733195	0.000000	7.512907	-.000038	-.000032
68	11.063485	0.000000	7.512907	-.000189	-.000173
69	8.054830	0.000000	8.709930	.000009	.000006
70	9.063082	0.000000	8.709930	.000009	.000007
71	10.071335	0.000000	8.709930	.000005	.000005
72	11.079587	0.000000	8.709930	-.000006	-.000005
73	3.127561	0.000000	-2.705077	.000744	.000947
74	5.751312	0.000000	-2.705077	.004171	.005203
75	8.375062	0.000000	-2.705077	.025486	.034387
76	10.998812	0.000000	-2.705077	.053276	.083382
77	4.114882	0.000000	-3.908323	.000220	.000285
78	6.414921	0.000000	-3.908323	.001734	.002110
79	8.714959	0.000000	-3.908323	.007530	.008794
80	11.014998	0.000000	-3.908323	.037019	.051479
81	5.101730	0.000000	-5.110993	.000060	.000079
82	7.078212	0.000000	-5.110993	.000469	.000568
83	9.054694	0.000000	-5.110993	.002280	.002581
84	11.031176	0.000000	-5.110993	.008325	.009077
85	6.087825	0.000000	-6.312745	.000018	.000024
86	7.740997	0.000000	-6.312745	.000094	.000115
87	9.394169	0.000000	-6.312745	.000435	.000491
88	11.047341	0.000000	-6.312745	.001729	.001819
89	7.072615	0.000000	-7.512907	.000010	.000014
90	8.402905	0.000000	-7.512907	.000018	.000023
91	9.733195	0.000000	-7.512907	.000057	.000067
92	11.063485	0.000000	-7.512907	.000209	.000224
93	8.054830	0.000000	-8.709930	.000009	.000013
94	9.063082	0.000000	-8.709930	.000009	.000013
95	10.071335	0.000000	-8.709930	.000011	.000014
96	11.079587	0.000000	-8.709930	.000020	.000023

*** STEP 3

FIN LOADING INFORMATION

MACH NUMBER =	.25000E+01
ANGLE OF ATTACK =	15.000 DEGREES
SIDE SLIP ANGLE =	.000 DEGREES
FIN AREA =	52.34373
REFERENCE AREA =	14.12000
REFERENCE LENGTH =	4.23000
EXPOSED FIN SPAN B/2=	7.23000
MOMENT CENTER: XM =	46.04000
ZM =	0.00000

LINEAR PRESSURE (U/VINF) LOADS IN BODY SYSTEM

	TOTAL	FIN 1 OR R	FIN 2 OR L	FIN 3 OR U	FIN 4 OR D	INTERF. SHELL
DEFL. ANGLE DEG. =		5.00000	-5.00000	0.00000	0.00000	
CTHR =	.68327E-01	.49335E-01	.19533E-01	-.27064E-03	-.27074E-03	
CZ =	4.1038	2.5707	1.5331	0.	0.	.58154
CY =	-.69007E-04	0.	0.	.29987E-01	-.30056E-01	-.10138E-04
CM =	22.666	14.176	8.4905	0.	0.	3.2168
CLN =	-.38198E-03	0.	0.	.15075	-.15113	-.56088E-04
CLL =	-1.2724	-3.1676	1.8489	.23113E-01	.23196E-01	.18681E-15

FOLLOWING ARE IN UNROLLED BODY-AXIS COORDINATE SYSTEM

CZU =	4.1038	2.5707	1.5331	-.52338E-06	.52458E-06	.58154
CYU =	.26187E-05	.44867E-04	.26758E-04	.29987E-01	-.30056E-01	.11440E-07
CMU =	22.666	14.176	8.4905	-.26310E-05	.26377E-05	3.2168
CLNU =	.13620E-04	.24742E-03	.14819E-03	.15075	-.15113	.55927E-07

NOTE: L.E. OF LEAD PANEL IN FIRST CHORDWISE ROW IS SUPERSONIC

SPANWISE DISTRIBUTIONS

-------------------UPPER RIGHT OR RIGHT HORIZONTAL FIN--------------------

I	Y/(B/2)	CN*C/(2*B)	CT*C/(2*B)	CY1*C/(2*B)	CYTOT*C/(2*B)	CS*C/(2*B)	CSINT	YBAR	GAMNET(I)	GAMMA,LE/VINF	XLE
1	.08162	.21764	0.00000	0.00000	.00250	0.00000	0.00000	0.00000	-3.15103	0.00000	.63500
2	.24804	.21391	0.00000	0.00000	.00460	0.00000	0.00000	0.00000	.05282	0.00000	1.92985
3	.41438	.20034	0.00000	0.00000	.00530	0.00000	0.00000	0.00000	.19480	0.00000	3.22407
4	.58060	.17563	0.00000	0.00000	.00435	0.00000	0.00000	0.00000	.35559	0.00000	4.51731
5	.74660	.13964	0.00000	0.00000	.00363	0.00000	0.00000	0.00000	.51857	0.00000	5.80884
6	.91216	.09444	0.00000	0.00000	0.00000	0.00000	0.00000	0.00000	.65163	0.00000	7.09699
7	1.00000	0.00000							1.37763		

THRUST- AND SIDE-FORCE COEFFICIENTS IN PLANE OF THE FIN

SUMFX =CX..ACTS ON LEADING EDGE
SUMFY1=CY..ACTS ON LEADING EDGE
SUMFY2=CY..ACTS ON LEADING AND SIDE EDGE
SUMFT2=CY..ACTS ON SIDE EDGE

SUMFX = 0.
SUMFY1 = 0.
SUMFY2 = .50274E-01
SUMFT2 = .21231E-01

SIDE EDGE DISTRIBUTION

JTIP	JSE	DISTANCE FROM LE /TIPCHORD	SUCTION FORCE PER UNIT LENGTH /(Q*TIPCHORD)	GAMMA,SE /VINF	YBAR	XSE
1	1	.25000	-.00110	.00020	7.23000	7.78041
2	2	.50000	-.00398	.00092	7.23000	8.61780
3	3	.75000	.01211	.00313	7.23000	9.45520
4	4	1.00000	.09984	.02130	7.23000	10.29260

S.E. AUGMENTATION OF FIN NORMAL FORCE FROM SUCTION CONVERSION IN PROPORTION WITH FACTOR
KVSE = 1.000

(LOCAL FIN)	(ROLLED BODY-AXIS)	(UNROLLED BODY-AXIS)
CNADD = .02325	CYADD = 0.00000	CYADD = .00000
	CZADD = .02325	CZADD = .02325
	CMADD = .11423	CMADD = .11425
	CLNADD = 0.00000	CLNADD = .00000

CLLADD	=	-.05136	CLLADD	=	-.05136
XCG	=	25.2552	XCG	=	25.2552
YCG	=	9.3450	YCG	=	9.3450
ZCG	=	0.0000	ZCG	=	-.0002

**** T.E. FIN VORTICITY DUE TO SIDE-EDGE FORCE AUGMENTATION

IVPT	GAMMA/VINF	Y.C.G. (LOCAL FIN)	Z.C.G. (LOCAL FIN)	Y.C.G. (BODY AXES)	Z.C.G. (BODY AXES)
1	.02130	7.23000	.59790	9.34500	.59790

------------------LOWER LEFT OR LEFT HORIZONTAL FIN--------------------

I	Y/(B/2)	CN*C/(2*B)	CT*C/(2*B)	CY1*C/(2*B)	CYTOT*C/(2*B)	CS*C/(2*B)	CSINT	YBAR	GAMNET(I)	GAMMA.LE/VINF	XLE
8	-.08162	.13939	0.00000	0.00000	-.00192	0.00000	0.00000	0.00000	2.01812	0.00000	.63500
9	-.24804	.13271	0.00000	0.00000	-.00182	0.00000	0.00000	0.00000	-.09593	0.00000	1.92985
10	-.41438	.11994	0.00000	0.00000	-.00166	0.00000	0.00000	0.00000	-.18401	0.00000	3.22407
11	-.58060	.10148	0.00000	0.00000	-.00111	0.00000	0.00000	0.00000	-.26612	0.00000	4.51731
12	-.74660	.07732	0.00000	0.00000	-.00087	0.00000	0.00000	0.00000	-.34850	0.00000	5.80884
13	-.91216	.05037	0.00000	0.00000	0.00000	0.00000	0.00000	0.00000	-.38878	0.00000	7.09699
14	-1.00000	0.00000							-.73479		

THRUST- AND SIDE-FORCE COEFFICIENTS IN PLANE OF THE FIN

SUMFX =CX..ACTS ON LEADING EDGE
SUMFY1=CY..ACTS ON LEADING EDGE
SUMFY2=CY..ACTS ON LEADING AND SIDE EDGE
SUMFT2=CY..ACTS ON SIDE EDGE

SUMFX = 0.
SUMFY1 = 0.
SUMFY2 = -.18233E-01
SUMFT2 = -.50575E-02

SIDE EDGE DISTRIBUTION

JTIP	JSE	DISTANCE FROM LE /TIPCHORD	SUCTION FORCE PER UNIT LENGTH /(Q*TIPCHORD)	GAMMA.SE /VINF	YBAR	XSE
1	5	.25000	.00057	-.00011	-7.23000	7.78041
2	6	.50000	.00209	-.00051	-7.23000	8.61780
3	7	.75000	-.00112	-.00072	-7.23000	9.45520
4	8	1.00000	-.02700	-.00588	-7.23000	10.29260

S.F. AUGMENTATION OF FIN NORMAL FORCE FROM SUCTION CONVERSION IN PROPORTION WITH FACTOR
KVSE = 1.000

(LOCAL FIN)		(ROLLED BODY-AXIS)		(UNROLLED BODY-AXIS)	
CNADD =	.00611	CYADD =	0.00000	CYADD =	.00000
		CZADD =	.00611	CZADD =	.00611
		CMADD =	.03003	CMADD =	.03005
		CLNADD =	0.00000	CLNADD =	.00000
		CLLADD =	.01350	CLLADD =	.01350
		XCG =	25.2552	XCG =	25.2552
		YCG =	-9.3450	YCG =	-9.3450
		ZCG =	-.0000	ZCG =	.0002

**** T.E. FIN VORTICITY DUE TO SIDE-EDGE FORCE AUGMENTATION

IVRT	GAMMA/VINF	Y.C.G. (LOCAL FIN)	Z.C.G. (LOCAL FIN)	Y.C.G. (BODY AXES)	Z.C.G. (BODY AXES)
2	-.00588	-7.23000	.28965	-9.34500	.28965

-------------------LOWER RIGHT OR UPPER VERTICAL FIN--------------------

I	Y/(B/2)	CN*C/(2*B)	CT*C/(2*B)	CY1*C/(2*B)	CYTOT*C/(2*B)	CS*C/(2*B)	CSINT	YBAR	GAMNET(I)	GAMMA.LE/VINF	XLE
15	.08162	-.00758	0.00000	0.00000	-.00001	0.00000	0.00000	0.00000	.10968	0.00000	.63500
16	.24804	-.00369	0.00000	0.00000	-.00002	0.00000	0.00000	0.00000	-.05629	0.00000	1.92985
17	.41438	-.00075	0.00000	0.00000	-.00000	0.00000	0.00000	0.00000	-.04247	0.00000	3.22407
18	.58060	-.00013	0.00000	0.00000	-.00000	0.00000	0.00000	0.00000	-.00911	0.00000	4.51731
19	.74660	-.00001	0.00000	0.00000	-.00000	0.00000	0.00000	0.00000	-.00167	0.00000	5.80884
20	.91216	.00000	0.00000	0.00000	0.00000	0.00000	0.00000	0.00000	-.00015	0.00000	7.09699
21	1.00000	0.00000							.00001		

THRUST- AND SIDE-FORCE COEFFICIENTS IN PLANE OF THE FIN

SUMFX =CX..ACTS ON LEADING EDGE
SUMFY1=CY..ACTS ON LEADING EDGE
SUMFY2=CY..ACTS ON LEADING AND SIDE EDGE
SUMFT2=CY..ACTS ON SIDE EDGE

SUMFX = 0.
SUMFY1 = 0.
SUMFY2 = -.65305E-04
SUMFT2 = .59962E-11

SIDE EDGE DISTRIBUTION

JTIP	JSF	DISTANCE FROM LE /TIPCHORD	SUCTION FORCE PER UNIT LENGTH /(Q*TIPCHORD)	GAMMA.SE /VINF	YBAR	XSE

1	9	.25000	.00000	0.00000	0.00000	7.78041
2	10	.50000	.00000	0.00000	0.00000	8.61780
3	11	.75000	.00000	0.00000	0.00000	9.45520
4	12	1.00000	.00000	0.00000	0.00000	10.29260

------------------UPPER LEFT OR LOWER VERTICAL FIN--------------------

I	Y/(B/2)	CN*C/(2*B)	CT*C/(2*B)	CY1*C/(2*B)	CYTOT*C/(2*B)	CS*C/(2*B)	CSINT	YBAR	GAMNET(I)	GAMMA,LE/VINF	XLE
22	-.08162	.00758	0.00000	0.00000	.00001	0.00000	0.00000	0.00000	.10977	0.00000	.63500
23	-.24804	.00369	0.00000	0.00000	.00002	0.00000	0.00000	0.00000	-.05629	0.00000	1.92985
24	-.41438	.00076	0.00000	0.00000	.00000	0.00000	0.00000	0.00000	-.04248	0.00000	3.22407
25	-.58060	.00013	0.00000	0.00000	.00000	0.00000	0.00000	0.00000	-.00912	0.00000	4.51731
26	-.74660	.00001	0.00000	0.00000	.00000	0.00000	0.00000	0.00000	-.00169	0.00000	5.80884
27	-.91216	.00000	0.00000	0.00000	0.00000	0.00000	0.00000	0.00000	-.00017	0.00000	7.09699
28	-1.00000	0.00000							-.00003		

THRUST- AND SIDE-FORCE COEFFICIENTS IN PLANE OF THE FIN

SUMFX =CX..ACTS ON LEADING EDGE
SUMFY1=CY..ACTS ON LEADING EDGE
SUMFY2=CY..ACTS ON LEADING AND SIDE EDGE
SUMFT2=CY..ACTS ON SIDE EDGE

SUMFX = 0.
SUMFY1 = 0.
SUMFY2 = .65226E-04
SUMFT2 = .26827E-11

SIDE EDGE DISTRIBUTION

JTIP	JSE	DISTANCE FROM LE /TIPCHORD	SUCTION FORCE PER UNIT LENGTH /(Q*TIPCHORD)	GAMMA,SE /VINF	YBAR	XSE
1	13	.25000	.00000	0.00000	0.00000	7.78041
2	14	.50000	.00000	0.00000	0.00000	8.61780
3	15	.75000	.00000	0.00000	0.00000	9.45520
4	16	1.00000	.00000	0.00000	0.00000	10.29260

FIN LOADING INFORMATION

*** STEP 3

```
          MACH NUMBER =    .25000E+01
      ANGLE OF ATTACK =   15.000 DEGREES
      SIDE SLIP ANGLE =     .000 DEGREES
             FIN AREA =   52.34373
       REFERENCE AREA =   14.12000
     REFERENCE LENGTH =    4.23000
  EXPOSED FIN SPAN B/2=    7.23000
  MOMENT CENTER:   XM =   46.04000
                   ZM =    0.00000
```

BERNOULLI PRESSURE LOADS IN BODY SYSTEM

	TOTAL	FIN 1 OR R	FIN 2 OR L	FIN 3 OR U	FIN 4 OR D	INTERF. SHELL
DEFL. ANGLE DEG. =		5.00000	-5.00000	0.00000	0.00000	
CTHR =	.68327E-01	.49335E-01	.19533E-01	-.27064E-03	-.27074E-03	
CZ =	4.4827	2.7760	1.7066	0.	0.	.58154
CY =	-.16259E-01	0.	0.	.26190E-01	-.42450E-01	-.10138E-04
CM =	24.663	15.233	9.4297	0.	0.	3.2168
CLN =	-.80453E-01	0.	0.	.13226	-.21271	-.56088E-04
CLL =	-1.3133	-3.4281	2.0623	.20344E-01	.32161E-01	.18681E-15

FOLLOWING ARE IN UNROLLED BODY-AXIS COORDINATE SYSTEM

	TOTAL	FIN 1 OR R	FIN 2 OR L	FIN 3 OR U	FIN 4 OR D	INTERF. SHELL
CZU =	4.4827	2.7760	1.7066	-.45711E-06	.74088E-06	.58154
CYU =	-.16181E-01	.48451E-04	.29786E-04	.26190E-01	-.42450E-01	.11440E-07
CMU =	24.663	15.233	9.4297	-.23084E-05	.37125E-05	3.2168
CLNU =	-.80022E-01	.26587E-03	.16458E-03	.13226	-.21271	.55927E-07

NOTE: L.E. OF LEAD PANEL IN FIRST CHORDWISE ROW IS SUPERSONIC

SPANWISE DISTRIBUTIONS

------------------UPPER RIGHT OR RIGHT HORIZONTAL FIN--------------------

I	Y/(B/2)	CN*C/(2*B)	CT*C/(2*B)	CY1*C/(2*B)	CYTOT*C/(2*B)	CS*C/(2*B)	CSINT	YBAR	GAMNET(I)	GAMMA.LE/VINF	XLE
1	.08162	.23373	0.00000	0.00000	.00250	0.00000	0.00000	0.00000	-3.15103	0.00000	.63500
2	.24804	.22936	0.00000	0.00000	.00460	0.00000	0.00000	0.00000	.05282	0.00000	1.92985
3	.41438	.21605	0.00000	0.00000	.00530	0.00000	0.00000	0.00000	.19480	0.00000	3.22407
4	.58060	.19066	0.00000	0.00000	.00435	0.00000	0.00000	0.00000	.35559	0.00000	4.51731
5	.74660	.15210	0.00000	0.00000	.00363	0.00000	0.00000	0.00000	.51857	0.00000	5.80884
6	.91216	.10289	0.00000	0.00000	0.00000	0.00000	0.00000	0.00000	.65163	0.00000	7.09699
7	1.00000	0.00000							1.37763		

THRUST- AND SIDE-FORCE COEFFICIENTS IN PLANE OF THE FIN

SUMFX =CX..ACTS ON LEADING EDGE
SUMFY1=CY..ACTS ON LEADING EDGE
SUMFY2=CY..ACTS ON LEADING AND SIDE EDGE
SUMFT2=CY..ACTS ON SIDE EDGE

SUMFX = 0.
SUMFY1 = 0.
SUMFY2 = .50274E-01
SUMFT2 = .21231E-01

SIDE EDGE DISTRIBUTION

JTIP	JSE	DISTANCE FROM LE /TIPCHORD	SUCTION FORCE PER UNIT LENGTH /(Q*TIPCHORD)	GAMMA.SE /VINF	YBAR	XSE
1	1	.25000	-.00110	.00020	7.23000	7.78041
2	2	.50000	-.00398	.00092	7.23000	8.61780
3	3	.75000	.01211	.00313	7.23000	9.45520
4	4	1.00000	.09984	.02130	7.23000	10.29260

****T.E. FIN VORTICITY DUE TO ATTACHED FLOW*****

IVRT	GAMMA/VINF	Y.C.G. (LOCAL FIN)	Y.C.G. (BODY AXES)	Z.C.G. (BODY AXES)
3	3.37977	5.79887	7.91387	0.00000

------------------LOWER LEFT OR LEFT HORIZONTAL FIN--------------------

I	Y/(B/2)	CN*C/(2*B)	CT*C/(2*B)	CY1*C/(2*B)	CYTOT*C/(2*B)	CS*C/(2*B)	CSINT	YBAR	GAMNET(I)	GAMMA,LE/VINF	XLE
8	-.08162	.15394	0.00000	0.00000	-.00192	0.00000	0.00000	0.00000	2.01812	0.00000	.63500
9	-.24804	.14719	0.00000	0.00000	-.00182	0.00000	0.00000	0.00000	-.09593	0.00000	1.92985
10	-.41438	.13373	0.00000	0.00000	-.00166	0.00000	0.00000	0.00000	-.18401	0.00000	3.22407
11	-.58060	.11355	0.00000	0.00000	-.00111	0.00000	0.00000	0.00000	-.26612	0.00000	4.51731
12	-.74660	.08656	0.00000	0.00000	-.00087	0.00000	0.00000	0.00000	-.34850	0.00000	5.80884
13	-.91216	.05652	0.00000	0.00000	0.00000	0.00000	0.00000	0.00000	-.38878	0.00000	7.09699
14	-1.00000	0.00000							-.73479		

THRUST- AND SIDE-FORCE COEFFICIENTS IN PLANE OF THE FIN

SUMFX =CX..ACTS ON LEADING EDGE
SUMFY1=CY..ACTS ON LEADING EDGE
SUMFY2=CY..ACTS ON LEADING AND SIDE EDGE
SUMFT2=CY..ACTS ON SIDE EDGE

SUMFX = 0.
SUMFY1 = 0.
SUMFY2 = -.18233E-01
SUMFT2 = -.50575E-02

SIDE EDGE DISTRIBUTION

JTIP	JSE	DISTANCE FROM LE /TIPCHORD	SUCTION FORCE PER UNIT LENGTH /(Q*TIPCHORD)	GAMMA,SE /VINF	YBAR	XSE
1	5	.25000	.00057	-.00011	-7.23000	7.78041
2	6	.50000	.00209	-.00051	-7.23000	8.61780
3	7	.75000	-.00112	-.00072	-7.23000	9.45520
4	8	1.00000	-.02700	-.00588	-7.23000	10.29260

****T.E. FIN VORTICITY DUE TO ATTACHED FLOW*****

IVRT	GAMMA/VINF	Y.C.G. (LOCAL FIN)	Y.C.G. (BODY AXES)	Z.C.G.
4	-2.22595	-5.41287	-7.52787	-.00000

------------------LOWER RIGHT OR UPPER VERTICAL FIN--------------------

I	Y/(B/2)	CN*C/(2*B)	CT*C/(2*B)	CY1*C/(2*B)	CYTOT*C/(2*B)	CS*C/(2*B)	CSINT	YBAR	GAMNET(I)	GAMMA.LE/VINF	XLE
15	.08162	-.00645	0.00000	0.00000	-.00001	0.00000	0.00000	0.00000	.10968	0.00000	.63500
16	.24804	-.00332	0.00000	0.00000	-.00002	0.00000	0.00000	0.00000	-.05629	0.00000	1.92985
17	.41438	-.00071	0.00000	0.00000	-.00000	0.00000	0.00000	0.00000	-.04247	0.00000	3.22407
18	.58060	-.00012	0.00000	0.00000	-.00000	0.00000	0.00000	0.00000	-.00911	0.00000	4.51731
19	.74660	-.00001	0.00000	0.00000	-.00000	0.00000	0.00000	0.00000	-.00167	0.00000	5.80884
20	.91216	.00000	0.00000	0.00000	0.00000	0.00000	0.00000	0.00000	-.00015	0.00000	7.09699
21	1.00000	0.00000							.00001		

THRUST- AND SIDE-FORCE COEFFICIENTS IN PLANE OF THE FIN

SUMFX =CX..ACTS ON LEADING EDGE
SUMFY1=CY..ACTS ON LEADING EDGE
SUMFY2=CY..ACTS ON LEADING AND SIDE EDGE
SUMFT2=CY..ACTS ON SIDE EDGE

SUMFX = 0.
SUMFY1 = 0.
SUMFY2 = -.65305E-04
SUMFT2 = .59962E-11

SIDE EDGE DISTRIBUTION

JTIP	JSE	DISTANCE FROM LE /TIPCHORD	SUCTION FORCE PER UNIT LENGTH /(Q*TIPCHORD)	GAMMA.SE /VINF	YBAR	XSE
1	9	.25000	.00000	0.00000	0.00000	7.78041
2	10	.50000	.00000	0.00000	0.00000	8.61780
3	11	.75000	.00000	0.00000	0.00000	9.45520
4	12	1.00000	.00000	0.00000	0.00000	10.29260

****T.E. FIN VORTICITY DUE TO ATTACHED FLOW*****

IVRT	GAMMA/VINF	Y.C.G. (LOCAL FIN)	Y.C.G. (BODY AXES)	Z.C.G. (BODY AXES)
5	-.09334	1.98101	-.00000	4.09601

-------------------UPPER LEFT OR LOWER VERTICAL FIN--------------------

I	Y/(B/2)	CN*C/(2*B)	CT*C/(2*B)	CY1*C/(2*B)	CYTOT*C/(2*B)	CS*C/(2*B)	CSINT	YBAR	GAMNET(I)	GAMMA.LE/VINF	XLE
22	-.08162	.01123	0.00000	0.00000	.00001	0.00000	0.00000	0.00000	.10977	0.00000	.63500
23	-.24804	.00498	0.00000	0.00000	.00002	0.00000	0.00000	0.00000	-.05629	0.00000	1.92985

24	-.41438	.00084	0.00000	0.00000	.00000	0.00000	0.00000	0.00000	-.04248	0.00000	3.22407
25	-.58060	.00014	0.00000	0.00000	.00000	0.00000	0.00000	0.00000	-.00912	0.00000	4.51731
26	-.74660	.00002	0.00000	0.00000	.00000	0.00000	0.00000	0.00000	-.00169	0.00000	5.80884
27	-.91216	.00000	0.00000	0.00000	0.00000	0.00000	0.00000	0.00000	-.00017	0.00000	7.09699
29	-1.00000	0.00000							-.00003		

THRUST- AND SIDE-FORCE COEFFICIENTS IN PLANE OF THE FIN

SUMFX =CX..ACTS ON LEADING EDGE
SUMFY1=CY..ACTS ON LEADING EDGE
SUMFY2=CY..ACTS ON LEADING AND SIDE EDGE
SUMFT2=CY..ACTS ON SIDE EDGE

SUMFX = 0.
SUMFY1 = 0.
SUMFY2 = .65226E-04
SUMFT2 = .26827E-11

SIDE EDGE DISTRIBUTION

JTIP	JSE	DISTANCE FROM LE /TIPCHORD	SUCTION FORCE PER UNIT LENGTH /(Q*TIPCHORD)	GAMMA.SE /VINF	YBAR	XSE
1	13	.25000	.00000	0.00000	0.00000	7.78041
2	14	.50000	.00000	0.00000	0.00000	8.61780
3	15	.75000	.00000	0.00000	0.00000	9.45520
4	16	1.00000	.00000	0.00000	0.00000	10.29260

****T.E. FIN VORTICITY DUE TO ATTACHED FLOW*****

IVRT	GAMMA/VINF	Y.C.G. (LOCAL FIN)	Y.C.G. (BODY AXES)	Z.C.G. (BODY AXES)
6	-.16236	-1.84585	.00000	-3.96085

VORTEX INFORMATION WRITTEN ON TAPE8 FROM SUBROUTINE SPNLD

I	Y	Z	GAMMA
6			
1	.93450E+01	.59790E+00	.21299E-01
2	-.93450E+01	.28965E+00	-.58798E-02
3	.79139E+01	0.	.33798E+01
4	-.75279E+01	-.36793E-12	-.22259E+01
5	-.18396E-12	.40960E+01	-.93338E-01
6	.56692E-12	-.39609E+01	-.16236E+00

****
AFT OF LEADING EDGE OF FIN ROOTCHORDS

BODY RING= 1

J	THETA, DEG.	XB	YB	ZB	UTOT	VTOT	WTOT	CP.LIN.	CP.BERN.	DR/DX	P/PINF. BERN.	P/PINF. LIN.
1	15.00000	18.44338	1.97332	.52875	.12150	-.09412	.07133	-.24299	-.18456	0.00000	.19255	-.06310
2	45.00000	18.44338	1.44457	1.44457	.01101	-.31132	.03086	-.02202	-.10902	0.00000	.52303	.90368
3	75.00000	18.44338	.52875	1.97332	.01144	-.15292	-.23957	-.02288	.02170	0.00000	1.09492	.89989
4	105.00000	18.44338	-.52875	1.97332	.01117	.15143	-.23997	-.02234	.02276	0.00000	1.09958	.90224
5	135.00000	18.44338	-1.44457	1.44457	.01053	.30773	.02726	-.02107	-.10570	0.00000	.53756	.90784
6	165.00000	18.44338	-1.97332	.52875	.08416	.11236	.13938	-.16832	-.17584	0.00000	.23068	.26360
7	195.00000	18.44338	-1.97332	-.52875	-.07320	-.11277	.13928	.14641	.03347	0.00000	1.14642	1.64054
8	225.00000	18.44338	-1.44457	-1.44457	.00042	-.30804	.02697	-.00084	-.09264	0.00000	.59469	.99630
9	255.00000	18.44338	-.52875	-1.97332	-.00021	-.15154	-.24038	.00043	.04722	0.00000	1.20657	1.00187
10	285.00000	18.44338	.52875	-1.97332	-.00049	.15303	-.23999	.00098	.04730	0.00000	1.20692	1.00429
11	315.00000	18.44338	1.44457	-1.44457	-.00005	.31162	.03054	.00011	-.09494	0.00000	.58464	1.00046
12	345.00000	18.44338	1.97332	-.52875	-.11054	.09454	.07121	.22108	.18924	0.00000	1.82793	1.96724

BODY LOADS ON RING 1 AT X= 18.44338

	UNROLLED BODY-AXIS COORDINATES LINEAR LOADING	UNROLLED BODY-AXIS COORDINATES BERNOULLI LOADING	FIXED OR ROLLED BODY-AXIS COORDINATES LINEAR LOADING	FIXED OR ROLLED BODY-AXIS COORDINATES BERNOULLI LOADING
CX			0.00000	0.00000
CZ	.06035	.04767	.06035	.04767
CY	-.00000	-.03007	-.00000	-.03008
CM	.39374	.31103	.39374	.31103
CLN	-.00000	-.19621	-.00001	-.19621

CUMULATIVE BODY LOADS TO THIS STATION

	UNROLLED BODY-AXIS COORDINATES LINEAR LOADING	UNROLLED BODY-AXIS COORDINATES BERNOULLI LOADING	FIXED OR ROLLED BODY-AXIS COORDINATES LINEAR LOADING	FIXED OR ROLLED BODY-AXIS COORDINATES BERNOULLI LOADING
CX			0.00000	0.00000
CZ	.06035	.04767	.06035	.04767
CY	-.00000	-.03007	-.00000	-.03008
CM	.39374	.31103	.39374	.31103
CLN	-.00000	-.19621	-.00001	-.19621

BODY RING= 2

J	THETA, DEG.	XB	YB	ZB	UTOT	VTOT	WTOT	CP.LIN.	CP.BERN.	DR/DX	P/PINF. BERN.	P/PINF. LIN.
1	15.00000	21.22588	1.97332	.52875	.14462	-.08574	.03987	-.28924	-.19301	0.00000	.15557	-.26544

2	45.00000	21.22588	1.44457	1.44457	.06974	-.21347	-.06669	-.13947	-.12106	0.00000	.47037	.38980
3	75.00000	21.22588	.52875	1.97332	.00434	-.16750	-.23528	-.00867	.03141	0.00000	1.13740	.96205
4	105.00000	21.22588	-.52875	1.97332	.00299	.15651	-.23823	-.00599	.03838	0.00000	1.16791	.97380
5	135.00000	21.22588	-1.44457	1.44457	.04798	.24110	-.03907	-.09595	-.10851	0.00000	.52529	.58020
6	165.00000	21.22588	-1.97332	.52875	.09556	.10807	.12315	-.19112	-.17942	0.00000	.21503	.16387
7	195.00000	21.22588	-1.97332	-.52875	-.08705	-.10807	.12315	.17411	.07800	0.00000	1.34123	1.76172
8	225.00000	21.22588	-1.44457	-1.44457	-.03947	-.24110	-.03907	.07894	.03724	0.00000	1.16293	1.34537
9	255.00000	21.22588	-.52875	-1.97332	.00551	-.15652	-.23823	-.01103	.03295	0.00000	1.14416	.95175
10	285.00000	21.22588	.52875	-1.97332	.00416	.16750	-.23529	-.00833	.03178	0.00000	1.13905	.96357
11	315.00000	21.22588	1.44457	-1.44457	-.06123	.21348	-.06670	.12247	.11535	0.00000	1.50464	1.53580
12	345.00000	21.22588	1.97332	-.52875	-.13612	.08576	.03986	.27223	.29699	0.00000	2.29933	2.19103

BODY LOADS ON RING 2 AT X= 21.22588

	UNROLLED BODY-AXIS COORDINATES		FIXED OR ROLLED BODY-AXIS COORDINATES	
	LINEAR LOADING	BERNOULLI LOADING	LINEAR LOADING	BERNOULLI LOADING
CX			0.00000	0.00000
CZ	.11876	.10012	.11876	.10012
CY	-.00000	-.05295	-.00000	-.05295
CM	.69668	.58733	.69668	.58733
CLN	-.00000	-.31062	-.00001	-.31063

CUMULATIVE BODY LOADS TO THIS STATION

	UNROLLED BODY-AXIS COORDINATES		FIXED OR ROLLED BODY-AXIS COORDINATES	
	LINEAR LOADING	BERNOULLI LOADING	LINEAR LOADING	BERNOULLI LOADING
CX			0.00000	0.00000
CZ	.17911	.14780	.17911	.14779
CY	-.00000	-.08303	-.00000	-.08303
CM	1.09042	.89836	1.09042	.89835
CLN	-.00000	-.50683	-.00002	-.50684

BODY RING= 3

J	THETA. DEG.	XB	YB	ZB	UTOT	VTOT	WTOT	CP.LIN.	CP.BERN.	DR/DX	P/PINF. BERN.	P/PINF. LIN.
1	15.00000	24.00838	1.97332	.52875	.11655	-.08062	.01968	-.23311	-.16924	0.00000	.25958	-.01985
2	45.00000	24.00838	1.44457	1.44457	.09482	-.17255	-.10893	-.18963	-.13353	0.00000	.41579	.17035
3	75.00000	24.00838	.52875	1.97332	.04560	-.10673	-.25292	-.09120	-.03278	0.00000	.85658	.60099
4	105.00000	24.00838	-.52875	1.97332	.02993	.11753	-.25003	-.05985	-.00556	0.00000	.97567	.73815
5	135.00000	24.00838	-1.44457	1.44457	.05846	.21100	-.07048	-.11692	-.10528	0.00000	.53938	.48846
6	165.00000	24.00838	-1.97332	.52875	.07382	.10339	.10460	-.14763	-.15610	0.00000	.31705	.35412
7	195.00000	24.00838	-1.97332	-.52875	-.06727	-.10358	.10455	.13454	.05362	0.00000	1.23461	1.58862
8	225.00000	24.00838	-1.44457	-1.44457	-.05192	-.21115	-.07062	.10383	.09636	0.00000	1.42157	1.45426
9	255.00000	24.00838	-.52875	-1.97332	-.02338	-.11759	-.25023	.04676	.11354	0.00000	1.49676	1.20457
10	285.00000	24.00838	.52875	-1.97332	-.03906	.10678	-.25312	.07812	.15785	0.00000	1.69059	1.34179
11	315.00000	24.00838	1.44457	-1.44457	-.08828	.17270	-.10908	.17655	.23232	0.00000	2.01639	1.77242
12	345.00000	24.00838	1.97332	-.52875	-.11001	.08083	.01962	.22002	.24207	0.00000	2.05905	1.96261

BODY LOADS ON RING 3 AT X= 24.00838

UNROLLED BODY-AXIS COORDINATES		FIXED OR ROLLED BODY-AXIS COORDINATES	
LINEAR LOADING	BERNOULLI LOADING	LINEAR LOADING	BERNOULLI LOADING

CX			0.00000	0.00000
CZ	.19027	.18794	.19027	.18794
CY	.00000	-.05454	-.00000	-.05454
CM	.99099	.97886	.99099	.97885
CLN	.00000	-.28405	-.00002	-.28406

CUMULATIVE BODY LOADS TO THIS STATION

	UNROLLED BODY-AXIS COORDINATES		FIXED OR ROLLED BODY-AXIS COORDINATES	
	LINEAR LOADING	BERNOULLI LOADING	LINEAR LOADING	BERNOULLI LOADING
CX			0.00000	0.00000
CZ	.36938	.33573	.36938	.33573
CY	.00000	-.13756	-.00001	-.13757
CM	2.08141	1.87722	2.08141	1.87721
CLN	.00000	-.79087	-.00004	-.79091

BODY RING= 4

J	THETA, DEG.	XB	YB	ZB	UTOT	VTOT	WTOT	CP.LIN.	CP.BERN.	DR/DX	P/PINF. BERN.	P/PINF. LIN.
1	15.00000	26.79088	1.97332	.52875	.10996	-.07833	.01105	-.21992	-.16153	0.00000	.29332	.03787
2	45.00000	26.79088	1.44457	1.44457	.08747	-.16555	-.11595	-.17494	-.12244	0.00000	.46434	.23465
3	75.00000	26.79088	.52875	1.97332	.08642	-.07421	-.26164	-.17284	-.09439	0.00000	.58702	.24384
4	105.00000	26.79088	-.52875	1.97332	.05534	.09270	-.25669	-.11069	-.04756	0.00000	.79192	.51575
5	135.00000	26.79088	-1.44457	1.44457	.04861	.20780	-.07371	-.09723	-.09010	0.00000	.60580	.57463
6	165.00000	26.79088	-1.97332	.52875	.06593	.10319	.10377	-.13186	-.14835	0.00000	.35098	.42313
7	195.00000	26.79088	-1.97332	-.52875	-.06072	-.10333	.10373	.12144	.04085	0.00000	1.17871	1.53129
8	225.00000	26.79088	-1.44457	-1.44457	-.04340	-.20791	-.07381	.08681	.07985	0.00000	1.34933	1.37979
9	255.00000	26.79088	-.52875	-1.97332	-.05013	-.09274	-.25684	.10027	.19272	0.00000	1.84315	1.43866
10	285.00000	26.79088	.52875	-1.97332	-.08121	.07425	-.26180	.16243	.29141	0.00000	2.27491	1.71063
11	315.00000	26.79088	1.44457	-1.44457	-.08226	.16566	-.11606	.16453	.22222	0.00000	1.97222	1.71981
12	345.00000	26.79088	1.97332	-.52875	-.10475	.07849	.01101	.20951	.23551	0.00000	2.03035	1.91659

BODY LOADS ON RING 4 AT X= 26.79088

	LINEAR LOADING	BERNOULLI LOADING	LINEAR LOADING	BERNOULLI LOADING
	UNROLLED BODY-AXIS COORDINATES		FIXED OR ROLLED BODY-AXIS COORDINATES	
CX			0.00000	0.00000
CZ	.23448	.24449	.23448	.24449
CY	.00000	-.05816	-.00000	-.05816
CM	1.06703	1.11260	1.06703	1.11260
CLN	.00000	-.26466	-.00002	-.26468

CUMULATIVE BODY LOADS TO THIS STATION

	UNROLLED BODY-AXIS COORDINATES		FIXED OR ROLLED BODY-AXIS COORDINATES	
	LINEAR LOADING	BERNOULLI LOADING	LINEAR LOADING	BERNOULLI LOADING
CX			0.00000	0.00000
CZ	.60386	.58023	.60386	.58022

CY	.00000	-.19572	-.00001	-.19573
CM	3.14844	2.98983	3.14844	2.98981
CLN	.00000	-1.05554	-.00005	-1.05559

***** SUMMARY OF TOTAL LOADS *****

*** STEP 3

ALPHA C = 15.00 DEG. PHI = .001 DEG. MACH = 2.50

(BODY AXIAL FORCE CONTRIBUTIONS NEGLECTED)

ROLLED BODY-AXIS COORDINATES			**	UNROLLED BODY-AXIS COORDINATES		
	LINEAR LOADING PRESSURE	BERNOULLI LOADING PRESSURE	**		LINEAR LOADING PRESSURE	BERNOULLI LOADING PRESSURE
CX(NOSE ONLY)	.1911E+00	.1937E+00	**	CX(NOSE ONLY)	.1911E+00	.1937E+00
CZB	.5517E+01	.6026E+01	**	CZU	.5517E+01	.6026E+01
CYB	-.9314E-04	-.2120E+00	**	CYU	.3140E-05	-.2119E+00
CMB	.3304E+02	.3644E+02	**	CMU	.3304E+02	.3644E+02
CLNB	-.5605E-03	-.1136E+01	**	CLNU	.1618E-04	-.1136E+01
CLLB	-.1310E+01	-.1351E+01	**	CLLU	-.1310E+01	-.1351E+01

(b) Step 3a, program BDYSHD

Figure A.7.- Continued.

(pages 170 through 210)

```
TF-4 AFTERBODY WITH SPECIFIED CANARD VORTICES
ALPHA=15.0  PHI=0.001   MACH=2.5   LAMINAR SEPARATION


     REFERENCE QUANTITIES
       REF. AREA ........  14.12
       REF. LENGTH ......   4.23
       X(MOMENT CENTER) .  46.04
       BODY LENGTH ...... 102.32
       BASE DIAMETER ....   4.23


     FLOW CONDITIONS
       MACH NUMBER.......   2.50
       ALPHA C (DEG.) ...  15.00
       PHI (DEG.) .......    .00
       REYNOLDS NUMBER ..   2.770E+05
       VISCOSITY RATIO ..   1.000E+00
       VORTEX FACTOR ....   1.00

       ALPHA (DEG.) .....  15.00
       BETA (DEG.) ......    .00
       U/V ..............   .966
       RE(2-DIM.) .......   7.169E+04
       F(RE) CROSSFLOW ..   1.695E+04

     INITIAL CONDITIONS      XI        XF        DX       TOL      EMKF      RGAM     RCORE
                           26.930    80.730    2.115   .10000    1.050     0.000    .25000


     OPTIONS...

  NCIR   NFC   ISYM  NRLSEP NSEPR  NSMOTH NDFUS  NDPHI   INP   NXFV   NFV   NVP   NVR   NVM   NVA  NASYM
    0     0     1     1      0      0      1      2      1     0      0     0     0     0     0     0


 NPRNTP NPRNTS NPRNTV NPLOTV NPLOTA NPRTVL NVTRNS
    0      1      1      3      0      0      0


     SHAPE DATA

  NXR
    1

  XR
 26.000

  R
 2.115

  DR
 0.000

       INITIAL FORCE AND MOMENT COEFFICIENT
      CN          CY          CM          CR          CSL          CA
    0.          0.          0.          0.          0.           0.
```

INITIAL VORTICITY DISTRIBUTION

GAMMA/V	Y	Z	XSHED
.02130	9.34500	.59790	0.00000
-.00588	-9.34500	.28965	0.00000
3.37980	7.91390	0.00000	0.00000
-2.22590	-7.52790	-.00000	0.00000
-.09334	-.00000	4.09600	0.00000
-.16236	.00000	-3.96090	0.00000

```
$BODY
NXBODY  = 50,

LNOSE   = .158E+02,

LBODY   = .10232E+03,

BCODE   = 2,

$END
```

PHYSICAL DIMENSIONS OF BODY AND LINE SINGULARITY STRENGTHS REPRESENTING THE BODY AT MACH= 2.5000 ALFAC= 15.0000

	Y	R	DR/DX	TX	T(I)	TC(I)
1	0.0000	-.14211E-13	.27261	.32561E-13	.76511E-01	.27824E-01
2	2.0882	.52921	.23444	.87558	-.31570E-01	-.76385E-02
3	4.1763	.97975	.19722	1.9314	-.18623E-01	-.45607E-02
4	6.2645	1.3534	.16077	3.1635	-.16238E-01	-.49524E-02
5	8.3527	1.6516	.12493	4.5684	-.12589E-01	-.44861E-02
6	10.4408	1.8755	.89567E-01	6.1436	-.98746E-02	-.43633E-02
7	12.5290	2.0259	.54531E-01	7.8871	-.73236E-02	-.42226E-02
8	14.6171	2.1034	.19694E-01	9.7978	-.48958E-02	-.40995E-02
9	16.7053	2.1150	0.	11.859	.17880E-01	-.22648E-02
10	18.7935	2.1150	0.	13.947	.16487E-02	.94869E-03
11	20.8816	2.1150	0.	16.036	.21093E-02	.12207E-02
12	22.9698	2.1150	0.	18.124	.91200E-03	.14718E-02
13	25.0580	2.1150	0.	20.212	.64126E-03	.13600E-02
14	27.1461	2.1150	0.	22.300	.40133E-03	.11683E-02
15	29.2343	2.1150	0.	24.388	.27490E-03	.93230E-03
16	31.3224	2.1150	0.	26.476	.18974E-03	.70422E-03
17	33.4106	2.1150	0.	28.565	.13469E-03	.50293E-03
18	35.4988	2.1150	0.	30.653	.97189E-04	.33763E-03
19	37.5869	2.1150	0.	32.741	.71295E-04	.20974E-03
20	39.6751	2.1150	0.	34.829	.53027E-04	.11549E-03
21	41.7633	2.1150	0.	36.917	.39939E-04	.49823E-04
22	43.8514	2.1150	0.	39.005	.30423E-04	.69259E-05
23	45.9396	2.1150	0.	41.094	.23417E-04	-.18747E-04
24	48.0278	2.1150	0.	43.182	.18198E-04	-.32039E-04
25	50.1159	2.1150	0.	45.270	.14269E-04	-.36920E-04
26	52.2041	2.1150	0.	47.358	.11281E-04	-.36474E-04
27	54.2922	2.1150	0.	49.446	.89894E-05	-.32981E-04
28	56.3804	2.1150	0.	51.534	.72160E-05	-.28041E-04
29	58.4686	2.1150	0.	53.622	.58330E-05	-.22713E-04
30	60.5567	2.1150	0.	55.711	.47462E-05	-.17642E-04
31	62.6449	2.1150	0.	57.799	.38862E-05	-.13180E-04
32	64.7331	2.1150	0.	59.887	.32011E-05	-.94700E-05
33	66.8212	2.1150	0.	61.975	.26518E-05	-.65282E-05
34	68.9094	2.1150	0.	64.063	.22087E-05	-.42921E-05
35	70.9976	2.1150	0.	66.151	.18492E-05	-.26613E-05
36	73.0857	2.1150	0.	68.240	.15559E-05	-.15227E-05
37	75.1739	2.1150	0.	70.328	.13153E-05	-.76652E-06
38	77.2620	2.1150	0.	72.416	.11170E-05	-.29469E-06
39	79.3502	2.1150	0.	74.504	.95276E-06	-.25860E-07
40	81.4384	2.1150	0.	76.592	.81604E-06	.10580E-06
41	83.5265	2.1150	0.	78.680	.70174E-06	.14975E-06
42	85.6147	2.1150	0.	80.769	.60577E-06	.14215E-06
43	87.7029	2.1150	0.	82.857	.52485E-06	.10810E-06
44	89.7910	2.1150	0.	84.945	.45635E-06	.64118E-07
45	91.8792	2.1150	0.	87.033	.39814E-06	.20287E-07
46	93.9673	2.1150	0.	89.121	.34948E-06	-.17884E-07
47	96.0555	2.1150	0.	91.209	.30598E-06	-.47977E-07
48	98.1437	2.1150	0.	93.298	.26946E-06	-.69542E-07
49	100.2318	2.1150	0.	95.386	.23900E-06	-.83264E-07
50	102.3200	2.1150	0.	97.474	0.	0.

BODY SURFACE PRESSURE DISTRIBUTION

X	R	DR/DX	M
26.9300	2.1150	0.0000	2.5000

J	Y	Z	BETA	U/VO	V/VO	W/VO	VT/VO	CP(M)	DPHI/DT	CP7	CP(I)
1	0.0000	-2.1150	0.000	.9743	-.0360	-.0030	-.0361	.0533	0.0000	.0494	.0494
2	.1843	-2.1070	5.000	.9743	-.0044	-.0034	-.0055	.0548	0.0000	.0507	.0507
3	.3673	-2.0829	10.000	.9743	.0248	.0014	.0248	.0542	0.0000	.0501	.0501
4	.5474	-2.0429	15.000	.9742	.0510	.0107	.0521	.0519	0.0000	.0482	.0482
5	.7234	-1.9874	20.000	.9741	.0737	.0238	.0774	.0483	0.0000	.0451	.0451
6	.8938	-1.9168	25.000	.9740	.0926	.0402	.1009	.0438	0.0000	.0411	.0411
7	1.0575	-1.8316	30.000	.9739	.1073	.0589	.1224	.0387	0.0000	.0366	.0366
8	1.2131	-1.7325	35.000	.9737	.1175	.0793	.1418	.0334	0.0000	.0318	.0318
9	1.3595	-1.6202	40.000	.9735	.1232	.1004	.1589	.0281	0.0000	.0270	.0270
10	1.4955	-1.4955	45.000	.9733	.1243	.1213	.1736	.0233	0.0000	.0225	.0225
11	1.6202	-1.3595	50.000	.9731	.1210	.1412	.1860	.0190	0.0000	.0185	.0185
12	1.7325	-1.2131	55.000	.9729	.1137	.1595	.1959	.0155	0.0000	.0152	.0152
13	1.8316	-1.0575	60.000	.9726	.1031	.1755	.2035	.0128	0.0000	.0126	.0126
14	1.9168	-.8938	65.000	.9724	.0895	.1890	.2092	.0110	0.0000	.0108	.0108
15	1.9874	-.7234	70.000	.9721	.0738	.1998	.2130	.0098	0.0000	.0097	.0097
16	2.0429	-.5474	75.000	.9718	.0565	.2080	.2155	.0093	0.0000	.0092	.0092
17	2.0829	-.3673	80.000	.9715	.0382	.2136	.2169	.0093	0.0000	.0091	.0091
18	2.1070	-.1843	85.000	.9712	.0192	.2167	.2176	.0096	0.0000	.0094	.0094
19	2.1150	0.0000	90.000	.9709	.0000	.2176	.2176	.0101	0.0000	.0100	.0100
20	2.1070	.1843	95.000	.9706	-.0192	.2163	.2172	.0110	0.0000	.0108	.0108
21	2.0829	.3673	100.000	.9703	-.0380	.2127	.2161	.0120	0.0000	.0118	.0118
22	2.0429	.5474	105.000	.9700	-.0562	.2067	.2142	.0135	0.0000	.0132	.0132
23	1.9874	.7234	110.000	.9697	-.0732	.1981	.2112	.0154	0.0000	.0150	.0150
24	1.9168	.8938	115.000	.9694	-.0885	.1869	.2068	.0179	0.0000	.0174	.0174
25	1.8316	1.0575	120.000	.9692	-.1016	.1730	.2006	.0211	0.0000	.0205	.0205
26	1.7325	1.2131	125.000	.9689	-.1117	.1565	.1923	.0251	0.0000	.0242	.0242
27	1.6202	1.3595	130.000	.9687	-.1182	.1379	.1816	.0300	0.0000	.0287	.0287
28	1.4955	1.4955	135.000	.9685	-.1205	.1176	.1684	.0355	0.0000	.0337	.0337
29	1.3595	1.6202	140.000	.9683	-.1183	.0963	.1526	.0416	0.0000	.0392	.0392
30	1.2131	1.7325	145.000	.9681	-.1113	.0750	.1342	.0480	0.0000	.0448	.0448
31	1.0575	1.8316	150.000	.9679	-.0995	.0545	.1135	.0543	0.0000	.0503	.0503
32	.8938	1.9168	155.000	.9678	-.0830	.0357	.0904	.0602	0.0000	.0552	.0552
33	.7234	1.9874	160.000	.9677	-.0622	.0197	.0653	.0651	0.0000	.0594	.0594
34	.5474	2.0429	165.000	.9676	-.0376	.0071	.0382	.0686	0.0000	.0623	.0623
35	.3673	2.0829	170.000	.9675	-.0097	-.0013	.0098	.0704	0.0000	.0638	.0638
36	.1843	2.1070	175.000	.9675	.0207	-.0048	-.0213	.0701	0.0000	.0635	.0635
37	-.0000	2.1150	180.000	.9675	.0528	-.0030	-.0529	.0673	0.0000	.0612	.0612
38	-.1843	2.1070	185.000	.9675	.0854	.0045	-.0855	.0619	0.0000	.0567	.0567
39	-.3673	2.0829	190.000	.9675	.1173	.0177	-.1186	.0539	0.0000	.0499	.0499
40	-.5474	2.0429	195.000	.9676	.1471	.0364	-.1515	.0435	0.0000	.0408	.0408
41	-.7234	1.9874	200.000	.9677	.1736	.0602	-.1837	.0313	0.0000	.0299	.0299
42	-.8938	1.9168	205.000	.9678	.1955	.0882	-.2145	.0179	0.0000	.0174	.0174
43	-1.0575	1.8316	210.000	.9679	.2121	.1195	-.2434	.0039	0.0000	.0039	.0039

ORIGINAL PAGE IS
OF POOR QUALITY

44	-1.2131	1.7325	215.000	.9681	.2226	.1529	-.2701	-.0100	0.0000	-.0101	-.0101
45	-1.3595	1.6202	220.000	.9683	.2268	.1874	-.2942	-.0232	0.0000	-.0241	-.0241
46	-1.4955	1.4955	225.000	.9685	.2247	.2217	-.3156	-.0354	0.0000	-.0375	-.0375
47	-1.6202	1.3595	230.000	.9687	.2163	.2547	-.3341	-.0462	0.0000	-.0500	-.0500
48	-1.7325	1.2131	235.000	.9689	.2021	.2856	-.3498	-.0556	0.0000	-.0612	-.0612
49	-1.8316	1.0575	240.000	.9692	.1827	.3134	-.3627	-.0634	0.0000	-.0709	-.0709
50	-1.9168	.8938	245.000	.9694	.1588	.3375	-.3730	-.0697	0.0000	-.0790	-.0790
51	-1.9874	.7234	250.000	.9697	.1312	.3575	-.3809	-.0746	0.0000	-.0854	-.0854
52	-2.0429	.5474	255.000	.9700	.1008	.3732	-.3866	-.0783	0.0000	-.0903	-.0903
53	-2.0829	.3673	260.000	.9703	.0683	.3843	-.3903	-.0809	0.0000	-.0938	-.0938
54	-2.1070	.1843	265.000	.9706	.0345	.3909	-.3924	-.0825	0.0000	-.0961	-.0961
55	-2.1150	-.0000	270.000	.9709	.0000	.3930	-.3930	-.0832	0.0000	-.0971	-.0971
56	-2.1070	-.1843	275.000	.9712	-.0344	.3905	-.3920	-.0831	0.0000	-.0969	-.0969
57	-2.0829	-.3673	280.000	.9715	-.0681	.3835	-.3895	-.0821	0.0000	-.0955	-.0955
58	-2.0429	-.5474	285.000	.9718	-.1005	.3720	-.3853	-.0801	0.0000	-.0928	-.0928
59	-1.9874	-.7234	290.000	.9721	-.1306	.3559	-.3791	-.0771	0.0000	-.0887	-.0887
60	-1.9168	-.8938	295.000	.9724	-.1578	.3355	-.3707	-.0727	0.0000	-.0829	-.0829
61	-1.8316	-1.0575	300.000	.9726	-.1812	.3109	-.3599	-.0670	0.0000	-.0755	-.0755
62	-1.7325	-1.2131	305.000	.9729	-.2000	.2827	-.3463	-.0598	0.0000	-.0664	-.0664
63	-1.6202	-1.3595	310.000	.9731	-.2135	.2515	-.3299	-.0511	0.0000	-.0558	-.0558
64	-1.4955	-1.4955	315.000	.9733	-.2210	.2180	-.3104	-.0408	0.0000	-.0437	-.0437
65	-1.3595	-1.6202	320.000	.9735	-.2221	.1834	-.2880	-.0293	0.0000	-.0307	-.0307
66	-1.2131	-1.7325	325.000	.9737	-.2165	.1486	-.2627	-.0167	0.0000	-.0171	-.0171
67	-1.0575	-1.8316	330.000	.9739	-.2044	.1150	-.2346	-.0034	0.0000	-.0035	-.0035
68	-.8938	-1.9168	335.000	.9740	-.1861	.0838	-.2041	.0098	0.0000	.0096	.0096
69	-.7234	-1.9874	340.000	.9741	-.1622	.0560	-.1716	.0224	0.0000	.0216	.0216
70	-.5474	-2.0429	345.000	.9742	-.1337	.0329	-.1377	.0336	0.0000	.0319	.0319
71	-.3673	-2.0829	350.000	.9743	-.1022	.0150	-.1033	.0427	0.0000	.0401	.0401
72	-.1843	-2.1070	355.000	.9743	-.0690	.0031	-.0691	.0493	0.0000	.0459	.0459
73	0.0000	-2.1150	360.000	.9743	-.0360	-.0030	-.0361	.0533	0.0000	.0494	.0494

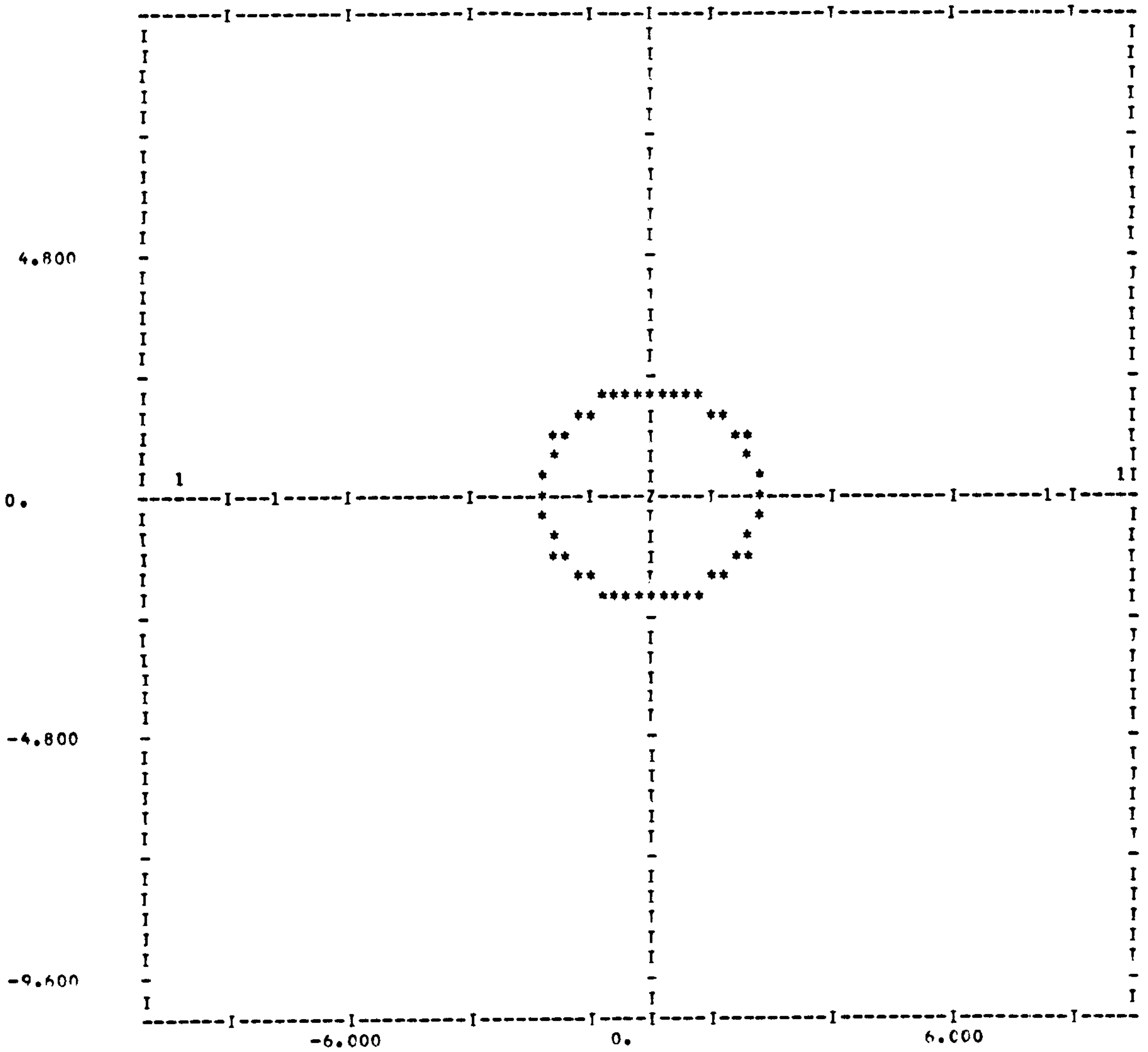

X	R	ALPHA	BETA	M
26.930	2.115	15.000	.000	2.500

X = 26.930

CN(X)	CY(X)	CP(0)	CP(90)	CP(180)
-1.042E-02	-7.370E-02	5.328E-02	1.014E-02	6.731E-02
CN	CM	CY	CR	CSL
-6.602E-03	-2.983E-02	-4.670E-02	2.110E-01	-2.559E-17

(SEPARATION POINTS)

Y	Z	BETA
1.255	1.700	143.6
-1.633	1.343	230.6

ORIGINAL PAGE IS
OF POOR QUALITY

STRATFORD SEPARATION CRITERION (LAMINAR) F(S) = .02252

SUMMARY OF PRESSURE DISTRIBUTION AND SEPARATION POINTS ON BODY ... X = 26.93

+Y SIDE*	Y	Z	BETA	ARC	CP	CP*	DCP*/DX
STAGNATION PT.	.184	-2.107	5.000	.049	.055		
MIN. PRESSURE	2.083	-.367	80.000	2.768	.009	0.000	0.000
SEPARATION	1.255	1.700	143.569	5.113	.046	.037	.035

-Y SIDE*	Y	Z	BETA	ARC	CP	CP*	DCP*/DX
STAGNATION PT.	.367	2.083	170.000	.049	.070		
MIN. PRESSURE	-2.115	-.000	270.000	3.506	-.083	0.000	0.000
SEPARATION	-1.633	1.343	230.570	4.961	-.047	.033	.050

INITIAL POSITIONS AND STRENGTHS OF SHED VORTICITY AT X = 26.930

	NV	GAM/V	M(K)	Y	Z	BETA	VT/V	YC	ZC	RG/R
+Y SIDE*	7	.0213	.0491	1.3188	1.7868	143.5695	.1394	1.3188	1.7868	1.0500
-Y SIDE*	8	-.1235	.1204	-1.7266	1.4197	230.5704	.3358	-1.7266	1.4197	1.0569

SUMMARY OF VORTEX FIELD AT X = 29.045 H = 2.11500

	NV	GAM/V	Y	Z	XSHED	BETA	YC	ZC	RG	RG/R
1	1	.02127	1.17594	1.90859	26.93000	148.362	1.17594	1.90859	2.24177	1.05994
1	2	.02130	8.95489	1.70166	0.00000	100.759	8.95489	1.70166	9.11514	4.30976
2	3	-.00588	-9.28184	1.25614	0.00000	262.293	-9.28184	1.25614	9.36646	4.42858
3	4	3.37980	7.91538	.48343	0.00000	93.495	7.91538	.48343	7.93013	3.74947
4	5	-2.22590	-7.50703	.56089	0.00000	265.727	-7.50703	.56089	7.52795	3.55931
5	6	-.03334	.06147	4.37243	0.00000	179.195	.06147	4.37243	4.37287	2.06755
6	7	-.16236	-.06502	-3.68560	0.00000	359.989	-.06502	-3.68560	3.68618	1.74287
1	8	-.12345	-1.44819	1.73425	26.93000	219.864	-1.44819	1.73425	2.25940	1.06827

CENTROID OF SHED VORTICITY

	GAM/V	Y	Z
+Y BODY*	.02127	1.17594	1.90859
-Y BODY*	-.12345	-1.44819	1.73425

X = 29.045

CN(X)	CY(X)	CP(0)	CP(90)	CP(180)
-1.046E-02	-5.363E-02	2.561E-03	-5.075E-02	1.373E-02

CN	CM	CY	CR	CSL
-1.323E-02	-5.646E-02	-8.068E-02	3.475E-01	-4.049E-17

(SEPARATION POINTS)

Y	Z	BETA
1.060	1.830	149.9
-1.731	1.216	234.9

SUMMARY OF VORTEX FIELD AT X = 37.505 H = 2.11500

	NV	GAM/V	Y	Z	YSHED	BETA	YC	ZC	RG	RG/R
1	1	.02127	.86641	2.24499	26.93000	158.897	.86641	2.24499	2.40638	1.13777
2	2	.00891	.80796	2.16758	29.04500	159.557	.80796	2.16758	2.31326	1.09374
3	3	.00226	.70686	2.12821	31.16000	161.627	.70686	2.12821	2.24253	1.06030
1	4	.02130	6.44785	3.16085	0.00000	116.115	6.44785	3.16085	7.18093	3.39524
2	5	-.00588	-8.09033	4.54707	0.00000	240.662	-8.09033	4.54707	9.28059	4.38799
3	6	3.37980	7.86366	2.41923	0.00000	107.100	7.86366	2.41923	8.22738	3.89001
4	7	-2.22590	-7.38233	2.78533	0.00000	249.329	-7.38233	2.78533	7.89030	3.73064
5	8	-.09334	.25459	5.49927	0.00000	177.349	.25459	5.49927	5.50516	2.60291
6	9	-.16236	-.45781	-2.73411	0.00000	350.494	-.45781	-2.73411	2.77217	1.31072
1	10	-.12345	-.88676	2.03230	26.93000	203.573	-.88676	2.03230	2.21734	1.04839
2	11	-.11374	-.92635	2.23850	29.04500	202.481	-.92635	2.23850	2.42260	1.14544
3	12	-.10674	-1.30721	2.03974	31.16000	212.655	-1.30721	2.03974	2.42267	1.14547
4	13	-.10560	-1.59190	1.72553	33.27500	222.693	-1.59190	1.72553	2.34768	1.11001
5	14	-.10994	-1.85701	1.32084	35.39000	234.577	-1.85701	1.32084	2.27884	1.07747

CENTROID OF SHED VORTICITY

	GAM/V	Y	Z
+Y BODY%	.03243	.83925	2.21560
-Y BODY%	-.55947	-1.29878	1.87793

ORIGINAL PAGE IS
OF POOR QUALITY

BODY SURFACE PRESSURE DISTRIBUTION

X	R	DR/DX	M
37.5050	2.1150	0.0000	2.5000

J	Y	Z	BETA	U/VO	V/VO	W/VO	VT/VO	CP(M)	DPHI/DT	CPZ	CP(I)
1	0.0000	-2.1150	0.000	.9714	-.0012	-.0030	-.0032	.0121	.0445	.0564	.0119
2	.1843	-2.1070	5.000	.9714	.0167	-.0015	.0168	.0131	.0433	.0562	.0128
3	.3673	-2.0829	10.000	.9713	.0377	.0037	.0379	.0133	.0420	.0551	.0130
4	.5474	-2.0429	15.000	.9713	.0607	.0133	.0622	.0118	.0411	.0528	.0116
5	.7234	-1.9874	20.000	.9712	.0835	.0274	.0879	.0085	.0407	.0491	.0084
6	.8938	-1.9168	25.000	.9711	.1041	.0456	.1137	.0035	.0406	.0441	.0035
7	1.0575	-1.8316	30.000	.9710	.1212	.0670	.1385	-.0028	.0409	.0381	-.0029
8	1.2131	-1.7325	35.000	.9708	.1338	.0907	.1616	-.0100	.0415	.0314	-.0101
9	1.3595	-1.6202	40.000	.9706	.1413	.1156	.1825	-.0174	.0424	.0246	-.0179
10	1.4955	-1.4955	45.000	.9704	.1434	.1404	.2007	-.0246	.0436	.0179	-.0256
11	1.6202	-1.3595	50.000	.9702	.1403	.1642	.2160	-.0313	.0449	.0120	-.0329
12	1.7325	-1.2131	55.000	.9700	.1322	.1858	.2280	-.0370	.0465	.0071	-.0394
13	1.8316	-1.0575	60.000	.9698	.1197	.2043	.2367	-.0417	.0482	.0035	-.0447
14	1.9168	-.8938	65.000	.9695	.1035	.2190	.2422	-.0451	.0501	.0013	-.0487
15	1.9874	-.7234	70.000	.9693	.0846	.2294	.2445	-.0473	.0521	.0007	-.0513
16	2.0429	-.5474	75.000	.9690	.0538	.2353	.2438	-.0484	.0541	.0016	-.0525
17	2.0829	-.3673	80.000	.9687	.0423	.2367	.2405	-.0483	.0562	.0037	-.0524
18	2.1070	-.1843	85.000	.9685	.0207	.2339	.2348	-.0473	.0582	.0070	-.0513
19	2.1150	0.0000	90.000	.9682	.0000	.2272	.2272	-.0455	.0602	.0110	-.0492
20	2.1070	.1843	95.000	.9679	-.0193	.2174	.2182	-.0432	.0620	.0156	-.0465
21	2.0829	.3673	100.000	.9676	-.0367	.2049	.2081	-.0404	.0637	.0204	-.0433
22	2.0429	.5474	105.000	.9673	-.0518	.1904	.1973	-.0373	.0650	.0253	-.0397
23	1.9874	.7234	110.000	.9671	-.0646	.1745	.1860	-.0340	.0662	.0302	-.0360
24	1.9168	.8938	115.000	.9668	-.0748	.1574	.1743	-.0305	.0670	.0349	-.0321
25	1.8316	1.0575	120.000	.9666	-.0924	.1397	.1622	-.0269	.0675	.0394	-.0281
26	1.7325	1.2131	125.000	.9663	-.0871	.1215	.1495	-.0230	.0678	.0439	-.0239
27	1.6202	1.3595	130.000	.9661	-.0889	.1030	.1360	-.0191	.0678	.0481	-.0197
28	1.4955	1.4955	135.000	.9659	-.0974	.0844	.1214	-.0150	.0677	.0523	-.0154
29	1.3595	1.6202	140.000	.9657	-.0821	.0659	.1052	-.0109	.0674	.0563	-.0111
30	1.2131	1.7325	145.000	.9655	-.0722	.0476	.0865	-.0068	.0671	.0602	-.0068
31	1.0575	1.8316	150.000	.9654	-.0560	.0293	.0632	-.0029	.0669	.0640	-.0029
32	.8938	1.9168	155.000	.9653	-.0321	.0120	.0343	-.0002	.0673	.0671	-.0002
33	.7234	1.9874	160.000	.9652	-.0101	.0007	.0101	-.0002	.0685	.0684	-.0002
34	.5474	2.0429	165.000	.9651	.0007	-.0032	-.0032	.0004	.0682	.0686	.0004
35	.3673	2.0829	170.000	.9650	.0111	-.0049	-.0121	.0008	.0678	.0686	.0008
36	.1843	2.1070	175.000	.9650	.0259	-.0052	-.0264	.0002	.0680	.0681	.0002
37	-.0000	2.1150	180.000	.9650	.0412	-.0030	-.0413	-.0018	.0689	.0671	-.0018
38	-.1843	2.1070	185.000	.9650	.0520	.0016	-.0521	-.0048	.0710	.0661	-.0048
39	-.3673	2.0829	190.000	.9650	.0504	.0059	-.0508	-.0085	.0748	.0662	-.0086
40	-.5474	2.0429	195.000	.9651	.0212	.0027	-.0213	-.0133	.0817	.0682	-.0135
41	-.7234	1.9874	200.000	.9652	-.0349	-.0157	.0383	-.0178	.0853	.0670	-.0183
42	-.8938	1.9168	205.000	.9653	-.0501	-.0263	.0566	-.0111	.0764	.0651	-.0113
43	-1.0575	1.8316	210.000	.9654	-.0136	-.0108	.0173	-.0388	.1092	.0677	-.0414

ORIGINAL PAGE IS
OF POOR QUALITY

44	-1.2131	1.7325	215.000	.9655	.0226	.0129	-.0260	-.0426	.1128	.0670	-.0457
45	-1.3595	1.6202	220.000	.9657	.0471	.0366	-.0597	-.0501	.1185	.0638	-.0546
46	-1.4955	1.4955	225.000	.9659	.0709	.0679	-.0982	-.0508	.1128	.0574	-.0554
47	-1.6202	1.3595	230.000	.9661	.0907	.1051	-.1388	-.0590	.1139	.0474	-.0665
48	-1.7325	1.2131	235.000	.9663	.1009	.1412	-.1735	-.0855	.1363	.0361	-.1002
49	-1.8316	1.0575	240.000	.9666	.1197	.2044	-.2369	-.0642	.0815	.0096	-.0719
50	-1.9168	.8938	245.000	.9668	.1259	.2669	-.2951	-.0743	.0632	-.0218	-.0850
51	-1.9874	.7234	250.000	.9671	.1140	.3102	-.3305	-.0866	.0573	-.0444	-.1017
52	-2.0429	.5474	255.000	.9673	.0923	.3414	-.3536	-.0958	.0542	-.0608	-.1150
53	-2.0829	.3673	260.000	.9676	.0649	.3651	-.3709	-.1020	.0519	-.0738	-.1258
54	-2.1070	.1843	265.000	.9679	.0337	.3827	-.3842	-.1085	.0499	-.0844	-.1343
55	-2.1150	-.0000	270.000	.9682	.0000	.3944	-.3944	-.1125	.0479	-.0929	-.1408
56	-2.1070	-.1843	275.000	.9685	-.0352	.3998	-.4014	-.1150	.0459	-.0990	-.1449
57	-2.0829	-.3673	280.000	.9687	-.0709	.3990	-.4052	-.1160	.0440	-.1026	-.1466
58	-2.0429	-.5474	285.000	.9690	-.1057	.3916	-.4056	-.1154	.0420	-.1035	-.1455
59	-1.9874	-.7234	290.000	.9693	-.1386	.3779	-.4025	-.1130	.0402	-.1015	-.1417
60	-1.9168	-.8938	295.000	.9695	-.1684	.3581	-.3957	-.1089	.0384	-.0966	-.1350
61	-1.8316	-1.0575	300.000	.9698	-.1938	.3327	-.3850	-.1028	.0368	-.0887	-.1255
62	-1.7325	-1.2131	305.000	.9700	-.2139	.3025	-.3705	-.0947	.0353	-.0782	-.1134
63	-1.6202	-1.3595	310.000	.9702	-.2277	.2684	-.3519	-.0847	.0339	-.0652	-.0992
64	-1.4955	-1.4955	315.000	.9704	-.2344	.2314	-.3294	-.0728	.0328	-.0502	-.0830
65	-1.3595	-1.6202	320.000	.9706	-.2332	.1927	-.3026	-.0591	.0319	-.0337	-.0656
66	-1.2131	-1.7325	325.000	.9708	-.2235	.1536	-.2712	-.0439	.0313	-.0160	-.0473
67	-1.0575	-1.8316	330.000	.9710	-.2045	.1151	-.2347	-.0278	.0313	.0022	-.0291
68	-.8938	-1.9168	335.000	.9711	-.1753	.0787	-.1921	-.0117	.0320	.0201	-.0119
69	-.7234	-1.9874	340.000	.9712	-.1357	.0464	-.1434	.0022	.0341	.0362	.0022
70	-.5474	-2.0429	345.000	.9713	-.0892	.0209	-.0916	.0107	.0377	.0482	.0105
71	-.3673	-2.0829	350.000	.9713	-.0469	.0053	-.0472	.0125	.0420	.0543	.0123
72	-.1843	-2.1070	355.000	.9714	-.0191	-.0013	-.0191	.0117	.0445	.0561	.0115
73	0.0000	-2.1150	360.000	.9714	-.0012	-.0030	-.0032	.0121	.0445	.0564	.0119

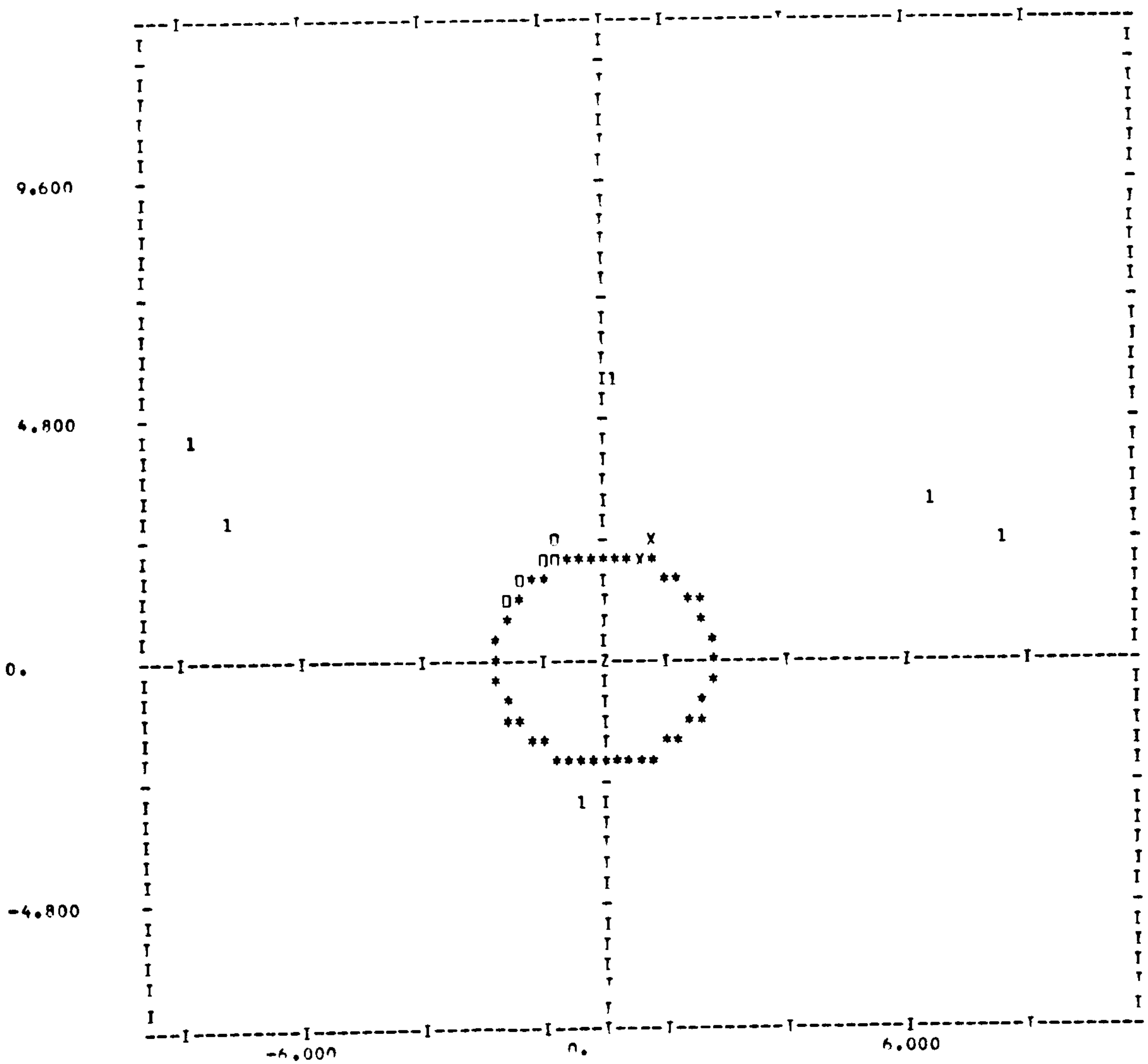

X	R	ALPHA	BETA	M
37.505	2.115	15.000	.000	2.500

X = 37.505

CN(X)	CY(X)	CP(0)	CP(90)	CP(180)
4.902E-05	-4.884E-02	1.208E-02	-4.554E-02	-1.790E-03

CN	CM	CY	CR	CSL
-2.251E-02	-8.628E-02	-2.093E-01	7.054E-01	-7.560E-17

(SEPARATION POINTS)

Y	Z	BETA
0.000	0.000	0.0
-1.955	.801	247.7

ORIGINAL PAGE IS OF POOR QUALITY

STRATFORD SEPARATION CRITERION (LAMINAR) F(S) = .02252

SUMMARY OF PRESSURE DISTRIBUTION AND SEPARATION POINTS ON BODY ... X = 37.51

+Y SIDE*	Y	Z	BETA	ARC	CP	CP*	DCP*/DX
STAGNATION PT.	0.000	-2.115	0.000	.056	.012		
MIN. PRESSURE	1.987	-.723	70.000	2.583	-.047	0.000	0.000
SEPARATION	0.000	0.000	0.000	0.000	0.000	0.000	0.000

-Y SIDE*	Y	Z	BETA	ARC	CP	CP*	DCP*/DX
STAGNATION PT.	-.547	2.043	195.000	.056	-.013		
MIN. PRESSURE	-2.043	-.547	285.000	2.768	-.115	0.000	0.000
SEPARATION	-1.955	.801	247.714	4.144	-.081	.031	.053

INITIAL POSITIONS AND STRENGTHS OF SHED VORTICITY AT X = 37.505

	NV	GAM/V	M(K)	Y	Z	BETA	VT/V	YC	ZC	RG/R
-Y SIDE*	15	-.1079	.1123	-2.0609	.8447	247.7136	.3140	-2.0609	.8447	1.0531

SUMMARY OF VORTEX FIELD AT X = 45.965 H = 2.11500

	NV	GAM/V	Y	Z	XSHED	BETA	YC	ZC	RG	RG/R
1	1	.02127	.73754	2.54816	26.93000	163.858	.73754	2.54816	2.65275	1.25425
2	2	.00691	.72252	2.39051	29.04500	163.183	.72252	2.39051	2.49731	1.18076
3	3	.00226	.66592	2.23770	31.16000	163.427	.66592	2.23770	2.33468	1.10387
1	4	.02130	7.48395	2.78594	0.00000	110.418	7.48395	2.78594	7.98567	3.77573
2	5	-.00588	-6.33608	6.56114	0.00000	224.000	-6.33608	6.56114	9.12111	4.31258
3	6	3.37980	7.81982	4.36317	0.00000	119.160	7.81982	4.36317	8.95471	4.23390
4	7	-2.22590	-7.22099	4.96015	0.00000	235.515	-7.22099	4.96015	8.76047	4.14207
5	8	-.09334	.39734	6.60621	0.00000	176.558	.39734	6.60621	6.61815	3.12915
6	9	-.16236	-1.41951	-1.82656	0.00000	322.147	-1.41951	-1.82656	2.31329	1.09376
1	10	-.12345	-1.29207	2.12242	26.93000	211.332	-1.29207	2.12242	2.48477	1.17483
2	11	-.11374	-1.28186	1.87219	29.04500	214.399	-1.28186	1.87219	2.26898	1.07280
3	12	-.10674	-.78220	2.17689	31.16000	199.764	-.78220	2.17689	2.31315	1.09369
4	13	-.10560	-.72802	2.45044	33.27500	196.547	-.72802	2.45044	2.55630	1.20865
5	14	-.10994	-1.10795	2.36154	35.39000	205.134	-1.10795	2.36154	2.60853	1.23335
6	15	-.10794	-1.47735	2.37177	37.50500	211.918	-1.47735	2.37177	2.79426	1.32116
7	16	-.11986	-1.75574	1.80784	39.62000	224.162	-1.75574	1.80784	2.52010	1.19154
8	17	-.12293	-1.94857	1.46949	41.73500	232.979	-1.94857	1.46949	2.44056	1.15393
9	18	-.13256	-2.09356	.99254	43.85000	244.635	-2.09356	.99254	2.31692	1.09547

CENTROID OF SHED VORTICITY

	GAM/V	Y	Z
+Y BODY*	.03243	.72843	2.48324
-Y BODY*	-1.04275	-1.41399	1.92817

BODY SURFACE PRESSURE DISTRIBUTION

X	R	DR/DX	M
45.9650	2.1150	0.0000	2.5000

J	Y	Z	BETA	U/VO	V/VO	W/VO	VT/VO	CP(M)	DPHI/DT	CPZ	CP(I)
1	0.0000	-2.1150	0.000	.9684	-.0539	-.0039	-.0540	.0360	.0251	.0593	.0341
2	.1843	-2.1070	5.000	.9684	-.0175	-.0045	-.0181	.0392	.0249	.0619	.0370
3	.3673	-2.0829	10.000	.9684	.0182	.0002	.0182	.0392	.0249	.0619	.0370
4	.5474	-2.0429	15.000	.9684	.0520	.0110	.0531	.0362	.0251	.0594	.0343
5	.7234	-1.9874	20.000	.9683	.0827	.0271	.0870	.0306	.0255	.0547	.0293
6	.8938	-1.9168	25.000	.9683	.1092	.0479	.1193	.0229	.0260	.0482	.0221
7	1.0575	-1.8316	30.000	.9683	.1308	.0725	.1495	.0136	.0268	.0401	.0134
8	1.2131	-1.7325	35.000	.9682	.1468	.0998	.1775	.0035	.0276	.0311	.0035
9	1.3595	-1.6202	40.000	.9681	.1568	.1285	.2027	-.0070	.0286	.0216	-.0070
10	1.4955	-1.4955	45.000	.9681	.1606	.1576	.2250	-.0171	.0298	.0122	-.0176
11	1.6202	-1.3595	50.000	.9680	.1584	.1858	.2441	-.0266	.0311	.0034	-.0277
12	1.7325	-1.2131	55.000	.9679	.1505	.2119	.2599	-.0349	.0326	-.0044	-.0370
13	1.8316	-1.0575	60.000	.9678	.1373	.2349	.2721	-.0419	.0342	-.0107	-.0449
14	1.9168	-.8938	65.000	.9678	.1197	.2539	.2807	-.0473	.0359	-.0153	-.0513
15	1.9874	-.7234	70.000	.9677	.0986	.2680	.2856	-.0511	.0378	-.0180	-.0558
16	2.0429	-.5474	75.000	.9676	.0750	.2771	.2870	-.0533	.0399	-.0186	-.0585
17	2.0829	-.3673	80.000	.9675	.0500	.2806	.2851	-.0540	.0420	-.0173	-.0593
18	2.1070	-.1843	85.000	.9674	.0247	.2788	.2799	-.0533	.0442	-.0142	-.0584
19	2.1150	0.0000	90.000	.9673	.0000	.2719	.2719	-.0514	.0465	-.0096	-.0561
20	2.1070	.1843	95.000	.9672	-.0230	.2603	.2613	-.0484	.0489	-.0037	-.0526
21	2.0829	.3673	100.000	.9671	-.0437	.2447	.2486	-.0448	.0512	.0029	-.0483
22	2.0429	.5474	105.000	.9670	-.0614	.2260	.2342	-.0406	.0535	.0101	-.0434
23	1.9874	.7234	110.000	.9669	-.0757	.2049	.2185	-.0361	.0557	.0174	-.0383
24	1.9168	.8938	115.000	.9668	-.0864	.1824	.2018	-.0316	.0578	.0245	-.0333
25	1.8316	1.0575	120.000	.9667	-.0935	.1590	.1845	-.0271	.0597	.0314	-.0283
26	1.7325	1.2131	125.000	.9666	-.0971	.1356	.1668	-.0228	.0615	.0378	-.0237
27	1.6202	1.3595	130.000	.9666	-.0971	.1127	.1487	-.0188	.0630	.0436	-.0194
28	1.4955	1.4955	135.000	.9665	-.0937	.0907	.1304	-.0152	.0644	.0489	-.0155
29	1.3595	1.6202	140.000	.9664	-.0869	.0700	.1116	-.0119	.0657	.0536	-.0121
30	1.2131	1.7325	145.000	.9664	-.0768	.0508	.0921	-.0090	.0668	.0576	-.0091
31	1.0575	1.8316	150.000	.9663	-.0632	.0335	.0715	-.0066	.0678	.0611	-.0067
32	.8938	1.9168	155.000	.9663	-.0456	.0183	.0491	-.0050	.0690	.0639	-.0051
33	.7234	1.9874	160.000	.9662	-.0255	.0063	.0262	-.0046	.0704	.0657	-.0047
34	.5474	2.0429	165.000	.9662	-.0096	-.0004	.0096	-.0056	.0720	.0664	-.0056
35	.3673	2.0829	170.000	.9662	-.0021	-.0026	.0033	-.0069	.0734	.0665	-.0069
36	.1843	2.1070	175.000	.9662	.0007	-.0030	-.0031	-.0083	.0749	.0665	-.0084
37	-.0000	2.1150	180.000	.9662	-.0022	-.0030	.0037	-.0102	.0769	.0665	-.0104
38	-.1843	2.1070	185.000	.9662	-.0184	-.0046	.0190	-.0133	.0798	.0662	-.0136
39	-.3673	2.0829	190.000	.9662	-.0599	-.0135	.0614	-.0201	.0835	.0627	-.0208
40	-.5474	2.0429	195.000	.9662	-.1286	-.0374	.1340	-.0339	.0843	.0485	-.0358
41	-.7234	1.9874	200.000	.9662	-.1781	-.0679	.1906	-.0515	.0864	.0301	-.0563
42	-.8938	1.9168	205.000	.9663	-.1796	-.0867	.1994	-.0779	.1163	.0265	-.0897
43	-1.0575	1.8316	210.000	.9663	-.1736	-.1032	.2020	-.0775	.1147	.0254	-.0893

ORIGINAL PAGE IS
OF POOR QUALITY

44	-1.2131	1.7325	215.000	.9664	-.1365	-.0985	.1683	-.0316	.0711	.0378	-.0333
45	-1.3595	1.6202	220.000	.9664	-.0665	-.0587	.0887	-.0369	.0974	.0581	-.0392
46	-1.4955	1.4955	225.000	.9665	-.0164	-.0194	.0254	-.0437	.1123	.0652	-.0471
47	-1.6202	1.3595	230.000	.9666	.0137	.0133	-.0191	-.0473	.1167	.0654	-.0513
48	-1.7325	1.2131	235.000	.9666	.0490	.0542	-.0674	-.0465	.1114	.0611	-.0503
49	-1.8316	1.0575	240.000	.9667	.0578	.0972	-.1131	-.0582	.1171	.0526	-.0645
50	-1.9168	.8938	245.000	.9668	.0675	.1417	-.1570	-.0761	.1281	.0406	-.0875
51	-1.9874	.7234	250.000	.9669	.0830	.2252	-.2400	-.0581	.0718	.0075	-.0643
52	-2.0429	.5474	255.000	.9670	.0926	.3054	-.3164	-.0725	.0474	-.0352	-.0826
53	-2.0829	.3673	260.000	.9671	.0633	.3563	-.3619	-.0891	.0391	-.0662	-.1053
54	-2.1070	.1843	265.000	.9672	.0342	.3878	-.3893	-.1006	.0351	-.0870	-.1221
55	-2.1150	-.0000	270.000	.9673	.0000	.4071	-.4071	-.1082	.0326	-.1014	-.1340
56	-2.1070	-.1843	275.000	.9674	-.0367	.4166	-.4182	-.1129	.0308	-.1107	-.1415
57	-2.0829	-.3673	280.000	.9675	-.0741	.4173	-.4238	-.1151	.0294	-.1156	-.1450
58	-2.0429	-.5474	285.000	.9676	-.1106	.4097	-.4243	-.1148	.0282	-.1163	-.1445
59	-1.9874	-.7234	290.000	.9677	-.1446	.3942	-.4199	-.1121	.0274	-.1127	-.1401
60	-1.9168	-.8938	295.000	.9678	-.1745	.3713	-.4103	-.1070	.0271	-.1049	-.1320
61	-1.8316	-1.0575	300.000	.9678	-.1987	.3412	-.3948	-.0992	.0275	-.0926	-.1201
62	-1.7325	-1.2131	305.000	.9679	-.2145	.3033	-.3715	-.0883	.0293	-.0749	-.1042
63	-1.6202	-1.3595	310.000	.9680	-.2164	.2550	-.3344	-.0736	.0351	-.0489	-.0840
64	-1.4955	-1.4955	315.000	.9681	-.1925	.1895	-.2701	-.0577	.0537	-.0102	-.0638
65	-1.3595	-1.6202	320.000	.9681	-.1460	.1195	-.1887	-.0730	.1104	.0271	-.0633
66	-1.2131	-1.7325	325.000	.9682	-.1383	.0939	-.1672	-.0677	.1104	.0346	-.0757
67	-1.0575	-1.8316	330.000	.9683	-.1706	.0955	-.1955	-.0336	.0598	.0243	-.0355
68	-.8938	-1.9168	335.000	.9683	-.1839	.0828	-.2017	-.0182	.0405	.0217	-.0188
69	-.7234	-1.9874	340.000	.9683	-.1741	.0604	-.1843	-.0043	.0327	.0284	-.0043
70	-.5474	-2.0429	345.000	.9684	-.1520	.0377	-.1566	.0090	.0289	.0377	.0088
71	-.3673	-2.0829	350.000	.9684	-.1229	.0187	-.1243	.0205	.0269	.0468	.0199
72	-.1843	-2.1070	355.000	.9684	-.0896	.0049	-.0897	.0297	.0257	.0541	.0284
73	0.0000	-2.1150	360.000	.9684	-.0539	-.0030	-.0540	.0360	.0251	.0593	.0341

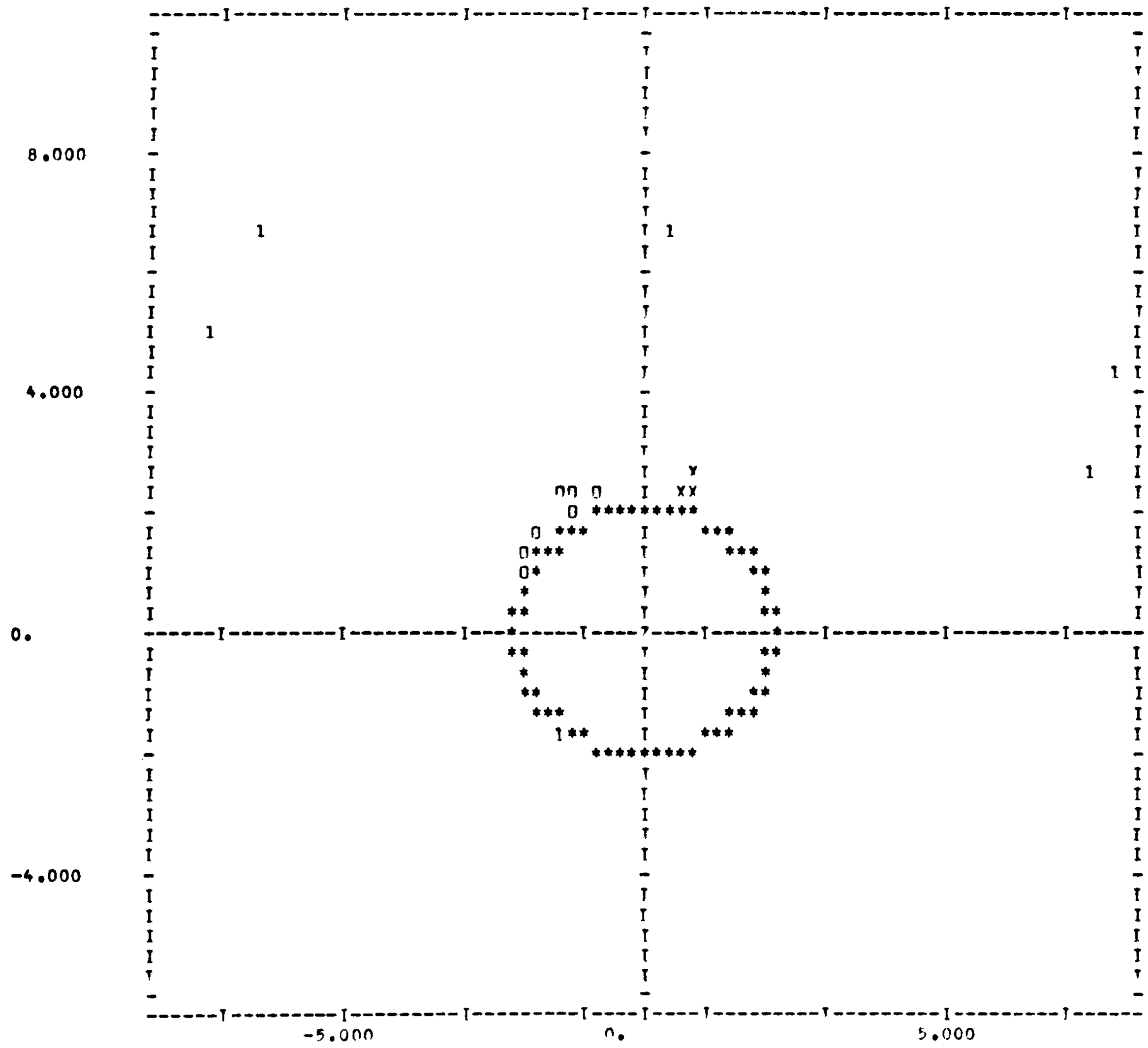

X	R	ALPHA	BETA	M
45.965	2.115	15.000	.000	2.500

X = 45.965

CN(X)	CY(X)	CP(0)	CP(90)	CP(180)
1.377E-02	-4.574E-02	3.600E-02	-5.136E-02	-1.021E-02

CN	CM	CY	CR	CSL
-5.953E-04	-7.460E-02	-3.289E-01	7.985E-01	-3.459E-17

(SEPARATION POINTS)

Y	Z	BETA
0.000	0.000	0.0
-2.075	.405	259.0

STRATFORD SEPARATION CRITERION (LAMINAR) F(S) = .02252

SUMMARY OF PRESSURE DISTRIBUTION AND SEPARATION POINTS ON BODY ... X = 45.96

		Y	Z	BETA	ARC	CP	CP*	DCP*/DX
+Y SIDE*	STAGNATION PT.	.184	-2.107	5.000	.059	.039		
	MIN. PRESSURE	2.043	-.547	75.000	2.583	-.053	0.000	0.000
	SEPARATION	0.000	0.000	0.000	0.000	0.000	0.000	0.000
-Y SIDE*	STAGNATION PT.	.184	2.107	175.000	.059	-.008		
	MIN. PRESSURE	-2.043	-.547	285.000	2.952	-.115	0.000	0.000
	SEPARATION	-2.075	.405	258.954	3.913	-.086	.026	.070

INITIAL POSITIONS AND STRENGTHS OF SHED VORTICITY AT X = 45.965

	NV	GAM/V	M(K)	Y	Z	BETA	VT/V	YC	ZC	RG/R
-Y SIDE*	19	-.1358	.1264	-2.1999	.4295	258.9538	.3521	-2.1999	.4295	1.0598

SUMMARY OF VORTEX FIELD AT X = 54.425 H = 2.11500

	NV	GAM/V	Y	Z	XSHED	BETA	YC	ZC	RG	RG/R
1	1	.02127	.59288	2.86634	26.93000	168.314	.59288	2.86634	2.92702	1.38393
2	2	.00891	.60482	2.67479	29.04500	167.259	.60482	2.67479	2.74232	1.29660
3	3	.00226	.51829	2.41920	31.16000	167.908	.51829	2.41920	2.47409	1.16978
4	4	.00539	-2.00259	2.16933	48.08000	222.711	-2.00259	2.16933	2.95234	1.39591
5	5	.01237	-1.91387	1.89930	50.19500	225.219	-1.91387	1.89930	2.69633	1.27486
6	6	.09896	-1.60969	1.75154	52.31000	222.583	-1.60969	1.75154	2.37886	1.12476
1	7	.02130	9.36145	6.39644	0.00000	124.344	9.36145	6.39644	11.33804	5.36078
2	8	-.00588	-5.23910	7.21491	0.00000	215.985	-5.23910	7.21491	8.91645	4.21582
3	9	3.37980	7.78047	6.27602	0.00000	128.891	7.78047	6.27602	9.99621	4.72634
4	10	-2.22590	-7.03760	7.07972	0.00000	224.829	-7.03760	7.07972	9.98250	4.71986
5	11	-.09334	.51539	7.66179	0.00000	176.152	.51539	7.66179	7.67911	3.63078
6	12	-.16236	-2.32476	.35511	0.00000	261.315	-2.32476	.35511	2.35172	1.11193
1	13	-.12345	-1.25200	2.25012	26.93000	209.092	-1.25200	2.25012	2.57499	1.21749
2	14	-.11374	-1.42120	2.47558	29.04500	209.860	-1.42120	2.47558	2.85453	1.34966
3	15	-.10674	-1.71419	2.34144	31.16000	216.208	-1.71419	2.34144	2.90186	1.37204
4	16	-.10560	-1.76190	1.96013	33.27500	221.951	-1.76190	1.96013	2.63560	1.24615
5	17	-.10994	-1.58457	1.97973	35.39000	218.674	-1.58457	1.97973	2.53579	1.19895
6	18	-.10794	-.86768	2.24170	37.50500	201.160	-.86768	2.24170	2.40376	1.13653
7	19	-.11986	-.89885	2.51398	39.62000	199.674	-.89885	2.51398	2.66984	1.26233
8	20	-.12293	-1.05079	2.91441	41.73500	199.827	-1.05079	2.91441	3.09805	1.46480
9	21	-.13256	-1.59343	2.73005	43.85000	210.270	-1.59343	2.73005	3.16104	1.49458
10	22	-.13576	-2.09458	2.38216	45.96500	221.324	-2.09458	2.38216	3.17205	1.49979
11	23	-.16777	-2.08429	1.43511	48.08000	235.451	-2.08429	1.43511	2.53057	1.19649
12	24	-.15944	-2.23561	1.02447	50.19500	245.380	-2.23561	1.02447	2.45916	1.16272
13	25	-.10112	-2.16729	.32409	52.31000	261.495	-2.16729	.32409	2.19139	1.03612

CENTROID OF SHED VORTICITY

	GAM/V	Y	Z
+Y BODY*	.14915	-1.17054	2.00311
-Y BODY*	-1.60684	-1.62484	2.02735

ORIGINAL PAGE IS
OF POOR QUALITY

BODY SURFACE PRESSURE DISTRIBUTION

X	R	DR/DX	M
54.4250	2.1150	0.0000	2.5000

J	Y	Z	BETA	U/VO	V/VO	W/VO	VT/VO	CP(M)	DPHI/DT	CPZ	CP(I)
1	0.0000	-2.1150	0.000	.9671	-.0471	-.0030	-.0471	.0513	.0148	.0625	.0477
2	.1843	-2.1070	5.000	.9671	-.0082	-.0037	-.0090	.0533	.0153	.0646	.0493
3	.3673	-2.0829	10.000	.9671	.0298	.0023	.0298	.0517	.0158	.0638	.0480
4	.5474	-2.0429	15.000	.9671	.0655	.0146	.0671	.0468	.0165	.0602	.0438
5	.7234	-1.9874	20.000	.9671	.0978	.0326	.1031	.0391	.0172	.0541	.0370
6	.8938	-1.9168	25.000	.9671	.1259	.0557	.1376	.0291	.0179	.0458	.0279
7	1.0575	-1.8316	30.000	.9671	.1487	.0829	.1702	.0175	.0188	.0358	.0170
8	1.2131	-1.7325	35.000	.9671	.1557	.1130	.2006	.0049	.0197	.0246	.0049
9	1.3595	-1.6202	40.000	.9670	.1764	.1450	.2284	-.0080	.0208	.0127	-.0081
10	1.4955	-1.4955	45.000	.9670	.1806	.1777	.2534	-.0205	.0219	.0007	-.0212
11	1.6202	-1.3595	50.000	.9670	.1784	.2096	.2753	-.0322	.0231	-.0109	-.0340
12	1.7325	-1.2131	55.000	.9670	.1700	.2397	.2939	-.0427	.0245	-.0214	-.0459
13	1.8316	-1.0575	60.000	.9670	.1558	.2669	.3090	-.0516	.0259	-.0305	-.0564
14	1.9168	-.8938	65.000	.9669	.1366	.2900	.3206	-.0589	.0275	-.0378	-.0652
15	1.9874	-.7234	70.000	.9669	.1133	.3084	.3285	-.0643	.0292	-.0429	-.0720
16	2.0429	-.5474	75.000	.9669	.0869	.3213	.3328	-.0679	.0310	-.0457	-.0766
17	2.0829	-.3673	80.000	.9669	.0584	.3283	.3335	-.0697	.0329	-.0461	-.0790
18	2.1070	-.1843	85.000	.9668	.0291	.3294	.3307	-.0698	.0350	-.0441	-.0791
19	2.1150	0.0000	90.000	.9668	.0000	.3245	.3245	-.0683	.0371	-.0401	-.0772
20	2.1070	.1843	95.000	.9668	-.0277	.3141	.3153	-.0655	.0394	-.0341	-.0735
21	2.0829	.3673	100.000	.9668	-.0532	.2987	.3034	-.0614	.0417	-.0267	-.0684
22	2.0429	.5474	105.000	.9668	-.0755	.2790	.2890	-.0564	.0441	-.0181	-.0622
23	1.9874	.7234	110.000	.9667	-.0942	.2558	.2726	-.0508	.0465	-.0089	-.0554
24	1.9168	.8938	115.000	.9667	-.1087	.2301	.2545	-.0448	.0490	.0007	-.0483
25	1.8316	1.0575	120.000	.9667	-.1189	.2029	.2352	-.0386	.0514	.0102	-.0412
26	1.7325	1.2131	125.000	.9667	-.1247	.1751	.2150	-.0327	.0538	.0193	-.0345
27	1.6202	1.3595	130.000	.9666	-.1263	.1476	.1942	-.0271	.0562	.0279	-.0284
28	1.4955	1.4955	135.000	.9666	-.1240	.1210	.1732	-.0221	.0585	.0356	-.0229
29	1.3595	1.6202	140.000	.9666	-.1180	.0961	.1522	-.0178	.0608	.0425	-.0183
30	1.2131	1.7325	145.000	.9666	-.1089	.0733	.1313	-.0143	.0630	.0484	-.0146
31	1.0575	1.8316	150.000	.9666	-.0972	.0531	.1108	-.0116	.0653	.0534	-.0118
32	.8938	1.9168	155.000	.9666	-.0834	.0359	.0908	-.0099	.0675	.0575	-.0101
33	.7234	1.9874	160.000	.9666	-.0686	.0220	.0720	-.0092	.0699	.0606	-.0094
34	.5474	2.0429	165.000	.9666	-.0552	.0118	.0565	-.0097	.0725	.0626	-.0099
35	.3673	2.0829	170.000	.9666	-.0471	.0053	.0475	-.0113	.0750	.0635	-.0115
36	.1843	2.1070	175.000	.9666	-.0472	.0012	.0472	-.0136	.0775	.0636	-.0139
37	-.0000	2.1150	180.000	.9665	-.0568	-.0030	.0569	-.0168	.0798	.0625	-.0173
38	-.1843	2.1070	185.000	.9666	-.0798	-.0100	.0804	-.0216	.0817	.0593	-.0224
39	-.3673	2.0829	190.000	.9666	-.1234	-.0247	.1258	-.0304	.0819	.0499	-.0319
40	-.5474	2.0429	195.000	.9666	-.1927	-.0546	.2003	-.0480	.0777	.0257	-.0521
41	-.7234	1.9874	200.000	.9666	-.2597	-.0975	.2774	-.0743	.0739	-.0112	-.0850
42	-.8938	1.9168	205.000	.9666	-.2693	-.1286	.2984	-.0965	.0926	-.0233	-.1160
43	-1.0575	1.8316	210.000	.9666	-.2325	-.1372	.2700	-.0957	.1077	-.0072	-.1149

ORIGINAL PAGE IS
OF POOR QUALITY

44	-1.2131	1.7325	215.000	.9666	-.1728	-.1240	.2127	-.0770	.1090	.0204	-.0886
45	-1.3595	1.6202	220.000	.9666	-.0953	-.0830	.1264	-.0544	.1095	.0497	-.0598
46	-1.4955	1.4955	225.000	.9666	-.0342	-.0372	.0506	-.0509	.1196	.0631	-.0555
47	-1.6202	1.3595	230.000	.9666	-.0151	-.0209	.0258	-.0504	.1199	.0649	-.0550
48	-1.7325	1.2131	235.000	.9667	-.0082	-.0147	.0168	-.0525	.1227	.0653	-.0574
49	-1.8316	1.0575	240.000	.9667	.0062	.0078	-.0100	-.0532	.1237	.0654	-.0583
50	-1.9168	.8938	245.000	.9667	.0229	.0462	-.0516	-.0522	.1200	.0628	-.0571
51	-1.9874	.7234	250.000	.9667	.0407	.1088	-.1161	-.0486	.1048	.0519	-.0528
52	-2.0429	.5474	255.000	.9668	.0388	.1419	-.1471	-.0684	.1210	.0437	-.0773
53	-2.0829	.3673	260.000	.9668	.0250	.1385	-.1408	-.1338	.2235	.0455	-.1780
54	-2.1070	.1843	265.000	.9668	.0183	.2060	-.2068	-.0655	.1227	.0225	-.1002
55	-2.1150	-.0000	270.000	.9668	.0000	.3114	-.3114	-.0746	.0537	-.0317	-.0854
56	-2.1070	-.1843	275.000	.9668	-.0320	.3727	-.3741	-.0902	.0321	-.0747	-.1068
57	-2.0829	-.3673	280.000	.9669	-.0706	.3971	-.4034	-.0999	.0235	-.0975	-.1211
58	-2.0429	-.5474	285.000	.9669	-.1084	.4017	-.4161	-.1040	.0194	-.1080	-.1274
59	-1.9874	-.7234	290.000	.9669	-.1443	.3936	-.4192	-.1043	.0171	-.1106	-.1278
60	-1.9168	-.8938	295.000	.9669	-.1767	.3759	-.4153	-.1013	.0157	-.1075	-.1232
61	-1.8316	-1.0575	300.000	.9670	-.2043	.3508	-.4059	-.0955	.0148	-.0998	-.1146
62	-1.7325	-1.2131	305.000	.9670	-.2261	.3199	-.3918	-.0873	.0142	-.0885	-.1027
63	-1.6202	-1.3595	310.000	.9670	-.2415	.2848	-.3734	-.0768	.0138	-.0745	-.0883
64	-1.4955	-1.4955	315.000	.9670	-.2499	.2470	-.3514	-.0643	.0135	-.0586	-.0721
65	-1.3595	-1.6202	320.000	.9670	-.2511	.2078	-.3259	-.0502	.0133	-.0414	-.0547
66	-1.2131	-1.7325	325.000	.9671	-.2451	.1687	-.2976	-.0349	.0133	-.0237	-.0370
67	-1.0575	-1.8316	330.000	.9671	-.2321	.1310	-.2666	-.0190	.0133	-.0063	-.0196
68	-.8938	-1.9168	335.000	.9671	-.2126	.0962	-.2334	-.0030	.0134	.0103	-.0031
69	-.7234	-1.9874	340.000	.9671	-.1873	.0652	-.1983	.0121	.0135	.0254	.0119
70	-.5474	-2.0429	345.000	.9671	-.1570	.0391	-.1617	.0258	.0138	.0386	.0248
71	-.3673	-2.0829	350.000	.9671	-.1227	.0187	-.1241	.0373	.0140	.0493	.0353
72	-.1843	-2.1070	355.000	.9671	-.0857	.0045	-.0858	.0459	.0144	.0574	.0430
73	0.0000	-2.1150	360.000	.9671	-.0471	-.0030	-.0471	.0513	.0148	.0625	.0477

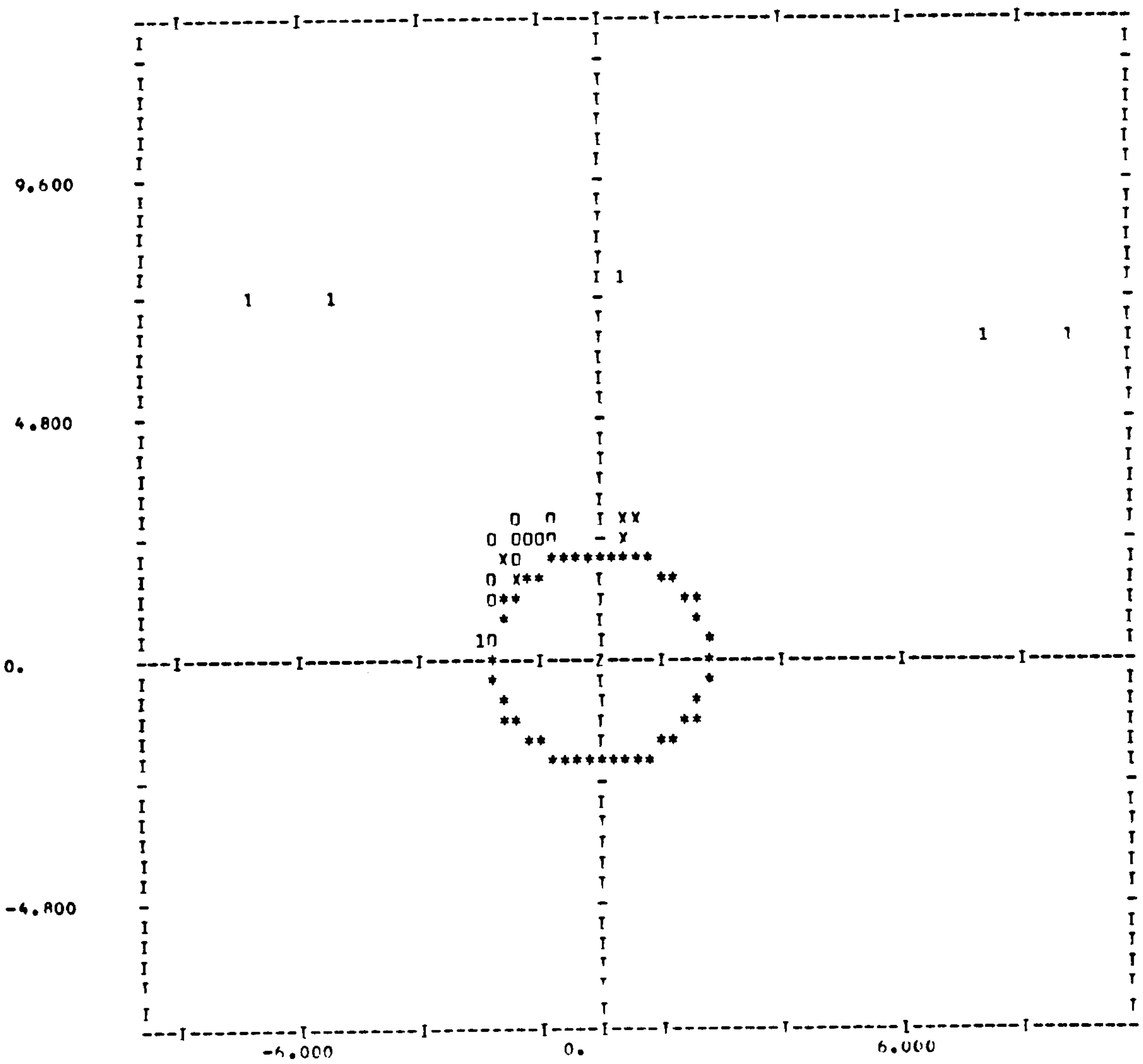

Y	R	ALPHA	BETA	M
54.425	2.115	15.000	.000	2.500

X = 54.425

CN(X)	CY(X)	CP(0)	CP(90)	CP(180)
3.116E-02	-3.291E-02	5.134E-02	-6.834E-02	-1.683E-02

CN	CM	CY	CR	CSL
6.194E-02	-1.592E-01	-4.289E-01	6.817E-01	-5.464E-17

(SEPARATION POINTS)

Y	Z	BETA
-1.782	1.679	217.4
-2.073	.414	258.7

STRATFORD SEPARATION CRITERION (LAMINAR) F(S) = .02252

SUMMARY OF PRESSURE DISTRIBUTION AND SEPARATION POINTS ON BODY ... X = 54.42

+Y SIDE		Y	Z	BETA	ARC	CP	CP*	DCP*/DX
	STAGNATION PT.	.184	-2.107	5.000	.062	.053		
	MIN. PRESSURE	2.107	-.184	85.000	2.952	-.070	0.000	0.000
	SEPARATION	-1.282	1.679	217.362	7.837	-.066	.003	.086

-Y SIDE		Y	Z	BETA	ARC	CP	CP*	DCP*/DX
	STAGNATION PT.	-1.832	1.057	240.000	.062	-.053		
	MIN. PRESSURE	-1.987	-.723	290.000	2.768	-.104	0.000	0.000
	SEPARATION	-2.073	.414	258.712	3.922	-.117	-.012	.085

INITIAL POSITIONS AND STRENGTHS OF SHED VORTICITY AT X = 54.425

	NV	GAM/V	M(K)	Y	Z	BETA	VT/V	YC	ZC	RG/R
+Y SIDE	26	.0323	.0607	-1.3477	1.7651	217.3618	.1717	-1.3477	1.7651	1.0500
-Y SIDE	27	-.0222	.0502	-2.1778	.4347	258.7119	.1423	-2.1778	.4347	1.0500

ORIGINAL PAGE IS OF POOR QUALITY

SUMMARY OF VORTEX FIELD AT X = 62.885   H = 2.11500

	NV	GAM/V	Y	Z	XSHED	BETA	YC	ZC	RG	RG/R
1	1	.02127	.30028	3.08424	26.93000	174.439	.30028	3.08424	3.09882	1.46516
2	2	.00891	.29206	2.88030	29.04500	174.210	.29206	2.88030	2.89507	1.36883
3	3	.00226	-.00493	2.46821	31.16000	180.115	-.00493	2.46821	2.46821	1.16700
4	4	.00539	-.72297	3.47343	48.08000	191.758	-.72297	3.47343	3.54787	1.67746
5	5	.01237	-1.12306	3.17096	50.19500	199.593	-1.12306	3.17096	3.36396	1.59053
6	6	.09896	-2.27944	2.15686	52.31000	226.583	-2.27944	2.15686	3.13814	1.48375
7	7	.03229	-2.05407	1.63970	54.42500	231.401	-2.05407	1.63970	2.62827	1.24268
8	8	.09281	-2.11124	1.79365	56.54000	229.650	-2.11124	1.79365	2.77029	1.30983
9	9	.04762	-1.79781	1.81310	58.65500	224.757	-1.79781	1.81310	2.55332	1.20724
10	10	.06218	-1.42366	1.83873	60.77000	217.749	-1.42366	1.83873	2.32545	1.09950
1	11	.02130	7.22290	9.69045	0.00000	143.301	7.22290	9.69045	12.08615	5.71449
2	12	-.00588	-5.59573	7.74297	0.00000	215.855	-5.59573	7.74297	9.55331	4.51693
3	13	3.37980	7.77353	8.18205	0.00000	136.467	7.77353	8.18205	11.28600	5.33617
4	14	-2.22590	-6.84751	9.15290	0.00000	216.801	-6.84751	9.15290	11.43083	5.40465
5	15	-.09334	.63552	8.66745	0.00000	175.806	.63552	8.66745	8.69071	4.10908
6	16	-.16236	-2.47960	2.30568	0.00000	227.082	-2.47960	2.30568	3.38593	1.60091
1	17	-.12345	-1.28218	3.39654	26.93000	200.681	-1.28218	3.39654	3.63049	1.71654
2	18	-.11374	-1.52596	2.94497	29.04500	207.391	-1.52596	2.94497	3.31683	1.56824
3	19	-.10674	-1.25187	2.69176	31.16000	204.942	-1.25187	2.69176	2.96863	1.40361
4	20	-.10560	-1.19121	3.21035	33.27500	200.357	-1.19121	3.21035	3.42423	1.61902
5	21	-.10994	-.98583	3.50117	35.39000	195.726	-.98583	3.50117	3.63732	1.71977
6	22	-.10794	-1.92601	2.84185	37.50500	214.127	-1.92601	2.84185	3.43301	1.62317
7	23	-.11986	-2.11571	2.35131	39.62000	221.981	-2.11571	2.35131	3.16305	1.49553
8	24	-.12293	-1.63265	2.50225	41.73500	213.123	-1.63265	2.50225	2.98777	1.41266
9	25	-.13256	-1.40216	2.36440	43.85000	210.669	-1.40216	2.36440	2.74890	1.29971
10	26	-.13576	-.86526	3.24422	45.96500	194.934	-.86526	3.24422	3.35762	1.58753
11	27	-.16777	-2.39231	2.09474	48.08000	228.794	-2.39231	2.09474	3.17979	1.50345
12	28	-.15944	-1.90505	3.17367	50.19500	210.975	-1.90505	3.17367	3.70154	1.75014
13	29	-.10112	-2.34853	2.38635	52.31000	224.542	-2.34853	2.38635	3.34817	1.58306
14	30	-.02216	-2.24412	1.54159	54.42500	235.513	-2.24412	1.54159	2.72261	1.28729
15	31	-.14577	-2.31020	1.36510	56.54000	239.421	-2.31020	1.36510	2.68338	1.26874
16	32	-.14717	-2.33043	.93469	58.65500	248.145	-2.33043	.93469	2.51089	1.18718
17	33	-.14067	-2.30052	.45317	60.77000	258.856	-2.30052	.45317	2.34473	1.10862

CENTROID OF SHED VORTICITY

	GAM/V	Y	Z
+Y BODY*	.38405	-1.74660	2.05257
-Y BODY*	-2.06261	-1.77484	2.39926

ORIGINAL PAGE IS
OF POOR QUALITY

BODY SURFACE PRESSURE DISTRIBUTION

X	R	DR/DX	M
62.8850	2.1150	0.0000	2.5000

J	Y	Z	BETA	U/VO	V/VO	W/VO	VT/VO	CP(M)	D2HI/DT	CPZ	CP(I)
1	0.0000	-2.1150	0.000	.9666	-.0315	-.0030	-.0317	.0590	.0104	.0646	.0542
2	.1843	-2.1070	5.000	.9666	.0084	-.0022	.0087	.0593	.0110	.0655	.0545
3	.3673	-2.0829	10.000	.9666	.0472	.0053	.0475	.0558	.0118	.0633	.0516
4	.5474	-2.0429	15.000	.9666	.0838	.0195	.0860	.0490	.0126	.0582	.0456
5	.7234	-1.9874	20.000	.9666	.1159	.0396	.1234	.0391	.0134	.0504	.0369
6	.8938	-1.9168	25.000	.9666	.1456	.0649	.1594	.0269	.0143	.0402	.0259
7	1.0575	-1.8316	30.000	.9666	.1690	.0946	.1936	.0131	.0153	.0281	.0128
8	1.2131	-1.7325	35.000	.9666	.1863	.1274	.2257	-.0016	.0163	.0147	-.0016
9	1.3595	-1.6202	40.000	.9666	.1971	.1624	.2554	-.0165	.0174	.0004	-.0170
10	1.4955	-1.4955	45.000	.9666	.2011	.1982	.2824	-.0310	.0186	-.0141	-.0327
11	1.6202	-1.3595	50.000	.9666	.1984	.2335	.3064	-.0446	.0198	-.0282	-.0481
12	1.7325	-1.2131	55.000	.9666	.1891	.2671	.3273	-.0569	.0212	-.0415	-.0626
13	1.8316	-1.0575	60.000	.9666	.1737	.2979	.3449	-.0673	.0226	-.0533	-.0759
14	1.9168	-.8938	65.000	.9666	.1529	.3249	.3590	-.0761	.0242	-.0632	-.0874
15	1.9874	-.7234	70.000	.9666	.1274	.3470	.3696	-.0830	.0258	-.0709	-.0967
16	2.0429	-.5474	75.000	.9666	.0982	.3636	.3766	-.0879	.0275	-.0761	-.1037
17	2.0829	-.3673	80.000	.9666	.0665	.3742	.3800	-.0910	.0294	-.0787	-.1081
18	2.1070	-.1843	85.000	.9666	.0334	.3785	.3799	-.0924	.0314	-.0786	-.1100
19	2.1150	0.0000	90.000	.9666	.0000	.3764	.3764	-.0920	.0335	-.0759	-.1094
20	2.1070	.1843	95.000	.9666	-.0325	.3683	.3697	-.0900	.0357	-.0709	-.1066
21	2.0829	.3673	100.000	.9665	-.0630	.3544	.3600	-.0866	.0380	-.0638	-.1018
22	2.0429	.5474	105.000	.9665	-.0907	.3356	.3476	-.0821	.0404	-.0550	-.0955
23	1.9874	.7234	110.000	.9665	-.1148	.3124	.3328	-.0765	.0430	-.0450	-.0879
24	1.9168	.8938	115.000	.9665	-.1347	.2859	.3161	-.0703	.0456	-.0341	-.0797
25	1.8316	1.0575	120.000	.9665	-.1502	.2571	.2978	-.0636	.0483	-.0228	-.0711
26	1.7325	1.2131	125.000	.9665	-.1610	.2270	.2783	-.0568	.0511	-.0116	-.0627
27	1.6202	1.3595	130.000	.9665	-.1673	.1964	.2580	-.0502	.0540	-.0007	-.0547
28	1.4955	1.4955	135.000	.9665	-.1695	.1665	.2375	-.0441	.0570	.0095	-.0475
29	1.3595	1.6202	140.000	.9665	-.1679	.1379	.2172	-.0388	.0601	.0187	-.0414
30	1.2131	1.7325	145.000	.9665	-.1632	.1113	.1975	-.0343	.0632	.0269	-.0364
31	1.0575	1.8316	150.000	.9665	-.1563	.0873	.1790	-.0310	.0665	.0339	-.0327
32	.8938	1.9168	155.000	.9665	-.1481	.0661	.1621	-.0290	.0700	.0396	-.0304
33	.7234	1.9874	160.000	.9665	-.1397	.0479	.1476	-.0283	.0737	.0441	-.0296
34	.5474	2.0429	165.000	.9665	-.1326	.0325	.1365	-.0290	.0777	.0473	-.0304
35	.3673	2.0829	170.000	.9665	-.1286	.0197	.1301	-.0313	.0819	.0490	-.0329
36	.1843	2.1070	175.000	.9665	-.1300	.0084	.1302	-.0352	.0863	.0490	-.0374
37	-.0000	2.1150	180.000	.9665	-.1383	-.0030	.1384	-.0411	.0908	.0468	-.0440
38	-.1843	2.1070	185.000	.9665	-.1539	-.0164	.1547	-.0486	.0949	.0420	-.0529
39	-.3673	2.0829	190.000	.9665	-.1738	-.0336	.1770	-.0575	.0982	.0346	-.0636
40	-.5474	2.0429	195.000	.9665	-.1941	-.0550	.2017	-.0662	.0997	.0252	-.0745
41	-.7234	1.9874	200.000	.9665	-.2090	-.0790	.2234	-.0723	.0983	.0160	-.0823
42	-.8938	1.9168	205.000	.9665	-.2084	-.1002	.2313	-.0714	.0937	.0124	-.0812
43	-1.0575	1.8316	210.000	.9665	-.1767	-.1050	.2055	-.0593	.0895	.0237	-.0658

44	-1.2131	1.7325	215.000	.9665	-.1103	-.0802	.1364	-.0462	.0973	.0473	-.0500
45	-1.3595	1.6202	220.000	.9665	-.0452	-.0409	.0610	-.0447	.1105	.0622	-.0483
46	-1.4955	1.4955	225.000	.9665	-.0051	-.0081	.0096	-.0378	.1061	.0658	-.0403
47	-1.6202	1.3595	230.000	.9665	.0146	.0144	-.0205	-.0377	.1056	.0655	-.0402
48	-1.7325	1.2131	235.000	.9665	.0181	.0229	-.0292	-.0394	.1071	.0650	-.0421
49	-1.8316	1.0575	240.000	.9665	.0165	.0255	-.0304	-.0408	.1086	.0649	-.0437
50	-1.9168	.8938	245.000	.9665	.0174	.0343	-.0385	-.0416	.1090	.0644	-.0446
51	-1.9874	.7234	250.000	.9665	.0237	.0620	-.0664	-.0400	.1042	.0614	-.0428
52	-2.0429	.5474	255.000	.9665	.0276	.1001	-.1038	-.0504	.1099	.0550	-.0549
53	-2.0829	.3673	260.000	.9665	.0283	.1574	-.1600	-.0525	.0977	.0402	-.0575
54	-2.1070	.1843	265.000	.9666	.0226	.2548	-.2558	-.0399	.0430	.0003	-.0426
55	-2.1150	-.0000	270.000	.9666	.0000	.3329	-.3329	-.0588	.0202	-.0450	-.0652
56	-2.1070	-.1843	275.000	.9666	-.0330	.3738	-.3753	-.0759	.0120	-.0751	-.0871
57	-2.0829	-.3673	280.000	.9666	-.0696	.3915	-.3976	-.0860	.0085	-.0924	-.1009
58	-2.0429	-.5474	285.000	.9666	-.1064	.3941	-.4082	-.0909	.0069	-.1009	-.1078
59	-1.9874	-.7234	290.000	.9666	-.1414	.3856	-.4107	-.0917	.0061	-.1030	-.1090
60	-1.9168	-.8938	295.000	.9666	-.1730	.3680	-.4067	-.0892	.0057	-.0997	-.1054
61	-1.8316	-1.0575	300.000	.9666	-.1999	.3432	-.3972	-.0836	.0056	-.0921	-.0976
62	-1.7325	-1.2131	305.000	.9666	-.2210	.3127	-.3829	-.0755	.0056	-.0809	-.0866
63	-1.6202	-1.3595	310.000	.9666	-.2357	.2779	-.3643	-.0649	.0058	-.0671	-.0729
64	-1.4955	-1.4955	315.000	.9666	-.2433	.2403	-.3420	-.0523	.0060	-.0513	-.0573
65	-1.3595	-1.6202	320.000	.9666	-.2436	.2015	-.3161	-.0381	.0063	-.0343	-.0406
66	-1.2131	-1.7325	325.000	.9666	-.2367	.1628	-.2873	-.0227	.0067	-.0169	-.0236
67	-1.0575	-1.8316	330.000	.9666	-.2228	.1256	-.2558	-.0068	.0071	.0002	-.0069
68	-.8938	-1.9168	335.000	.9666	-.2023	.0913	-.2219	.0090	.0075	.0164	.0088
69	-.7234	-1.9874	340.000	.9666	-.1759	.0610	-.1862	.0238	.0080	.0309	.0229
70	-.5474	-2.0429	345.000	.9666	-.1445	.0357	-.1489	.0368	.0085	.0434	.0349
71	-.3673	-2.0829	350.000	.9666	-.1092	.0163	-.1104	.0475	.0091	.0534	.0443
72	-.1843	-2.1070	355.000	.9666	-.0712	.0032	-.0712	.0550	.0097	.0605	.0508
73	0.0000	-2.1150	360.000	.9666	-.0315	-.0030	-.0317	.0590	.0104	.0646	.0542

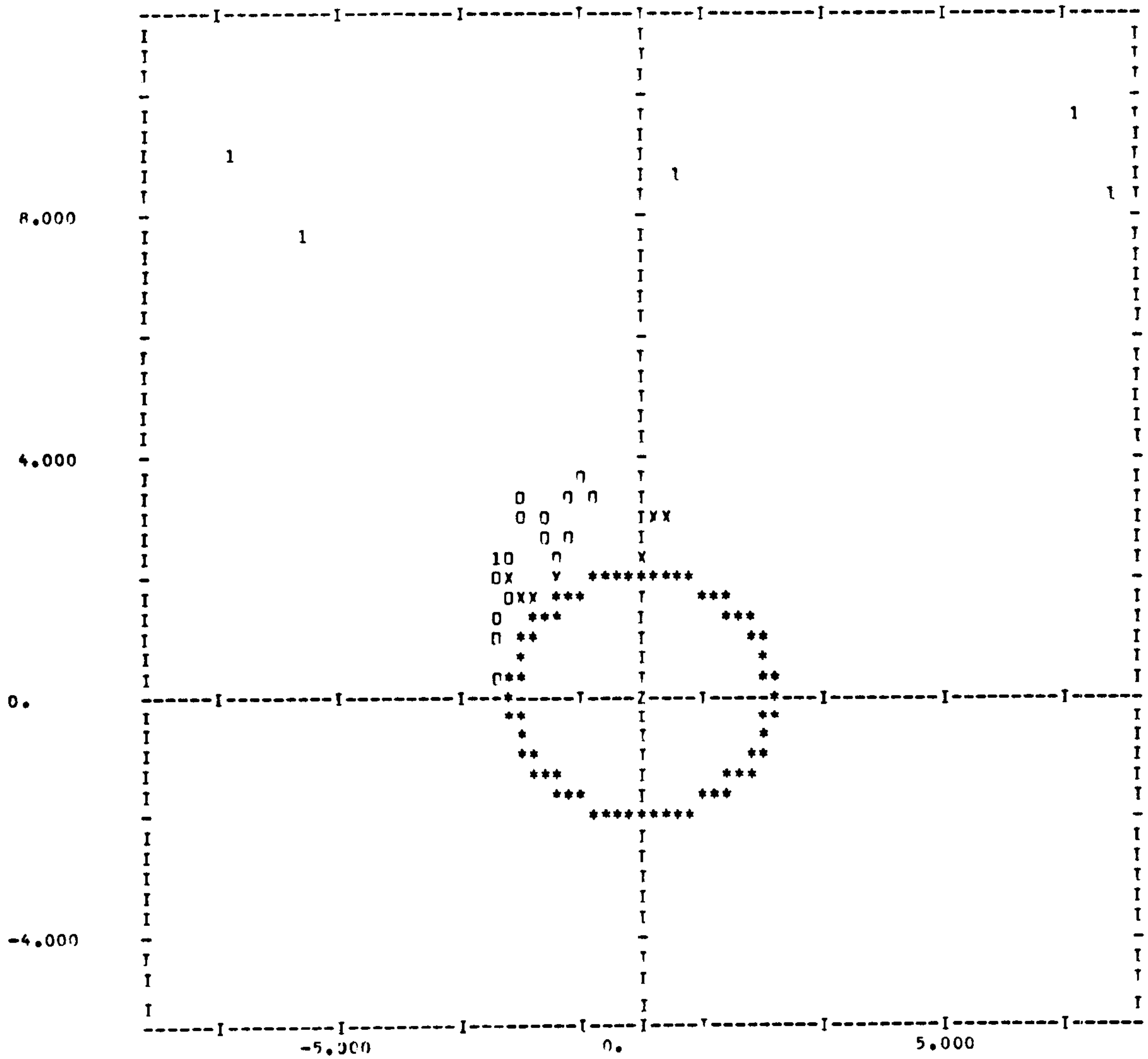

X	R	ALPHA	BETA	M
62.885	2.115	15.000	.000	2.500

X = 62.885

CN(X)	CY(X)	CP(0)	CP(90)	CP(180)
4.215E-02	2.923E-03	5.899E-02	-9.196E-02	-4.106E-02

CN	CM	CY	CR	CSL
1.610E-01	-4.836E-01	-4.551E-01	6.109E-01	-6.310E-17

(SEPARATION POINTS)

Y	Z	BETA
-.885	1.920	204.8
-2.112	-.062	271.7

STRATFORD SEPARATION CRITERION (LAMINAR) F(S) = .02252

SUMMARY OF PRESSURE DISTRIBUTION AND SEPARATION POINTS ON BODY ... X = 62.88

		Y	Z	BETA	ARC	CP	CP*	DCP*/DX
+Y SIDE:	STAGNATION PT.	.184	-2.107	5.000	.065	.059		
	MIN. PRESSURE	2.107	-.184	85.000	2.952	-.092	0.000	0.000
	SEPARATION	-.885	1.920	204.750	7.371	-.071	.019	.030
-Y SIDE:	STAGNATION PT.	-1.496	1.496	225.000	.065	-.038		
	MIN. PRESSURE	-1.987	-.723	290.000	2.768	-.092	0.000	0.000
	SEPARATION	-2.112	-.062	271.673	3.444	-.065	.025	.082

INITIAL POSITIONS AND STRENGTHS OF SHED VORTICITY AT X = 62.885

	NV	GAM/V	M(K)	Y	Z	BETA	VT/V	YC	ZC	RG/R
+Y SIDE:	34	.0583	.0820	-.9297	2.0168	204.7502	.2308	-.9297	2.0168	1.0500
-Y SIDE:	35	-.1316	.1244	-2.2384	-.0654	271.6730	.3468	-2.2384	-.0654	1.0588

SUMMARY OF VORTEX FIELD AT X = 71.345   H = 2.11500

	NV	GAM/V	Y	Z	XSHED	BETA	YC	ZC	RG	RG/R
1	1	.02127	-.60640	2.78484	26.93000	192.284	-.60640	2.78484	2.85010	1.34756
2	2	.00891	-.73481	2.56118	29.04500	196.008	-.73481	2.56118	2.66450	1.25981
3	3	.00226	-1.52299	2.17994	31.16000	214.940	-1.52299	2.17994	2.65926	1.25733
4	4	.00539	-1.92682	3.65644	48.08000	207.788	-1.92682	3.65644	4.13306	1.95417
5	5	.01237	-1.52670	3.27679	50.19500	204.981	-1.52670	3.27679	3.61499	1.70922
6	6	.09896	-1.64146	4.48221	52.31000	200.114	-1.64146	4.48221	4.77332	2.25689
7	7	.03229	-2.32083	1.69860	54.42500	233.800	-2.32083	1.69860	2.87602	1.35982
8	8	.09281	-2.82769	3.97391	56.54000	215.434	-2.82769	3.97391	4.87728	2.30604
9	9	.04762	-2.56965	3.76176	58.65500	214.337	-2.56965	3.76176	4.55565	2.15397
10	10	.06218	-2.20044	1.76136	60.77000	231.324	-2.20044	1.76136	2.81856	1.33265
11	11	.05834	-1.75140	1.79586	62.88500	224.282	-1.75140	1.79586	2.50849	1.18605
12	12	.04154	-1.63326	1.92579	65.00000	220.301	-1.63326	1.92579	2.52512	1.19391
13	13	.04002	-1.34085	1.97883	67.11500	214.121	-1.34065	1.97883	2.39033	1.13018
1	14	.02130	6.52328	9.11073	0.00000	144.397	6.52328	9.11073	11.20529	5.29801
2	15	-.00588	-6.83423	9.31935	0.00000	216.254	-6.83423	9.31935	11.55668	5.46415
3	16	3.37980	7.76467	10.09983	0.00000	142.447	7.76467	10.09983	12.73957	6.02344
4	17	-2.22590	-6.65663	11.19299	0.00000	210.741	-6.65663	11.19299	13.02282	6.15736
5	18	-.09334	.78464	9.63909	0.00000	175.346	.78464	9.63909	9.67097	4.57256
6	19	-.16236	-1.72297	4.13574	0.00000	202.617	-1.72297	4.13574	4.48028	2.11834
1	20	-.12345	-1.69545	3.03134	26.93000	209.219	-1.69545	3.03134	3.47326	1.64220
2	21	-.11374	-1.46613	3.55345	29.04500	202.421	-1.46613	3.55345	3.84403	1.81751
3	22	-.10674	-2.58311	4.29233	31.16000	211.039	-2.58311	4.29233	5.00965	2.36863
4	23	-.10560	-1.55714	3.18024	33.27500	206.088	-1.55714	3.18024	3.54099	1.67423
5	24	-.10994	-1.84735	3.53146	35.39000	207.615	-1.84735	3.53145	3.98546	1.88438
6	25	-.10794	-.92621	3.59682	37.50500	194.440	-.92621	3.59682	3.71416	1.75610
7	26	-.11986	-1.59292	4.38347	39.62000	199.971	-1.59292	4.38347	4.66392	2.20517
8	27	-.12293	-2.31802	4.23834	41.73500	208.675	-2.31802	4.23834	4.83081	2.28407
9	28	-.13256	-2.11207	4.51071	43.85000	205.091	-2.11207	4.51071	4.98070	2.35494
10	29	-.13576	-1.76072	3.75001	45.96500	205.151	-1.76072	3.75001	4.14279	1.95876
11	30	-.16777	-1.83691	4.74012	48.08000	201.183	-1.83691	4.74012	5.08359	2.40359
12	31	-.15944	-1.18756	3.25017	50.19500	200.071	-1.18756	3.25017	3.46033	1.63609
13	32	-.10112	-1.61171	4.11858	52.31000	201.372	-1.61171	4.11858	4.42271	2.09111
14	33	-.02216	-2.49272	1.94466	54.42500	232.041	-2.49272	1.94466	3.16154	1.49482
15	34	-.14577	-2.43956	2.12410	56.54000	228.954	-2.43956	2.12410	3.23470	1.52941
16	35	-.14717	-2.35834	2.69661	58.65500	221.172	-2.35834	2.69661	3.58238	1.69380
17	36	-.14067	-2.58588	2.28721	60.77000	228.507	-2.58588	2.28721	3.45226	1.63227
18	37	-.13164	-2.57385	1.67732	62.88500	236.909	-2.57385	1.67732	3.07215	1.45255
19	38	-.12939	-2.41858	1.20849	65.00000	243.450	-2.41858	1.20849	2.70369	1.27834
20	39	-.12775	-2.37428	.80507	67.11500	251.269	-2.37428	.80507	2.50706	1.18537
21	40	-.12478	-2.30872	.35890	69.23000	261.164	-2.30872	.35890	2.33645	1.10470

CENTROID OF SHED VORTICITY

	GAM/V	Y	Z
+Y BODY*	.52395	-1.97506	2.99080
-Y BODY*	-2.57616	-1.99502	3.03876

ORIGINAL PAGE IS
OF POOR QUALITY

BODY SURFACE PRESSURE DISTRIBUTION

X	R	DR/DX	M
71.3450	2.1150	0.0000	2.5000

J	Y	Z	BETA	U/VO	V/VO	W/VO	VT/VO	CP(M)	DPHI/DT	CPZ	CP(I)
1	0.0000	-2.1150	0.000	.9665	-.0119	-.0030	-.0122	.0643	.0071	.0658	.0587
2	.1843	-2.1070	5.000	.9665	.0287	-.0005	.0287	.0624	.0080	.0651	.0571
3	.3673	-2.0829	10.000	.9665	.0681	.0070	.0686	.0567	.0089	.0612	.0523
4	.5474	-2.0429	15.000	.9665	.1051	.0252	.1081	.0475	.0099	.0543	.0444
5	.7234	-1.9874	20.000	.9665	.1386	.0475	.1465	.0354	.0109	.0445	.0336
6	.8938	-1.9168	25.000	.9665	.1675	.0751	.1836	.0209	.0120	.0323	.0203
7	1.0575	-1.8316	30.000	.9665	.1909	.1072	.2190	.0050	.0131	.0180	.0049
8	1.2131	-1.7325	35.000	.9664	.2081	.1428	.2524	-.0117	.0142	.0023	-.0120
9	1.3595	-1.6202	40.000	.9664	.2186	.1805	.2835	-.0285	.0155	-.0144	-.0299
10	1.4955	-1.4955	45.000	.9664	.2222	.2192	.3121	-.0446	.0167	-.0314	-.0481
11	1.6202	-1.3595	50.000	.9664	.2186	.2576	.3379	-.0596	.0181	-.0481	-.0662
12	1.7325	-1.2131	55.000	.9664	.2082	.2944	.3606	-.0732	.0195	-.0640	-.0835
13	1.8316	-1.0575	60.000	.9664	.1914	.3285	.3802	-.0850	.0209	-.0785	-.0995
14	1.9168	-.8938	65.000	.9664	.1687	.3588	.3964	-.0949	.0225	-.0911	-.1136
15	1.9874	-.7234	70.000	.9664	.1409	.3842	.4093	-.1029	.0242	-.1015	-.1256
16	2.0429	-.5474	75.000	.9664	.1091	.4041	.4186	-.1089	.0259	-.1092	-.1351
17	2.0829	-.3673	80.000	.9664	.0742	.4179	.4245	-.1131	.0277	-.1141	-.1418
18	2.1070	-.1843	85.000	.9664	.0375	.4252	.4268	-.1155	.0297	-.1161	-.1458
19	2.1150	0.0000	90.000	.9664	.0000	.4259	.4259	-.1163	.0317	-.1153	-.1470
20	2.1070	.1843	95.000	.9664	-.0370	.4201	.4217	-.1154	.0338	-.1117	-.1456
21	2.0829	.3673	100.000	.9664	-.0725	.4081	.4145	-.1131	.0361	-.1057	-.1418
22	2.0429	.5474	105.000	.9664	-.1054	.3906	.4045	-.1095	.0384	-.0975	-.1360
23	1.9874	.7234	110.000	.9664	-.1351	.3681	.3921	-.1047	.0409	-.0876	-.1285
24	1.9168	.8938	115.000	.9664	-.1607	.3416	.3775	-.0990	.0435	-.0764	-.1198
25	1.8316	1.0575	120.000	.9664	-.1819	.3121	.3612	-.0927	.0461	-.0643	-.1104
26	1.7325	1.2131	125.000	.9664	-.1985	.2804	.3436	-.0858	.0488	-.0519	-.1007
27	1.6202	1.3595	130.000	.9664	-.2104	.2478	.3250	-.0789	.0517	-.0395	-.0911
28	1.4955	1.4955	135.000	.9663	-.2180	.2150	.3061	-.0721	.0546	-.0275	-.0821
29	1.3595	1.6202	140.000	.9663	-.2216	.1829	.2873	-.0657	.0575	-.0164	-.0739
30	1.2131	1.7325	145.000	.9663	-.2219	.1524	.2691	-.0601	.0605	-.0062	-.0667
31	1.0575	1.8316	150.000	.9663	-.2196	.1238	.2521	-.0553	.0635	.0026	-.0609
32	.8938	1.9168	155.000	.9663	-.2157	.0976	.2368	-.0516	.0666	.0101	-.0564
33	.7234	1.9874	160.000	.9663	-.2111	.0739	.2236	-.0491	.0696	.0162	-.0534
34	.5474	2.0429	165.000	.9663	-.2066	.0524	.2132	-.0477	.0725	.0208	-.0517
35	.3673	2.0829	170.000	.9663	-.2030	.0328	.2056	-.0474	.0753	.0239	-.0514
36	.1843	2.1070	175.000	.9663	-.2005	.0146	.2010	-.0480	.0779	.0258	-.0521
37	-.0000	2.1150	180.000	.9663	-.1988	-.0030	.1989	-.0493	.0803	.0267	-.0536
38	-.1843	2.1070	185.000	.9663	-.1968	-.0202	.1979	-.0506	.0922	.0271	-.0551
39	-.3673	2.0829	190.000	.9663	-.1929	-.0370	.1964	-.0511	.0834	.0276	-.0558
40	-.5474	2.0429	195.000	.9663	-.1850	-.0526	.1923	-.0498	.0834	.0292	-.0542
41	-.7234	1.9874	200.000	.9663	-.1694	-.0646	.1813	-.0454	.0824	.0333	-.0491
42	-.8938	1.9168	205.000	.9663	-.1396	-.0681	.1553	-.0373	.0817	.0421	-.0397
43	-1.0575	1.8316	210.000	.9663	-.0926	-.0565	.1085	-.0285	.0843	.0544	-.0299

44	-1.2131	1.7325	215.000	.9663	-.0416	-.0321	.0526	-.0262	.0908	.0634	-.0273
45	-1.3595	1.6202	220.000	.9663	-.0041	-.0064	.0076	-.0255	.0927	.0661	-.0266
46	-1.4955	1.4955	225.000	.9663	.0151	.0121	-.0193	-.0251	.0920	.0658	-.0262
47	-1.6202	1.3595	230.000	.9664	.0184	.0189	-.0263	-.0225	.0888	.0655	-.0233
48	-1.7325	1.2131	235.000	.9664	.0171	.0214	-.0274	-.0196	.0856	.0654	-.0202
49	-1.8316	1.0575	240.000	.9664	.0154	.0237	-.0283	-.0180	.0839	.0653	-.0185
50	-1.9168	.8938	245.000	.9664	.0147	.0285	-.0321	-.0177	.0834	.0651	-.0183
51	-1.9874	.7234	250.000	.9664	.0168	.0433	-.0464	-.0173	.0818	.0640	-.0178
52	-2.0429	.5474	255.000	.9664	.0212	.0762	-.0791	-.0196	.0801	.0599	-.0202
53	-2.0829	.3673	260.000	.9664	.0218	.1209	-.1229	-.0347	.0878	.0510	-.0368
54	-2.1070	.1843	265.000	.9664	.0180	.2022	-.2030	-.0183	.0437	.0249	-.0188
55	-2.1150	-.0000	270.000	.9664	.0000	.2900	-.2900	-.0290	.0124	-.0180	-.0304
56	-2.1070	-.1843	275.000	.9664	-.0302	.3418	-.3432	-.0497	.0025	-.0517	-.0542
57	-2.0829	-.3673	280.000	.9664	-.0650	.3654	-.3711	-.0633	-.0010	-.0717	-.0707
58	-2.0429	-.5474	285.000	.9664	-.1004	.3717	-.3850	-.0705	-.0022	-.0822	-.0800
59	-1.9874	-.7234	290.000	.9664	-.1342	.3657	-.3895	-.0730	-.0024	-.0857	-.0833
60	-1.9168	-.8938	295.000	.9664	-.1647	.3501	-.3869	-.0716	-.0023	-.0837	-.0814
61	-1.8316	-1.0575	300.000	.9664	-.1905	.3270	-.3784	-.0669	-.0019	-.0772	-.0753
62	-1.7325	-1.2131	305.000	.9664	-.2107	.2979	-.3648	-.0593	-.0013	-.0671	-.0658
63	-1.6202	-1.3595	310.000	.9664	-.2244	.2644	-.3468	-.0492	-.0007	-.0542	-.0535
64	-1.4955	-1.4955	315.000	.9664	-.2311	.2281	-.3247	-.0370	-.0001	-.0394	-.0394
65	-1.3595	-1.6202	320.000	.9664	-.2305	.1904	-.2990	-.0232	.0006	-.0234	-.0241
66	-1.2131	-1.7325	325.000	.9664	-.2227	.1529	-.2702	-.0083	.0014	-.0070	-.0084
67	-1.0575	-1.8316	330.000	.9665	-.2079	.1170	-.2385	.0070	.0021	.0091	.0069
68	-.8938	-1.9168	335.000	.9665	-.1865	.0840	-.2045	.0220	.0029	.0241	.0212
69	-.7234	-1.9874	340.000	.9665	-.1593	.0550	-.1685	.0357	.0037	.0376	.0339
70	-.5474	-2.0429	345.000	.9665	-.1271	.0311	-.1308	.0475	.0045	.0488	.0443
71	-.3673	-2.0829	350.000	.9665	-.0910	.0131	-.0919	.0566	.0053	.0575	.0522
72	-.1843	-2.1070	355.000	.9665	-.0522	.0016	-.0522	.0623	.0062	.0632	.0570
73	0.0000	-2.1150	360.000	.9665	-.0119	-.0030	-.0122	.0643	.0071	.0658	.0587

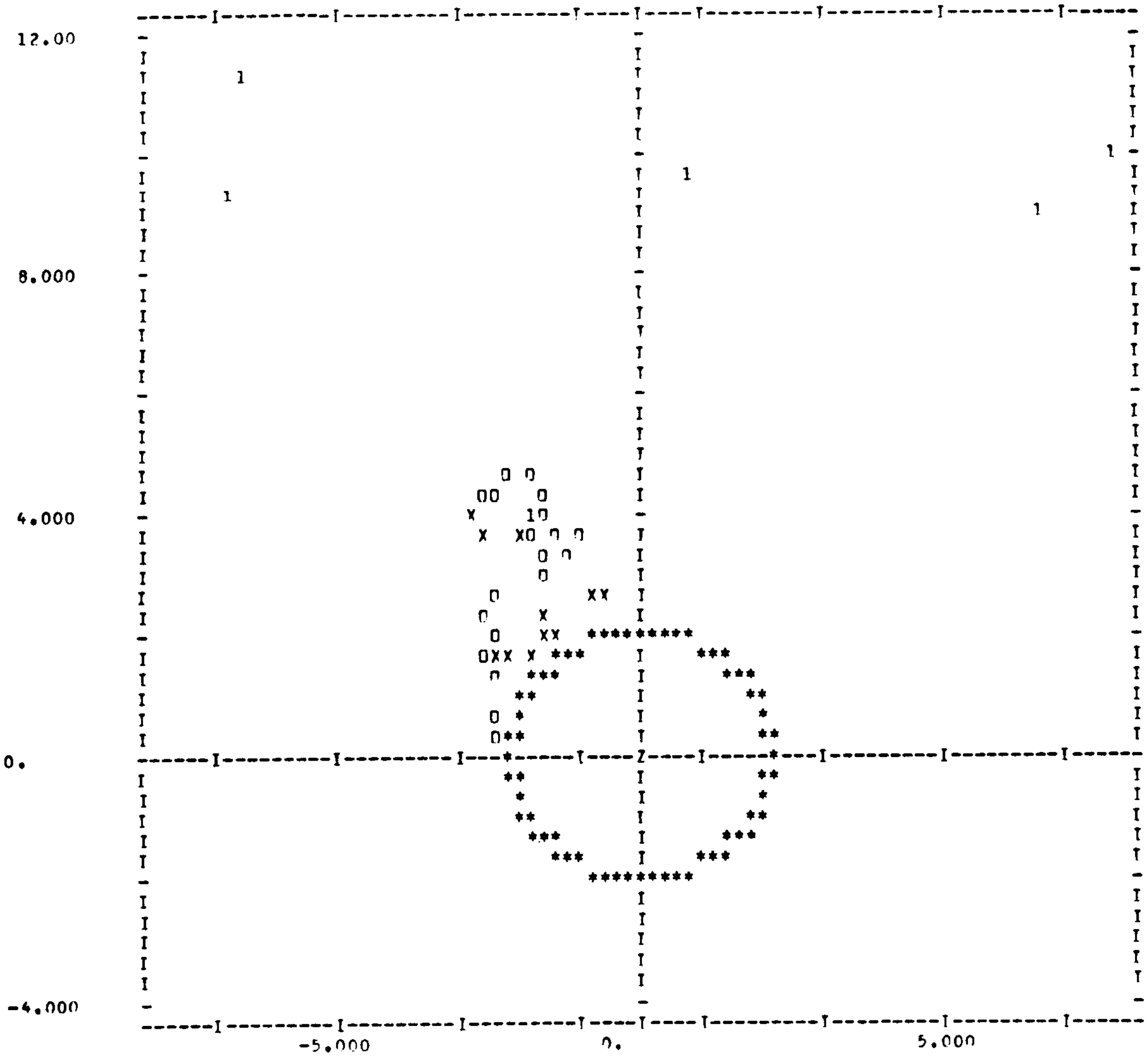

X	R	ALPHA	BETA	M
71.345	2.115	15.000	.000	2.500

X = 71.345

CN(X)	CY(X)	CP(0)	CP(90)	CP(180)
4.720E-02	4.411E-02	6.431E-02	-1.163E-01	-4.928E-02
CN	CM	CY	CR	CSL
2.725E-01	-1.070E+00	-3.866E-01	9.867E-01	-4.619E-17

(SEPARATION POINTS)

Y	Z	BETA
-.595	2.028	196.4
-2.109	-.132	273.6

STRATFORD SEPARATION CRITERION (LAMINAR) F(S) = .02252

SUMMARY OF PRESSURE DISTRIBUTION AND SEPARATION POINTS ON BODY ... X = 71.34

+Y SIDE:	Y	Z	BETA	ARC	CP	CP*	DCP*/DX
STAGNATION PT.	0.000	-2.115	0.000	.066	.064		
MIN. PRESSURE	2.115	0.000	90.000	3.321	-.116	0.000	0.000
SEPARATION	-.595	2.028	196.358	7.246	-.049	.061	.018

-Y SIDE:	Y	Z	BETA	ARC	CP	CP*	DCP*/DX
STAGNATION PT.	-1.359	1.620	220.000	.066	-.026		
MIN. PRESSURE	-1.987	-.723	290.000	2.583	-.073	0.000	0.000
SEPARATION	-2.109	-.132	273.571	3.189	-.044	.027	.085

INITIAL POSITIONS AND STRENGTHS OF SHED VORTICITY AT X = 71.345

	NV	GAM/V	M(K)	Y	Z	BETA	VT/V	YC	ZC	RG/R
+Y SIDE:	41	.0392	.0670	-.6254	2.1309	196.3577	.1892	-.6254	2.1309	1.0500
-Y SIDE:	42	-.1176	.1174	-2.2280	-.1390	273.5706	.3277	-2.2280	-.1390	1.0555

ORIGINAL PAGE IS
OF POOR QUALITY

SUMMARY OF VORTEX FIELD AT X = 79.805   H = 2.11500

	NV	GAM/V	Y	Z	YSHED	BETA	YC	ZC	RG	RG/P
1	1	.02127	-2.28223	3.00595	26.93000	217.207	-2.28223	3.00595	3.77416	1.76447
2	2	.00891	-2.14644	2.80768	29.04500	217.397	-2.14644	2.80768	3.53415	1.67099
3	3	.00226	-2.91968	3.04716	31.16000	223.776	-2.91968	3.04716	4.22016	1.99535
4	4	.00539	-1.26996	5.00404	48.08000	194.240	-1.26996	5.00404	5.16267	2.44098
5	5	.01237	-2.23791	4.51013	50.19500	206.390	-2.23791	4.51013	5.03483	2.38053
6	6	.09896	-2.30788	3.89505	52.31000	210.647	-2.30788	3.89505	4.52744	2.14064
7	7	.03229	-2.72285	2.73514	54.42500	224.871	-2.72285	2.73514	3.85939	1.82477
8	8	.09281	-2.18110	6.51199	56.54000	198.518	-2.18110	6.51199	6.86755	3.24707
9	9	.04762	-1.97444	6.78719	58.65500	196.220	-1.97444	6.78719	7.06855	3.34210
10	10	.06218	-2.61385	2.74374	60.77000	223.611	-2.61385	2.74374	3.78950	1.79173
11	11	.05834	-1.88502	1.81367	62.88500	226.105	-1.88502	1.81367	2.61586	1.23681
12	12	.04154	-2.01781	1.96260	65.00000	225.795	-2.01781	1.96260	2.81485	1.33090
13	13	.04002	-2.08762	2.39162	67.11500	221.117	-2.08762	2.39162	3.17458	1.50099
14	14	.03919	-1.37723	1.93342	71.34500	215.463	-1.37723	1.93342	2.37379	1.12236
15	15	.03660	-1.27047	2.07840	73.46000	211.436	-1.27047	2.07840	2.43595	1.15175
16	16	.04529	-.76379	2.15040	75.57500	199.554	-.76379	2.15040	2.28202	1.07897
17	17	.05570	-.17923	2.23544	77.69000	184.584	-.17923	2.23544	2.24262	1.06034
1	18	.02130	9.02307	11.04027	0.00000	140.741	9.02307	11.04027	14.25845	6.74159
2	19	-.00588	-8.00517	12.24965	0.00000	213.165	-8.00517	12.24965	14.63341	6.91887
3	20	3.37980	7.74475	11.98644	0.00000	147.132	7.74475	11.98644	14.27081	6.74743
4	21	-2.22590	-6.46846	13.21080	0.00000	206.088	-6.46846	13.21080	14.70939	6.95479
5	22	-.09334	.99179	10.59940	0.00000	174.654	.99179	10.59940	10.64570	5.03343
6	23	-.16236	-2.20691	4.11103	0.00000	208.228	-2.20691	4.11103	4.66595	2.20612
1	24	-.12345	-1.90863	4.47787	26.93000	203.085	-1.90863	4.47787	4.86767	2.30150
2	25	-.11374	-2.54129	4.38456	29.04500	210.097	-2.54129	4.38456	5.06779	2.39612
3	26	-.10674	-1.41170	6.54601	31.16000	192.170	-1.41170	6.54601	6.69650	3.16620
4	27	-.10560	-2.05504	4.62947	33.27500	203.937	-2.05504	4.62947	5.06510	2.39484
5	28	-.10994	-1.02226	5.24090	35.39000	191.037	-1.02226	5.24090	5.33966	2.52466
6	29	-.10794	-2.53378	3.61129	37.50500	215.055	-2.53378	3.61129	4.41152	2.08582
7	30	-.11986	-2.40243	4.15536	39.62000	210.034	-2.40243	4.15536	4.79986	2.26944
8	31	-.12293	-1.57198	6.57306	41.73500	193.450	-1.57198	6.57306	6.75842	3.19547
9	32	-.13256	-.79863	5.21618	43.85000	188.705	-.79863	5.21618	5.27697	2.49502
10	33	-.13576	-1.23340	5.16975	45.96500	193.419	-1.23340	5.16975	5.31485	2.51293
11	34	-.16777	-1.31382	4.60854	48.08000	195.912	-1.31382	4.60854	4.79215	2.26579
12	35	-.15944	-2.51267	4.61455	50.19500	208.569	-2.51267	4.61455	5.25429	2.48430
13	36	-.10112	-1.73285	4.37214	52.31000	201.620	-1.73285	4.37214	4.70302	2.22365
14	37	-.02216	-3.18388	4.28738	54.42500	216.598	-3.18388	4.28738	5.34029	2.52496
15	38	-.14577	-3.27858	4.25360	56.54000	217.624	-3.27858	4.25360	5.37049	2.53924
16	39	-.14717	-1.89225	4.90645	58.65500	201.090	-1.89225	4.90645	5.25869	2.48638
17	40	-.14067	-2.41322	5.07488	60.77000	205.432	-2.41322	5.07488	5.61943	2.65694
18	41	-.13164	-3.50383	4.38461	62.88500	218.629	-3.50383	4.38461	5.61263	2.65373
19	42	-.12939	-2.22766	1.75989	65.00000	231.691	-2.22766	1.75989	2.83895	1.34230
20	43	-.12775	-2.22491	2.10256	67.11500	226.619	-2.22491	2.10256	3.06121	1.44738
21	44	-.12478	-2.50860	2.01943	69.23000	231.166	-2.50860	2.01943	3.22043	1.52266
22	45	-.11758	-2.53070	1.51467	71.34500	239.099	-2.53070	1.51467	2.94935	1.39449
23	46	-.09861	-2.53394	1.18094	73.46000	245.012	-2.53394	1.18094	2.79562	1.32180
24	47	-.10995	-2.33359	.71352	75.57500	252.998	-2.33359	.71352	2.44024	1.15378
25	48	-.08637	-2.31361	.42201	77.69000	259.663	-2.31361	.42201	2.35179	1.11196

CENTROID OF SHED VORTICITY

	GAM/V	Y	Z
+Y BODY%	.70073	-1.86441	3.43545
-Y BODY%	-2.98866	-2.12334	3.92863

BODY SURFACE PRESSURE DISTRIBUTION

X	R	DR/DX	M
79.8050	2.1150	0.0000	2.5000

J	Y	Z	BETA	U/VO	V/VO	W/VO	VT/VO	CP(M)	DPHI/DT	CPZ	CP(I)
1	0.0000	-2.1150	0.000	.9663	.0108	-.0030	.0112	.0656	.0063	.0661	.0598
2	.1843	-2.1070	5.000	.9663	.0517	.0015	.0518	.0615	.0071	.0635	.0564
3	.3673	-2.0829	10.000	.9663	.0915	.0132	.0924	.0535	.0081	.0576	.0496
4	.5474	-2.0429	15.000	.9663	.1288	.0315	.1326	.0421	.0090	.0486	.0396
5	.7234	-1.9874	20.000	.9663	.1624	.0561	.1718	.0278	.0100	.0367	.0267
6	.8938	-1.9168	25.000	.9663	.1912	.0862	.2097	.0114	.0110	.0222	.0112
7	1.0575	-1.8316	30.000	.9663	.2144	.1208	.2461	-.0063	.0120	.0056	-.0064
8	1.2131	-1.7325	35.000	.9663	.2313	.1590	.2806	-.0247	.0131	-.0126	-.0257
9	1.3595	-1.6202	40.000	.9663	.2412	.1994	.3129	-.0428	.0142	-.0317	-.0460
10	1.4955	-1.4955	45.000	.9663	.2439	.2409	.3428	-.0601	.0154	-.0513	-.0667
11	1.6202	-1.3595	50.000	.9663	.2393	.2822	.3700	-.0761	.0167	-.0707	-.0873
12	1.7325	-1.2131	55.000	.9663	.2276	.3220	.3943	-.0904	.0180	-.0892	-.1072
13	1.8316	-1.0575	60.000	.9663	.2091	.3591	.4155	-.1020	.0193	-.1064	-.1257
14	1.9168	-.8938	65.000	.9663	.1844	.3924	.4335	-.1135	.0207	-.1217	-.1424
15	1.9874	-.7234	70.000	.9663	.1543	.4209	.4482	-.1221	.0222	-.1347	-.1569
16	2.0429	-.5474	75.000	.9663	.1197	.4437	.4596	-.1288	.0238	-.1449	-.1687
17	2.0829	-.3673	80.000	.9663	.0817	.4603	.4675	-.1337	.0254	-.1523	-.1777
18	2.1070	-.1843	85.000	.9663	.0414	.4703	.4721	-.1369	.0271	-.1566	-.1837
19	2.1150	0.0000	90.000	.9663	.0000	.4733	.4733	-.1384	.0289	-.1578	-.1867
20	2.1070	.1843	95.000	.9663	-.0413	.4696	.4714	-.1384	.0308	-.1559	-.1868
21	2.0829	.3673	100.000	.9663	-.0815	.4593	.4665	-.1371	.0328	-.1513	-.1841
22	2.0429	.5474	105.000	.9663	-.1195	.4429	.4588	-.1344	.0348	-.1442	-.1790
23	1.9874	.7234	110.000	.9663	-.1544	.4211	.4485	-.1305	.0369	-.1348	-.1718
24	1.9168	.8938	115.000	.9663	-.1854	.3946	.4360	-.1256	.0391	-.1238	-.1629
25	1.8316	1.0575	120.000	.9663	-.2121	.3644	.4216	-.1197	.0414	-.1114	-.1528
26	1.7325	1.2131	125.000	.9663	-.2340	.3313	.4056	-.1132	.0437	-.0982	-.1419
27	1.6202	1.3595	130.000	.9662	-.2512	.2963	.3885	-.1061	.0461	-.0845	-.1307
28	1.4955	1.4955	135.000	.9662	-.2635	.2605	.3705	-.0988	.0485	-.0709	-.1195
29	1.3595	1.6202	140.000	.9662	-.2713	.2246	.3522	-.0914	.0510	-.0577	-.1086
30	1.2131	1.7325	145.000	.9662	-.2748	.1894	.3338	-.0842	.0534	-.0450	-.0984
31	1.0575	1.8316	150.000	.9662	-.2746	.1556	.3156	-.0773	.0558	-.0332	-.0890
32	.8938	1.9168	155.000	.9662	-.2710	.1234	.2978	-.0709	.0582	-.0223	-.0805
33	.7234	1.9874	160.000	.9662	-.2644	.0933	.2804	-.0649	.0605	-.0122	-.0728
34	.5474	2.0429	165.000	.9662	-.2548	.0653	.2630	-.0592	.0629	-.0028	-.0656
35	.3673	2.0829	170.000	.9662	-.2417	.0396	.2444	-.0535	.0654	.0067	-.0587
36	.1843	2.1070	175.000	.9662	-.2206	.0163	.2212	-.0475	.0690	.0175	-.0515
37	-.0000	2.1150	180.000	.9662	-.1888	-.0030	.1889	-.0453	.0797	.0307	-.0490
38	-.1843	2.1070	185.000	.9662	-.1587	-.0169	.1596	-.0616	.1097	.0409	-.0687
39	-.3673	2.0829	190.000	.9662	-.1423	-.0281	.1451	-.0352	.0827	.0454	-.0373
40	-.5474	2.0429	195.000	.9662	-.1162	-.0341	.1211	-.0265	.0794	.0517	-.0277
41	-.7234	1.9874	200.000	.9662	-.0820	-.0328	.0883	-.0288	.0888	.0586	-.0302
42	-.8938	1.9168	205.000	.9662	-.0544	-.0284	.0614	-.0178	.0809	.0626	-.0183
43	-1.0575	1.8316	210.000	.9662	-.0220	-.0157	.0270	-.0143	.0803	.0657	-.0146

44	-1.2131	1.7325	215.000	.9662	.0014	-.0020	.0024	-.0162	.0830	.0664	-.0166
45	-1.3595	1.6202	220.000	.9662	.0035	-.0000	-.0035	-.0157	.0824	.0664	-.0161
46	-1.4955	1.4955	225.000	.9662	-.0001	-.0031	.0031	-.0143	.0810	.0664	-.0146
47	-1.6202	1.3595	230.000	.9662	-.0030	-.0066	.0072	-.0123	.0788	.0663	-.0125
48	-1.7325	1.2131	235.000	.9663	-.0008	-.0042	.0042	-.0095	.0760	.0663	-.0097
49	-1.8316	1.0575	240.000	.9663	.0070	.0091	-.0114	-.0072	.0735	.0662	-.0073
50	-1.9168	.8938	245.000	.9663	.0130	.0250	-.0282	-.0076	.0732	.0655	-.0077
51	-1.9874	.7234	250.000	.9663	.0137	.0347	-.0373	-.0122	.0774	.0649	-.0125
52	-2.0429	.5474	255.000	.9663	.0166	.0591	-.0614	-.0143	.0772	.0626	-.0147
53	-2.0829	.3673	260.000	.9663	.0223	.1236	-.1256	-.0100	.0607	.0505	-.0102
54	-2.1070	.1843	265.000	.9663	.0191	.2151	-.2159	-.0036	.0233	.0197	-.0037
55	-2.1150	-.0000	270.000	.9663	.0000	.2884	-.2884	-.0227	.0066	-.0169	-.0235
56	-2.1070	-.1843	275.000	.9663	-.0291	.3294	-.3307	-.0410	.0009	-.0431	-.0439
57	-2.0829	-.3673	280.000	.9663	-.0620	.3487	-.3541	-.0527	-.0014	-.0591	-.0578
58	-2.0429	-.5474	285.000	.9663	-.0955	.3534	-.3661	-.0591	-.0022	-.0678	-.0655
59	-1.9874	-.7234	290.000	.9663	-.1274	.3471	-.3698	-.0611	-.0025	-.0705	-.0680
60	-1.9168	-.8938	295.000	.9663	-.1561	.3319	-.3668	-.0594	-.0024	-.0683	-.0659
61	-1.8316	-1.0575	300.000	.9663	-.1803	.3094	-.3581	-.0545	-.0020	-.0620	-.0600
62	-1.7325	-1.2131	305.000	.9663	-.1990	.2812	-.3444	-.0469	-.0016	-.0524	-.0508
63	-1.6202	-1.3595	310.000	.9663	-.2112	.2487	-.3263	-.0368	-.0011	-.0403	-.0392
64	-1.4955	-1.4955	315.000	.9663	-.2166	.2136	-.3042	-.0248	-.0005	-.0263	-.0258
65	-1.3595	-1.6202	320.000	.9663	-.2148	.1772	-.2785	-.0113	.0002	-.0113	-.0115
66	-1.2131	-1.7325	325.000	.9663	-.2058	.1411	-.2495	.0031	.0008	.0039	.0031
67	-1.0575	-1.8316	330.000	.9663	-.1899	.1067	-.2178	.0177	.0015	.0188	.0172
68	-.8938	-1.9168	335.000	.9663	-.1675	.0751	-.1836	.0317	.0023	.0325	.0302
69	-.7234	-1.9874	340.000	.9663	-.1394	.0478	-.1474	.0442	.0030	.0445	.0415
70	-.5474	-2.0429	345.000	.9663	-.1064	.0255	-.1094	.0545	.0038	.0542	.0504
71	-.3673	-2.0829	350.000	.9663	-.0696	.0093	-.0702	.0619	.0046	.0612	.0567
72	-.1843	-2.1070	355.000	.9663	-.0301	-.0003	-.0301	.0657	.0054	.0653	.0599
73	0.0000	-2.1150	360.000	.9663	.0108	-.0030	.0112	.0656	.0063	.0661	.0598

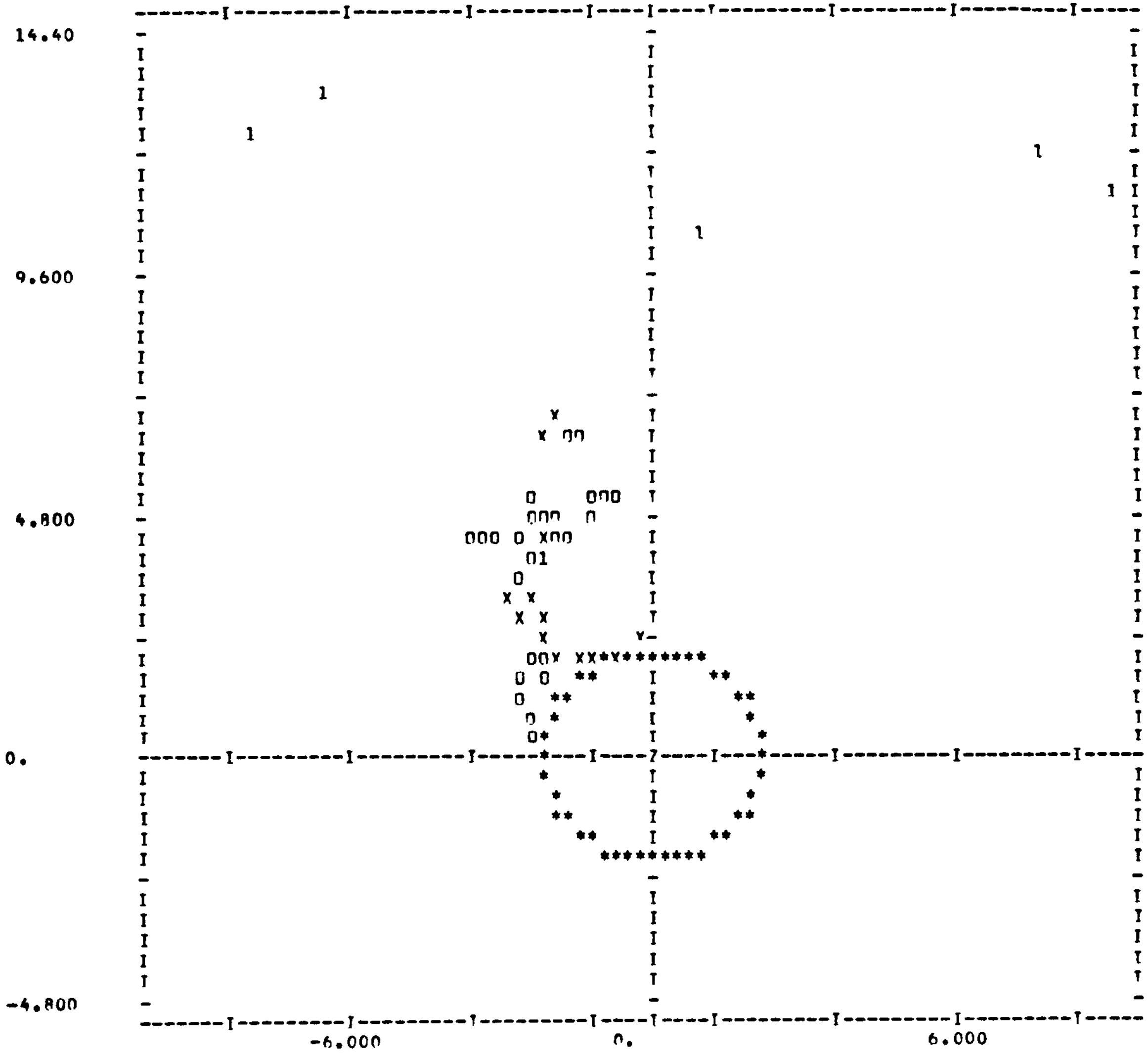

X	R	ALPHA	BETA	M
79.805	2.115	15.000	.000	2.500

X = 79.805

CN(X)	CY(X)	CP(0)	CP(90)	CP(180)
4.977E-02	7.567E-02	6.558E-02	-1.384E-01	-4.534E-02

CN	CM	CY	CR	CSL
3.956E-01	-1.961E+00	-2.226E-01	2.185E+00	-7.741E-17

(SEPARATION POINTS)

Y	Z	BETA
1.052	1.835	150.2
-2.110	-.115	273.1

STRATFORD SEPARATION CRITERION (LAMINAR) F(S) = .02252

SUMMARY OF PRESSURE DISTRIBUTION AND SEPARATION POINTS ON BODY ... X = 79.80

+Y SIDE*	Y	Z	BETA	ARC	CP	CP*	DCP*/DX
STAGNATION PT.	0.000	-2.115	360.000	.066	.066		
MIN. PRESSURE	2.107	.184	95.000	3.506	-.138	0.000	0.000
SEPARATION	1.052	1.635	150.177	5.542	-.077	.054	.032

-Y SIDE*	Y	Z	BETA	ARC	CP	CP*	DCP*/DX
STAGNATION PT.	-1.496	1.496	225.000	.066	-.014		
MIN. PRESSURE	-1.987	-.723	290.000	2.583	-.061	0.000	0.000
SEPARATION	-2.110	-.115	273.110	3.206	-.034	.025	.084

INITIAL POSITIONS AND STRENGTHS OF SHED VORTICITY AT X = 79.805

	NV	GAM/V	M(K)	Y	Z	BETA	VT/V	YC	ZC	RG/R
+Y SIDE*	49	.1086	.1127	1.1079	1.9326	150.1767	.3149	1.1079	1.9326	1.0533
-Y SIDE*	50	-.1082	.1125	-2.2242	-.1209	273.1101	.3144	-2.2242	-.1209	1.0532

SUMMARY OF VORTEX FIELD AT X = 80.730 H = .92500

	NV	GAM/V	Y	Z	YSHED	BETA	YC	ZC	RC	RG/R
1	1	.02127	-2.43271	3.16549	26.93000	217.543	-2.43271	3.16549	3.99229	1.88761
2	2	.00891	-2.24056	2.94373	29.04500	217.276	-2.24056	2.94373	3.69941	1.74913
3	3	.00226	-3.05995	3.26092	31.16000	223.179	-3.05995	3.26092	4.47179	2.11432
4	4	.00539	-1.27347	5.06187	48.08000	194.121	-1.27347	5.06187	5.21960	2.46790
5	5	.01237	-2.26829	4.70342	50.19500	205.746	-2.26829	4.70342	5.22181	2.46894
6	6	.09896	-2.57866	4.10138	52.31000	212.159	-2.57866	4.10138	4.84466	2.29062
7	7	.03229	-2.79264	2.90923	54.42500	223.829	-2.79264	2.90923	4.03267	1.90670
8	8	.09281	-2.05780	6.72255	56.54000	197.020	-2.05780	6.72255	7.03045	3.32409
9	9	.04762	-1.87990	7.02098	58.65500	194.990	-1.87990	7.02098	7.26830	3.43655
10	10	.06218	-2.68653	2.92695	60.77000	222.548	-2.68653	2.92695	3.97297	1.87847
11	11	.05834	-1.91249	1.76600	62.88500	227.280	-1.91249	1.76600	2.60315	1.23080
12	12	.04154	-2.05302	1.89579	65.00000	227.280	-2.05302	1.89579	2.79444	1.32125
13	13	.04002	-2.08121	2.43884	67.11500	220.476	-2.08121	2.43884	3.20614	1.51591
14	14	.03919	-1.41496	1.92133	71.34500	216.370	-1.41496	1.92133	2.38613	1.12820
15	15	.03660	-1.35033	2.07690	73.46000	213.031	-1.35033	2.07690	2.47728	1.17129
16	16	.04529	-.85986	2.13995	75.57500	201.891	-.85986	2.13995	2.30624	1.09042
17	17	.05570	-.32228	2.23371	77.69000	188.210	-.32228	2.23371	2.25684	1.06706
18	18	.10858	.92927	2.03541	79.80500	155.461	.92927	2.03541	2.23750	1.05792
1	19	.02130	9.18453	11.52835	0.00000	141.456	9.18453	11.52835	14.73969	6.96912
2	20	-.00588	-8.07550	12.64102	0.00000	212.572	-8.07550	12.64102	15.00030	7.09234
3	21	3.37980	7.74394	12.19013	0.00000	147.574	7.74394	12.19013	14.44188	6.82831
4	22	-2.22590	-6.44797	13.43016	0.00000	205.646	-6.44797	13.43016	14.89783	7.04389
5	23	-.09334	1.01847	10.70497	0.00000	174.565	1.01847	10.70497	10.75331	5.08431
6	24	-.16236	-2.46655	4.28695	0.00000	209.914	-2.46655	4.28695	4.94589	2.33848
1	25	-.12345	-2.01868	4.57137	26.93000	203.826	-2.01868	4.57137	4.99725	2.36277
2	26	-.11374	-2.57953	4.71331	29.04500	208.691	-2.57953	4.71331	5.37301	2.54043
3	27	-.10674	-1.31888	6.65612	31.16000	191.208	-1.31888	6.65612	6.78553	3.20829
4	28	-.10560	-2.03579	4.77974	33.27500	203.070	-2.03579	4.77974	5.19522	2.45637
5	29	-.10994	-.94649	5.24126	35.39000	190.236	-.94649	5.24126	5.32604	2.51822
6	30	-.10794	-2.73324	3.82067	37.50500	215.579	-2.73324	3.82067	4.69767	2.22112
7	31	-.11986	-2.59128	4.43610	39.62000	210.291	-2.59128	4.43610	5.13748	2.42907
8	32	-.12293	-1.44098	6.77846	41.73500	192.001	-1.44098	6.77846	6.92994	3.27657
9	33	-.13256	-.79522	5.13163	43.85000	188.809	-.79522	5.13163	5.19288	2.45526
10	34	-.13576	-1.15947	5.25894	45.96500	192.433	-1.15947	5.25894	5.38524	2.54621
11	35	-.16777	-1.42316	4.57716	48.08000	197.272	-1.42316	4.57716	4.79330	2.26634
12	36	-.15944	-2.43213	4.90083	50.19500	206.394	-2.43213	4.90083	5.47114	2.58683
13	37	-.10112	-1.94014	4.39741	52.31000	203.807	-1.94014	4.39741	4.80639	2.27252
14	38	-.02216	-3.24068	4.57248	54.42500	215.327	-3.24068	4.57248	5.60442	2.64985
15	39	-.14577	-3.35519	4.57810	56.54000	216.237	-3.35519	4.57810	5.67594	2.68366
16	40	-.14717	-1.77692	4.98414	58.65500	199.622	-1.77692	4.98414	5.29142	2.50185
17	41	-.14067	-2.21914	5.31214	60.77000	202.673	-2.21914	5.31214	5.75703	2.72200
18	42	-.13164	-3.46894	4.77985	62.88500	215.970	-3.46894	4.77985	5.90597	2.79242
19	43	-.12939	-2.27140	1.76698	65.00000	232.088	-2.27140	1.76898	2.87898	1.36122
20	44	-.12775	-2.20426	2.11355	67.11500	226.204	-2.20426	2.11355	3.05382	1.44389
21	45	-.12478	-2.47403	2.21170	69.23000	228.204	-2.47403	2.21170	3.31850	1.56903
22	46	-.11758	-2.57104	1.71627	71.34500	236.275	-2.57104	1.71627	3.09125	1.46158
23	47	-.09861	-2.60907	1.37536	73.46000	242.204	-2.60907	1.37536	2.94938	1.39451
24	48	-.10995	-2.34119	.85690	75.57500	249.897	-2.34119	.85690	2.49308	1.17876
25	49	-.08637	-2.36212	.60005	77.69000	255.747	-2.36212	.60005	2.43714	1.15231
26	50	-.10822	-2.25216	.08482	79.80500	267.843	-2.25216	.08482	2.25376	1.06561

CENTROID OF SHED VORTICITY

	GAM/V	Y	Z
+Y BODY*	.80931	-1.54137	3.33550
-Y BODY*	-3.09689	-2.13468	3.94057

ORIGINAL PAGE IS
OF POOR QUALITY

BODY SURFACE PRESSURE DISTRIBUTION

X	R	DR/DX	M
80.7300	2.1150	0.0000	2.5000

J	Y	Z	BETA	U/VO	V/VO	W/VO	VT/VO	CP(M)	DPHI/DT	CPZ	CP(I)
1	0.0000	-2.1150	0.000	.9663	.0132	-.0030	.0135	.0657	.0062	.0660	.0598
2	.1843	-2.1070	5.000	.9663	.0542	.0018	.0542	.0613	.0070	.0633	.0562
3	.3673	-2.0829	10.000	.9663	.0940	.0136	.0949	.0532	.0079	.0572	.0493
4	.5474	-2.0429	15.000	.9663	.1312	.0322	.1351	.0415	.0089	.0479	.0391
5	.7234	-1.9874	20.000	.9663	.1648	.0570	.1744	.0271	.0098	.0359	.0260
6	.8938	-1.9168	25.000	.9663	.1936	.0873	.2124	.0104	.0108	.0211	.0103
7	1.0575	-1.8316	30.000	.9663	.2168	.1222	.2489	-.0075	.0118	.0043	-.0076
8	1.2131	-1.7325	35.000	.9663	.2336	.1606	.2835	-.0259	.0129	-.0141	-.0270
9	1.3595	-1.6202	40.000	.9663	.2434	.2013	.3159	-.0441	.0140	-.0335	-.0476
10	1.4955	-1.4955	45.000	.9663	.2460	.2430	.3458	-.0615	.0152	-.0534	-.0686
11	1.6202	-1.3595	50.000	.9663	.2413	.2846	.3731	-.0776	.0164	-.0730	-.0894
12	1.7325	-1.2131	55.000	.9663	.2294	.3247	.3975	-.0920	.0177	-.0918	-.1095
13	1.8316	-1.0575	60.000	.9663	.2107	.3620	.4189	-.1045	.0190	-.1092	-.1282
14	1.9168	-.8938	65.000	.9663	.1858	.3955	.4370	-.1151	.0204	-.1247	-.1451
15	1.9874	-.7234	70.000	.9663	.1555	.4243	.4519	-.1238	.0219	-.1379	-.1598
16	2.0429	-.5474	75.000	.9663	.1207	.4473	.4633	-.1305	.0234	-.1484	-.1718
17	2.0829	-.3673	80.000	.9663	.0824	.4641	.4714	-.1354	.0250	-.1559	-.1809
18	2.1070	-.1843	85.000	.9663	.0418	.4742	.4761	-.1386	.0267	-.1603	-.1871
19	2.1150	0.0000	90.000	.9663	.0000	.4775	.4775	-.1402	.0285	-.1617	-.1901
20	2.1070	.1843	95.000	.9663	-.0417	.4739	.4756	-.1402	.0303	-.1599	-.1902
21	2.0829	.3673	100.000	.9663	-.0823	.4635	.4708	-.1388	.0323	-.1553	-.1876
22	2.0429	.5474	105.000	.9663	-.1206	.4471	.4630	-.1362	.0343	-.1481	-.1824
23	1.9874	.7234	110.000	.9663	-.1558	.4251	.4527	-.1322	.0364	-.1386	-.1750
24	1.9168	.8938	115.000	.9663	-.1871	.3982	.4400	-.1272	.0387	-.1272	-.1659
25	1.8316	1.0575	120.000	.9662	-.2139	.3675	.4252	-.1213	.0410	-.1144	-.1554
26	1.7325	1.2131	125.000	.9662	-.2357	.3337	.4085	-.1145	.0435	-.1005	-.1440
27	1.6202	1.3595	130.000	.9662	-.2522	.2976	.3901	-.1070	.0462	-.0858	-.1320
28	1.4955	1.4955	135.000	.9662	-.2630	.2600	.3698	-.0990	.0493	-.0704	-.1197
29	1.3595	1.6202	140.000	.9662	-.2668	.2209	.3464	-.0903	.0534	-.0536	-.1070
30	1.2131	1.7325	145.000	.9662	-.2600	.1791	.3157	-.0808	.0605	-.0332	-.0937
31	1.0575	1.8316	150.000	.9662	-.2353	.1328	.2702	-.0768	.0818	-.0066	-.0884
32	.8938	1.9168	155.000	.9662	-.2083	.0941	.2286	-.1212	.1694	.0142	-.1553
33	.7234	1.9874	160.000	.9662	-.2158	.0756	.2286	-.0752	.1003	.0142	-.0862
34	.5474	2.0429	165.000	.9662	-.2332	.0595	.2407	-.0594	.0744	.0085	-.0659
35	.3673	2.0829	170.000	.9662	-.2342	.0383	.2373	-.0540	.0694	.0101	-.0593
36	.1843	2.1070	175.000	.9662	-.2220	.0164	.2226	-.0480	.0690	.0169	-.0522
37	-.0000	2.1150	180.000	.9662	-.1975	-.0030	.1975	-.0414	.0718	.0274	-.0444
38	-.1843	2.1070	185.000	.9662	-.1607	-.0170	.1616	-.0421	.0855	.0403	-.0452
39	-.3673	2.0829	190.000	.9662	-.1311	-.0261	.1336	-.0458	.0981	.0486	-.0496
40	-.5474	2.0429	195.000	.9662	-.1103	-.0325	.1150	-.0261	.0804	.0532	-.0272
41	-.7234	1.9874	200.000	.9662	-.0781	-.0314	.0842	-.0230	.0832	.0593	-.0238
42	-.8938	1.9168	205.000	.9662	-.0492	-.0259	.0556	-.0199	.0939	.0633	-.0206
43	-1.0575	1.8316	210.000	.9662	-.0230	-.0163	.0282	-.0149	.0808	.0656	-.0152

44	-1.2131	1.7325	215.000	.9662	.0004	-.0027	.0027	-.0161	.0829	.0664	-.0165
45	-1.3595	1.6202	220.000	.9662	.0048	.0010	-.0049	-.0164	.0832	.0664	-.0168
46	-1.4955	1.4955	225.000	.9662	.0023	-.0007	.0024	-.0150	.0818	.0664	-.0154
47	-1.6202	1.3595	230.000	.9662	.0013	-.0014	.0019	-.0126	.0792	.0664	-.0129
48	-1.7325	1.2131	235.000	.9662	.0029	.0011	.0031	-.0093	.0758	.0664	-.0094
49	-1.8316	1.0575	240.000	.9662	.0072	.0095	-.0119	-.0076	.0739	.0662	-.0076
50	-1.9168	.8938	245.000	.9663	.0086	.0154	-.0177	-.0096	.0757	.0660	-.0097
51	-1.9874	.7234	250.000	.9663	.0100	.0246	-.0266	-.0113	.0771	.0656	-.0115
52	-2.0429	.5474	255.000	.9663	.0182	.0649	-.0674	-.0062	.0681	.0618	-.0063
53	-2.0829	.3673	260.000	.9663	.0234	.1297	-.1318	-.0050	.0540	.0490	-.0050
54	-2.1070	.1843	265.000	.9663	.0158	.1780	-.1787	-.0442	.0820	.0344	-.0476
55	-2.1150	-.0000	270.000	.9663	.0000	.2283	-.2283	-.0519	.0709	.0142	-.0567
56	-2.1070	-.1843	275.000	.9663	-.0258	.2923	-.2934	-.0328	.0149	-.0198	-.0347
57	-2.0829	-.3673	280.000	.9663	-.0590	.3314	-.3366	-.0463	.0031	-.0470	-.0501
58	-2.0429	-.5474	285.000	.9663	-.0930	.3441	-.3564	-.0550	-.0003	-.0607	-.0605
59	-1.9874	-.7234	290.000	.9663	-.1252	.3411	-.3633	-.0581	-.0015	-.0657	-.0643
60	-1.9168	-.8938	295.000	.9663	-.1541	.3275	-.3619	-.0570	-.0018	-.0647	-.0629
61	-1.8316	-1.0575	300.000	.9663	-.1783	.3059	-.3541	-.0525	-.0017	-.0591	-.0574
62	-1.7325	-1.2131	305.000	.9663	-.1970	.2783	-.3410	-.0451	-.0014	-.0500	-.0486
63	-1.6202	-1.3595	310.000	.9663	-.2092	.2463	-.3232	-.0352	-.0009	-.0382	-.0373
64	-1.4955	-1.4955	315.000	.9663	-.2145	.2116	-.3013	-.0233	-.0004	-.0246	-.0242
65	-1.3595	-1.6202	320.000	.9663	-.2127	.1755	-.2757	-.0099	.0002	-.0098	-.0100
66	-1.2131	-1.7325	325.000	.9663	-.2037	.1396	-.2469	.0044	.0008	.0052	.0044
67	-1.0575	-1.8316	330.000	.9663	-.1877	.1054	-.2153	.0189	.0015	.0199	.0184
68	-.8938	-1.9168	335.000	.9663	-.1653	.0741	-.1811	.0327	.0022	.0334	.0312
69	-.7234	-1.9874	340.000	.9663	-.1371	.0469	-.1449	.0451	.0030	.0452	.0422
70	-.5474	-2.0429	345.000	.9663	-.1041	.0249	-.1070	.0552	.0037	.0547	.0510
71	-.3673	-2.0829	350.000	.9663	-.0672	.0089	-.0678	.0624	.0045	.0616	.0571
72	-.1843	-2.1070	355.000	.9663	-.0277	-.0006	-.0277	.0660	.0053	.0654	.0601
73	0.0000	-2.1150	360.000	.9663	.0132	-.0030	.0135	.0657	.0062	.0660	.0598

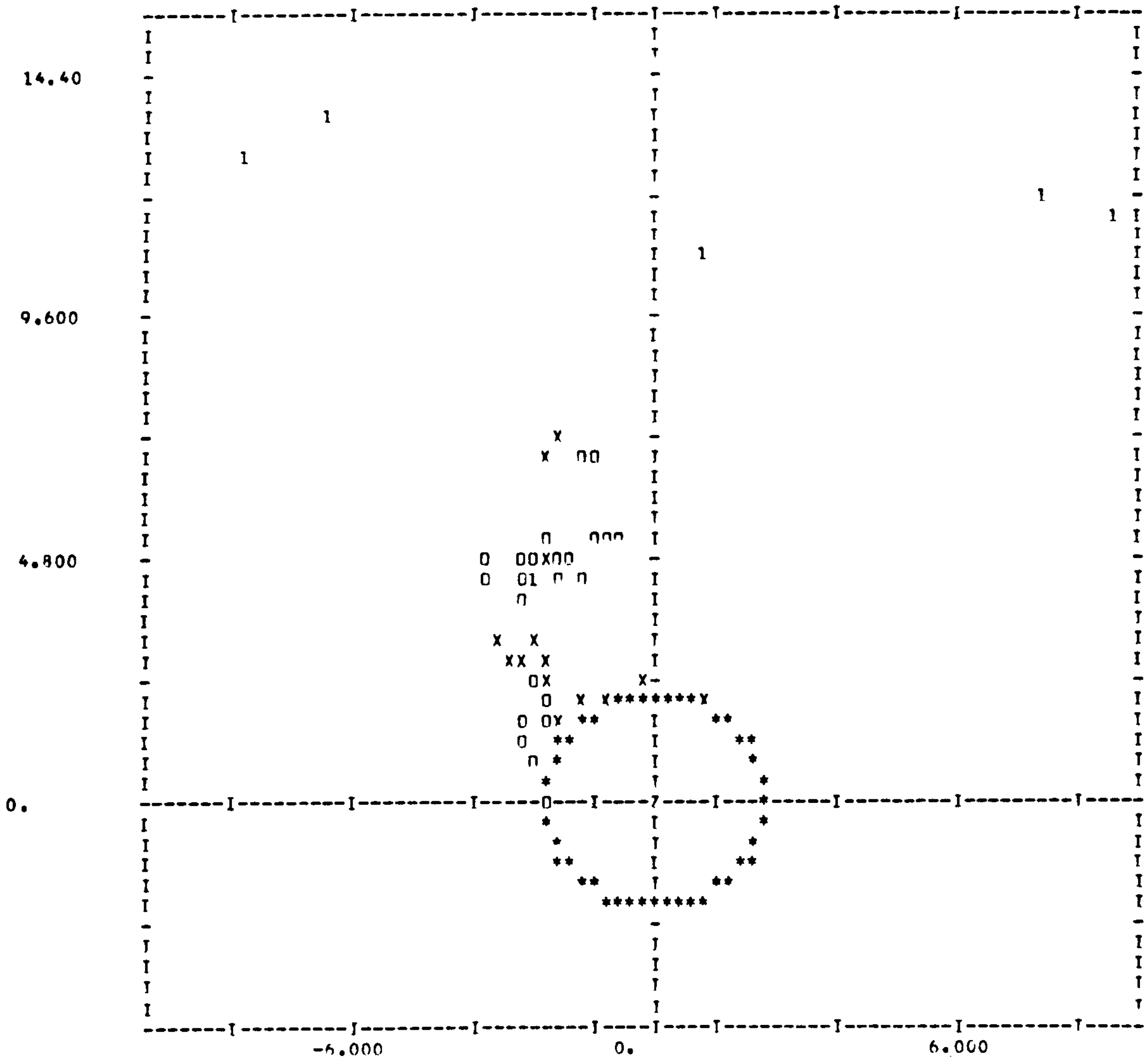

X	R	ALPHA	BETA	M
80.730	2.115	15.000	.000	2.500

X = 80.730

CN(X)	CY(X)	CP(0)	CP(90)	CP(180)
5.181E-02	7.679E-02	6.565E-02	-1.402E-01	-4.138E-02
CN	CM	CY	CR	CSL
4.099E-01	-2.078E+00	-2.014E-01	2.359E+00	-3.361E-17

(SEPARATION POINTS)

Y	Z	BETA
1.404	1.580	138.4
-2.108	.159	265.7

STRATFORD SEPARATION CRITERION (LAMINAR) F(S) = .02252

SUMMARY OF PRESSURE DISTRIBUTION AND SEPARATION POINTS ON BODY ... X = 80.73

+Y SIDE*	Y	Z	BETA	ARC	CP	CP*	DCP*/DX
STAGNATION PT.	0.000	-2.115	360.000	.066	.066		
MIN. PRESSURE	2.107	.184	95.000	3.506	-.140	0.000	0.000
SEPARATION	1.404	1.580	138.369	5.106	-.093	.041	.042

-Y SIDE*	Y	Z	BETA	ARC	CP	CP*	DCP*/DX
STAGNATION PT.	-1.496	1.496	225.000	.066	-.015		
MIN. PRESSURE	-1.987	-.723	290.000	2.583	-.058	0.000	0.000
SEPARATION	-2.108	.159	265.701	3.480	-.045	.012	.099

INITIAL POSITIONS AND STRENGTHS OF SHED VORTICITY AT X = 80.730

	NV	GAM/V	M(K)	Y	Z	BETA	VT/V	YC	ZC	RG/R
+Y SIDE*	51	.0599	.0546	1.4753	1.6599	138.3695	.3537	1.4753	1.6599	1.0500
-Y SIDE*	52	-.0165	.0285	-2.2145	.1665	265.7006	.1855	-2.2145	.1665	1.0500

CENTROID OF SHED VORTICITY

	GAM/V	Y	Z
+Y BODY*	.86923	-1.33343	3.22000
-Y BODY*	-3.11337	-2.13510	3.92059

** CONTRIBUTION OF BODY SECTION TO TOTAL LOADS **

STRENGTHS AND POSITIONS OF VORTICES AT END OF BODY SECTION

A = 2.1150

I	GAMMA/2PIVA	YO/A	ZO/A
1	.06541	-.6305	1.5225
2	-.23428	-1.0095	1.8537

FORCE AND MOMENT COEFFICIENTS

BERNOULLI LOADING PRESSURE

	UNROLLED BODY COORDINATES	ROLLED BODY COORDINATES
CX	0.00000	0.00000
CZ	.40995	.40994
CY	-.20136	-.20137

CM	-2.07853	-2.07849
CLN	2.35915	2.35919
CLL	-.00000	-.00000

VORTEX INFORMATION WRITTEN TO TAPE8

	Y	Z	GAMMA/V
8			
1	-.13334E+01	.32200E+01	.86923E+00
2	-.21351E+01	.39206E+01	-.31134E+01
3	.91845E+01	.11528E+02	.21299E-01
4	-.80755E+01	.12641E+02	-.58799E-02
5	.77439E+01	.12190E+02	.33798E+01
6	-.64480E+01	.13430E+02	-.22259E+01
7	.10185E+01	.10705E+02	-.93338E-01
8	-.24665E+01	.42869E+01	-.16236E+00

(c) Steps 4-6, program LRCDM2

Figure A.7.- Concluded.

(pages 212 through 259)

*** STEP 4

***** SUMMARY OF TOTAL LOADS *****

ALPHA C = 15.00 DEG. PHI = .001 DEG. MACH = 2.50

(BODY AXIAL FORCE CONTRIBUTIONS NEGLECTED)

ROLLED BODY-AXIS COORDINATES			**	UNROLLED BODY-AXIS COORDINATES		
CX(NOSE ONLY)	.1911E+00	.1937E+00	**	CX(NOSE ONLY)	.1911E+00	.1937E+00
CZB	.5517E+01	.6436E+01	**	CZU	.5517E+01	.6436E+01
CYB	-.9314E-04	-.4134E+00	**	CYU	.3140E-05	-.4133E+00
CMB	.3304E+02	.3436E+02	**	CMU	.3304E+02	.3436E+02
CLNB	-.5605E-03	.1223E+01	**	CLNU	.1618E-04	.1223E+01
CLLB	-.1310E+01	-.1351E+01	**	CLLU	-.1310E+01	-.1351E+01

NOTE: THESE LOADS HAVE BEEN READ FROM TAPE9 AND ARE VALID FOR CONFIGURATION UP TO TAIL FINS.

STEP 4 LOADS ON TAIL FINS WITHOUT VORTEX EFFECTS

NASA/LRC TF-4 WITH KING TAIL (D), AFTERBODY AND TAIL SECTION

```
$INPUT
BIL     = .2159E+02,
B2      = .904E+01,
B2V     = .904E+01,
CRP     = .2159E+02,
CRPV    = .2159E+02,
DELD    = 0.0,
DELL    = 0.0,
DELR    = 0.0,
DELU    = 0.0,
ERATIO  = .1E+01,
FAC     = .95E+00,
FKLE    = .5E+00,
FKSE    = .1E+01,
FMACH   = .25E+01,
ITAIL   = 1,
JCPT    = 0,
LVSWP   = 0,
MINPRN  = 0,
MSWD    = 6,
MSWL    = 6,
MSWR    = 6,
MSWU    = 6,
NBDCR   = 12,
NBDYPR  = 1,
NBSHED  = 1,
NCPOUT  = 1,
NCRX    = 1,
NC4     = 4,
NCWB    = 4,
NCWT    = 0,
NDRAG   = 1,
NFVNPR  = 0,
NOLINP  = 1,
NOUT    = 0,
NPR     = 0,
NPRESS  = 0,
NTDAT   = 0,
NTPR    = 0,
NVLIN   = 0,
NVRTPL  = 1,
NVRTX   = 0,
N2DPRB  = 0,
N2DPRF  = 0,
PHIDIH  = 0.0,
PHIFR   = 0.0,
PHIFL   = 0.0,
PHIFU   = .9E+02,
PHIFD   = .9E+02,
PHIINT  = 0.0,
RA      = .2115E+01,
RB      = .2115E+01,
REFL    = .423E+01,
SREF    = .1412E+02,
SWLEP   = .45E+02,
SWLEV   = .45E+02,
SWTEP   = 0.0,
SWTEV   = 0.0,
THETIT  = 0.0,
THETR   = 0.0,
THETL   = 0.0,
THETU   = .9E+02,
THETD   = .9E+02,
TOLFAC  = .1E+01,
VRTMAX  = .35E+00,
XM      = .4604E+02,
XSTART  = .8073E+02,
XWLE    = .8073E+02,
ZM      = 0.0,
$END
```

FIN SECTION GEOMETRY DESCRIPTION

NO. OF CHORDWISE PANELS ON FINS PRESENT (NCW) = 4

FIN PROPERTY		FIN 1 OR R	FIN 2 OR L	FIN 3 OR U	FIN 4 OR D
NO. OF PANELS - SPANWISE	(MSW) =	6	6	6	6
ROOT CHORD	(CR) =	21.590	21.590	21.590	21.590
LEADING EDGE SWEEP	(SWLE) =	45.000	45.000	45.000	45.000
TRAILING EDGE SWEEP	(SWTE) =	0.000	0.000	0.000	0.000
EXPOSED SEMISPAN	(B2) =	9.040	9.040	9.040	9.040
FIN DIHEDRAL	(PHIF) =	0.000	0.000	90.000	90.000
BODY ANGLE OF FIN ATTACHMENT	(THET) =	0.000	0.000	90.000	90.000
FIN DEFLECTION	(DEL) =	0.000	0.000	0.000	0.000
Y-INTERSECTION OF FIN TO BODY	(YBOD) =	2.115	-2.115	-.000	.000
Z-INTERSECTION OF FIN TO BODY	(ZBOD) =	0.000	-.000	2.115	-2.115

FIN GEOMETRY

TIP CHORD = 12.55000

ROOT CHORD = 21.59000

FIN SEMISPAN = 9.04000

LEADING EDGE SWEEP = 45.00000 DEGREES

TRAILING EDGE SWEEP = 0.00000 DEGREES

FLOW CONDITIONS

MACH = 2.50000 ALPHAC= 15.00000 PHI = .00100 ALFA = 15.00000 BETA = .00026

CRPT = 21.59000
CRPTV = 21.59000

```
$BODY
NXBODY = 50.

LNOSE  = .9518E+01.

LBODY  = .10232E+03.

BCODE  = 2.

$END
```

PHYSICAL DIMENSIONS OF BODY AND LINE SINGULARITY STRENGTHS REPRESENTING THE BODY AT MACH= 2.5000 ALFAC= 15.0000

	X	R	DR/DX	TX	T(I)	TC(I)
1	0.0000	0.	.46751	0.	.34589	.11034
2	3.1314	1.1884	.29640	.40834	-.31104	-.80658E-01
3	5.1978	1.6959	.19588	1.3121	-.30893E-01	-.72376E-02
4	7.2643	2.0017	.10079	2.6778	-.41636E-01	-.15486E-01
5	9.3307	2.1142	.83352E-02	4.4864	.62544E-02	-.11892E-01
6	11.3971	2.1150	0.	6.5510	.25497E-01	-.46221E-02
7	13.4635	2.1150	0.	8.6175	.34224E-03	-.32877E-03
8	15.5300	2.1150	0.	10.684	.26558E-02	.85085E-03
9	17.5964	2.1150	0.	12.750	.88314E-03	.15202E-02
10	19.6628	2.1150	0.	14.817	.67952E-03	.16413E-02
11	21.7293	2.1150	0.	16.883	.40031E-03	.15407E-02
12	23.7957	2.1150	0.	18.950	.27314E-03	.13180E-02
13	25.8621	2.1150	0.	21.016	.18473E-03	.10582E-02
14	27.9285	2.1150	0.	23.082	.12958E-03	.80390E-03
15	29.9950	2.1150	0.	25.149	.92336E-04	.57904E-03
16	32.0614	2.1150	0.	27.215	.67019E-04	.39330E-03
17	34.1278	2.1150	0.	29.282	.49355E-04	.24817E-03
18	36.1943	2.1150	0.	31.348	.36838E-04	.14040E-03
19	38.2607	2.1150	0.	33.415	.27826E-04	.64483E-04
20	40.3271	2.1150	0.	35.481	.21249E-04	.14158E-04
21	42.3935	2.1150	0.	37.547	.16391E-04	-.16619E-04
22	44.4600	2.1150	0.	39.614	.12761E-04	-.33185E-04
23	46.5264	2.1150	0.	41.680	.10021E-04	-.39960E-04
24	48.5928	2.1150	0.	43.747	.79342E-05	-.40416E-04
25	50.6593	2.1150	0.	45.813	.63298E-05	-.37149E-04
26	52.7257	2.1150	0.	47.880	.50863E-05	-.32007E-04
27	54.7921	2.1150	0.	49.946	.41151E-05	-.26235E-04
28	56.8586	2.1150	0.	52.012	.33509E-05	-.20612E-04
29	58.9250	2.1150	0.	54.079	.27455E-05	-.15575E-04
30	60.9914	2.1150	0.	56.145	.22627E-05	-.11327E-04
31	63.0578	2.1150	0.	58.212	.18753E-05	-.79112E-05
32	65.1243	2.1150	0.	60.278	.15625E-05	-.52800E-05
33	67.1907	2.1150	0.	62.345	.13086E-05	-.33338E-05
34	69.2571	2.1150	0.	64.411	.11013E-05	-.19537E-05
35	71.3236	2.1150	0.	66.477	.93116E-06	-.10201E-05
36	73.3900	2.1150	0.	68.544	.79087E-06	-.42402E-06
37	75.4564	2.1150	0.	70.610	.67461E-06	-.72300E-07
38	77.5228	2.1150	0.	72.677	.57782E-06	.11041E-06
39	79.5893	2.1150	0.	74.743	.49688E-06	.18248E-06
40	81.6557	2.1150	0.	76.810	.42891E-06	.18719E-06
41	83.7221	2.1150	0.	78.876	.37159E-06	.15520E-06
42	85.7886	2.1150	0.	80.942	.32306E-06	.10720E-06
43	87.8550	2.1150	0.	83.009	.28181E-06	.56229E-07
44	89.9214	2.1150	0.	85.075	.24663E-06	.98192E-08
45	91.9879	2.1150	0.	87.142	.21651E-06	-.28342E-07
46	94.0543	2.1150	0.	89.208	.19064E-06	-.57081E-07
47	96.1207	2.1150	0.	91.275	.16835E-06	-.76742E-07
48	98.1871	2.1150	0.	93.341	.14907E-06	-.88497E-07
49	100.2536	2.1150	0.	95.407	.13236E-06	-.93853E-07
50	102.3200	2.1150	0.	97.474	0.	0.

COORDINATES AT POINTS ON BODY MERIDIANS

144 CONTROL POINTS AND PRESSURE POINTS WRITTEN TO TAPE 4 FROM SUBROUTINE BDYPR

	XCP	YCP	ZCP
1	.86425E+02	.28593E+01	0.
2	.91637E+02	.28593E+01	0.
3	.96848E+02	.28593E+01	0.
4	.10206E+03	.28593E+01	0.
5	.87573E+02	.43652E+01	0.
6	.92408E+02	.43652E+01	0.
7	.97243E+02	.43652E+01	0.
8	.10208E+03	.43652E+01	0.
9	.88722E+02	.58711E+01	0.
10	.93180E+02	.58711E+01	0.
11	.97639E+02	.58711E+01	0.
12	.10210E+03	.58711E+01	0.
13	.89870E+02	.73767E+01	0.
14	.93952E+02	.73767E+01	0.
15	.98034E+02	.73767E+01	0.
16	.10212E+03	.73767E+01	0.
17	.91018E+02	.88822E+01	0.
18	.94723E+02	.88822E+01	0.
19	.98429E+02	.88822E+01	0.
20	.10213E+03	.88822E+01	0.
21	.92165E+02	.10387E+02	0.
22	.95495E+02	.10387E+02	0.
23	.98824E+02	.10387E+02	0.
24	.10215E+03	.10387E+02	0.
25	.86425E+02	-.28593E+01	0.
26	.91637E+02	-.28593E+01	0.
27	.96848E+02	-.28593E+01	0.
28	.10206E+03	-.28593E+01	0.
29	.87573E+02	-.43652E+01	0.
30	.92408E+02	-.43652E+01	0.
31	.97243E+02	-.43652E+01	0.
32	.10208E+03	-.43652E+01	0.
33	.88722E+02	-.58711E+01	0.
34	.93180E+02	-.58711E+01	0.
35	.97639E+02	-.58711E+01	0.
36	.10210E+03	-.58711E+01	0.
37	.89870E+02	-.73767E+01	0.
38	.93952E+02	-.73767E+01	0.
39	.98034E+02	-.73767E+01	0.
40	.10212E+03	-.73767E+01	0.
41	.91018E+02	-.88822E+01	0.
42	.94723E+02	-.88822E+01	0.
43	.98429E+02	-.88822E+01	0.
44	.10213E+03	-.88822E+01	0.
45	.92165E+02	-.10387E+02	0.
46	.95495E+02	-.10387E+02	0.
47	.98824E+02	-.10387E+02	0.
48	.10215E+03	-.10387E+02	0.
49	.86425E+02	0.	.28593E+01
50	.91637E+02	0.	.28593E+01
51	.96848E+02	0.	.28593E+01
52	.10206E+03	0.	.28593E+01
53	.87573E+02	0.	.43652E+01
54	.92408E+02	0.	.43652E+01
55	.97243E+02	0.	.43652E+01
56	.10208E+03	0.	.43652E+01
57	.88722E+02	0.	.58711E+01
58	.93180E+02	0.	.58711E+01
59	.97639E+02	0.	.58711E+01
60	.10210E+03	0.	.58711E+01
61	.89870E+02	0.	.73767E+01
62	.93952E+02	0.	.73767E+01
63	.98034E+02	0.	.73767E+01
64	.10212E+03	0.	.73767E+01
65	.91018E+02	0.	.88822E+01
66	.94723E+02	0.	.88822E+01
67	.98429E+02	0.	.88822E+01
68	.10213E+03	0.	.88822E+01
69	.92165E+02	0.	.10387E+02
70	.95495E+02	0.	.10387E+02
71	.98824E+02	0.	.10387E+02
72	.10215E+03	0.	.10387E+02
73	.86425E+02	0.	-.28593E+01
74	.91637E+02	0.	-.28593E+01
75	.96848E+02	0.	-.28593E+01
76	.10206E+03	0.	-.28593E+01
77	.87573E+02	0.	-.43652E+01
78	.92408E+02	0.	-.43652E+01
79	.97243E+02	0.	-.43652E+01
80	.10208E+03	0.	-.43652E+01
81	.88722E+02	0.	-.58711E+01
82	.93180E+02	0.	-.58711E+01
83	.97639E+02	0.	-.58711E+01
84	.10210E+03	0.	-.58711E+01
85	.89870E+02	0.	-.73767E+01
86	.93952E+02	0.	-.73767E+01
87	.98034E+02	0.	-.73767E+01
88	.10212E+03	0.	-.73767E+01
89	.91018E+02	0.	-.88822E+01
90	.94723E+02	0.	-.88822E+01
91	.98429E+02	0.	-.88822E+01
92	.10213E+03	0.	-.88822E+01
93	.92165E+02	0.	-.10387E+02
94	.95495E+02	0.	-.10387E+02
95	.98824E+02	0.	-.10387E+02
96	.10215E+03	0.	-.10387E+02
97	.85858E+02	.19733E+01	.52875E+00
98	.85858E+02	.14446E+01	.14446E+01
99	.85858E+02	.52875E+00	.19733E+01
100	.85858E+02	-.52875E+00	.19733E+01
101	.85858E+02	-.14446E+01	.14446E+01
102	.85858E+02	-.19733E+01	.52875E+00
103	.85858E+02	-.19733E+01	-.52875E+00
104	.85858E+02	-.14446E+01	-.14446E+01
105	.85858E+02	-.52875E+00	-.19733E+01
106	.85858E+02	.52875E+00	-.19733E+01
107	.85858E+02	.14446E+01	-.14446E+01
108	.85858E+02	.19733E+01	-.52875E+00
109	.91255E+02	.19733E+01	.52875E+00
110	.91255E+02	.14446E+01	.14446E+01
111	.91255E+02	.52875E+00	.19733E+01
112	.91255E+02	-.52875E+00	.19733E+01
113	.91255E+02	-.14446E+01	.14446E+01
114	.91255E+02	-.19733E+01	.52875E+00
115	.91255E+02	-.19733E+01	-.52875E+00
116	.91255E+02	-.14446E+01	-.14446E+01
117	.91255E+02	-.52875E+00	-.19733E+01
118	.91255E+02	.52875E+00	-.19733E+01
119	.91255E+02	.14446E+01	-.14446E+01
120	.91255E+02	.19733E+01	-.52875E+00
121	.96653E+02	.19733E+01	.52875E+00
122	.96653E+02	.14446E+01	.14446E+01
123	.96653E+02	.52875E+00	.19733E+01
124	.96653E+02	-.52875E+00	.19733E+01
125	.96653E+02	-.14446E+01	.14446E+01
126	.96653E+02	-.19733E+01	.52875E+00
127	.96653E+02	-.19733E+01	-.52875E+00
128	.96653E+02	-.14446E+01	-.14446E+01
129	.96653E+02	-.52875E+00	-.19733E+01
130	.96653E+02	.52875E+00	-.19733E+01
131	.96653E+02	.14446E+01	-.14446E+01
132	.96653E+02	.19733E+01	-.52875E+00
133	.10205E+03	.19733E+01	.52875E+00
134	.10205E+03	.14446E+01	.14446E+01
135	.10205E+03	.52875E+00	.19733E+01
136	.10205E+03	-.52875E+00	.19733E+01
137	.10205E+03	-.14446E+01	.14446E+01
138	.10205E+03	-.19733E+01	.52875E+00
139	.10205E+03	-.19733E+01	-.52875E+00
140	.10205E+03	-.14446E+01	-.14446E+01
141	.10205E+03	-.52875E+00	-.19733E+01
142	.10205E+03	.52875E+00	-.19733E+01
143	.10205E+03	.14446E+01	-.14446E+01
144	.10205E+03	.19733E+01	-.52875E+00

ORIGINAL PAGE IS
OF POOR QUALITY

CONTROL POINT COORDINATES FOR 4 CHORDWISE BY 6 SPANWISE PANELS ON FIN 1 OR R, 6 SPANWISE ON FIN 2 OR L
AND 6 SPANWISE PANELS ON FIN 3 OR U 6 SPANWISE ON FIN 4 OR D

J	X(J)	Y(J)	Z(J)	BU(J)	BV(J)	BW(J)	VVRTX	WVRTX
1	5.69512	2.85925	0.00000	.18448E-03	-.13612E-04	.14396E+00	0.	0.
2	10.90656	2.85925	0.00000	.16205E-03	-.10867E-04	.14387E+00	0.	0.
3	16.11799	2.85925	0.00000	.14340E-03	-.85591E-05	.14380E+00	0.	0.
4	21.32943	2.85925	0.00000	.12783E-03	-.68288E-05	.14375E+00	0.	0.
5	6.84341	4.36521	0.00000	.18075E-03	-.38997E-04	.62013E-01	0.	0.
6	11.67836	4.36521	0.00000	.16032E-03	-.32485E-04	.61953E-01	0.	0.
7	16.51331	4.36521	0.00000	.14315E-03	-.27267E-04	.61902E-01	0.	0.
8	21.34825	4.36521	0.00000	.12859E-03	-.23044E-04	.61858E-01	0.	0.
9	7.99162	5.87105	0.00000	.17834E-03	-.58917E-04	.34473E-01	0.	0.
10	12.45010	5.87105	0.00000	.15960E-03	-.49900E-04	.34424E-01	0.	0.
11	16.90859	5.87105	0.00000	.14369E-03	-.42624E-04	.34381E-01	0.	0.
12	21.36708	5.87105	0.00000	.13005E-03	-.36683E-04	.34344E-01	0.	0.
13	9.13970	7.37674	0.00000	.17701E-03	-.76693E-04	.21991E-01	0.	0.
14	13.22177	7.37674	0.00000	.15978E-03	-.65926E-04	.21948E-01	0.	0.
15	17.30383	7.37674	0.00000	.14497E-03	-.57073E-04	.21911E-01	0.	0.
16	21.38590	7.37674	0.00000	.13214E-03	-.49729E-04	.21878E-01	0.	0.
17	10.28764	8.88223	0.00000	.17666E-03	-.93536E-04	.15296E-01	0.	0.
18	13.99333	8.88223	0.00000	.16079E-03	-.81509E-04	.15259E-01	0.	0.
19	17.69902	8.88223	0.00000	.14696E-03	-.71404E-04	.15226E-01	0.	0.
20	21.40472	8.88223	0.00000	.13488E-03	-.62923E-04	.15196E-01	0.	0.
21	11.43537	10.38745	0.00000	.17720E-03	-.10997E-03	.11294E-01	0.	0.
22	14.76475	10.38745	0.00000	.16253E-03	-.96970E-04	.11262E-01	0.	0.
23	18.09414	10.38745	0.00000	.14970E-03	-.86063E-04	.11232E-01	0.	0.
24	21.42353	10.38745	0.00000	.13837E-03	-.76768E-04	.11206E-01	0.	0.
25	5.69512	-2.85925	0.00000	.18448E-03	.18604E-04	.14396E+00	0.	0.
26	10.90656	-2.85925	0.00000	.16205E-03	.15860E-04	.14387E+00	0.	0.
27	16.11799	-2.85925	0.00000	.14340E-03	.13553E-04	.14380E+00	0.	0.
28	21.32943	-2.85925	0.00000	.12783E-03	.11824E-04	.14375E+00	0.	0.
29	6.84341	-4.36521	0.00000	.18075E-03	.41130E-04	.62013E-01	0.	0.
30	11.67836	-4.36521	0.00000	.16032E-03	.34620E-04	.61953E-01	0.	0.
31	16.51331	-4.36521	0.00000	.14315E-03	.29402E-04	.61902E-01	0.	0.
32	21.34825	-4.36521	0.00000	.12859E-03	.25180E-04	.61858E-01	0.	0.
33	7.99162	-5.87105	0.00000	.17834E-03	.60089E-04	.34473E-01	0.	0.
34	12.45010	-5.87105	0.00000	.15960E-03	.51073E-04	.34424E-01	0.	0.
35	16.90859	-5.87105	0.00000	.14368E-03	.43798E-04	.34381E-01	0.	0.
36	21.36708	-5.87105	0.00000	.13005E-03	.37859E-04	.34344E-01	0.	0.
37	9.13970	-7.37674	0.00000	.17701E-03	.77429E-04	.21991E-01	0.	0.
38	13.22177	-7.37674	0.00000	.15978E-03	.66664E-04	.21948E-01	0.	0.
39	17.30383	-7.37674	0.00000	.14496E-03	.57812E-04	.21911E-01	0.	0.
40	21.38590	-7.37674	0.00000	.13213E-03	.50469E-04	.21878E-01	0.	0.
41	10.28764	-8.88223	0.00000	.17666E-03	.94039E-04	.15296E-01	0.	0.
42	13.99333	-8.88223	0.00000	.16078E-03	.82013E-04	.15259E-01	0.	0.
43	17.69902	-8.88223	0.00000	.14696E-03	.71910E-04	.15226E-01	0.	0.
44	21.40472	-8.88223	0.00000	.13488E-03	.63429E-04	.15196E-01	0.	0.
45	11.43537	-10.38745	0.00000	.17719E-03	.11033E-03	.11294E-01	0.	0.
46	14.76475	-10.38745	0.00000	.16253E-03	.97335E-04	.11262E-01	0.	0.
47	18.09414	-10.38745	0.00000	.14969E-03	.86429E-04	.11232E-01	0.	0.
48	21.42353	-10.38745	0.00000	.13836E-03	.77134E-04	.11206E-01	0.	0.
49	5.69512	0.00000	2.85925	.13489E-03	-.25125E-05	-.14305E+00	0.	0.
50	10.90656	0.00000	2.85925	.12038E-03	-.25111E-05	-.14307E+00	0.	0.
51	16.11799	0.00000	2.85925	.10851E-03	-.25099E-05	-.14309E+00	0.	0.
52	21.32943	0.00000	2.85925	.98452E-04	-.25088E-05	-.14311E+00	0.	0.
53	6.84341	0.00000	4.36521	.12231E-03	-.10823E-05	-.61141E-01	0.	0.
54	11.67836	0.00000	4.36521	.11043E-03	-.10813E-05	-.61173E-01	0.	0.
55	16.51331	0.00000	4.36521	.10075E-03	-.10804E-05	-.61202E-01	0.	0.
56	21.34825	0.00000	4.36521	.92404E-04	-.10796E-05	-.61226E-01	0.	0.
57	7.99162	0.00000	5.87105	.10855E-03	0.	-.33630E-01	0.	0.

58	12.45010	0.00000	5.87105	.99025E-04	0.	-.33661E-01	0.	0.
59	16.90859	0.00000	5.87105	.91374E-04	0.	-.33690E-01	0.	0.
60	21.36708	0.00000	5.87105	.84823E-04	0.	-.33715E-01	0.	0.
61	9.13970	0.00000	7.37674	.95310E-04	0.	-.21172E-01	0.	0.
62	13.22177	0.00000	7.37674	.87634E-04	0.	-.21199E-01	0.	0.
63	17.30383	0.00000	7.37674	.81659E-04	0.	-.21225E-01	0.	0.
64	21.38590	0.00000	7.37674	.76647E-04	0.	-.21249E-01	0.	0.
65	10.28764	0.00000	8.88223	.83087E-04	0.	-.14498E-01	0.	0.
66	13.99333	0.00000	8.88223	.76727E-04	0.	-.14521E-01	0.	0.
67	17.69902	0.00000	8.88223	.72017E-04	0.	-.14544E-01	0.	0.
68	21.40472	0.00000	8.88223	.68239E-04	0.	-.14566E-01	0.	0.
69	11.43537	0.00000	10.38745	.72062E-04	0.	-.10514E-01	0.	0.
70	14.76475	0.00000	10.38745	.66518E-04	0.	-.10533E-01	0.	0.
71	18.09414	0.00000	10.38745	.62676E-04	0.	-.10552E-01	0.	0.
72	21.42353	0.00000	10.38745	.59789E-04	0.	-.10571E-01	0.	0.
73	5.69512	0.00000	-2.85925	.23406E-03	-.25125E-05	-.14302E+00	0.	0.
74	10.90656	0.00000	-2.85925	.20372E-03	-.25111E-05	-.14304E+00	0.	0.
75	16.11799	0.00000	-2.85925	.17828E-03	-.25099E-05	-.14307E+00	0.	0.
76	21.32943	0.00000	-2.85925	.15720E-03	-.25088E-05	-.14309E+00	0.	0.
77	6.84341	0.00000	-4.36521	.23919E-03	-.10823E-05	-.61061E-01	0.	0.
78	11.67836	0.00000	-4.36521	.21020E-03	-.10813E-05	-.61106E-01	0.	0.
79	16.51331	0.00000	-4.36521	.18555E-03	-.10804E-05	-.61145E-01	0.	0.
80	21.34825	0.00000	-4.36521	.16477E-03	-.10796E-05	-.61178E-01	0.	0.
81	7.99162	0.00000	-5.87105	.24812E-03	0.	-.33511E-01	0.	0.
82	12.45010	0.00000	-5.87105	.22018E-03	0.	-.33560E-01	0.	0.
83	16.90859	0.00000	-5.87105	.19600E-03	0.	-.33603E-01	0.	0.
84	21.36708	0.00000	-5.87105	.17527E-03	0.	-.33640E-01	0.	0.
85	9.13970	0.00000	-7.37674	.25871E-03	0.	-.21018E-01	0.	0.
86	13.22177	0.00000	-7.37674	.23192E-03	0.	-.21067E-01	0.	0.
87	17.30383	0.00000	-7.37674	.20827E-03	0.	-.21110E-01	0.	0.
88	21.38590	0.00000	-7.37674	.18762E-03	0.	-.21149E-01	0.	0.
89	10.28764	0.00000	-8.88223	.27024E-03	0.	-.14310E-01	0.	0.
90	13.99333	0.00000	-8.88223	.24484E-03	0.	-.14358E-01	0.	0.
91	17.69902	0.00000	-8.88223	.22191E-03	0.	-.14401E-01	0.	0.
92	21.40472	0.00000	-8.88223	.20152E-03	0.	-.14439E-01	0.	0.
93	11.43537	0.00000	-10.38745	.28233E-03	0.	-.10294E-01	0.	0.
94	14.76475	0.00000	-10.38745	.25854E-03	0.	-.10338E-01	0.	0.
95	18.09414	0.00000	-10.38745	.23671E-03	0.	-.10379E-01	0.	0.
96	21.42353	0.00000	-10.38745	.21694E-03	0.	-.10417E-01	0.	0.

CONTROL POINT COORDINATES FOR BIP*S (FIN FRAME)

J	X(J)	Y(J)	Z(J)	THU(J)	THV(J)	THW(J)
97	5.12763	1.97332	.52875	0.	0.	0.
98	5.12763	1.44457	1.44457	0.	0.	0.
99	5.12763	.52875	1.97332	0.	0.	0.
100	5.12763	-.52875	1.97332	0.	0.	0.
101	5.12763	-1.44457	1.44457	0.	0.	0.
102	5.12763	-1.97332	.52875	0.	0.	0.
103	5.12763	-1.97332	-.52875	0.	0.	0.
104	5.12763	-1.44457	-1.44457	0.	0.	0.
105	5.12763	-.52875	-1.97332	0.	0.	0.
106	5.12763	.52875	-1.97332	0.	0.	0.
107	5.12763	1.44457	-1.44457	0.	0.	0.
108	5.12763	1.97332	-.52875	0.	0.	0.
109	10.52513	1.97332	.52875	0.	0.	0.
110	10.52513	1.44457	1.44457	0.	0.	0.
111	10.52513	.52875	1.97332	0.	0.	0.
112	10.52513	-.52875	1.97332	0.	0.	0.
113	10.52513	-1.44457	1.44457	0.	0.	0.
114	10.52513	-1.97332	.52875	0.	0.	0.
115	10.52513	-1.97332	-.52875	0.	0.	0.
116	10.52513	-1.44457	-1.44457	0.	0.	0.
117	10.52513	-.52875	-1.97332	0.	0.	0.
118	10.52513	.52875	-1.97332	0.	0.	0.
119	10.52513	1.44457	-1.44457	0.	0.	0.
120	10.52513	1.97332	-.52875	0.	0.	0.
121	15.92263	1.97332	.52875	0.	0.	0.
122	15.92263	1.44457	1.44457	0.	0.	0.
123	15.92263	.52875	1.97332	0.	0.	0.
124	15.92263	-.52875	1.97332	0.	0.	0.
125	15.92263	-1.44457	1.44457	0.	0.	0.
126	15.92263	-1.97332	.52875	0.	0.	0.
127	15.92263	-1.97332	-.52875	0.	0.	0.
128	15.92263	-1.44457	-1.44457	0.	0.	0.
129	15.92263	-.52875	-1.97332	0.	0.	0.
130	15.92263	.52875	-1.97332	0.	0.	0.
131	15.92263	1.44457	-1.44457	0.	0.	0.
132	15.92263	1.97332	-.52875	0.	0.	0.
133	21.32013	1.97332	.52875	0.	0.	0.
134	21.32013	1.44457	1.44457	0.	0.	0.
135	21.32013	.52875	1.97332	0.	0.	0.
136	21.32013	-.52875	1.97332	0.	0.	0.
137	21.32013	-1.44457	1.44457	0.	0.	0.
138	21.32013	-1.97332	.52875	0.	0.	0.
139	21.32013	-1.97332	-.52875	0.	0.	0.
140	21.32013	-1.44457	-1.44457	0.	0.	0.
141	21.32013	-.52875	-1.97332	0.	0.	0.
142	21.32013	.52875	-1.97332	0.	0.	0.
143	21.32013	1.44457	-1.44457	0.	0.	0.
144	21.32013	1.97332	-.52875	0.	0.	0.

** SPECPR **

VELOCITIES AND BERNOULLI PRESSURES AT CONTROL POINTS IMMEDIATELY ABOVE AND BELOW FIN SURFACE *** STEP 4

J	X(J)	Y(J)	Z(J)	UTOTA	VTOTA	WTOTA	PRESSA	UTOTB	VTOTB	WTOTB	PRESSB
1	5.695119	2.859255	0.000000	.140266	-.140094	-.258819	-.164315	-.139897	.140068	-.258819	.463890
2	10.906555	2.859255	0.000000	.092677	-.069396	-.258819	-.102754	-.092355	.069378	-.258819	.328842
3	16.117992	2.859255	0.000000	.085936	-.042903	-.258819	-.091160	-.085652	.042890	-.258819	.312414
4	21.329428	2.859255	0.000000	.082224	-.020530	-.258819	-.084647	-.081971	.020519	-.258819	.303079
5	6.843413	4.365214	0.000000	.147087	-.146945	-.258819	-.170963	-.146725	.146867	-.258819	.484599
6	11.678359	4.365214	0.000000	.103991	-.077904	-.258819	-.118531	-.103671	.077842	-.258819	.364399
7	16.513306	4.365214	0.000000	.089994	-.044950	-.258819	-.097137	-.089711	.044902	-.258819	.325389
8	21.348253	4.365214	0.000000	.084721	-.021169	-.258819	-.088397	-.084466	.021128	-.258819	.311128
9	7.991615	5.871053	0.000000	.143603	-.143483	-.258819	-.167627	-.143246	.143365	-.258819	.474068
10	12.450102	5.871053	0.000000	.121491	-.091048	-.258819	-.140476	-.121172	.090949	-.258819	.420873
11	16.908589	5.871053	0.000000	.096968	-.048453	-.258819	-.107031	-.096683	.048373	-.258819	.348004
12	21.367076	5.871053	0.000000	.081758	-.020441	-.258819	-.083941	-.081500	.020374	-.258819	.301572
13	9.139701	7.376740	0.000000	.138917	-.138816	-.258819	-.162956	-.138563	.138663	-.258819	.459895
14	13.221767	7.376740	0.000000	.133074	-.099751	-.258819	-.153394	-.132755	.099620	-.258819	.459144
15	17.303832	7.376740	0.000000	.103745	-.051857	-.258819	-.116196	-.103455	.051743	-.258819	.370365
16	21.385897	7.376740	0.000000	.070087	-.017536	-.258819	-.065544	-.069825	.017442	-.258819	.264809
17	10.287635	8.882227	0.000000	.134870	-.134787	-.258819	-.158751	-.134516	.134599	-.258819	.447660
18	13.993329	8.882227	0.000000	.131009	-.098218	-.258819	-.151185	-.130687	.098055	-.258819	.452273
19	17.699022	8.882227	0.000000	.095942	-.047969	-.258819	-.105608	-.095648	.047826	-.258819	.344627
20	21.404715	8.882227	0.000000	.057964	-.014519	-.258819	-.044988	-.057696	.014396	-.258819	.228080
21	11.435366	10.387447	0.000000	.128314	-.128247	-.258819	-.151598	-.127960	.128027	-.258819	.427864
22	14.764754	10.387447	0.000000	.089457	-.067068	-.258819	-.098041	-.089132	.066874	-.258819	.318885
23	18.094142	10.387447	0.000000	.066760	-.033391	-.258819	-.060722	-.066460	.033219	-.258819	.253058
24	21.423531	10.387447	0.000000	.044655	-.011206	-.258819	-.020693	-.044378	.011053	-.258819	.189495
25	5.695119	-2.859255	0.000000	.140266	.140100	-.258819	-.164315	-.139897	-.140062	-.258819	.463888
26	10.906555	-2.859255	0.000000	.092679	.069405	-.258819	-.102757	-.092353	-.069370	-.258819	.328834
27	16.117992	-2.859255	0.000000	.085939	.042912	-.258819	-.091165	-.085649	-.042881	-.258819	.312404
28	21.329428	-2.859255	0.000000	.082226	.020538	-.258819	-.084650	-.081968	-.020511	-.258819	.303070
29	6.843413	-4.365214	0.000000	.147087	.146947	-.258819	-.170963	-.146725	-.146865	-.258819	.484594
30	11.678359	-4.365214	0.000000	.103992	.077909	-.258819	-.118532	-.103670	-.077837	-.258819	.364393
31	16.513306	-4.365214	0.000000	.089997	.044959	-.258819	-.097142	-.089707	-.044893	-.258819	.325377
32	21.348253	-4.365214	0.000000	.084723	.021176	-.258819	-.088401	-.084464	-.021120	-.258819	.311119
33	7.991615	-5.871053	0.000000	.143603	.143484	-.258819	-.167627	-.143246	-.143364	-.258819	.474063
34	12.450102	-5.871053	0.000000	.121491	.091050	-.258819	-.140476	-.121172	-.090947	-.258819	.420869
35	16.908589	-5.871053	0.000000	.096970	.048459	-.258819	-.107035	-.096680	-.048366	-.258819	.347995
36	21.367076	-5.871053	0.000000	.081761	.020448	-.258819	-.083945	-.081498	-.020366	-.258819	.301563
37	9.139701	-7.376740	0.000000	.138917	.138817	-.258819	-.162955	-.138563	-.138662	-.258819	.459890
38	13.221767	-7.376740	0.000000	.133074	.099753	-.258819	-.153394	-.132754	-.099619	-.258819	.459140
39	17.303832	-7.376740	0.000000	.103745	.051858	-.258819	-.116196	-.103455	-.051742	-.258819	.370363
40	21.385897	-7.376740	0.000000	.070089	.017543	-.258819	-.065548	-.069822	-.017435	-.258819	.264800
41	10.287635	-8.882227	0.000000	.134870	.134787	-.258819	-.158750	-.134516	-.134599	-.258819	.447655
42	13.993329	-8.882227	0.000000	.131009	.098218	-.258819	-.151184	-.130687	-.098054	-.258819	.452270
43	17.699022	-8.882227	0.000000	.095942	.047969	-.258819	-.105607	-.095648	-.047825	-.258819	.344625
44	21.404715	-8.882227	0.000000	.057966	.014522	-.258819	-.044990	-.057695	-.014393	-.258819	.228076
45	11.435366	-10.387447	0.000000	.128314	.128247	-.258819	-.151597	-.127960	-.128027	-.258819	.427859
46	14.764754	-10.387447	0.000000	.089457	.067068	-.258819	-.098040	-.089132	-.066874	-.258819	.318883
47	18.094142	-10.387447	0.000000	.066760	.033391	-.258819	-.060721	-.066460	-.033219	-.258819	.253057
48	21.423531	-10.387447	0.000000	.044655	.011207	-.258819	-.020694	-.044378	-.011052	-.258819	.189494
49	5.695119	0.000000	2.859255	.005733	.000005	-.158504	.049190	.005728	.000005	-.158499	.049200
50	10.906555	0.000000	2.859255	.062902	.000005	-.238471	-.053678	.062899	.000005	-.238469	-.053673
51	16.117992	0.000000	2.859255	.087578	.000005	-.263486	-.092296	.087575	.000005	-.263485	-.092292
52	21.329428	0.000000	2.859255	.079211	.000005	-.234664	-.080183	.079209	.000005	-.234663	-.080179
53	6.843413	0.000000	4.365214	.006142	.000005	-.076069	.022432	.006137	.000005	-.076064	.022441
54	11.678359	0.000000	4.365214	.035437	.000005	-.133235	-.017971	.035434	.000005	-.133232	-.017965
55	16.513306	0.000000	4.365214	.102836	.000005	-.269206	-.113448	.102833	.000005	-.269204	-.113444
56	21.348253	0.000000	4.365214	.081837	.000005	-.226378	-.084517	.081834	.000005	-.226378	-.084513
57	7.991615	0.000000	5.871053	.000111	.000005	-.033633	.016471	.000106	.000005	-.033628	.016479

ORIGINAL PAGE IS
OF POOR QUALITY

58	12.450102	0.000000	5.871053	.003535	.000005	-.042908	.013817	.003531	.000005	-.042905	.013823
59	16.908589	0.000000	5.871053	.069600	.000005	-.184850	-.068785	.069597	.000005	-.184848	-.068780
60	21.367076	0.000000	5.871053	.083330	.000005	-.217744	-.087208	.083328	.000005	-.217743	-.087204
61	9.139701	0.000000	7.376740	.000098	.000005	-.021174	.010491	.000093	.000005	-.021170	.010498
62	13.221767	0.000000	7.376740	.005119	.000005	-.033095	.006180	.005114	.000005	-.033092	.006187
63	17.303832	0.000000	7.376740	.002969	.000005	-.028576	.008338	.002965	.000005	-.028574	.008344
64	21.385897	0.000000	7.376740	.080494	.000005	-.201760	-.084079	.080492	.000005	-.201759	-.084075
65	10.287635	0.000000	8.882227	.000085	.000005	-.014500	.007211	.000081	.000005	-.014496	.007217
66	13.993329	0.000000	8.882227	.000079	.000005	-.014523	.007235	.000075	.000005	-.014520	.007241
67	17.699022	0.000000	8.882227	.004670	.000005	-.025587	.003565	.004667	.000005	-.025585	.003571
68	21.404715	0.000000	8.882227	.032419	.000005	-.087629	-.024959	.032417	.000005	-.087628	-.024956
69	11.435366	0.000000	10.387447	.000074	.000005	-.010516	.005232	.000070	.000005	-.010512	.005238
70	14.764754	0.000000	10.387447	.000068	.000005	-.010534	.005253	.000065	.000005	-.010531	.005258
71	18.094142	0.000000	10.387447	.000064	.000005	-.010553	.005271	.000062	.000005	-.010551	.005274
72	21.423531	0.000000	10.387447	.004447	.000005	-.021076	.001861	.004445	.000005	-.021076	.001864
73	5.695119	0.000000	-2.859255	-.005359	.000005	-.158467	.074606	-.005364	.000005	-.158472	.074619
74	10.906555	0.000000	-2.859255	-.062575	.000005	-.238442	.242386	-.062578	.000005	-.238444	.242396
75	16.117992	0.000000	-2.859255	-.087288	.000005	-.263462	.321153	-.087291	.000005	-.263464	.321162
76	21.329428	0.000000	-2.859255	-.078953	.000005	-.234644	.293082	-.078956	.000005	-.234645	.293091
77	6.843413	0.000000	-4.365214	-.005775	.000005	-.075984	.047889	-.005780	.000005	-.075989	.047903
78	11.678359	0.000000	-4.365214	-.035113	.000005	-.133165	.141106	-.035117	.000005	-.133168	.141116
79	16.513306	0.000000	-4.365214	-.102547	.000005	-.269147	.372363	-.102550	.000005	-.269149	.372374
80	21.348253	0.000000	-4.365214	-.081577	.000005	-.226329	.300650	-.081579	.000005	-.226330	.300659
81	7.991615	0.000000	-5.871053	.000250	.000005	-.033509	.016130	.000246	.000005	-.033514	.016141
82	12.450102	0.000000	-5.871053	-.003212	.000005	-.042804	.027636	-.003216	.000005	-.042807	.027646
83	16.908589	0.000000	-5.871053	-.069309	.000005	-.184762	.254312	-.069313	.000005	-.184763	.254323
84	21.367076	0.000000	-5.871053	-.083067	.000005	-.217669	.304296	-.083070	.000005	-.217669	.304305
85	9.139701	0.000000	-7.376740	.000261	.000005	-.021015	.010088	.000256	.000005	-.021020	.010099
86	13.221767	0.000000	-7.376740	-.004795	.000005	-.032959	.026224	-.004799	.000005	-.032962	.026234
87	17.303832	0.000000	-7.376740	-.002675	.000005	-.028459	.019658	-.002679	.000005	-.028461	.019666
88	21.385897	0.000000	-7.376740	-.080227	.000005	-.201659	.292318	-.080230	.000005	-.201660	.292326
89	10.287635	0.000000	-8.882227	.000272	.000005	-.014308	.006745	.000268	.000005	-.014313	.006756
90	13.993329	0.000000	-8.882227	.000247	.000005	-.014356	.006819	.000243	.000005	-.014359	.006829
91	17.699022	0.000000	-8.882227	-.004373	.000005	-.025442	.021647	-.004377	.000005	-.025444	.021654
92	21.404715	0.000000	-8.882227	-.032147	.000005	-.087502	.114885	-.032149	.000005	-.087502	.114890
93	11.435366	0.000000	-10.387447	.000284	.000005	-.010292	.004706	.000280	.000005	-.010296	.004716
94	14.764754	0.000000	-10.387447	.000260	.000005	-.010337	.004777	.000257	.000005	-.010339	.004784
95	18.094142	0.000000	-10.387447	.000238	.000005	-.010379	.004841	.000236	.000005	-.010380	.004846
96	21.423531	0.000000	-10.387447	-.004168	.000005	-.020922	.018964	-.004170	.000005	-.020922	.018968

PRESSURE LOADINGS AT CONTROL POINTS

J	X(J)	Y(J)	Z(J)	DELTP.LIN.	DELTP.BERN.
1	5.695119	2.859255	0.000000	.560325	.628205
2	10.906555	2.859255	0.000000	.370065	.431596
3	16.117992	2.859255	0.000000	.343175	.403574
4	21.329428	2.859255	0.000000	.328388	.387725
5	6.843413	4.365214	0.000000	.587624	.655562
6	11.678359	4.365214	0.000000	.415323	.482929
7	16.513306	4.365214	0.000000	.359409	.422526
8	21.348253	4.365214	0.000000	.338374	.399524
9	7.991615	5.871053	0.000000	.573698	.641696
10	12.450102	5.871053	0.000000	.485326	.561349
11	16.908589	5.871053	0.000000	.387300	.455035
12	21.367076	5.871053	0.000000	.326516	.385513
13	9.139701	7.376740	0.000000	.554959	.622851
14	13.221767	7.376740	0.000000	.531657	.612538
15	17.303832	7.376740	0.000000	.414400	.486561
16	21.385897	7.376740	0.000000	.279823	.330352
17	10.287635	8.882227	0.000000	.538772	.606411
18	13.993329	8.882227	0.000000	.523393	.603458
19	17.699022	8.882227	0.000000	.383179	.450234
20	21.404715	8.882227	0.000000	.231320	.273068
21	11.435366	10.387447	0.000000	.512548	.579462
22	14.764754	10.387447	0.000000	.357178	.416926
23	18.094142	10.387447	0.000000	.266440	.313780
24	21.423531	10.387447	0.000000	.178067	.210188
25	5.695119	-2.859255	0.000000	.560325	.628202
26	10.906555	-2.859255	0.000000	.370065	.431591
27	16.117992	-2.859255	0.000000	.343175	.403569
28	21.329428	-2.859255	0.000000	.328388	.387721
29	6.843413	-4.365214	0.000000	.587624	.655557
30	11.678359	-4.365214	0.000000	.415323	.482925
31	16.513306	-4.365214	0.000000	.359409	.422520
32	21.348253	-4.365214	0.000000	.338374	.399519
33	7.991615	-5.871053	0.000000	.573698	.641690
34	12.450102	-5.871053	0.000000	.485326	.561345
35	16.908589	-5.871053	0.000000	.387300	.455030
36	21.367076	-5.871053	0.000000	.326516	.385508
37	9.139701	-7.376740	0.000000	.554959	.622845
38	13.221767	-7.376740	0.000000	.531657	.612534
39	17.303832	-7.376740	0.000000	.414400	.486558
40	21.385897	-7.376740	0.000000	.279823	.330348
41	10.287635	-8.882227	0.000000	.538772	.606405
42	13.993329	-8.882227	0.000000	.523393	.603454
43	17.699022	-8.882227	0.000000	.383179	.450232
44	21.404715	-8.882227	0.000000	.231320	.273066
45	11.435366	-10.387447	0.000000	.512548	.579456
46	14.764754	-10.387447	0.000000	.357178	.416923
47	18.094142	-10.387447	0.000000	.266440	.313778
48	21.423531	-10.387447	0.000000	.178067	.210187
49	5.695119	0.000000	2.859255	.000010	.000010
50	10.906555	0.000000	2.859255	.000006	.000005
51	16.117992	0.000000	2.859255	.000006	.000004
52	21.329428	0.000000	2.859255	.000005	.000004
53	6.843413	0.000000	4.365214	.000010	.000009
54	11.678359	0.000000	4.365214	.000007	.000006
55	16.513306	0.000000	4.365214	.000006	.000004
56	21.348253	0.000000	4.365214	.000006	.000004
57	7.991615	0.000000	5.871053	.000009	.000007
58	12.450102	0.000000	5.871053	.000008	.000007
59	16.908589	0.000000	5.871053	.000006	.000005
60	21.367076	0.000000	5.871053	.000005	.000004
61	9.139701	0.000000	7.376740	.000009	.000007
62	13.221767	0.000000	7.376740	.000009	.000007
63	17.303832	0.000000	7.376740	.000007	.000006
64	21.385897	0.000000	7.376740	.000005	.000003
65	10.287635	0.000000	8.882227	.000009	.000007
66	13.993329	0.000000	8.882227	.000009	.000007
67	17.699022	0.000000	8.882227	.000006	.000006
68	21.404715	0.000000	8.882227	.000004	.000003
69	11.435366	0.000000	10.387447	.000009	.000006
70	14.764754	0.000000	10.387447	.000006	.000005
71	18.094142	0.000000	10.387447	.000004	.000004
72	21.423531	0.000000	10.387447	.000003	.000003
73	5.695119	0.000000	-2.859255	.000010	.000013
74	10.906555	0.000000	-2.859255	.000006	.000010
75	16.117992	0.000000	-2.859255	.000006	.000009
76	21.329428	0.000000	-2.859255	.000005	.000009
77	6.843413	0.000000	-4.365214	.000010	.000013
78	11.678359	0.000000	-4.365214	.000007	.000010
79	16.513306	0.000000	-4.365214	.000006	.000010
80	21.348253	0.000000	-4.365214	.000006	.000009
81	7.991615	0.000000	-5.871053	.000009	.000012
82	12.450102	0.000000	-5.871053	.000008	.000010
83	16.908589	0.000000	-5.871053	.000006	.000010
84	21.367076	0.000000	-5.871053	.000005	.000009
85	9.139701	0.000000	-7.376740	.000009	.000011
86	13.221767	0.000000	-7.376740	.000009	.000011
87	17.303832	0.000000	-7.376740	.000007	.000008
88	21.385897	0.000000	-7.376740	.000005	.000008
89	10.287635	0.000000	-8.882227	.000009	.000011
90	13.993329	0.000000	-8.882227	.000009	.000010
91	17.699022	0.000000	-8.882227	.000006	.000007
92	21.404715	0.000000	-8.882227	.000004	.000005
93	11.435366	0.000000	-10.387447	.000009	.000010
94	14.764754	0.000000	-10.387447	.000006	.000007
95	18.094142	0.000000	-10.387447	.000004	.000005
96	21.423531	0.000000	-10.387447	.000003	.000003

FIN LOADING INFORMATION

*** STEP 4

MACH NUMBER =	.25000E+01
ANGLE OF ATTACK =	15.000 DEGREES
SIDE SLIP ANGLE =	.000 DEGREES
FIN AREA =	154.31280
REFERENCE AREA =	14.12000
REFERENCE LENGTH =	4.23000
EXPOSED FIN SPAN B/2=	9.04000
MOMENT CENTER: XM =	46.04000
ZM =	0.00000

LINEAR PRESSURE (U/VINF) LOADS IN BODY SYSTEM

	TOTAL	FIN 1 OR R	FIN 2 OR L	FIN 3 OR U	FIN 4 OR D	INTERF. SHELL
DEFL. ANGLE DEG. =		0.00000	0.00000	0.00000	0.00000	
CTHR =	.19363	.96815E-01	.96815E-01	.27469E-10	.27469E-10	
CZ =	9.0285	4.5143	4.5143	0.	0.	1.5129
CY =	-.15083E-03	0.	0.	-.75414E-04	-.75414E-04	-.25725E-04
CM =	-98.932	-49.466	-49.466	0.	0.	-16.953
CLN =	.16519E-02	0.	0.	.82593E-03	.82593E-03	.28780E-03
CLL =	.71452E-13	-6.5648	6.5648	-.10922E-03	.10922E-03	.34202E-15

FOLLOWING ARE IN UNROLLED BODY-AXIS COORDINATE SYSTEM

CZU =	9.0285	4.5143	4.5143	.13162E-08	.13162E-08	1.5129
CYU =	.67486E-05	.78789E-04	.78789E-04	-.75414E-04	-.75414E-04	.68036E-06
CMU =	-98.932	-49.466	-49.466	-.14415E-07	-.14415E-07	-16.953
CLNU =	-.74842E-04	-.86335E-03	-.86335E-03	.82593E-03	.82593E-03	-.80887E-05

NOTE: L.E. OF LEAD PANEL IN FIRST CHORDWISE ROW IS SUPERSONIC

SPANWISE DISTRIBUTIONS

-------------------UPPFR RIGHT OR RIGHT HORIZONTAL FIN--------------------

I	Y/(B/2)	CN*C/(2*B)	CT*C/(2*B)	CY1*C/(2*B)	CYTOT*C/(2*B)	CS*C/(2*B)	CSINT	YBAR	GAMNET(I)	GAMMA.LE/VINF	XLE
1	.08233	.23078	0.00000	0.00000	.00084	0.00000	0.00000	0.00000	-4.17424	0.00000	.74425
2	.24892	.22729	0.00000	0.00000	.00202	0.00000	0.00000	0.00000	.06277	0.00000	2.25021
3	.41549	.21846	0.00000	0.00000	.00331	0.00000	0.00000	0.00000	.15938	0.00000	3.75605
4	.58205	.20089	0.00000	0.00000	.00439	0.00000	0.00000	0.00000	.31734	0.00000	5.26174
5	.74859	.17168	0.00000	0.00000	.00513	0.00000	0.00000	0.00000	.52815	0.00000	6.76723
6	.91509	.12088	0.00000	0.00000	0.00000	0.00000	0.00000	0.00000	.91881	0.00000	8.27245
7	1.00000	0.00000							2.18780		

THRUST- AND SIDE-FORCE COEFFICIENTS IN PLANE OF THE FIN

SUMFX =CX..ACTS ON LEADING EDGE
SUMFY1=CY..ACTS ON LEADING EDGE
SUMFY2=CY..ACTS ON LEADING AND SIDE EDGE
SUMFT2=CY..ACTS ON SIDE EDGE

SUMFX = 0.
SUMFY1 = 0.
SUMFY2 = .60527E-01
SUMFT2 = .36408E+00

SIDE EDGE DISTRIBUTION

JTIP	JSE	DISTANCE FROM LE /TIPCHORD	SUCTION FORCE PER UNIT LENGTH /(Q*TIPCHORD)	GAMMA.SE /VINF	YBAR	XSE
1	1	.25000	.00078	.00165	9.04000	9.04000
2	2	.50000	.02282	.04965	9.04000	12.17750
3	3	.75000	.05391	.16305	9.04000	15.31500
4	4	1.00000	.05305	.27465	9.04000	18.45250

S.E. AUGMENTATION OF FIN NORMAL FORCE FROM SUCTION CONVERSION IN PROPORTION WITH FACTOR
KVSE = 1.000

(LOCAL FIN)		(ROLLED BODY-AXIS)		(UNROLLED BODY-AXIS)	
CNADD =	.36408	CYADD =	0.00000	CYADD =	.00001
		CZADD =	.36408	CZADD =	.36408
		CMADD =	-4.30397	CMADD =	-4.30395
		CLNADD =	0.00000	CLNADD =	-.00008

CLLADD	= -.96012		CLLADD	= -.96012
XCG	= 96.0450		XCG	= 96.0450
YCG	= 11.1550		YCG	= 11.1550
ZCG	= 0.0000		ZCG	= -.0002

**** T.E. FIN VORTICITY DUE TO SIDE-EDGE FORCE AUGMENTATION

IVRT	GAMMA/VINF	Y.C.G. (LOCAL FIN)	Z.C.G. (LOCAL FIN)	Y.C.G. (BODY AXES)	Z.C.G. (BODY AXES)
1	.27465	9.04000	1.65224	11.15500	1.65224

------------------LOWER LEFT OR LEFT HORIZONTAL FIN--------------------

I	Y/(B/2)	CN*C/(2*B)	CT*C/(2*B)	CY1*C/(2*B)	CYTOT*C/(2*B)	CS*C/(2*B)	CSINT	YBAR	GAMNET(I)	GAMMA,LE/VINF	XLE
8	-.08233	.23078	0.00000	0.00000	-.00084	0.00000	0.00000	0.00000	4.17424	0.00000	.74425
9	-.24892	.22729	0.00000	0.00000	-.00202	0.00000	0.00000	0.00000	-.06277	0.00000	2.25021
10	-.41549	.21846	0.00000	0.00000	-.00331	0.00000	0.00000	0.00000	-.15938	0.00000	3.75605
11	-.58205	.20089	0.00000	0.00000	-.00439	0.00000	0.00000	0.00000	-.31734	0.00000	5.26174
12	-.74859	.17168	0.00000	0.00000	-.00513	0.00000	0.00000	0.00000	-.52815	0.00000	6.76723
13	-.91509	.12088	0.00000	0.00000	0.00000	0.00000	0.00000	0.00000	-.91881	0.00000	8.27245
14	-1.00000	0.00000							-2.18780		

THRUST- AND SIDE-FORCE COEFFICIENTS IN PLANE OF THE FIN

SUMFX =CX..ACTS ON LEADING EDGE
SUMFY1=CY..ACTS ON LEADING EDGE
SUMFY2=CY..ACTS ON LEADING AND SIDE EDGE
SUMFT2=CY..ACTS ON SIDE EDGE

SUMFX = 0.
SUMFY1 = 0.
SUMFY2 = -.60527E-01
SUMFT2 = -.36408E+00

SIDE EDGE DISTRIBUTION

JTIP	JSE	DISTANCE FROM LE /TIPCHORD	SUCTION FORCE PER UNIT LENGTH /(Q*TIPCHORD)	GAMMA,SE /VINF	YBAR	XSE
1	5	.25000	-.00078	-.00165	-9.04000	9.04000
2	6	.50000	-.02282	-.04965	-9.04000	12.17750
3	7	.75000	-.05391	-.16305	-9.04000	15.31500
4	8	1.00000	-.05305	-.27465	-9.04000	18.45250

```
S.F. AUGMENTATION OF FIN NORMAL FORCE FROM SUCTION CONVERSION IN PROPORTION WITH FACTOR
                                   KVSE =  1.000

 (LOCAL FIN)                     (ROLLED BODY-AXIS)           (UNROLLED BODY-AXIS)
CNADD   =     .36408              CYADD    =   0.00000          CYADD    =     .00001
                                  CZADD    =    .36408          CZADD    =    .36408
                                  CMADD    =  -4.30397          CMADD    =  -4.30395
                                 CLNADD    =   0.00000         CLNADD    =   -.00008
                                 CLLADD    =    .96012         CLLADD    =    .96012
                                    XCG    =   96.0450            XCG    =   96.0450
                                    YCG    =  -11.1550            YCG    =  -11.1550
                                    ZCG    =     -.0000           ZCG    =     .0002


**** T.E. FIN VORTICITY DUE TO SIDE-EDGE FORCE AUGMENTATION

       IVRT   GAMMA/VINF    Y.C.G.        Z.C.G.       Y.C.G.        Z.C.G.
                                 (LOCAL FIN)                (BODY AXES)
        2      -.27465    -9.04000      1.65224    -11.15500      1.65224



-------------------LOWER RIGHT OR UPPER VERTICAL FIN--------------------
```

I	Y/(B/2)	CN*C/(2*B)	CT*C/(2*B)	CY1*C/(2*B)	CYTOT*C/(2*B)	CS*C/(2*B)	CSINT	YBAR	GAMNET(I)	GAMMA,LE/VINF	XLE
15	.08233	.00000	0.00000	0.00000	.00000	0.00000	0.00000	0.00000	-.00007	0.00000	.74425
16	.24892	.00000	0.00000	0.00000	-.00000	0.00000	0.00000	0.00000	.00000	0.00000	2.25021
17	.41549	.00000	0.00000	0.00000	.00000	0.00000	0.00000	0.00000	.00000	0.00000	3.75605
18	.58205	.00000	0.00000	0.00000	.00000	0.00000	0.00000	0.00000	.00001	0.00000	5.26174
19	.74859	.00000	0.00000	0.00000	.00000	0.00000	0.00000	0.00000	.00001	0.00000	6.76723
20	.91509	.00000	0.00000	0.00000	0.00000	0.00000	0.00000	0.00000	.00002	0.00000	8.27245
21	1.00000	0.00000							.00004		

```
   THRUST- AND SIDE-FORCE COEFFICIENTS IN PLANE OF THE FIN

   SUMFX =CX..ACTS ON LEADING EDGE
   SUMFY1=CY..ACTS ON LEADING EDGE
   SUMFY2=CY..ACTS ON LEADING AND SIDE EDGE
   SUMFT2=CY..ACTS ON SIDE EDGE


        SUMFX  =  0.
        SUMFY1 =  0.
        SUMFY2 =   .14602E-10
        SUMFT2 =   .10179E-09


        SIDE EDGE DISTRIBUTION

JTIP  JSE  DISTANCE        SUCTION FORCE       GAMMA,SE      YBAR       XSE
           FROM LE         PER UNIT LENGTH     /VINF
           /TIPCHORD       /(Q*TIPCHORD)
```

1	9	.25000	.00000	0.00000	0.00000	9.04000
2	10	.50000	.00000	0.00000	0.00000	12.17750
3	11	.75000	.00000	0.00000	0.00000	15.31500
4	12	1.00000	.00000	0.00000	0.00000	18.45250

------------------UPPER LEFT OR LOWER VERTICAL FIN--------------------

I	Y/(B/2)	CN*C/(2*B)	CT*C/(2*B)	CY1*C/(2*B)	CYTOT*C/(2*B)	CS*C/(2*B)	CSINT	YBAR	GAMNET(I)	GAMMA,LE/VINF	XLE
22	-.08233	.00000	0.00000	0.00000	-.00000	0.00000	0.00000	0.00000	.00007	0.00000	.74425
23	-.24892	.00000	0.00000	0.00000	.00000	0.00000	0.00000	0.00000	-.00000	0.00000	2.25021
24	-.41549	.00000	0.00000	0.00000	-.00000	0.00000	0.00000	0.00000	-.00000	0.00000	3.75605
25	-.58205	.00000	0.00000	0.00000	-.00000	0.00000	0.00000	0.00000	-.00001	0.00000	5.26174
26	-.74859	.00000	0.00000	0.00000	-.00000	0.00000	0.00000	0.00000	-.00001	0.00000	6.76723
27	-.91509	.00000	0.00000	0.00000	0.00000	0.00000	0.00000	0.00000	-.00002	0.00000	8.27245
28	-1.00000	0.00000							-.00004		

THRUST- AND SIDE-FORCE COEFFICIENTS IN PLANE OF THE FIN

SUMFX =CX..ACTS ON LEADING EDGE
SUMFY1=CY..ACTS ON LEADING EDGE
SUMFY2=CY..ACTS ON LEADING AND SIDE EDGE
SUMFT2=CY..ACTS ON SIDE EDGE

SUMFX = 0.
SUMFY1 = 0.
SUMFY2 = -.14602E-10
SUMFT2 = -.10179E-09

SIDE EDGE DISTRIBUTION

JTIP	JSE	DISTANCE FROM LE /TIPCHORD	SUCTION FORCE PER UNIT LENGTH /(Q*TIPCHORD)	GAMMA,SE /VINF	YBAR	XSE
1	13	.25000	-.00000	0.00000	0.00000	9.04000
2	14	.50000	-.00000	0.00000	0.00000	12.17750
3	15	.75000	-.00000	0.00000	0.00000	15.31500
4	16	1.00000	-.00000	0.00000	0.00000	18.45250

*** STEP 4

FIN LOADING INFORMATION

MACH NUMBER =	.25000E+01
ANGLE OF ATTACK =	15.000 DEGREES
SIDE SLIP ANGLE =	.000 DEGREES
FIN AREA =	154.31280
REFERENCE AREA =	14.12000
REFERENCE LENGTH =	4.23000
EXPOSED FIN SPAN B/2=	9.04000
MOMENT CENTER: XM =	46.04000
ZM =	0.00000

BERNOULLI PRESSURE LOADS IN BODY SYSTEM

	TOTAL	FIN 1 OR R	FIN 2 OR L	FIN 3 OR U	FIN 4 OR D	INTERF. SHELL
DEFL. ANGLE DEG. =		0.00000	0.00000	0.00000	0.00000	
CTHR =	.19363	.96815E-01	.96815E-01	.27469E-10	.27469E-10	
CZ =	10.416	5.2081	5.2080	0.	0.	1.5129
CY =	-.16347E-03	0.	0.	-.60925E-04	-.10255E-03	-.25725E-04
CM =	-114.38	-57.188	-57.187	0.	0.	-16.953
CLN =	.17940E-02	0.	0.	.66454E-03	.11294E-02	.28780E-03
CLL =	-.10219E-04	-7.5738	7.5738	-.87655E-04	.14329E-03	.34202E-15

FOLLOWING ARE IN UNROLLED BODY-AXIS COORDINATE SYSTEM

CZU =	10.416	5.2081	5.2080	.10633E-08	.17898E-08	1.5129
CYU =	.18323E-04	.90898E-04	.90898E-04	-.60925E-04	-.10255E-03	.68036E-06
CMU =	-114.38	-57.188	-57.187	-.11598E-07	-.19712E-07	-16.953
CLNU =	-.20225E-03	-.99812E-03	-.99811E-03	.66454E-03	.11294E-02	-.80887E-05

NOTE: L.E. OF LEAD PANEL IN FIRST CHORDWISE ROW IS SUPERSONIC

SPANWISE DISTRIBUTIONS

------------------UPPER RIGHT OR RIGHT HORIZONTAL FIN--------------------

I	Y/(B/2)	CN*C/(2*B)	CT*C/(2*B)	CY1*C/(2*B)	CYTOT*C/(2*B)	CS*C/(2*B)	CSINT	YBAR	GAMNET(I)	GAMMA,LE/VINF	XLE
1	.08233	.26667	0.00000	0.00000	.00084	0.00000	0.00000	0.00000	-4.17424	0.00000	.74425
2	.24892	.26201	0.00000	0.00000	.00202	0.00000	0.00000	0.00000	.06277	0.00000	2.25021
3	.41549	.25182	0.00000	0.00000	.00331	0.00000	0.00000	0.00000	.15938	0.00000	3.75605
4	.58205	.23152	0.00000	0.00000	.00439	0.00000	0.00000	0.00000	.31734	0.00000	5.26174
5	.74859	.19794	0.00000	0.00000	.00513	0.00000	0.00000	0.00000	.52815	0.00000	6.76723
6	.91509	.13984	0.00000	0.00000	0.00000	0.00000	0.00000	0.00000	.91881	0.00000	8.27245
7	1.00000	0.00000							2.18780		

THRUST- AND SIDE-FORCE COEFFICIENTS IN PLANE OF THE FIN

SUMFX =CX..ACTS ON LEADING EDGE
SUMFY1=CY..ACTS ON LEADING EDGE
SUMFY2=CY..ACTS ON LEADING AND SIDE EDGE
SUMFT2=CY..ACTS ON SIDE EDGE

SUMFX = 0.
SUMFY1 = 0.
SUMFY2 = .60527E-01
SUMFT2 = .36408E+00

SIDE EDGE DISTRIBUTION

JTIP	JSE	DISTANCE FROM LE /TIPCHORD	SUCTION FORCE PER UNIT LENGTH /(Q*TIPCHORD)	GAMMA,SE /VINF	YBAR	XSE
1	1	.25000	.00078	.00165	9.04000	9.04000
2	2	.50000	.02282	.04965	9.04000	12.17750
3	3	.75000	.05391	.16305	9.04000	15.31500
4	4	1.00000	.05305	.27465	9.04000	18.45250

****T.E. FIN VORTICITY DUE TO ATTACHED FLOW*****

IVRT	GAMMA/VINF	Y.C.G. (LOCAL FIN)	Y.C.G. (BODY AXES)	Z.C.G.
3	4.82135	7.62633	9.74133	0.00000

--------------------LOWER LEFT OR LEFT HORIZONTAL FIN--------------------

I	Y/(B/2)	CN*C/(2*B)	CT*C/(2*B)	CY1*C/(2*B)	CYTOT*C/(2*B)	CS*C/(2*B)	CSINT	YBAR	GAMNET(I)	GAMMA,LE/VINF	XLE
8	-.08233	.26666	0.00000	0.00000	-.00084	0.00000	0.00000	0.00000	4.17424	0.00000	.74425
9	-.24892	.26201	0.00000	0.00000	-.00202	0.00000	0.00000	0.00000	-.06277	0.00000	2.25021
10	-.41549	.25182	0.00000	0.00000	-.00331	0.00000	0.00000	0.00000	-.15938	0.00000	3.75605
11	-.58205	.23152	0.00000	0.00000	-.00439	0.00000	0.00000	0.00000	-.31734	0.00000	5.26174
12	-.74859	.19794	0.00000	0.00000	-.00513	0.00000	0.00000	0.00000	-.52815	0.00000	6.76723
13	-.91509	.13983	0.00000	0.00000	0.00000	0.00000	0.00000	0.00000	-.91881	0.00000	8.27245
14	-1.00000	0.00000							-2.18780		

THRUST- AND SIDE-FORCE COEFFICIENTS IN PLANE OF THE FIN

SUMFX =CX..ACTS ON LEADING EDGE
SUMFY1=CY..ACTS ON LEADING EDGE
SUMFY2=CY..ACTS ON LEADING AND SIDE EDGE
SUMFT2=CY..ACTS ON SIDE EDGE

SUMFX = 0.
SUMFY1 = 0.
SUMFY2 = -.60527E-01
SUMFT2 = -.36408E+00

SIDE EDGE DISTRIBUTION

JTIP	JSE	DISTANCE FROM LE /TIPCHORD	SUCTION FORCE PER UNIT LENGTH /(Q*TIPCHORD)	GAMMA,SE /VINF	YBAR	XSE
1	5	.25000	-.00078	-.00165	-9.04000	9.04000
2	6	.50000	-.02282	-.04965	-9.04000	12.17750
3	7	.75000	-.05391	-.16305	-9.04000	15.31500
4	8	1.00000	-.05305	-.27465	-9.04000	18.45250

****T.E. FIN VORTICITY DUE TO ATTACHED FLOW*****

IVRT	GAMMA/VINF	Y.C.G. (LOCAL FIN)	Y.C.G. (BODY AXES)	Z.C.G. (BODY AXES)
4	-4.82130	-7.62633	-9.74133	-.00000

--------------------LOWER RIGHT OR UPPER VERTICAL FIN--------------------

I	Y/(B/2)	CN*C/(2*B)	CT*C/(2*B)	CY1*C/(2*B)	CYTOT*C/(2*B)	CS*C/(2*B)	CSINT	YBAR	GAMNET(I)	GAMMA,LE/VINF	XLE
15	.08233	.00000	0.00000	0.00000	.00000	0.00000	0.00000	0.00000	-.00007	0.00000	.74425
16	.24892	.00000	0.00000	0.00000	-.00000	0.00000	0.00000	0.00000	.00000	0.00000	2.25021
17	.41549	.00000	0.00000	0.00000	.00000	0.00000	0.00000	0.00000	.00000	0.00000	3.75605
18	.58205	.00000	0.00000	0.00000	.00000	0.00000	0.00000	0.00000	.00001	0.00000	5.26174
19	.74859	.00000	0.00000	0.00000	.00000	0.00000	0.00000	0.00000	.00001	0.00000	6.76723
20	.91509	.00000	0.00000	0.00000	0.00000	0.00000	0.00000	0.00000	.00002	0.00000	8.27245
21	1.00000	0.00000							.00004		

THRUST- AND SIDE-FORCE COEFFICIENTS IN PLANE OF THE FIN

SUMFX =CX..ACTS ON LEADING EDGE
SUMFY1=CY..ACTS ON LEADING EDGE
SUMFY2=CY..ACTS ON LEADING AND SIDE EDGE
SUMFT2=CY..ACTS ON SIDE EDGE

SUMFX = 0.
SUMFY1 = 0.
SUMFY2 = .14602E-10
SUMFT2 = .10179E-09

SIDE EDGE DISTRIBUTION

JTIP	JSE	DISTANCE FROM LE /TIPCHORD	SUCTION FORCE PER UNIT LENGTH /(Q*TIPCHORD)	GAMMA,SE /VINF	YBAR	XSE
1	9	.25000	.00000	0.00000	0.00000	9.04000
2	10	.50000	.00000	0.00000	0.00000	12.17750
3	11	.75000	.00000	0.00000	0.00000	15.31500
4	12	1.00000	.00000	0.00000	0.00000	18.45250

****T.E. FIN VORTICITY DUE TO ATTACHED FLOW*****

IVRT	GAMMA/VINF	Y.C.G. (LOCAL FIN)	Y.C.G. (BODY AXES)	Z.C.G.
5	.00006	7.04686	-.00000	9.16186

-------------------UPPER LEFT OR LOWER VERTICAL FIN--------------------

I	Y/(B/2)	CN*C/(2*B)	CT*C/(2*B)	CY1*C/(2*B)	CYTOT*C/(2*B)	CS*C/(2*B)	CSINT	YBAR	GAMNET(I)	GAMMA,LE/VINF	XLE
22	-.08233	.00001	0.00000	0.00000	-.00000	0.00000	0.00000	0.00000	.00007	0.00000	.74425
23	-.24892	.00001	0.00000	0.00000	.00000	0.00000	0.00000	0.00000	-.00000	0.00000	2.25021

24	-.41549	.00001	0.00000	0.00000	-.00000	0.00000	0.00000	0.00000	-.00000	0.00000	3.75605
25	-.54205	.00000	0.00000	0.00000	-.00000	0.00000	0.00000	0.00000	-.00001	0.00000	5.26174
26	-.74859	.00000	0.00000	0.00000	-.00000	0.00000	0.00000	0.00000	-.00001	0.00000	6.76723
27	-.91509	.00000	0.00000	0.00000	0.00000	0.00000	0.00000	0.00000	-.00002	0.00000	8.27245
28	-1.00000	0.00000							-.00004		

THRUST- AND SIDE-FORCE COEFFICIENTS IN PLANE OF THE FIN

SUMFX =CX..ACTS ON LEADING EDGE
SUMFY1=CY..ACTS ON LEADING EDGE
SUMFY2=CY..ACTS ON LEADING AND SIDE EDGE
SUMFT2=CY..ACTS ON SIDE EDGE

SUMFX = 0.
SUMFY1 = 0.
SUMFY2 = -.14602E-10
SUMFT2 = -.10179E-09

SIDE EDGE DISTRIBUTION

JTIP	JSE	DISTANCE FROM LE /TIPCHORD	SUCTION FORCE PER UNIT LENGTH /(Q*TIPCHORD)	GAMMA,SE /VINF	YBAR	XSE
1	13	.25000	-.00000	0.00000	0.00000	9.04000
2	14	.50000	-.00000	0.00000	0.00000	12.17750
3	15	.75000	-.00000	0.00000	0.00000	15.31500
4	16	1.00000	-.00000	0.00000	0.00000	18.45250

****T.E. FIN VORTICITY DUE TO ATTACHED FLOW*****

IVRT	GAMMA/VINF	Y.C.G. (LOCAL FIN)	Y.C.G. (BODY AXES)	Z.C.G. (BODY AXES)
6	-.00011	-6.84231	.00000	-8.95731

STEP 5 PATHS OF VORTICES OVER AFTERBODY AND TAIL FINS

TRACK VORTICES ALONG AFTERBODY AND TAIL SECTION, TF-4, KING TAIL (D)

```
          FIN GEOMETRY
FIN SEMISPAN            =   11.15500
FIN ROOTCHORD           =   21.59100
FIN ROOT L.E. X-STATION=    80.73000
         L.E. Y-STATION=     2.11500
FIN TIP L.E. X-STATION =    89.77000
         L.E. Y-STATION =   11.15500
FIN TIP T.E. X-STATION =   102.32000
         T.E. Y-STATION =   11.15500
FIN ROOT T.E. X-STATION=   102.32100
         T.E. Y-STATION=     2.11500
```

INCLUDED ANGLE OF ATTACK(DEG) = 15.00000 ROLL ANGLE(DEG) = .00100

PANEL DEFL.(DEG)

DELTA1= 0.000 DELTA2= 0.000 DELTA3= 0.000 DELTA4= 0.000

****PERMISSIBLE RELATIVE ERROR,E5,USED IN INTEGRATION SCHEME = .10000E-02

VORTEX COORDINATES IN CROSS-FLOW PLANE

INITIAL VORTEX POSITIONS AT X = 80.730

LOCAL BODY RADIUS = 2.11500 LOCAL SEMI SPAN S = 2.11500

VORTEX	Y,VRTX	Z,VRTX	GAMMA/VINF
1	-.13334E+01	.32200E+01	.86923E+00
2	-.21351E+01	.39206E+01	-.31134E+01
3	.91845E+01	.11528E+02	.21299E-01
4	-.80755E+01	.12641E+02	-.58798E-02
5	.77439E+01	.12190E+02	.33798E+01
6	-.64480E+01	.13430E+02	-.22259E+01
7	.10185E+01	.10705E+02	-.93338E-01
8	-.24665E+01	.42869E+01	-.16236E+00

CROSSFLOW VELOCITIES AT CONTROL POINTS INDUCED BY VORTICES AND THEIR IMAGES *** STEP 5

IC	X,BODY	Y,BODY	Z,BODY	V	W
1	.86425E+02	.28593E+01	0.	.18694E-02	-.38187E-01
2	.91637E+02	.28593E+01	0.	.18694E-02	-.38187E-01
3	.96848E+02	.28593E+01	0.	.18694E-02	-.38187E-01
4	.10206E+03	.28593E+01	0.	.18694E-02	-.38187E-01
5	.87573E+02	.43652E+01	0.	.82526E-02	-.33910E-01
6	.92408E+02	.43652E+01	0.	.82526E-02	-.33910E-01
7	.97243E+02	.43652E+01	0.	.82526E-02	-.33910E-01
8	.10208E+03	.43652E+01	0.	.82526E-02	-.33910E-01
9	.88722E+02	.58711E+01	0.	.15017E-01	-.30279E-01
10	.93180E+02	.58711E+01	0.	.15017E-01	-.30279E-01
11	.97639E+02	.58711E+01	0.	.15017E-01	-.30279E-01
12	.10210E+03	.58711E+01	0.	.15017E-01	-.30279E-01
13	.89870E+02	.73767E+01	0.	.20176E-01	-.25295E-01
14	.93952E+02	.73767E+01	0.	.20176E-01	-.25295E-01
15	.98034E+02	.73767E+01	0.	.20176E-01	-.25295E-01
16	.10212E+03	.73767E+01	0.	.20176E-01	-.25295E-01
17	.91018E+02	.88822E+01	0.	.23308E-01	-.19595E-01
18	.94723E+02	.88822E+01	0.	.23308E-01	-.19595E-01
19	.98429E+02	.88822E+01	0.	.23308E-01	-.19595E-01
20	.10213E+03	.88822E+01	0.	.23308E-01	-.19595E-01
21	.92165E+02	.10387E+02	0.	.24540E-01	-.13919E-01
22	.95495E+02	.10387E+02	0.	.24540E-01	-.13919E-01
23	.98824E+02	.10387E+02	0.	.24540E-01	-.13919E-01
24	.10215E+03	.10387E+02	0.	.24540E-01	-.13919E-01
25	.86425E+02	-.28593E+01	0.	-.48111E-01	-.12413E+00
26	.91637E+02	-.28593E+01	0.	-.48111E-01	-.12413E+00
27	.96848E+02	-.28593E+01	0.	-.48111E-01	-.12413E+00
28	.10206E+03	-.28593E+01	0.	-.48111E-01	-.12413E+00
29	.87573E+02	-.43652E+01	0.	-.64826E-01	-.53363E-01
30	.92408E+02	-.43652E+01	0.	-.64826E-01	-.53363E-01
31	.97243E+02	-.43652E+01	0.	-.64826E-01	-.53363E-01
32	.10208E+03	-.43652E+01	0.	-.64826E-01	-.53363E-01
33	.88722E+02	-.58711E+01	0.	-.54095E-01	-.21210E-01
34	.93180E+02	-.58711E+01	0.	-.54095E-01	-.21210E-01
35	.97639E+02	-.58711E+01	0.	-.54095E-01	-.21210E-01
36	.10210E+03	-.58711E+01	0.	-.54095E-01	-.21210E-01
37	.89870E+02	-.73767E+01	0.	-.42625E-01	-.75657E-02
38	.93952E+02	-.73767E+01	0.	-.42625E-01	-.75657E-02
39	.98034E+02	-.73767E+01	0.	-.42625E-01	-.75657E-02
40	.10212E+03	-.73767E+01	0.	-.42625E-01	-.75657E-02
41	.91018E+02	-.88822E+01	0.	-.34287E-01	-.13057E-02
42	.94723E+02	-.88822E+01	0.	-.34287E-01	-.13057E-02
43	.98429E+02	-.88822E+01	0.	-.34287E-01	-.13057E-02
44	.10213E+03	-.88822E+01	0.	-.34287E-01	-.13057E-02
45	.92165E+02	-.10387E+02	0.	-.28355E-01	.20259E-02
46	.95495E+02	-.10387E+02	0.	-.28355E-01	.20259E-02
47	.98824E+02	-.10387E+02	0.	-.28355E-01	.20259E-02
48	.10215E+03	-.10387E+02	0.	-.28355E-01	.20259E-02
49	.86425E+02	0.	.28593E+01	-.17061E+00	-.82941E-01
50	.91637E+02	0.	.28593E+01	-.17061E+00	-.82941E-01
51	.96848E+02	0.	.28593E+01	-.17061E+00	-.82941E-01
52	.10206E+03	0.	.28593E+01	-.17061E+00	-.82941E-01
53	.87573E+02	0.	.43652E+01	-.60893E-01	-.20438E+00
54	.92408E+02	0.	.43652E+01	-.60893E-01	-.20438E+00
55	.97243E+02	0.	.43652E+01	-.60893E-01	-.20438E+00
56	.10208E+03	0.	.43652E+01	-.60893E-01	-.20438E+00
57	.88722E+02	0.	.58711E+01	.38837E-01	-.16639E+00
58	.93180E+02	0.	.58711E+01	.38837E-01	-.16639E+00
59	.97639E+02	0.	.58711E+01	.38837E-01	-.16639E+00

60	.10210E+03	0.	.58711E+01	.38837E-01	-.16639E+00
61	.89870E+02	0.	.73767E+01	.44811E-01	-.13017E+00
62	.93952E+02	0.	.73767E+01	.44811E-01	-.13017E+00
63	.98034E+02	0.	.73767E+01	.44811E-01	-.13017E+00
64	.10212E+03	0.	.73767E+01	.44811E-01	-.13017E+00
65	.91018E+02	0.	.88822E+01	.31335E-01	-.12100E+00
66	.94723E+02	0.	.88822E+01	.31335E-01	-.12100E+00
67	.98429E+02	0.	.88822E+01	.31335E-01	-.12100E+00
68	.10213E+03	0.	.88822E+01	.31335E-01	-.12100E+00
69	.92165E+02	0.	.10387E+02	.21249E-01	-.11555E+00
70	.95495E+02	0.	.10387E+02	.21249E-01	-.11555E+00
71	.98824E+02	0.	.10387E+02	.21249E-01	-.11555E+00
72	.10215E+03	0.	.10387E+02	.21249E-01	-.11555E+00
73	.86425E+02	0.	-.28593E+01	.89920E-02	-.11978E-01
74	.91637E+02	0.	-.28593E+01	.89920E-02	-.11978E-01
75	.96848E+02	0.	-.28593E+01	.89920E-02	-.11978E-01
76	.10206E+03	0.	-.28593E+01	.89920E-02	-.11978E-01
77	.87573E+02	0.	-.43652E+01	.38046E-02	-.17893E-01
78	.92408E+02	0.	-.43652E+01	.38046E-02	-.17893E-01
79	.97243E+02	0.	-.43652E+01	.38046E-02	-.17893E-01
80	.10208E+03	0.	-.43652E+01	.38046E-02	-.17893E-01
81	.88722E+02	0.	-.58711E+01	.14017E-02	-.17591E-01
82	.93180E+02	0.	-.58711E+01	.14017E-02	-.17591E-01
83	.97639E+02	0.	-.58711E+01	.14017E-02	-.17591E-01
84	.10210E+03	0.	-.58711E+01	.14017E-02	-.17591E-01
85	.89870E+02	0.	-.73767E+01	.27213E-03	-.16052E-01
86	.93952E+02	0.	-.73767E+01	.27213E-03	-.16052E-01
87	.98034E+02	0.	-.73767E+01	.27213E-03	-.16052E-01
88	.10212E+03	0.	-.73767E+01	.27213E-03	-.16052E-01
89	.91018E+02	0.	-.88822E+01	-.26587E-03	-.14365E-01
90	.94723E+02	0.	-.88822E+01	-.26587E-03	-.14365E-01
91	.98429E+02	0.	-.88822E+01	-.26587E-03	-.14365E-01
92	.10213E+03	0.	-.88822E+01	-.26587E-03	-.14365E-01
93	.92165E+02	0.	-.10387E+02	-.51597E-03	-.12805E-01
94	.95495E+02	0.	-.10387E+02	-.51597E-03	-.12805E-01
95	.98824E+02	0.	-.10387E+02	-.51597E-03	-.12805E-01
96	.10215E+03	0.	-.10387E+02	-.51597E-03	-.12805E-01
97	.85858E+02	.19733E+01	.52875E+00	.12922E-01	-.44158E-01
98	.85858E+02	.14446E+01	.14446E+01	.33960E-02	.46072E-02
99	.85858E+02	.52875E+00	.19733E+01	-.12725E+00	.46383E-01
100	.85858E+02	-.52875E+00	.19733E+01	-.30716E+00	-.70830E-01
101	.85858E+02	-.14446E+01	.14446E+01	-.29139E+00	-.29875E+00
102	.85858E+02	-.19733E+01	.52875E+00	-.56079E-01	-.25042E+00
103	.85858E+02	-.19733E+01	-.52875E+00	.40598E-01	-.12932E+00
104	.85858E+02	-.14446E+01	-.14446E+01	.51672E-01	-.47024E-01
105	.85858E+02	-.52875E+00	-.19733E+01	.28884E-01	-.54379E-02
106	.85858E+02	.52875E+00	-.19733E+01	-.79913E-03	.16193E-02
107	.85858E+02	.14446E+01	-.14446E+01	-.18855E-01	-.16718E-01
108	.85858E+02	.19733E+01	-.52875E+00	-.12376E-01	-.42660E-01
109	.91255E+02	.19733E+01	.52875E+00	.12922E-01	-.44158E-01
110	.91255E+02	.14446E+01	.14446E+01	.33960E-02	.46072E-02
111	.91255E+02	.52875E+00	.19733E+01	-.12725E+00	.46383E-01
112	.91255E+02	-.52875E+00	.19733E+01	-.30716E+00	-.70830E-01
113	.91255E+02	-.14446E+01	.14446E+01	-.29139E+00	-.29875E+00
114	.91255E+02	-.19733E+01	.52875E+00	-.56079E-01	-.25042E+00
115	.91255E+02	-.19733E+01	-.52875E+00	.40598E-01	-.12932E+00
116	.91255E+02	-.14446E+01	-.14446E+01	.51672E-01	-.47024E-01
117	.91255E+02	-.52875E+00	-.19733E+01	.28884E-01	-.54379E-02
118	.91255E+02	.52875E+00	-.19733E+01	-.79913E-03	.16193E-02
119	.91255E+02	.14446E+01	-.14446E+01	-.18855E-01	-.16718E-01
120	.91255E+02	.19733E+01	-.52875E+00	-.12376E-01	-.42660E-01
121	.96653E+02	.19733E+01	.52875E+00	.12922E-01	-.44158E-01
122	.96653E+02	.14446E+01	.14446E+01	.33960E-02	.46072E-02
123	.96653E+02	.52875E+00	.19733E+01	-.12725E+00	.46383E-01
124	.96653E+02	-.52875E+00	.19733E+01	-.30716E+00	-.70830E-01
125	.96653E+02	-.14446E+01	.14446E+01	-.29139E+00	-.29875E+00

126	.96653E+02	-.19733E+01	.52875E+00	-.56079E-01	-.25042E+00
127	.96653E+02	-.19733E+01	-.52875E+00	.40598E-01	-.12932E+00
128	.96653E+02	-.14446E+01	-.14446E+01	.51672E-01	-.47024E-01
129	.96653E+02	-.52875E+00	-.19733E+01	.28884E-01	-.54379E-02
130	.96653E+02	.52875E+00	-.19733E+01	-.79913E-03	.16193E-02
131	.96653E+02	.14446E+01	-.14446E+01	-.18855E-01	-.16718E-01
132	.96653E+02	.19733E+01	-.52875E+00	-.12376E-01	-.42660E-01
133	.10205E+03	.19733E+01	.52875E+00	.12922E-01	-.44158E-01
134	.10205E+03	.14446E+01	.14446E+01	.33960E-02	.46072E-02
135	.10205E+03	.52875E+00	.19733E+01	-.12725E+00	.46383E-01
136	.10205E+03	-.52875E+00	.19733E+01	-.30716E+00	-.70830E-01
137	.10205E+03	-.14446E+01	.14446E+01	-.29139E+00	-.29875E+00
138	.10205E+03	-.19733E+01	.52875E+00	-.56079E-01	-.25042E+00
139	.10205E+03	-.19733E+01	-.52875E+00	.40598E-01	-.12932E+00
140	.10205E+03	-.14446E+01	-.14446E+01	.51672E-01	-.47024E-01
141	.10205E+03	-.52875E+00	-.19733E+01	.28884E-01	-.54379E-02
142	.10205E+03	.52875E+00	-.19733E+01	-.79913E-03	.16193E-02
143	.10205E+03	.14446E+01	-.14446E+01	-.18855E-01	-.16718E-01
144	.10205E+03	.19733E+01	-.52875E+00	-.12376E-01	-.42660E-01

STEP 6 LOADS ON TAIL FINS WITH VORTEX EFFECTS

NASA/LRC TF-4 WITH KING TAIL (D), AFTERBODY AND TAIL SECTION

```
$INPUT
BIL     = .2159E+02,
B2      = .904E+01,
B2V     = .904E+01,
CRP     = .2159E+02,
CRPV    = .2159E+02,
DELD    = 0.0,
DELL    = 0.0,
DELR    = 0.0,
DELU    = 0.0,
ERATIO  = .1E+01,
FAC     = .95E+00,
FKLE    = .5E+00,
FKSE    = .1E+01,
FMACH   = .25E+01,
ITAIL   = 1,
JCPT    = 144,
LVSWP   = 0,
MINPRN  = 0,
MSWD    = 6,
MSWL    = 6,
MSWR    = 6,
MSWU    = 6,
NBDCR   = 12,
NBDYPR  = 1,
NBSHED  = 1,
NCPOUT  = 0,
NCRX    = 1,
NCW     = 4,
NCWB    = 4,
NCWT    = 0,
NDRAG   = 1,
NFVNPR  = 0,
NOLINP  = 1,
NOUT    = 0,
NPR     = 0,
NPRESS  = 0,
NTDAT   = 0,
NTPR    = 0,
NVLIN   = 1,
NVRTPL  = 1,
NVRTX   = 0,
N2DPRB  = 0,
N2DPRF  = 0,
PHIDIH  = 0.0,
PHIFR   = 0.0,
PHIFL   = 0.0,
PHIFU   = .9E+02,
PHIFD   = .9E+02,
PHIINT  = 0.0,
RA      = .2115E+01,
RB      = .2115E+01,
REFL    = .423E+01,
SREF    = .1412E+02,
SWLEP   = .45E+02,
SWLEV   = .45E+02,
SWTEP   = 0.0,
SWTEV   = 0.0,
THETIT  = 0.0,
THETR   = 0.0,
THETL   = 0.0,
THETU   = .9E+02,
THETD   = .9E+02,
TOLFAC  = .1E+01,
VRTMAX  = .35E+00,
XM      = .4604E+02,
XSTART  = .8073E+02,
XWLE    = .8073E+02,
ZM      = 0.0,
$END
```

FIN SECTION GEOMETRY DESCRIPTION

NO. OF CHORDWISE PANELS ON FINS PRESENT (NCW) = 4

FIN PROPERTY		FIN 1 OR R	FIN 2 OR L	FIN 3 OR U	FIN 4 OR D
NO. OF PANELS - SPANWISE	(MSW) =	6	6	6	6
ROOT CHORD	(CR) =	21.590	21.590	21.590	21.590
LEADING EDGE SWEEP	(SWLE) =	45.000	45.000	45.000	45.000
TRAILING EDGE SWEEP	(SWTE) =	0.000	0.000	0.000	0.000
EXPOSED SEMISPAN	(B2) =	9.040	9.040	9.040	9.040
FIN DIHEDRAL	(PHIF) =	0.000	0.000	90.000	90.000
BODY ANGLE OF FIN ATTACHMENT	(THET) =	0.000	0.000	90.000	90.000
FIN DEFLECTION	(DEL) =	0.000	0.000	0.000	0.000
Y-INTERSECTION OF FIN TO BODY	(YBOD) =	2.115	-2.115	-.000	.000
Z-INTERSECTION OF FIN TO BODY	(ZBOD) =	0.000	-.000	2.115	-2.115

FLOW CONDITIONS

MACH = 2.50000 ALPHAC= 15.00000 PHI = .00100 ALFA = 15.00000 BETA = .00026

CRPT = 21.59000
CRPTV = 21.59000

POINT COORDINATES AND PERTURBATION VELOCITIES CALCULATED BY PROGRAM VPATH

IC	XCP	YCP	ZCP	VVEL(IC)	WVEL(IC)
1	86.42500	2.85930	0.00000	.18694E-02	-.38187E-01
2	91.63700	2.85930	0.00000	.18694E-02	-.38187E-01
3	96.84800	2.85930	0.00000	.18694E-02	-.38187E-01
4	102.06000	2.85930	0.00000	.18694E-02	-.38187E-01
5	87.57300	4.36520	0.00000	.82526E-02	-.33910E-01
6	92.40800	4.36520	0.00000	.82526E-02	-.33910E-01
7	97.24300	4.36520	0.00000	.82526E-02	-.33910E-01
8	102.08000	4.36520	0.00000	.82526E-02	-.33910E-01
9	88.72200	5.87110	0.00000	.15017E-01	-.30279E-01
10	93.18000	5.87110	0.00000	.15017E-01	-.30279E-01
11	97.63900	5.87110	0.00000	.15017E-01	-.30279E-01
12	102.10000	5.87110	0.00000	.15017E-01	-.30279E-01
13	89.87000	7.37670	0.00000	.20176E-01	-.25295E-01
14	93.95200	7.37670	0.00000	.20176E-01	-.25295E-01
15	98.03400	7.37670	0.00000	.20176E-01	-.25295E-01
16	102.12000	7.37670	0.00000	.20176E-01	-.25295E-01
17	91.01800	8.88220	0.00000	.23308E-01	-.19595E-01
18	94.72300	8.88220	0.00000	.23308E-01	-.19595E-01
19	98.42900	8.88220	0.00000	.23308E-01	-.19595E-01
20	102.13000	8.88220	0.00000	.23308E-01	-.19595E-01
21	92.16500	10.38700	0.00000	.24540E-01	-.13919E-01
22	95.49500	10.38700	0.00000	.24540E-01	-.13919E-01
23	98.82400	10.38700	0.00000	.24540E-01	-.13919E-01
24	102.15000	10.38700	0.00000	.24540E-01	-.13919E-01
25	86.42500	-2.85930	0.00000	-.48111E-01	-.12413E+00
26	91.63700	-2.85930	0.00000	-.48111E-01	-.12413E+00
27	96.84800	-2.85930	0.00000	-.48111E-01	-.12413E+00
28	102.06000	-2.85930	0.00000	-.48111E-01	-.12413E+00
29	87.57300	-4.36520	0.00000	-.64826E-01	-.53363E-01
30	92.40800	-4.36520	0.00000	-.64826E-01	-.53363E-01
31	97.24300	-4.36520	0.00000	-.64826E-01	-.53363E-01
32	102.08000	-4.36520	0.00000	-.64826E-01	-.53363E-01
33	88.72200	-5.87110	0.00000	-.54095E-01	-.21210E-01
34	93.18000	-5.87110	0.00000	-.54095E-01	-.21210E-01
35	97.63900	-5.87110	0.00000	-.54095E-01	-.21210E-01
36	102.10000	-5.87110	0.00000	-.54095E-01	-.21210E-01
37	89.87000	-7.37670	0.00000	-.42625E-01	-.75657E-02
38	93.95200	-7.37670	0.00000	-.42625E-01	-.75657E-02
39	98.03400	-7.37670	0.00000	-.42625E-01	-.75657E-02
40	102.12000	-7.37670	0.00000	-.42625E-01	-.75657E-02
41	91.01800	-8.88220	0.00000	-.34287E-01	-.13057E-02
42	94.72300	-8.88220	0.00000	-.34287E-01	-.13057E-02
43	98.42900	-8.88220	0.00000	-.34287E-01	-.13057E-02
44	102.13000	-8.88220	0.00000	-.34287E-01	-.13057E-02
45	92.16500	-10.38700	0.00000	-.28355E-01	.20259E-02
46	95.49500	-10.38700	0.00000	-.28355E-01	.20259E-02
47	98.82400	-10.38700	0.00000	-.28355E-01	.20259E-02
48	102.15000	-10.38700	0.00000	-.28355E-01	.20259E-02
49	86.42500	0.00000	2.85930	-.17061E+00	-.82941E-01
50	91.63700	0.00000	2.85930	-.17061E+00	-.82941E-01
51	96.84800	0.00000	2.85930	-.17061E+00	-.82941E-01
52	102.06000	0.00000	2.85930	-.17061E+00	-.82941E-01
53	87.57300	0.00000	4.36520	-.60893E-01	-.20438E+00
54	92.40800	0.00000	4.36520	-.60893E-01	-.20438E+00
55	97.24300	0.00000	4.36520	-.60893E-01	-.20438E+00
56	102.08000	0.00000	4.36520	-.60893E-01	-.20438E+00
57	88.72200	0.00000	5.87110	.38837E-01	-.16639E+00
58	93.18000	0.00000	5.87110	.38837E-01	-.16639E+00

59	97.63900	0.00000	5.87110	.38837E-01	-.16639E+00
60	102.10000	0.00000	5.87110	.38837E-01	-.16639E+00
61	89.87000	0.00000	7.37670	.44811E-01	-.13017E+00
62	93.95200	0.00000	7.37670	.44811E-01	-.13017E+00
63	98.03400	0.00000	7.37670	.44811E-01	-.13017E+00
64	102.12000	0.00000	7.37670	.44811E-01	-.13017E+00
65	91.01800	0.00000	8.88220	.31335E-01	-.12100E+00
66	94.72300	0.00000	8.88220	.31335E-01	-.12100E+00
67	98.42900	0.00000	8.88220	.31335E-01	-.12100E+00
68	102.13000	0.00000	8.88220	.31335E-01	-.12100E+00
69	92.16500	0.00000	10.38700	.21249E-01	-.11555E+00
70	95.49500	0.00000	10.38700	.21249E-01	-.11555E+00
71	98.82400	0.00000	10.38700	.21249E-01	-.11555E+00
72	102.15000	0.00000	10.38700	.21249E-01	-.11555E+00
73	86.42500	0.00000	-2.85930	.89920E-02	-.11978E-01
74	91.63700	0.00000	-2.85930	.89920E-02	-.11978E-01
75	96.84800	0.00000	-2.85930	.89920E-02	-.11978E-01
76	102.06000	0.00000	-2.85930	.89920E-02	-.11978E-01
77	87.57300	0.00000	-4.36520	.38046E-02	-.17893E-01
78	92.40800	0.00000	-4.36520	.38046E-02	-.17893E-01
79	97.24300	0.00000	-4.36520	.38046E-02	-.17893E-01
80	102.08000	0.00000	-4.36520	.38046E-02	-.17893E-01
81	88.72200	0.00000	-5.87110	.14017E-02	-.17591E-01
82	93.18000	0.00000	-5.87110	.14017E-02	-.17591E-01
83	97.63900	0.00000	-5.87110	.14017E-02	-.17591E-01
84	102.10000	0.00000	-5.87110	.14017E-02	-.17591E-01
85	89.87000	0.00000	-7.37670	.27213E-03	-.16052E-01
86	93.95200	0.00000	-7.37670	.27213E-03	-.16052E-01
87	98.03400	0.00000	-7.37670	.27213E-03	-.16052E-01
88	102.12000	0.00000	-7.37670	.27213E-03	-.16052E-01
89	91.01800	0.00000	-8.88220	-.26587E-03	-.14365E-01
90	94.72300	0.00000	-8.88220	-.26587E-03	-.14365E-01
91	98.42900	0.00000	-8.88220	-.26587E-03	-.14365E-01
92	102.13000	0.00000	-8.88220	-.26587E-03	-.14365E-01
93	92.16500	0.00000	-10.38700	-.51597E-03	-.12805E-01
94	95.49500	0.00000	-10.38700	-.51597E-03	-.12805E-01
95	98.82400	0.00000	-10.38700	-.51597E-03	-.12805E-01
96	102.15000	0.00000	-10.38700	-.51597E-03	-.12805E-01
97	85.85800	1.97330	.52875	.12922E-01	-.44158E-01
98	85.85800	1.44460	1.44460	.33960E-02	.46072E-02
99	85.85800	.52875	1.97330	-.12725E+00	.46383E-01
100	85.85800	-.52875	1.97330	-.30716E+00	-.70830E-01
101	85.85800	-1.44460	1.44460	-.29139E+00	-.29875E+00
102	85.85800	-1.97330	.52875	-.56079E-01	-.25042E+00
103	85.85800	-1.97330	-.52875	.40598E-01	-.12932E+00
104	85.85800	-1.44460	-1.44460	.51672E-01	-.47024E-01
105	85.85800	-.52875	-1.97330	.28884E-01	-.54379E-02
106	85.85800	.52875	-1.97330	-.79913E-03	.16193E-02
107	85.85800	1.44460	-1.44460	-.18855E-01	-.16718E-01
108	85.85800	1.97330	-.52875	-.12376E-01	-.42660E-01
109	91.25500	1.97330	.52875	.12922E-01	-.44158E-01
110	91.25500	1.44460	1.44460	.33960E-02	.46072E-02
111	91.25500	.52875	1.97330	-.12725E+00	.46383E-01
112	91.25500	-.52875	1.97330	-.30716E+00	-.70830E-01
113	91.25500	-1.44460	1.44460	-.29139E+00	-.29875E+00
114	91.25500	-1.97330	.52875	-.56079E-01	-.25042E+00
115	91.25500	-1.97330	-.52875	.40598E-01	-.12932E+00
116	91.25500	-1.44460	-1.44460	.51672E-01	-.47024E-01
117	91.25500	-.52875	-1.97330	.28884E-01	-.54379E-02
118	91.25500	.52875	-1.97330	-.79913E-03	.16193E-02
119	91.25500	1.44460	-1.44460	-.18855E-01	-.16718E-01
120	91.25500	1.97330	-.52875	-.12376E-01	-.42660E-01
121	96.65300	1.97330	.52875	.12922E-01	-.44158E-01
122	96.65300	1.44460	1.44460	.33960E-02	.46072E-02
123	96.65300	.52875	1.97330	-.12725E+00	.46383E-01
124	96.65300	-.52875	1.97330	-.30716E+00	-.70830E-01

125	96.65300	-1.44460	1.44460	-.29139E+00	-.29875E+00
126	96.65300	-1.97330	.52875	-.56079E-01	-.25042E+00
127	96.65300	-1.97330	-.52875	.40598E-01	-.12932E+00
128	96.65300	-1.44460	-1.44460	.51672E-01	-.47024E-01
129	96.65300	-.52875	-1.97330	.28884E-01	-.54379E-02
130	96.65300	.52875	-1.97330	-.79913E-03	.16193E-02
131	96.65300	1.44460	-1.44460	-.18855E-01	-.16718E-01
132	96.65300	1.97330	-.52875	-.12376E-01	-.42660E-01
133	102.05000	1.97330	.52875	.12922E-01	-.44158E-01
134	102.05000	1.44460	1.44460	.33960E-02	.46072E-02
135	102.05000	.52875	1.97330	-.12725E+00	.46383E-01
136	102.05000	-.52875	1.97330	-.30716E+00	-.70830E-01
137	102.05000	-1.44460	1.44460	-.29139E+00	-.29875E+00
138	102.05000	-1.97330	.52875	-.56079E-01	-.25042E+00
139	102.05000	-1.97330	-.52875	.40598E-01	-.12932E+00
140	102.05000	-1.44460	-1.44460	.51672E-01	-.47024E-01
141	102.05000	-.52875	-1.97330	.28884E-01	-.54379E-02
142	102.05000	.52875	-1.97330	-.79913E-03	.16193E-02
143	102.05000	1.44460	-1.44460	-.18855E-01	-.16718E-01
144	102.05000	1.97330	-.52875	-.12376E-01	-.42660E-01

** SPECPR **
*** STEP 6

VELOCITIES AND BERNOULLI PRESSURES AT CONTROL POINTS IMMEDIATELY ABOVE AND BELOW FIN SURFACE

J	X(J)	Y(J)	Z(J)	UTOTA	VTOTA	WTOTA	PRESSA	UTOTB	VTOTB	WTOTB	PRESSB
1	5.695119	2.859255	0.000000	.124663	-.120799	-.258819	-.146983	-.126365	.130229	-.258819	.420997
2	10.906555	2.859255	0.000000	.062575	-.036994	-.258819	-.053911	-.084426	.073257	-.258819	.301964
3	16.117992	2.859255	0.000000	.059437	-.020379	-.258819	-.047729	-.076744	.047711	-.258819	.283029
4	21.329428	2.859255	0.000000	.070861	-.014781	-.258819	-.066732	-.071405	.020785	-.258819	.269505
5	6.843413	4.365214	0.000000	.130415	-.120372	-.258819	-.152806	-.132280	.142323	-.258819	.435024
6	11.678359	4.365214	0.000000	.081347	-.045367	-.258819	-.084503	-.092709	.085175	-.258819	.325403
7	16.513306	4.365214	0.000000	.054672	.005390	-.258819	-.039009	-.085545	.075498	-.258819	.304961
8	21.348253	4.365214	0.000000	.068518	.003550	-.258819	-.062745	-.077040	.039940	-.258819	.285179
9	7.991615	5.871053	0.000000	.128782	-.113645	-.258819	-.150439	-.128425	.143561	-.258819	.420586
10	12.450102	5.871053	0.000000	.106490	-.063547	-.258819	-.120490	-.107442	.096902	-.258819	.370661
11	16.908589	5.871053	0.000000	.065574	.002706	-.258819	-.057852	-.089898	.080442	-.258819	.317663
12	21.367076	5.871053	0.000000	.062518	.013133	-.258819	-.052824	-.074042	.047273	-.258819	.274597
13	9.139701	7.376740	0.000000	.125849	-.105573	-.258819	-.146572	-.125495	.145772	-.258819	.408953
14	13.221767	7.376740	0.000000	.119005	-.067521	-.258819	-.135767	-.120546	.112143	-.258819	.409639
15	17.303832	7.376740	0.000000	.089548	-.023490	-.258819	-.095507	-.090326	.066448	-.258819	.322907
16	21.385897	7.376740	0.000000	.041523	.034775	-.258819	-.015758	-.065988	.061653	-.258819	.247045
17	10.287635	8.882227	0.000000	.124249	-.100858	-.258819	-.144405	-.123896	.147287	-.258819	.402453
18	13.993329	8.882227	0.000000	.119855	-.066544	-.258819	-.136665	-.119533	.112997	-.258819	.405678
19	17.699022	8.882227	0.000000	.084670	-.017407	-.258819	-.088219	-.086077	.067967	-.258819	.308664
20	21.404715	8.882227	0.000000	.040725	.024175	-.258819	-.013629	-.051509	.047233	-.258819	.206646
21	11.435366	10.387447	0.000000	.120575	-.095968	-.258819	-.139934	-.120221	.144828	-.258819	.391199
22	14.764754	10.387447	0.000000	.082245	-.037119	-.258819	-.085365	-.081920	.086005	-.258819	.290281
23	18.094142	10.387447	0.000000	.060055	-.005499	-.258819	-.048475	-.059756	.054407	-.258819	.229698
24	21.423531	10.387447	0.000000	.037296	.016915	-.258819	-.006669	-.038643	.035899	-.258819	.171655
25	5.695119	-2.859255	0.000000	.101817	.055364	-.258819	-.113924	-.099377	-.145830	-.258819	.320874
26	10.906555	-2.859255	0.000000	.094710	.030773	-.258819	-.103039	-.072211	-.094418	-.258819	.257329
27	16.117992	-2.859255	0.000000	.090216	.004345	-.258819	-.096102	-.072335	-.076930	-.258819	.262865
28	21.329428	-2.859255	0.000000	.075477	-.028223	-.258819	-.074541	-.074421	-.065697	-.258819	.272130
29	6.843413	-4.365214	0.000000	.118504	.055187	-.258819	-.134394	-.115916	-.179233	-.258819	.354380
30	11.678359	-4.365214	0.000000	.098904	.016569	-.258819	-.108330	-.086901	-.122785	-.258819	.292258
31	16.513306	-4.365214	0.000000	.104180	.011651	-.258819	-.115216	-.072734	-.076806	-.258819	.264132
32	21.348253	-4.365214	0.000000	.082672	-.031747	-.258819	-.085741	-.073636	-.070824	-.258819	.268463
33	7.991615	-5.871053	0.000000	.125873	.071660	-.258819	-.143670	-.125517	-.179730	-.258819	.386316
34	12.450102	-5.871053	0.000000	.107530	.027718	-.258819	-.119881	-.105940	-.132385	-.258819	.349596
35	16.908589	-5.871053	0.000000	.108219	.020433	-.258819	-.120542	-.083319	-.075336	-.258819	.297848
36	21.367076	-5.871053	0.000000	.084428	-.019233	-.258819	-.087907	-.072383	-.058435	-.258819	.267354
37	9.139701	-7.376740	0.000000	.129983	.087259	-.258819	-.149191	-.129629	-.172354	-.258819	.405779
38	13.221767	-7.376740	0.000000	.120462	.049171	-.258819	-.136303	-.118281	-.129886	-.258819	.392867
39	17.303832	-7.376740	0.000000	.097883	.007395	-.258819	-.106810	-.096525	-.089809	-.258819	.336466
40	21.385897	-7.376740	0.000000	.083957	.003379	-.258819	-.086952	-.058963	-.032351	-.258819	.230479
41	10.287635	-8.882227	0.000000	.131363	.096993	-.258819	-.151432	-.131009	-.165379	-.258819	.415497
42	13.993329	-8.882227	0.000000	.122276	.057381	-.258819	-.138799	-.121954	-.125791	-.258819	.407826
43	17.699022	-8.882227	0.000000	.087316	.010987	-.258819	-.091983	-.085321	-.075331	-.258819	.304280
44	21.404715	-8.882227	0.000000	.061785	-.007734	-.258819	-.051478	-.050461	-.035796	-.258819	.205113
45	11.435366	-10.387447	0.000000	.127869	.099447	-.258819	-.148079	-.127515	-.155937	-.258819	.409620
46	14.764754	-10.387447	0.000000	.085240	.035550	-.258819	-.089736	-.084915	-.092066	-.258819	.297872
47	18.094142	-10.387447	0.000000	.059497	.001405	-.258819	-.047483	-.059198	-.057942	-.258819	.227384
48	21.423531	-10.387447	0.000000	.040162	-.016531	-.258819	-.012244	-.038262	-.036137	-.258819	.170576
49	5.695119	0.000000	2.859255	.058743	.000005	-.292553	-.047135	-.049440	.000005	-.184370	.195503
50	10.906555	0.000000	2.859255	.068561	.000005	-.316844	-.065465	.033568	.000005	-.290600	.000002
51	16.117992	0.000000	2.859255	.081586	.000005	-.332035	-.087218	.067458	.000005	-.324971	-.064465
52	21.329428	0.000000	2.859255	.073954	.000005	-.308469	-.073406	.067442	.000005	-.306841	-.062798
53	6.843413	0.000000	4.365214	.040323	.000005	-.312912	-.015094	-.030367	.000005	-.242222	.150573
54	11.678359	0.000000	4.365214	.040378	.000005	-.333117	-.017657	.017587	.000005	-.316024	.030809
55	16.513306	0.000000	4.365214	.088356	.000005	-.438451	-.114314	.081247	.000005	-.434896	-.104130
56	21.348253	0.000000	4.365214	.075736	.000005	-.408064	-.090519	.066360	.000005	-.405720	-.075953
57	7.991615	0.000000	5.871053	.002825	.000005	-.202737	.063897	-.002608	.000005	-.197304	.075823

58	12.450102	0.000000	5.871053	.011980	.000005	-.214345	.044514	-.006239	.000005	-.200681	.084983
59	16.908589	0.000000	5.871053	.058050	.000005	-.323578	-.048520	.054908	.000005	-.322007	-.042870
60	21.367076	0.000000	5.871053	.075208	.000005	-.358778	-.080957	.068754	.000005	-.357164	-.070673
61	9.139701	0.000000	7.376740	-.011562	.000005	-.139684	.084202	.011753	.000005	-.162999	.036915
62	13.221767	0.000000	7.376740	.008723	.000005	-.164401	.043859	-.000430	.000005	-.157536	.062924
63	17.303832	0.000000	7.376740	.005371	.000005	-.158807	.050070	-.000550	.000005	-.155847	.062790
64	21.385897	0.000000	7.376740	.067810	.000005	-.300363	-.062942	.064891	.000005	-.299633	-.058055
65	10.287635	0.000000	8.882227	-.013513	.000005	-.121902	.083161	.013679	.000005	-.149094	.029611
66	13.993329	0.000000	8.882227	-.002888	.000005	-.133298	.062024	.003041	.000005	-.137744	.049913
67	17.699022	0.000000	8.882227	.009399	.000005	-.147265	.038402	-.001835	.000005	-.141647	.062022
68	21.404715	0.000000	8.882227	.029773	.000005	-.195924	.004662	.023059	.000005	-.194246	.018237
69	11.435366	0.000000	10.387447	-.010915	.000005	-.115077	.074669	.011059	.000005	-.137051	.032171
70	14.764754	0.000000	10.387447	-.005267	.000005	-.122082	.063970	.005400	.000005	-.130083	.042510
71	18.094142	0.000000	10.387447	.003624	.000005	-.127883	.045772	-.003499	.000005	-.124321	.060652
72	21.423531	0.000000	10.387447	.009806	.000005	-.136151	.034626	-.002606	.000005	-.133048	.061307
73	5.695119	0.000000	-2.859255	-.006531	.000005	-.169715	.080000	-.002033	.000005	-.165217	.068422
74	10.906555	0.000000	-2.859255	-.049071	.000005	-.231480	.201940	-.052410	.000005	-.233984	.211832
75	16.117992	0.000000	-2.859255	-.072233	.000005	-.256517	.272839	-.076238	.000005	-.258519	.285477
76	21.329428	0.000000	-2.859255	-.068467	.000005	-.236179	.260244	-.072417	.000005	-.237167	.272604
77	6.843413	0.000000	-4.365214	-.006408	.000005	-.092792	.056084	-.002825	.000005	-.089209	.046732
78	11.678359	0.000000	-4.365214	-.027588	.000005	-.137211	.123012	-.029736	.000005	-.138822	.129054
79	16.513306	0.000000	-4.365214	-.081266	.000005	-.248505	.301378	-.087765	.000005	-.251754	.322668
80	21.348253	0.000000	-4.365214	-.070015	.000005	-.220162	.263336	-.071567	.000005	-.220551	.268211
81	7.991615	0.000000	-5.871053	-.000842	.000005	-.052192	.026985	.001338	.000005	-.050013	.021485
82	12.450102	0.000000	-5.871053	-.002662	.000005	-.058696	.033713	-.002441	.000005	-.058530	.033170
83	16.908589	0.000000	-5.871053	-.053176	.000005	-.172399	.203182	-.059208	.000005	-.175415	.221548
84	21.367076	0.000000	-5.871053	-.070743	.000005	-.208853	.263860	-.072698	.000005	-.209342	.270021
85	9.139701	0.000000	-7.376740	-.000225	.000005	-.037553	.019002	.000742	.000005	-.036586	.016578
86	13.221767	0.000000	-7.376740	-.004305	.000005	-.047077	.031927	-.003349	.000005	-.046359	.029580
87	17.303832	0.000000	-7.376740	-.001043	.000005	-.042555	.023014	-.003198	.000005	-.043633	.027995
88	21.385897	0.000000	-7.376740	-.063455	.000005	-.185122	.236668	-.068717	.000005	-.186438	.252919
89	10.287635	0.000000	-8.882227	.000189	.000005	-.028757	.013989	.000352	.000005	-.028594	.013583
90	13.993329	0.000000	-8.882227	-.000114	.000005	-.028992	.014713	.000603	.000005	-.028454	.013009
91	17.699022	0.000000	-8.882227	-.003434	.000005	-.037650	.025661	-.003542	.000005	-.037705	.025912
92	21.404715	0.000000	-8.882227	-.024348	.000005	-.087874	.095879	-.027944	.000005	-.088773	.105045
93	11.435366	0.000000	-10.387447	.000423	.000005	-.022958	.010714	.000142	.000005	-.023239	.011414
94	14.764754	0.000000	-10.387447	.000095	.000005	-.023266	.011521	.000422	.000005	-.023020	.010746
95	18.094142	0.000000	-10.387447	-.000004	.000005	-.023305	.011737	.000477	.000005	-.023064	.010658
96	21.423531	0.000000	-10.387447	-.002923	.000005	-.031600	.021695	-.003723	.000005	-.031800	.023440

PRESSURE LOADINGS AT CONTROL POINTS

J	X(J)	Y(J)	Z(J)	DELTP.LIN.	DELTP.BERN.
1	5.695119	2.859255	0.000000	.502055	.567980
2	10.906555	2.859255	0.000000	.294002	.355875
3	16.117992	2.859255	0.000000	.272362	.330758
4	21.329428	2.859255	0.000000	.284533	.336238
5	6.843413	4.365214	0.000000	.525391	.587831
6	11.678359	4.365214	0.000000	.348112	.409906
7	16.513306	4.365214	0.000000	.280435	.343971
8	21.348253	4.365214	0.000000	.291117	.347923
9	7.991615	5.871053	0.000000	.514413	.571024
10	12.450102	5.871053	0.000000	.427864	.491151
11	16.908589	5.871053	0.000000	.310944	.375516
12	21.367076	5.871053	0.000000	.273120	.327420
13	9.139701	7.376740	0.000000	.502690	.555524
14	13.221767	7.376740	0.000000	.479102	.545407
15	17.303832	7.376740	0.000000	.359749	.418415
16	21.385897	7.376740	0.000000	.215023	.262803
17	10.287635	8.882227	0.000000	.496291	.546858
18	13.993329	8.882227	0.000000	.478775	.542343
19	17.699022	8.882227	0.000000	.341493	.396883
20	21.404715	8.882227	0.000000	.184468	.220275
21	11.435366	10.387447	0.000000	.481593	.531132
22	14.764754	10.387447	0.000000	.328331	.375646
23	18.094142	10.387447	0.000000	.239623	.278173
24	21.423531	10.387447	0.000000	.151877	.178324
25	5.695119	-2.859255	0.000000	.402387	.434798
26	10.906555	-2.859255	0.000000	.333841	.360368
27	16.117992	-2.859255	0.000000	.325100	.358966
28	21.329428	-2.859255	0.000000	.299795	.346671
29	6.843413	-4.365214	0.000000	.468839	.488774
30	11.678359	-4.365214	0.000000	.371609	.400588
31	16.513306	-4.365214	0.000000	.353828	.379348
32	21.348253	-4.365214	0.000000	.312618	.354204
33	7.991615	-5.871053	0.000000	.502780	.529986
34	12.450102	-5.871053	0.000000	.426941	.469476
35	16.908589	-5.871053	0.000000	.383076	.418390
36	21.367076	-5.871053	0.000000	.313621	.355261
37	9.139701	-7.376740	0.000000	.519226	.554971
38	13.221767	-7.376740	0.000000	.477486	.529170
39	17.303832	-7.376740	0.000000	.388815	.443276
40	21.385897	-7.376740	0.000000	.285841	.317432
41	10.287635	-8.882227	0.000000	.524743	.566928
42	13.993329	-8.882227	0.000000	.488459	.546625
43	17.699022	-8.882227	0.000000	.345273	.396263
44	21.404715	-8.882227	0.000000	.224493	.256591
45	11.435366	-10.387447	0.000000	.510768	.557699
46	14.764754	-10.387447	0.000000	.340309	.387608
47	18.094142	-10.387447	0.000000	.237390	.274867
48	21.423531	-10.387447	0.000000	.156848	.182820
49	5.695119	0.000000	2.859255	.216366	.242638
50	10.906555	0.000000	2.859255	.069985	.065467
51	16.117992	0.000000	2.859255	.028255	.022754
52	21.329428	0.000000	2.859255	.013025	.010608
53	6.843413	0.000000	4.365214	.141380	.165667
54	11.678359	0.000000	4.365214	.045581	.048466
55	16.513306	0.000000	4.365214	.014220	.010184
56	21.348253	0.000000	4.365214	.018751	.014566
57	7.991615	0.000000	5.871053	.010866	.011926
58	12.450102	0.000000	5.871053	.036437	.040469
59	16.908589	0.000000	5.871053	.006284	.005650
60	21.367076	0.000000	5.871053	.012909	.010285
61	9.139701	0.000000	7.376740	-.046630	-.047287
62	13.221767	0.000000	7.376740	.018305	.019065
63	17.303832	0.000000	7.376740	.011842	.012719
64	21.385897	0.000000	7.376740	.005838	.004887
65	10.287635	0.000000	8.882227	-.054385	-.053550
66	13.993329	0.000000	8.882227	-.011858	-.012111
67	17.699022	0.000000	8.882227	.022470	.023621
68	21.404715	0.000000	8.882227	.013428	.013575
69	11.435366	0.000000	10.387447	-.043949	-.042498
70	14.764754	0.000000	10.387447	-.021334	-.021460
71	18.094142	0.000000	10.387447	.014245	.014880
72	21.423531	0.000000	10.387447	.024825	.026680
73	5.695119	0.000000	-2.859255	-.008996	-.011579
74	10.906555	0.000000	-2.859255	.006678	.009893
75	16.117992	0.000000	-2.859255	.008009	.012639
76	21.329428	0.000000	-2.859255	.007900	.012361
77	6.843413	0.000000	-4.365214	-.007166	-.009353
78	11.678359	0.000000	-4.365214	.004296	.006042
79	16.513306	0.000000	-4.365214	.012997	.021290
80	21.348253	0.000000	-4.365214	.003105	.004874
81	7.991615	0.000000	-5.871053	-.004360	-.005499
82	12.450102	0.000000	-5.871053	-.000442	-.000543
83	16.908589	0.000000	-5.871053	.012064	.018366
84	21.367076	0.000000	-5.871053	.003911	.006162
85	9.139701	0.000000	-7.376740	-.001935	-.002424
86	13.221767	0.000000	-7.376740	-.001913	-.002347
87	17.303832	0.000000	-7.376740	.004310	.004981
88	21.385897	0.000000	-7.376740	.010524	.016251
89	10.287635	0.000000	-8.882227	-.000325	-.000406
90	13.993329	0.000000	-8.882227	-.001434	-.001703
91	17.699022	0.000000	-8.882227	.000216	.000251
92	21.404715	0.000000	-8.882227	.007193	.009166
93	11.435366	0.000000	-10.387447	.000563	.000700
94	14.764754	0.000000	-10.387447	-.000656	-.000775
95	18.094142	0.000000	-10.387447	-.000962	-.001079
96	21.423531	0.000000	-10.387447	.001600	.001745

FIN LOADING INFORMATION

*** STEP 6

```
         MACH NUMBER =    .25000E+01
     ANGLE OF ATTACK =   15.000 DEGREES
     SIDE SLIP ANGLE =     .000 DEGREES
            FIN AREA =  154.31280
      REFERENCE AREA =   14.12000
    REFERENCE LENGTH =    4.23000
  EXPOSED FIN SPAN B/2=   9.04000
  MOMENT CENTER:   XM =  46.04000
                   ZM =   0.00000
```

LINEAR PRESSURE (U/VINF) LOADS IN BODY SYSTEM

	TOTAL	FIN 1 OR R	FIN 2 OR L	FIN 3 OR U	FIN 4 OR D	INTERF. SHELL
DEFL. ANGLE DEG. =		0.00000	0.00000	0.00000	0.00000	
CTHR =	.15764	.81136E-01	.68580E-01	.79303E-02	-.56527E-05	
CZ =	8.0215	3.9198	4.1017	0.	0.	1.2898
CY =	-.32811	0.	0.	-.30121	-.26898E-01	-.14415
CM =	-88.030	-42.837	-45.193	0.	0.	-14.504
CLN =	3.3889	0.	0.	3.0373	.35156	1.5181
CLL =	.10050	-5.7583	6.0537	-.22791	.33023E-01	.55021E-15

FOLLOWING ARE IN UNROLLED BODY-AXIS COORDINATE SYSTEM

	TOTAL	FIN 1 OR R	FIN 2 OR L	FIN 3 OR U	FIN 4 OR D	INTERF. SHELL
CZU =	8.0215	3.9198	4.1017	.52571E-05	.46946E-06	1.2899
CYU =	-.32797	.68413E-04	.71588E-04	-.30121	-.26898E-01	-.14413
CMU =	-88.030	-42.837	-45.193	-.53012E-04	-.61360E-05	-14.504
CLNU =	3.3874	-.74765E-03	-.78877E-03	3.0373	.35156	1.5179

NOTE: L.E. OF LEAD PANEL IN FIRST CHORDWISE ROW IS SUPERSONIC

SPANWISE DISTRIBUTIONS

-------------------UPPER RIGHT OR RIGHT HORIZONTAL FIN--------------------

I	Y/(B/2)	CN*C/(2*B)	CT*C/(2*B)	CY1*C/(2*B)	CYTOT*C/(2*B)	CS*C/(2*B)	CSINT	YBAR	GAMNET(I)	GAMMA.LE/VINF	XLE
1	.08233	.19490	0.00000	0.00000	.00020	0.00000	0.00000	0.00000	-3.52541	0.00000	.74425
2	.24892	.19312	0.00000	0.00000	.00076	0.00000	0.00000	0.00000	.03203	0.00000	2.25021
3	.41549	.18808	0.00000	0.00000	.00168	0.00000	0.00000	0.00000	.09080	0.00000	3.75605
4	.58205	.17559	0.00000	0.00000	.00291	0.00000	0.00000	0.00000	.22559	0.00000	5.26174
5	.74859	.15369	0.00000	0.00000	.00423	0.00000	0.00000	0.00000	.39582	0.00000	6.76723
6	.91509	.11050	0.00000	0.00000	0.00000	0.00000	0.00000	0.00000	.78117	0.00000	8.27245
7	1.00000	0.00000							2.00000		

THRUST- AND SIDE-FORCE COEFFICIENTS IN PLANE OF THE FIN

SUMFX =CX..ACTS ON LEADING EDGE
SUMFY1=CY..ACTS ON LEADING EDGE
SUMFY2=CY..ACTS ON LEADING AND SIDE EDGE
SUMFT2=CY..ACTS ON SIDE EDGE

SUMFX = 0.
SUMFY1 = 0.
SUMFY2 = .37733E-01
SUMFT2 = .32015E+00

SIDE EDGE DISTRIBUTION

JTIP	JSE	DISTANCE FROM LE /TIPCHORD	SUCTION FORCE PER UNIT LENGTH /(Q*TIPCHORD)	GAMMA.SE /VINF	YBAR	XSE
1	1	.25000	.00093	.00195	9.04000	9.04000
2	2	.50000	.02075	.04560	9.04000	12.17750
3	3	.75000	.04773	.14600	9.04000	15.31500
4	4	1.00000	.04540	.24151	9.04000	18.45250

S.F. AUGMENTATION OF FIN NORMAL FORCE FROM SUCTION CONVERSION IN PROPORTION WITH FACTOR
KVSE = 1.000

(LOCAL FIN)	(ROLLED BODY-AXIS)	(UNROLLED BODY-AXIS)
CNADD = .32015	CYADD = 0.00000	CYADD = .00001
	CZADD = .32015	CZADD = .32015
	CMADD = -3.78470	CMADD = -3.78468
	CLNADD = 0.00000	CLNADD = -.00007

CLLADD	=	-.84428	CLLADD	=	-.84428
XCG	=	96.0450	XCG	=	96.0450
YCG	=	11.1550	YCG	=	11.1550
ZCG	=	0.0000	ZCG	=	-.0002

**** T.E. FIN VORTICITY DUE TO SIDE-EDGE FORCE AUGMENTATION

IVRT	GAMMA/VINF	Y.C.G. (LOCAL FIN)	Z.C.G. (LOCAL FIN)	Y.C.G. (BODY AXES)	Z.C.G. (BODY AXES)
1	.24151	9.04000	1.65224	11.15500	1.65224

------------------LOWER LEFT OR LEFT HORIZONTAL FIN--------------------

I	Y/(B/2)	CN*C/(2*B)	CT*C/(2*B)	CY1*C/(2*B)	CYTOT*C/(2*B)	CS*C/(2*B)	CSINT	YBAR	GAMNET(I)	GAMMA.LE/VINF	XLE
8	-.08233	.19608	0.00000	0.00000	-.00055	0.00000	0.00000	0.00000	3.54671	0.00000	.74425
9	-.24892	.20138	0.00000	0.00000	-.00008	0.00000	0.00000	0.00000	.09617	0.00000	2.25021
10	-.41549	.20042	0.00000	0.00000	-.00204	0.00000	0.00000	0.00000	-.01720	0.00000	3.75605
11	-.58205	.18855	0.00000	0.00000	-.00387	0.00000	0.00000	0.00000	-.21436	0.00000	5.26174
12	-.74859	.16208	0.00000	0.00000	-.00497	0.00000	0.00000	0.00000	-.47832	0.00000	6.76723
13	-.91509	.11454	0.00000	0.00000	0.00000	0.00000	0.00000	0.00000	-.85993	0.00000	8.27245
14	-1.00000	0.00000							-2.07307		

THRUST- AND SIDE-FORCE COEFFICIENTS IN PLANE OF THE FIN

SUMFX =CX..ACTS ON LEADING EDGE
SUMFY1=CY..ACTS ON LEADING EDGE
SUMFY2=CY..ACTS ON LEADING AND SIDE EDGE
SUMFT2=CY..ACTS ON SIDE EDGE

SUMFX = 0.
SUMFY1 = 0.
SUMFY2 = -.44408E-01
SUMFT2 = -.35423E+00

SIDE EDGE DISTRIBUTION

JTIP	JSE	DISTANCE FROM LE /TIPCHORD	SUCTION FORCE PER UNIT LENGTH /(Q*TIPCHORD)	GAMMA.SE /VINF	YBAR	XSE
1	5	.25000	-.00110	-.00231	-9.04000	9.04000
2	6	.50000	-.02392	-.05263	-9.04000	12.17750
3	7	.75000	-.05360	-.16538	-9.04000	15.31500
4	8	1.00000	-.04841	-.26722	-9.04000	18.45250

S.F. AUGMENTATION OF FIN NORMAL FORCE FROM SUCTION CONVERSION IN PROPORTION WITH FACTOR
KVSE = 1.000

(LOCAL FIN)			(ROLLED BODY-AXIS)			(UNROLLED BODY-AXIS)		
CNADD	=	.35423	CYADD	=	0.00000	CYADD	=	.00001
			CZADD	=	.35423	CZADD	=	.35423
			CMADD	=	-4.18757	CMADD	=	-4.18755
			CLNADD	=	0.00000	CLNADD	=	-.00007
			CLLADD	=	.93415	CLLADD	=	.93415
			XCG	=	96.0450	XCG	=	96.0450
			YCG	=	-11.1550	YCG	=	-11.1550
			ZCG	=	-.0000	ZCG	=	.0002

**** T.E. FIN VORTICITY DUE TO SIDE-EDGE FORCE AUGMENTATION

IVRT	GAMMA/VINF	Y.C.G. (LOCAL FIN)	Z.C.G. (LOCAL FIN)	Y.C.G. (BODY AXES)	Z.C.G. (BODY AXES)
2	-.26722	-9.04000	1.65224	-11.15500	1.65224

------------------LOWER RIGHT OR UPPER VERTICAL FIN--------------------

I	Y/(B/2)	CN*C/(2*B)	CT*C/(2*B)	CY1*C/(2*B)	CYTOT*C/(2*B)	CS*C/(2*B)	CSINT	YBAR	GAMNET(I)	GAMMA.LE/VINF	XLE
15	.08233	.04720	0.00000	0.00000	.01119	0.00000	0.00000	0.00000	-.85371	0.00000	.74425
16	.24892	.02939	0.00000	0.00000	.00581	0.00000	0.00000	0.00000	.32203	0.00000	2.25021
17	.41549	.00819	0.00000	0.00000	-.00150	0.00000	0.00000	0.00000	.38344	0.00000	3.75605
18	.58205	-.00120	0.00000	0.00000	-.00037	0.00000	0.00000	0.00000	.16996	0.00000	5.26174
19	.74859	-.00311	0.00000	0.00000	.00003	0.00000	0.00000	0.00000	.03450	0.00000	6.76723
20	.91509	-.00241	0.00000	0.00000	0.00000	0.00000	0.00000	0.00000	-.01259	0.00000	8.27245
21	1.00000	0.00000							-.04364		

THRUST- AND SIDE-FORCE COEFFICIENTS IN PLANE OF THE FIN

SUMFX =CX..ACTS ON LEADING EDGE
SUMFY1=CY..ACTS ON LEADING EDGE
SUMFY2=CY..ACTS ON LEADING AND SIDE EDGE
SUMFT2=CY..ACTS ON SIDE EDGE

SUMFX = 0.
SUMFY1 = 0.
SUMFY2 = .58546E-01
SUMFT2 = .16360E-02

SIDE EDGE DISTRIBUTION

JTIP	JSE	DISTANCE FROM LE /TIPCHORD	SUCTION FORCE PER UNIT LENGTH /(Q*TIPCHORD)	GAMMA.SE /VINF	YBAR	XSE

1	9	.25000	-.00001	.00002	9.04000	9.04000
2	10	.50000	.00021	.00048	9.04000	12.17750
3	11	.75000	.00034	.00123	9.04000	15.31500
4	12	1.00000	.00004	.00132	9.04000	18.45250

S.E. AUGMENTATION OF FIN NORMAL FORCE FROM SUCTION CONVERSION IN PROPORTION WITH FACTOR
KVSE = 1.000

(LOCAL FIN)		(ROLLED BODY-AXIS)		(UNROLLED BODY-AXIS)	
CNADD =	.00169	CYADD =	-.00169	CYADD =	-.00169
		CZADD =	0.00000	CZADD =	.00000
		CMADD =	0.00000	CMADD =	-.02002
		CLNADD =	.02004	CLNADD =	.02004
		CLLADD =	-.00447	CLLADD =	-.00447
		XCG =	96.0450	XCG =	96.0450
		YCG =	-.0000	YCG =	.0002
		ZCG =	11.1550	ZCG =	11.1550

**** T.E. FIN VORTICITY DUE TO SIDE-EDGE FORCE AUGMENTATION

IVRT	GAMMA/VINF	Y.C.G. (LOCAL FIN)	Z.C.G. (LOCAL FIN)	Y.C.G. (BODY AXES)	Z.C.G. (BODY AXES)
3	.00132	9.04000	.00003	-.00003	11.15500

-------------------UPPER LEFT OR LOWER VERTICAL FIN---------------------

I	Y/(B/2)	CN*C/(2*B)	CT*C/(2*B)	CY1*C/(2*B)	CYTOT*C/(2*B)	CS*C/(2*B)	CSINT	YBAR	GAMNET(I)	GAMMA.LE/VINF	XLE
22	-.08233	.00196	0.00000	0.00000	-.00001	0.00000	0.00000	0.00000	.03542	0.00000	.74425
23	-.24892	.00177	0.00000	0.00000	.00001	0.00000	0.00000	0.00000	-.00343	0.00000	2.25021
24	-.41549	.00138	0.00000	0.00000	.00000	0.00000	0.00000	0.00000	-.00708	0.00000	3.75605
25	-.58205	.00124	0.00000	0.00000	-.00000	0.00000	0.00000	0.00000	-.00248	0.00000	5.26174
26	-.74859	.00058	0.00000	0.00000	.00000	0.00000	0.00000	0.00000	-.01196	0.00000	6.76723
27	-.91509	.00005	0.00000	0.00000	0.00000	0.00000	0.00000	0.00000	-.00956	0.00000	8.27245
28	-1.00000	0.00000							-.00091		

THRUST- AND SIDE-FORCE COEFFICIENTS IN PLANE OF THE FIN

SUMFX =CX..ACTS ON LEADING EDGE
SUMFY1=CY..ACTS ON LEADING EDGE
SUMFY2=CY..ACTS ON LEADING AND SIDE EDGE
SUMFT2=CY..ACTS ON SIDE EDGE

SUMFX = 0.
SUMFY1 = 0.
SUMFY2 = .69140E-05
SUMFT2 = .39971E-06

SIDE EDGE DISTRIBUTION

JTIP	JSE	DISTANCE FROM LE /TIPCHORD	SUCTION FORCE PER UNIT LENGTH /(Q*TIPCHORD)	GAMMA.SE /VINF	YBAR	XSE
1	13	.25000	-.00000	0.00000	0.00000	9.04000
2	14	.50000	.00000	0.00000	0.00000	12.17750
3	15	.75000	.00000	0.00000	0.00000	15.31500
4	16	1.00000	.00000	0.00000	0.00000	18.45250

FIN LOADING INFORMATION

MACH NUMBER =	.25000E+01
ANGLE OF ATTACK =	15.000 DEGREES
SIDE SLIP ANGLE =	.000 DEGREES
FIN AREA =	154.31280
REFERENCE AREA =	14.12000
REFERENCE LENGTH =	4.23000
EXPOSED FIN SPAN B/2=	9.04000
MOMENT CENTER: XM =	46.04000
ZM =	0.00000

BERNOULLI PRESSURE LOADS IN BODY SYSTEM

	TOTAL	FIN 1 OR R	FIN 2 OR L	FIN 3 OR U	FIN 4 OR D	INTERF. SHELL
DEFL. ANGLE DEG. =		0.00000	0.00000	0.00000	0.00000	
CTHR =	.15764	.81136E-01	.68580E-01	.79303E-02	-.56527E-05	
CZ =	9.0413	4.5284	4.5129	0.	0.	1.2898
CY =	-.36545	0.	0.	-.32165	-.43793E-01	-.14415
CM =	-99.466	-49.613	-49.853	0.	0.	-14.504
CLN =	3.7630	0.	0.	3.2018	.56117	1.5181
CLL =	-.12915	-6.6180	6.6860	-.24931	.52190E-01	.55021E-15

FOLLOWING ARE IN UNROLLED BODY-AXIS COORDINATE SYSTEM

CZU =	9.0413	4.5284	4.5129	.56139E-05	.76433E-06	1.2899
CYU =	-.36529	.79035E-04	.78764E-04	-.32165	-.43793E-01	-.14413
CMU =	-99.466	-49.613	-49.853	-.55882E-04	-.97942E-05	-14.504
CLNU =	3.7612	-.86591E-03	-.87010E-03	3.2018	.56117	1.5179

NOTE: L.E. OF LEAD PANEL IN FIRST CHORDWISE ROW IS SUPERSONIC

SPANWISE DISTRIBUTIONS

------------------UPPER RIGHT OR RIGHT HORIZONTAL FIN--------------------

I	Y/(B/2)	CN*C/(2*B)	CT*C/(2*B)	CY1*C/(2*B)	CYTOT*C/(2*B)	CS*C/(2*B)	CSINT	YBAR	GAMNET(I)	GAMMA.LE/VINF	XLE
1	.08233	.22918	0.00000	0.00000	.00020	0.00000	0.00000	0.00000	-3.52541	0.00000	.74425
2	.24892	.22581	0.00000	0.00000	.00076	0.00000	0.00000	0.00000	.03203	0.00000	2.25021
3	.41549	.21751	0.00000	0.00000	.00168	0.00000	0.00000	0.00000	.09080	0.00000	3.75605
4	.58205	.20104	0.00000	0.00000	.00291	0.00000	0.00000	0.00000	.22559	0.00000	5.26174
5	.74859	.17472	0.00000	0.00000	.00423	0.00000	0.00000	0.00000	.39582	0.00000	6.76723
6	.91509	.12539	0.00000	0.00000	0.00000	0.00000	0.00000	0.00000	.78117	0.00000	8.27245
7	1.00000	0.00000							2.00000		

THRUST- AND SIDE-FORCE COEFFICIENTS IN PLANE OF THE FIN

SUMFX =CX..ACTS ON LEADING EDGE
SUMFY1=CY..ACTS ON LEADING EDGE
SUMFY2=CY..ACTS ON LEADING AND SIDE EDGE
SUMFT2=CY..ACTS ON SIDE EDGE

SUMFX = 0.
SUMFY1 = 0.
SUMFY2 = .37733E-01
SUMFT2 = .32015E+00

SIDE EDGE DISTRIBUTION

JTIP	JSE	DISTANCE FROM LE /TIPCHORD	SUCTION FORCE PER UNIT LENGTH /(Q*TIPCHORD)	GAMMA,SE /VINF	YBAR	XSE
1	1	.25000	.00093	.00195	9.04000	9.04000
2	2	.50000	.02075	.04560	9.04000	12.17750
3	3	.75000	.04773	.14600	9.04000	15.31500
4	4	1.00000	.04540	.24151	9.04000	18.45250

****T.E. FIN VORTICITY DUE TO ATTACHED FLOW*****

IVRT	GAMMA/VINF	Y.C.G. (LOCAL FIN)	Y.C.G. (BODY AXES)	Z.C.G. (BODY AXES)
	4.14350	7.71581	9.83081	0.00000

------------------LOWER LEFT OR LEFT HORIZONTAL FIN--------------------

I	Y/(B/2)	CN*C/(2*B)	CT*C/(2*B)	CY1*C/(2*B)	CYTOT*C/(2*B)	CS*C/(2*B)	CSINT	YBAR	GAMNET(I)	GAMMA.LE/VINF	XLE
8	-.08233	.21620	0.00000	0.00000	-.00055	0.00000	0.00000	0.00000	3.54671	0.00000	.74425
9	-.24892	.21689	0.00000	0.00000	-.00008	0.00000	0.00000	0.00000	.09617	0.00000	2.25021
10	-.41549	.21849	0.00000	0.00000	-.00204	0.00000	0.00000	0.00000	-.01720	0.00000	3.75605
11	-.58205	.20812	0.00000	0.00000	-.00387	0.00000	0.00000	0.00000	-.21436	0.00000	5.26174
12	-.74859	.18087	0.00000	0.00000	-.00497	0.00000	0.00000	0.00000	-.47832	0.00000	6.76723
13	-.91509	.12904	0.00000	0.00000	0.00000	0.00000	0.00000	0.00000	-.85993	0.00000	8.27245
14	-1.00000	0.00000							-2.07307		

THRUST- AND SIDE-FORCE COEFFICIENTS IN PLANE OF THE FIN

SUMFX =CX..ACTS ON LEADING EDGE
SUMFY1=CY..ACTS ON LEADING EDGE
SUMFY2=CY..ACTS ON LEADING AND SIDE EDGE
SUMFT2=CY..ACTS ON SIDE EDGE

SUMFX = 0.
SUMFY1 = 0.
SUMFY2 = -.44408E-01
SUMFT2 = -.35423E+00

SIDE EDGE DISTRIBUTION

JTIP	JSE	DISTANCE FROM LE /TIPCHORD	SUCTION FORCE PER UNIT LENGTH /(Q*TIPCHORD)	GAMMA,SE /VINF	YBAR	XSE
1	5	.25000	-.00110	-.00231	-9.04000	9.04000
2	6	.50000	-.02392	-.05263	-9.04000	12.17750
3	7	.75000	-.05360	-.16538	-9.04000	15.31500
4	8	1.00000	-.04841	-.26722	-9.04000	18.45250

****T.E. FIN VORTICITY DUE TO ATTACHED FLOW*****

IVRT	GAMMA/VINF	Y.C.G. (LOCAL FIN)	Y.C.G. (BODY AXES)	Z.C.G. (BODY AXES)
5	-3.90897	-8.15069	-10.26569	-.00000

------------------LOWER RIGHT OR UPPER VERTICAL FIN--------------------

I	Y/(B/2)	CN*C/(2*B)	CT*C/(2*B)	CY1*C/(2*B)	CYTOT*C/(2*B)	CS*C/(2*B)	CSINT	YBAR	GAMNET(I)	GAMMA,LE/VINF	XLE
15	.08233	.04919	0.00000	0.00000	.01119	0.00000	0.00000	0.00000	-.85371	0.00000	.74425
16	.24892	.03192	0.00000	0.00000	.00581	0.00000	0.00000	0.00000	.32203	0.00000	2.25021
17	.41549	.00842	0.00000	0.00000	-.00150	0.00000	0.00000	0.00000	.38344	0.00000	3.75605
18	.58205	-.00120	0.00000	0.00000	-.00037	0.00000	0.00000	0.00000	.16996	0.00000	5.26174
19	.74859	-.00291	0.00000	0.00000	.00003	0.00000	0.00000	0.00000	.03450	0.00000	6.76723
20	.91509	-.00206	0.00000	0.00000	0.00000	0.00000	0.00000	0.00000	-.01259	0.00000	8.27245
21	1.00000	0.00000							-.04364		

THRUST- AND SIDE-FORCE COEFFICIENTS IN PLANE OF THE FIN

SUMFX =CX..ACTS ON LEADING EDGE
SUMFY1=CY..ACTS ON LEADING EDGE
SUMFY2=CY..ACTS ON LEADING AND SIDE EDGE
SUMFT2=CY..ACTS ON SIDE EDGE

SUMFX = 0.
SUMFY1 = 0.
SUMFY2 = .58546E-01
SUMFT2 = .16360E-02

SIDE EDGE DISTRIBUTION

JTIP	JSE	DISTANCE FROM LE /TIPCHORD	SUCTION FORCE PER UNIT LENGTH /(Q*TIPCHORD)	GAMMA,SE /VINF	YBAR	XSE
1	9	.25000	-.00001	.00002	9.04000	9.04000
2	10	.50000	.00021	.00048	9.04000	12.17750
3	11	.75000	.00034	.00123	9.04000	15.31500
4	12	1.00000	.00004	.00132	9.04000	18.45250

****T.E. FIN VORTICITY DUE TO ATTACHED FLOW*****

IVRT	GAMMA/VINF	Y.C.G. (LOCAL FIN)	Y.C.G. (BODY AXES)	Z.C.G.
6	.94208	2.89146	-.00000	5.00646
7	-.05270	8.59823	-.00000	10.71323

-------------------UPPER LEFT OR LOWER VERTICAL FIN--------------------

I	Y/(B/2)	CN*C/(2*B)	CT*C/(2*B)	CY1*C/(2*B)	CYTOT*C/(2*B)	CS*C/(2*B)	CSINT	YBAR	GAMNET(I)	GAMMA,LE/VINF	XLE
22	-.08233	.00336	0.00000	0.00000	-.00001	0.00000	0.00000	0.00000	.03542	0.00000	.74425

23	-.24892	.00305	0.00000	0.00000	.00001	0.00000	0.00000	0.00000	-.00343	0.00000	2.25021
24	-.41549	.00228	0.00000	0.00000	.00000	0.00000	0.00000	0.00000	-.00708	0.00000	3.75605
25	-.58205	.00186	0.00000	0.00000	-.00000	0.00000	0.00000	0.00000	-.00248	0.00000	5.26174
26	-.74859	.00075	0.00000	0.00000	.00000	0.00000	0.00000	0.00000	-.01196	0.00000	6.76723
27	-.91509	.00005	0.00000	0.00000	0.00000	0.00000	0.00000	0.00000	-.00956	0.00000	8.27245
28	-1.00000	0.00000							-.00091		

THRUST- AND SIDE-FORCE COEFFICIENTS IN PLANE OF THE FIN

SUMFX =CX..ACTS ON LEADING EDGE
SUMFY1=CY..ACTS ON LEADING EDGE
SUMFY2=CY..ACTS ON LEADING AND SIDE EDGE
SUMFT2=CY..ACTS ON SIDE EDGE

SUMFX = 0.
SUMFY1 = 0.
SUMFY2 = .69140E-05
SUMFT2 = .39971E-06

SIDE EDGE DISTRIBUTION

JTIP	JSE	DISTANCE FROM LE /TIPCHORD	SUCTION FORCE PER UNIT LENGTH /(Q*TIPCHORD)	GAMMA.SE /VINF	YBAR	XSE
1	13	.25000	-.00000	0.00000	0.00000	9.04000
2	14	.50000	.00000	0.00000	0.00000	12.17750
3	15	.75000	.00000	0.00000	0.00000	15.31500
4	16	1.00000	.00000	0.00000	0.00000	18.45250

****T.E. FIN VORTICITY DUE TO ATTACHED FLOW*****

IVRT	GAMMA/VINF	Y.C.G. (LOCAL FIN)	Y.C.G. (BODY AXES)	Z.C.G. (BODY AXES)
8	-.06072	-5.09178	.00000	-7.20678

****
AFT OF LEADING EDGE OF FIN ROOTCHORDS

BODY RING= 1

J	THETA. DEG.	XB	YB	ZB	UTOT	VTOT	WTOT	CP.LIN.	CP.BERN.	DR/DX	P/PINF. BERN.	P/PINF. LIN.
1	15.00000	85.85763	1.97332	.52875	.08917	-.08262	.03180	-.17834	-.14724	0.00000	.35583	.21977
2	45.00000	85.85763	1.44457	1.44457	.02274	-.19902	-.07360	-.04548	-.04738	0.00000	.79271	.80103
3	75.00000	85.85763	.52875	1.97332	-.03962	-.20361	-.21378	.07925	.11458	0.00000	1.50127	1.34671
4	105.00000	85.85763	-.52875	1.97332	.03679	-.08605	-.29221	-.07358	-.01366	0.00000	.94023	.67807
5	135.00000	85.85763	-1.44457	1.44457	.04913	-.03259	-.32058	-.09827	-.03332	0.00000	.85420	.57009
6	165.00000	85.85763	-1.97332	.52875	.07008	.04513	-.15335	-.14017	-.07541	0.00000	.67006	.38677
7	195.00000	85.85763	-1.97332	-.52875	-.07042	-.06161	-.02849	.14085	.17520	0.00000	1.76651	1.61621
8	225.00000	85.85763	-1.44457	-1.44457	-.03235	-.18398	-.09199	.06470	.07401	0.00000	1.32380	1.28306
9	255.00000	85.85763	-.52875	-1.97332	.00002	-.12007	-.24616	-.00003	.05681	0.00000	1.24854	.99987
10	285.00000	85.85763	.52875	-1.97332	.00356	.14773	-.23922	-.00713	.04018	0.00000	1.17578	.96881
11	315.00000	85.85763	1.44457	-1.44457	-.03877	.20671	-.07179	.07755	.06907	0.00000	1.30216	1.33928
12	345.00000	85.85763	1.97332	-.52875	-.08808	.08217	.02953	.17616	.17260	0.00000	1.75513	1.77071

BODY LOADS ON RING 1 AT X= 85.85763

	UNROLLED BODY-AXIS COORDINATES LINEAR LOADING	UNROLLED BODY-AXIS COORDINATES BERNOULLI LOADING	FIXED OR ROLLED BODY-AXIS COORDINATES LINEAR LOADING	FIXED OR ROLLED BODY-AXIS COORDINATES BERNOULLI LOADING
CX			0.00000	0.00000
CZ	.14999	.12788	.14999	.12788
CY	-.03444	.02389	-.03445	.02389
CM	-1.41191	-1.20375	-1.41190	-1.20375
CLN	.32423	-.22491	.32425	-.22489

CUMULATIVE BODY LOADS TO THIS STATION

	UNROLLED BODY-AXIS COORDINATES LINEAR LOADING	UNROLLED BODY-AXIS COORDINATES BERNOULLI LOADING	FIXED OR ROLLED BODY-AXIS COORDINATES LINEAR LOADING	FIXED OR ROLLED BODY-AXIS COORDINATES BERNOULLI LOADING
CX			0.00000	0.00000
CZ	.14999	.12788	.14999	.12788
CY	-.03444	.02389	-.03445	.02389
CM	-1.41191	-1.20375	-1.41190	-1.20375
CLN	.32423	-.22491	.32425	-.22489

BODY RING= 2

J	THETA. DEG.	XB	YB	ZB	UTOT	VTOT	WTOT	CP.LIN.	CP.BERN.	DR/DX	P/PINF. BERN.	P/PINF. LIN.
1	15.00000	91.25513	1.97332	.52875	.06149	-.07385	-.00093	-.12298	-.10411	0.00000	.54450	.46195

2	45.00000	91.25513	1.44457	1.44457	.04636	-.17486	-.09775	-.09271	-.07144	0.00000	.68744	.59437
3	75.00000	91.25513	.52875	1.97332	.02793	-.15648	-.22641	-.05586	-.01301	0.00000	.94307	.75562
4	105.00000	91.25513	-.52875	1.97332	.05980	-.13983	-.30662	-.11961	-.06580	0.00000	.71211	.47671
5	135.00000	91.25513	-1.44457	1.44457	.07856	-.06055	-.34854	-.15712	-.08724	0.00000	.61832	.31258
6	165.00000	91.25513	-1.97332	.52875	.09435	.04774	-.14361	-.18869	-.11183	0.00000	.51075	.17446
7	195.00000	91.25513	-1.97332	-.52875	-.07484	-.05826	-.04098	.14968	.19644	0.00000	1.85943	1.65485
8	225.00000	91.25513	-1.44457	-1.44457	-.05949	-.15671	-.11926	.11897	.16494	0.00000	1.72162	1.52050
9	255.00000	91.25513	-.52875	-1.97332	-.03992	-.07891	-.25718	.07983	.16781	0.00000	1.73419	1.34926
10	285.00000	91.25513	.52875	-1.97332	-.04716	.08797	-.25522	.09433	.18566	0.00000	1.81225	1.41269
11	315.00000	91.25513	1.44457	-1.44457	-.06478	.18186	-.09663	.12956	.15650	0.00000	1.68469	1.56683
12	345.00000	91.25513	1.97332	-.52875	-.08035	.07936	.01904	.16069	.16188	0.00000	1.70821	1.70302

BODY LOADS ON RING 2 AT X= 91.25513

	UNROLLED BODY-AXIS COORDINATES LINEAR LOADING	BERNOULLI LOADING	FIXED OR ROLLED BODY-AXIS COORDINATES LINEAR LOADING	BERNOULLI LOADING
CX			0.00000	0.00000
CZ	.36029	.38339	.36029	.38339
CY	-.06239	.00105	-.06239	.00104
CM	-3.85123	-4.09816	-3.85122	-4.09816
CLN	.66687	-.01117	.66694	-.01110

CUMULATIVE BODY LOADS TO THIS STATION

	UNROLLED BODY-AXIS COORDINATES LINEAR LOADING	BERNOULLI LOADING	FIXED OR ROLLED BODY-AXIS COORDINATES LINEAR LOADING	BERNOULLI LOADING
CX			0.00000	0.00000
CZ	.51029	.51127	.51028	.51127
CY	-.09683	.02494	-.09684	.02493
CM	-5.26314	-5.30191	-5.26312	-5.30191
CLN	.99110	-.23608	.99119	-.23599

BODY RING= 3

J	THETA. DEG.	XB	YB	ZB	UTOT	VTOT	WTOT	CP.LIN.	CP.BERN.	DR/DX	P/PINF. BERN.	P/PINF. LIN.
1	15.00000	96.65262	1.97332	.52875	.05740	-.07315	-.00354	-.11480	-.09762	0.00000	.57290	.49776
2	45.00000	96.65262	1.44457	1.44457	.06019	-.16794	-.10468	-.12038	-.08880	0.00000	.61150	.47334
3	75.00000	96.65262	.52875	1.97332	.06199	-.16068	-.22528	-.12399	-.07321	0.00000	.67969	.45756
4	105.00000	96.65262	-.52875	1.97332	.07266	-.14598	-.30826	-.14532	-.08706	0.00000	.61912	.36424
5	135.00000	96.65262	-1.44457	1.44457	.07359	-.07484	-.36282	-.14718	-.08319	0.00000	.63606	.35608
6	165.00000	96.65262	-1.97332	.52875	.08666	.04380	-.15832	-.17332	-.09913	0.00000	.56632	.24172
7	195.00000	96.65262	-1.97332	-.52875	-.06972	-.05704	-.04553	.13943	.18555	0.00000	1.81180	1.61001
8	225.00000	96.65262	-1.44457	-1.44457	-.06534	-.14820	-.12778	.13068	.18824	0.00000	1.82354	1.57173
9	255.00000	96.65262	-.52875	-1.97332	-.06479	-.07430	-.25841	.12959	.24054	0.00000	2.05236	1.56694
10	285.00000	96.65262	.52875	-1.97332	-.06928	.09063	-.25451	.13857	.24956	0.00000	2.09183	1.60623
11	315.00000	96.65262	1.44457	-1.44457	-.06786	.16917	-.10933	.13573	.17715	0.00000	1.77503	1.59381
12	345.00000	96.65262	1.97332	-.52875	-.07377	.07593	.00627	.14754	.15572	0.00000	1.68126	1.64547

BODY LOADS ON RING 3 AT X= 96.65262

UNROLLED BODY-AXIS COORDINATES LINEAR LOADING	BERNOULLI LOADING	FIXED OR ROLLED BODY-AXIS COORDINATES LINEAR LOADING	BERNOULLI LOADING

CX			0.00000	0.00000
CZ	.44261	.48573	.44260	.48573
CY	-.04009	.01409	-.04010	.01408
CM	-5.29584	-5.81187	-5.29584	-5.81187
CLN	.47969	-.16857	.47978	-.16847

CUMULATIVE BODY LOADS TO THIS STATION

	UNROLLED BODY-AXIS COORDINATES		FIXED OR ROLLED BODY-AXIS COORDINATES	
	LINEAR LOADING	BERNOULLI LOADING	LINEAR LOADING	BERNOULLI LOADING
CX			0.00000	0.00000
CZ	.95289	.99701	.95289	.99701
CY	-.13692	.03903	-.13694	.03901
CM	-10.55898	-11.11378	-10.55896	-11.11378
CLN	1.47079	-.40466	1.47097	-.40446

BODY RING= 4

J	THETA. DEG.	XB	YB	ZB	UTOT	VTOT	WTOT	CP.LIN.	CP.BERN.	DR/DX	P/PINF. BERN.	P/PINF. LIN.
1	15.00000	102.05013	1.97332	.52875	.06858	-.07588	.00665	-.13715	-.11592	0.00000	.49286	.39996
2	45.00000	102.05013	1.44457	1.44457	.07257	-.17029	-.10232	-.14513	-.10695	0.00000	.53210	.36505
3	75.00000	102.05013	.52875	1.97332	.07274	-.16525	-.22405	-.14549	-.09053	0.00000	.60392	.36349
4	105.00000	102.05013	-.52875	1.97332	.08129	-.14938	-.30917	-.16258	-.10016	0.00000	.56182	.28873
5	135.00000	102.05013	-1.44457	1.44457	.08089	-.07316	-.36115	-.16178	-.09351	0.00000	.59090	.29220
6	165.00000	102.05013	-1.97332	.52875	.08086	.04542	-.15226	-.16172	-.09180	0.00000	.59836	.29247
7	195.00000	102.05013	-1.97332	-.52875	-.07272	-.05903	-.03811	.14545	.18851	0.00000	1.82475	1.63632
8	225.00000	102.05013	-1.44457	-1.44457	-.07413	-.15175	-.12422	.14826	.20973	0.00000	1.91758	1.64863
9	255.00000	102.05013	-.52875	-1.97332	-.07517	-.07436	-.25839	.15034	.27235	0.00000	2.19152	1.65775
10	285.00000	102.05013	.52875	-1.97332	-.07835	.09174	-.25421	.15670	.27717	0.00000	2.21261	1.68555
11	315.00000	102.05013	1.44457	-1.44457	-.07882	.16964	-.10884	.15763	.20689	0.00000	1.90516	1.68965
12	345.00000	102.05013	1.97332	-.52875	-.07620	.07830	.01509	.15241	.15459	0.00000	1.67632	1.66678

BODY LOADS ON RING 4 AT X= 102.05013

	LINEAR LOADING	BERNOULLI LOADING	LINEAR LOADING	BERNOULLI LOADING
	UNROLLED BODY-AXIS COORDINATES		FIXED OR ROLLED BODY-AXIS COORDINATES	
CX			0.00000	0.00000
CZ	.50032	.54773	.50032	.54773
CY	-.02324	.02703	-.02325	.02702
CM	-6.62489	-7.25253	-6.62488	-7.25254
CLN	.30777	-.35794	.30789	-.35782

CUMULATIVE BODY LOADS TO THIS STATION

	UNROLLED BODY-AXIS COORDINATES		FIXED OR ROLLED BODY-AXIS COORDINATES	
	LINEAR LOADING	BERNOULLI LOADING	LINEAR LOADING	BERNOULLI LOADING
CX			0.00000	0.00000
CZ	1.45322	1.54473	1.45321	1.54473

CY	-.16017	.06606	-.16019	.06603
CM	-17.18387	-18.36630	-17.18384	-18.36632
CLN	1.77856	-.76260	1.77886	-.76228

***** SUMMARY OF TOTAL LOADS *****

*** STEP 6

ALPHA C = 15.00 DEG. PHI = .001 DEG. MACH = 2.50

(BODY AXIAL FORCE CONTRIBUTIONS NEGLECTED)

ROLLED BODY-AXIS COORDINATES			**	UNROLLED BODY-AXIS COORDINATES		
	LINEAR LOADING PRESSURE	BERNOULLI LOADING PRESSURE	**		LINEAR LOADING PRESSURE	BERNOULLI LOADING PRESSURE
CX(NOSE ONLY)	.1911E+00	.1937E+00	**	CX(NOSE ONLY)	.1911E+00	.1937E+00
CZB	.1567E+02	.1770E+02	**	CZU	.1567E+02	.1770E+02
CYB	-.4901E+00	-.7145E+00	**	CYU	-.4898E+00	-.7142E+00
CMB	-.8015E+02	-.9144E+02	**	CMU	-.8017E+02	-.9146E+02
CLNB	.5187E+01	.4244E+01	**	CLNU	.5186E+01	.4242E+01
CLLB	-.1124E+01	-.1395E+01	**	CLLU	-.1124E+01	-.1395E+01

ORIGINAL PAGE IS
OF POOR QUALITY

APPENDIX B
COMPANION PROGRAM BDYSHD

TABLE OF CONTENTS

APPENDIX B

PROGRAM BDYSHD

B.1 INTRODUCTION

This appendix provides user-oriented information for the optional application of vortex-shedding program BDYSHD to the afterbody of a complete supersonic configuration consisting of a set of forward fins and a set of tail fins mounted on an axisymmetric body. The afterbody is the length of body between the forward- and tail-finned sections.

Program BDYSHD has been specifically designed to be used as a companion program in an optional step (step 3a) of the stepwise procedure of program LRCDM2 as described in section 2.3 and in Appendix A of this report. Program BDYSHD should be engaged for cases with included angles of attack in excess of 10° and for afterbody lengths longer than about 10 diameters.

In essence, BDYSHD is a modified version of forebody vortex-shedding program NOSEVTX referred to in reference 5 and described in detail in reference 6. The major differences between program BDYSHD and program NOSEVTX are listed in section 2.2 of this report.

A general description of the method of analysis and the optional use of program BDYSHD in conjunction with program LRCDM2 will be given. This is followed by descriptions of the program input and output. A sample case involving program LRCDM2 and companion program BDYSHD is given in section A.9 of Appendix A.

B.2 GENERAL DESCRIPTION

Program BDYSHD calculates pressure distributions and forces and moments acting on axisymmetric afterbodies under the influences of vortices generated by the forebody and the forward fins and additional vortices shed from the afterbody surface (step 3a). The development of the afterbody shed vortices is the main feature of this program and the essential theoretical methods are summarized next. Detailed descriptions are provided in reference 6. A subroutine calling sequence chart for BDYSHD is shown in figure B.1. The common block cross reference map and subroutine cross reference map are given in figure B.2 and figure B.3 respectively.

Immediately aft of the trailing edge of the forward-finned section, the circumferential pressure distribution is computed on the afterbody on the basis of the compressible Bernoulli pressure calculation method. In this calculation, velocities induced by linearly varying line sources/sinks and line doublets used to model axisymmetric bodies in supersonic flow are added to contributions from the body-nose vortices (if present) and forward-fin wake vortices. Program BDYSHD performs the body modeling (it is the same as used in LRCDM2) and the vortex information at the beginning station is transferred on TAPE8 from LRCDM2 to BDYSHD at the completion of step 3. Once the circumferential pressure distribution is determined, program BDYSHD applies a modified Stratford criteria to the pressure profile. If certain conditions related to the circumferential pressure gradient and pressure coefficient are satisfied (details in ref. 6), separation points on the circumference of this axial station are computed and vortices shed from these points. All the vortices are tracked to the next axial location and the circumferential pressure distribution is calculated again including effects of the body singularities, body-nose, fin-wake vortices and the additional shed vortices if they were formed at the previous station.

The above process is repeated at many axial stations along the afterbody length up to to the leading edge of the tail-finned section. Note that the vortex paths are calculated on the basis of vortex tracking methods involving slender body theory for vortices in the presence of one another and the afterbody. At each axial station, the circumferential pressure distribution is integrated to obtain force and moment coefficients for a body ring, and the accummulated values are calculated up to the axial station under consideration. Towards the tail section, the vorticity shed from the afterbody forms two vortex clouds which can be asymmetric depending on the lateral locations and strengths of the upstream vorticity at the beginning station as transferred from LRCDM2.

At the last axial station immediately ahead of the tail section, program BDYSHD transfers the vortex strengths and crossflow coordinates to LRCDM2. In this transfer on TAPE8, the body-shed vorticity in the vortex clouds are represented by their centroids of vorticity if the number of shed vortices exceeds number NVTRNS specified in the input of BDYSHD. However, the forebody vortices (if any) and the forward-fin wake vortices are kept separate from the additional afterbody-shed vortices. Finally, at the conclusion of step 3a, program BDYSHD computes the forces and moments acting on the afterbody and these loads are added to the total forces and moments calculated by LRCDM2 up to the end of the forward-finned section. This information is stored on TAPE9.

Program BDYSHD has internal error messages. In most cases, they are self explanatory. In addition, there are execution stops at numbered STOP locations within the program. They are described on page 26 of reference 6. Messages concerned with the body paneling scheme do not apply to program BDYSHD.

B.3 DESCRIPTION OF INPUT

The input for program BDYSHD is a simplified version of the input for NOSEVTX described in detail in reference 6. The simplifications are the result of eliminating the body-paneling scheme used in NOSEVTX which is applicable to various body cross sectional shapes. The paneling method is replaced with the much simpler line singularities distributed along the body centerline for bodies with axisymmetric cross section and pointed noses. Therefore, the amount of input has been decreased appreciably.

The program user can refer to reference 6 for the original NOSEVTX input description. New items in the input for program BDYSHD are indicated with (NEW) in the list of variables given below. References are made to the body coordinate system (x_B, y_B, z_B,) which has its origin at the body nose, refer to figure A.4 in Appendix A. Note that new input Item 19, namelist $BODY, is the same as the step 1, Item 9 input for LRCDM2, Appendix A.

INPUT VARIABLES FOR PROGRAM BDYSHD

Program Variable	Format	Comments
Item 1	(16I5)	Single card containing 16 integers, each right justified in a five column field.
NCIR		NCIR = 0
NFC		NFC = 0
ISYM		Symmetry index. = 0, right-left flow symmetry = 1, no symmetry
NBLSEP		Body vortex separation index. = 0, no separation (required if $\alpha_c = 0$ in item 5). = 1, laminar separation, Preferred. = 2, turbulent separation.
NSEPR		Reverse flow separation index. = 0, no separation = 1, laminar separation in reverse flow region
NSMOTH		Vortex induced velocity smoothing index. = 0, no smoothing = 1, vortex smoothing in pressure calculation = 2, vortex smoothing in velocity field calculation = 3, combination
NDFUS		Vortex core model index. = 0, potential vortex = 1, diffusion core model, preferred.
NDPHI		Unsteady pressure term index. = 0, omit $\delta\phi/\delta t$ from C_p calculation = 1, include $\delta\phi/\delta t$ term = 2, include $\delta\phi/\delta t$ term at all axial stations except first station XI, item 6 below, use NDPHI = 2 (NEW)

INP		Nose force index = 0, slender body theory force on portion of nose ahead of starting point (XI) = 1, zero force on nose ahead of XI. Use this value
NXFV		Number of x_B-stations at which flow field is calculated or special output is generated. See Item 12, below. $0 < NXFV < 8$
NFV		Number of field points for flow field calculation See Item 13, below. $0 < NFV < 200$; set NFV=0
NVP		Number of $+\Gamma$ vortices on $+y_B$ side of body to be input for restart calculation. See Item 15, below. $0 < NVP < 70$; normally not used, set NVP=0.
NVR		Number of $-\Gamma$ vortices on $-y_B$ side of body to be input for restart calculation. See Item 16, below. $0 < NVR < 30$; normally not used, set NVR=0.
NVM		Number of $-\Gamma$ vortices on $-y_B$ side of body to be input for restart calculation. See Item 17. NVM = 0 if ISYM = 0. $0 < NVM < 70$; normally not used, set NVM = 0
NVA		Number of $+\Gamma$ reverse flow vortices on $-y_B$ side of body to be input for restart calculation. See Item 18. NVA = 0 if ISYM = 0. $0 < NVA < 30$; Normally not used, set NVA = 0.
NASYM		Asymmetric vortex shedding index. See Item 7. = 0, no forced asymmetry. Use this value. = 1, forced asymmetry.
<u>Item 2</u>	(16I5)	A single card defining seven integer output option indices.
NHEAD		Number of title cards in Item 3. NHEAD > 1

NPRNTP — Pressure distribution print index.

- = 0, no pressure output except at special x_B-stations specified by Item 12 below.
- = 1, pressure distribution at each x_B-station calculated by the progam.

NPRNTS — Vortex separation print index.

- = 0, no output
- = 1, output at each x_B-station. Preferred.
- = 2, detailed separation calculation output. For debugging purposes only.

NPRNTV — Vortex cloud summary output index.

- = 0, no vortex cloud output.
- = 1, vortex cloud output. Preferred.

NPLOTV — Vortex cloud printer-plot option.

- = 0, no plot
- = 1, plot full cross section on a constant scale.
- = 2, plot upper half cross section on a constant scale.
- = 3, plot full cross section on a variable scale.

NPLOTA — Plot frequency index.

- = 0, no plots
- = 1, plot vortex cloud at specified x_B-stations. See Item 12.
- = 2, plot vortex cloud at each x_B-station.

NPRTVL — Velocity calculation auxiliary output for debugging purposes only.

- = 0, no output. Preferred.
- = 1, print velocity components at field points. See Items 12 and 13.
- = 2, print velocity components at body control points during pressure calculation. This option can produce massive quantities of output. (Not recommended)

NVTRNS		Maximum number of body-shed and specified vortices transferred to program LRCDM2 on TAPE8. If NVTRNS=0, the afterbody vortices are represented by centroids of vorticity, preferred value (NEW).
<u>Item 3</u>	(20A4)	A series of cards containing Hollerith information identifying the run.
TITLE		NHEAD cards of identification. Information to be printed at top of output.
<u>Item 4</u>	(8F10.5)	Reference information used in forming aerodynamic coefficients.
REFS		Reference area. REFS > 0; set equal to reference area SREF of LRCDM2 input in Item 2 of step 1, Appendix A.
REFL		Reference length. REFL > 0; set equal to reference length REFL of LRCDM2 input in Item 2 of step 1, Appendix A.
XM		Moment center; set equal to moment center XM of LRCDM2 input in Item 2 of step 1, Appendix A.
SL		Body length (L), same as LBODY in item 19 below.
SD	D	Body maximum diameter
<u>Item 5</u>	(8F10.5)	Flow condition parameters
ALPHAC	α_c	Angle of incidence, degrees ($0° \leq \alpha_c < 90^0$). If $\alpha_c = 0°$, set NBLSEP = 0 in Item 1. Note: Value for ALPHAC should be the same as the (one) value for ALFS input for LRCDM2, Appendix A, item 3 of input required for all runs.

PHI	ϕ	Angle of roll, degrees. Note: Value for PHI should be the same as the (one) value for FEES input for LRCDM2, Appendix A, item 5 of input required for all runs.
RE		Reynolds Number ($V_\infty D/\nu$)
VISR		Viscosity ratio (ν_e/ν). To be used to increase diffusion effect of vortex model. Preferred value = 1.0.
XMACH		Mach number, M_∞ ; set equal to Mach number FMACH of LRCDM2 input in Item 2 of step 1, Appendix A.
Item 6	(8F10.5)	A single card containing the specification of the axial extent of the run and certain parameters associated with the vortex wake.
XI		Initial x_B-station. XI > 0, use axial location of canard trailing edge.
XF		Final x_B-station. XF > XI, use axial location of tail-section leading edge.
DX		Increment in x_B for vortex shedding calculation. Typical value, DX $\tilde{\sim}$ D/2
EMKF		Minimum distance of shed-vortex starting position from body surface. = 1.0, vortices positioned such that separation point is a stagnation point in the crossflow plane. > 1.0, minimum radii away from body surface for shed vortices. Typical value, EMKF = 1.05.
RGAM		Vortex combination factor. = 0.0, vortices not combined. Preferred. > 0.0, radial distance within which vortices are combined. Typical value, RGAM = 0.05 D

VRF		Vortex reduction factor to account for observed decrease in vortex strength. = 6.0, for subsonic flow, not applicable to BDYSHD = 1.0, for closed bodies, or supersonic flow. Use this value.
RCORE		Vortex core radius, normally use 0.25 (NEW).
<u>Item 7</u>	(8F10.5)	Contains only one variable that is of general use in program BDYSHD, and that is the integration error tolerance, E5. The next three variables concern the use of forced asymmetry for bodies at very high angles of attack in subsonic flow, not applicable to BDYSHD
E5		Error tolerance for vortex trajectory calculation. Typical range, E5 = 0.01 to 0.05
XTABL		XTABL = 0.0
XASYMI		Initial x_B-location at which forced asymmetry of separation points is used. Typical value, XASYMI = 0.0
XASYMF		Final x_B-location at which forced asymmetry of separation points is used. Typical value, XASYMF = 0.0
DBETA		Amount of forced asymmetry for separation points on body, degrees. Typical value, DBETA = 0.0

<u>Items 8, 9, 10, and 11</u> provide a table of geometric characteristics that must be input for the afterbody.

<u>Item 8</u>	(I5)	
NXR		Number of entries in body table. (1 < NXR < 50); normally NXR=1 for constant radius afterbody.
<u>Item 9</u>	(8F10.5)	

XR		x_B-stations for geometry table (NXR values, 8 per card)
<u>Item 10</u>	(8F10.5)	
R		Body radius at x_B-stations (NXR values, 8 per card)
<u>Item 11</u>	(8F10.5)	
DR		Body slope, dr_o/dx at x_B-stations (NXR values, 8 per card). For constant radius afterbody DR = 0.0.
<u>Item 12</u>	(8F10.5)	
		This item is included only if NXFV > 0 in Item 1 above
XFV		X_B-stations at which field point velocities are calculated or at which optional output is generated, 8 stations maximum.
<u>Item 13</u>		This item is included only if NFV > 0, Item 1 above
YFV, ZFV		y_B, z_B coordinates of field points at which velocity field is calculated. These are expressed in terms of local body radius, y/r_o, z/r_o. (NFV cards with one set of coordinates per card)
<u>Item 14</u>	(8F10.5)	Contains the nose force and moment coefficients at the first axial station upstream of the restart point. When program BDYSHD is used in conjunction with program LRDCM2, these values are set to zero.
CN		Normal force coefficient
CY		Side force coefficient
CM		Pitching moment coefficient
CR		Yawing moment coefficient
CSL		Rolling moment coefficient
CA		Axial force coefficient

Item 15	(8F10.5)	A block of NVP cards to specify the positive separation vorticity on the right side of the body. Omitted if NVP = 0, Item 1 above
GAMP		Γ/V_∞, positive separation vorticity on right side of body.
YP, ZP		Coordinates of discrete vortices on right side of body at XI.
XSHEDP		x_B-location at which vortex was shed.
Item 16	(8F10.5)	A block of NVR cards to specify the secondary vorticity on the right side of the body. Omitted if NVR = 0, item 1 above
GAMR		Γ/V_∞, reverse flow or additional vorticity on right side of body.
YR, ZR		Coordinates of discrete vortices on right side of body at starting point (XI).
XSHEDR		x_B-location at which individual vortex was shed (may be 0.0).
Item 17	(8F10.5)	Specifies the negative separation vorticity on the left side of the body, analogous to Item 15. Omitted if NVM = 0 or ISYM = 0, Item 1 above.
GAMM		Γ/V_∞, negative separation vorticity on left side of body.
YM, ZM		Coordinates of discrete vortices on left side of body at starting point (XI).
XSHEDM		X_B-location at which individual vortex was shed (may be 0.0).
Item 18	(8F10.5)	Specifies the secondary vorticity on the left side of the body. This item is analogous to Item 16, and is omitted if NVA = 0 or ISYM = 0
GAMA		Γ/V_∞, reverse flow or additional vorticity on left side of body

YA, ZA		Coordinates of discrete vortices on left side of body at starting point (XI)
XSHEDA		x_B-location at which individual vortex was shed (may be 0.0).
<u>Item 19</u>	(namelist)	Namelist $BODY read in by subroutine BDYGEN. Consists of four variables describing the body. (NEW).
NXBODY		Number of line sources/sinks and line doublet singularities distributed along body centerline.
LNOSE		Length of nose part of body measured from nose tip, dimensional (real variable).
LBODY		Length of body, dimensional (real variable).
BCODE		Control index (integer) for specifying forebody shape over length of LNOSE = 0, Parabolic = 1, Sears-Haack = 2, Tangent ogive = 3, Ellipsiodal = 4, Conical

B.4 DESCRIPTION OF OUTPUT

The output of program BDYSHD is essentially the same as the output of program NOSEVTX described in detail in reference 6. In that output description, however, any references to source panels do not apply to BDYSHD. In what follows, the output of BDYSHD will be summarized for the normally used output options NPRNTP=0, NPRNTS=1, NPRNTV=1, NPLOTV=3, NPLOTA=1 and NPRTVL=0 specified in Item 2 of the input for this program. Output for a sample case is shown in figure A.7 of Appendix A.

The output of BDYSHD opens with reference quantities, flow conditions, initial conditions and options chosen in the input. Of importance is the list of vortex strengths and locations transferred from LRCDM2 at the end of step 3 on TAPE8. This is followed by the input supplied to flow model the afterbody which in fact starts at $x_B = 26.93$ and ends at $x_B = 80.73$ inches in the sample case. Program BDYSHD distributes line singularities from the body nose, $x_B = 0.0$, to the body base, $x_B = 102.32$ inches. The solution for the complete body follows, and it is characterized by the linearly varying line source strength constants, T (I), the linearly varying line doublet strength constants, TC (I), and the line singularity starting locations X ($\equiv x_B$).

The following pages of the output contain pressure distributions, vortex positions in the cross flow plane, separation data and integrated forces and moments at the first station XI specified in Item 6 of the input. Detailed descriptions are given on pages 52 through 55 of reference 6. The same information is given at many axial locations along the afterbody. In particular, the pressure distributions are given at axial stations closest to the stations XFV specified in Item 12 of the input. These axial locations do not coincide necessarily since the program-calculated stations depend on an integration step Δx_B set by the integration routine DASCRU. At the end of the output, x_B = 80.75 in the sample case, the important information includes the total forces and moments acting on the afterbody calculated on the basis of Bernoulli pressures listed under the heading "CONTRIBUTION OF BODY SECTION TO TOTAL LOADS". In addition, the body-shed vortex strengths and lateral locations at the end of the afterbody are given in nondimensionalized form. The output concludes with a list of all the vortices (including body-nose vortices, if present, and the fin-wake vortices), their locations in the crossflow plane ($Y \equiv Y_B$, $Z \equiv z_B$) and strenghts (Γ divided by free stream). This information is transferred back to LRCDM2 on TAPE8 prior to analysis of the tail section.

Figure B.1 -

SUBROUTINE CALLING SEQUENCE OF PROGRAM BDYSHD

(Pages 1 through 4)

FLOW CHART OF PROGRAM - BDYSHD

```
PROGRAM
 BDYSHD

   |-- INPUT
   |-- OUTPUT
   |-- TAPE10
   |-- TAPE5
   |-- TAPE6
   |-- TAPE7
   |-- TAPE8
   |-- TAPE9
   |-- INPT   ---- TAPE5
   |            |-- TAPE6
   |            |-- TAPE8
   |            |-- EOF
   |            |-- SIN
   |            |-- COS
   |            |-- ASIN
   |            |-- SQRT
   |-- ELNOSE ---- TAPE6
                |-- TAPE8
                |-- TAPE9
                |-- F      ---- SHAPE
                |            |-- BMAP   ---- TAPE6
                |            |            |-- COS
                |            |            |-- SIN
                |            |            |-- ATAN2
                |            |            |-- SQRT
                |            |            |-- SUM    ---- CEXP
                |            |-- ATAN2
                |            |-- DMAP   ---- SIN
                |            |            |-- COS
                |            |-- CMAP   ---- CSQRT
                |            |            |-- SQRT
                |            |            |-- ATAN2
                |            |            |-- COS
                |            |            |-- SIN
                |            |            |-- SUM    ---- CEXP
                |            |-- VELCAL ---- SQRT
                |            |            |-- ATAN2
                |            |            |-- SOURCE ---- TAPE6
                |            |            |            |-- SQRT
                |            |            |            |-- ALOG
                |            |            |-- DOUBLT ---- TAPE6
                |            |            |            |-- SQRT
                |            |            |            |-- ALOG
                |            |            |-- COS
                |            |            |-- SIN
                |            |-- VLOCTY ---- TAPE6
                |                         |-- SUM    ---- CEXP
                |                         |-- SMOOTH ---- CLOG
                |                         |            |-- CABS
                |                         |            |-- EXP
                |                         |-- EXP
```

(a) Page 1

Figure B.1 - Subroutine calling sequence of program BDYSHD.

```
 |                                  |-- ASUM
 |                                  |-- SQRT
 |-- SIN
 |-- COS
 |-- SQRT
 |-- SHAPE
 |-- BMAP     ---- TAPE6
 |                |-- COS
 |                |-- SIN
 |                |-- ATAN2
 |                |-- SQRT
 |                |-- SUM     ---- CEXP
 |-- ATAN2
 |-- DMAP     ---- SIN
 |                |-- COS
 |-- CMAP     ---- CSQRT
 |                |-- SQRT
 |                |-- ATAN2
 |                |-- COS
 |                |-- SIN
 |                |-- SUM     ---- CEXP
 |-- BDYGEN   ---- TAPE5
 |                |-- TAPE6
 |                |-- SIN
 |                |-- SQRT
 |                |-- ASIN
 |                |-- BODYR   ---- SQRT
 |                |-- SOURCE  ---- TAPE6
 |                |                |-- SQRT
 |                |                |-- ALOG
 |                |-- DOUBLT  ---- TAPE6
 |                                 |-- SQRT
 |                                 |-- ALOG
 |-- BODYR    ---- SQRT
 |-- VLOCTY   ---- TAPE6
 |                |-- SUM     ---- CEXP
 |                |-- SMOOTH  ---- CLOG
 |                |                |-- CABS
 |                |                |-- EXP
 |                |-- EXP
 |                |-- ASUM
 |                |-- SQRT
 |-- VELCAL   ---- SQRT
 |                |-- ATAN2
 |                |-- SOURCE  ---- TAPE6
 |                |                |-- SQRT
 |                |                |-- ALOG
 |                |-- DOUBLT  ---- TAPE6
 |                |                |-- SQRT
 |                |                |-- ALOG
 |                |-- COS
 |                |-- SIN
 |-- DPHIDT   ---- VELCAL  ---- SQRT
 |                |                |-- ATAN2
 |                |                |-- SOURCE  ---- TAPE6
 |                |                |                |-- SQRT
 |                |                |                |-- ALOG
 |                |                |-- DOUBLT  ---- TAPE6
 |                |                |                |-- SQRT
 |                |                |                |-- ALOG
```

(b) Page 2

Figure B.1 - Continued.

```
|              |              |-- COS
|              |              |-- SIN
|              |-- VLOCTY ---- TAPE6
|                             |-- SUM      ---- CEXP
|                             |-- SMOOTH ---- CLOG
|                             |              |-- CABS
|                             |              |-- EXP
|                             |-- EXP
|                             |-- ASUM
|                             |-- SQRT
|-- FORCEP
|-- PLOTV  ---- PLOTA2 ---- TAPE6
|                             |-- PLOTA8 ---- PLOTA6 ---- ALOG10
|                             |              |-- PLOTA5
|                             |-- PLOTA7
|-- FPVEL  ---- TAPE6
|              |-- ATAN2
|              |-- DMAP   ---- SIN
|              |              |-- COS
|              |-- CMAP   ---- CSQRT
|              |              |-- SQRT
|              |              |-- ATAN2
|              |              |-- COS
|              |              |-- SIN
|              |              |-- SUM      ---- CEXP
|              |-- VELCAL ---- SQRT
|              |              |-- ATAN2
|              |              |-- SOURCE ---- TAPE6
|              |              |              |-- SQRT
|              |              |              |-- ALOG
|              |              |-- DOUBLT ---- TAPE6
|              |              |              |-- SQRT
|              |              |              |-- ALOG
|              |              |-- COS
|              |              |-- SIN
|              |-- VLOCTY ---- TAPE6
|              |              |-- SUM      ---- CEXP
|              |              |-- SMOOTH ---- CLOG
|              |              |              |-- CABS
|              |              |              |-- EXP
|              |              |-- EXP
|              |              |-- ASUM
|              |              |-- SQRT
|              |-- SQRT
|-- SEPRAT ---- TAPE6
|              |-- SQRT
|-- VTABLE
|-- DASCPU ---- F       ---- SHAPE
|                             |-- BMAP   ---- TAPE6
|                             |              |-- COS
|                             |              |-- SIN
|                             |              |-- ATAN2
|                             |              |-- SQRT
|                             |              |-- SUM      ---- CEXP
|                             |-- ATAN2
|                             |-- DMAP   ---- SIN
|                             |              |-- COS
|                             |-- CMAP   ---- CSQRT
|                             |              |-- SQRT
|                             |              |-- ATAN2
```

(c) Page 3

Figure B.1 - Continued.

```
                |                       |           |-- COS
                |                       |           |-- SIN
                |                       |           |-- SUM     ---- CEXP
                |                       |-- VELCAL ---- SQRT
                |                       |           |-- ATAN2
                |                       |           |-- SOURCE ---- TAPE6
                |                       |           |           |-- SQRT
                |                       |           |           |-- ALOG
                |                       |           |-- DOUBLT ---- TAPE6
                |                       |           |           |-- SQRT
                |                       |           |           |-- ALOG
                |                       |           |-- COS
                |                       |           |-- SIN
                |                       |-- VLOCTY ---- TAPE6
                |                                   |-- SUM     ---- CEXP
                |                                   |-- SMOOTH ---- CLOG
                |                                   |           |-- CABS
                |                                   |           |-- EXP
                |                                   |-- EXP
                |                                   |-- ASUM
                |                                   |-- SQRT
                |
                |-- VCENTR
                |-- COMBIN ---- TAPE6
                            |-- SQRT

PROGRAM
  END
```

(d) Page 4

Figure B.1 - Concluded.

Figure B.2 -

COMMON BLOCK CROSS REFERENCE MAP FOR PROGRAM BDYSHD

(Pages 1 through 2)

CROSS REFERENCE MAP

PAGE = 1

SUBROUTINE NAME / COMMON BLOCKS	ASUM	BDYGFN	BDYSHD	BMAP	BUDYR	CMAP	COMBIN	DASCRU	DMAP	DOUBLT	DPHIDT	FLNOSE	FORCEP	FPVEL	F
BLREV												X			
BLSEP												X			
BODYGN		X													
BPLTA1															
BPLTA2															
BSCALE															
BVEL															
CBODY												X			
CFLAG												X			
CFLT												X			
CLDS			X									X			
CNTROD												X			
CONST				X		X			X		X	X	X	X	X
COP												X			
CTRANS		X													
CVRTX			X									X			
FLOW											X	X	X	X	
JOPTNS												X			
LOADP												X	X		
MAPB				X		X			X			X		X	X
MAPC				X		X			X			X		X	X
MAPN	X			X		X									
MAPX												X			X
MAP1	X			X		X			X			X	X	X	X
MAP2				X					X			X	X		
ONE		X													
PARAM		X										X			
PHI											X	X			
PRESS												X	X		
PRINT		X													

SUBROUTINE NAME / COMMON BLOCKS	INPT	PLOTA2	PLOTA5	PLOTA6	PLOTA7	PLOTA8	PLOTV	SEPRAT	SHAPE	SMOOTH	SOURCE	SUM	VCENTR	VELCAL	VLOCTY	VTABLE
BLREV	X							X								
BLSEP	X							X								
BODYGN	X															
BPLTA1		X			X	X										
BPLTA2		X														
BSCALE		X				X	X									
BVEL														X		
CBODY	X															
CFLAG	X														X	
CFLT	X															
CLDS													X			
CNTROD															X	
CONST																
COP	X															
CTRANS																
CVRTX													X			
FLOW	X									X					X	
JOPTNS																
LOADP	X															
MAPB																
MAPC																
MAPN	X								X			X				
MAPX																
MAP1	X							X	X			X			X	
MAP2							X	X								
ONE														X		
PARAM																
PHI															X	
PRESS								X								
PRINT																

(a) Page 1

Figure B.2 - Common block cross reference map for program BDYSHD.

CROSS REFERENCE MAP PAGE = 2

SUBROUTINE NAME / COMMON BLOCKS	ASUM	HDYGFN	HDYSHD	HMAP	HODYR	CMAP	COMBIN	DASCRU	DMAP	DOUBLT	DPHIDT	ELNOSE	FORCEP	FPVEL	F	INPT	PLOTA2	PLOTA5	PLOTA6	PLOTA7	PLOTA8	PLOTVT	SFPRAT	SHAPE	SMOOTH	SOURCE	SUM	VCENTR	VELCAL	VLOCTY	VTABLE
RFF												X	X			X						X	X								
SHPF												X				X								X							
SPSANG		X																													
STACK		X																											X		
SYMTRY												X			X	X							X								
TRANS																X															
TWO		X			X					X																X			X		
VFL											X	X		X	X	X														X	
VFPTS												X		X		X															
VORTFX							X				X	X	X		X	X						X			X			X		X	X
VTXTPL							X					X				X						X			X			X			X
WBTRI		X										X																			
WBTP		X																													
ZFLOW												X				X							X								

(b) Page 2

Figure B.2 - Concluded.

Figure B.3 -

SUBROUTINE CROSS REFERENCE MAP FOR PROGRAM BDYSHD

(Pages 1 through 2)

CROSS REFERENCE MAP PAGE = 1

SUBROUTINE NAME / EXTERNAL REFERENCES	ASUM	BDYGEN	BDYSHD	BMAP	BODYR	CMAP	COMBIN	DASCRU	DMAP	DOUBLT	DPHIDT	ELNOSE	FORCEP	FPVEL	F
ALOG10															
ALOG										X					
ASIN		X													
ASUM															
ATAN2				X		X						X		X	X
BDYGEN												X			
BMAP												X			X
BODYR		X										X			
CABS															
CEXP															
CLOG															
CMAP												X		X	X
COMBIN												X			
COS				X		X			X			X			
CSQRT						X									
DASCRU												X			
DMAP												X		X	X
DOUBLT		X													
DPHIDT												X			
ELNOSE			X												
EOF															
EXP															
FORCEP												X			
FPVEL												X			
F								X				X			
INPT			X												
INPUT			X												
OUTPUT			X												
PLOTA2															
PLOTA5															

SUBROUTINE NAME / EXTERNAL REFERENCES	INPT	PLOTA2	PLOTA5	PLOTA6	PLOTA7	PLOTAB	PLOTV	SEPRAT	SHAPE	SMOOTH	SOURCE	SUM	VCENTR	VELCAL	VLOCTY	VTABLE
ALOG10				X												
ALOG											X					
ASIN	X															
ASUM															X	
ATAN2														X		
BDYGEN																
BMAP																
BODYR																
CABS										X						
CEXP												X				
CLOG										X						
CMAP																
COMBIN																
COS	X													X		
CSQRT																
DASCRU																
DMAP																
DOUBLT														X		
DPHIDT																
ELNOSE																
EOF	X															
EXP										X					X	
FORCEP																
FPVEL																
F																
INPT																
INPUT																
OUTPUT																
PLOTA2							X									
PLOTA5						X										

(a) Page 1

Figure B.3 - Subroutine cross reference map for program BDYSHD.

CROSS REFERENCE MAP PAGE = 2

SUBROUTINE NAME / EXTERNAL REFERENCES	ASUM	BDYGEN	BDYSHD	HMAP	RODYR	CMAP	COMRIN	DASCHU	DMAP	DOUBLT	DPHIDT	ELNOSE	FORCEP	FPVEL	F	INPT	PLOTA2	PLOTA5	PLOTA6	PLOTA7	PLOTA8	PLOTV	SEPRAT	SHAPE	SMOOTH	SOURCE	SUM	VCENTR	VELCAL	VLOCTY	VTABLE
PLOTA6																					X										
PLOTA7																	X														
PLOTA8																	X														
PLOTV												X																			
SEPRAT												X																			
SHAPE												X			X																
SIN		X		X		X			X			X				X													X		
SMOOTH																														X	
SOURCE		X																											X		
SORT		X		X	X	X	X			X		X		X		X							X			X			X	X	
SUM				X		X																								X	
TAPE10			X																												
TAPE5		X	X													X															
TAPE6		X	X	X			X			X		X		X		X	X						X			X				X	
TAPE7			X																												
TAPE8			X									X				X															
TAPE9			X									X																			
VCENTR												X																			
VELCAL											X	X		X	X																
VLOCTY											X	X		X	X																
VTABLE												X																			

(b) Page 2

Figure B.3 - Concluded.

APPENDIX C

FIN-EDGE VORTICITY, EFFECTS OF EXTERNAL VORTICES, BODY FORCES AND MOMENTS

C.1 INTRODUCTION

This appendix contains descriptions of the updated analytical treatment of leading- and side-edge force augmentations and vorticity characteristics. This is followed by the updated calculation of fin trailing-edge vorticity for a fin with arbitrary dihedral or cant angle. The updates refer to improvements and changes since the descriptions of the above characteristics in Appendices C and B, respectively, in Reference 1. The updates are related to the formulation of the spanwise loading distributions in the local fin coordinate system in order to allow for arbitrary fin location and cant angle.

A short description is given of the approach used to account for external vortex effects on the body and fin loads. Finally, the expressions used to integrate the pressures acting on the axisymmetric body for obtaining the body forces and moments are discussed. References are made to variable names and routines of program LRCDM2 (refer to Appendix A of this report for routine calling sequence chart).

C.2 ANALYTICAL TREATMENT OF LEADING- AND SIDE-EDGE VORTICITY CHARACTERISTICS

For fins with sharp edges and subjected to sufficiently high angles of attack, lift augmentation and vortex formation occurs at those edges due to flow separation. The vortices due to the forward-finned section are introduced into the flow along the afterbody and tail fins. It is therefore necessary to estimate these vortex characteristics and to include effects induced by these vortices on the afterbody and tail fins.

One of the simplest approaches is to relate the strength and location of the leading- and side-edge vortices to the suction distributions by means of the Polhamus analogy (refer to Appendix C of Ref. 1). The suction distributions are related to the in-plane forces calculated as an extension to the constant u-velocity panel theory. Effects of leading-edge sweep breaks in the vortex formation and effects of vortex bursting are presently not accounted for.

The basic methods involved in the determination of leading- and side-edge vortex characteristics are described in Appendix C of Reference 1 for cruciform or planar fins. In program LRCDM2, geometrical restrictions concerning fin dihedral angle and position on the body circumference have been relaxed. In essence, the fin plane does not have to be a radial plane passing through the body centerline. This means that span-load and suction distributions need to be computed as a function of the local fin spanwise coordinate, y_F. The following sketch shows the lateral components (y_F,z_F) of the fin local coordinate system for all fins of a cruciform fin layout and for one fin of an arbitrary layout. Note that fin location angle THETR or THETL etc. need not be equal to fin dihedral or cant angle PHIFR or PHIFL, etc. The local fin y_F-coordinate lies in the plane of the fin and is measured normal from the fin root chord. The directions can be outboard or inboard depending on the location of the fin (or equivalently its number designation).

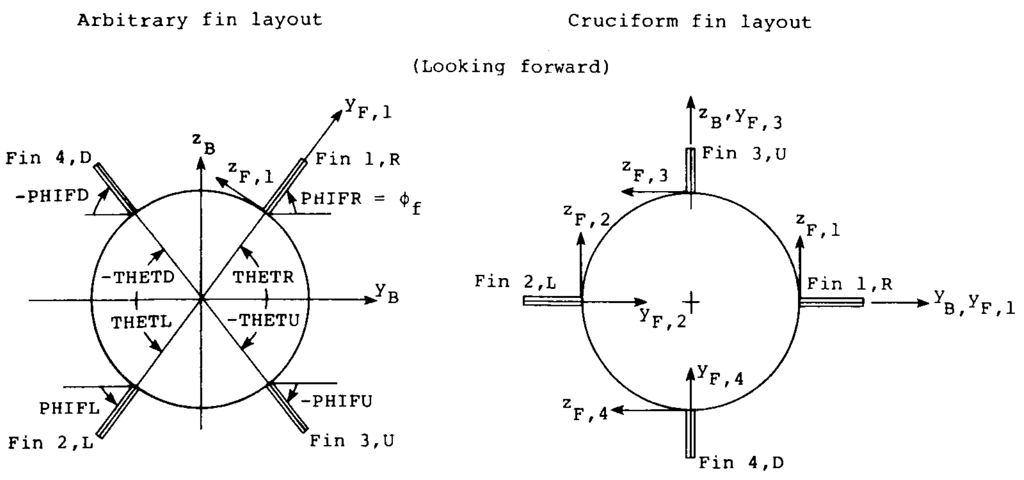

The updated method for calculating the normal force and lift augmentation and the attendant vortex characteristics associated with the leading and/or side edge will now be described. For the leading edge the integration of suction in the spanwise direction is specified as CSINT.

$$\text{CSINT} = 2b \sum_{i=1}^{\text{MSW}} \left. \frac{c_s c}{2b} \right|_i \Delta y_{F,i} \qquad \text{(C-1)}$$

where MSW is the number of constant u-velocity panels in the spanwise direction. The moment with respect to the fin root is calculated as

$$\text{CSMOM} = 2b \sum_{i=1}^{\text{MSW}} y_{F,i} \left. \frac{c_s c}{2b} \right|_i \Delta y_{F,i} \qquad \text{(C-2)}$$

The meanings of the terms appearing in the above equations are shown in the sketch below. This sketch shows a fin in planform with root chord c_r mounted on a body. A two-chordwise (NCW=2) by three-spanwise (MSW=3) paneling layout is indicated on the fin planform. Also depicted are the distributions of suction along the leading and side edges. In routine SPNLD of

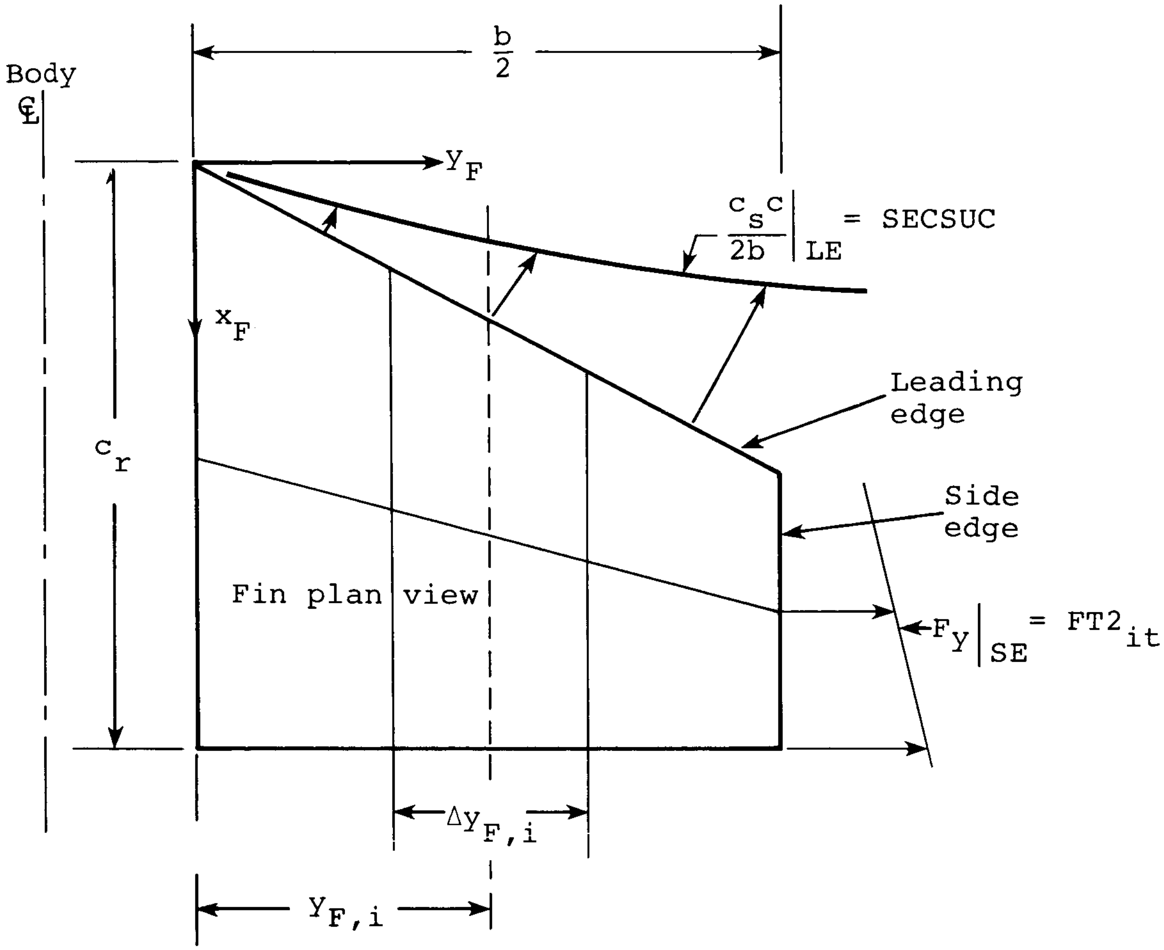

program LRCDM2, variables CSINT and CSMOM are computed as positive (or zero for supersonic edge) quantities. The spanwise center of gravity (or pressure) of the suction distribution is designated CGLOC. In the fin coordinate system it is given by the ratio of the moment over the suction force.

$$y_{c.g.suction}\Big|_{LE} = \text{CGLOC} = \left(\frac{\text{CSMOM}}{\text{CSINT}}\right)(\text{SIGN}) \qquad \text{(C-3)}$$

Quantity SIGN equals positive one (+1) for fins 1 or R and 3 or U, and equals negative one (-1) for fins 2 or L and 4 or D. In this way, the c.g. location is consistent with the fin coordinate system.

In accordance with Polhamus' analogy relating the augmentation of normal force on the leading edge to suction, the added normal force in coefficient form is given by

$$C_N\Big|_{LE\ suction} = K_{v,LE}\ \frac{(CSINT)}{S_{ref}} \qquad (C-4)$$

where $K_{v,LE}$ is the vortex-lift factor for the leading edge and S_{ref} is the reference area. Factor $K_{v,LE}$ has default value 0.5 in program LRCDM2. Refined values on the basis of experimental data can be obtained from Figure 9(a) in Reference 8 as a function of Mach number and aspect ratio. The additional lift can be related approximately to the normal force in accordance with

$$C_L\Big|_{LE\ suction} = C_N\Big|_{LE\ suction} \cos(\alpha_F + \delta) \qquad (C-5)$$

Here α_F is the angle of attack seen by the fin and δ is the angle of deflection of the fin. The quantity α_F is related to angle of pitch α and angle of sideslip β defined in Equation (3) in this report as follows.

$$\alpha_F = \sin^{-1}(-\sin\beta\ \sin\phi_F + \sin\alpha\ \cos\phi_F) \qquad (C-6)$$

Angle ϕ_F is the dihedral angle (PHIFR, etc.) of the fin.

If the fin has a side edge with nonzero length, additional normal force is produced that is related to the suction along the side edge. If this is the case, the integration of suction is continued from the leading edge onto the side edge using quantity CSINT and suction forces $FT2_{it}$ shown in the previous sketch.

$$CSINT|_{TOTAL} = CSINT|_{LE} + \underbrace{\sum_{it=1}^{NCW} FT2_{it}}_{CSINT|_{SE}} \qquad (C-7)$$

Similarly, the moment associated with the side-edge suction is added to the moment determined for the leading edge (b/2 is the exposed fin semispan).

$$CSMOM|_{TOTAL} = CSMOM|_{LE} + \underbrace{\sum_{it=1}^{NCW} \left(\frac{b}{2}\right) FT2_{it}}_{CSMOM|_{SE}} \qquad (C-8)$$

The suction forces acting on each panel outboard aft corner of the panels nearest the fin side edge are designated $FT2_{it}$. Two are shown in the previous sketch.

The spanwise center of gravity (or pressure) of the total distribution of the suction along the leading and side edges is given by

$$y_{c.g.,suction}\Big|_{LE+SE} = CGSELC = \frac{CSMOM|_{TOTAL}}{CSINT|_{TOTAL}} \text{ (SIGN)} \qquad (C-9)$$

with SIGN having the meaning given previously in connection with Equation (C-3). If the fin does not develop suction along the leading edge (i.e., when the leading edge is supersonic), the above treatment is to be applied to the side edge only. In that case,

$$\begin{aligned} CSINT|_{LE} &= 0.0 \\ CSMOM|_{LE} &= 0.0 \end{aligned} \qquad (C-10)$$

and the spanwise center of gravity is located at the fin side edge. By another application of Polhamus' analogy, the total increment in normal and lift force acting on the fin with leading- and side-edge suction can be expressed as

$$\left.\begin{aligned} C_N\Big|_{LE+SE\ suction} &= K_{v,LE}\ \frac{CSINT|_{LE}}{S_{ref}} + K_{v,SE}\ \frac{CSINT|_{SE}}{S_{ref}} \\ C_L\Big|_{LE+SE\ suction} &= C_N\Big|_{LE+SE\ suction}\ \cos(\alpha_F + \delta) \end{aligned}\right\} \quad (C\text{-}11)$$

where $K_{v,SE}$ is the vortex lift factor for the side edge. In program LRCDM2, factor $K_{v,SE}$ has default value 1.0. For supersonic flow, there are few experimental data from which side-edge normal force or lift augmentation can be deduced. For sharp side edges, it is assumed that all of the suction is converted to additional normal force.

The vorticity associated with the total lift augmentation for the fin can be represented as follows. A horseshoe vortex is positioned with its bound leg in the plane of the fin and the outboard trailing leg at the center of gravity of the suction distribution. The inboard leg lies along the fin root as shown in the following sketch. Assuming that

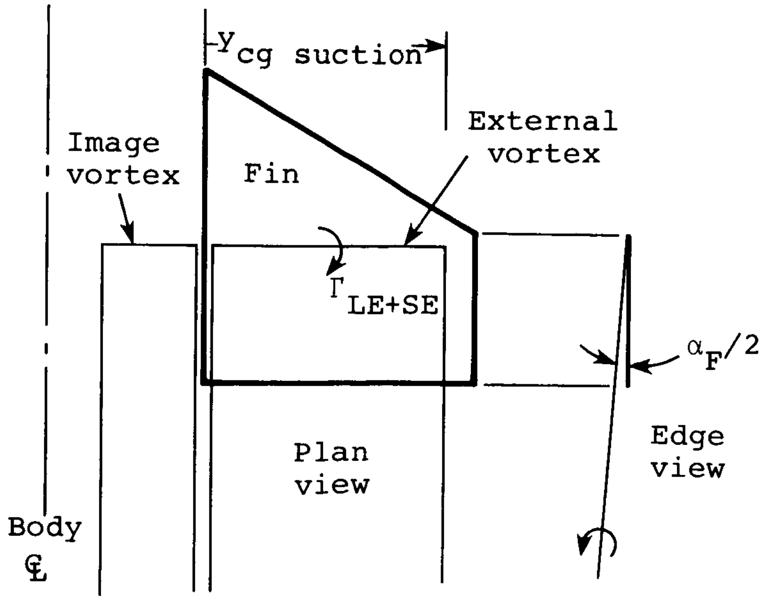

*In any event, the incremental force on the side edge is assumed to act at mid chord.

the additional (augmented) lift generated on (or actually near) the leading and side edges acts on the bound leg of the representative horseshoe vortex, the Kutta-Joukowski law for lift provides the following expression for the vortex strength

$$y_{c.g.,suction} \frac{\Gamma_{LE+SE}}{V_\infty} = \left[K_{v,LE} CSINT|_{LE} + K_{v,SE} CSINT|_{SE} \right] \cos(\alpha_F + \delta) \tag{C-12}$$

or

$$\frac{\Gamma_{LE+SE}}{V_\infty} = \left[\frac{K_{v,LE} CSINT|_{LE} + K_{v,SE} CSINT|_{SE}}{y_{c.g.,suction}} \right] \cos(\alpha_F + \delta) \tag{C-13}$$

The elevation of this vortex above the fin plane is related to angle $\alpha_F/2 (= \alpha_\ell/2)$ as described in Section 2.4 in this report.

In summary, the above method provides a simple model for the vorticity associated with leading- and side-edge flow separation. In reality a rolled up sheet of vorticity appears on top of the fin at its trailing edge. It is represented here by a concentrated, discrete vortex.

The force and moment augmentations due to leading- and side-edge flow separation are included in the summing of overall forces and moments acting on the complete configuration.

C.3 CALCULATION OF FIN TRAILING-EDGE VORTEX CHARACTERISTICS FOR FINS WITH ARBITRARY CANT (OR DIHEDRAL) ANGLE AND ARBITRARY LOCATION ON THE BODY

This section is concerned with the changes to the method described in Appendix B of Reference 1 for cruciform and planar cases. The purpose of the method is to represent the trailing-edge wake of the fin by discrete, concentrated vortices. In this account, the vortices emanating from the trailing edge are related to the span-load distribution associated with attached flow on the fin. Leading- and side-edge flow separation and the attendant augmentation to normal force and moments acting on the fin are not included. A separate analysis, given in the previous section, describes the representation of the vortices associated with the leading and side edges.

The principal modification to the original method consists of referring all calculations relative to the fin-body junction instead of the body centerline. This allows for arbitrary fin location and cant angle. Thus, coordinate transformations will be added to account for the fact that the fins may be in planes other than the major planes.

Consider a fin with exposed semispan b/2 attached to a body as shown in the following sketch. An external vortex

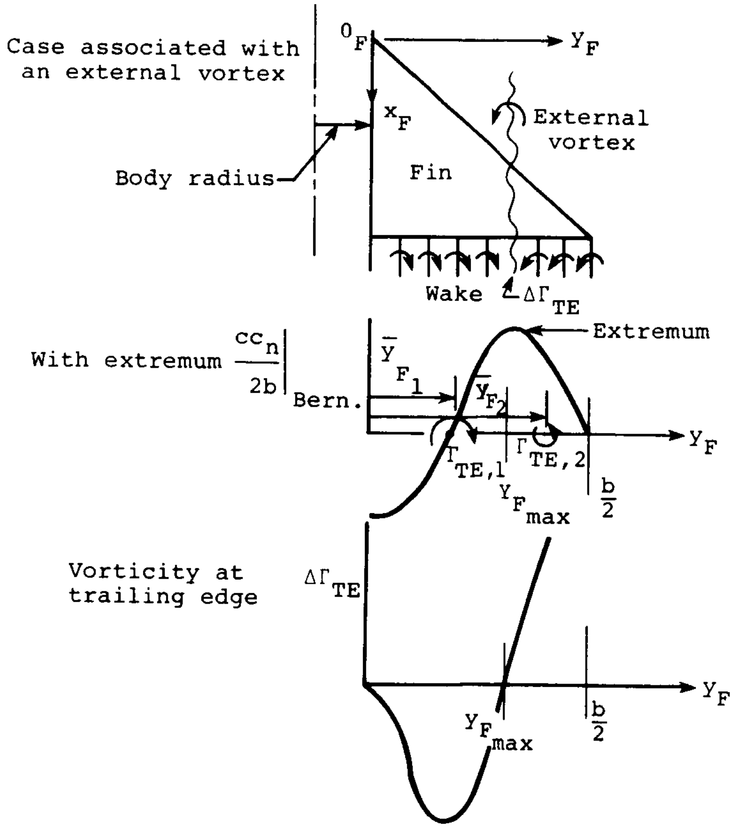

passes over the fin. The resulting span load distribution is indicated. The distribution of the vorticity at the trailing edge is also shown. It is desired to determine the strength(s) and location(s) of the concentrated vortex (vortices) representing the wake.

In the preceeding section, the fin local coordinate system (x_F, y_F, z_F) was introduced with the y_F-axis in the plane of the fin and directed outboard or inboard depending on the fin designation. The z_F-axis is normal to the plane of the fin and x_F extends aft along the fin root. Origin O_F is at the leading edge of the root chord. The spanwise load distribution will be calculated as a function of coordinate y_F.

It can be shown* that under the assumptions of no sideslip and the pressure being linearly related to the potential, the trailing-edge vorticity Γ_{TE} can be related to the span loading as follows.

$$\frac{1}{V_\infty} \frac{\partial \Gamma_{TE}}{\partial y_F} = -\frac{1}{2} \frac{\partial}{\partial y_F} (cc_n) \qquad \text{(C-13)}$$

This relationship will be used here for fins with sideslip as an approximation. The approximation is valid provided the actual span loading is used (i.e., cc_n is representative of the fin load including effects of sideslip).

In order to represent the distributed trailing-edge vorticity by concentrated vortices, the spanwise load distribution based on the Bernoulli pressure expressions is calculated first in routine SPNLD. For the case when this distribution exhibits extrema in between the root and side

---

*Nielsen, J. N., Spangler, S. B., and Hemsch, M. J.: A Study of Induced Rolling Moments for Cruciform-Winged Missiles. Nielsen Engineering & Research, Inc. TR 61, Dec. 1973, p. 36.

edge, as in the previous sketch, the number of concentrated vortices is given by number of extrema plus 1. The trailing-edge vortex strength and spanwise position for the inboard portion of the span load distribution are then given by

$$\frac{\Gamma_{TE,1}}{V_\infty} = -\frac{1}{2}\int_o^{y_{F_{max}}} \frac{\partial}{\partial y_F}(cc_n)\,dy_F = -\frac{1}{2}\int_o^{y_{F_{max}}} d(cc_n) \tag{C-14}$$

$$y_{F_1} = \frac{-\frac{1}{2}\int_o^{y_{F_{max}}} y_F \frac{\partial}{\partial y_F}(cc_n)\,dy_F}{-\frac{1}{2}\int_o^{y_{F_{max}}} \frac{\partial}{\partial y_F}(cc_n)\,dy_F} \tag{C-15}$$

Integrating Equation (C-14) yields

$$\frac{\Gamma_{TE,1}}{V} = -\frac{1}{2}\left[cc_n\Big|_{y_{F_{max}}} - cc_n\Big|_o\right] \tag{C-16}$$

Equation (C-15) is integrated by parts with the following result.

$$\bar{y}_{F_1} = \frac{-\frac{1}{2}\left[y_F cc_n\Big|_o^{y_{F_{max}}} - \int_o^{y_{F_{max}}} (cc_n)\,dy_F\right]}{-\frac{1}{2}\int_o^{y_{F_{max}}} d(cc_n)} \tag{C-17}$$

or

$$\bar{y}_{F_1} = \frac{y_{F_{max}} cc_n \Big|_{y_{F_{max}}} - \int_0^{y_{F_{max}}} (cc_n)\, dy_F}{cc_n \Big|_{y_{F_{max}}} - cc_n \Big|_0} \qquad \text{(C-18)}$$

In routine SPNLD, the integral in Equation (C-18) is designated VALNUM and the denominator is DIFMAX. Quantity $cc_n \Big|_{y_{F_{max}}}$ is called VALMAX.

The strength and position of the outboard vortex is obtained in the same fashion with a change in the limits of integration.

$$\frac{\Gamma_{TE,2}}{V_\infty} = -\frac{1}{2} \int_{y_{F_{max}}}^{b/2} d(cc_n)$$

$$= -\frac{1}{2} \left[cc_n \Big|_{\frac{b}{2}} - cc_n \Big|_{y_{F_{max}}} \right] \qquad \text{(C-19)}$$

(the term $cc_n \Big|_{\frac{b}{2}}$ is struck through with an arrow to "o")

Since the span load vanishes at the side edge (not accounting for side-edge lift augmentation), Equation (C-19) simplifies to

$$\frac{\Gamma_{TE,2}}{V_\infty} = \frac{1}{2}\, cc_n \Big|_{y_{F_{max}}} \qquad \text{(C-20)}$$

The spanwise location of the outboard vortex on the trailing edge is given by Equation (C-15) with the proper limits of integration.

$$\bar{y}_{F_2} = \frac{-\frac{1}{2}\int_{y_{F_{max}}}^{b/2} y_F \frac{\partial}{\partial y_F}(cc_n)\,dy_F}{-\frac{1}{2}\int_{y_{F_{max}}}^{b/2} d(cc_n)} \tag{C-21}$$

After integration by parts, the result is

$$\bar{y}_{F_2} = \frac{cc_n\, y_F\Big|_{y_{F_{max}}}^{b/2} - \int_{y_{F_{max}}}^{b/2}(cc_n)\,dy_F}{cc_n\Big|_{\frac{b}{2}} - cc_n\Big|_{y_{F_{max}}}}$$

or

$$\bar{y}_{F_2} = \frac{-cc_n\Big|_{y_{F_{max}}} y_{F_{max}} - \int_{y_{F_{max}}}^{b/2}(cc_n)\,dy_F}{-cc_n\Big|_{y_{F_{max}}}} \tag{C-22}$$

and finally,

$$\bar{y}_{F_2} = y_{F_{max}} + \frac{\int_{y_{F_{max}}}^{b/2}(cc_n)\,dy_F}{cc_n\Big|_{y_{F_{max}}}} \tag{C-23}$$

In the above equation, the integral is called VALINT in routine SPNLD.

If the span load distribution exhibits additional extrema, Equations (C-16) through (18) must be applied again with the appropriate limits of integration $y_{F_{max,1}}$ to $y_{F_{max,2}}$. For the outboard vortex, Equations (C-19) through (C-23) hold. The vorticity for a fin with fully attached flow always leaves from the fin trailing edge.

It should be noted here that the span load distribution $cc_n/2b$ need not be limited to the attached flow type loading. The above treatment holds for any distribution. However, the position above the fin for a vortex (or vortices) representing leading- and/or side-edge flow separation requires further consideration (see Section 2.4 in this report).

C.4 INCLUSION OF EXTERNAL VORTEX INDUCED EFFECTS IN BODY AND FIN LOADING CALCULATIONS

This section describes the approaches used to account for the influence of external vortices (i.e., body nose and/or wake vortices from the forward fins) on body and fin loadings. The description of the treatment will cover the body first and the fin next. Certain approximations are pointed out. The treatment only applies to program LRCDM2 and not to the methods by which vortex effects are calculated in companion program BDYSHD. Refer to References 5 and 6 for the latter.

Consider first the portions of the body without the fins (i.e., the axisymmetric forebody and afterbody). For the forebody, program LRCDM2 is equipped with a data base (in subroutine BDYVTX) containing strengths and lateral locations of a symmetrical pair of concentrated vortices as a function of distance from the nose. These vortices are representative of forebody flow separation. Over the length of the afterbody, canard wake and forebody vortices influence the body loadings. If afterbody vortex shedding is to be considered, program BDYSHD is engaged as an option.

Thus, on the forebody the vortex locations are supplied as a function of axial distance by the built-in data base and vortex tracking is not required. Vortex induced effects are therefore determined directly from standard crossflow plane theory (employing vortex images inside the body contour) implemented in the routines of module VPATH2. A typical situation for a case involving nonzero roll angle is shown in the sketch below. The external forebody vortices

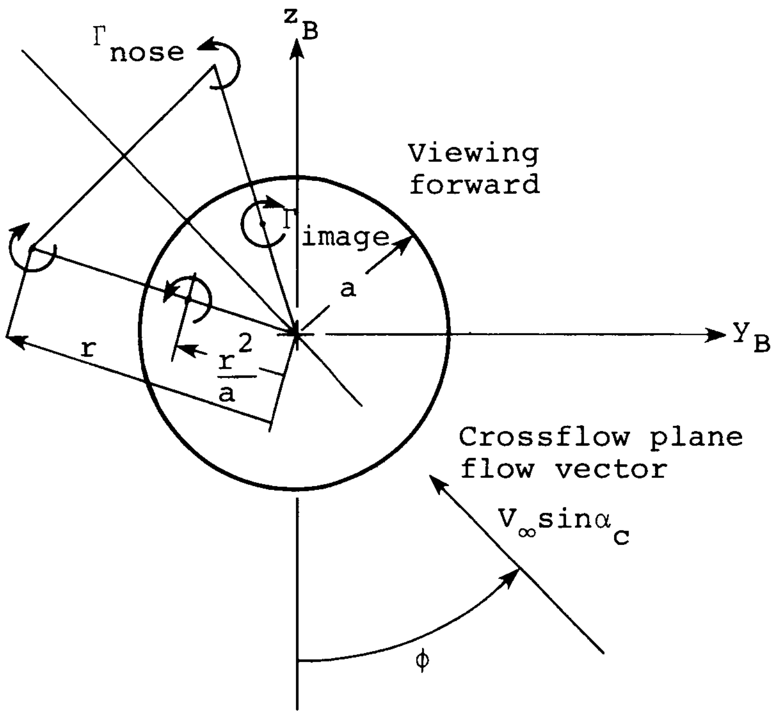

are always symmetrically positioned relative to the crossflow plane flow vector. The lateral body coordinates (y_B,z_B) are also shown. The actual crossflow plane solution for this case is a degenerate version (body without fins) of the theory discussed in Section 1 of Appendix I of Reference 1.

The flow-tangency condition due to the presence of the symmetrical vortex pair is satisfied in the slender-body-theory sense at any point on the surface of the forebody. Therefore, on the basis of the superposition principle associated with linear or potential theory, the vortex induced perturbation velocities can be added to those induced by the line-source and line-doublet singularities used to flow model the axisymmetric body. These supersonic line singularities are described in Appendix I of Reference 7. The sum of the perturbation velocities are then substituted in the compressible (isentropic) Bernoulli pressure/velocity relationship, for example, as in Equation (6) in this report. Loads are obtained from integrating the pressures over the body surface as described in the next section. In this treatment the vortices are assumed to be parallel to the body centerline and therefore only induce lateral velocity components. Within the framework of this simplest crossflow analysis, the effects of the external vortices on the axial perturbation flow component are not accounted for. Note that in the computation of the Bernoulli pressure coefficient, the u/V component is the most important one [refer to Equations (6) and (7) of Section 2.6.1 of this report]. Consequently, the Bernoulli pressures on the leeward side of the body are not predicted well. In fact, the present scheme usually overpredicts these pressures. On the windward side where the flow is attached, the calculated Bernoulli pressures are valid provided the Mach number and/or angle of attack are within the range for linear supersonic theory (also refer to Section 2.6 in this report). The normal force acting on the forebody is based on the pressure distributions and is underestimated when vortices are present. Without vortices (low angles of attack), the predicted forebody loads are valid.

In reality, the external vortices are inclined with respect to the body centerline and induce an axial flow component. The present method does not include this contribution which may be most important when the vortices lie close to the body.

Over the length of the afterbody, the paths of the external (body nose and/or canard vortices) vortices are first determined by module VPATH2, the vortex tracker. Once the lateral vortex positions are known as a function of axial distance, the procedure described above for the forebody is employed to compute pressure coefficients at points on the afterbody. These calculations are performed in subroutine BDYPR. Again, only vortex-induced lateral velocity components are included and the contribution to the axial component is neglected. The same remarks made above apply to the afterbody loads under the influence of external vortices. Note that if companion program BDYSHD is engaged, the afterbody pressure distributions and loads include all effects of external vortices including the axial flow components induced by afterbody vortices.

The paths of external vortices over the finned portions of a configuration are calculated by module VPATH2. The vortices will move from one axial station to the next in accordance with crossflow plane theory for external vortices in the vicinity of a finned body, at angle of pitch and sideslip. Details are given in Appendix I of Reference 1. When a vortex lies close to the surface of the body or a fin, an unrealistic vortex path may result. At the present time, this is due in part to the absence of a vortex-core model in the routines of VPATH2. In a case such as this, it is better to make the vortices act as if their paths lie parallel to the body centerline throughout the length of the finned section by means of the input to VPATH2 for steps 2 and/or 5 of the stepwise procedure (Section 2.3). In any event, the flow-tangency condition due to the presence of the external vortices is satisfied in the slender-body theory (two-dimensional) sense at any point on the body or fin surfaces. Then, in order to satisfy the flow-tangency condition in the three-dimensional linear theory sense, the effects of the vortices with their paths known from the slender-body theory calculation are determined at the control points of the constant u-velocity panels distributed over the fins. In this process, the vortices are assumed to be in the presence of the body without the fins (i.e., as shown for two vortices in the previous sketch). In this way, the vortex-induced flow components normal to the fins are included in the fin flow-tangency condition and directly influence the strengths of the constant u-velocity panels on the fins. The Bernoulli pressure calculations on the fins include effects of all the panels on the fins and interference shell, body line singularities and also the velocity lateral components from the external vortices calculated with the vortices in the presence cf the finned body. On the body surface next to the fins, the slender-body-theory flow-tangency boundary condition is retained and the Bernoulli pressure calculations receive contributions from body line singularities, all panels on fins and interference shell and the lateral velocity components from the external vortices calculated with the vortices in the presence of the finned body.

C.5 BODY LOADS CALCULATED FROM PRESSURE DISTRIBUTIONS

In this section, expressions are given for the three components of force acting on axisymmetric bodies in the body coordinate system (x_B,y_B,z_B) shown in the sketch below. The circumferential pressure-coefficient distributions are integrated to give loads acting on a body ring. The forces and moments acting on the rings are added over all body rings to give overall body forces and moments.

Consider an axisymmetric body as shown in the sketch below. At points on body meridians, pressure coefficients are computed in subroutine BDYPR in accordance with the linear and Bernoulli expressions, Equations (5) and (6) in Section 2.6.1, respectively. The geometrical layout of the pressure points provides for a circumferential distribution of calculated pressures at many axial stations from the body nose to the base including the body portions of the forward- and tail-finned sections.

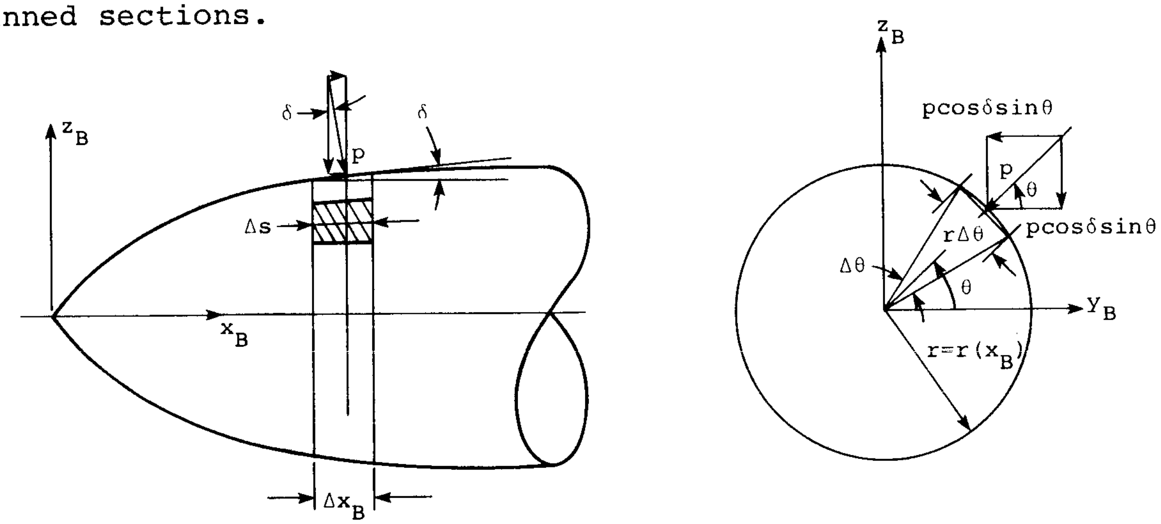

A shaded area is indicated on which pressure p is exerted resulting in elemental force ΔF

$$\Delta F = p(r\Delta\theta)ds \tag{C-24}$$

This elemental force has the following components in the x_B, y_B, and z_B directions.

$$\left.\begin{aligned} \Delta F_{x_B} &= p(r\Delta\theta)\Delta s \sin\delta \\ \Delta F_{y_B} &= -p(r\Delta\theta)\Delta s \cos\delta \cos\theta \\ \Delta F_{z_B} &= -p(r\Delta\theta)\Delta s \cos\delta \sin\theta \end{aligned}\right\} \qquad \text{(C-25)}$$

Noting that

$$\Delta s = \frac{\Delta x_B}{\cos\delta} \qquad \text{(C-26)}$$

and integrating around the circumference gives the forces acting on a ring with thickness Δx_B.

$$\left.\begin{aligned} \Delta F_{x_B}\Big|_{\Delta x_B} &= \frac{r(x_B)\Delta x_B}{\cos\delta}\left[\int_o^{2\pi} p\, d\theta\right]\sin\delta \\ \Delta F_{y_B}\Big|_{\Delta x_B} &= \frac{r(x_B)\Delta x_B}{\cos\delta}\left[\int_o^{2\pi} p \sin\theta\, d\theta\right]\cos\delta \\ \Delta F_{z_B}\Big|_{\Delta x_B} &= \frac{r(x_B)\Delta x_B}{\cos\delta}\left[\int_o^{2\pi} p \sin\theta\, d\theta\right]\cos\delta \end{aligned}\right\} \qquad \text{(C-27)}$$

It is clear that

$$\left.\begin{aligned} &\int_o^{2\pi} p_\infty \begin{Bmatrix}\sin\\ \text{or}\\ \cos\end{Bmatrix} d\theta = 0 \\ &\frac{\sin\delta}{\cos\delta} = \tan\delta = \frac{dr}{dx_B} \end{aligned}\right\} \qquad \text{(C-28)}$$

Thus, the pressure p can be replaced with the pressure coefficient C_p. With the pressure coefficients known, the following expressions are employed to calculate force and moment coefficients acting on a body ring with length Δx_B.

$$\left.\begin{aligned}
\Delta C_X &= \frac{r(x_B)}{S_{ref}} \frac{dr(x_B)}{dx_B} \left[\int_o^{2\pi} C_p d\theta \right] \Delta x_B \\
\Delta C_Z &= - \frac{r(x_B)}{S_{ref}} \left[\int_o^{2\pi} C_p \sin\theta \, d\theta \right] \Delta x_B \\
\Delta C_Y &= - \frac{r(x_B)}{S_{ref}} \left[\int_o^{2\pi} C_p \cos\theta \, d\theta \right] \Delta x_B \\
\Delta C_m &= - \frac{x_B - x_M}{L_{ref}} \Delta C_Z \\
\Delta C_n &= - \frac{x_B - x_M}{L_{ref}} \Delta C_Y \\
\Delta C_\ell &= 0.0
\end{aligned}\right\} \qquad \text{(C-29)}$$

The terms inside the brackets are integrated numerically. Program BDYPR sums these quantities based on the linear and Bernoulli pressure coefficients to give the loads on the forebody, body portion of the forward finned section, afterbody (unless optional program BDYSHD is engaged) and the body portion of the tail section.

APPENDIX D

PRESSURE COEFFICIENTS CALCULATED BY SHOCK-EXPANSION THEORY

D.1 INTRODUCTION

This appendix contains a description of a method for calculating pressure coefficients based on two-dimensional nonlinear shock-expansion (or tangent wedge) theory. It is applied to the calculation of chordwise pressure distributions on an airfoil using strips on the top and the bottom. This method can also be applied to "strips" laid out along the meridians of a body. However, in the application to a body, the two-dimensional tangent wedge theory is only a first approximation. As an improvement, the tangent-cone method can be applied to the body nose tip and Prandtl-Meyer expansion theory used on the rest of the ogive cylinder type bodies.

In the main body of this report, the nonlinear shock-expansion (tangent wedge) method described below is modified to account for three-dimensional interference effects.

D.2 CALCULATION OF PRESSURE DISTRIBUTIONS ON AN AIRFOIL USING SHOCK-EXPANSION THEORY*

The method of calculating the pressure distribution on an airfoil using shock-expansion theory will be described. This method is valid up to the angle of attack at which the leading-edge shock wave becomes detached.

*This portion of the work is due to Mr. F. K. Goodwin at Nielsen Engineering & Research, Inc. and is described in Reference D.1.

Figure D.1 shows an airfoil section whose surface is approximated by a series of straight line segments. The number of segments on the upper or lower surface equals N. The value of x at which a given segment ends, x_n, is specified as is its surface angle, θ_n, measured from the chordal plane. Near the leading edge of the airfoil, θ_n is positive. Downstream of the point of maximum thickness θ_n is negative.

On the lower surface, the flow in each region is characterized by

$C_{p_{\ell_n}}$ = pressure coefficient, $(p_{\ell_n} - p_\infty)/q_\infty$

M_{ℓ_n} = Mach number

ν_{ℓ_n} = local Prandtl-Meyer angle

Similarly, the flow in each region on the upper surface is characterized by

$C_{p_{u_n}}$ = pressure coefficient, $(p_{u_n} - p_\infty)/q_\infty$

M_{u_n} = Mach number

ν_{u_n} = local Prandtl-Meyer angle

The calculation of the N values of Cp_ℓ and the N values of Cp_u will now be described for the lower surface and for the upper surface, respectively. Most of the equations used are taken from Reference D.2.

D.2.1 Lower Surface

Region 1 (behind shock)

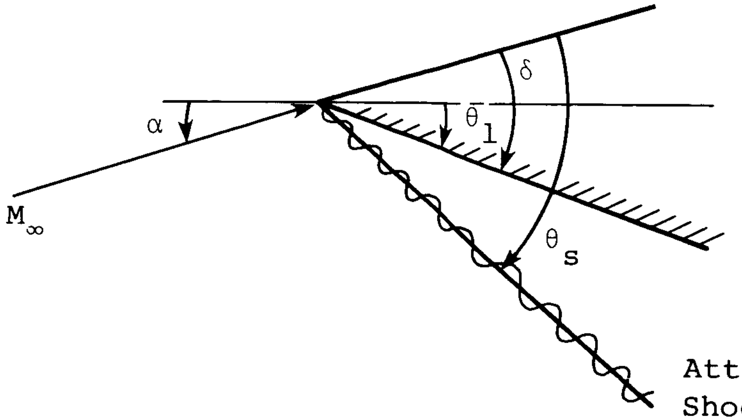

On the lower surface in region 1 shown in figure D.1, the free-stream flow is deflected through an angle δ where

$$\delta = \alpha + \theta_1 \tag{D-1}$$

Angle α is the angle of attack seen by the airfoil section at its leading edge.

To calculate the flow quantities in region 1, the shock wave angle, θ_s, which is a function of M_∞ and δ must be determined. This angle can be determined by an iterative solution of the following equation (γ = 1.4 for air).

$$\mathrm{ctn}\,\delta = \tan\theta_s \left[\frac{(\gamma + 1)M_\infty^2}{2(M_\infty^2 \sin^2\theta_s - 1)} - 1 \right] \tag{D-2}$$

This equation [Equation (138) in Ref. D.2] is double-valued in θ_s. Also, for a given value of M_∞, there is a value of δ above which no solution can be found, this is the case of a detached shock wave. The maximum value of the wedge angle, δ , which will allow an attached shock occurs when, from Equation (D.2),

$$\frac{d\delta}{d\theta_s} = 0 \tag{D-3}$$

Therefore, the maximum value of θ_s for an attached shock wave for a given M_∞ can be found by differentiating Equation (D.2) and setting the derivative, $d\delta/d\theta_s$, to zero. If this is done, the result is

$$\sin\theta_{s_{max}} = \left[\frac{-[4 - (\gamma+1)M_\infty^2] + \sqrt{(\gamma+1)^2 M_\infty^4 + 8(\gamma+1)(\gamma-1)M_\infty^2 + 16(\gamma+1)}}{4\gamma M_\infty^2}\right]^{1/2} \tag{D-4}$$

which is the same as Equation (168) in Reference D.2 for the shock wave angle for maximum stream deflection. Using $\theta_{s_{max}}$ and M_∞, Equation (D-2) can be used to find the maximum value of δ for an attached shock wave.

The procedure to be used in solving Equation (D-2) for θ_s for given values of M_∞ and δ is:

1. Determine $\theta_{s_{max}}$ using Equation (D-4).
2. Using $\theta_{s_{max}}$ in Equation (D-2) compute δ_{max}.
3. If $\delta < \delta_{max}$ solve Equation (D-2) for the value of θ_s which will be less than $\theta_{s_{max}}$.

With θ_s determined, the following quantities in region 1 on the lower surface of the airfoil can be calculated.

Pressure Coefficient [Eq. (145), Ref. D.2]

$$C_{P_{\ell_1}} \equiv \frac{p_{\ell_1} - p_\infty}{q_\infty} = \frac{4(M_\infty^2 \sin^2\theta_s - 1)}{(\gamma + 1)M_\infty^2} \tag{D-5}$$

C-5

Mach Number [Eq. (132), Ref. D.2]

$$M_{\ell_1} = \left\{ \frac{(\gamma+1)^2 M_\infty^4 \sin^2\theta_s - 4(M_\infty^2 \sin^2\theta_s - 1)(\gamma M_\infty^2 \sin^2\theta_s + 1)}{[2\gamma M_\infty^2 \sin^2\theta_s - (\gamma-1)][(\gamma-1)M_\infty^2 \sin^2\theta_s + 2]} \right\}^{1/2} \quad \text{(D-6)}$$

Prandtl-Meyer Angle ν_{ℓ_1} for M_{ℓ_1} [Eq. (171c), Ref. D.2]

$$\nu_{\ell_1} = \sqrt{\frac{\gamma+1}{\gamma-1}} \tan^{-1} \sqrt{\frac{\gamma-1}{\gamma+1} (M_{\ell_1}^2 - 1)} - \tan^{-1}\sqrt{M_{\ell_1}^2 - 1} \quad \text{(D-7)}$$

Ratio of Total Pressure to Free-Stream Total Pressure [Eq. (142), Ref. D.2]

$$\frac{p_{t_{\ell_1}}}{p_{t_\infty}} = \left[\frac{(\gamma+1) M_\infty^2 \sin^2\theta_s}{(\gamma-1) M_\infty^2 \sin^2\theta_s + 2} \right]^{\frac{\gamma}{\gamma-1}} \left[\frac{\gamma+1}{2\gamma M_\infty^2 \sin^2\theta_s - (\gamma-1)} \right]^{\frac{1}{\gamma-1}} \quad \text{(D-8)}$$

Region n:

The procedure used to calculate the pressure coefficients in regions 2, 3,...N on the lower surface is identical so that the following equations are written for region n where n=2,3,...N.

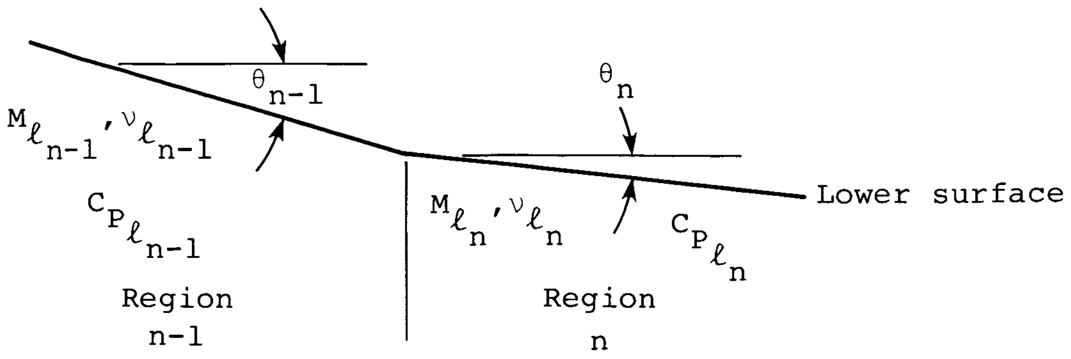

The calculation is repeated sequentially for all these regions as described next.

The flow, in going from region n-1 to region n, expands through angle $(\theta_{n-1} - \theta_n)$. Therefore, the Prandtl-Meyer angle is

$$\nu_{\ell_n} = \nu_{\ell_{n-1}} + (\theta_{n-1} - \theta_n) \quad \text{(D-9)}$$

With this angle known, the Mach number in region n can be calculated using equations given in Reference D.3 and repeated below.

$$M_{\ell_n} = \frac{1 + 1.3604\bar{\nu} + 0.0962\bar{\nu}^2 - 0.5127\bar{\nu}^3}{1 - 0.6722\bar{\nu} - 0.3278\bar{\nu}^2} \quad \text{(D-10)}$$

where

$$\bar{\nu} = \left(\frac{\nu_{\ell_n}}{\nu_{max}}\right)^{2/3} \quad ; \quad \nu_{max} = \frac{\pi}{2}\left(\sqrt{\frac{\gamma+1}{\gamma-1}} - 1\right) \quad \text{(D-11)}$$

The ratio of static pressure to total pressure in region n is then [Eq. (44), Ref. D.2]:

$$\frac{p_{\ell_n}}{p_{t_{\ell_n}}} = \left(1 + \frac{\gamma-1}{2} M_{\ell_n}^2\right)^{-\frac{\gamma}{\gamma-1}} \quad \text{(D-12)}$$

and the pressure coefficient is

$$C_{p_{\ell_n}} \equiv \frac{p_{\ell_n} - p_\infty}{q_\infty} = \frac{\left(\frac{p_{\ell_n}}{p_{t_{\ell_n}}}\right)\left(\frac{p_{t_{\ell_1}}}{p_{t_\infty}}\right) - \frac{p_\infty}{p_{t_\infty}}}{\frac{q_\infty}{p_{t_\infty}}} \qquad \text{(D-13)}$$

This expression uses the fact that $p_{t_{\ell_n}} = p_{t_{\ell_1}}$, i.e., the total pressure is constant behind the oblique shock. The ratio $p_{t_{\ell_1}}/p_{t_\infty}$ is given by Equation (D-8) and

$$\frac{p_\infty}{p_{t_\infty}} = \left(1 + \frac{\gamma-1}{2} M_\infty^2\right)^{-\frac{\gamma}{\gamma-1}} \qquad \text{(D-14)}$$

$$\frac{q_\infty}{p_{t_\infty}} = \frac{\pi}{2} M_\infty^2 \left(\frac{p_\infty}{p_{t_\infty}}\right) \qquad \text{(D-15)}$$

from Equations (44) and (31a) in Reference D.2, respectively.

After the calculations given by Equations (D-9) through (D-15) have been done sequentially for n=2,3,...N, the two-dimensional pressure distribution on the lower surface has been determined.

D.2.2 Upper Surface

Region 1:

Two separate methods are used in calculating the pressure coefficient, $C_{p_{u_1}}$, in region 1 shown in Figure D.1 on the upper surface depending on whether the angle of attack, α, is less than or greater than the surface angle, θ_1, shown also in Figure D.1. The two methods will now be discussed.

Method for $\alpha < \theta_1$

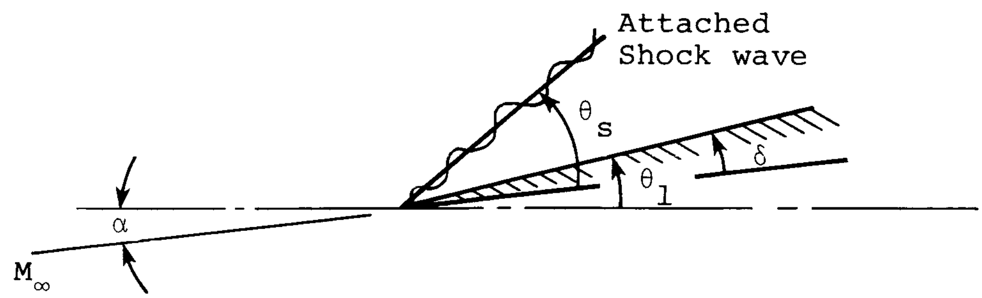

If $\alpha < \theta_1$ the free-stream flow is deflected through an angle δ where

$$\delta = -(\alpha - \theta_1) \tag{D-16}$$

and a shock wave exists on the upper surface. For this case the procedure described for region 1 on the lower surface is followed. The value of δ given by Equation (D-16) is used along with the free-stream Mach number, M_∞, in Equation (D-2) to find the shock-wave angle, θ_s. Analogous to Equations (D-5), (D-6), (D-7), and (D-8) the following expressions hold.

Pressure Coefficient

$$C_{P_{u_1}} \equiv \frac{p_{u_1} - p_\infty}{q_\infty} = \frac{4(M_\infty^2 \sin^2\theta_s - 1)}{(\gamma+1)M_\infty^2} \tag{D-17}$$

Mach Number

$$M_{u_1} = \left\{ \frac{(\gamma+1)^2 M_\infty^4 \sin^2\theta_s - 4(M_\infty^2 \sin^2\theta_s - 1)(\gamma M_\infty^2 \sin^2\theta_s + 1)}{[2\gamma M_\infty^2 \sin^2\theta_s - (\gamma-1)][(\gamma-1)(M_\infty^2 \sin^2\theta_s + 2]} \right\}^{1/2}$$

(D-18)

Prandtl-Meyer Angle for M_{u_1}

$$\nu_{u_1} = \sqrt{\frac{\gamma+1}{\gamma-1}} \tan^{-1}\sqrt{\frac{\gamma-1}{\gamma+1}(M_{u_1}^2 - 1)} - \tan^{-1}\sqrt{M_{u_1}^2 - 1} \quad \text{(D-19)}$$

Ratio of Total Pressure to Free-Stream Total Pressure

$$\frac{p_{t_{u_1}}}{p_{t_\infty}} = \left[\frac{(\gamma+1) M_\infty^2 \sin^2\theta_s}{(\gamma-1) M_\infty^2 \sin^2\theta_s + 2} \right]^{\frac{\gamma}{\gamma-1}} \left[\frac{\gamma+1}{2\gamma M_\infty^2 \sin^2\theta_s - (\gamma-1)} \right]^{\frac{1}{\gamma-1}}$$

(D-20)

Method for $\alpha > \theta_1$

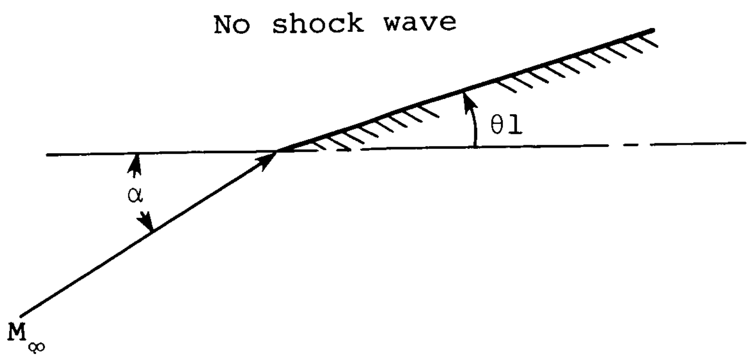

If $\alpha > \theta_1$ the flow expands through angle $(\alpha - \theta_1)$ in going from the free stream to region 1 on the upper surface and the procedure for the expansion flow on the lower surface is repeated. Therefore, the Prandtl-Meyer angle in region 1 is

$$\nu_{u_1} = \nu_\infty + (\alpha - \theta_1) \tag{D-21}$$

where

$$\nu_\infty = \sqrt{\frac{\gamma+1}{\gamma-1}} \tan^{-1}\sqrt{\frac{\gamma-1}{\gamma+1} (M_\infty^2 - 1)} - \tan^{-1}\sqrt{M_\infty^2 - 1} \tag{D-22}$$

and the Mach number is

$$M_{u_1} = \frac{1 + 1.3604\bar{\nu} + 0.0962\bar{\nu}^2 - 0.5127\bar{\nu}^3}{1 - 0.6722\bar{\nu} - 0.3278\bar{\nu}^2} \tag{D-23}$$

where

$$\bar{\nu} = \left(\frac{\nu_{u_1}}{\nu_{max}}\right)^{2/3} \quad ; \quad \nu_{max} = \frac{\pi}{2}\left(\sqrt{\frac{\gamma+1}{\gamma-1}} - 1\right) \tag{D-24}$$

The ratio of static pressure to total pressure in region 1 is

$$\frac{p_{u_1}}{p_{t_{u_1}}} = \left(1 + \frac{\gamma-1}{2} M_{u_1}^2\right)^{-\frac{\gamma}{\gamma-1}} \tag{D-25}$$

and the ratio of total pressure in region 1 to free-stream total pressure, since in this case $(\alpha > \theta_1)$ there is no shock wave, is given by

$$\frac{p_{t_{u_1}}}{p_{t_\infty}} = 1.0 \tag{D-26}$$

The pressure coefficient in region 1 on the upper surface is given by

$$C_{P_{u_1}} = \frac{\left(\frac{p_{u_1}}{p_{t_{u_1}}}\right)\left(\frac{p_{t_{u_1}}}{p_{t_\infty}}\right) - \frac{p_\infty}{p_{t_\infty}}}{\frac{q_\infty}{p_{t_\infty}}} \qquad \text{(D-27)}$$

the quantities p_∞/p_{t_∞} and q_∞/p_{t_∞} are obtained from Equations (D-14) and (D-15).

Region n:

The procedure for calculating the pressure coefficients in regions 2,3,...N on the upper surface is the same as that described previously for the expanding flow regions on the lower surface. The following equations are written for region n where n=2,3,...N.

The flow in going from region n-1 to region n expands through the angle $(\theta_{n-1} - \theta_n)$. The Prandtl-Meyer angle in region n is

$$\nu_{u_n} = \nu_{u_{n-1}} + (\theta_{n-1} - \theta_n) \qquad \text{(D-28)}$$

If n=2, either Equation (D-19) or (D-21) is used to determine $\nu_{u_{n-1}}$ depending on whether α is less than or greater than θ_1.

With ν_{u_n} known, the Mach number in region n is

$$M_{u_n} = \frac{1 + 1.3604\bar{\nu} + 0.0962\bar{\nu}^2 - 0.5127\bar{\nu}^3}{1 - 0.6722\bar{\nu} - 0.3278\bar{\nu}^2} \qquad \text{(D-29)}$$

where

$$\bar{\nu} = \left(\frac{\nu_{u_n}}{\nu_{max}}\right)^{2/3} \quad ; \quad \nu_{max} = \frac{\pi}{2}\left(\sqrt{\frac{\gamma+1}{\gamma-1}} - 1\right) \tag{D-30}$$

The ratio of static pressure to total pressure in region n is

$$\frac{p_{u_n}}{p_{t_{u_n}}} = \left(1 + \frac{\gamma-1}{2} M_{u_n}^2\right)^{-\frac{\gamma}{\gamma-1}} \tag{D-31}$$

and the pressure coefficient is

$$C_{p_{u_n}} = \frac{\left(\frac{p_{u_n}}{p_{t_{u_n}}}\right)\left(\frac{p_{t_{u_1}}}{p_{t_\infty}}\right) - \frac{p_\infty}{p_{t_\infty}}}{\frac{q_\infty}{p_{t_\infty}}} \tag{D-32}$$

Since the total pressure is constant behind the oblique shock (if there is a shock), $p_{t_{u_n}} = p_{t_{u_1}}$. The ratio $p_{t_{u_1}}/p_{t_\infty}$ is given by Equation (D-20) if $\alpha \leq \theta_1$, or by Equation (D-26) if $\alpha > \theta_1$. Quantities p_∞/p_{t_∞} and q_∞/p_{t_∞} are specified by Equations (D-14) and (D-15), respectively. After the calculations given by Equations (D-28) through (D-32) have been repeated sequentially for n=2,3,...N, the two-dimensional pressure distribution on the upper surface of the airfoil has been determined.

All of the above is programmed in subroutines SHKAGL and SHKEXP of program LRCDM2.

REFERENCES

D.1 Nielsen, J. N. and Goodwin, F. K.: Preliminary Method for Estimating Hinge Moments of All Movable Controls. Nielsen Engineering & Research, Inc. TR 268, Mar. 1982.

D.2 NACA Ames Research Staff: Equations, Tables, and Charts for Compressible Flow. NACA Report 1135, 1953.

D.3 Hall, I. M.: Inversions of the Prandtl-Meyer Relation. Aero. Jour., Roy. Aero. Soc., UK, Sept. 1975, pp. 417-418.

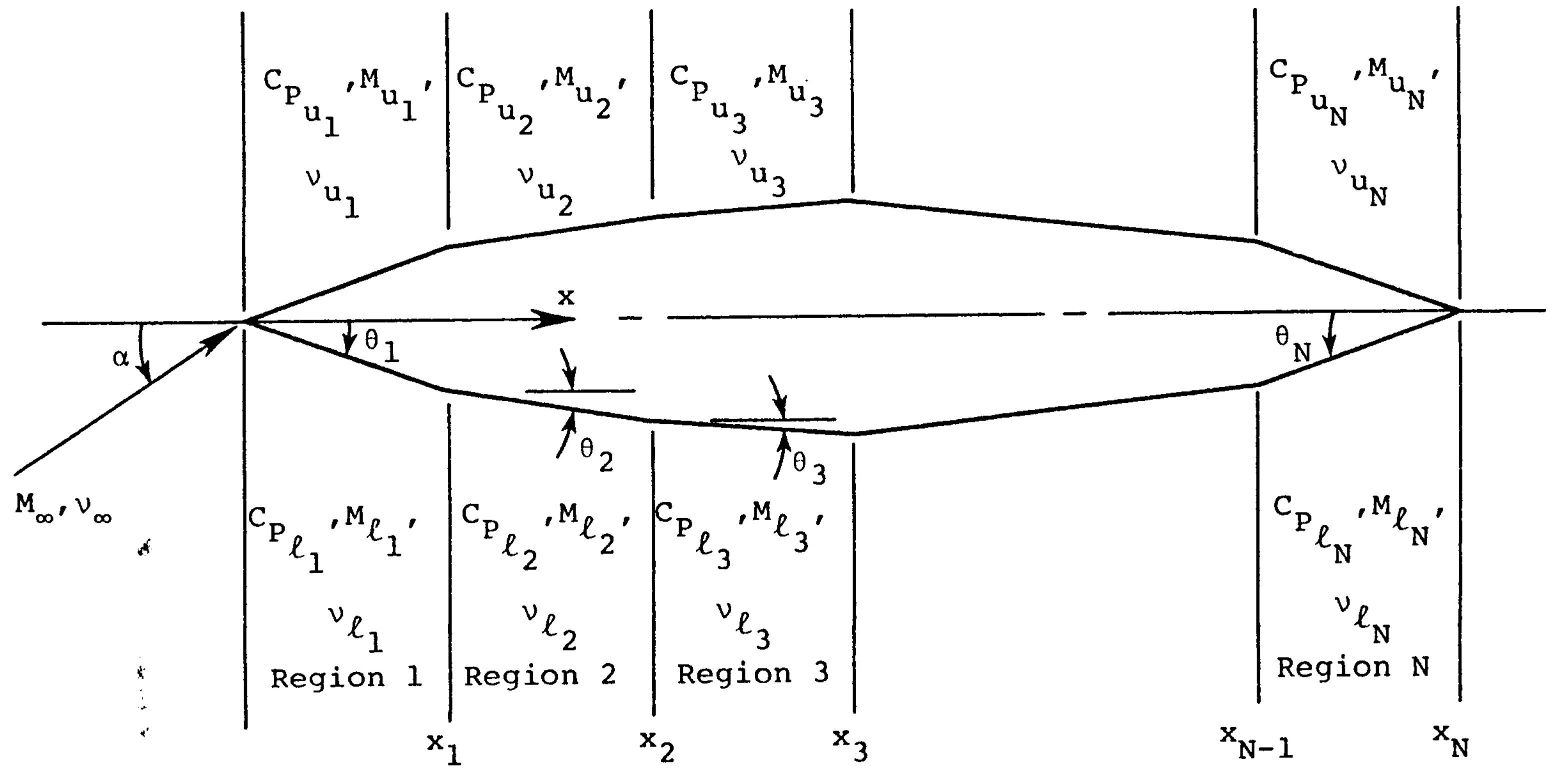

Figure D.1.- Symmetric airfoil section made up of straight line segments.

1. Report No. NASA CR-3883	2. Government Accession No.	3. Recipient's Catalog No.
4. Title and Subtitle Program LRCDM2, Improved Aerodynamic Prediction Program for Supersonic Canard-Tail Missiles With Axisymmetric Bodies		5. Report Date April 1985 6. Performing Organization Code 769/C
7. Author(s) Marnix F. E. Dillenius		8. Performing Organization Report No. NEAR TR 287
9. Performing Organization Name and Address Nielsen Engineering & Research, Inc. 510 Clyde Avenue Mountain View, CA 94043		10. Work Unit No. 11. Contract or Grant No. NAS1-16770
12. Sponsoring Agency Name and Address National Aeronautics and Space Administration Washington, DC 20546		13. Type of Report and Period Covered Contractor Report 08/31/81-02/15/83 14. Sponsoring Agency Code 505-43-23-02

15. Supplementary Notes

Langley Technical Monitor: Jerry M. Allen
Final Report

16. Abstract

Program LRCDM2 was developed for supersonic missiles with axisymmetric bodies and up to two finned sections. This program predicts pressure distributions and loads acting on a complete configuration including effects of body separated-flow vorticity and fin-edge vortices. The analysis embodied in the computer program is based on supersonic paneling and line-singularity methods coupled with vortex-tracking theory. Effects of afterbody shed vorticity on the afterbody and tail-fin pressure distributions can be optionally treated by companion program BDYSHD. Preliminary versions of combined shock-expansion/linear theory and Newtonian/linear theory have been implemented as optional pressure calculation methods to extend the Mach number and angle-of-attack ranges of applicability into the nonlinear supersonic flow regime.

Comparisons between program results and experimental data are given for a triform tail-finned configuration and for a canard-controlled configuration with a long afterbody for Mach numbers up to 2.5. For the latter, the afterbody vortex-shedding option improves prediction of the highly nonlinear total rolling moment for the case with roll control. Initial tests of the nonlinear/linear theory approaches show good agreement for pressures acting on a rectangular wing and a delta wing with attached shocks for Mach numbers up to 4.6 and angles of attack up to 20°. Recommendations are given in the conclusions.

17. Key Words (Suggested by Author(s)) Axisymmetric bodies, finned sections Pressure distributions, overall loads Supersonic panel and line singularity methods Body vortices, canard-fin wakes Nonlinear/linear pressure calculation methods	18. Distribution Statement [redacted] Until April 1987 Subject Category 02

19. Security Classif. (of this report)	20. Security Classif. (of this page)	21. No. of Pages	22. Price
Unclassified	Unclassified	418	